2010

Metamorphic rocks in the Sawtooth Mountains, Idaho, USA: a window into the Precambrian basement of southwest Laurentia

Kyle Michael Metz
Louisiana State University and Agricultural and Mechanical College

METAMORPHIC ROCKS IN THE SAWTOOTH MOUNTAINS, IDAHO, USA: A WINDOW INTO THE PRECAMBRIAN BASEMENT OF SOUTHWEST LAURENTIA

A Thesis

Submitted to the Graduate Faculty of the
Louisiana State University and
Agricultural and Mechanical College
In partial fulfillment of the
Requirements for the degree of
Master of Science

In

The Department of Geology and Geophysics

By
Kyle Metz
B.S., Texas Tech University, 2007
August 201

ACKNOWLEDGEMENTS

I wish to thank my committee, Dr. Barbara Dutrow, Dr. Darrell Henry, and Dr. Alexander Webb, for their guidance and support throughout my graduate career. I am especially grateful towards Dr. Dutrow for introducing me to the Sawtooth Mountains, a place of unrivaled beauty. Drs. Dutrow and Henry have been instrumental in providing scholarship opportunities towards funding this project. My committee has always had an open door for questions and comments which were instrumental in completion of this project.

I am sincerely thankful to Dr. Dennis Norton and Dr. Dana Perkins for introducing me to the field area and making me feel like a local to the region. Many thanks go to Philip Bergeron for keeping me relatively sane during the first field season. I'd also like to thank Amy Spaziani for support in the field and in the office. Without her encouragement I would have been lost. I thank Rick Young for the many hours spent preparing and polishing thin sections and Dr. Xiaogang Xie for assistance with the electron microprobe.

I also thank the monetary support for this project: the American Federation of Mineralogical Societies, the Southeastern Geophysical Society, the New Orleans Geological Society, the Advanced Depositional Geosystems program at LSU along with the Department of Geology and Geophysics.

Thanks to the Sawtooth National Recreation Area administered through the National Forest Service for providing a collection permit for the study area in the Sawtooth Wilderness Area.

TABLE OF CONTENTS

LIST OF TABLES

LIST OF FIGURES

ABSTRACT

The western North American craton consists of a mosaic of Precambrian basement terranes that developed through episodes of microcontinent collision and magmatic-arc accretion. Defining the extent and boundaries of these terranes is critical to deciphering the Precambrian development of Laurentia. The poorly exposed Selway terrane occurs between the Archean Wyoming province and the Neoproterozoic rifted margin of Laurentia. A rare exposure of Precambrian metamorphic rocks, the Sawtooth Metamorphic Complex (SMC), crops out over 33 km^2 in the Sawtooth Mountains of Idaho, USA, and potentially provides a window into the deep crust of the region.

Field mapping, petrographic analyses, and mineral chemical data characterize the nature of the SMC rocks. Nine rock types occur in the SMC: quartzite, quartzofeldspathic gneiss, calc-silicate gneiss, marble mylonite, titanite-hornblende-biotite gneiss, metagabbro, biotite-amphibolite, peraluminous gneiss, and amphibole-pyroxene gneiss.

Cross-cutting relationships and mineral-replacement textures in the Iron Creek peraluminous gneiss indicate the rocks passed through muscovite stability in the sillimanite field during prograde metamorphism but dehydrated to produce sillimanite + K-feldspar + H_2O. Fine-grained biotite and sillimanite are included in cordierite suggesting the reaction: phlogopite + sillimanite $\rightarrow$ Mg-cordierite + garnet + H_2O. These two dehydration reactions contribute to partial melting of the rocks at peak metamorphic conditions interpreted to be near T = 800°C and P = 7 kbar based on presence of migmatites. Tabular muscovite and euhedral andalusite cross-cut the main foliation in Iron Creek peraluminous gneisses, indicating a clock-wise decrease in pressure and temperature during retrograde metamorphism.

Thompson Peak rocks share similar prograde, peak, and post-peak conditions, but different retrograde paths. Thompson Peak rocks contain pseudomorphs of kyanite indicating the rocks remained at relatively high-presssure during retrograde metamorphism.

Based on several geothermobarometers, calculated metamorphic conditions, T = 680 – 750 ±40 °C and P = 5 – 7 ± 0.5 kbar, indicate the rocks are transitional granulites to amphibolites from the mid-lower crust. Clock-wise P-T paths suggest the SMC is composed of multiple tectonic slices from the mid-lower crust metamorphosed in a collisional tectonic setting. This suggests the SMC is a western exposure of the Selway terrane.

CHAPTER I. INTRODUCTION

1.1 Background Geology

In the last three decades, numerous advances have been made in understanding the nature of Archean – Proterozoic terranes in North America and the timing of orogenic events associated with the accretion of these terranes. Through isotope geochronologic and geophysical studies, multiple Archean and Proterozoic terranes have been identified across North America and used in tectonic reconstructions of Laurentia (e.g. Thomas et al., 1987; Hoffman, 1988; Lemieux et al., 2000; Ross, 2002;).

The assembly history of Laurentia was first summarized by Hoffman (1988). Since this historic paper, other studies have refined the tectonic and paleogeographic history of Laurentia (Percival et al., 2004; Corrigan et al., 2005; Whitmeyer and Karlstrom, 2007), but the basic model still stands (Fig. 1.1); that is a series of Archean continents and smaller Archean continental fragments sutured together by Paleoproterozoic orogens. The formation of Laurentia can be interpreted from evidence in magmatic and metamorphic events found in Archean - Proterozoic crustal blocks and in the Paleoproterozoic suture zones between these blocks (Mueller and Wooden, 1988; Mogk et al., 1992; Mueller et al., 1993; Frost et al., 1998; Frost et al., 2000; Chamberlain et al., 2003; Mueller et al., 2005).

The initial amalgamation of Laurentia is inferred to be a series of collisional events, referred to as the Trans-Hudson orogeny, which occurred from ca. 1.96 to 1.80 Ga. This orogeny is comparable in spatial and temporal scale to the modern accretionary growth of the Tibetan Plateau (e.g. Whitmeyer and Karlstrom, 2007). Some of these Paleoproterozoic collisions are interpreted to have consumed large amounts of oceanic crust as suggested by the remnants of 1.96-1.86 Ga juvenile volcanic arcs occurring within the orogens (Mueller et al., 2002; Bleeker, 2003; Corrigan et al., 2005; Bleeker and Ernst, 2006). After the initial amalgamation of

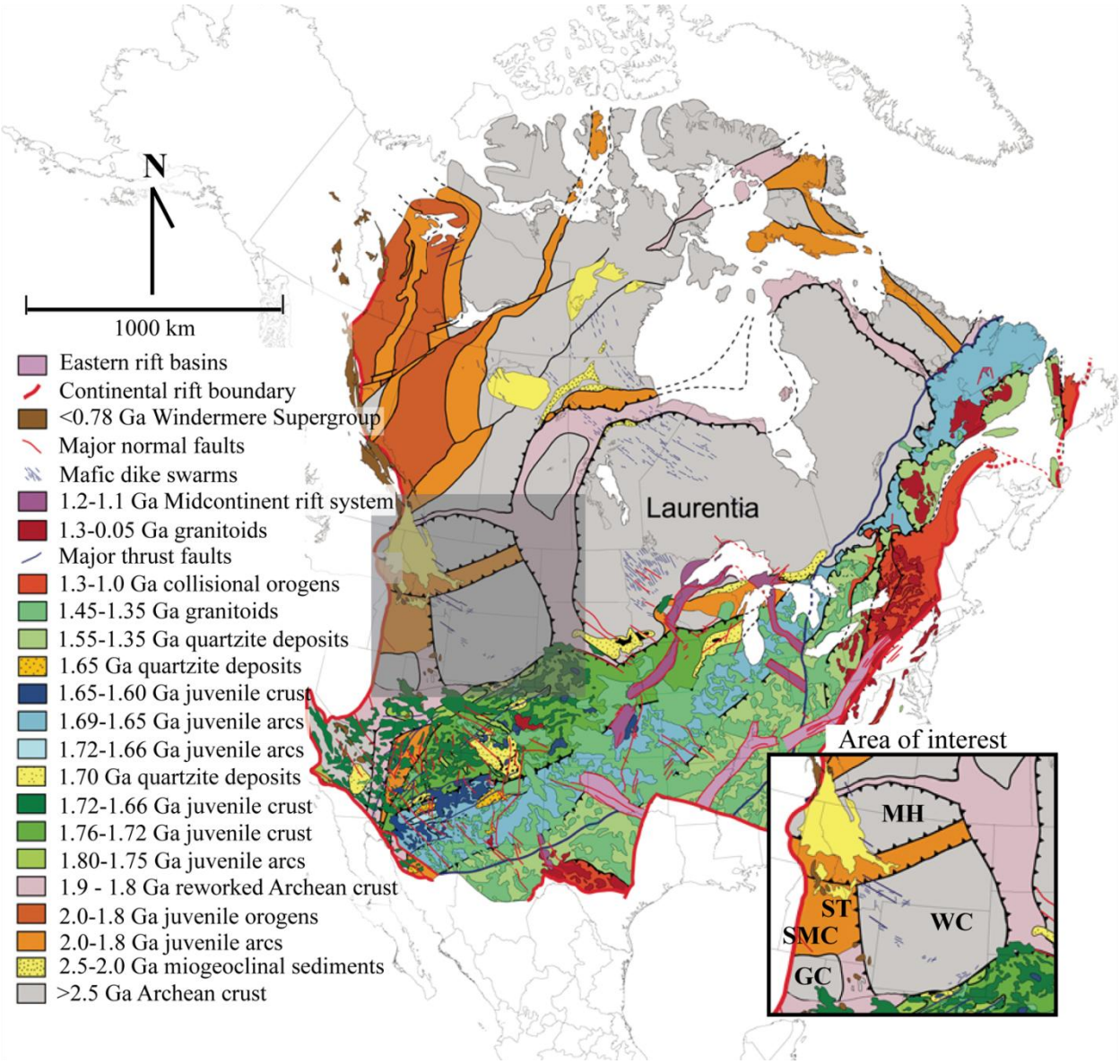

Figure 1.1: Schematic map of Archean through Neoproterozoic basement terranes of Laurentia, modified from Whitmeyer and Karlstrom (2007). The box is the area of interest, and includes the Wyoming Craton (WC), Medicine Hat block (MH), Grouse Creek block (GC), and Selway terrane (ST) that includes the Sawtooth Metamorphic Complex (SMC).

Laurentia (ca 1.80 Ga), new crust was added along the southern margin by the progressive accretion of juvenile magmatic arcs and oceanic terranes (i.e. Yavapai, Mazatzal), analogous to present-day convergence between Australia and Indonesia (Whitmeyer and Karlstrom, 2007).

The tectonic framework occurring along the southwestern margin of Laurentia (west of the Wyoming Craton) remains enigmatic due to the lack of Precambrian basement-rock exposures (Fig. 1.2). Exposures are rare because abundant Cretaceous – Tertiary magmatic/volcanic activity such as the Idaho batholith, Snake River Plain basalts, and the Yellowstone hotspot has obliterated or covered most of the older rocks. Despite this, various Archean crustal blocks and Proterozoic provinces have been proposed. These include: the Medicine Hat, Priest River, and Grouse Creek blocks, the Great Falls Tectonic zone and Selway terrane (e.g. Foster et al., 2006).

Two theories for the tectonic framework of southwestern Laurentia have been proposed based on isolated Precambrian outcrops. Geochronologic data from the proposed Selway terrane suggest new crust was added through the accretion of magmatic arc-like terranes, and this terrane extends from the western margin of the Wyoming Craton to the Salmon River suture (Fig. 1.3, e.g. Foster et al., 2006). However, isotopic and geochronologic data from the Grouse Creek block, suggest there could be a previously un-identified Archean crustal block west of the Wyoming Craton (Fig. 1.3, e.g. Stroud et al., 2009). Cross sections across the western margin of Laurentian provide insight into tectonic processes occurring in the region (Fig. 1.3). A western exposure of mid-lower crust is critical to understanding and building these cross sections.

The Sawtooth Metamorphic Complex (SMC) crops out at the intersection of these ambiguous terranes and may provide a window into the middle-lower crust of central Idaho. Determining the metamorphic P-T conditions of the SMC potentially yields information on

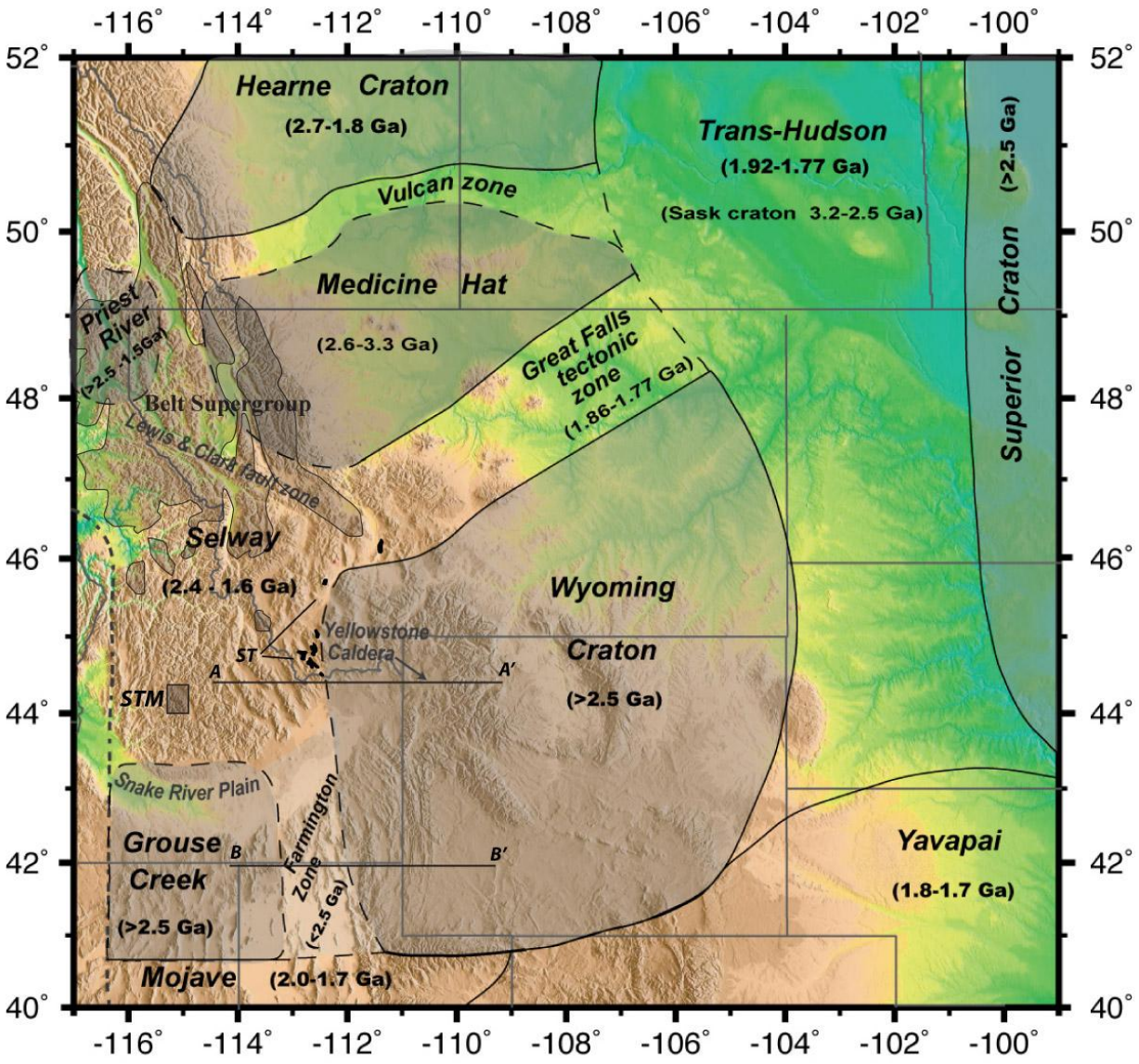

Figure 1.2: Schematic map of the Archean and Proterozoic basement terranes of southwest Laurentia (slightly modified from Foster et al., 2006). Dashed lines indicate uncertainty in contacts of crustal provinces surrounding the Selway terrane (ST). The Sawtooth Mountains (STM) are denoted by the grey rectangle and the definitive outcrops of Selway terrane (ST) are shown in black (Foster et al., 2006). Current state boundaries are shown with grey lines. The dotted line to the west is the Salmon River suture/Sr = 0.706 line. The cross section lines (A-A' and B-B') relate to the schematics in Fig. 1.3.

tectonic processes occurring along the southwestern margin of Laurentia. In addition, mineral-assemblage data and ages aid in constraining the extent of Proterozoic terranes in this region. This study tests the hypothesis that the SMC is a remnant of the Selway terrane suggesting that crust was added to the southwestern margin of Laurentia by accretionary processes during the Proterozoic (Fig. 1.3, A-A'). To test this, detailed field mapping and petrologic investigation were undertaken to determine the extent of the SMC, the mineral assemblages present, and pressure-temperature conditions recorded in the rocks. Additionally, the SMC likely represents a sample of original middle-lower crust entrained into the Sawtooth batholith at intrusion and can be used as a model for middle-lower crust for recent Earthscope investigations in the region (Fig. 1.2, www.earthscope.org).

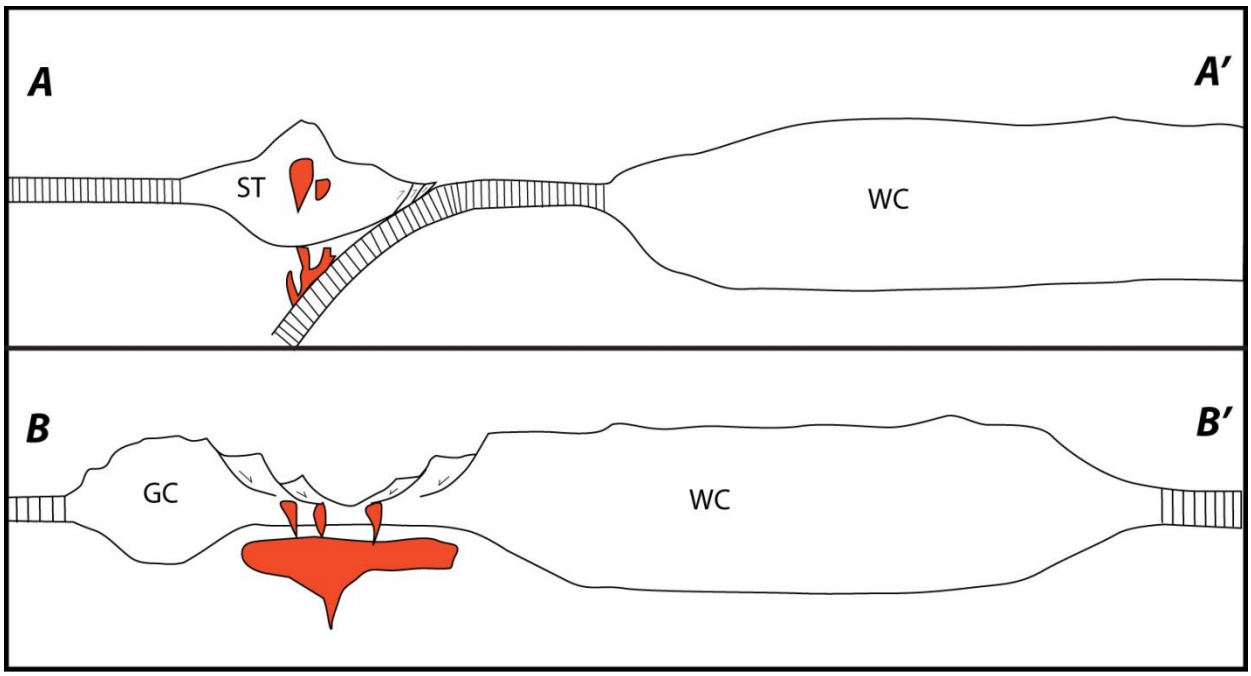

Figure 1.3: Schematic cross sections of leading hypotheses for the tectonic evolution of basement rock along the southwestern margin of Laurentia. Cross section locations are shown in Figure 1.2. The top model shows the Selway terrane (ST) as a magmatic arc accreting to the western margin of the Wyoming Craton (WC). The lower model suggests the Grouse Creek block (GC) is a partially rifted fragment of the WC.

1.2 Study Area

The Sawtooth Metamorphic Complex (SMC) occurs within the Sawtooth Mountains (STM), a basin and range, fault-bounded mountain range located in central Idaho (Fig. 1.4). The STM consist primarily of rocks of the Idaho batholith, a biotite-muscovite granodiorite emplaced at ~4 km from 100-75 Ma (e.g. Lewis et al. 1987; King and Valley, 2001; Evans and Green, 2003). The Sawtooth batholith intruded into the Idaho batholith ca. 45 Ma. The Sawtooth batholith is an alkali-feldspar and volatile-rich granite with widespread aplite and pegmatite dikes, indicative of shallow intrusion (e.g. Norton, pers. comm., Williams et al., 2004). During the Tertiary, the STM were uplifted as a horst block by basin and range extension and are bound on the east by the Sawtooth (normal) Fault, separating them from the adjacent Stanley Basin (Reid, 1963). Pleistocene glaciation deposited large moraines (Fig. 1.5, 2-3 km long and >300 m in elevation) that cover the Sawtooth fault. A regional fracture system, coupled with frost wedging, give the Sawtooth Mountains their characteristic appearance of steep-sided ridges with serrated, peaks above broad glacial valleys (Fig. 1.6).

Within the Sawtooth Mountains, the Sawtooth Metamorphic Complex (SMC) occurs as an isolated outcrop of metamorphic rock largely on top of the Sawtooth batholith (Reid, 1963). The SMC is bound on the north and south by the Sawtooth batholith, on the west by the Idaho batholith, and on the east by the Sawtooth fault. Initial studies in the area mapped the metamorphic rocks as undifferentiated Precambrian metamorphic rocks (Fig. 1.7, Reid, 1963).

Subsequently, multiple metasedimentary and metaigneous lithologies were differentiated within the SMC (Dutrow et al., 1995). These lithologies include meta-pelities, amphibolites, calc-silicate gneisses, marbles, and pyroxene gneisses. Peak conditions are suggested by the presence of migmatites. Based on the partial melting curve of a Ca-bearing granite with $X(H_2O) = 0.5$, conditions are estimated at 800 °C and 7 kbar (Fig. 1.9, ibid).

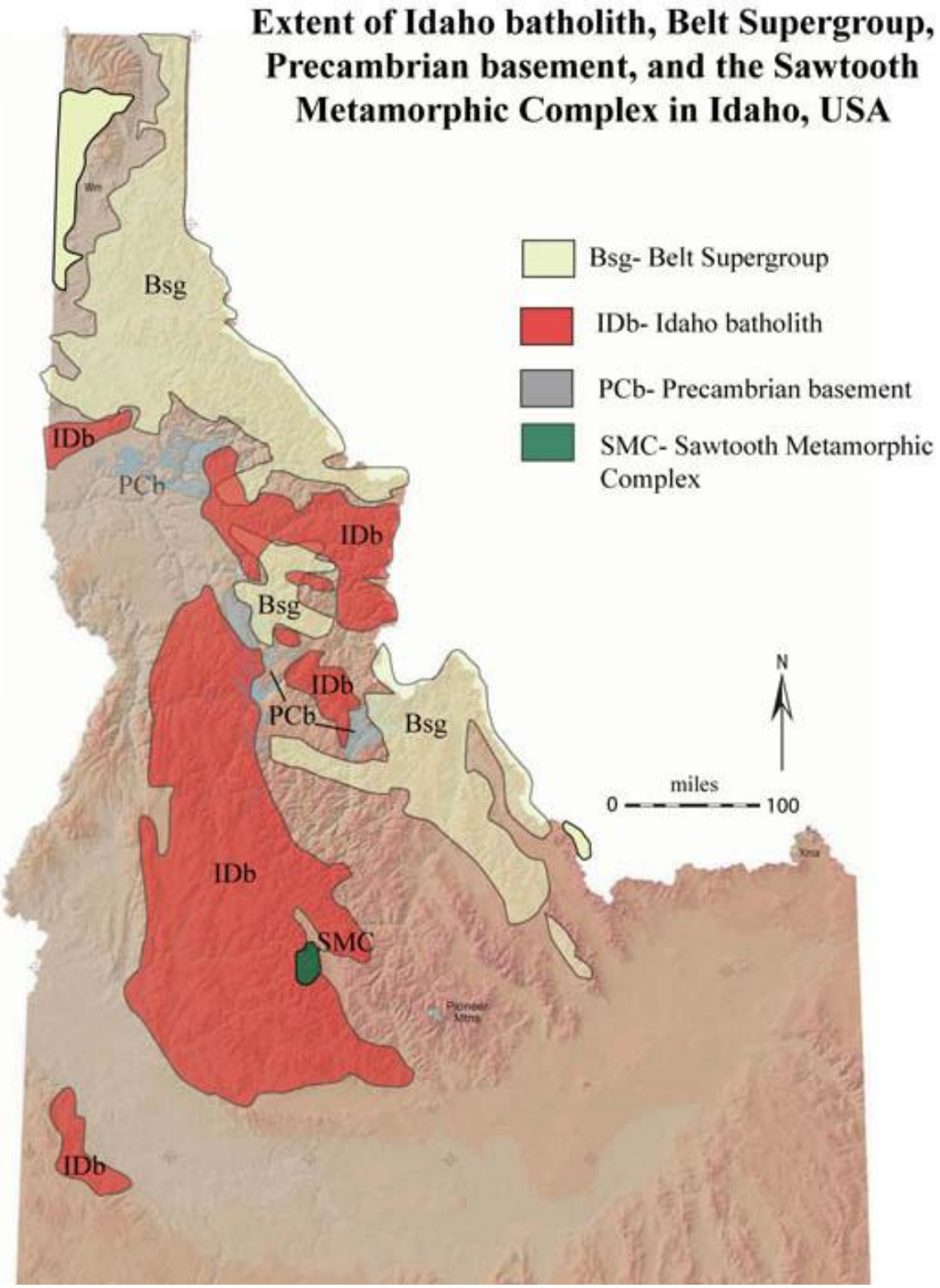

Figure 1.4: Digital elevation map of Idaho displaying the extent of the Idaho batholith (IDb), Belt Supergroup (Bsg), Precambrian basement (PCb) and the Sawtooth Metamorphic Complex (SMC). Modified from Digital atlas of Idaho (http://imnh.isu.edu/digitalatlas).

Figure 1.5: Photo of Thompson Peak, the highest peak in the range at 10,751 feet, taken from a lateral moraine with greater than 1000 feet of relief. Large U-shaped valleys and moraines were created by relatively recent glacial processes (Photo from K. Metz).

Figure 1.6: Panoramic view of the Sawtooth Mountains front range taken to the southwest from the town of Stanley, ID. The Stanley basin, a basin-and-range graben structure, is in the foreground. Serrated peaks are created by jointing in the rocks, giving the Sawtooth Mountains their name (Photo from B. Dutrow).

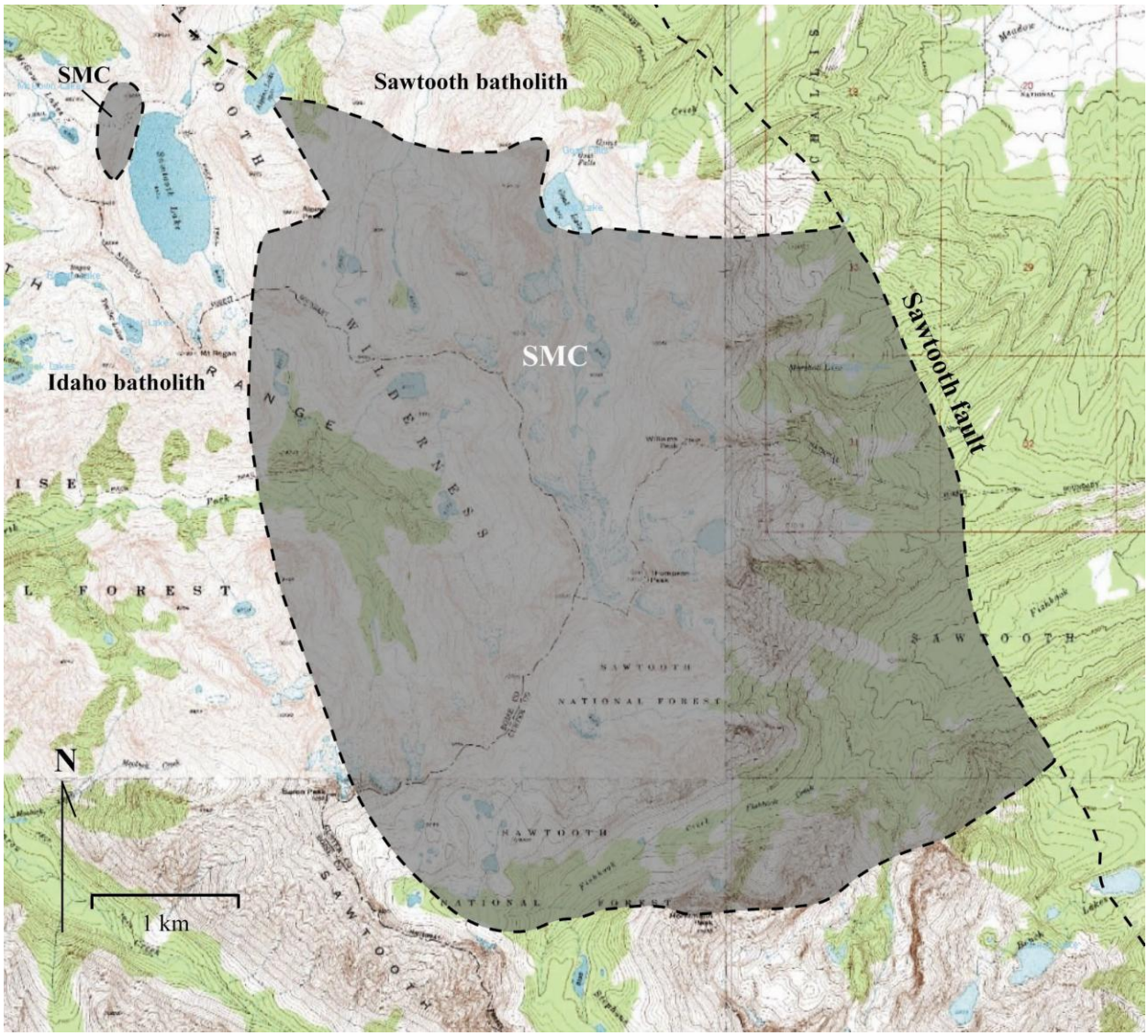

Figure 1.7: Topographic map of the Sawtooth Mountains displaying original extent of the SMC mapped as undifferentiated Precambrian metamorphic rock (Reid, 1963). Basemap is USGS topographic quadrangles: Stanley Lake (west) and Stanley (east) from NASA's Worldwind program.

Preliminary thermo-barometric and mineral-chemical data from the Thompson Peak area record post-peak metamorphic conditions of 650-775°C and 5 – 7 kbar (Fig. 1.9, Table 1.1, Anderson, 1995; Dutrow et al., 1995). Such conditions suggest that these rocks are transitional granulites and remnants of the middle-lower crust. A margarite pseudomorph after kyanite indicates the rocks passed into the kyanite stability field during prograde metamorphism. A composite clock-wise pressure-temperature (P-T) path for the Thompson Peak rocks expresses these conditions, suggesting metamorphism through collisional processes (Fig. 1.9). One Nd/Sm model age of 2.4 Ga suggests these rocks might represent the Paleoproterozoic Selway terrane (Dutrow et al., 1995).

1.3 Geologic Setting of Associated Crustal Blocks

The following sections briefly describe the Archean and Proterozoic basement terranes of southwestern Laurentia relevant to the SMC (Fig. 1.2). Archean crustal blocks include the Wyoming craton, Medicine Hat block, Priest River complex, and Grouse Creek block. Accretionary terranes including the Great Falls Tectonic zone and Selway terrane are discussed subsequently, followed by Precambrian metamorphic and basement rocks found in Idaho.

1.3.1 Wyoming Craton

The Wyoming craton (WC, Fig. 1.2) is perhaps the most well – understood Archean crustal province in Laurentia. In part, this is due to the relative abundance of basement rock exposures and the fact that these rocks represent some of the oldest crust (~3.5 Ga) known in the North American continent (e.g. Wooden and Mueller, 1988; Mogk et al., 1992; Frost, 1993; Frost et al., 1998; Frost et al., 2000; Mueller and Frost, 2006).

The Wyoming craton can be summarized as a series of Archean magmatic belts which nucleated around Middle- to Late Archean core, and can be divided into five sub-provinces (e.g.

Chamberlain et al., 2003). The continental nucleus, Beartooth-Bighorn Magmatic Province (BBMP), is a predominantly granitic-tonalitic-dioritic terrane that was relatively rapidly intruded

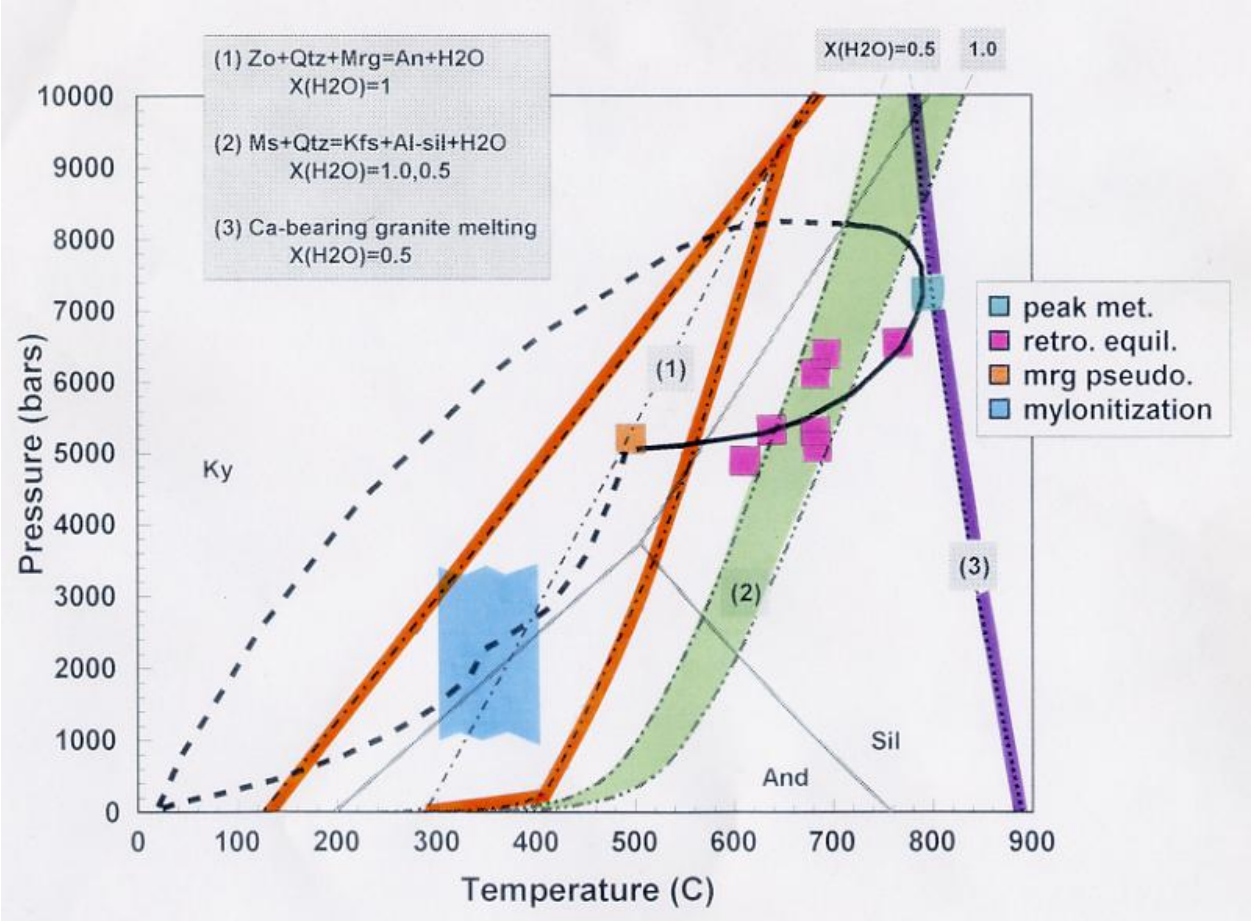

Figure 1.8: Petrogenetic grid displaying a composite clockwise P-T path for the Thompson Peak rocks of the SMC (from Dutrow et al., 1995). Peak conditions are estimated by the Ca-bearing granite melting curve with $X(H_2O) = 0.5$ at ~800°C and 7 kbar. Post-peak conditions calculated define a range from 650-775°C and 5 – 7 kbar (Dutrow et al., 1995). A margarite pseudomorph after kyanite indicates the rocks passed through the kyanite field. This clockwise P-T path suggests metamorphism through collisional processes.

at ~2.8 Ga associated with subduction processes (D. Henry, pers. comm.). These plutonic rocks contain earlier xenoliths as old as 3.7 Ga with detrital zircons over 4.0 Ga (D. Henry, pers. comm.). The northwest portion of the Wyoming craton consists of 3.5 – 3.2 Ga gneisses known as the Montana metasedimentary terrane (MMT) and represents older metasedimentary crust (3.5-3.2 Ga) accreted onto the BBMP at 2.55 Ga (e.g. Mueller et al., 1993; Chamberlain et al., 2003).

The MMT consists of quartzofeldspathic gneisses, banded iron formations, marbles, calcareous gneisses, and pelitic to mafic schists (e.g. Mogk and Henry, 1988). Peak metamorphic conditions of ~800°C and 6 -7 kbar are recorded in trondhjemitic gneisses. A clockwise P-T-*t* path is suggested by mineral inclusions, reaction textures and P-T estimates based on core-rim mineral compositions (e.g. Mogk 1990). South of the MMT is a suite of 2.90 – 2.75 Ga high-Na, tonalite-trondjemite-granodiorite and calc-alkaline plutons in the Teton Range (e.g. Chamberlain et al., 2003). South of this pluton suite are three, roughly concentric, zones of calc-alkaline magmatism that contain juvenile rocks. These zones of calc-alkaline magmatism become progressively younger to the south and consist of 2.71-2.67, 2.63-2.60 and 2.55-2.50 Ga age rocks respectively. The curvilinear forms of these magmatic belts, along with chemical and isotopic data, have been interpreted as evidence for a long-lived active margin surrounding the Wyoming craton during the Archean (Frost et al., 1998, 2000; Chamberlain et al., 2003). The lithosphere of the Wyoming craton is ~60 km thick and possesses seismic velocity of 8.1-8.4km/s (Thomas et al., 1987; Henstock et al., 1998). These properties coupled with enriched Pb isotopic signatures (Mueller and Wooden, 1988; Frost, 1993), and Archean U/Pb ages distinguish it from adjacent terranes (Table 1.2) and aid tectonic correlations.

The Wyoming craton has been variously interpreted to be (1) a southward continuation of the Medicine Hat-Hearne province (Ross, 2002); (2) a separate, unique, Archean terrane based on geochemical and geophysical data (Wooden and Mueller, 1988; Mogk et al., 1992; Frost et al., 1998; Henstock et al., 1998; Chamberlain et al., 2003; Foster et al., 2006; Mueller and Frost, 2006); and (3) an Archean continental fragment rifted off the southern margin of the Superior province based on mafic dike swarms and miogeosynclinal sediment packages in both terranes (Dahl et al., 2006).

Table 1.1: Pressure and Temperature calculations of SMC rocks from the Thompson Peak area (from Anderson, 1995 and Dutrow et al., 1995).

Sample	Rock type	position	Temperature (˚C)	Pressure (kbar)	Calculation
95-08	grt-sil-bt gneiss	Inner rim	765 ± 10	6.54 ± 0.11	TWQ
		Outer rim	684 ± 19	5.09 ± 0.04	
94-06	Amphibolite	Core	655	7 (assumed)	H&B
		Inner rim	764	7 (assumed)	
		Core	683	7 (assumed)	H&B
		Inner rim	704	7 (assumed)	
94-28	Amphibolite	Core	687	7 (assumed)	H&B, rxn A
		Inner rim	682	7 (assumed)	
		Core	729	7 (assumed)	H&B, rxn B
		Inner rim	710	7 (assumed)	
95-06	Amphibolite	Inner rim	682 ± 16	6.11 ± 0.23	TWQ
		Outer rim	611 ± 10	4.9 ± 0.15	
95-05	Grt-hbl gneiss		693 ± 11	6.4 ± 0.15	TWQ
94-36	Calc-silicate	Core	490	7 (assumed)	H&B, rxn A
		Inner Rim	476	7 (assumed)	
		Core	652	7 (assumed)	H&B, rxn B
		Inner Rim	652	7 (assumed)	
95-02	Grt-hbl gneiss		490	5.3	TWQ

TWQ = multi-equilibria of Berman, 1991; H&B = Holland and Blundy, 1994
rxn A = edenite + quartz = tremolite + albite
rxn B = edenite + albite = richerite + anorthite

Table 1.2: Summary of Archean and Proterozoic basement crustal province ages in southwestern Laurentia (refer to Fig. 1.2 for locations).

Terrane Name	age (Ga)	method	Source
Wyoming Province	>2.5	all	*Chamberlain et al., 2003; Mueller et al., 1993*
Medicine Hat Block	2.6-3.3	not specified	*Ross et al., 1991*
Priest River Complex	2.65 & 1.58	U/Pb SHRIMP	*Soughty et al., 1998*
Great Falls Tectonic Zone	1.86 - 1.77	U/Pb SHRIMP	*Cheney et al., 2004; Mueller et al., 2005*
Grouse Creek Block	3.2 - 2.6	U/Pb SHRIMP	*Leeman et al., 1985; Wolf et al., 2005*
Selway Terrane	2.4 - 1.6	U/Pb SHRIMP	*Foster et al., 2006*
Belt-Purcell Supergroup	1.47 - 1.4	U/Pb SHRIMP	*Evans et al., 2000; Luepke et al., 2001*
Pioneer Mountains	2.6-2.2 & 1.8-1.4	not specified	*Link et al., 2007; Link, 2009*
Idaho roof pendants	1.44 w/ ~0.1 meta	not specified	*Lund, 1993; Lund et al., 2005; Lund et al., 2008*

all methods = U/Pb SHRIMP, LA-ICPMS, and TIMS

1.3.2 Medicine Hat Block

The basement terrane of northwestern Montana and southern Alberta is known as the Medicine Hat block (MH, Fig. 1.2). The Medicine Hat block has been defined by borehole intersections and geophysical data because no known outcrops exist (e.g. Ross et al., 1991; Lemieux et al., 2000). No detailed mineralogic or petrologic work has been conducted on these rocks; although, U/Pb zircon analyses of crystalline basement from drill core give 3.3 – 2.6 Ga crustal ages (Table 1.2, Ross et al., 1992). The Medicine Hat block may be the southern extension of the Hearne province (Hoffman, 1989), but it has also been proposed as part of the Wyoming craton based on seismic studies (e.g. Henstock et al., 1998).

Currently, the most accepted model interprets the Medicine Hat block as a separate crustal block that accreted to the Hearne province along the Paleoproterozoic Vulcan zone and to the Wyoming craton along the Great Falls Tectonic Zone ca. 1.77 Ga (e.g. Mueller et al., 2002, 2005). The Medicine Hat block is bounded on the north by the Vulcan zone, on the east by the Trans-Hudson Orogeny, and on the south by the Great Falls Tectonic zone. The western extent of the Medicine Hat block is poorly defined.

1.3.3 Priest River Complex

The Priest River metamorphic core complex in northern Idaho (PR, Fig. 1.2) contains Archean and Proterozoic outcrops. Metaigneous rock units in the Priest River complex include the Pend Oreille gneiss, a medium- to coarse-grained quartzofeldspathic gneiss with quartz + plagioclase + biotite + K-feldspar, and the Laclede augen gneiss, a megacrystic augen gneiss (e.g. Doughty et al., 1997). U – Pb TIMS zircon geochronology of the Pend Oreille gneiss and Laclede ortho-augen gneiss (Table 1.2) reveals 2.65 Archean basement rock with 1.58 Ga felsic meta-intrusive rock, respectively (Evans and Fischer, 1986; Doughty et al., 1998). Metasedimentary rocks in the region include the Hauser Lake gneiss, a coarse-grained migmatitic paragneiss composed of interlayered granofels and pelitic schist with disseminated sulfides, and the Gold Cup quartzite, a medium- to coarse-grained quartzite containing quartz + K-feldspar + sillimanite + biotite (Doughty et al., 1997). Metasedimentary rocks contain upper amphibolite – granulite facies mineral assemblages that record P-T conditions of 675 - 930°C and 7 – 10 kbar (Doughty, 1995).

Interpretations of the Priest River complex have implications for constraining the Belt-Supergroup and reconstructions of the supercontinent Rodinia. Metaigneous rocks are interpreted as Precambrian basement, and metasedimentary rocks are interpreted as the lower-most sections of the Belt-Purcell Supergroup (e.g. Doughty et al., 1998). The co-occurrence of 2.65 Ga and 1.58 Ga orthogneiss has been used as a piercing point for the reconstruction of the supercontinent Rodinia (Doughty et al., 1998). A similar assemblage of 2.55-2.65 Ga crust with 1.59 Ga felsic volcanic and plutonic rock is found in the Gawler craton of eastern Australia (Fanning et al., 1988). This supports the model proposed by Ross et al. (1992) that east Australia's Gawler craton was once adjacent to the western margin of Laurentia (Doughty et al., 1998).

1.3.4 Grouse Creek Block

The Grouse Creek block is an Archean basement terrane that occurs west of the Wyoming craton and south of the SMC (Fig. 1.2, Foster et al., 2006). Isolated outcrops of Archean rock have been noted in the Albion, Raft River, East Humbolt, and Grouse Creek ranges of Idaho, Utah, and northeastern Nevada (Wright and Snoke, 1993; Nelson et al., 2002; Egger et al., 2003), but no detailed mineralogic/petrologic studies have been published on these Archean exposures.

The extent of the Grouse Creek block is unclear. Cenozoic lavas of the Snake River Plain include metaigneous xenoliths with Sm – Nd model ages between 3.2 – 2.6 Ga. This suggests the Grouse Creek block extends beneath the Snake River Plain (Leeman et al., 1985; Wolf et al., 2005). The Grouse Creek block appears to be separate from the Wyoming craton based on exposures of Paleoproterozoic rocks with 2.45 – 1.6 Ga zircon ages in the Farmington Canyon complex, Utah that lie between these blocks (Bryant, 1988; Nelson et al., 2002). Although the Grouse Creek block is separate from the Wyoming craton on the surface, it is unclear if they are disconnected at deeper crustal levels (Nelson et al., 2002; Foster et al., 2006). Isotopic U/Pb and Ar^{40}/Ar^{39} monazite ages in the Farmington Canyon complex suggests orogeny and magmatism at ca. 2.45 and 1.80 Ga (Barnett et al., 1993; Nelson et al., 2002). These dates suggest the Grouse Creek block was accreted to the Wyoming craton in Paleoproterozoic time. Therefore, the Grouse Creek block could be a separate Archean crustal province, a rifted piece of the Wyoming craton which re-accreted (Fig. 1.3), or a piece of the Wyoming craton which is partially separated by a failed rift (Foster et al., 2006).

1.3.5 Great Falls Tectonic Zone

The Great Falls Tectonic Zone (GFTZ) marks the Paleoproterozoic suture between the Medicine Hat and Wyoming craton (Mueller et al., 2002; Mueller et al., 2005). The eastern

portion of the GFTZ, in the Little Belt Mountains, Montana, is dominated by the Pinto diorite. The Pinto diorite intrudes two quartzofeldspathic gneisses. U/Pb SHRIMP ages on zircons from the Pinto diorite yield an average age of 1.86 Ga, whereas the quartzofeldspathic gneisses yielded U/Pb SHRIMP zircon ages of 1.85 – 1.87 Ga (Mueller et al., 2002). Metaigneous rocks exhibit trace element and Nd isotopic data similar to those found in convergent margins where juvenile lithosphere is consumed (Mueller et al., 2002; Vogl, 2004; Mueller et al., 2005). The western GFTZ possesses a different tectonic history than the Little Belt Mountains (Giletti, 1966; Roberts et al., 2002; Mueller et al., 2005).

The western GFTZ outcrops in the Tobacco Root and the Highland Mountains, Montana. Rock samples in the Tobacco Root Mountains, Montana include quartz + biotite + sillimanite garnet schist and a metabasaltic dike (Mueller et al., 2005). U/Pb SHRIMP ages on zircons from the Tobacco Root Mountains give 1.77 Ga ages on the garnet-schist and 1.77-2.06 Ga ages for the metabasalt (Mueller et al., 2005). P-T conditions of the metabasalt record a granulite facies metamorphic event at 600-730°C and 7-11 kbar (Cheney et al., 2004). Monazites from a leucogranite in the Highland Mountains give ID-TIMS ages of 1.77 Ga for leucogranite generation (Cheney et al., 2004; Mueller et al., 2005). These data provide insight into the tectonic development of the GFTZ.

The GFTZ is interpreted to have been an active convergent margin up to ~1.86 Ga where juvenile crust was created through an arc-like system in the Little Belt Mountains, Montana (Mueller et al., 2002). Magmatism along this margin ceased prior to the ca. 1.77 Ga collision between the Medicine Hat block and Wyoming craton. This collision is recorded by the regional granulite facies metamorphism (Mueller et al., 2005). Geophysical data identified a north-dipping paleosubducted slab beneath the Medicine Hat block which has been interpreted to represent the closure of an ocean basin at the inception of continental collision (Gorman et al.,

2002; Ross, 2002). The western extent of the GFTZ is poorly constrained and has been inferred to extend underneath the Belt Supergroup to the Idaho batholith (Foster and Fanning, 1997; Mueller et al., 2005).

1.3.6 Selway Terrane

The Selway terrane (ST) corresponds to the region west of the Wyoming craton (ST, Fig. 1.2), and was defined based on small outcrops in the Pioneer Range, Biltmore anticline, Tendoy Range, Highland Mountains, Beaverhead Range, Bitterroot Range, and at Boehls Butte, Montana. These outcrops occur in the basement-cored Laramide uplifts of southwest Montana and define the western boundary of the Wyoming craton (Foster et al., 2006). These metamorphic rocks include a kilometer-scale diorite orthogneiss roof pendant, a biotite quartzofeldspathic orthogneiss, and an amphibolite. No detailed mineralogic or metamorphic data have been published. Archean rocks have only been found in the Highland Mountains, Montana (O'Neill et al., 1988). Based on these isolated rock outcrops, Foster et al. (2006) proposed the Selway terrane to extend from the Wyoming craton west, beneath the Idaho batholith, to the Sr = 0.706 line, south to the Grouse Creek block, and north to the Medicine Hat block (Fig. 1.2). Basement rock exposures in the Selway terrane are rare due to voluminous Cretaceous and Tertiary volcanic and magmatic activity.

Consequently, work has focused on defining the Paleoproterozoic basement of the Selway terrane by examining crustal xenoliths of basement and inherited zircons incorporated into the Idaho batholith (e.g. Gaschnig et al., 2008). These rocks provide U-Pb SHRIMP and LA-ICP-MS zircon ages from ca. 2700 to 669 Ma scattered throughout the region with no definitive age for the basement crust (Fig. 1.9, Leeman et al., 1985; Wolf et al., 2005; Alexander et al., 2006; Durk et al., 2007; Link et al., 2007; Gaschnig et al., 2008).

The scattering of 2.7 – 1.6 Ga Paleoproterozoic metamorphic and igneous rocks in the Selway terrane suggests a heterogeneous basement in the region, that could be produced through the accretion of an arc-like terrane to the western Wyoming craton during the Proterozoic (Foster et al., 2006).

1.3.7 Belt-Purcell Supergroup

The Belt-Purcell Supergroup is a thick Mesoproterozoic succession of siliciclastic and carbonate metasedimentary rocks in northwestern United States and adjacent Canada (Fig. 1.2, Fig 1.4, e.g. Ross et al., 1992). These rocks have been studied and discussed in great detail (e.g. Harrison, 1972; Ross et al., 1992; Link, 1993). The Belt strata range from ~20 km thick in the west to ~5 km thick in the east and record a range of metamorphic grades from sub-greenschist facies in the upper sequence through greenschist facies in the northeast to amphibolite facies in the southwest (e.g. Harrison, 1972, Gonzalez-Alvarez et al., 2006). U-Pb SHRIMP zircon dates from volcanic deposits and mafic sills within the Belt-Purcell Supergroup bracket the age of deposition between 1500 and 900 Ma with ~60% of the deposition occurring between 1470-1440 Ma as indicated by lower Belt-Purcell synsedimentary mafic intrusive and upper Belt-Purcell mafic extrusive rocks (Link, 1993; Evans et al., 2000). Based on paleo-current data, grain-size variation, and sedimentary-facies successions, most units are interpreted as continental and shallow-water deposits. A western source area and a tectonically active basin margin is inferred through westward coarsening and thickening of clastic units coupled with U/Pb SHRIMP detrital zircon ages ca. 1700 Ma (e.g. Ross et al., 1992; Gonzalez-Alvarez et al., 2005). Sulfur isotope trends in black shales in the Helena Embayment, Montana, provide evidence that the Belt strata were deposited in a restricted marine setting (Luepke and Lyons, 2001). The Belt Supergroup has been, dominantly, subjected to greenschist-grade metamorphism, but local variations in metamorphic grade are described.

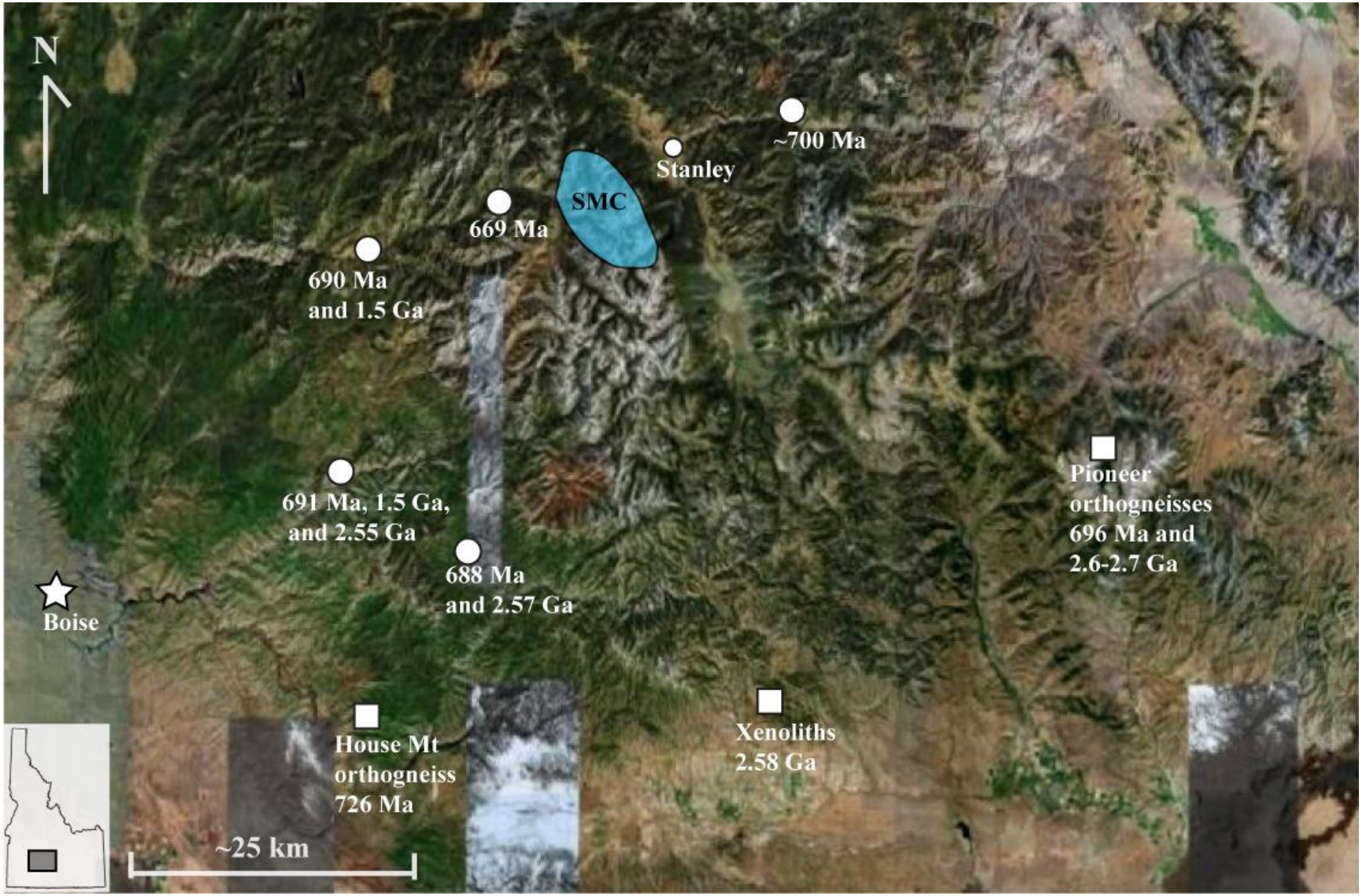

Figure 1.9: Map showing the spread of zircon ages from 2700 – 699 Ma throughout south-central Idaho. Ages are based primarily on inherited zircons and crustal xenoliths within the Idaho batholith. Modes of ages are given. The Sawtooth Metamorphic Complex (SMC) is shown in blue. Basemap is from GoogleEarth. Modified after Gaschnig et al. (2008).

The lower most units of the Belt Supergroup and the pre-Beltian basement crop out in the Goat Mountain-Boehls Butte area of northern Idaho. They contain mineral assemblages that record a complex pressure and temperature history (e.g. Carey et al., 1992; Grover et al., 1992). At approximately 1625 Ma (Reid et al., 1973), anorthositic magma intruded and partially melted the basement complex in the area resulting in a melt rich in aluminum and magnesium (M1). The second metamorphic event (M2) produced kyanite and sillimanite at peak metamorphic conditions between 650 – 750°C and 8 – 11 kbar calculated by garnet-biotite and garnet-aluminosilicate-quartz-plagioclase geothermobarometry (Grover et al., 1992). The resulting mineral assemblage consists of kyanite ± sillimanite ± biotite ± plagioclase ± rutile ± garnet ± muscovite ± staurolite ± corundum ± quartz (e.g. Carey et al., 1992; Grover et al., 1992). Isothermal decompression resulted (M3) resulted in the growth of low-pressure andalusite from polymorphic inversion of strained kyanite (Carey et al., 1992; Grover et al., 1992).

1.3.8 Other Metamorphic Basement Rocks of Uncertain Affinity in Idaho

Metamorphic rocks crop out sporadically throughout north-central Idaho as roof pendants in the Idaho batholith (Fig. 1.8, Lund, 1993). Due to limited accessibility, only a small percentage of the metamorphic roof pendants have been studied and few in detail. General aspects of these pendants have been described. They are dominantly metasedimentary siliciclastic and calc-silicate rocks including: pure quartzite, sillimanite-muscovite-biotite-feldspar quartzite, garnet-sillimanite-muscovite-biotite quartzitic gneiss, biotite-quartz-feldspar gneiss, biotite-quartzitic phyllites, garnet-muscovite schist, biotite-calc-silicate, and marbles that range from greenschist to amphibolite facies and record multiple episodes of deformation (e.g. Lund, 1993). In many units, stratigraphic succession can be documented via sedimentary structures and primary bedding features, but in some outcrops contacts between units are structural and stratigraphic relationships cannot be determined (ibid).

The structure of the roof pendants studied in detail can be divided into a lower and upper suite. The lower suites are lithologically consistent through kilometers of section and are similar to the Middle Proterozoic rocks of the Belt Supergroup (Lund, 1993). The upper suite lithologic units are hundreds of kilometers thick, laterally continuous, and relatively pure when compared to Middle Proterozoic units of the Belt Supergroup (Lund, 1993). No detailed mineralogy or P-T calculations have been published on these rocks.

The Pioneer Mountains of south-central Idaho (Fig. 1.8) are a metamorphic core complex comprised of Archean and Precambrian basement (e.g. Link et al., 2007; Link 2009). Archean and Mesoproterozoic U-Pb SHRIMP zircon ages from the lower structural levels of the Pioneer Mountains metamorphic complex indicate Archean and Mesoproterozoic protoliths (Link et al., 2007; Link, 2009). An Archean orthogneiss, 2608 – 2674 Ma (Wetherill regression ages), is structurally overlain by quartzite, calc-silicate, and pelitic metasedimentary rocks containing Paleoproterozoic zircons with U-Pb SHRIMP zircon ages between 1450-1800 Ma (Link, 2009). The middle structural levels of the Pioneer Mountains metamorphic complex contain metasedimentary rocks with zircon core ages 1050-1330 Ma and metamorphic rims approximately 50 m.y. younger. These metamorphic rims are of Grenville age and are interpreted to represent a western extension of Grenville tectonic activity (Link, 2009). The Pioneer Mountains metamorphic complex is interpreted as the northern extension of the Grouse Creek block based on the ages of Archean orthogneiss. The calc-silicate gneiss and pelitic metasedimentary rocks are interpreted as the southern extension of the Lower Belt Supergroup based on similarities in lithology and U/Pb age dates (Link, 2009). Despite the detailed age dates in the Pioneer Mountains metamorphic complex, no detailed mineralogic or petrologic work has been published.

CHAPTER II. METHODS

2.1 Field Methods

Field work in the Sawtooth Mountains, Idaho was conducted over a seven week period in the summer of 2008 and a two week period in the summer of 2009. UTM coordinates were recorded for 84 sample locations (Appendix A). These points were overlain on a topographic map in NASA's World Wind program (Fig. 2.1). Detailed field mapping and sample collection focused in the Thompson Peak-Marshall Lake and Iron Creek areas (Fig. 2.2a,b). Due to the rugged terrain, limited accessibility and the designation of the Wilderness area, it was necessary to backpack samples out at five-day intervals. A collection permit was granted by the Sawtooth National Recreation Area administered by the National Forest Service.

2.2 Analytical Methods

Eighty-four samples were selected for thin-section preparation and petrographic analysis based on location, rock type, and amount of alteration present. Petrographic analyses were conducted using an Olympus BH-2 petrographic microscope. Mineral assemblage data, metamorphic texture(s), presence of alteration and desirable minerals for chemical analysis and P-T calculations and U/Pb zircon, titanite, and monazite geochronology, were recorded. Ten thin sections were polished and carbon coated for mineral chemical analyses on the electron microprobe. These were supplemented by samples previously collected by Dutrow et al. (1995) and Anderson (1995). Prior to any microanalytical work, backscattered electron images were taken of minerals for analysis: amphibole, biotite, cordierite, garnet, plagioclase, and pyroxene grains. These images provided additional textural and chemical zoning information and were used as a basemap for electron microprobe analyses.

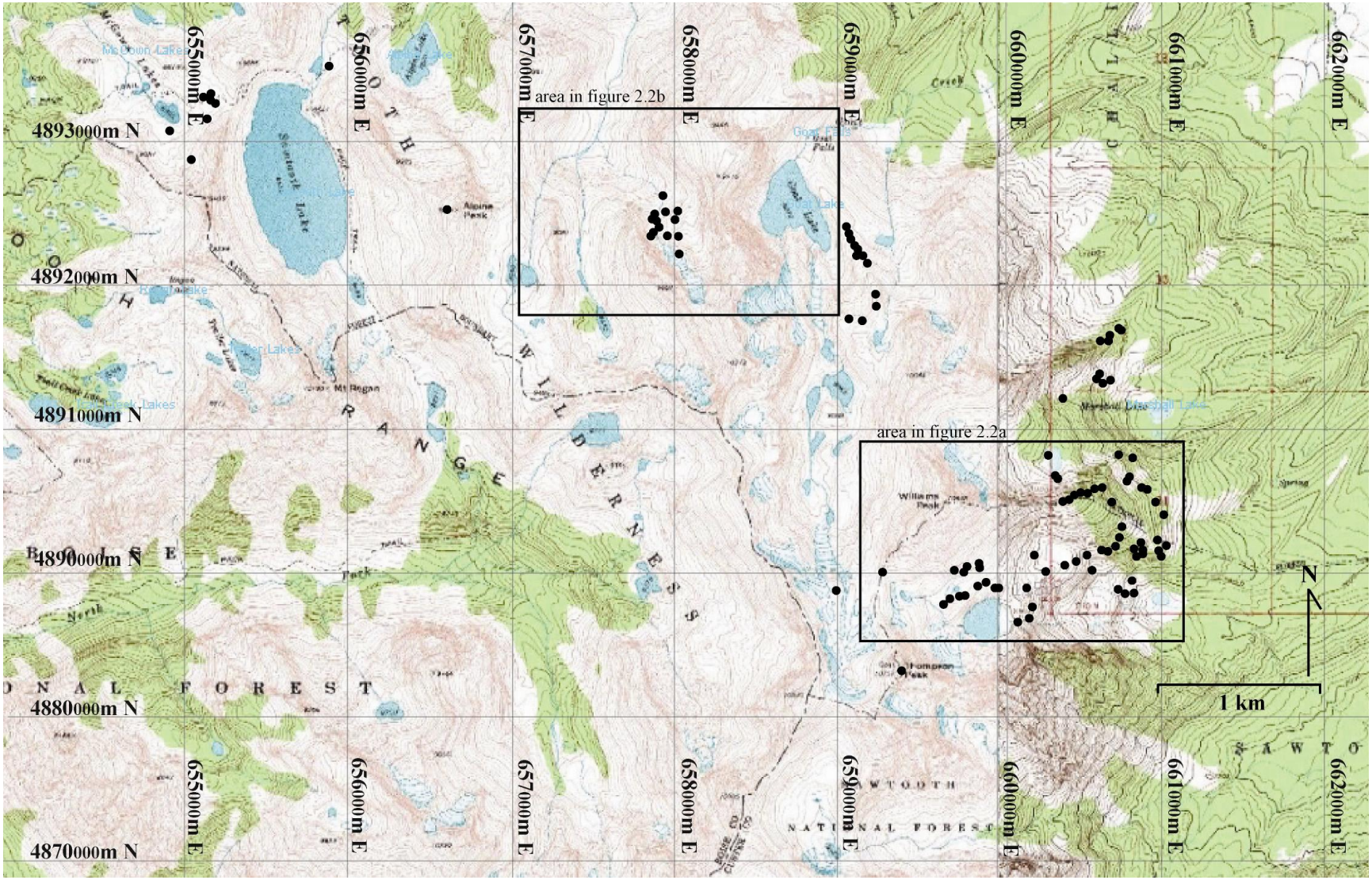

Figure 2.1: Topographic map of the northeastern portion of the Sawtooth Mountains. Each dot represents a site where one or more samples (UTM locations are given in Appendix A). Rectangles outline areas of detailed mapping and sampling. Basemap consists of USGS quadrangles: Stanley Lake (west) and Stanley (east) from NASA's WorldWind program.

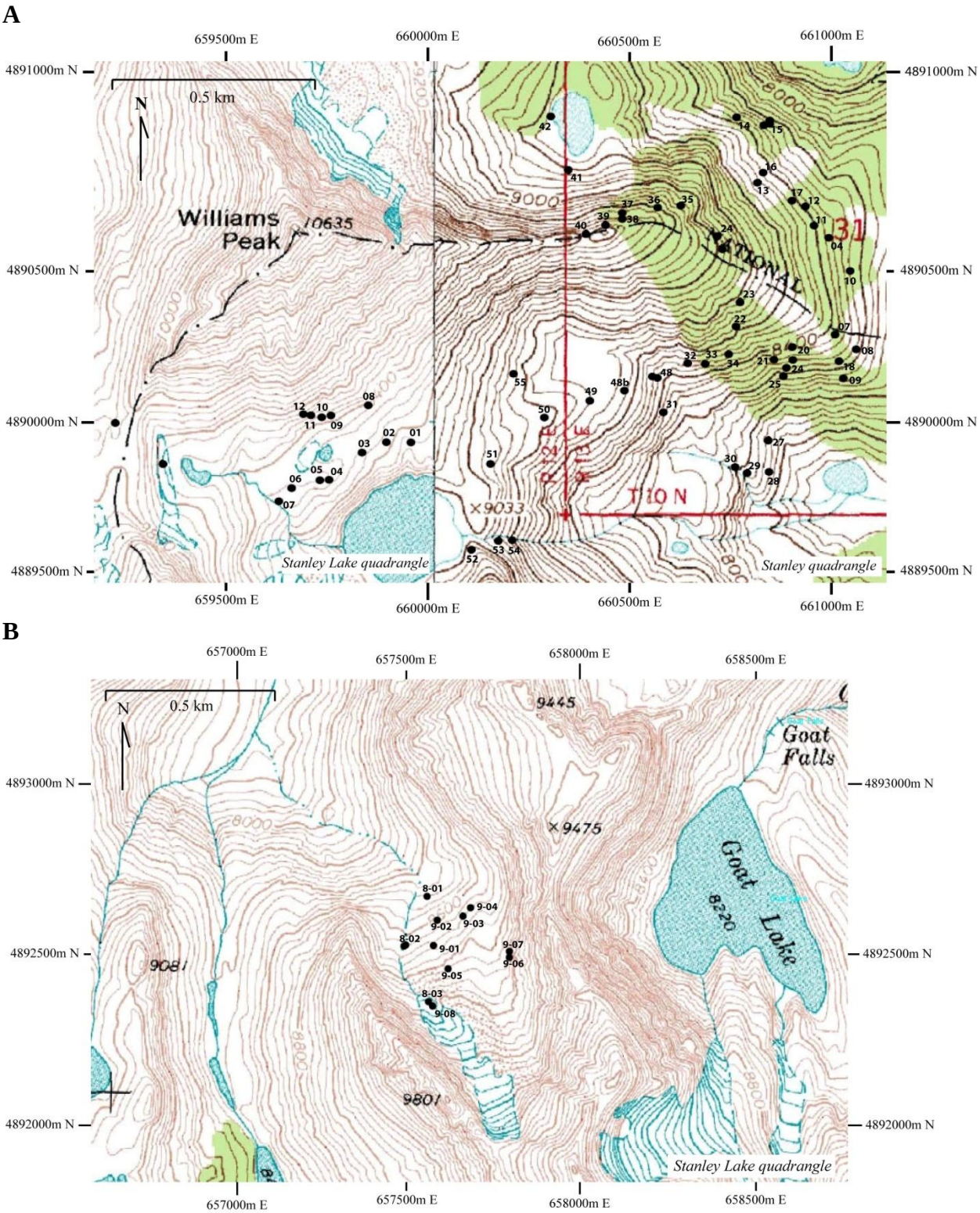

Figure 2.2a, b: Subset of sample locations shown in Fig. 2.1. (A) Enlarged topographic map of Thompson Peak – Marshall Lake area. (B) Enlarged topographic map of Iron Creek area. Sample prefixes are ST08- (A) and IC0 (B). Basemap is from USGS Stanley and Stanley Lake quadrangles.…..

2.2.1 Mineral Chemical Analyses

Quantitative microanalytical electron microprobe analyses (EMPA) were obtained using wavelength-dispersive spectrometry on the JEOL 733 Superprobe at LSU. Samples were analyzed using an accelerating potential of 15 kV, a beam current of 10 nA, and a 2 μm focused electron beam for anhydrous phases and a 10-15 μm focused electron beam for hydrous phases. Garnet was analyzed for the elements: Si, Ti, Al, Cr, Fe, Mn, Mg, and Ca, plagioclase for the elements: Si, Al, Ca, Ba, Na, K, Fe, and Mg; biotite, muscovite, and cordierite for the elements: Si, Ti, Al, Cr, Fe, Mn, Mg, Ca, Ba, Na, K, and F; and pyroxenes for the elements: Si, Ti, Al, Cr, Fe, Mn, Mg, Ca, Na, and K, as were amphiboles with the addition of Cl and F. A series of well-characterized minerals were used as standards (Table 2.1). Secondary standards were analyzed as unknowns before and after each sample suite to maintain quality and check for instrument drift.

Pelitic samples were analyzed for: garnet, plagioclase, biotite, muscovite, and cordierite, if present. For garnet analyses, traverses across grains encompassed ten to thirty spot analyses to check for chemical zoning. For all other phases, two to three grains of each mineral were analyzed per sample and ten to fifteen spots were analyzed on each grain.

Amphibolite samples were analyzed for: amphibole, plagioclase, biotite, and pyroxene. Traverses across amphibole, plagioclase, and pyroxene grains used ten to twenty spot analyses on two to three grains in each sample.

Weight-percent oxide analyses were normalized to atoms per formula unit based on oxygen content or the sum of cations. Garnet analyses were normalized on the basis of 12 oxygen atoms, feldspar on the basis of 8 oxygen atoms, and pyroxene on the basis of 6 oxygen atoms. Cordierite analyses were normalized to the anhydrous basis of 18 oxygen atoms, biotite and muscovite normalization assumed full occupancy of the hydroxyl site with OH^- and F^-

Table 2.1: Mineral standards used for Electron Microprobe analyses.

Element	Standard for garnet analysis	Standard for feldspar analysis	Standard for Biotite/Muscovite/ Cordierite analyses	Standard for amphibole analysis	Standard for pyroxene analysis
Si	Toronto almandine	Toronto albite	Kakanui hornblende	Kakanui hornblende	Toronto diopside
Ti	Kakanui hornblende	*	Kakanui hornblende	Kakanui hornblende	Kakanui hornblende
Al	Toronto almandine	Lake County plagioclase	Kakanui hornblende	Kakanui hornblende	Kakanui augite
Cr	Smithsonian chromite	*	Smithsonian chromite	Smithsonian chromite	Smithsonian chromite
Fe	Toronto almandine	Kakanui hornblende	Kakanui hornblende	Kakanui hornblende	Johnstown hypersthene
Mn	Toronto rhodonite	*	Toronto rhodonite	Toronto Rhodonite	Smithsonian ilmenite
Mg	Kakanui pyrope	Kakanui hornblende	Kakanui hornblende	Kakanui hornblende	Toronto diopside
Ca	Grossular 55	Lake County plagioclase	Kakanui hornblende	Kakanui hornblende	Kakanui augite
Ba	*	Toronto sanidine	Toronto sanadine	Toronto sanadine	*
Na	*	Toronto albite	Kakanui hornblende	Kakanui hornblende	Kakanui hornblende
K	*	Toronto sanidine	Toronto biotite	Kakanui hornblende	Kakanui hornblende
F	*	*	Smithsonian fluorapatite	Smithsonian fluorapatite	*
Cl	*	*	*	Toronto tugtupite	*

anions and all Fe as FeO and analyses were normalized on the basis of 22 oxygen atoms. Amphibole analyses were normalized on the basis of 23 oxygen atoms using the Stoich program developed by D.J. Henry (pers. comm.).

2.2.2 Geothermobarometry

Geothermobarometric calculations utilized various exchange thermometers, net transfer barometers and the multiequilibria approach. Assumptions inherent in geothermobarometry include: the mineral phases involved in any given calculation are in chemical equilibrium, record a single event, and that no retrograde alteration is present. P-T estimates were obtained using averages of multiple analyses on single mineral grains in close proximity. For calculations involving garnet, the inner rims of grains were used to avoid areas of retrograde re-equilibration (B. Dutrow, pers. comm.).

Temperatures were calculated for Iron Creek metapelites using garnet-biotite (GB) calibrations of Holdaway and Lee (1977), Dasgupta et al. (1991), and Bhattacharya et al. (1992). Garnet-muscovite (GM) temperatures were calculated with Wu and Zhao's (2006) calibration, and the Ti-in-biotite (TIB) thermometer calibration of Henry et al. (2005).

The GB thermometer is described by the reaction: $Fe_3Al_2Si_3O_{12} + KMg_3AlSi_3O_{10}(OH)_2 = Mg_3Al_2Si_3O_{12} + KFe_3AlSi_3O_{10}(OH)_2$. This reaction represents the Fe-Mg exchange between garnet and biotite and is temperature sensitive. Holdaway and Lee's (1977) calibration of the GB thermometer accounts for Fe/Mg exchange in the presence of cordierite and has an absolute error of ±50˚C. The calibration of Dasgupta et al. (1991) accounts for Fe-Mg-Ca-Mn components in garnet and Al and Ti substitution in the octahedral site of biotite. This calibration has an absolute error of ±50˚C. The calibration of Bhattacharya et al. (1992) accounts for Fe-Mg non-ideal mixing in the phlogopite – annite binary with an absolute error of ±20˚C.

The GM thermometer is described by the reaction: $Mg_3Al_2Si_3O_{12}$ *(pyrope)* + $3K(FeAl)Si_4O_{10}(OH)_2$ *(Fe-celadonite)* = $Fe_3Al_2Si_3O_{12}$ *(almandine)* + $3K(MgAl)Si_4O_{10}(OH)_2$ *(Mg-celadonite)*. This reaction represents the Fe-Mg exchange between garnet and muscovite (celadonite) and is temperature dependent. The thermometer of Wu and Zhao (2006) is calibrated for conditions of T = 450 – 750 ˚C and 0.8 – 11.1 kbar using a compositional range of X_{Fe}^{grt} = 0.53 – 0.81, X_{Mg}^{grt} = 0.05 – 0.24, X_{Ca}^{grt} = 0.03 – 0.23, X_{an} = 0.17 – 0.74, and Fe = 0.04 – 0.16, Mg = 0.04 – 0.13, and Al^{iv} = 1.74 – 1.96 in muscovite.

The TiB thermometer of Henry et al. (2005) relies on a non-linear relationship between Ti concentration in biotite with $Mg/(Mg+Fe^{2+})$ and temperature. This relationship results in higher Ti concentrations at higher temperatures for a given $Mg/(Mg+Fe^{2+})$ value, and is described by the equation: $T = \{[ln(Ti) - a - c(X_{Mg})^3]/b\}^{0.333}$, where T is temperature in ˚C, a = -2.3594, b = $4.6482e^{-9}$, and c = -1.7283 (Henry et al., 2005). This expression is valid for X_{Mg} = 0.275 – 1.000, Ti = 0.04 – 0.60 apfu and *T* = 480 – 800 ˚C and calibrated for pressures from 4 – 6 kbar. Error associated with this thermometer is ±24 ˚C at temperatures below 600 ˚C, improving to ±12 ˚C at temperatures above 700˚C.

Geobarometers used for calculating pressures of Iron Creek metapelites include the garnet – alumino-silicate – plagioclase – quartz (GASP) barometer and garnet – muscovite – plagioclase – quartz (GMPQ) calibration of Wu and Zhao (2006).

The GASP barometer relies on the reaction: $Ca_3Al_2Si_3O_{12}$ (*grossular*) + Al_2SiO_5 (*sillimanite*) + SiO_2 (*quartz*) = $3CaAl_2Si_2O_8$ (*anorthite*) developed by Ghent (1976). Pressures were calculated using Waters' program using the calibration: P = *A* + *BT* + *CTln*K, where P = pressure in kbar, *T* = temperature in K, *A* = -5240, *B* = 21.79, and *C* = -1.574 (*http://www.earth.ox.ac.uk/~davewa/pt/index.html*). Winters' program (ibid.) utilizes the garnet activity model of Hackler and Wood (1989) and plagioclase activity model of Holland and

Powell (1992). The input temperature is from the GB thermometer of Bhattacharya et al. (1992). This barometer has an assumed error of ±1.5 kbar.

The GMPQ barometer of Wu and Zhao (2006) is based on the reactions: $Mg_3Al_2Si_3O_{12}$ *(pyrope)* + $2Ca_3Al_2Si_3O_{12}$ *(grossular)* + $3KAl_2(AlSi_3)O_{10}(OH)_2$ *(muscovite)* + $6SiO_2$ *(quartz)* = $6CaAl_2Si_2O_8$ *(anorthite)* + $3K(MgAl)Si_4O_{10}(OH)_2$ *(Mg-celadonite)* for the magnesium (Mg) model and $Fe_3Al_2Si_3O_{12}$ *(pyrope)* + $2Ca_3Al_2Si_3O_{12}$ *(grossular)* + $3KAl_2(AlSi_3)O_{10}(OH)_2$ *(muscovite)* + $6SiO_2$ *(quartz)* = $6CaAl_2Si_2O_8$ *(anorthite)* + $3K(FeAl)Si_4O_{10}(OH)_2$ *(Fe-celadonite)* for the iron (Fe) model. This barometer was calibrated simultaneously with the GM thermometer of Wu and Zhao (2006) under the same conditions listed above. An absolute error of ±1.5 kbar is reported.

Pressure-temperature conditions of amphibole-bearing rocks were calculated using the hornblende-plagioclase thermometer of Holland and Blundy (1994), barometer of Bhadra and Bhattacharya (2007), and hornblende thermobarometer of Gerya et al. (1997).

Values of the hornblende-plagioclase thermometer of Holland and Blundy (1994) were calculated using Waters' program (*http://www.earth.ox.ac.uk/~davewa/pt/index.html*). These equilibria are defined as: edenite + albite = richterite + anorthite for non-quartz bearing phases and edenite + 4 quartz = tremolite + albite for quartz bearing assemblages, and are valid for calcic-amphiboles in conditions 400 – 1000 ˚C and 1 – 15 kbar. This thermometer has an absolute error of ±40˚C.

The hornblende-plagioclase barometer of Bhadra and Bhattacharya (2007) is based on the reaction: $Ca_2Mg_5Si_8O_{22}$ (*tremolite component)* + $Ca_2Mg_3Al_4Si_6O_{22}(OH)_2$ *(tschermakite)* + $2NaAlSi_3O_8$ *(albite)* = $2NaCa_2Mg_4Al_3Si_6O_{22}(OH)_2$ *(paragasite)* + $8SiO_2$ *(quartz)*, and is valid for plagioclase = $0.20 \leq X_{Ab} \leq 0.82$, and amphibole composition between: $6.09 \leq Si \leq 7.27$, $0.90 \leq Al \leq 2.65$, $0.0 \leq Ti \leq 0.29$, $1.79 \leq Mg \leq 4.32$, $0.76 \leq Fe \leq 2.63$, $0.0 \leq Mn \leq 0.09$, $1.38 \leq$

$Ca \leq 1.88$, $0.23 \leq Na \leq 0.77$, $0.0 \leq K \leq 0.27$, and $1.73 \leq Ca+Na+K \leq 2.67$ apfu. The absolute error associated with this calibration is ±2.0 kbar.

The hornblende thermobarometer of Gerya et al. (1997) uses the following reactions: $T(K) = (6119 - 28.4(P) + 114X_{Mg}^{Hbl}) / [8.181 - Rln(8.489 - Si^{Hbl})]$ and $P(kbar) = [2543 - 4.744(T) + 175X_{Mg}^{Hbl} + RTln(Al^{Hbl} + 1.433)] / 148.1$. This thermobarometer is valid for calcic-amphiboles and plagioclase with X_{An} higher than 0.1, and gives results within an absolute error of ±40˚C and 1.2 kbar (Gerya et al., 1997).

In addition, the multi-equilibria approach was used on peraluminous gneisses. P-T conditions were calculated using TWQ 2.32 computer program developed by Berman (1991), together with the most recent database by Berman and Aranovich (in prep). No error values are given for specific thermometers or barometers, but INTERSX, a sub-program within TWQ, determines the uncertainty of the pressure-temperature point based on the degree of convergence between equilibria reactions in pressure-temperature space and gives a weighted preference to those reactions most affected by changes in pressure and temperature (Berman, 1991). This allows for accurate estimation of error between the intersecting equilibria.

These data provide information on conditions of formation of the SMC rocks. P-T data coupled with metamorphic textures allow the history of rock formation to be estimated.

CHAPTER III: RESULTS

3.1 Petrology of the SMC

Geologic field mapping refined the north and west contacts of the SMC originally mapped by Reid (1963). The northern contact was moved south of Alpine Peak, where a sample of granodiorite was collected. Due to the topography in the region, the contact west of Iron Creek was not physically crossed, but was mapped through distal observation from Alpine Peak. The western contact was shifted eastward based on sampling float south of Alpine Peak (Fig. 3.1). The northern contact was shifted southward based on insitu sampling, but the southern and eastern contacts were left unchanged. These changes result in the SMC cropping out over approximately 33 km^2 (Fig. 3.3).

Rock units are heterogeneous across an outcrop, or hand sample; therefore, units were mapped based on the dominant rock type. Mineral abbreviations used in this study are taken from Kretz (1983; Table 3.1).

Table 3.1: Mineral symbols and abbreviations used in this study (after Kretz, 1983).

Abbreviation	Mineral Name
Ab	albite
Aln	allanite
Alm	almandine
Amp	amphibole
And	andalusite
Ann	annite
An	anorthite
Ap	apatite
As	aluminosilicate
Bt	biotite
Cpx	Ca clinopyroxene
Cal	calcite
Chl	chlorite
Cld	chloritoid
Czo	clinozoisite
Crd	cordierite
Di	diopside
Ep	epidote
Grt	garnet
Gr	graphite

Abbreviation	Mineral Name
Grs	grossularite
Hem	hematite
Hbl	hornblende
Kfs	K-feldspar
Ky	kyanite
Mnz	monazite
Ms	muscovite
Opx	orthopyroxene
Phl	phlogopite
Pl	plagioclase
Py	pyrite
Pyp	pyrope
Po	pyrrhotite
Qtz	quartz
Rt	rutile
Sil	sillimanite
Tlc	talc
Ttn	titanite
Zrn	zircon

Between Thompson Peak and Marshall Lake, in the southeast portion of the SMC, nineteen metamorphic units were mapped (Fig. 3.2, Table 3.2). These units are: (1) coarse-grained biotite-muscovite-alkali-feldspar quartzite, (2) medium-grained biotite amphibolite, (3) coarse-grained biotite-plagioclase metagabbro, (4) medium-grained titanite-amphibole-biotite gneiss, (5) coarse-grained biotite-muscovite-alkali-feldspar quartzite with lenses of medium-grained biotite-plagioclase-clinozoisite-alkali-feldspar-amphibole calc-silicate gneiss, (6) mixed fine-grained mylonitic amphibole-clinozoisite-clinopyroxene calc-silicate gneiss with medium-grained biotite quartzofeldspathic gneiss, (7) coarse-grained pyroxene-biotite-amphibole metagabbro, (8) mixed biotite-K-feldspar quartzofeldspathic gneiss with trace allanite, (9) medium-grained ilmenite-titanite-amphibole-biotite gneiss, (10) fine-grained impure marble-mylonite with porphyroblasts of alkali-feldspar-plagioclase-quartz-clinopyroxene, (11) medium grained mylonitic titanite-clinozoisite-clinopyroxene calc-silicate gneiss, (12) granoblastic biotite-clinozoisite calc-silicate gneiss, (13) medium-grained muscovite and orthopyroxene bearing biotite-clinopyroxene calc-silicate gneiss, (14) medium-grained biotite-orthopyroxene-clinopyroxene gneiss, (15) medium-grained mylonitic biotite-muscovite alkali-feldspar quartzite, (16) mixed marble mylonite with megaboudins of calc-silicate gneiss, (17) medium-grained impure marble-mylonite with porphyroblasts of plagioclase-clinozoisite-clinopyroxene-quartz, (18) medium-grained ilmenite-biotiteamphibolite, and (19) medium-grained mylonitic Cr-muscovite quartzite with accessory rutile (Appendix B). Units strike approximately north-south, and dip near vertically (Fig. 3.2). The dip varies less than 20° east – west largely due to local deformation within units. Contacts between units appear to be a mixture of stratigraphic and tectonic. In some locations, contacts are preferentially intruded by Tertiary and Miocene dikes. Additional mapping was conducted in the northwestern portion of the SMC, in the Iron Creek region.

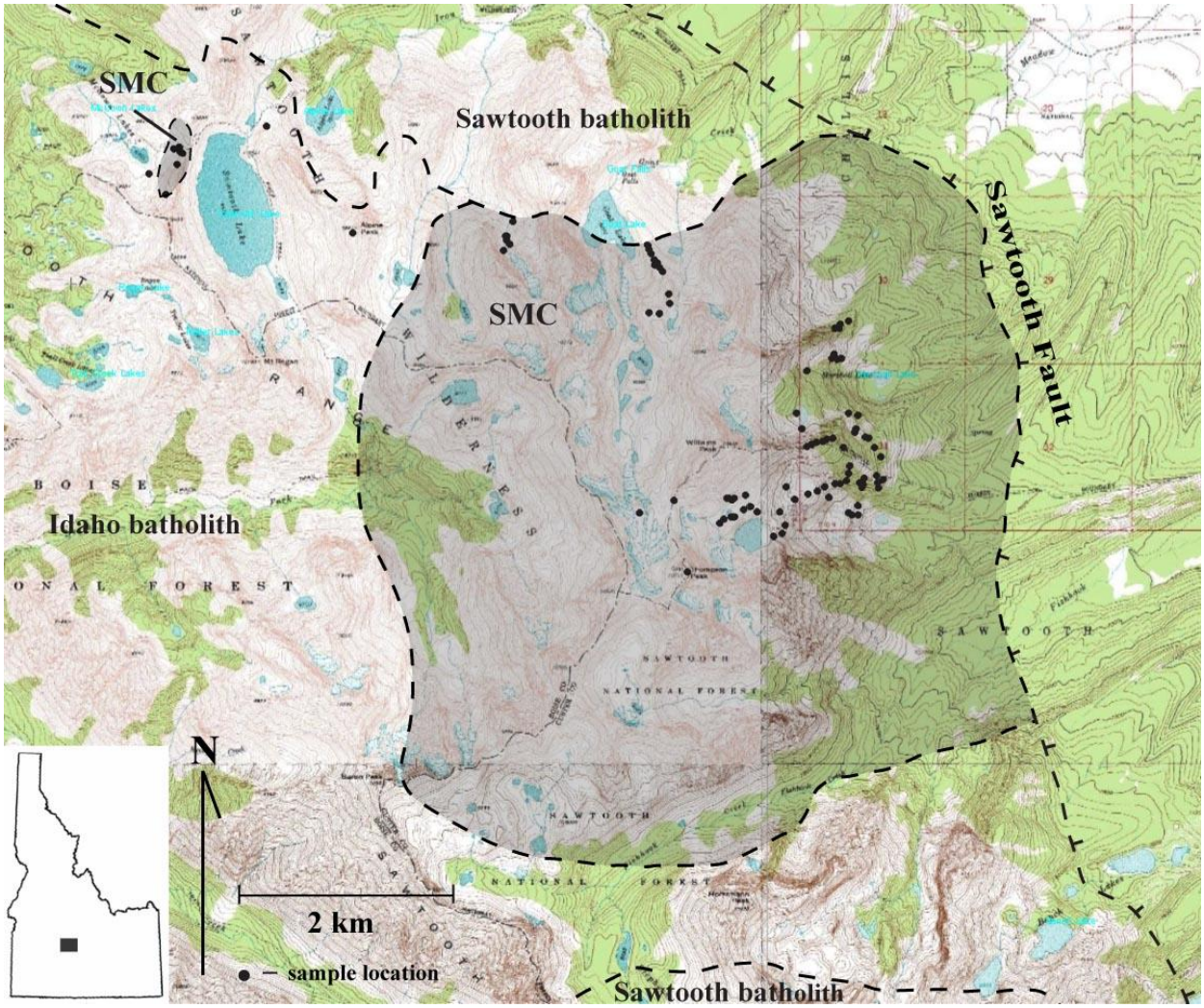

Figure 3.1: Topographic map of the Sawtooth Mountains, Idaho, displaying the areal extent of the SMC refined by this study on the north and west from Reid (1963). The SMC crops out over ~33 km^2. Sample localities are denoted by black dots. Basemap is from USGS quadrangles Stanley, and Stanley Lake with samples locations plotted in NASA's Worldwind program.

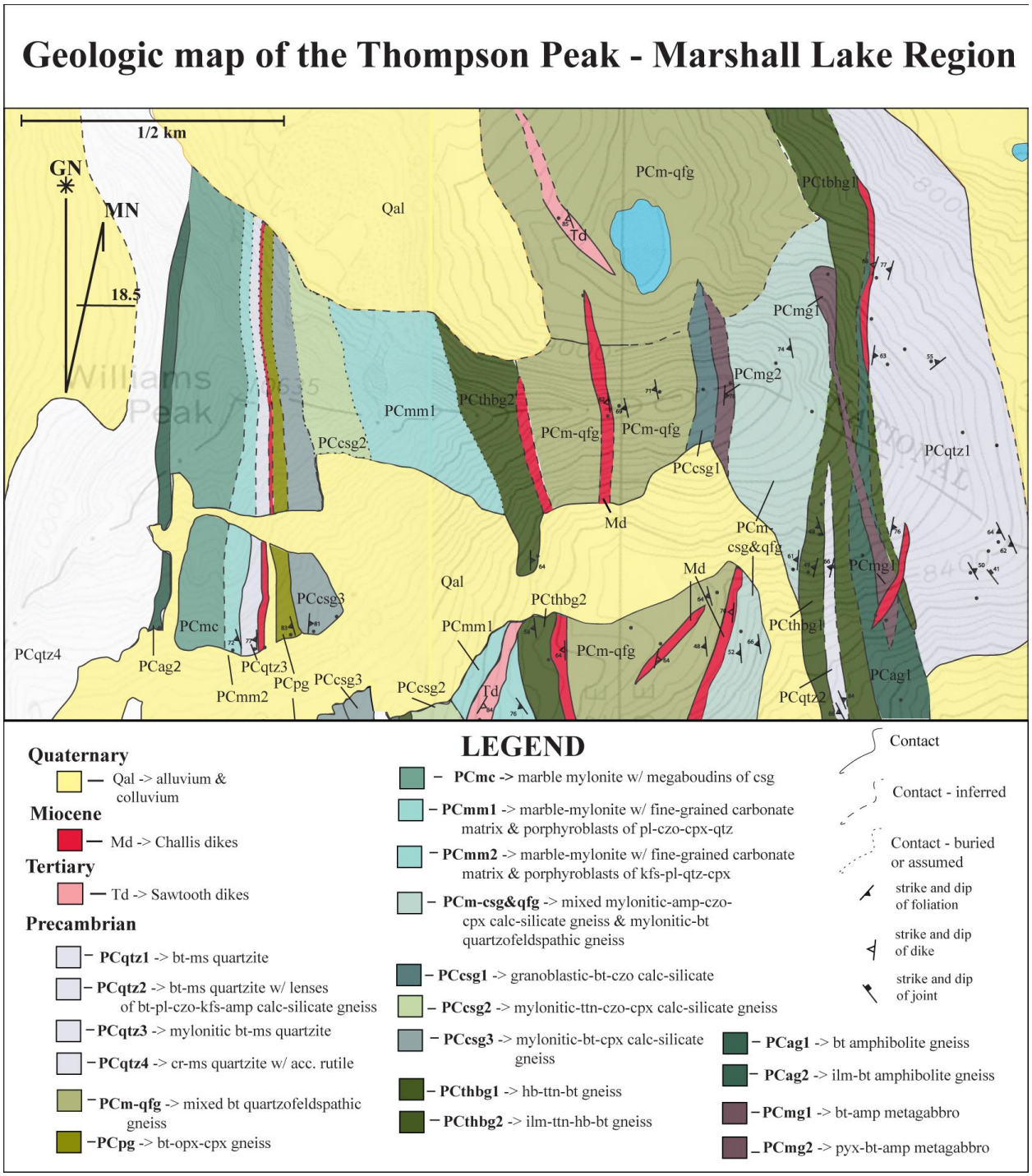

Figure 3.2: Geologic map of the Thompson Peak – Marshall Lake area in the eastern SMC. Nineteen metamorphic units were identified (see text for details). Units strike N-S and dip near vertical. Miocene dikes preferentially intrude along some contacts. Seven units originally mapped by Dutrow et al. (1995) were extended to the north in this study. These units are: PCcsg3, PCpg, PCqtz3, PCmm2, PCmc, PCag2, and PCqtz4.

Table 3.2: List of units mapped in Thompson Peak – Marshall Lake and Iron Creek.

Location	map symbol	rock name
Thompson Peak - Marshall		
	PCqtz1	coarse-grained mylonitic biotite-muscovite-alkali-feldspar quartzite
	PCqtz2	coarse-grained biotite-muscovite-alkali-feldspar quartzite with lenses of medium-grained biotite-plagiclase-clinozoisite-alkali-feldspar-amphibole calc-silicate gneiss
	PCqtz3	medium-grained muscovite-biotite-alkali-feldspar quartzite
	PCqtz4	medium-grained mylonitic Cr-muscovite quartzite with accessor rutile
	PCm-qfg	mixed-dominantly medium-grained biotite-alkali-feldspar-plagioclase-quartzofeldspathic gneiss with trace allanite
	PCm-csg&qfg	medium-grained mylonitic biotite-alkali-feldspar-plagioclase quartzofeldspathic gneiss interlayered with fine-grained mylonitic amphibole-plagioclase-clinozoisite-clinopyroxene-quartz calc-silicate gneiss with trace titanite
	PCcsg1	fine-grained granoblastic biotite-clinozoisite-clinopyroxene calc-silicate gneiss
	PCcsg2	medium-grained mylonitic titanite-clinozoisite-clinopyroxene calc-silicate gneiss
	PCcsg3	medium-grained muscovite and orthopyroxene bearing biotite-clinopyroxene calc-silicate gneiss
	PCmc	fine-grained mylonitic alkali-feldspar-plagioclase-quartz-clinopyroxene marble with megaboudins of medium-grained clinozoisite-clinopyroxene calc-silicate gneiss
	PCmm1	fine-grained mylonitic alkali-feldspar-plagioclase-quartz-clinopyroxene marble
	PCmm2	medium-grained mylonitic plagioclase-clinozoisite-clinopyroxene-quartz marble
	PCthbg1	medium-grained ilmenite-bearing amphibole-titanite-biotite gneiss with accessory rutile
	PCthbg2	medium-grained ilmenite-titanite-amphibole-biotite gneiss with accessory rutile
	PCag1	medium-grained ilmenite-biotite-amphibolite gneiss
	PCag2	medium-grained ilmenite-biotite-amphibolite gneiss
	PCmg1	coarse-grained granoblastic biotite-bearing plagioclase-amphibole metagabbro
	PCmg2	coarse-grained clinopyroxene-ilmenite-biotite-hornblende metagabbro with relict igneous texture
	PCpg	medium-grained biotite-orthopyroxene-clinopyroxene gneiss
Iron Creek		
	PCal-g	fine- to coarse-grained alkali-feldspar-garnet-muscovite-sillimanite-biotite-cordierite migmatite
	PCqfg	muscovite-biotite quartzofeldspathic gneiss with trace ilmenite and pyrrhotite

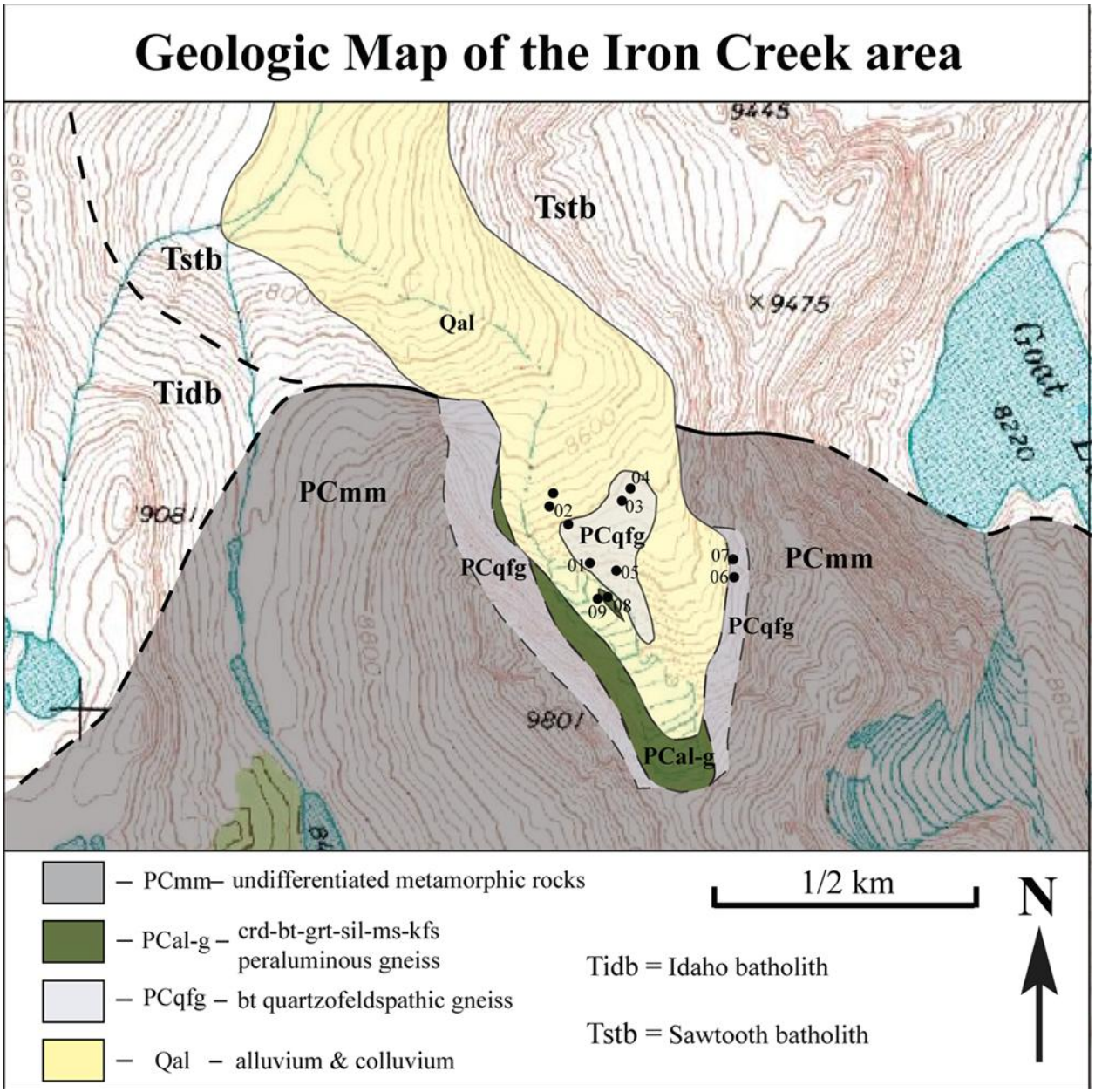

Figure 3.3: Geologic map of the Iron Creek area of the SMC. Quartzofeldspathic and peraluminous gneisess were mapped in this region. The western quartzo-feldspathic gneiss was mapped through far-field observation and float due to topography and unstable slopes.

Two lithologies were identified in the Iron Creek area (Fig. 3.3, Table 3.2). These lithologies are: fine- to coarse-grained alkali-feldspar-garnet-muscovite-sillimanite-biotite-cordierite migmatites and gneisses and medium-grained biotite-alkali-feldspar quartzofeldspathic gneiss (Appendix B). Samples from this region were critical for geothermobarometry because of the presence of garnet.

The twenty-one rock units mapped in the Thompson Peak – Marshall Lake and Iron Creek areas based on their spatial distribution and mineralogy. Units of similar lithology tend to share similar mineralogy, outcrop features, and metamorphic textures. For example, all quartzites in the SMC outcrop as white ridge-forming units (Fig. 3.4). Therefore, the metamorphic rocks of the SMC can be grouped into nine general litho-types: quartzites, quartzofeldspathic gneisses, calc-silicate gneisses, marble mylonites, titanite-hornblende-biotite gneisses, metagabbros, biotite-hornblende gneisses, peraluminous gneisses, and amphibole-pyroxene gneisses (Table 3.3). Although the units in the SMC are heterogeneous and occurs on a centimeter to meter scale, they can be grouped such that the general rock types in the SMC are described subsequently.

3.1.1 Quartzites

Quartzites contain >75 modal amount quartz, and are medium- to coarse-grained (Fettes and Desmons, 2007). Due to the quartz content, these rocks are resistant to weathering and crop out as distinctive white ridges in the field (Fig. 3.4). Lenses of darker, quartzofeldspathic gneiss, less than one-meter thick, occur intermittently throughout quartzite units and more frequently near contacts with other units. These layers are fine- to medium-grained and contain 25 – 35 modal proportion of feldspar, biotite, and/or muscovite.

Four quartzite units were separated based on mineralogy and spatial distribution and were mapped in the Thompson Peak – Marshall Lake area (Fig. 3.4). These units are: *qtz1* = coarse-

grained mylonitic biotite-muscovite-alkali-feldspar quartzite; *qtz2* = coarse-grained biotite-muscovite-alkali-feldspar quartzite with lenses of medium-grained biotite-plagioclase-clinozoisite-alkali-feldspar-amphibole calc-silicate gneiss; *qtz3* = medium-grained muscovite-biotite-alkali-feldspar quartzite; and *qtz4* = medium-grained mylonitic Cr-muscovite quartzite with accessory rutile. The map units PCqtz3 and 4 were originally defined by Dutrow et al. (1995).

The characteristic mineral assemblage of all quartzites is: qtz + kfs + bt + ms ± pl ± mnz ± zrn (Table 3.3). Stretched grains of quartz, present from 75 – 90 modal amount, are > 3 mm long and possess strong undulose extinction (Fig. 3.5). Five of the eleven samples of quartzite contain ribbon quartz with neoblasts of quartz occurring along grain boundaries. Equant feldspar grains, < 1 mm across, are present from 5 – 20 modal amount throughout the samples and may be partially to completely altered to sericite. Deformed laths of pleochroic-brown biotite, ~0.5 mm long and < 0.1 mm wide, are present up to 5 modal amount and define a moderate foliation. Moderate alteration of biotite to chlorite is present in all samples. Tabular muscovite is present in most samples up to 5 percent, and is commonly associated with feldspar. Green chromian-muscovite is seen in hand samples of quartzites in the Thompson Peak area (Fig. 3.6). No detailed mineral chemical analyses were conducted on quartzites.

3.1.2 Quartzofeldspathic Gneisses

Quartzofeldspathic gneisses are defined as rocks whose primary constituents are quartz and alkali-feldspar. Quartzofeldspathic gneisses contain similar minerals to the quartzites, but less than 75 percent quartz. Consequently, quartzites and quartzofeldspathic gneisses are often interlayered, and crop out together as light, ridge-forming units (Fig. 3.4). Quartzofeldspathic gneisses are more fine-grained than quartzites, with a stronger foliation indicated by the greater

Table 3.3: Mineral modes of SMC lithologies.

Lithology	**Mineral**																						
	grt	**bt**	**ms**	**sil**	**qtz**	**pl**	**kfs**	**amp**	**cpx**	**opx**	**ep**	**czo**	**crd**	**cal**	**ttn**	**chl**	**ilm**	**rt**	**po**	**apt**	**aln**	**gr**	**mnz**	**zrn**
quartzite	-	<5%	<5%	-	>75%	-	5 - 20%	-	-	-	-	-	-	-	-	(s)	-	-	-	-	-	-	-	tr
quartzo-feldspathic gneiss	-	<8%	<5%	-	30-65%	-	25 - 60%	-	-	-	-	-	-	-	tr	(s)	-	-	-	-	tr	-	tr	tr
mylonitic calc-silicate gneiss (matrix = 25 - 50 %)	-	-	-	-	85% of mtx*	25% of prb	-	-	50% of prb	-	10% of prb	15% of prb	-	<15% of mtx	-	-	-	-	-	-	-	tr	-	tr
granoblastic calc-silicate gneiss	-	acc.	-	-	5-25%	20-40%	-	<5%	<55%	-	-	-	-	-	tr	(s)	-	-	-	tr	-	-	-	tr
marble mylonite	-	-	-	-	<5%	<5%	<5%	-	10%	tr	-	tr	-	~75%	tr	-	-	-	-	-	-	tr	-	-
titanite-hornblende-biotite gneiss	-	15-35%	-	-	10-15%	30-40%	-	15 - 25%	-	-	-	-	-	-	~5 %	-	tr	tr	-	-	-	-	-	tr
metagabbro	-	5-10%	-	-	-	5-40%	-	35 - 90%	tr	-	-	-	-	-	-	-	tr - 10 %	-	-	-	-	-	-	-
biotite-amphibolite gneiss	-	<5%	-	-	-	35-50%	-	40-50%	-	-	-	-	-	-	acc.	-	<5 %	-	-	-	-	-	-	tr
peraluminous gneiss (Fe-Mg**/felsic)	10% FeMg	10-25% FeMg	10% FeMg / 15% felsic (s)	10-20% FeMg	-	5% FeMg / 40% felsic	<5% felsic (s)	-	-	-	-	-	30-35% FeMg	-	-	-	acc.	-	tr	-	-	-	tr	tr
amphibole-pyroxene-biotite gneiss	-	30%	-	-	-	35%	-	>5% (s)	25%	-	-	-	-	-	<5 %	-	tr	-	-	-	-	-	tr	tr

*mtx = matrix assemblage versus prb = porphyroclast/blastic assemblage
**FeMg indicates the ferromagnesian assemblage versus the felsic leucosome assemblage
(s) indicates secondary mineral

Figure 3.4: Distinctive light-colored ridge-forming quartzite outcrop on the eastern portion of William's ridge (ST08-04a). Prevalent fracturing occurs throughout the unit (Photo from B. Dutrow).

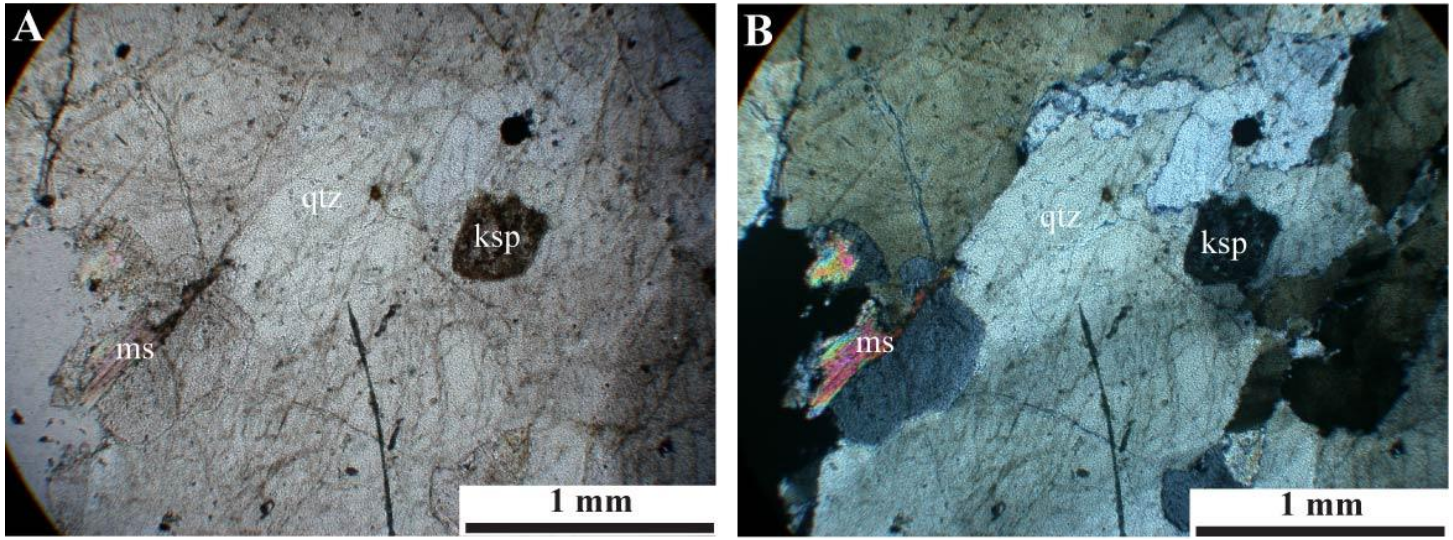

Figure 3.5: Photomicrographs of quartzite sample ST08-04c in PPL (a) and XPL (b). Proto-mylonitic fabric is defined by stretched quartz grains.

Figure 3.6: Hand sample of quartzite TP89-50 displaying green Cr-muscovite.

abundance of elongate mica. Map units of quartzofeldspathic gneiss are tens of meters thick and include layers or lenses of quartzite, calc-silicate gneiss, and/or hornblende-biotite gneiss.

Two mixed quartzofeldspathic gneiss units were mapped in the Thompson Peak – Marshall Lake area (Fig. 3.2), and one quartzofeldspathic gneiss was mapped in the Iron Creek area (Fig. 3.3). These units are: *m-csg&qfg* = medium-grained mylonitic biotite-K-feldspar-plagioclase quartzofeldspathic gneiss interlayered with fine-grained mylonitic amphibole-plagioclase-clinozoisite-clinopyroxene-quartz calc-silicate gneiss with trace titanite, *m-qfg* = mixed-dominantly medium-grained biotite-K-feldspar-plagioclase-quartzofeldspathic gneiss with trace allanite, and *qfg* = muscovite-biotite quartzofeldspathic gneiss with trace ilmenite and pyrrhotite.

Based on petrographic analysis of twelve samples, the characteristic mineral assemblage of quartzofeldspathic gneisses is: qtz + kfs + bt + ms ± pl ± ttn ± aln ± mnz ± zrn (Fig. 3.7 and 3.8, Table 3.3). Elongate ribbon quartz grains are > 1 mm in length, possess strong undulose extinction, and account for 30 – 65 modal amount. Neoblasts of quartz occur along sutured grain boundaries of quartz and feldspar. Alkali-feldspar, present from 15 – 30 modal amount, ranges in size from ~0.5 mm to > 3.5 mm in diameter and possesses grid twinning. Moderate alteration

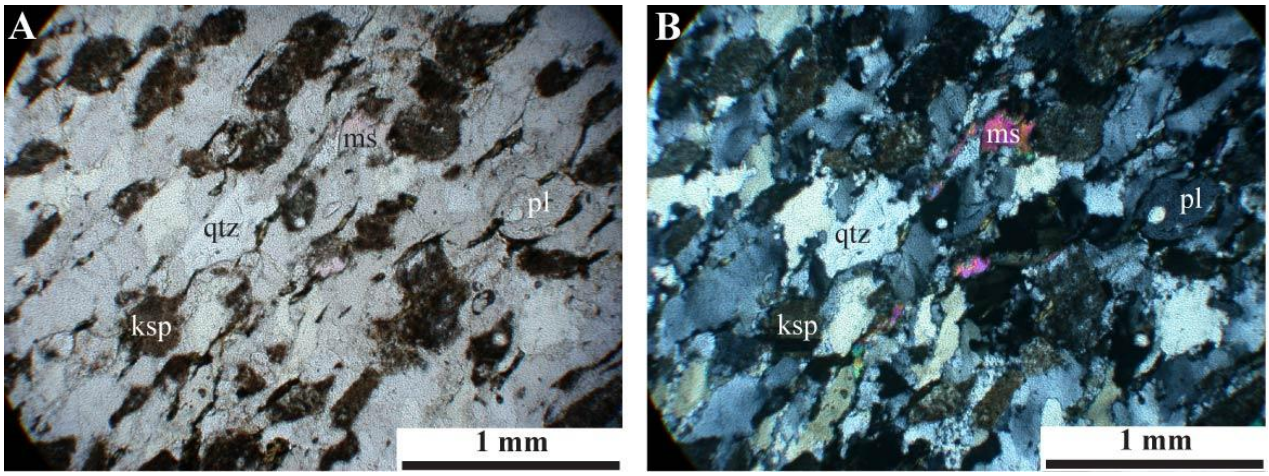

Figure 3.7: Photomicrographs of deformed quartzofeldspathic gneiss (ST08-35a) in PPL (a) and XPL (b). Ribbon quartz and biotite laths define a mylonitic fabric.

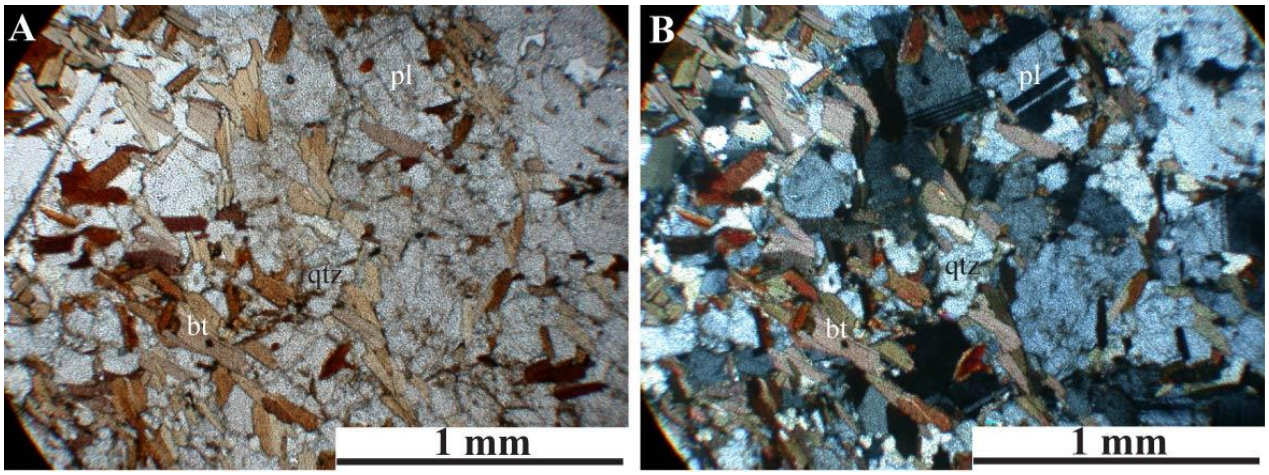

Figure 3.8: Photomicrograph of biotite-rich quartzofeldspathic gneiss (ST08-48b) in PPL (a) and XPL (b). Compositional variation exists among the quartzofeldspathic gneisses (cf. ST08-35a;Fig. 3.7).

of sericite after K-feldspar is present. Equant plagioclase, present from 10 – 30 modal amount, ranges in size from ~0.5 – 1 mm in diameter and displays deformation lamellae. Deformed biotite laths, present from 5 – 8 modal amount, are < 1 mm long by 0.2 mm wide, display brown pleochroism, and define a moderate – strong foliation. Minor chlorite alteration of biotite is present in all samples. Tabular muscovite, ~0.2 – 0.1 mm, accounts for < 5 percent of the rock.

3.1.3 Calc-Silicate Gneisses

Rocks containing abundant calcium-rich silicate minerals and < 5 percent carbonate are considered calc-silicates (Fettes and Desmons, 2007). Although mineral assemblages are similar

for all calc-silicates, textural differences from granoblastic to mylonitic occur in the SMC. All calc-silicates outcrop as light-colored grey-green ridge-forming units. Granoblastic calc-silicates have a "sugary" texture (Fig. 3.9), whereas the mylonitized calc-silicates are compositionally segregated and banded with a "classic" gneissic appearance (Fig. 3.10). A slight green color is imparted to hand samples by diopside and clinoamphibole grains.

Figure 3.9: Hand sample of granoblastic calc-silicate gneiss from Goat Creek (GC08-04) displaying "sugary" texture.


Figure 3.10: Outcrop of mylonitic calc-silicate gneiss from Thompson Peak region displaying compositional segregation and banding.

Nine samples of calc-silicate were taken from the Thompson Peak – Marshall Lake area, where three calc-silicate units were mapped based on mineral distribution (Fig. 3.2). These units are: *mixed-csg&qfg* = fine-grained mylonitic amphibole-plagioclase-clinozoisite-clinopyroxene-

quartz calc-silicate gneiss with trace titanite interlayered with medium-grained mylonitic biotite-K-feldspar-plagioclase quartzofeldspathic gneiss, *csg1* = fine-grained granoblastic biotite-clinozoisite-clinopyroxene calc-silicate gneiss, *csg2* = medium-grained mylonitic titanite-clinozoisite-clinopyroxene-quartz calc-silicate gneiss, *csg3* = medium-grained muscovite and orthopyroxene-bearing biotite-plagioclase-clinopyroxene-quartz calc-silicate gneiss.

The characteristic mineral assemblage of calc-silicates is qtz + cpx + pl ± czo ± ep ± amp ± kfs ± bt ± cal ± chl ± ttn ± apt ± zrn (Table 3.3). In mylonitic samples, a matrix of quartz and calcite comprises 25 – 50 modal amount of the total rock (Fig. 3.11). Ribbon and fine-grained quartz grains comprise ~85 percent of the matrix and fine-grained calcite comprises < 15 percent. Porphyroclasts account for 50 – 75 modal amount of the rock and are composed of diopside, clinozoisite, plagioclase, and/or amphibole, epidote, and alkali-feldspar. Diopside makes up 35 – 50 modal amount of the porphyroclasts, and is euhedral to slightly elongate, colorless, and possesses deformation lamellae. Elongate clinozoisite and epidote, present as 25 – 35 modal amount of porphyroclasts, exhibit anomalous yellow and blue birefringence, have sutured grain boundaries, and are ~ 1.5 mm long by 0.5 mm wide. Rounded plagioclase grains, < 0.5 mm in diameter, account for 25 – 30 modal amount of the porphyroclasts.

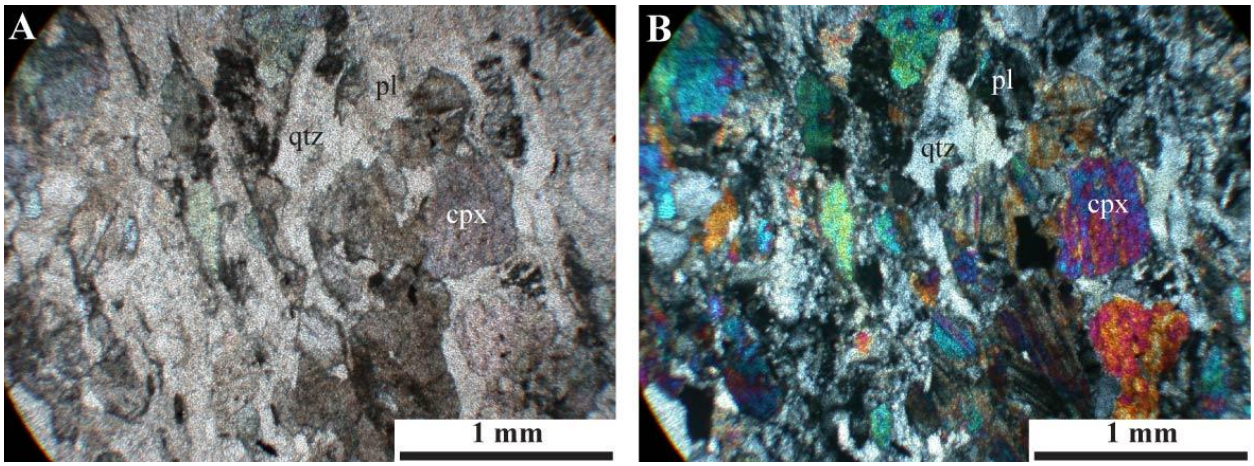

Figure 3.11: Photomicrographs of mylonitic calc-silicate gneiss (ST08-32c) in PPL (a) and XPL (b). Ribbon-quartz defines the strong mylonitic fabric. Porphyroclasts of clinopyroxene displaying deformation lamellae.

Granoblastic calc-silicates contain similar minerals as mylonitic samples, but in different modal amount (Fig. 3.12). Equant diopside grains ~ 0.5 mm in diameter dominate the mineral assemblage making up < 55 modal amount of the rock. Medium-grained, equant plagioclase grains comprise 30 – 40 modal amount and range from < 0.5 mm to 0.8 mm in length. Fine-grained equant quartz accounts for 5 – 15 percent of the rock, and is < 0.3 mm in diameter. Accessory minerals include euhedral wedges of titanite, equant grains of apatite, clino-amphibole, zircon, biotite, and chlorite.

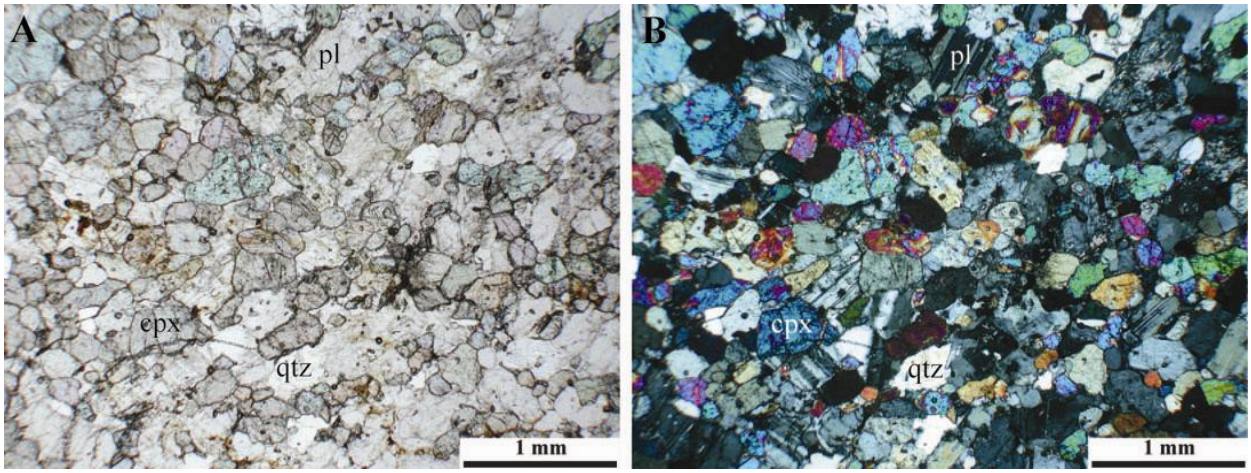

Figure 3.12: Photomicrographs of granoblastic calc-silicate gneiss (csg) (ST08-35a from PCm csg&qfg, Fig. 3.2) in PPL (a) and XPL (b). Lower modal amounts of quartz are present in granoblastic versus mylonitic csgs.

Biotite occurs in quantities up to 20 modal percent in two samples collected near quartzofeldspathic gneisses. Two samples contain the mineral assemblage pl + kfs + bt + qtz + cpx + czo ± ep (Fig. 3.13). These samples have a weak gneissic texture. Equant plagioclase, < 1 mm in diameter, makes up ~30 modal amount and exhibits polysynthetic twinning. Equant alkali-feldspar, < 1 mm in diameter, make up ~30 percent of the rock and exhibits scotch-plaid twinning. Tabular biotite, < 0.5 mm long by < 0.2 mm wide, is the next most abundant mineral accounting for ~20 modal amount, and defines a weak foliation. Equant quartz grains, < 0.5 mm in diameter, account for < 10 modal amount. Quartz grains have sutured boundaries and exhibit

undulose extinction. Anhedral diopside grains make up < 10 percent of the rock and exhibit deformation lamellae. Anhedral grains of clinozoisite and/or epidote make up < 3 percent and possess anomalous blue and yellow birefringence suggesting the presence of Fe^{3+}.

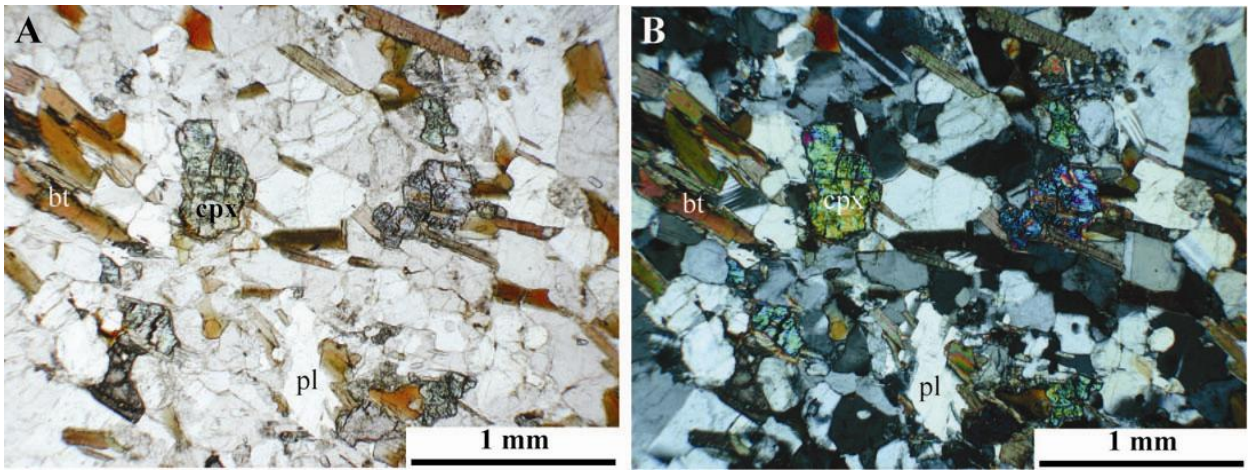

Figure 3.13: Photomicrographs of biotite-rich calc-silicate gneiss (ST08-35b from PCm csg&qfg, Fig. 3.2) in PPL (a) and XPL (b). A weak gneissic texture is defined by laths of biotite.

3.1.4 Marble Mylonites

Marble mylonites contain > 50 percent carbonate and possess a strong mylonitic fabric. Marble mylonites are light grey in hand sample and exhibit a distinctive outcrop pattern due to the differential weathering of carbonate and included calc-silicate minerals (Fig. 3.14). Extreme mylonitization has led to chemical segregation and banding of carbonate-rich and silica-rich layers on a 1 – 15 cm scale.

Two marble mylonite units were mapped based on spatial distribution in the Thompson Peak – Marshall Lake area (Fig. 3.2). These units are: *mm1* = fine-grained mylonitic alkali-feldspar-plagioclase-quartz-clinopyroxene marble and *mm2* = medium-grained mylonitic plagioclase-clinozoisite-clinopyroxene-quartz marble.

Petrographic analyses on six samples have identified the characteristic mineral assemblage of silica-rich layers to be similar to calc-silicates described above, and the carbonate-rich layers as: cal + cpx + qtz + pl + kfs + gr ± czo ± opx ± ttn ± ilm (Fig. 3.15, Table 3.3).

The matrix is composed of fine-grained carbonate and accounts for ~75 modal amount. Fine- to coarse-grained, undeformed, porphyroclasts of: clinopyroxene (~10 percent), quartz (~3 percent), plagioclase (~3 percent), and alkali-feldspar (~ 3 percent) account for > 20 modal amount. Trace amounts of orthopyroxene and clinozoisite occur as fine to medium-grained porphyroclasts. Trace amounts of euhedral titanite occur as small, < 0.3 mm, wedge-shaped porphyroclasts. Disseminated flecks of graphite and/or ilmenite, < 0.01 mm, occur throughout the fine-grained carbonate matrix and account for < 5 modal amount. The grey color is due to the ubiquitous presence of graphite.

3.1.5 Titanite-Amphibole-Biotite Gneisses

Titanite-amphibole-biotite gneisses are classified by the presence of titanium-saturating phases such as ilmenite, titanite, and/or rutile. These gneisses are fine- to medium-grained and possess a strong foliation plane. Amphibole is distinguishable in hand sample by diagnostic cleavage and, with biotite, imparts a dark color to these rocks. These gneisses weather to rusty red-brown, are typically slope-forming units, and include felsic layers <5 – 100 cm thick (Fig. 3.16).

Two titanite-amphibole-biotite gneiss units were mapped based on spatial distribution in the Thompson Peak – Marshall Lake area. These units are referred to as: *thbg1* = medium-grained ilmenite bearing hornblende-titanite-biotite gneiss with accessory rutile, and *thbg2* = medium-grained ilmenite-titanite-hornblende-biotite gneiss with accessory rutile.

Petrographic analyses of nine samples identify the characteristic mineral assemblage of titanium-hornblende-biotite gneisses as: pl($An_{\sim 83}$) + bt ± hb + qtz + ttn ± ilm ± rutile (Fig. 3.17, Table 3.3). Equant grains of plagioclase, present from 30 – 40 modal amount, are ~0.5 mm in

Petrographic analyses of nine samples identify the characteristic mineral assemblage of titanite-hornblende-biotite gneisses as: pl($An_{\sim 83}$) + bt ± hb + qtz + ttn ± ilm ± rutile (Fig. 3.17,

Figure 3.14: Marble mylonite (PCmm1) with deformation folding and uneven weathering caused by the preferential dissolution of calcite compared with silicate minerals.

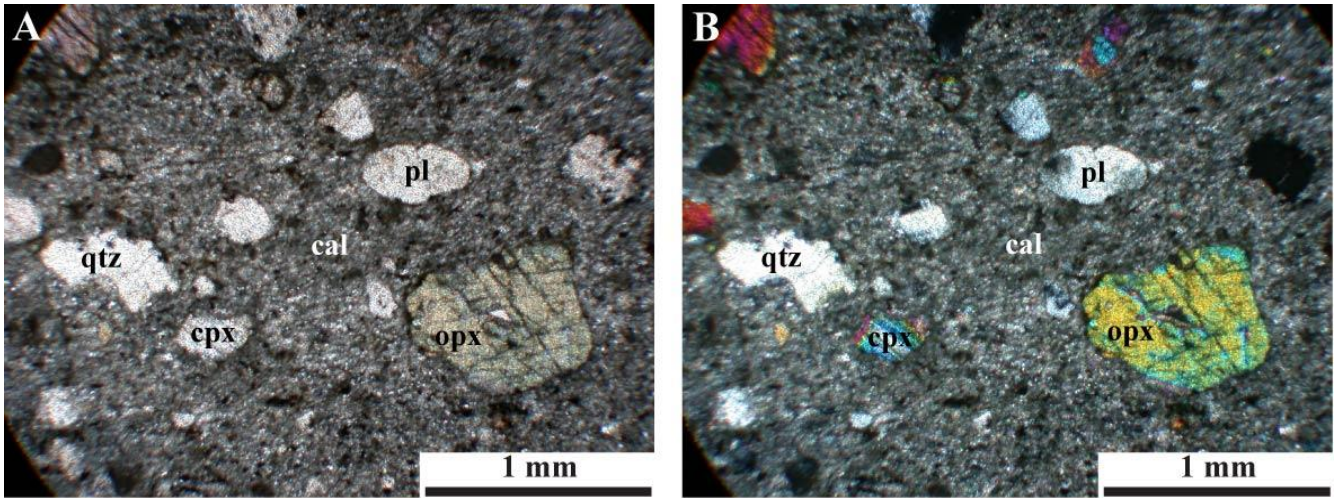

Figure 3.15: Photomicrographs of marble mylonite (ST08-53a) in PPL (a) and XPL (b) showing rounded porphyroclasts in a fine-grained calcite matrix.

Figure 3.16: Outcrop of titanite-hornblende-biotite gneiss along south face of William's ridge (ST08-55, PCthbg2, see Fig. 3.2) displaying red-brown color and occurrence as slope-forming units. Quartzofeldspathic gneiss (lighter unit) is interlayered with the gneiss.

Table 3.3). Equant grains of plagioclase, present from 30 – 40 modal amount, are ~0.5 mm in diameter. Plagioclase grains have sutured grain boundaries and polysynthetic twinning. Tabular biotite, 0.5 – 4 mm long, accounts for 5 – 35 modal amount, and defines a strong foliation. Biotite exhibits deep red-to-brown pleochroism indicative of Ti-rich biotites. Subhedral hornblende is found in half of the samples and accounts for 15 – 25 modal amount. These grains range from 0.3 – 1.5 mm in diameter with an average size of ~0.5 mm. Hornblendes exhibit strong pleochroism of green rims and brown cores. This suggests the hornblendes are compositionally zoned, with Ti-rich cores and Mg-rich rims. Medium-grained anhedral quartz crystals are distributed throughout, with 10 – 15 modal amount. Fine- to medium-grained, subhedral to euhedral titanite grains, 0.1 – 0.5 mm in length, are scattered throughout the sample, accounting for 10 – 15 modal amount and are easily identified by their wedge-shaped crystals. Ilmenite flakes account for ~5 modal amount and are found in the center of larger, anhedral

titanite grains suggesting a reaction of ilmenite to titanite. Accessory rutile occurs as very fine-grained prismatic needles throughout the samples.

ST08-45 contains a different mineral assemblage, lacking biotite and containing a clinopyroxene-rich vein approximately 5 mm thick. The mineral assemblage of ST08-45a is: plagioclase + amphibole + quartz + titanite + clinopyroxene + monazite + ilmenite + rutile (Fig. 3.18, Table 3.3). Rounded plagioclase are 0.4 – 1 mm in diameter and account for 40 modal percent. Subhedral amphiboles account for 25 modal percent and are 0.3 – 2 mm in length. Elongate amphiboles and stretched quartz define a moderate-gneissic texture. Stretched quartz accounts for 15 modal percent. Euhedral- to subhedral-wedges of titanite account for 10 modal percent and range from 0.1 – 0.5 mm. Large titanite grains contain ilmenite cores. Clinopyroxene accounts for approximately < 10 modal percent and ranges from 0.3 – 0.7 mm in diameter. Accessory minerals include fine-grained rutile and monazite.

These rocks possess a strong gneissic texture with foliation defined by aligned tabular biotite, elongate hornblende, stretched quartz, and needles of rutile. In approximately half the samples, biotite appears kinked. Minor – moderate alteration of biotite to chlorite is present. Sample ST08-45a contains a lens of medium-grained pyroxene and plagioclase ~4 mm wide.

Electron microprobe analyses of two samples from two localities provide mineral chemical data for titanite-hornblende-biotite gneisses. ST08-30a is typical of all samples of titanite-hornblende-biotite gneiss except for ST08-45a. Plagioclase compositions were calculated with 25 analyses on three grains in ST08-30a that range from $Ab_{9\text{-}18}An_{76\text{-}90}Or_{0\text{-}1,}$ $Ab_{61\text{-}67}An_{31\text{-}38}Or_{1\text{-}5,}$ and $Ab_{17\text{-}21}An_{79\text{-}82}Or_{0\text{-}1}$ for grains 1 – 3 respectively (Fig. 3.19, Appendix C). Two, subhedral plagioclase grains average ~83 percent anorthite, and a third grain is ~35 percent anorthite (andesine, Fig. 3.20, Table 3.4). The andesine grain is darker in the back-scatter electron image than other plagioclase grains due to increased Na, and appears to fill fractures

between grains (Fig. 3.19). No relationship is detected between composition and spatial distribution of the plagioclases.

Compositions of amphibole grains were calculated with 40 analyses from four grains in ST08-30a (Fig. 3.19, Appendix D). Optical zoning was observed though the presence of brown cores and green rims, so core-rim traverses were conducted to characterize the chemical zoning. Cores are slightly enriched in Ti and Al (Fig. 3.21). Composition of amphibole rims range from Al = 1.69 – 2.10 apfu and Ti = 0.06 – 0.13 apfu, whereas cores range from Al = 1.68 – 2.08 apfu and Ti = 0.07 – 0.20 apfu (Table 3.5). All rim and core compositions are classified as magnesio-hornblende except the core of grain one, which is a tschermakitic hornblende (Fig. 3.22, Leake et al., 1997). Structural formulae range from $(K_{0.21}Na_{0.21})(Ca_{1.88}Na_{0.12})(Mg_{2.21}Fe_{2.05}Al_{0.82}Mn_{0.04})(Si_{6.55}Al_{1.25}Ti_{0.20})O_{22}(OH)_2$ for core to $(K_{0.15}Na_{0.05})(Ca_{1.83}Na_{0.17})(Mg_{2.14}Fe_{1.97}Al_{1.08}Mn_{0.03})(Si_{6.563}Al_{1.28}Ti_{0.09})O_{22}(OH)_2$ for rim compositions.

Biotite compositions were calculated using 21 analyses from two grains in ST08-30a (Fig. 3.19, Appendix E). These grains plot as intermediate biotites (Fig. 3.23, Table 3.6), and range from Ti = 0.11 – 0.29 apfu, with structural formulas from $\square_{0.50}K_{1.44}Na_{0.03}(Fe^{2+}_{2.57}Mg_{2.56}Al_{1.14}Ti_{0.11}Ca_{0.03}Mn_{0.03})(Al_{2.12}Si_{5.33})O_{20}(OH,F)_4$ to $\square_{0.17}Na_{0.02}K_{1.81}(Fe^{2+}_{2.65}Mg_{2.53}\ Al_{0.77}Ti_{0.29}Mn_{0.03}Ca_{0.02})(Al_{2.37}Si_{5.63})O_{20}(OH,F)_4$.

Plagioclase compositions for ST08-45a were calculated using 21 analyses from two grains (Fig. 3.24, Appendix C). Compositions are andesine and range from $Ab_{62\text{-}66}An_{32\text{-}36}Or_{01\text{-}02}$ (Fig. 3.20). No compositional zoning was detected, so grain averages were calculated using all analyses per grain (Table 3.4).

Composition of amphibole in ST08-45a was calculated with 21 analyses from two grains (Fig. 3.25, Appendix D). Optical zoning of brown cores and green rims was observed so core-

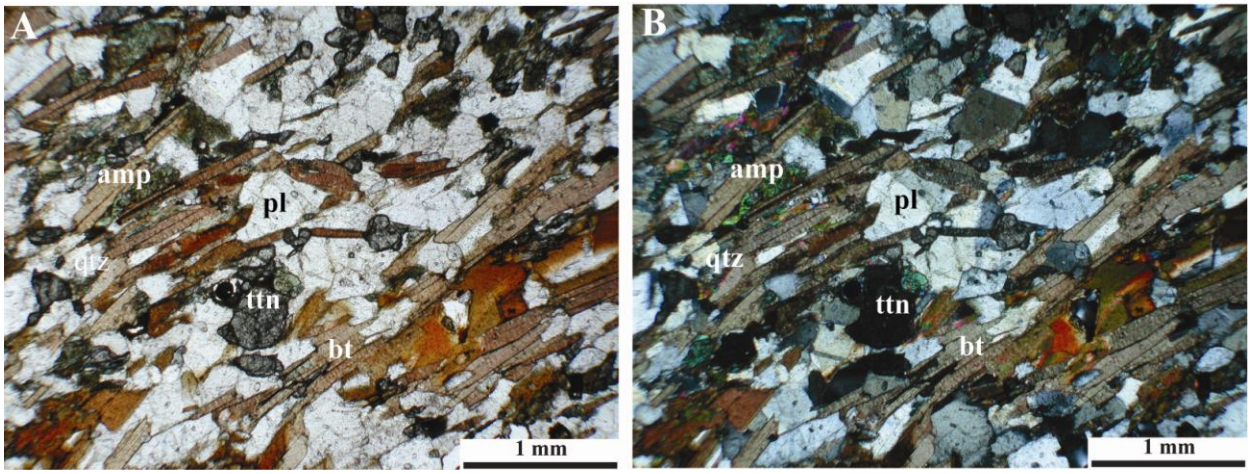

Figure 3.17: Photomicrographs of titanite-amphibole-biotite gneiss (ST08-26b) in PPL (a) and XPL (b). Aligned biotite (bt) and amphibole (amp) with elongate plagioclase (pl) define a gneissic texture. Anhedral titanite (ttn) grains are common throughout.

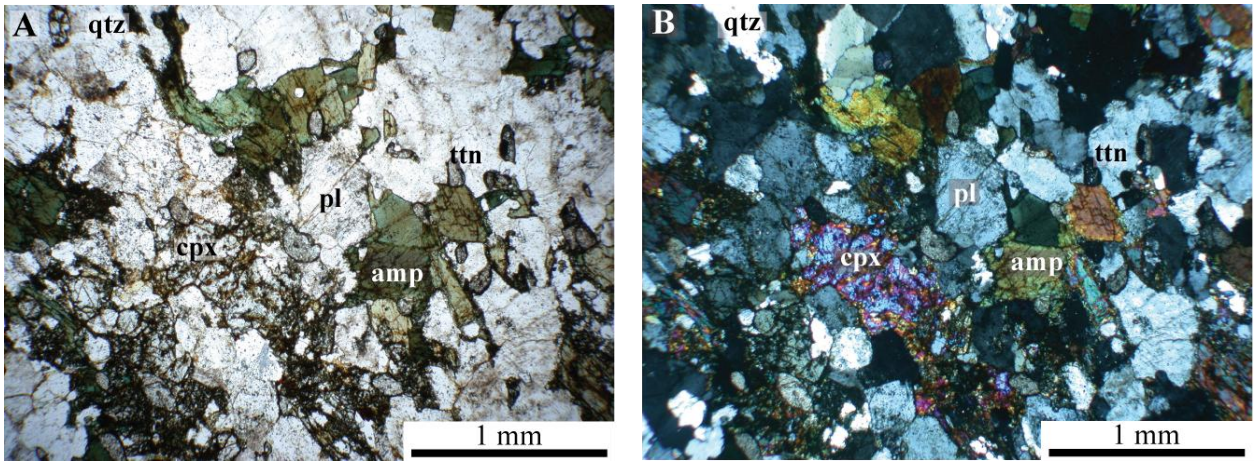

Figure 3.18: Photomicrographs of titanite-amphibole-biotite gneiss (ST08-45a) in PPL (a) and XPL (b) displaying dominant minerals: plagioclase (pl), amphibole (amp), clinopyroxene (cpx), titanite (ttn), and quartz (qtz).

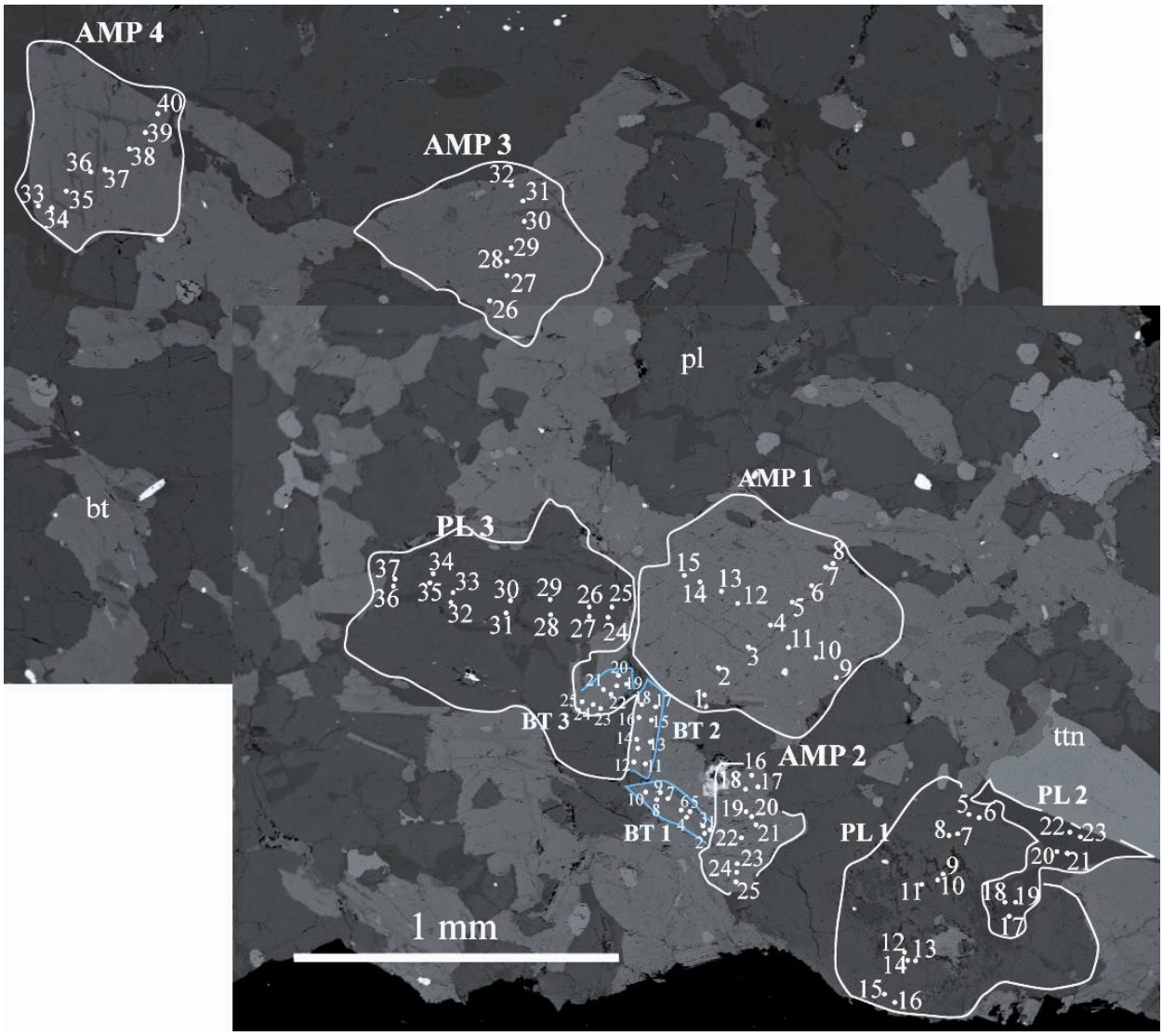

Figure 3.19: Backscattered electron (BSE) image of ST08-30a showing electron microprobe analysis (EMPA) points of amphibole (AMP), plagioclase (PL), and biotite (BT) grains. PL2 is darker than PL1 and PL3 indicating different composition.

rim traverses were conducted to check for chemical zoning (Fig. 3.26). Composition of amphiboles rims and cores are similar. Rims range from X_{Mg} = 0.31 – 0.32, Ti = 0.15 – 0.19 apfu, and Al = 2.14 – 2.27, whereas cores range from X_{Mg} = 0.30-0.34, Ti = 0.14 – 0.24 apfu, and Al = 2.15 – 2.28 apfu (Table 3.5). The core of grain two has higher (peak) Ti values averaging 0.23 apfu, and plots as ferro-tschermakite, but grain two rim and grain one rim and core plot as ferro-tschermakitic-hornblendes (Fig. 3.22, Leake, 1997). ST08-45a amphiboles contain higher iron and aluminum components than those of ST08-30a. Structural formulae range from $(K_{0.35-0.38}Na_{0.09-0.37})(Ca_{1.73-1.96}Na_{0.04-0.27})(Fe_{2.94-3.00}Mg_{1.27-1.29}Al_{0.59-0.61})(Si_{6.19-6.24}Al_{1.57-1.65}Ti_{0.14-0.24})O_{22}(OH)_2$ for core to rim compositions

Composition of pyroxene in ST08-45a was calculated with 24 analyses from three grains (Fig. 3.27, Appendix F). Pyroxenes are dominantly calcic with $Wo_{48-50}En_{22-25}Fs_{25-29}$ (Table 3.7). No zoning was noted. Structural formulae range from $Ca_{0.95-1.00}(Fe_{0.50-0.58}Mg_{0.44-0.50}Al_{0.01-0.11})Si_2O_6$, and are classifiedas diopside (Fig. 3.28).

3.1.6 Metagabbros

Metagabbros in the SMC are coarse-grained rocks containing 35 – 80 percent amphibole with relict igneous or granoblastic textures. Outcrops are easily identified by their coarse-grains, dark-green to black color, homogeneous appearance, and rounded weathering profile (Fig. 3.29). Amphiboles are identified in hand sample by diagnostic 60°/120° cleavage.

Two metagabbro units were mapped in the Thompson Peak – Marshall Lake area (Fig. 3.2). These units are: *mg1* = coarse-grained granoblastic biotite-bearing plagioclase-amphibole metagabbro and *mg2* = coarse-grained granoblastic clinopyroxene-ilmenite-biotite-hornblende metagabbro.

Petrographic analyses of six samples identified the characteristic mineral assemblage of *mg1* as: amp + pl + bt ± cpx ± ttn (Fig. 3.30, Table 3.3). Subhedral, equant amphibole grains

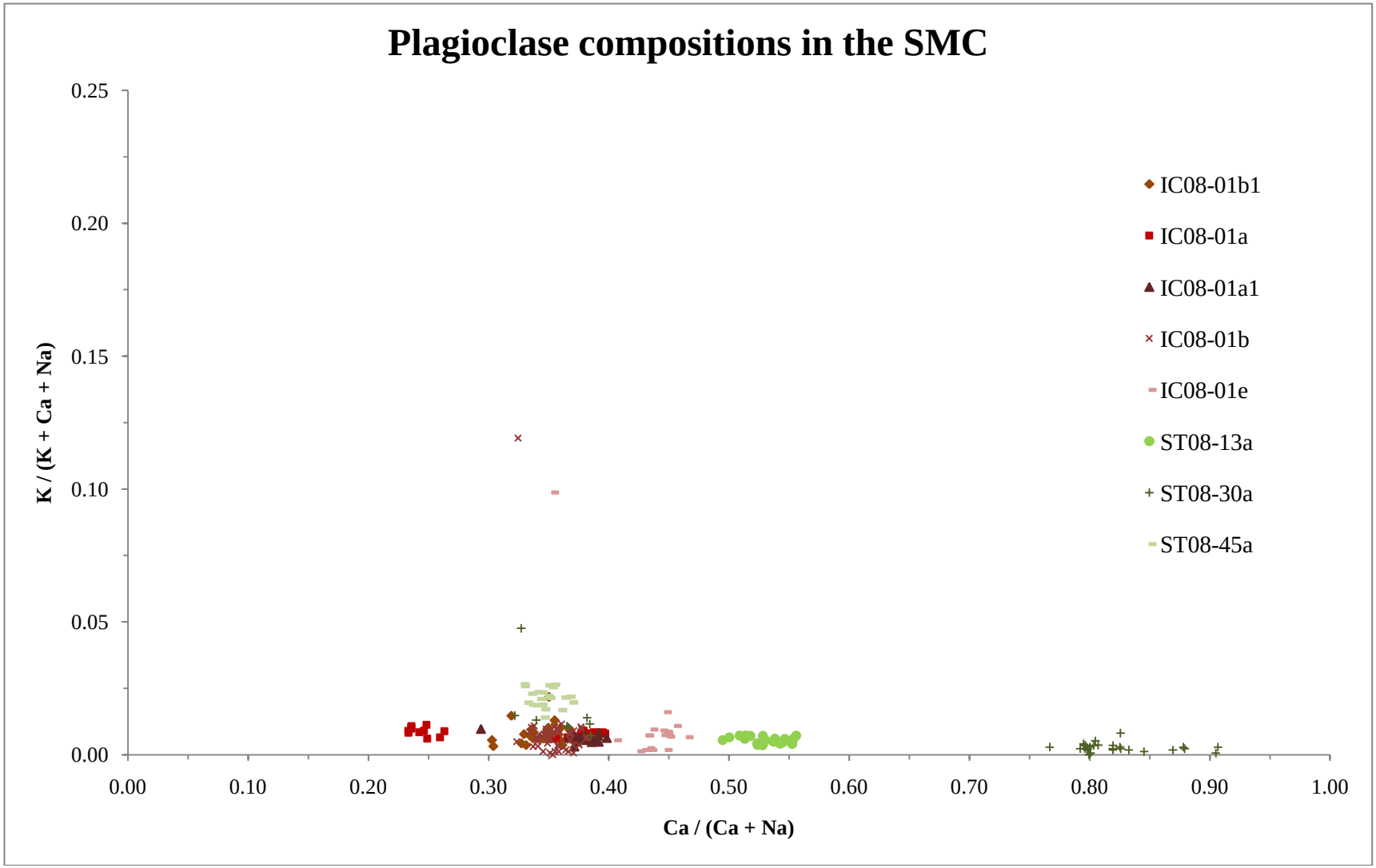

Figure 3.20: Compositions of plagioclase in the SMC. Plagioclase from peraluminous gneiss are oligoclase to andesite. Plagioclase in ST08-45a plot is also andesine. Two modes of plagioclase are present in ST08-30a: most contain $An_{>80}$, but one grain averages $An_{\sim 35}$. Plagioclase in ST08-13a is labradorite. Little-to-no zoning was noted in all analyzed grains. However, three analyses contained high potassium concentrations.

Table 3.4: Plagioclase grain averages in titanite-amphibole-biotite gneisses.

	ST08-30a			st08-45a	
	Grain 1	Grain 2	Grain 3	Grain 1	Grain 2
wt %					
SiO_2	46.55	59.44	47.67	59.96	59.65
Al_2O_3	34.45	25.61	33.67	25.50	25.73
CaO	17.45	6.84	16.36	6.55	6.81
BaO	0.01	0.03	0.02	0.02	0.02
Na_2O	1.73	6.77	2.22	7.05	6.91
K_2O	0.04	0.27	0.05	0.35	0.36
FeO	0.05	0.09	0.05	0.04	0.06
MgO	0.00	0.01	0.01	0.01	0.01
Total	100.28	99.06	100.05	99.48	99.56

Oxygens = 8

Feldspar

	ST08-30a			st08-45a	
	Grain 1	Grain 2	Grain 3	Grain 1	Grain 2
apfu					
Si	2.13	2.67	2.18	2.68	2.66
Al	1.86	1.35	1.82	1.34	1.35
Ca	0.86	0.33	0.80	0.31	0.33
Ba	0.00	0.00	0.00	0.00	0.00
Na	0.15	0.59	0.20	0.61	0.60
K	0.00	0.02	0.00	0.02	0.02
Fe^{2+}	0.00	0.00	0.00	0.00	0.00
Mg	0.00	0.00	0.00	0.00	0.00
X_{Ab}	0.15	0.63	0.20	0.65	0.63
X_{Or}	0.00	0.02	0.00	0.02	0.02
X_{An}	0.85	0.35	0.80	0.33	0.35

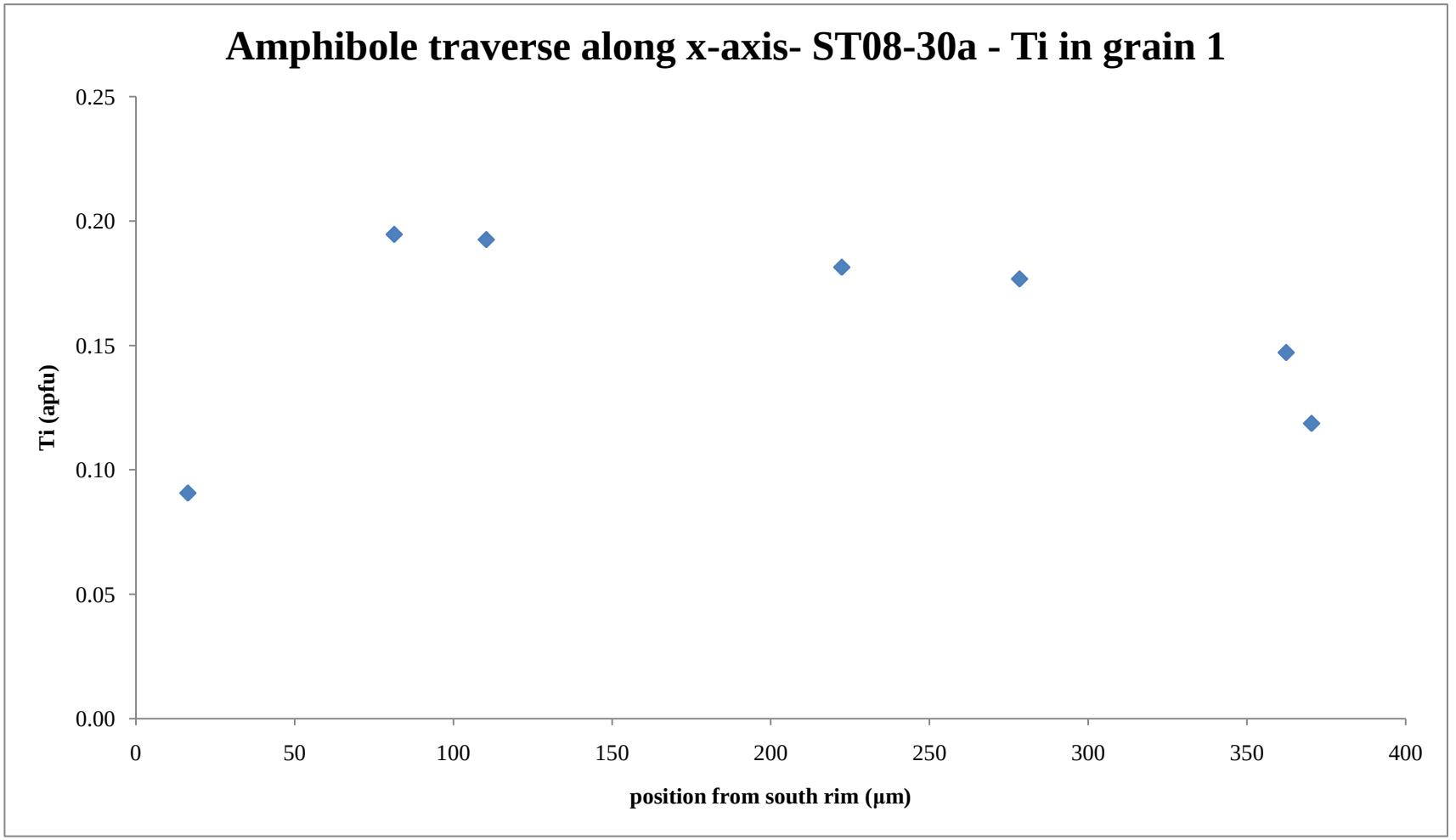

Figure 3.21: Core-to-rim traverse of Ti concentration of amphibole grain one in titanite-amphibole-biotite gneiss (ST08-30a). Cores are slightly Ti-enriched with respect to rims.

Table 3.5: Compositional averages of amphibole rims and cores from titanite-amphibole-biotite gneisses.

	ST08-30a		ST08-30a		ST08-30a		ST08-30a		ST08-45a		ST08-45a	
	Rim_1	Core_1	Rim_2	Core_2	Rim_3	Core_3	Rim_4	Core_4	Rim_1	Core_1	Rim_2	Core_2
wt %												
SiO_2	45.50	44.27	45.48	45.16	46.23	45.98	45.96	46.64	40.31	39.90	39.88	39.61
TiO_2	0.95	1.71	1.07	1.09	1.01	1.00	0.89	0.62	1.62	1.29	1.35	2.00
Al_2O_3	11.77	11.78	11.09	10.78	10.20	10.07	9.97	10.25	12.03	12.40	12.25	12.07
Cr_2O_3	0.01	0.01	0.09	0.04	0.07	0.04	0.06	0.04	0.05	0.07	0.05	0.11
FeO	15.90	16.75	15.76	15.94	15.51	15.54	15.33	14.73	22.01	21.14	21.48	22.41
MnO	0.28	0.28	0.25	0.27	0.25	0.29	0.29	0.26	0.28	0.36	0.33	0.34
MgO	10.37	10.08	10.55	10.48	11.24	11.07	11.21	11.36	5.69	5.73	5.57	5.43
CaO	12.02	11.81	12.36	12.12	12.15	12.22	12.09	12.51	11.90	11.66	11.84	11.71
BaO	0.04	0.03	0.00	0.04	0.02	0.03	0.02	0.01	0.01	0.03	0.01	0.02
Na_2O	0.86	1.08	0.93	0.93	0.90	0.97	0.97	0.92	1.28	1.23	1.26	1.32
K_2O	0.81	1.14	0.86	0.88	0.85	0.81	0.79	0.69	1.84	1.72	1.82	1.87
Cl	0.13	0.14	0.14	0.14	0.15	0.15	0.13	0.07	0.36	0.27	0.38	0.43
Total	99.05	99.21	99.34	98.73	99.64	99.24	99.18	99.98	99.54	98.75	98.90	98.82

stoiched on 15 cations

	ST08-30a		ST08-30a		ST08-30a		ST08-30a		ST08-45a		ST08-45a	
	Rim_1	Core_1	Rim_2	Core_2	Rim_3	Core_3	Rim_4	Core_4	Rim_1	Core_1	Rim_2	Core_2
apfu												
Si	6.67	6.54	6.66	6.67	6.74	6.74	6.74	6.76	6.22	6.18	6.19	6.17
Ti	0.10	0.19	0.12	0.12	0.11	0.11	0.10	0.07	0.19	0.15	0.16	0.23
Al	2.04	2.05	1.92	1.88	1.75	1.74	1.72	1.75	2.19	2.26	2.24	2.22
Cr	0.00	0.00	0.01	0.00	0.01	0.01	0.01	0.00	0.01	0.01	0.01	0.01
Fe^{3+}	0.05	0.01	0.08	0.10	0.12	0.12	0.16	0.21	0.25	0.35	0.31	0.18
Fe^{2+}	1.95	2.07	1.93	1.97	1.89	1.91	1.88	1.79	2.84	2.74	2.79	2.92
Mn^{2+}	0.04	0.03	0.03	0.03	0.03	0.04	0.04	0.03	0.04	0.05	0.04	0.04
Mg	2.27	2.22	2.30	2.31	2.44	2.42	2.45	2.45	1.31	1.32	1.29	1.26
Ca	1.89	1.87	1.94	1.92	1.90	1.92	1.90	1.94	1.97	1.94	1.97	1.96
Ba	0.00	0.00	0.00	0.00	0.00	0.00	0.00	0.00	0.00	0.00	0.00	0.00
Na	0.25	0.31	0.27	0.27	0.25	0.27	0.28	0.26	0.38	0.37	0.38	0.40
K	0.15	0.22	0.16	0.17	0.16	0.15	0.15	0.13	0.36	0.34	0.36	0.37
Cl	0.03	0.03	0.03	0.03	0.04	0.04	0.03	0.02	0.09	0.07	0.10	0.11
X_{Mg}	0.54	0.52	0.54	0.54	0.56	0.56	0.57	0.58	0.32	0.33	0.32	0.30

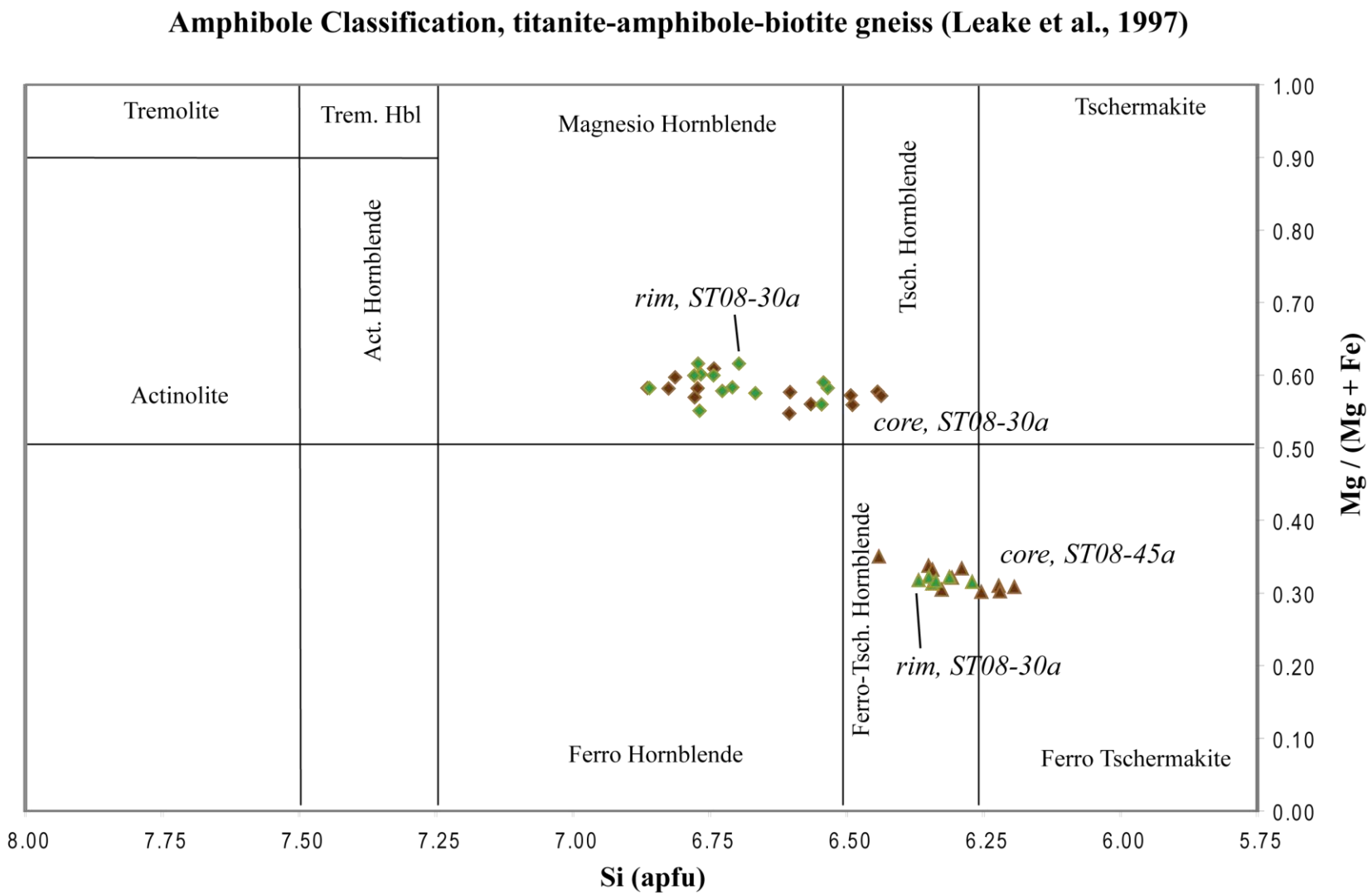

Figure 3.22: Rim and core compositions for four amphibole grains from ST08-30a and two amphiboles in ST08-45a. ST08-30a compositions are magnesio-hornblende with the exception of one core that is a tschermakitic hornblende. ST08-45a amphiboles contain higher iron concentrations and plot as Ferro-tschermakitic hornblende with the exception of core analyses from grain two which plot as ferro-tschermakite. Classification after Leake (1997).

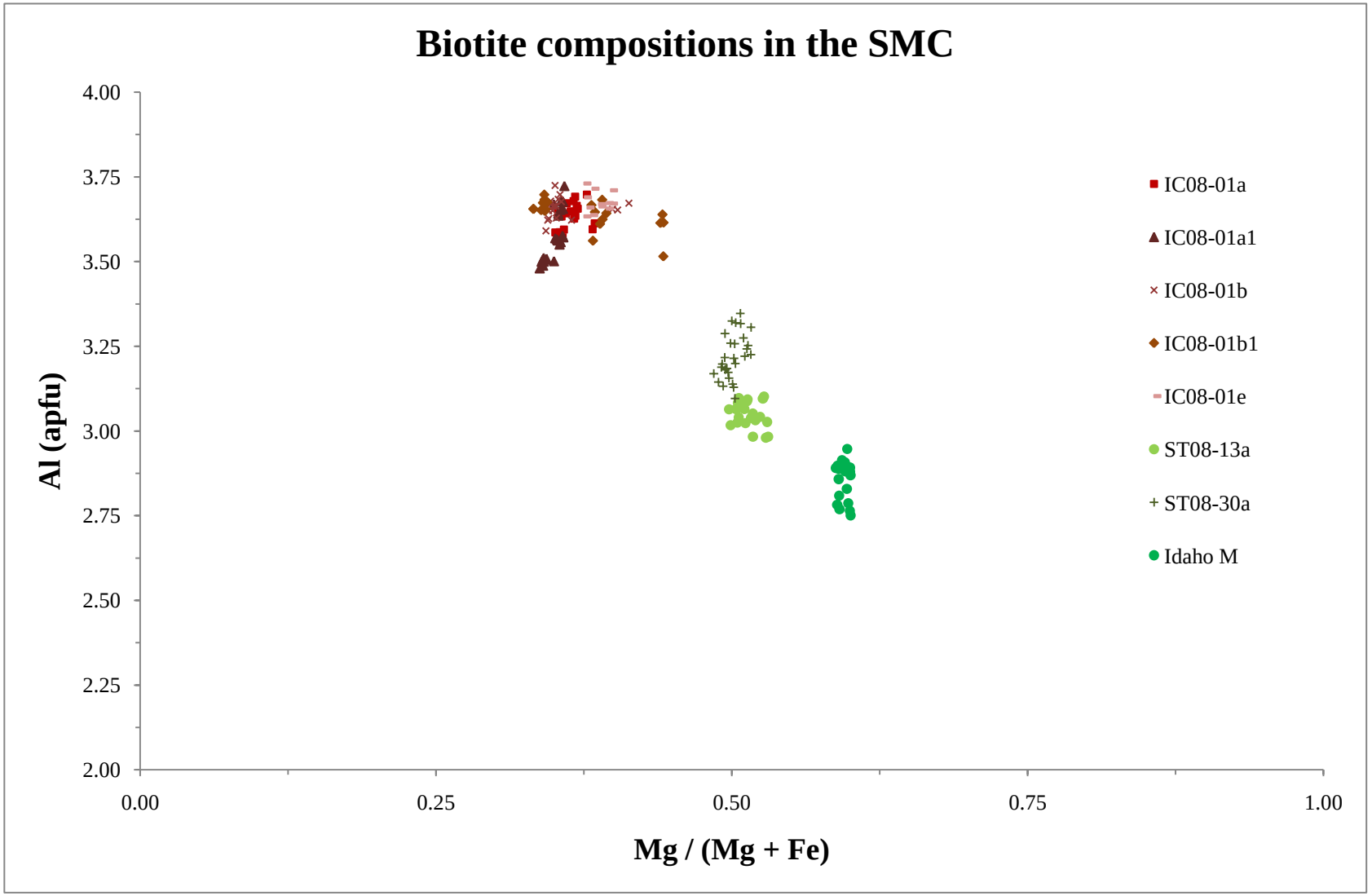

Figure 3.23: Composition of biotite from the SMC. Biotites from Iron Creek have higher concentrations of aluminum 3.48 – 3.72 apfu with Mg/(Mg+Fe) ranging from 0.33 – 0.44. Biotite in ST08-13a and ST08-30a have intermediate aluminum 2.98 – 3.10 apfu with Mg/(Mg+Fe) ~0.50. Biotites in Idaho M contain 2.75 – 2.91 apfu Al and Mg/(Mg+Fe) ~0.60.

Table 3.6: Compositional ranges (based on titanium content) of biotites in ST08-30a.

	st08-30a					
	Grain 1 - low-Ti	Grain 1 - High-Ti	Grain 2 - low-Ti	Grain 2 - High-Ti	Grain 3 - low-Ti	Grain 3 - High-Ti
wt %						
SiO_2	36.35	36.24	35.65	36.08	35.81	36.82
TiO_2	1.46	2.46	0.99	1.56	1.38	2.22
Al_2O_3	17.73	17.18	18.51	17.42	18.14	17.45
Cr_2O_3	0.07	0.03	0.02	0.03	0.03	0.00
FeO	20.34	20.41	20.55	20.75	20.54	20.39
MnO	0.24	0.20	0.23	0.23	0.25	0.22
MgO	11.49	10.94	11.48	11.78	11.87	11.17
CaO	0.07	0.09	0.19	0.07	0.05	0.02
BaO	0.49	0.81	0.10	0.95	0.54	0.74
Na_2O	0.14	0.06	0.11	0.12	0.15	0.10
K_2O	8.83	9.15	7.53	8.79	8.93	9.25
Total	97.21	97.57	95.36	97.78	97.69	98.38

Oxygens = 22

Biotite

	st08-30a					
	Grain 1 - low-Ti	Grain 1 - High-Ti	Grain 2 - low-Ti	Grain 2 - High-Ti	Grain 3 - low-Ti	Grain 3 - High-Ti
apfu						
Si	5.45	5.44	5.40	5.41	5.36	5.47
Ti	0.16	0.28	0.11	0.18	0.16	0.25
Al	3.13	3.04	3.31	3.08	3.20	3.06
Cr	0.01	0.00	0.00	0.00	0.00	0.00
Fe^{2+}	2.55	2.56	2.60	2.60	2.57	2.53
Mn^{2+}	0.03	0.03	0.03	0.03	0.03	0.03
Mg	2.57	2.45	2.59	2.64	2.65	2.47
Ca	0.01	0.01	0.03	0.01	0.01	0.00
Ba	0.03	0.05	0.01	0.06	0.03	0.04
Na	0.04	0.02	0.03	0.03	0.04	0.03
K	1.69	1.75	1.46	1.68	1.71	1.75
X_{Mg}	0.50	0.49	0.50	0.50	0.51	0.49

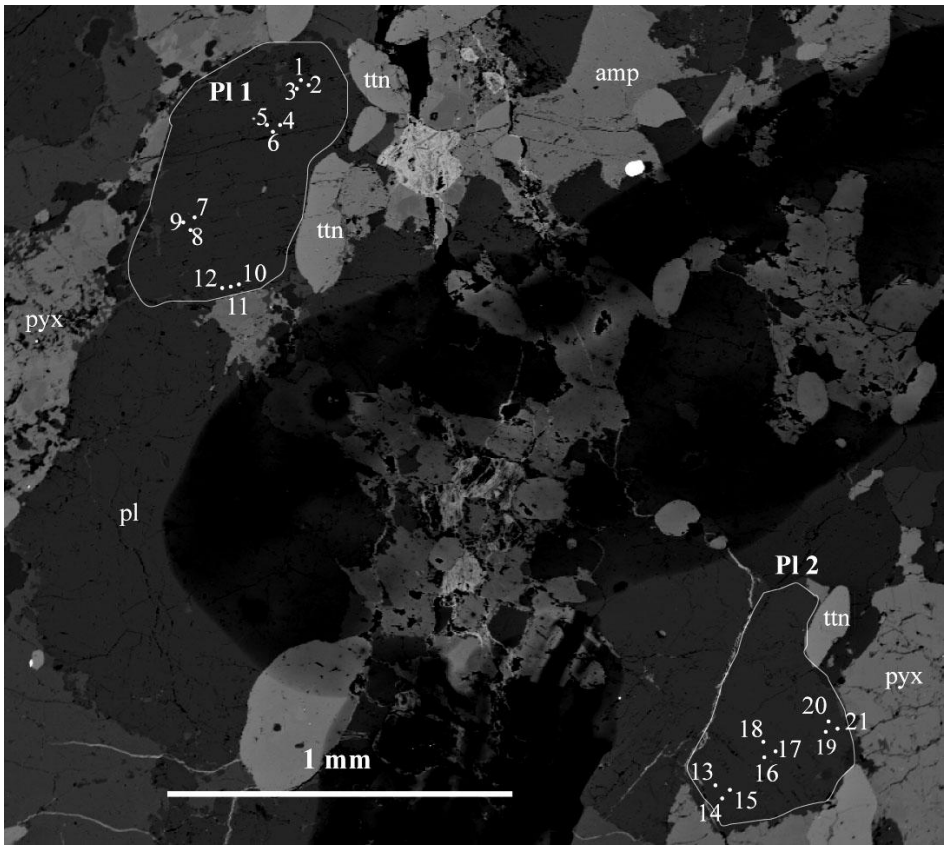

Figure 3.24: BSE image displaying analysis points of plagioclase (Pl) in ST08-45a. Two grains were analyzed with n = 21 points. No zoning was detected.

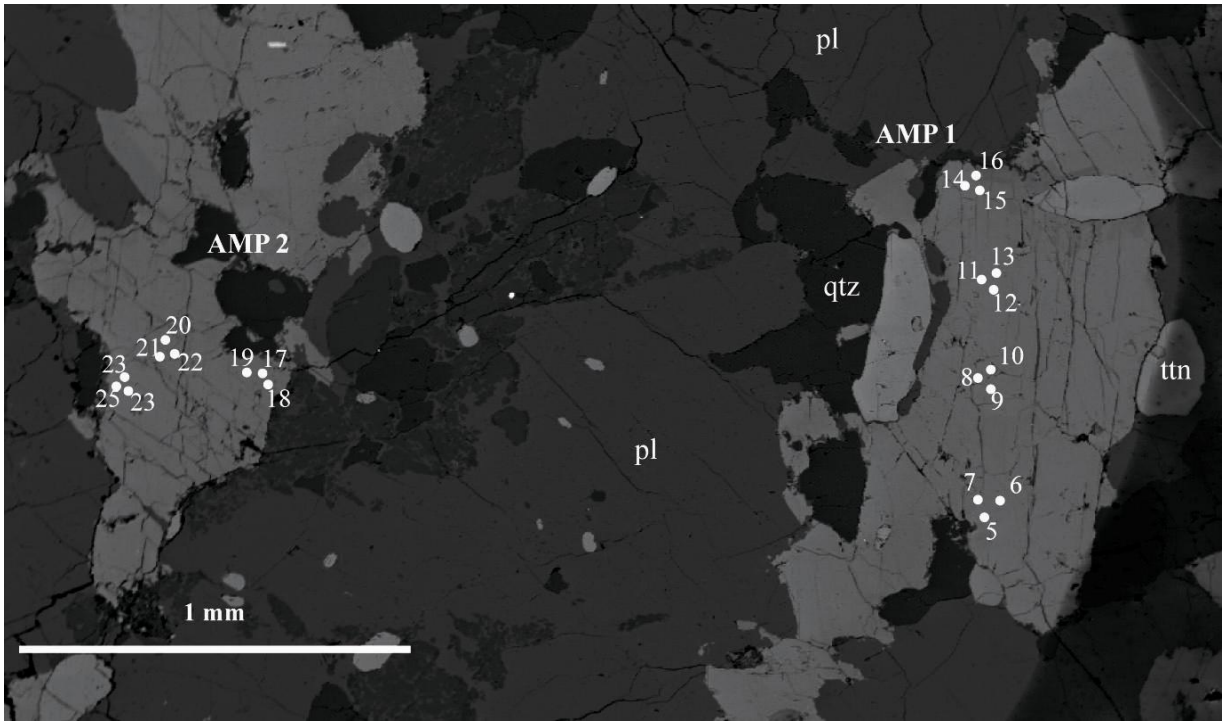

Figure 3.25: BSE image displaying points analyzed for amphibole (AMP) in ST08-45a. Two grains were analyzed with n = 21 points.

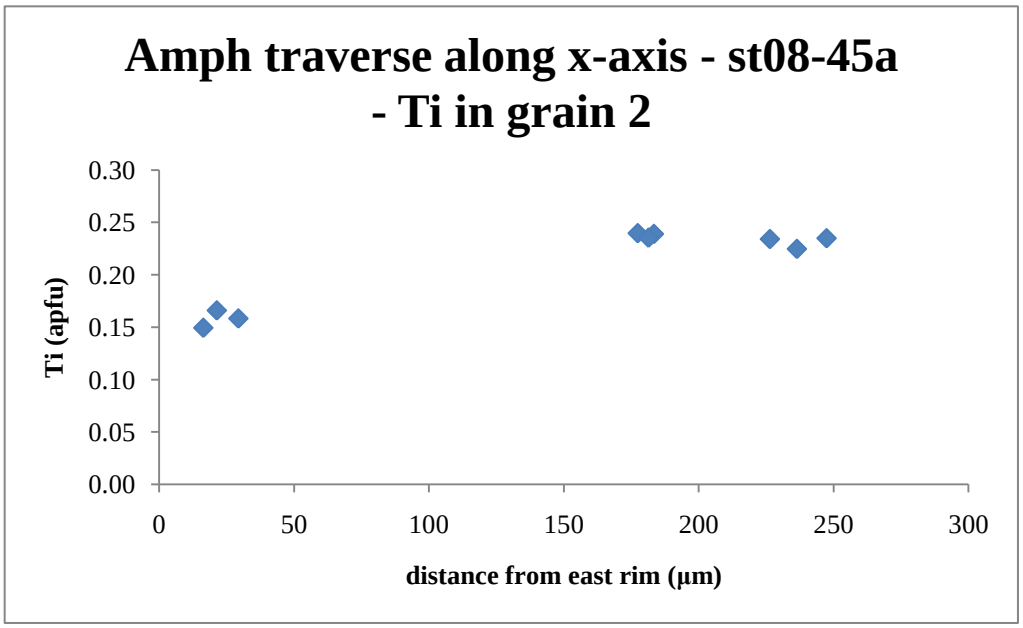

Figure 3.26: Core to rim traverse of Ti across amphibole grain 2 in ST08-45a showing slight Ti decrease along the grain boundary with a Ti-enriched core.

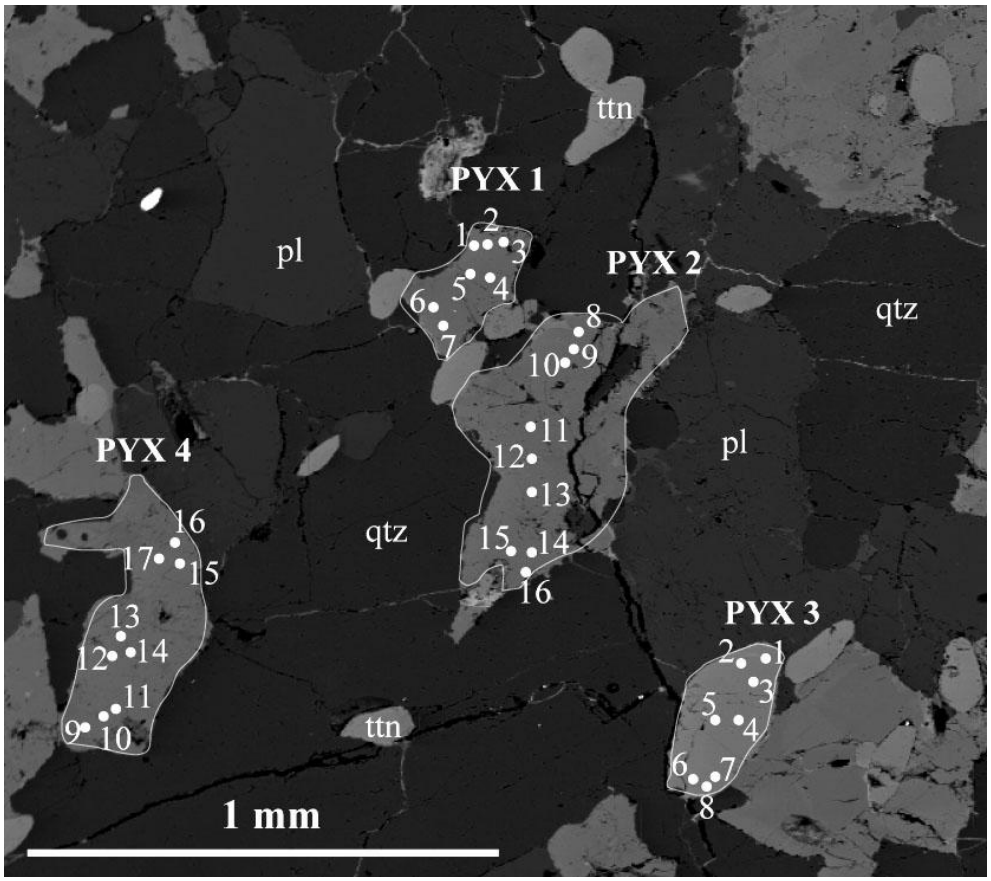

Figure 3.27: BSE image displaying points for pyroxene (pyx) analyses in ST08-45a. Four pyroxene grains were analyzed with n = 32 points. Analyses on pyx 3 had errors of ~2 wt % so compositions were calculated for three grains: pyx 1, pyx 2, and pyx 4.

Table 3.7: Compositional averages of pyroxene grains in ST08-45a. No zoning was detected in these grains.

	ST08-45a		
	Grain 1	Grain 2	Grain 4
wt %			
SiO_2	51.01	50.74	50.85
TiO_2	0.05	0.06	0.09
Al_2O_3	0.59	0.79	0.75
Cr_2O_3	0.03	0.05	0.03
FeO	16.22	16.27	17.03
MnO	0.43	0.46	0.45
MgO	8.49	8.42	7.94
CaO	23.59	23.61	23.64
Na_2O	0.22	0.24	0.25
K_2O	0.00	0.01	0.01
Total	100.61	100.63	101.04

Oxygens = 6

	ST08-45a		
	Grain 1	Grain 2	Grain 4
apfu			
Si	1.97	1.96	1.97
Ti	0.00	0.00	0.00
Al	0.03	0.04	0.03
Cr	0.00	0.00	0.00
Fe^{2+}	0.52	0.53	0.55
Mn^{2+}	0.01	0.01	0.01
Mg	0.49	0.49	0.46
Ca	0.98	0.98	0.98
Na	0.02	0.02	0.02
K	0.00	0.00	0.00
Fe^{3+}	0.00	0.00	0.00
X_{Mg}	0.48	0.48	0.45

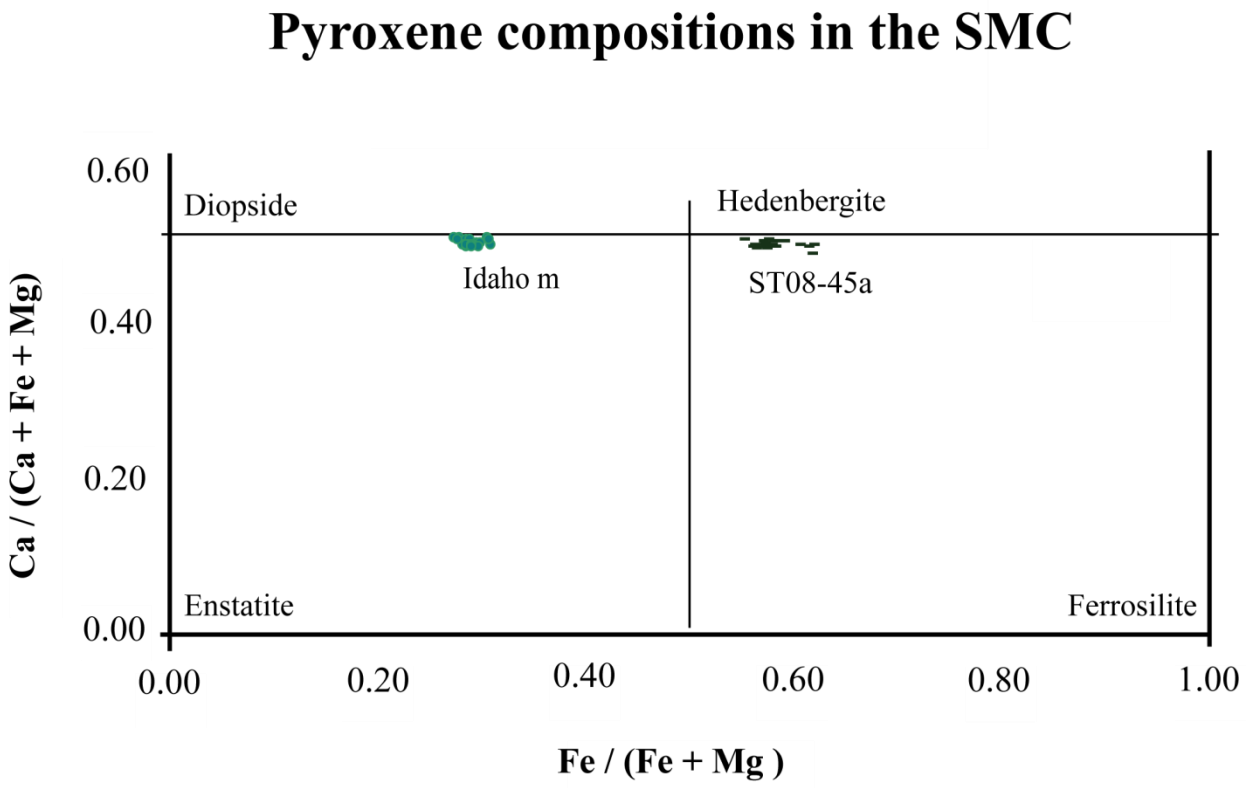

Figure 3.28: Pyroxene compositions from the SMC. Pyroxene in ST08-45a are hedenbergite. Pyroxene analyses from Idaho M are diopside.

range in size from < 1 mm to ~6 mm and compose >90 modal amount. These grains display tan-brown pleochroism with high-birefringent rims suggesting resetting. Anhedral plagioclase, 0.3 – 1 mm, composes ~5 modal amount and is near completely altered to sericite. Tabular biotite, < 0.4 mm by < 1 mm, occurs throughout and makes up < 5 modal amount. No EMP analyses were conducted on plagioclase or biotite due to major sericite and chlorite alteration, respectively.

One sample from *mg2* on William's ridge, ST08-36a, contains different mineral modal amount and a relict igneous texture. This sample contains pl + amp + bt + ilm + cpx (Fig. 3.31, Table 3.3). Coarse-grained, 0.5 – 2 mm, euhedral plagioclase grains are the dominant mode composing > 40 modal amount. Plagioclase in ST08-36a has an average composition of An_{54}

Figure 3.29: Hand sample of metagabbro [ST08-27(left) and ST08-20 (right)] displaying dark color, coarse grains and homogeneous appearance. Light areas are percussion marks from the hammer.

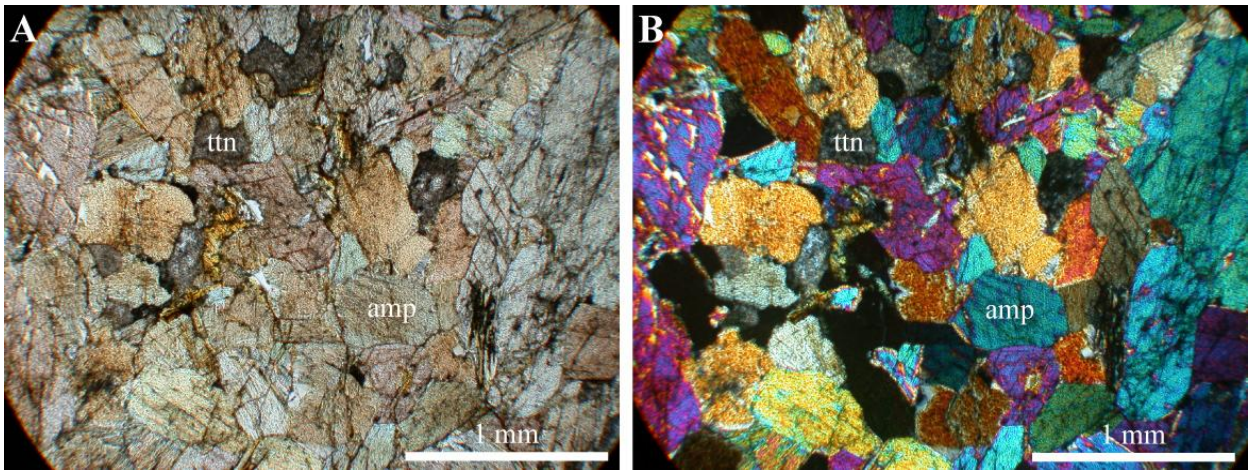

Figure 3.30: Photomicrographs of metagabbro (ST08-15d) in PPL (a) and XPL (b) displaying abundant amphibole with high-birefringent rims and granoblastic texture.

measured through the Michel-Lévy method. Coarse-grained subhedral amphibole, 0.3 – 1.5 mm, accounts for 35 modal amount. Medium-grained, tabular biotite, from 0.2 – 1 mm long accounts for ~10 modal amount. Ilmenite accounts for ~10 modal amount and occurs as needles within biotite. Medium-grained, highly-fractured, poikiloblastic clinopyroxene grains, 0.3 – 0.5 mm in diameter, occur within amphibole and account for ~5 modal amount (Fig. 3.31).

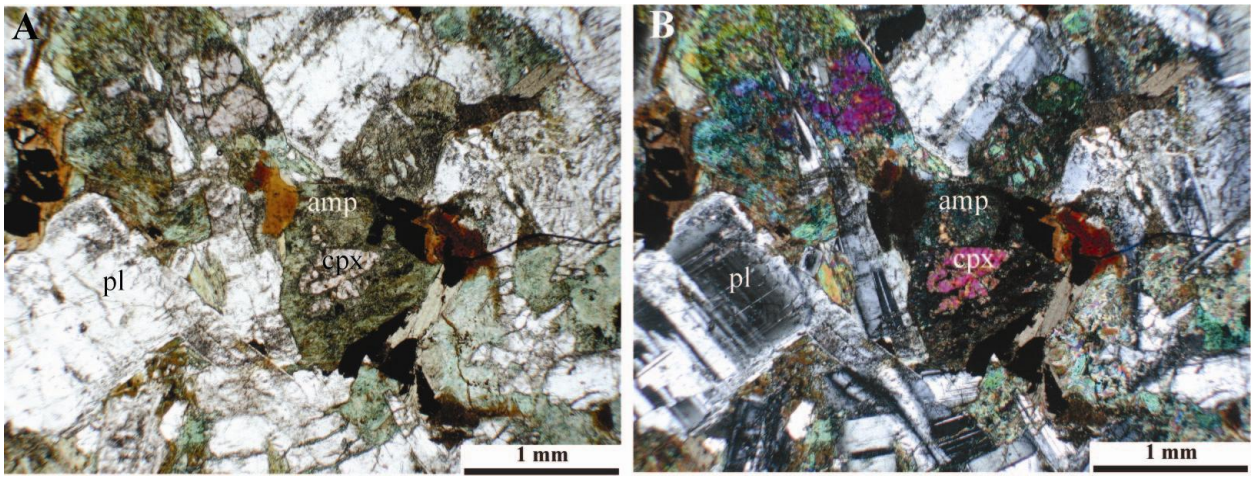

Figure 3.31: Photomicrographs of metagabbro (ST08-36a) in PPL (a) and XPL (b) displaying relict igneous texture with coarse-grained equant plagioclase and amphibole rimming clinopyroxene cores.

These rocks retain original igneous textures. Approximately one third of the amphibole grains possess high-birefringent rims, suggestive of a different composition (Fig. 3.30). In ST08-36a, ilmenite occurs within the biotite. Cores of clinopyroxene are surrounded by subhedral amphibole, suggesting amphiboles are replacing clinopyroxene.

Analyses of three amphibole grains in ST08-15d provide mineral chemical data (Fig. 3.32, Appendix D). Due to the apparent rims, traverses across grains were conducted to characterize zoning. These reveal slight Ti-enriched cores from 0.10 – 0.12, 0.11 – 0.11, and 0.12 – 0.15 apfu for grains one through three with respect to rim compositions of 0.04 – 0.11, 0.07 – 0.09, 0.04 – 0.11 apfu(Fig. 3.33). The average core composition plots as actinolitic hornblende: $(\square_{0.58}Na_{0.31}K_{0.11})(Ca_{1.93}Mn_{0.02}Mg_{0.03})\ (Mg_{3.14}Fe^{2+}_{1.31}Fe^{3+}_{0.02}Al_{0.53})(Si_{6.91}Al_{0.98}Ti_{0.11})O_{22}(OH)_{2,}$ and the average rim composition plots as magnesiohornblende: $(\square_{0.62}Na_{0.28}K_{0.08})(Ca_{1.85}Mn_{0.03}Mg_{0.09})$ $(Mg_{3.17}Fe^{2+}_{1.34}Al_{0.49})(Si_{7.11}Al_{0.81}Ti_{0.08})O_{22}(OH)_2$ (Table 3.8, Fig. 3.34, Leake et al., 1997).

3.1.7 Biotite-Amphibole Gneisses

Biotite-amphibole gneisses are medium-grained rocks containing >40% amphibole with a weakly gneissic to granoblastic texture. Due to the abundance of amphibole, these rocks are

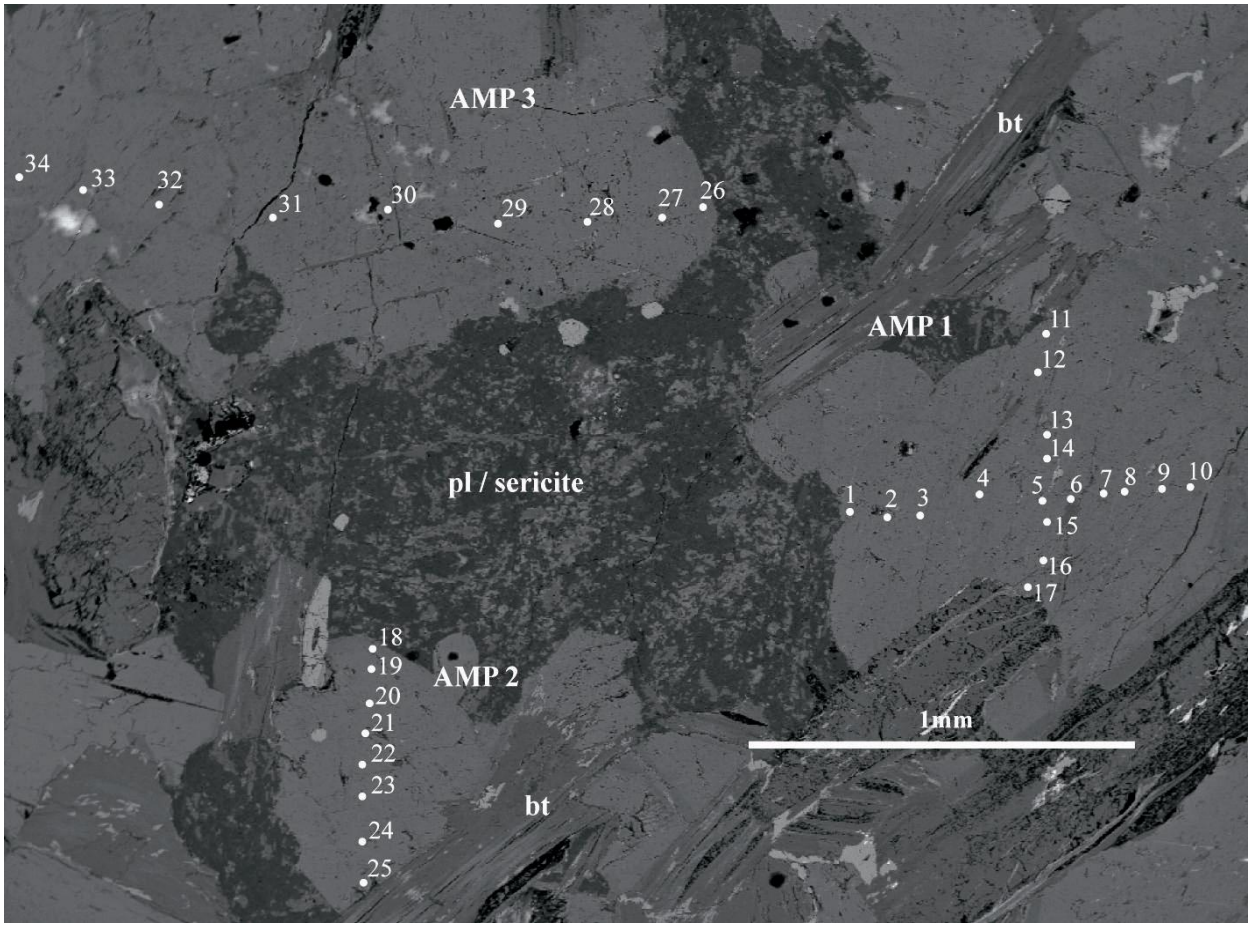

Figure 3.32: BSE image of electron microprobe analysis points of amphibole grains in metagabbro (ST08-15d). A total of 34 analyses were conducted on traverses across three grains.

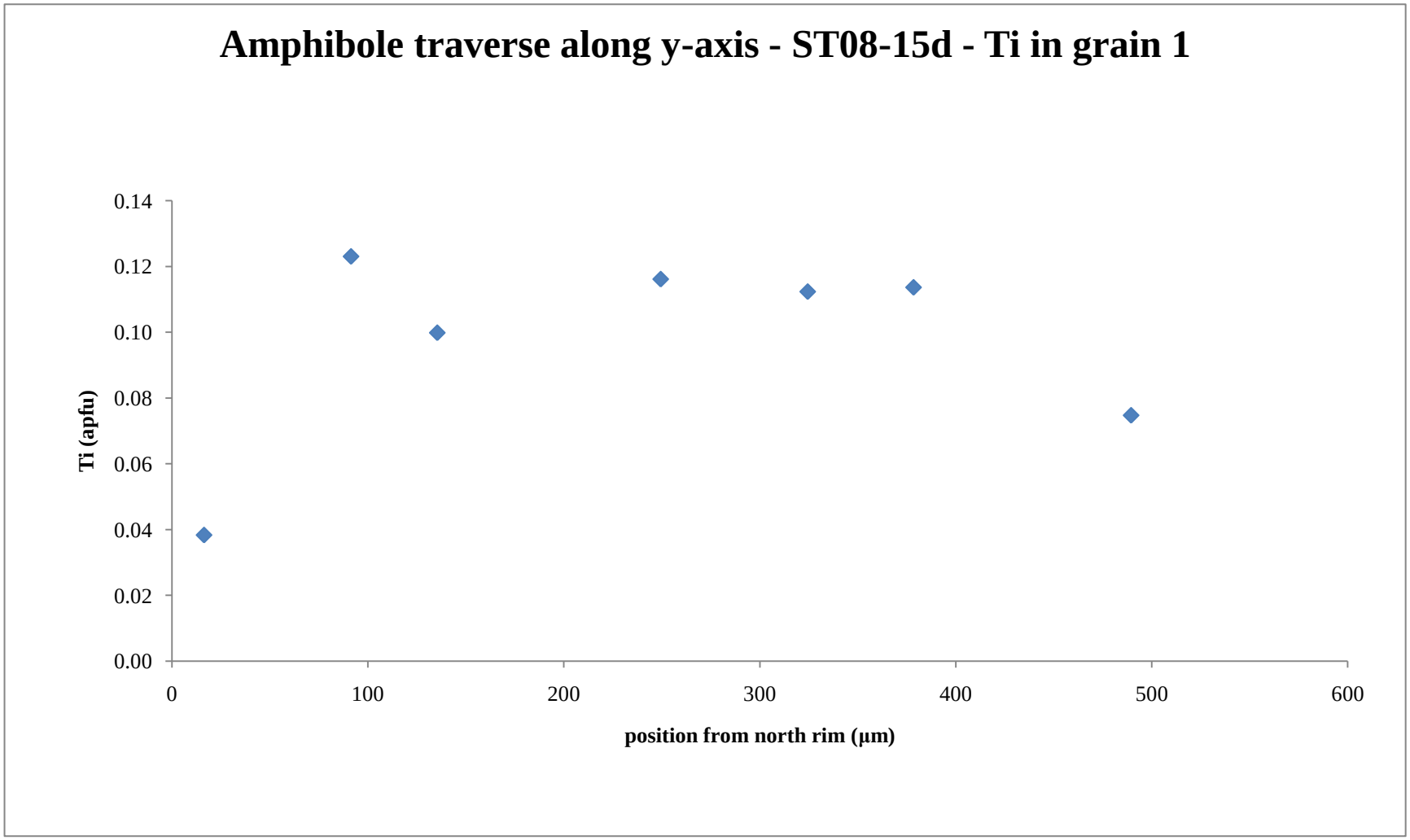

Figure 3.33: Rim to rim traverse of Ti concentration across amphibole grain 1 in vertical axis from ST08-15d. Cores are Ti-rich with respect to amphibole rims.

Table 3.8: Core and rim compositional averages for amphibole grains from ST08-15d.

	ST08-15d		ST08-15d		ST08-15d	
	Rim_1	Core_1	Rim_2	Core_2	Rim_3	Core_3
wt %						
SiO_2	47.73	48.44	49.45	47.24	49.55	47.57
TiO_2	0.96	1.06	0.77	1.00	0.70	1.26
Al_2O_3	9.10	9.31	8.24	9.06	7.92	9.52
Cr_2O_3	0.11	0.13	0.11	0.15	0.14	0.12
FeO	10.72	11.22	10.84	11.16	11.12	11.13
MnO	0.22	0.24	0.22	0.20	0.21	0.21
MgO	14.66	14.92	15.41	14.28	15.19	14.52
CaO	12.03	12.13	12.08	12.01	12.11	12.01
BaO	0.00	0.02	0.04	0.02	0.01	0.02
Na_2O	1.04	1.10	1.01	1.08	1.02	1.19
K_2O	0.52	0.56	0.47	0.60	0.43	0.63
Cl	0.07	0.04	0.05	0.08	0.08	0.07
Total	97.58	99.25	98.66	96.95	98.54	98.24

stoiched on 15 cations

	ST08-15d		ST08-15d		ST08-15d	
	Rim_1	Core_1	Rim_2	Core_2	Rim_3	Core_3
apfu						
Si	6.92	6.91	7.07	6.92	7.10	6.87
Ti	0.10	0.11	0.08	0.11	0.08	0.14
Al	1.56	1.57	1.39	1.56	1.34	1.62
Cr	0.01	0.01	0.01	0.02	0.02	0.01
Fe^{3+}	0.05	0.01	0.00	0.01	0.01	0.00
Fe^{2+}	1.30	1.34	1.29	1.37	1.33	1.34
Mn^{2+}	0.03	0.03	0.03	0.03	0.03	0.03
Mg	3.17	3.17	3.28	3.11	3.24	3.13
Ca	1.87	1.85	1.85	1.88	1.86	1.86
Ba	0.00	0.00	0.00	0.00	0.00	0.00
Na	0.29	0.30	0.28	0.31	0.28	0.33
K	0.10	0.10	0.09	0.11	0.08	0.12
Cl	0.02	0.01	0.01	0.02	0.02	0.02
X_{Mg}	0.71	0.70	0.72	0.69	0.71	0.70

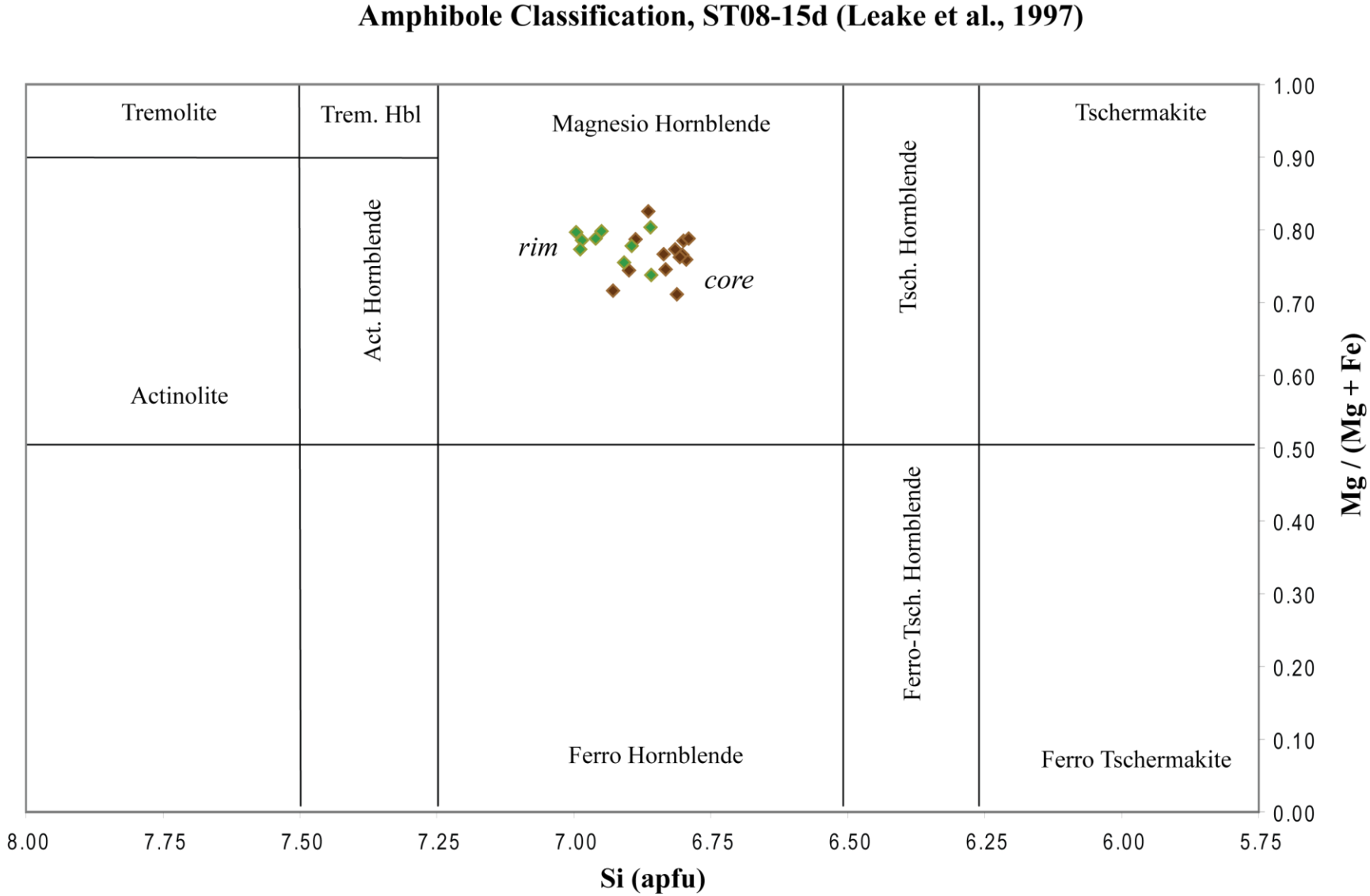

Figure 3.34: Classification of amphibole grains in ST08-15d after Leake et al. (1997). Core and rim compositional averages plot as magnesio-hornblende.

dark-grey to black, but weather to a rusty red-brown due to the presence of sulfides. In some hand samples, large amphibole grains, >20 mm long are visible with diagnostic cleavage (Fig. 3.35). Quartz and feldspar are not readily observable in hand sample.

Figure 3.35: Hand sample of biotite-amphibole (ST08-28) displaying dark color, gneissic texture and large black amphibole crystals ~2 cm long.

Two biotite-amphibole gneiss units were mapped in the Thompson Peak – Marshall Lake region (Fig. 3.2). These units map designations and names are: *ag1* = medium-grained ilmenite-biotite-amphibolite gneiss and *ag2* = medium-grained ilmenite-biotite-amphibolite gneiss.

Petrographic analysis of five samples of biotite-amphibole gneiss identified the characteristic mineral assemblage as: pl + amp + bt + ilm + chl ± hem(s) ± ttn (Fig. 3.36, Table. 3.3). Amphibole makes up 40 – 50 modal amount and occurs as equant to elongate grains. Equant, subhedral-hornblende grains range from ~0.3 to 3 mm in diameter with an average of 0.4 mm, and display brown – green pleochroism, with dark brown cores lightening to green rims (Fig. 3.37). This suggests compositional zoning related to Ti-rich cores. Equant plagioclase, present from 35 – 50 percent, measures from 0.2 to 2 mm in diameter with an average grain size

of ~0.6 mm and display polysynthetic twins. Deformed laths of biotite range from 0.5 - >1 mm long by 0.2 – 0.5 mm wide, account for 5 – 10 modal amount, and define a weak gneissic texture. Biotites exhibit deep red – brown pleochroism indicative of Ti-rich biotite. Moderate alteration of biotite to chlorite is present throughout. Accessory, < 3 modal percent, titanite grains are found sporadically throughout the samples. Fine-grained ilmenite < 0.2 mm in diameter make up < 5 modal amount with minor alteration of hematite.

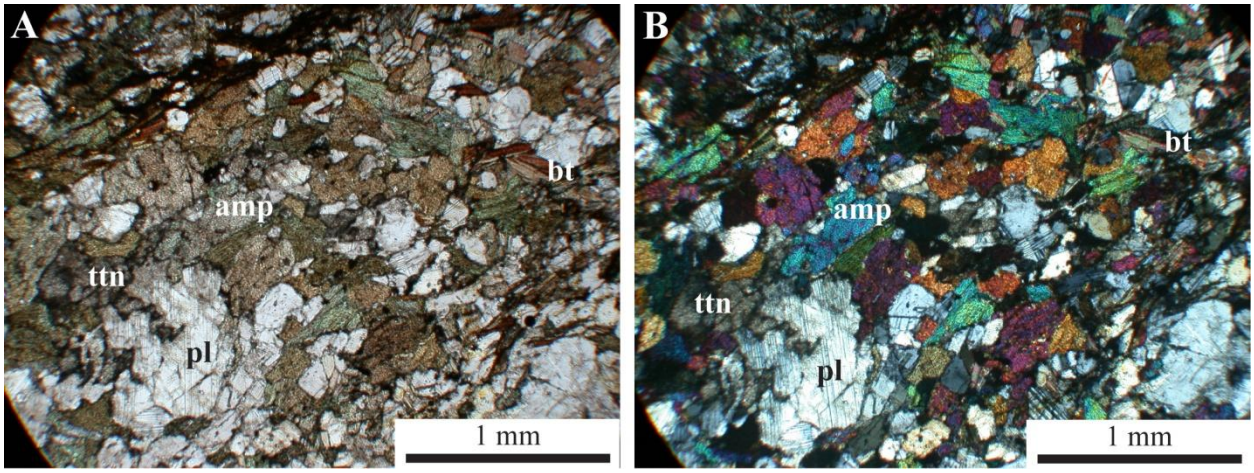

Figure 3.36: Photomicrographs of biotite-amphibole gneiss (ST08-13a) in PPL (a) and XPL (b) displaying weak gneissic texture defined by aligned biotite with elongate plagioclase and amphibole.

The texture of biotite-amphibole gneisses ranges from granoblastic to gneissic. Hornblende and plagioclase, < 1 mm long by < 0.3 mm wide and aligned with tabular biotite defining a moderate-weak foliation (Fig. 3.36).

Plagioclase compositions were calculated from twenty EMP analyses on two grains (Fig. 3.38, 3.39, Appendix C). Plagioclase grain compositions range from $Ab_{44\text{-}50}An_{49\text{-}55}Or_{0\text{-}1}$ (andesine-labradorite). No compositional zoning was detected. The average plagioclase composition is: $(Ca_{0.51}Na_{0.45}\ K_{0.01})(\ Si_{2.48}Al_{1.52})O_8$ (Fig. 3.20, Table 3.9).

Amphibole compositions were calculated using 41 analyses on five grains in ST08-13a (Fig. 3.38, 3.39, Appendix D). Chemical traverses reveal little change between core/rim

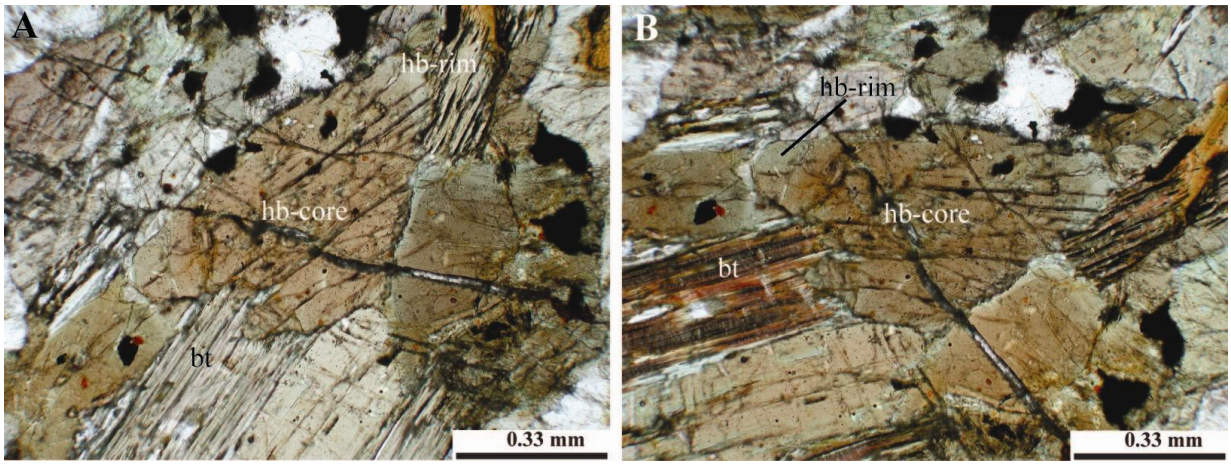

Figure 3.37: Photomicrographs in PPL displaying pleochroism in ST08-13a. Amphibole grains display optical zoning with pleochroic brown cores and green rims, suggestive of Ti-richer cores.

compositions (Fig. 3.40). Rim compositions range from Ti = 0.10 – 0.18 apfu, Al = 2.16 – 2.38 apfu, and Si = 6.31 – 6.70 apfu. Core compositions range from Ti = 0.13 – 0.21 apfu, Al = 2.24 – 2.40 apfu, and Si = 6.28 – 6.55 apfu. Core and rim compositions are characterized as magnesio hornblende for all grains expect the core of grain two, which is a tschermakitic hornblende (Fig. 3.41, Leake, 1997). Rim and core compositions of magnesio hornblende range from $(\square_{0.43\text{-}0.47}Na_{0.38\text{-}0.40}K_{0.15\text{-}0.17})Ca_{1.83}(Mg_{2.20\text{-}2.23}Fe^{2+}_{1.52\text{-}1.56})(Al_{0.62\text{-}0.66}Fe^{3+}_{0.40\text{-}0.44})Al_{1.52\text{-}1.64}Si_{6.36\text{-}6.43}O_{22}(OH)_2$, and the tschermakitic hornblende core composition is $(\square_{0.40}Na_{0.41}K_{0.19})Ca_{1.85}(Mg_{2.15}Fe^{2+}_{1.60})(Al_{0.64}Fe^{3+}_{0.36})Al_{1.72}Si_{6.28}O_{22}(OH)_2$ (Table 3.10).

Biotite compositions were calculated using 24 analyses from three grains in ST08-13a (Fig. 3.38, 3.39, Appendix E). Analyses range from X_{Mg} = 0.50 – 0.53, Al = 2.98 – 3.10 apfu, and Ti = 0.18 – 0.26 apfu (Fig. 3.23, Table 3.11). Structural formulae calculated with high- and low-Ti biotite compositions range from: $\square_{0.70}Na_{0.06}K_{1.24}(Mn_{0.01}Ca_{0.03}Mg_{2.76}Fe^{2+}_{2.70})(Al_{0.19}Ti_{0.18})(Al_{2.85}Si_{5.15})O_{22}(OH)_4$ to $\square_{0.25}Na_{0.04}K_{1.71}(Mn_{0.03}Mg_{2.69}Fe^{2+}_{2.62})(Al_{0.70}Ti_{0.26})(Al_{2.39}Si_{5.61})O_{22}(OH)_4$.

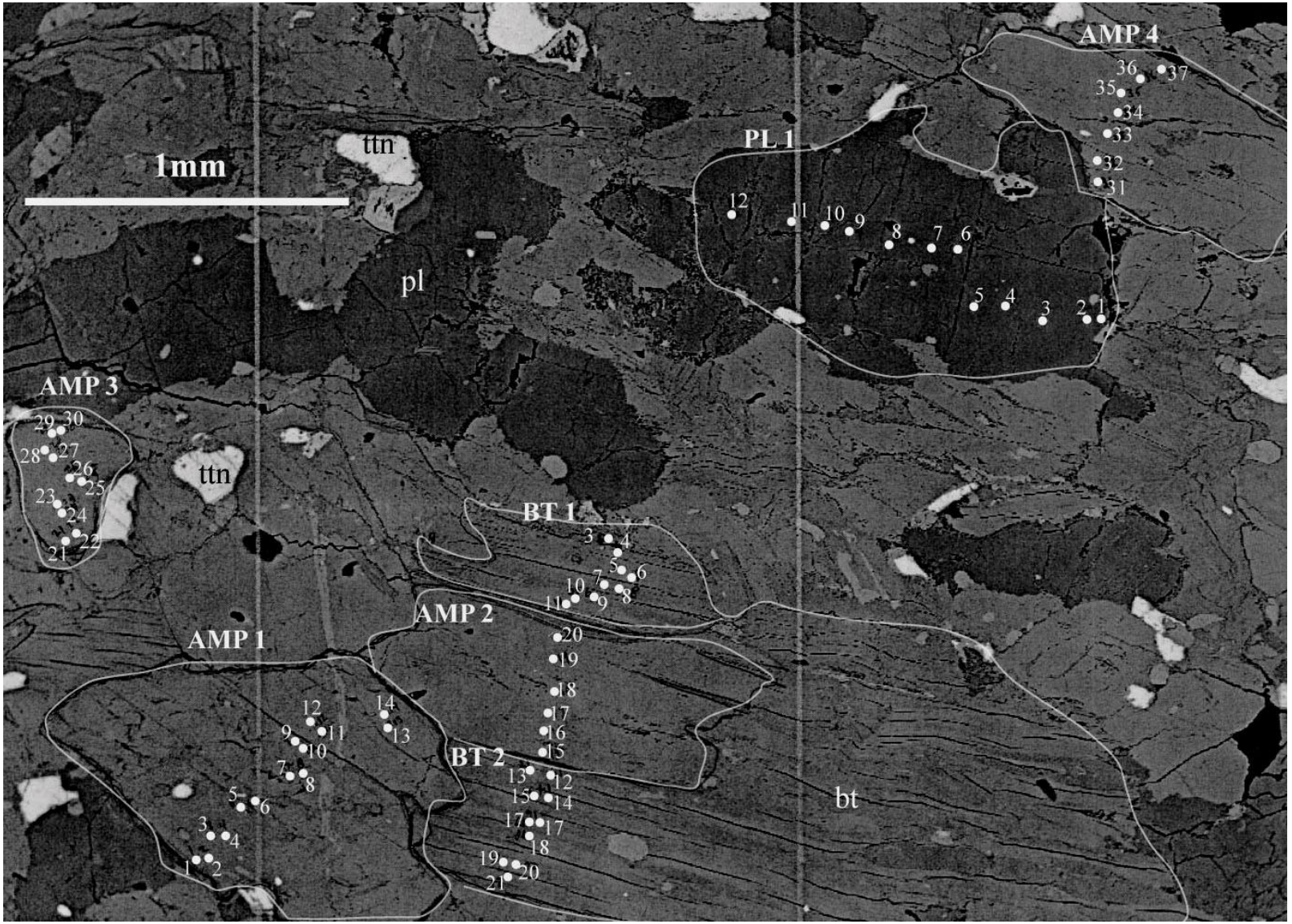

Figure 3.38: BSE image displaying EMPA points of amphibole (AMP), biotite (BT), and plagioclase (PL) in ST08-13a.

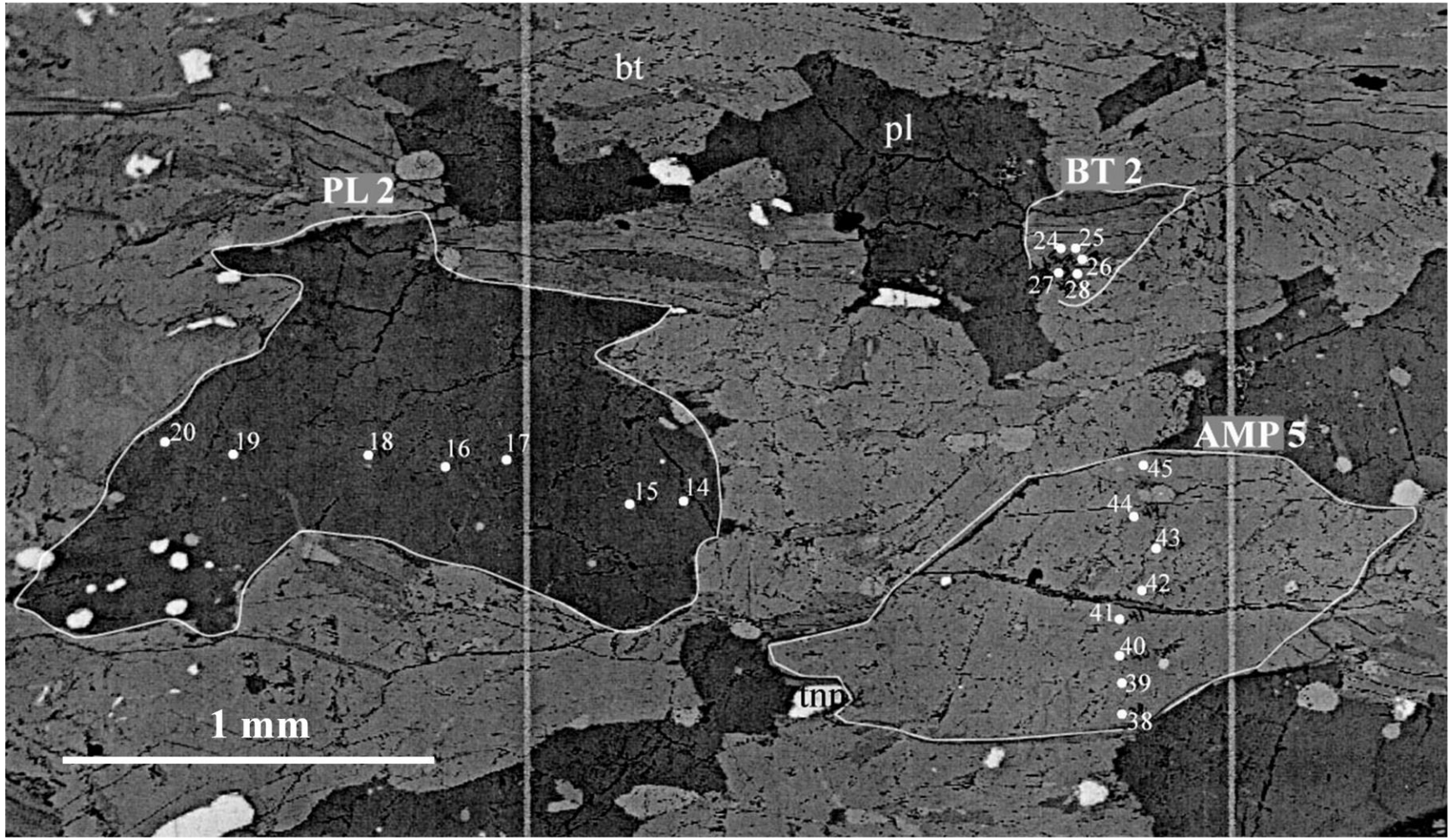

Figure 3.39: BSE image displaying EMPA points of amphibole (AMP), biotite (BT), and plagioclase (PL) in ST08-13a. Slight Ti zoning was observed in amphiboles, but no zoning was observed in other phases. Note cleavage development in the amphiboles.

Table 3.9: Compositional averages of plagioclase grains analyzed in biotite-amphibole gneiss (ST08-13a).

	ST08-13a	
	Grain 1	Grain 2
wt %		
SiO_2	54.34	54.99
Al_2O_3	28.72	28.6
CaO	10.56	10.33
BaO	0.02	0.02
Na_2O	5.14	5.19
K_2O	0.1	0.09
FeO	0.05	0.06
MgO	0.01	0.01
Total	98.94	99.29

Oxygens = 8

Feldspar

	ST08-13a	
	Grain 1	Grain 2
apfu		
Si	2.47	2.49
Al	1.54	1.53
Ca	0.51	0.50
Ba	0.00	0.00
Na	0.45	0.46
K	0.01	0.01
Fe^{2+}	0.00	0.00
Mg	0.00	0.00
X_{Ab}	0.47	0.47
X_{Or}	0.01	0.01
X_{An}	0.53	0.52

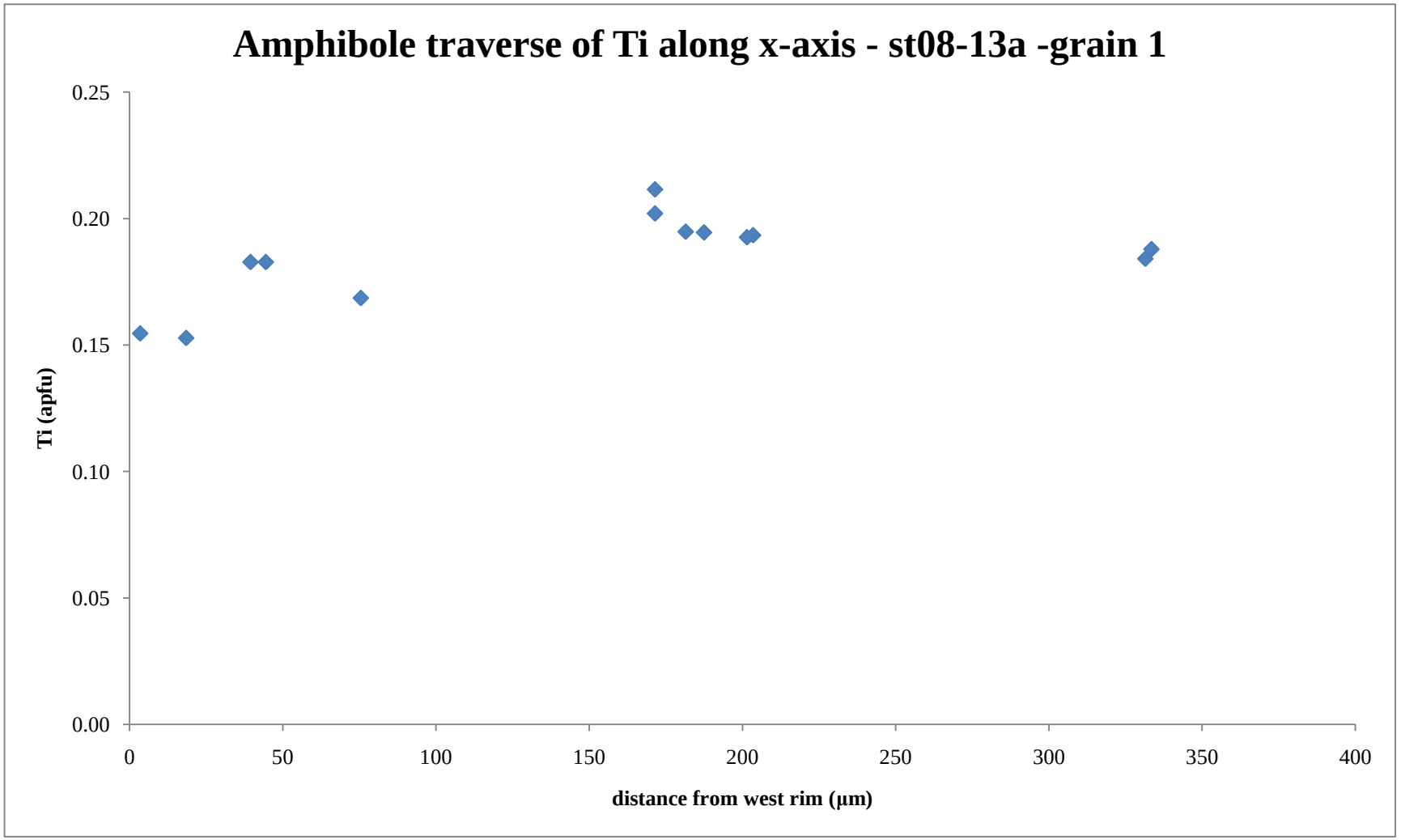

Figure 3.40: Rim to core traverse of titanium compositional variation of amphibole grain 1 in ST08-13a, displaying slight Ti-depletion in amphibole rims with respect to cores.

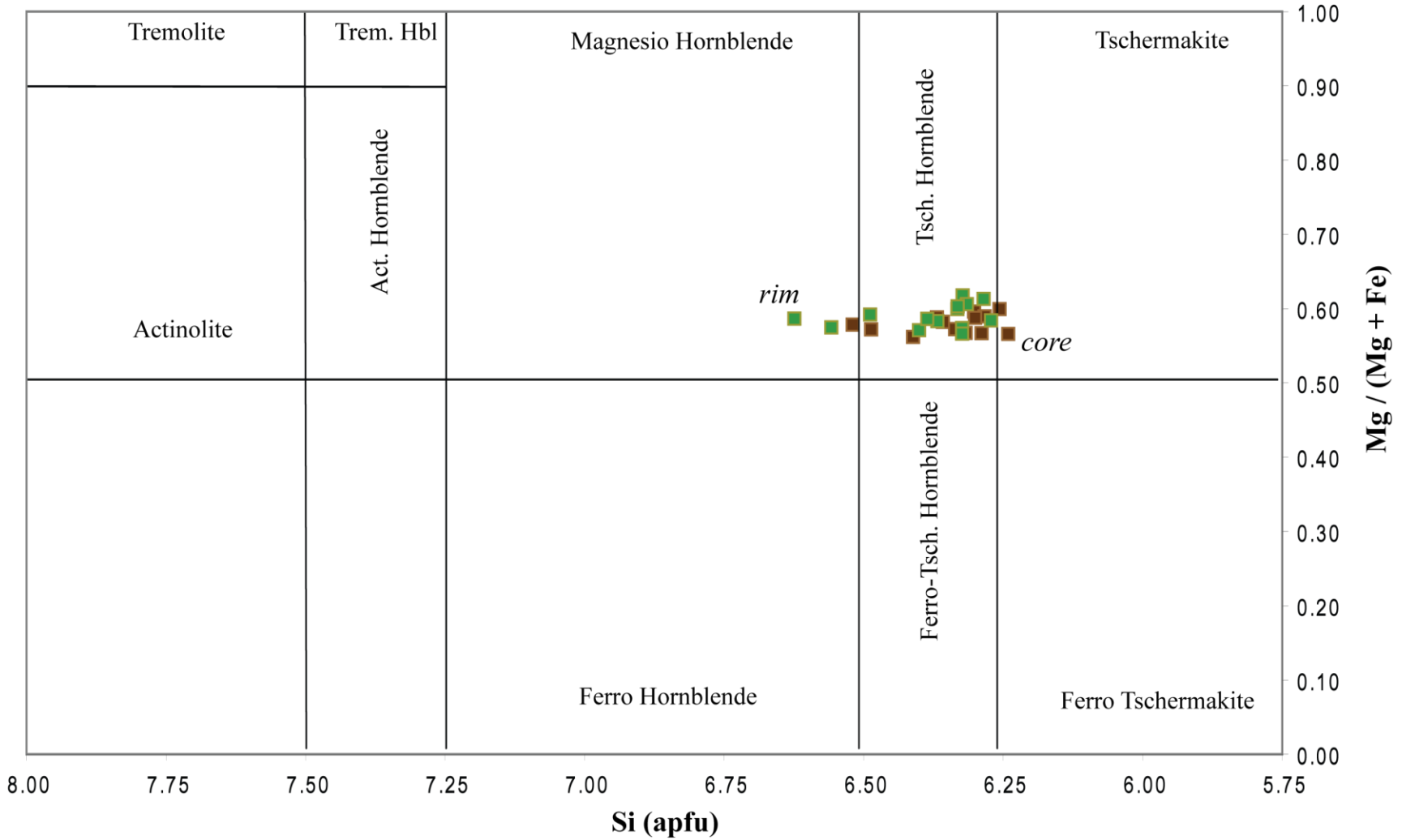

Figure 3.41: Classification of amphibole rim and core analyses in ST08-13a, after Leake et al. (1997). Most analyses are tschermakitic hornblende, except for two rim and one core analysis of amphibole 3, that are magnesio-hornblende. Two core analyses of grain 1 are tschermakite.

Table 3.10: Core and rim compositional averages of amphibole grains in biotite-amphibole gneiss (ST08-13a).

	ST08-13a		ST08-13a		ST08-13a		ST08-13a		ST08-13a	
	Rim_1	Core_1	Rim_2	Core_2	Rim_3	Core_3	Rim_4	Core_4	Rim_5	Core_5
wt %										
SiO_2	42.67	42.44	42.99	42.70	44.62	43.49	43.11	43.70	43.71	43.45
TiO_2	1.51	1.73	1.64	1.83	1.01	1.21	1.30	1.57	1.34	1.59
Al_2O_3	13.34	13.37	13.75	13.61	12.48	13.18	13.34	13.53	13.40	13.41
Cr_2O_3	0.05	0.05	0.09	0.08	0.03	0.05	0.02	0.03	0.01	0.05
FeO	15.63	15.90	16.15	15.92	14.98	15.51	15.87	15.77	16.01	15.96
MnO	0.24	0.25	0.26	0.26	0.29	0.28	0.26	0.23	0.24	0.28
MgO	10.11	9.94	10.03	9.82	10.17	9.90	10.20	10.12	10.21	10.07
CaO	11.76	11.64	11.85	11.72	11.81	11.57	11.65	11.70	11.84	12.03
BaO	0.03	0.01	0.00	0.06	0.03	0.00	0.06	0.00	0.04	0.02
Na_2O	1.39	1.37	1.37	1.45	1.10	1.40	1.56	1.43	1.47	1.38
K_2O	0.89	0.97	1.02	1.01	0.68	0.76	0.88	0.87	0.88	0.95
Cl	0.19	0.20	0.19	0.22	0.16	0.18	0.19	0.17	0.18	0.19
Total	98.28	98.10	99.58	98.66	97.32	97.52	98.44	99.10	99.32	99.48

stoiched on 15 cations

	ST08-13a		ST08-13a		ST08-13a		ST08-13a		ST08-13a	
	Rim_1	Core_1	Rim_2	Core_2	Rim_3	Core_3	Rim_4	Core_4	Rim_5	Core_5
apfu										
Si	6.35	6.33	6.32	6.35	6.65	6.50	6.40	6.44	6.43	6.39
Ti	0.17	0.19	0.18	0.20	0.11	0.14	0.15	0.17	0.15	0.18
Al	2.34	2.35	2.38	2.38	2.19	2.32	2.33	2.35	2.32	2.32
Cr	0.01	0.01	0.01	0.01	0.00	0.01	0.00	0.00	0.00	0.01
Fe^{3+}	0.06	0.03	0.03	0.00	0.00	0.00	0.00	0.00	0.00	0.01
Fe^{2+}	1.94	1.98	1.99	1.98	1.87	1.94	1.97	1.94	1.97	1.96
Mn^{2+}	0.03	0.03	0.03	0.03	0.04	0.04	0.03	0.03	0.03	0.03
Mg	2.24	2.21	2.20	2.18	2.26	2.21	2.26	2.22	2.24	2.21
Ca	1.87	1.86	1.87	1.87	1.88	1.85	1.85	1.85	1.86	1.89
Ba	0.00	0.00	0.00	0.00	0.00	0.00	0.00	0.00	0.00	0.00
Na	0.40	0.39	0.39	0.42	0.32	0.40	0.45	0.41	0.42	0.39
K	0.17	0.19	0.19	0.19	0.13	0.15	0.17	0.16	0.16	0.18
Cl	0.05	0.05	0.05	0.06	0.04	0.04	0.05	0.04	0.04	0.05
X_{Mg}	0.54	0.53	0.53	0.52	0.55	0.53	0.53	0.53	0.53	0.53

3.1.8 Peraluminous Gneisses

Peraluminous gneisses are found in the Iron Creek region of the northwestern SMC (Fig 3.1) and are classified by the presence of an aluminosilicate polymorph, sillimanite (primary) and/or andalusite (secondary). These gneisses are medium- to coarse-grained, and exhibit a strong gneissic texture with bands of dark ferromagnesian minerals (melanosomes), and light bands of felsic minerals (leucosomes). The melanosomes compose >70% of the rock. In hand sample, sillimanite and biotite are identifiable as major constituents in the melanosomes and define a strong foliation. Felsic bands composed of quartz and plagioclase are coarser-grained than their mafic counterparts and are generally < 3 mm wide. Some outcrops are migmatitic and record deformation (Fig. 3.42). Garnets are easily identifiable by their pink color and rounded-dodecahedral habit. In most samples, plagioclase halos are visible surrounding garnets in the melanosomes (Fig. 3.43).

One aluminous gneiss unit was mapped in the Iron Creek area as "al-g" (Fig. 3.3). This unit's formal rock name is: medium- to coarse-grained migmatitic K-feldspar-garnet-muscovite-sillimanite-biotite-cordierite gneiss.

Petrographic analyses of six samples from four localities (Fig. 3.3) identified the characteristic mineral assemblage as: crd + bt + pl + qtz + grt + sil + ms + kfs + and + ilm ± ttn + ccp + po ± py ± mnz ± zrn (Fig. 3.44, Table 3.3). Due to the migmatitic texture of the aluminous gneisses, mineral modes of the melanosome and leucosome assemblages are calculated and described separately.

The melanosome consists of primary crd + bt + sil + grt + ms + pl + qtz + ilm ± ttn with secondary, ms + pl + po ± py and accessory mnz ± zrn (Fig. 3.45, Table 3.3, Henry, pers. comm.). Biotite grains exhibit deep red-brown pleochroism indicative of Ti. Sillimanite

Table 3.11: Compositional ranges (based on titanium content) for biotites in ST08-13a.

	st08-13a					
	Grain 1 - low-Ti	Grain 1 - High-Ti	Grain 2 - low-Ti	Grain 2 - High-Ti	Grain 3 - low-Ti	Grain 3 - High-Ti
wt %						
SiO_2	36.32	36.45	34.14	36.54	34.51	35.56
TiO_2	1.73	2.28	1.77	2.22	1.59	1.99
Al_2O_3	17.45	17.03	17.31	17.03	17.29	17.07
Cr_2O_3	0.04	0.01	0.06	0.00	0.01	0.00
FeO	19.39	20.40	22.02	20.60	21.65	20.87
MnO	0.17	0.14	0.14	0.11	0.10	0.14
MgO	12.26	11.74	12.59	11.80	12.43	11.66
CaO	0.25	0.03	0.08	0.03	0.16	0.14
BaO	0.26	0.33	0.24	0.32	0.29	0.24
Na_2O	0.26	0.15	0.17	0.15	0.19	0.20
K_2O	6.64	8.72	5.81	8.48	6.52	7.45
Total	94.77	97.28	94.33	97.28	94.74	95.32

Oxygens = 22

	Biotite					
	st08-13a					
	Grain 1 - low-Ti	Grain 1 - High-Ti	Grain 2 - low-Ti	Grain 2 - High-Ti	Grain 3 - low-Ti	Grain 3 - High-Ti
apfu						
Si	5.49	5.46	5.25	5.46	5.30	5.42
Ti	0.20	0.26	0.20	0.25	0.18	0.23
Al	3.11	3.00	3.14	3.00	3.13	3.06
Cr	0.00	0.00	0.01	0.00	0.00	0.00
Fe^{2+}	2.45	2.55	2.83	2.58	2.78	2.66
Mn^{2+}	0.02	0.02	0.02	0.01	0.01	0.02
Mg	2.76	2.62	2.89	2.63	2.84	2.65
Ca	0.04	0.00	0.01	0.00	0.03	0.02
Ba	0.02	0.02	0.01	0.02	0.02	0.01
Na	0.08	0.04	0.05	0.04	0.06	0.06
K	1.28	1.66	1.14	1.62	1.28	1.45
X_{Mg}	0.53	0.51	0.50	0.51	0.51	0.50

Figure 3.42: Outcrop of peraluminous migmatite in Iron Creek (IC08-01a) displaying migmatitic texture with melanosomes and leucosomes. Backpack is for scale.

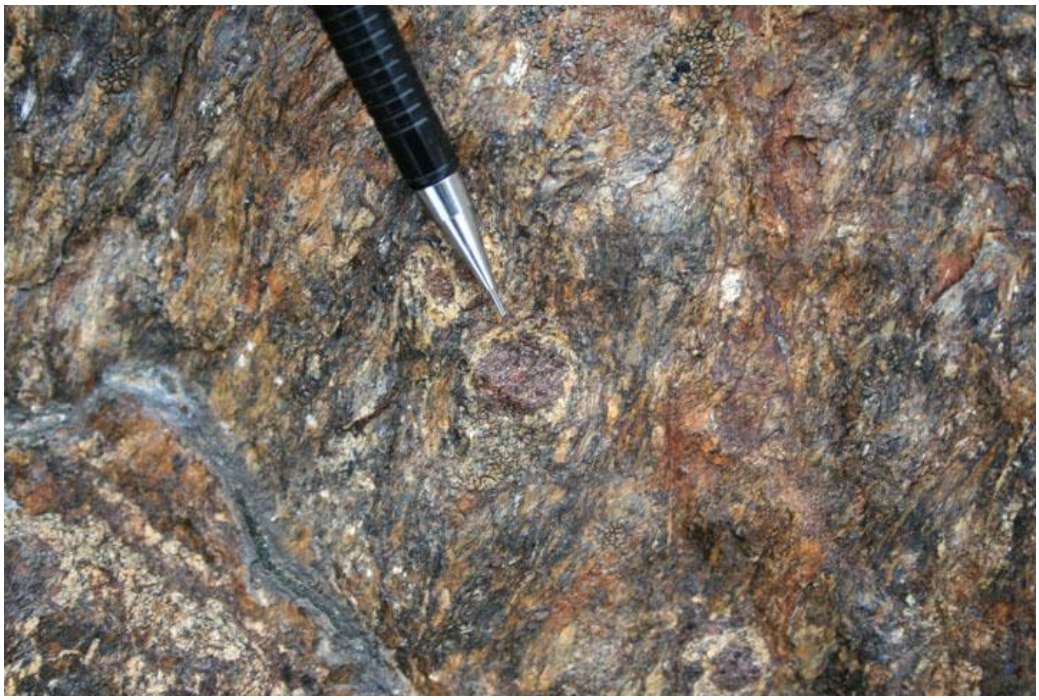

Figure 3.43: Outcrop of peraluminous gneiss displaying dark garnets surrounded by light-colored plagioclase halos (IC08-01b). Pencil is for scale.

accounts for 10 – 20% modal amount. Acicular needles of sillimanite are very-fine to coarse-grained, < 1.5 mm in length, while mats of fibrolite are as large as 4 mm^2 and appear to be replacing cordierite. In samples with low modal amounts of sillimanite, cordierite and biotite are more abundant. Poikiloblastic primary-muscovite accounts for 10 modal amount and occurs as fine-grained flakes within cordierite and, more rarely, tabular grains near garnets. Large, > 2 mm, poikiloblastic garnet account for ~10% modal amount. Garnets are fractured and surrounded by halos of subhedral equant-plagioclase grains. Plagioclase grains are 0.3 – >1 mm in diameter and account for ~5% modal amount. Ilmenite with pyrrhotite cores are scattered throughout the rock and account for < 3% modal amount.

Felsic leucosomes are coarser-grained than pelitic layers and contain: pl + qtz + ms + kfs (Fig. 3.46, Table 3.3). Equant plagioclase grains from 0.2 – 0.8 mm account for ~40% modal amount. Stretched quartz grains from 0.2 – 0.7 mm account for ~40% modal amount. Tabular muscovite, from 0.5 – 3 mm long, account for ~15% modal amount, cuts across boundaries with the ferromagnesian assemblage and the main foliation. Anhedral alkali-feldspar, from 0.2 – 0.8 mm, accounts for < 5% modal amount. Alkali-feldspar grains are associated with muscovite, exhibit microcline-twinning and myrmekite.

Electron microprobe analyses of garnet, biotite, muscovite, plagioclase, and cordierite provide mineral chemical data. Backscattered electron (BSE) images showing locations of analyses points were obtained for all analyses in all peraluminous samples (Appendix J). One BSE image showing points of analyses for each mineral in IC08-01b is provided.

Garnet compositions were determined from 114 electron microprobe analyses of six garnets from five samples of peraluminous gneiss. These data were used to determine garnet compositions (Fig. 3.47, Appendix G). In all samples, almandine (alm) was the dominant

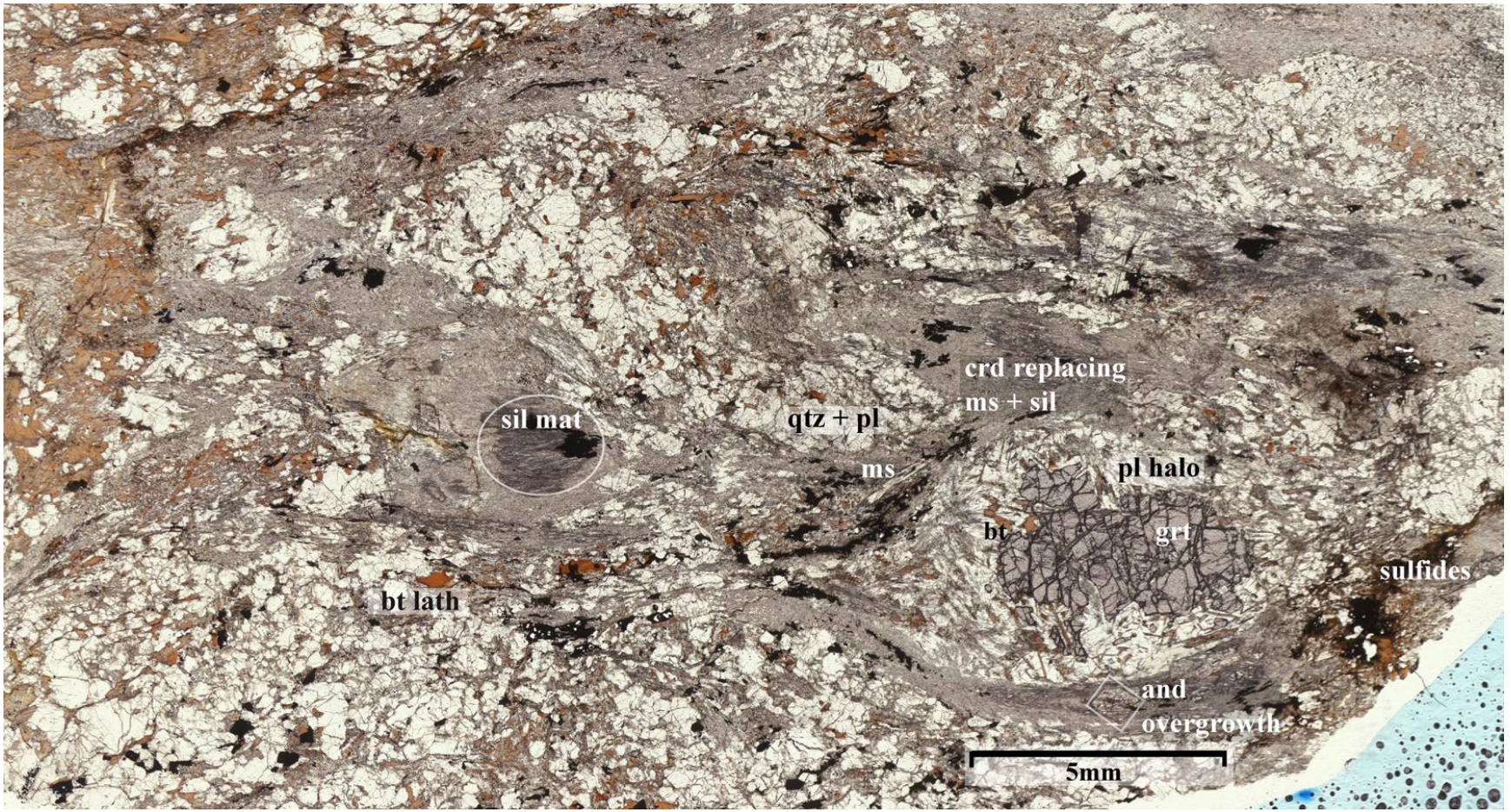

Figure 3.44: Thin-section scan of peraluminous gneiss sample IC08-01b1. The main foliation bends around garnet grains and includes biotite, quartz, plagioclase, muscovite, sillimanite, and poikiloblastic cordierite. Opaque minerals include ilmenite, chalcocite, chalcopyrite, pyrite, and pyrrhotite.

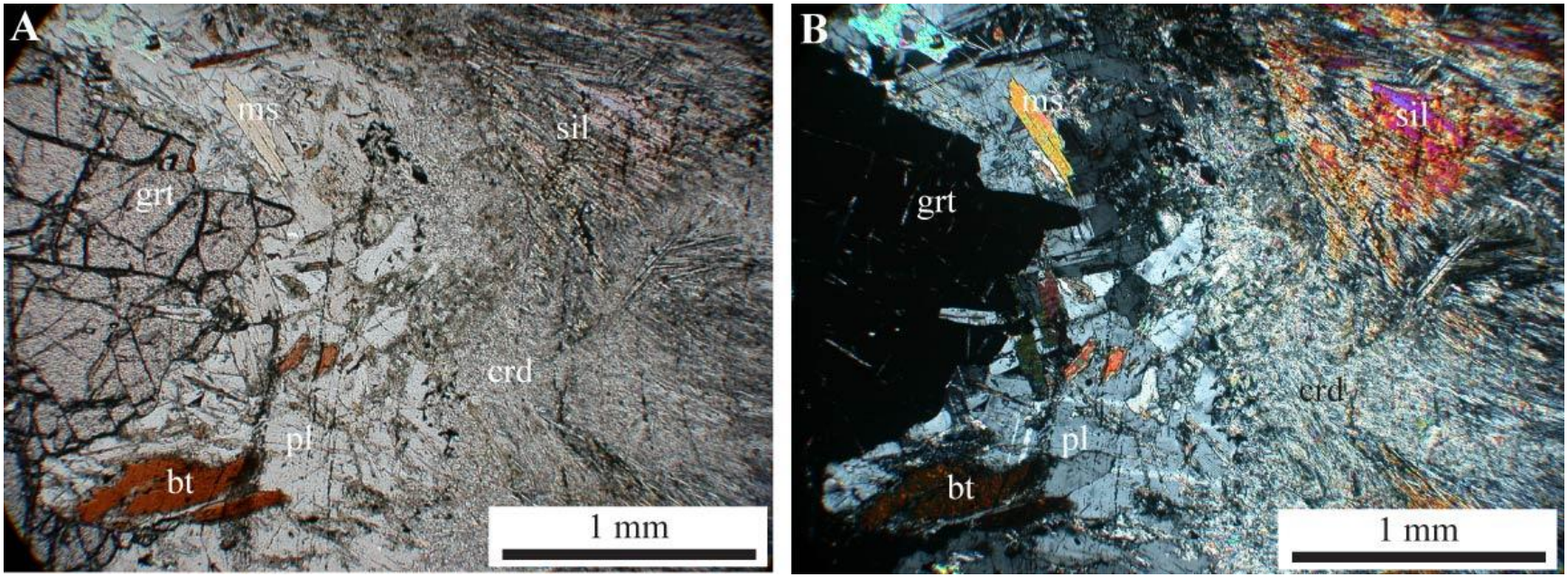

Figure 3.45: Photomicrographs of pelitic mineral assemblage in PPL (a) and XPL (b). This assemblage contains: crd + bt + sil + grt + ms + pl + qtz + ilm ± ttn + po ± py ± mnz ± zrn. Cordierite and sillimanite appear to deform around garnet, and plagioclase halos surround garnet grains (IC08-01b).

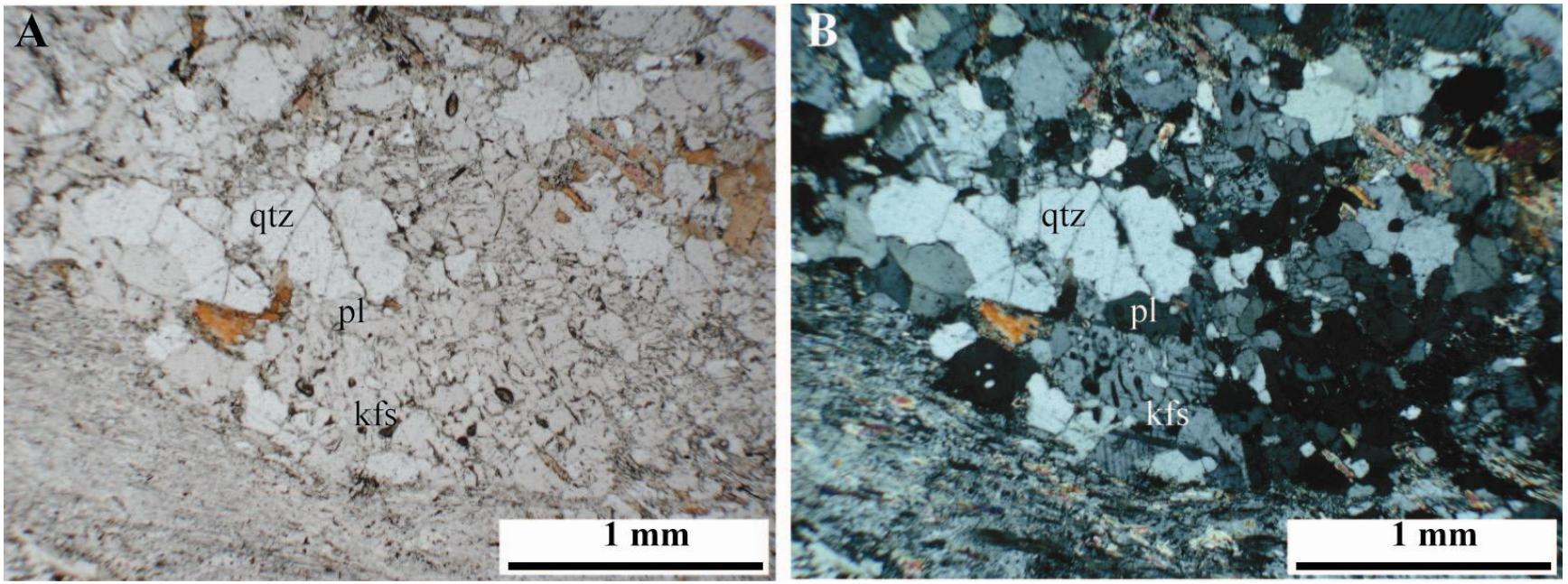

Figure 3.46: Photomicrographs of felsic leucosome in contact with fine-grained pelitic mineral assemblage in PPL (a) and XPL (b). The leucosome assemblage contains: plagioclase + quartz + muscovite + K-feldspar (IC08-01b1).

component followed by pyrope (pyp), grossular (grs) and spessartine (sps). The garnet from sample IC08-01b is typical of garnets from Iron Creek, with homogeneous alm and grs components and an antithetical relationship between sps and pyp where manganese is enriched and magnesium is depleted at garnet rims resulting in a range of compositions from $Alm_{79-80}Pyp_{8-15}Grs_{\sim 12}Sps_{2-8}$ (Fig. 3.48). Garnet analyses were grouped into rim, inner-rim and core analyses and averaged per grain. These values provide a range of $Alm_{76-79}Pyp_{10-12}Grs_{5-6}Sps_{6-8}$ for rim averages, $Alm_{76-79}Py_{12-15}Grs_{4-6}Sps_{4-6}$ for inner-rim averages, and $Alm_{75-78}Pyp_{12-16}Grs_{4-6}Sps_{4-6}$ for core averages (Table 3.12).

Biotite compositions were determined from 97 analyses of 16 grains in five samples of peraluminous-gneiss (Fig. 3.49, Fig. 3.50, Appendix E). No chemical zoning of biotite was detected. All biotite grains are Fe and Al-rich containing X_{Mg} = 0.33 – 0.41, Al = 3.48 – 3.72 apfu, and Ti = 0.15 – 0.32 apfu (Fig. 3.51, Table 3.13). The chemical composition of biotites range from $\square_{0.26}K_{1.70}\ Na_{0.04}(Fe^{2+}_{3.01}Mg_{1.75}\ Mn_{0.01})(\ Al_{3.69}Ti_{0.15}Si_{5.25})O_{20}(OH)_4$ to $\square_{0.17}K_{1.75}\ Na_{0.08}(Fe^{2+}_{3.04}Mg_{1.57}Mn_{0.03})(\ Al_{3.49}Ti_{0.32}Si_{5.28})O_{20}(OH)_4$. All biotite grains from peraluminous gneisses contain high Al- and low Mg/(Mg+Fe) contents (Fig. 3.23).

Muscovite compositions were determined with 109 analyses on eleven grains in five samples of peraluminous gneiss from Iron Creek (Fig. 3.49, Appendix H). Analyses range from Al = 2.79 – 3.08 apfu, Na = 0.03 – 0.20 apfu, K = 0.59 – 0.85 apfu, and Mg/(Fe+Mg) = 0.40 – 0.58 (Appendix H). Chromium content was below detection in all analyses. No spatial relationship with muscovite composition was detected. Grain averages range from $K_{0.79}Na_{0.11}(Al_{3.70}Fe^{2+}_{0.14}Ti_{0.14}\ Mg_{0.12})\ (Al_{2.04}Si_{5.96})O_{20}(OH)_4$ to $K_{0.64}Na_{0.11}\ (Al_{3.98}\ Fe^{2+}_{0.07}Mg_{0.05}Ti_{0.02})(Al_{2.10}Si_{5.90})O_{20}(OH)_4$ (Table 3.14).

Cordierite compositions were calculated using 79 analyses in five samples of peraluminous gneiss from Iron Creek (Fig. 3.52, Appendix I). Cordierites have intermediate X_{Mg}

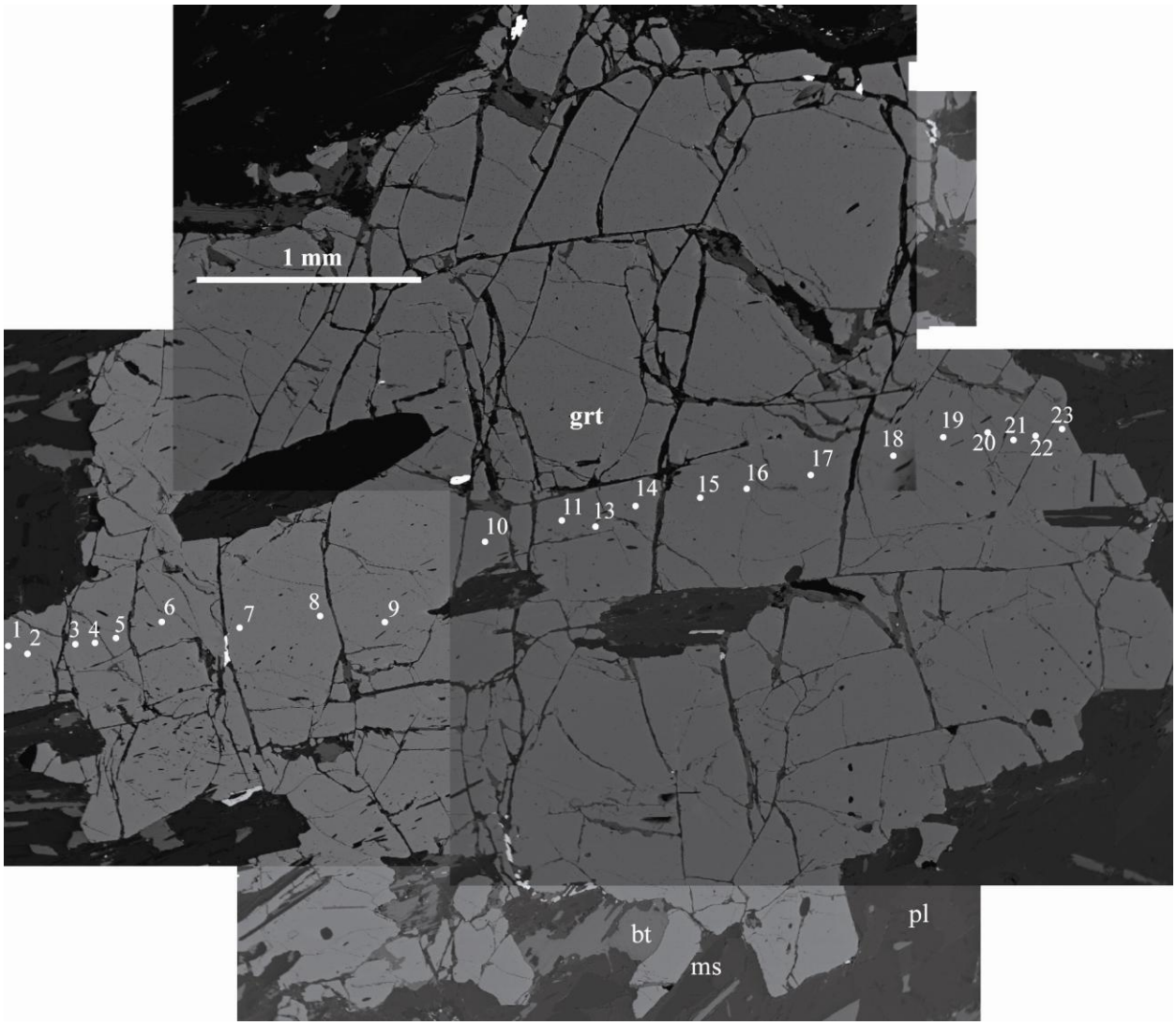

Figure 3.47: Composite BSE image displaying traverse of EMPA point on garnet in IC08-01b. Twenty-three analyses were recorded and used to plot chemical variation across the grain.

= 0.42 – 0.50 (Fig. 3.53), and low Na = 0.29 – 0.43 apfu, and Mn = 0.02 – 0.06 apfu. Cordierite contains the following X_{Mg} ranges: IC08-01a = 0.45 – 0.49, IC08-01a1 = 0.42 – 0.44, IC08-01b = 0.43 – 0.46, IC08-01b1 = 0.44 – 0.48, and IC08-01e = 0.49 – 0.50 (Table 3.15).

Plagioclase compositions were determined with 174 analyses on 16 grains in five samples of peraluminous gneiss from Iron Creek (Fig. 3.50, Appendix C). Plagioclase compositions of Iron Creek peraluminous gneisses ranged from IC08-01a = $Ab_{60-76}An_{23-39}Or_{0-1,}$ IC08-01a1 = $Ab_{60-70}An_{29-39}Or_{0-1,}$ IC08-01b = $Ab_{61-66}An_{32-38}Or_{0-1,}$ IC08-01b1 = $Ab_{63-69}An_{30-37}Or_{0-2}$, IC08-01e = $Ab_{53-59}An_{40-46}Or_{0-2}$ (Fig. 3.20, Table 3.16). One analysis in each IC08-01b and IC08-01e contained $Ab_{58}An_{32}Or_{10}$ and $Ab_{60}An_{29}Or_{12}$ respectively (Appendix C). Together these data provide temperature and pressure constraints on metamorphic conditions.

3.1.9 Amphibole-Pyroxene Gneiss

Amphibole-pyroxene gneiss is characterized by an abundance of amphibole, pyroxene, biotite, and plagioclase, and a lack of quartz and other felsic components. These gneisses have a dark color, imparted by ferromagnesian phases. One unit was sampled (Idaho M) near Sawtooth Lake and is separated from the main SMC (Fig. 3.1). No detailed mapping was conducted on this unit because it was interpreted, in the field, as the Idaho batholith based on a weak gneissic texture and high abundance of anastamosing felsic dikes cross-cutting the unit (Fig. 3.54).

Petrographic analysis of one sample identified the characteristic mineral assemblage as: pl + bt + cpx + amp + ttn + mnz + zrn (Fig. 3.55, Table 3.3). Medium-grained equant plagioclase, from 0.5 – 1.5 mm, accounts for 35 modal percent of the rock. Plagioclase exhibits polysynthetic twinning and slight sutured grain boundaries. Tabular biotite, from 0.2 – 1.5 mm with an average of 0.7 mm long, exhibits deep-red pleochroism and accounts for ~30 modal percent. Subhedral clinopyroxene grains from 0.25 to 1 mm account for ~25 modal percent, are highly fractured, and display deformation lamellae. Euhedral amphibole grains are < 0.4 mm and

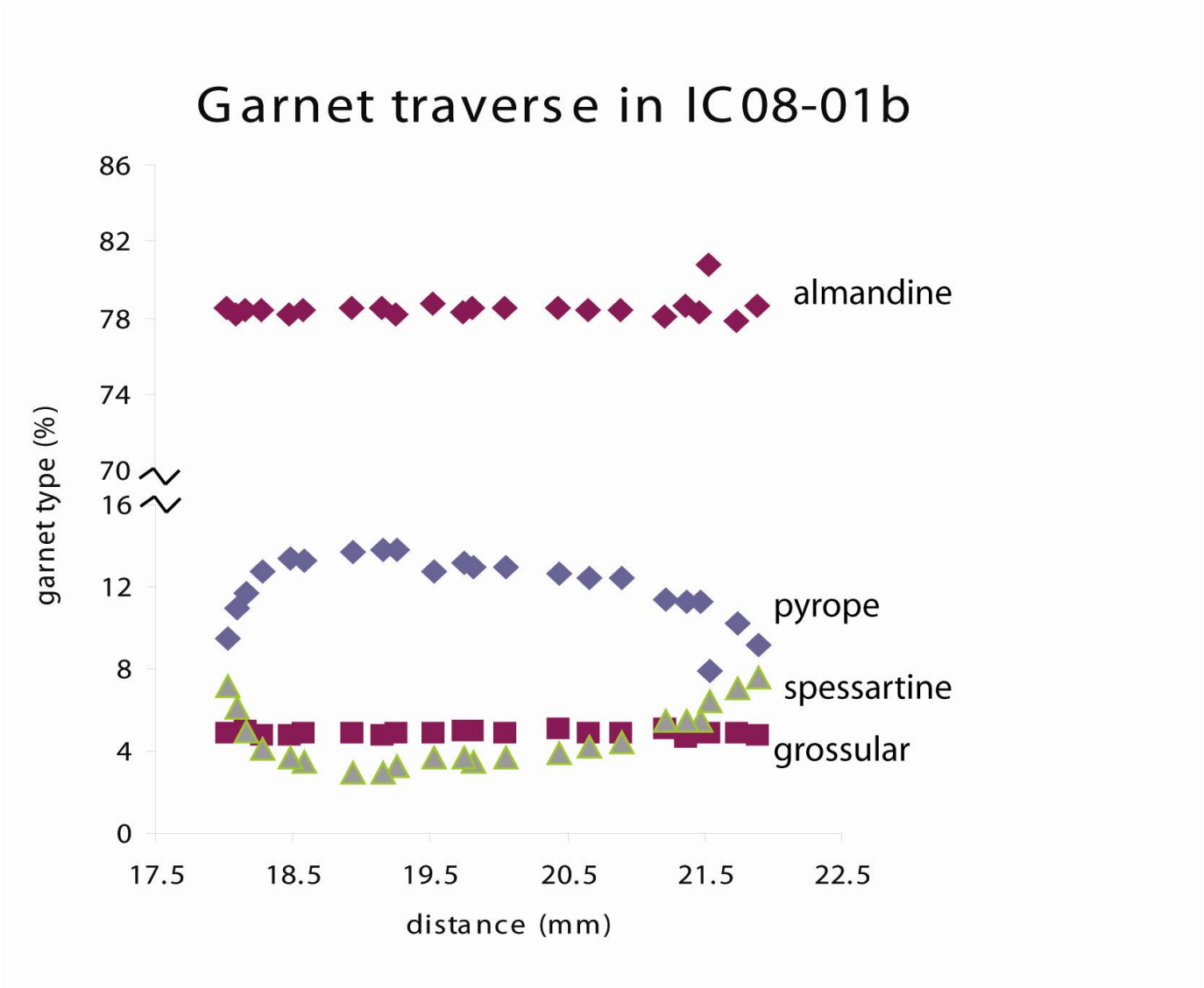

Figure 3.48: Compositional changes across garnet in Fig. 3.54 (IC08-01b). Mg-Mn substitution is evident by the antithetic relationship. Substitution is more pronounced at rims with respect to cores.

Table 3.12: Average compositions of rim, inner rim, and core analyses of garnets in Peraluminous gneisses from Iron Creek.

	IC08-01a			IC08-01a1			IC08-01b			IC08-01b1			IC08-01b1			IC08-01e		
	Grain 1 - rim	Grain 1 - inner rim	Grain 1 - core	Grain 1 - rim	Grain 1 - inner rim	Grain 1 - core	Grain 1 - rim	Grain 1 - inner rim	Grain 1 - core	Grain 1 - rim	Grain 1 - inner rim	Grain 1 - core	Grain 2 - rim	Grain 2 - inner rim	Grain 2 - core	Grain 5 - rim	Grain 5 - inner rim	Grain 5 - core
wt %																		
SiO_2	36.87	37.12	37.03	37.04	37.32	37.15	36.85	36.93	36.93	36.71	37.27	37.25	37.12	36.87	37.39	37.15	37.21	37.22
TiO_2	0.01	0.01	0.01	0.02	0.01	0.01	0.01	0.01	0.01	0.00	0.01	0.01	0.01	0.01	0.01	0.01	0.02	0.01
Al_2O_3	20.74	21.02	20.96	20.70	20.67	20.61	20.58	20.87	21.01	20.94	21.20	21.41	20.94	20.93	21.19	20.80	21.11	20.81
Cr_2O_3	0.03	0.02	0.02	0.03	0.01	0.00	0.03	0.01	0.01	0.03	0.02	0.03	0.02	0.01	0.02	0.02	0.00	0.01
FeO	33.49	33.79	33.58	33.50	34.16	34.34	34.54	34.76	34.77	34.87	35.06	35.16	34.02	34.03	34.03	34.02	34.17	34.26
MnO	3.38	2.36	2.09	3.61	1.67	2.58	3.01	1.95	1.58	3.27	2.07	1.79	2.39	1.58	1.57	3.48	2.61	2.00
MgO	2.68	3.34	3.90	2.83	3.66	3.09	2.43	2.93	3.24	2.42	3.04	3.25	2.97	3.47	3.40	2.35	2.90	3.21
CaO	1.70	1.74	1.53	1.71	1.50	1.49	1.64	1.68	1.70	1.63	1.63	1.64	1.73	1.66	1.78	1.92	2.06	2.03
Total	98.87	99.39	99.12	99.43	99.00	99.27	99.09	99.15	99.25	99.87	100.29	100.54	99.19	98.56	99.40	99.75	100.07	99.55

Garnet

	IC08-01a			IC08-01a1			IC08-01b			IC08-01b1			IC08-01b1			IC08-01e		
	Grain 1 - rim	Grain 1 - inner rim	Grain 1 - core	Grain 1 - rim	Grain 1 - inner rim	Grain 1 - core	Grain 1 - rim	Grain 1 - inner rim	Grain 1 - core	Grain 1 - rim	Grain 1 - inner rim	Grain 1 - core	Grain 2 - rim	Grain 2 - inner rim	Grain 2 - core	Grain 5 - rim	Grain 5 - inner rim	Grain 5 - core
apfu																		
Si	3.01	3.00	2.99	3.01	3.02	3.02	3.01	3.00	2.99	2.98	2.99	2.98	3.01	3.00	3.01	3.01	3.00	3.01
Ti	0.00	0.00	0.00	0.00	0.00	0.00	0.00	0.00	0.00	0.00	0.00	0.00	0.00	0.00	0.00	0.00	0.00	0.00
Al	1.99	2.00	2.00	1.98	1.97	1.97	1.98	2.00	2.01	2.00	2.01	2.02	2.00	2.01	2.01	1.99	2.00	1.98
Cr	0.00	0.00	0.00	0.00	0.00	0.00	0.00	0.00	0.00	0.00	0.00	0.00	0.00	0.00	0.00	0.00	0.00	0.00
Fe^{2+}	2.28	2.28	2.27	2.27	2.31	2.33	2.36	2.36	2.36	2.37	2.35	2.35	2.31	2.32	2.29	2.31	2.30	2.31
Mn^{2+}	0.23	0.16	0.14	0.25	0.11	0.18	0.21	0.13	0.11	0.22	0.14	0.12	0.16	0.11	0.11	0.24	0.18	0.14
Mg	0.33	0.40	0.47	0.34	0.44	0.37	0.30	0.35	0.39	0.29	0.36	0.39	0.36	0.42	0.41	0.28	0.35	0.39
Ca	0.15	0.15	0.13	0.15	0.13	0.13	0.14	0.15	0.15	0.14	0.14	0.14	0.15	0.14	0.15	0.17	0.18	0.18
Fe^{3+}	0.00	0.00	0.00	0.00	0.00	0.00	0.00	0.00	0.00	0.00	0.00	0.00	0.00	0.00	0.00	0.00	0.00	0.00
molar % garnet composition																		
almandine	76.3	76.2	75.3	75.5	77.1	77.4	78.5	78.8	78.4	78.2	78.5	78.4	77.4	77.4	77.4	77.0	76.6	76.8
pyrope	10.9	13.4	15.6	11.4	14.7	12.4	9.8	11.8	13.0	9.7	12.1	12.9	12.0	14.1	13.8	9.5	11.6	12.8
grossular	5.0	5.0	4.4	4.9	4.3	4.3	4.8	4.9	4.9	4.7	4.7	4.7	5.0	4.8	5.2	5.6	5.9	5.8
spessartine	7.8	5.4	4.7	8.2	3.8	5.9	6.9	4.5	3.6	7.4	4.7	4.0	5.5	3.6	3.6	8.0	5.9	4.5

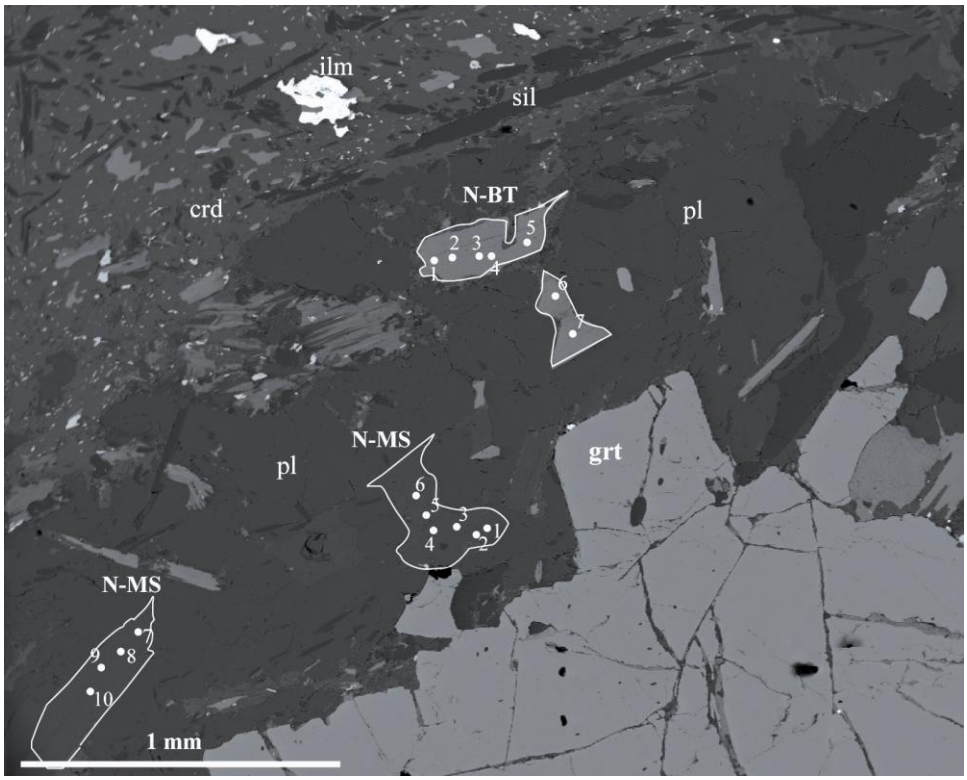

Figure 3.49: BSE image displaying analyses points of biotite and muscovite near garnet in IC08-01b.

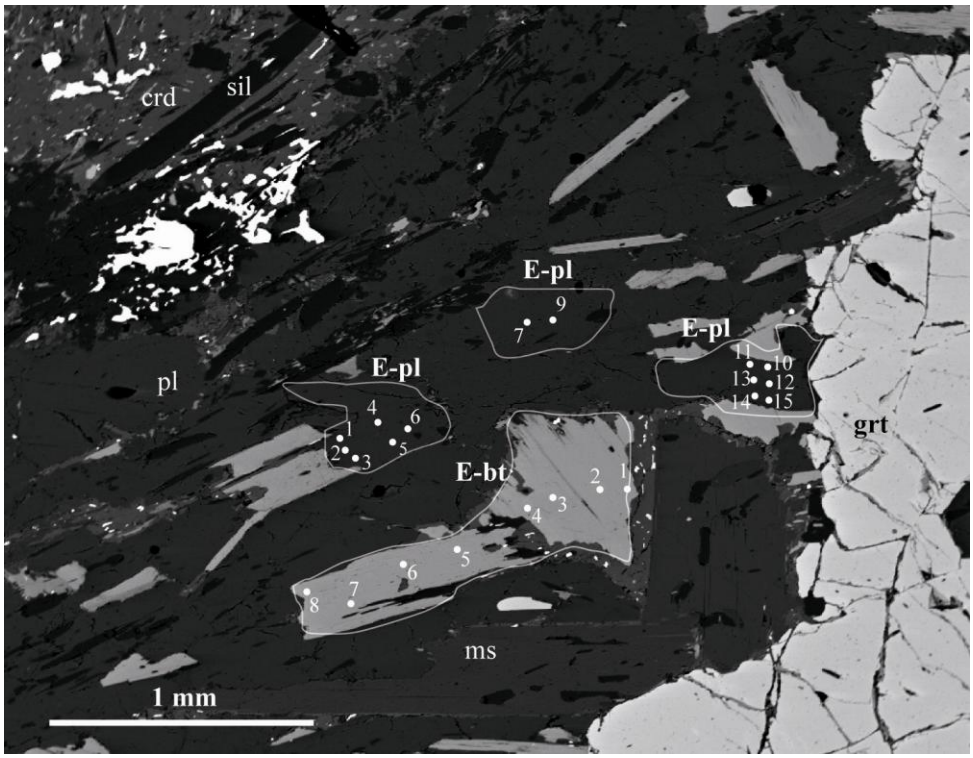

Figure 3.50: BSE image displaying analyses points of biotite and plagioclase near garnet in IC08-01b. Cordierite is associated with tabular biotite.

Table 3.13: Compositional ranges of biotite grains based on titanium in Iron Creek peraluminous gneiss.

	IC08-01a				IC08-01a1						IC08-01b					
	Grain 1 - low-Ti	Grain 1 - High-Ti	Matrix - low-Ti	Matrix - high-Ti	Grain 1 - low-Ti	Grain 1 - High-Ti	Grain 2 - low-Ti	Grain 2 - High-Ti	Matrix - low-Ti	Matrix - high-Ti	Grain 1 - low-Ti	Grain 1 - High-Ti	Grain 2 - low-Ti	Grain 2 - High-Ti	Matrix - low-Ti	Matrix - high-Ti
wt %																
SiO_2	35.43	34.67	34.88	34.64	34.50	34.44	34.04	34.04	33.92	34.17	34.81	33.70	34.50	34.28	34.81	34.53
TiO_2	1.46	2.37	1.32	1.78	2.62	2.76	1.70	2.06	2.22	2.37	1.79	2.01	1.84	2.06	1.68	1.71
Al_2O_3	20.34	20.00	20.83	20.32	19.45	19.46	20.21	20.02	19.46	19.75	20.64	20.49	20.48	20.36	20.37	20.33
Cr_2O_3	0.06	0.12	0.07	0.06	0.09	0.08	0.08	0.10	0.04	0.08	0.04	0.09	0.10	0.07	0.07	0.07
FeO	22.93	23.64	23.95	23.35	24.13	23.84	23.09	23.10	23.28	22.99	23.33	23.45	23.52	23.11	21.77	22.19
MnO	0.12	0.15	0.11	0.12	0.21	0.20	0.18	0.17	0.11	0.13	0.09	0.08	0.05	0.04	0.06	0.06
MgO	8.02	7.36	7.81	7.62	6.95	6.92	7.20	7.08	7.17	7.18	7.20	7.10	7.29	7.08	8.26	8.27
CaO	0.02	0.03	0.01	0.00	0.02	0.00	0.00	0.00	0.03	0.04	0.09	0.01	0.01	0.03	0.01	0.00
BaO	0.14	0.19	0.16	0.20	0.19	0.18	0.19	0.18	0.18	0.23	0.18	0.20	0.20	0.16	0.26	0.21
Na_2O	0.20	0.23	0.15	0.16	0.23	0.10	0.24	0.27	0.61	0.72	0.29	0.28	0.28	0.27	0.31	0.25
K_2O	8.42	8.75	8.86	9.01	8.80	8.75	8.65	8.55	8.67	8.74	8.02	8.22	8.46	8.30	8.43	8.34
Total	97.14	97.51	98.15	97.26	97.19	96.73	95.58	95.57	95.69	96.40	96.48	95.63	96.73	95.76	96.03	95.96

Oxygens = 22

Biotite

	IC08-01a				IC08-01a1						IC08-01b					
	Grain 1 - low-Ti	Grain 1 - High-Ti	Matrix - low-Ti	Matrix - high-Ti	Grain 1 - low-Ti	Grain 1 - High-Ti	Grain 2 - low-Ti	Grain 2 - High-Ti	Matrix - low-Ti	Matrix - high-Ti	Grain 1 - low-Ti	Grain 1 - High-Ti	Grain 2 - low-Ti	Grain 2 - High-Ti	Matrix - low-Ti	Matrix - high-Ti
apfu																
Si	5.34	5.25	5.25	5.26	5.27	5.27	5.26	5.26	5.25	5.24	5.29	5.20	5.26	5.26	5.30	5.27
Ti	0.17	0.27	0.15	0.20	0.30	0.32	0.20	0.24	0.26	0.27	0.20	0.23	0.21	0.24	0.19	0.20
Al	3.61	3.57	3.69	3.64	3.50	3.51	3.68	3.64	3.55	3.57	3.70	3.73	3.68	3.68	3.65	3.65
Cr	0.01	0.01	0.01	0.01	0.01	0.01	0.01	0.01	0.00	0.01	0.00	0.01	0.01	0.01	0.01	0.01
Fe^{2+}	2.89	3.00	3.01	2.96	3.08	3.05	2.98	2.98	3.01	2.95	2.97	3.03	3.00	2.97	2.77	2.83
Mn^{2+}	0.02	0.02	0.01	0.02	0.03	0.03	0.02	0.02	0.01	0.02	0.01	0.01	0.01	0.01	0.01	0.01
Mg	1.80	1.66	1.75	1.72	1.58	1.58	1.66	1.63	1.65	1.64	1.63	1.63	1.66	1.62	1.87	1.88
Ca	0.00	0.00	0.00	0.00	0.00	0.00	0.00	0.00	0.01	0.01	0.01	0.00	0.00	0.00	0.00	0.00
Ba	0.01	0.01	0.01	0.01	0.01	0.01	0.01	0.01	0.01	0.01	0.01	0.01	0.01	0.01	0.02	0.01
Na	0.06	0.07	0.04	0.05	0.07	0.03	0.07	0.08	0.18	0.21	0.09	0.08	0.08	0.08	0.09	0.07
K	1.62	1.69	1.70	1.74	1.71	1.71	1.70	1.68	1.71	1.71	1.56	1.62	1.64	1.63	1.64	1.62
X_{Mg}	0.38	0.36	0.37	0.37	0.34	0.34	0.36	0.35	0.35	0.36	0.35	0.35	0.36	0.35	0.40	0.40

Table 3.13 cont'd.

	IC08-01b1						IC08-01e	
	Grain 1 - low-Ti	Grain 1 - High-Ti	Grain 2 - low-Ti	Grain 2 - High-Ti	Matrix - low-Ti	Matrix - high-Ti	Grain 1 - low-Ti	Grain 1 - High-Ti
wt %								
SiO_2	34.70	36.12	34.80	34.82	35.05	34.96	34.25	34.43
TiO_2	1.95	2.29	1.81	2.18	1.73	2.31	1.67	2.01
Al_2O_3	20.57	20.73	20.61	20.24	20.40	20.51	20.74	20.27
Cr_2O_3	0.08	0.10	0.06	0.04	0.03	0.08	0.07	0.06
FeO	24.18	22.50	22.21	21.93	21.09	20.42	22.59	22.62
MnO	0.07	0.07	0.06	0.08	0.08	0.04	0.12	0.11
MgO	7.00	6.47	7.98	7.89	9.38	9.05	7.61	7.81
CaO	0.00	0.21	0.02	0.01	0.00	0.00	0.03	0.00
BaO	0.23	0.20	0.25	0.21	0.19	0.19	0.14	0.21
Na_2O	0.29	0.73	0.35	0.29	0.31	0.24	0.31	0.22
K_2O	8.31	8.16	8.32	8.59	8.53	8.58	8.86	9.00
Total	97.38	97.58	96.47	96.28	96.79	96.38	96.39	96.74

Oxygens = 22

Biotite

	IC08-01b1						IC08-01e	
	Grain 1 - low-Ti	Grain 1 - High-Ti	Grain 2 - low-Ti	Grain 2 - High-Ti	Matrix - low-Ti	Matrix - high-Ti	Grain 1 - low-Ti	Grain 1 - High-Ti
apfu								
Si	5.26	5.40	5.28	5.29	5.27	5.26	5.23	5.24
Ti	0.22	0.26	0.21	0.25	0.20	0.26	0.19	0.23
Al	3.67	3.65	3.68	3.63	3.62	3.64	3.73	3.64
Cr	0.01	0.01	0.01	0.00	0.00	0.01	0.01	0.01
Fe^{2+}	3.06	2.81	2.82	2.79	2.65	2.57	2.88	2.88
Mn^{2+}	0.01	0.01	0.01	0.01	0.01	0.01	0.02	0.01
Mg	1.58	1.44	1.80	1.79	2.10	2.03	1.73	1.77
Ca	0.00	0.03	0.00	0.00	0.00	0.00	0.00	0.00
Ba	0.01	0.01	0.01	0.01	0.01	0.01	0.01	0.01
Na	0.09	0.21	0.10	0.09	0.09	0.07	0.09	0.07
K	1.61	1.56	1.61	1.67	1.64	1.65	1.73	1.75
X_{Mg}	0.34	0.34	0.39	0.39	0.44	0.44	0.38	0.38

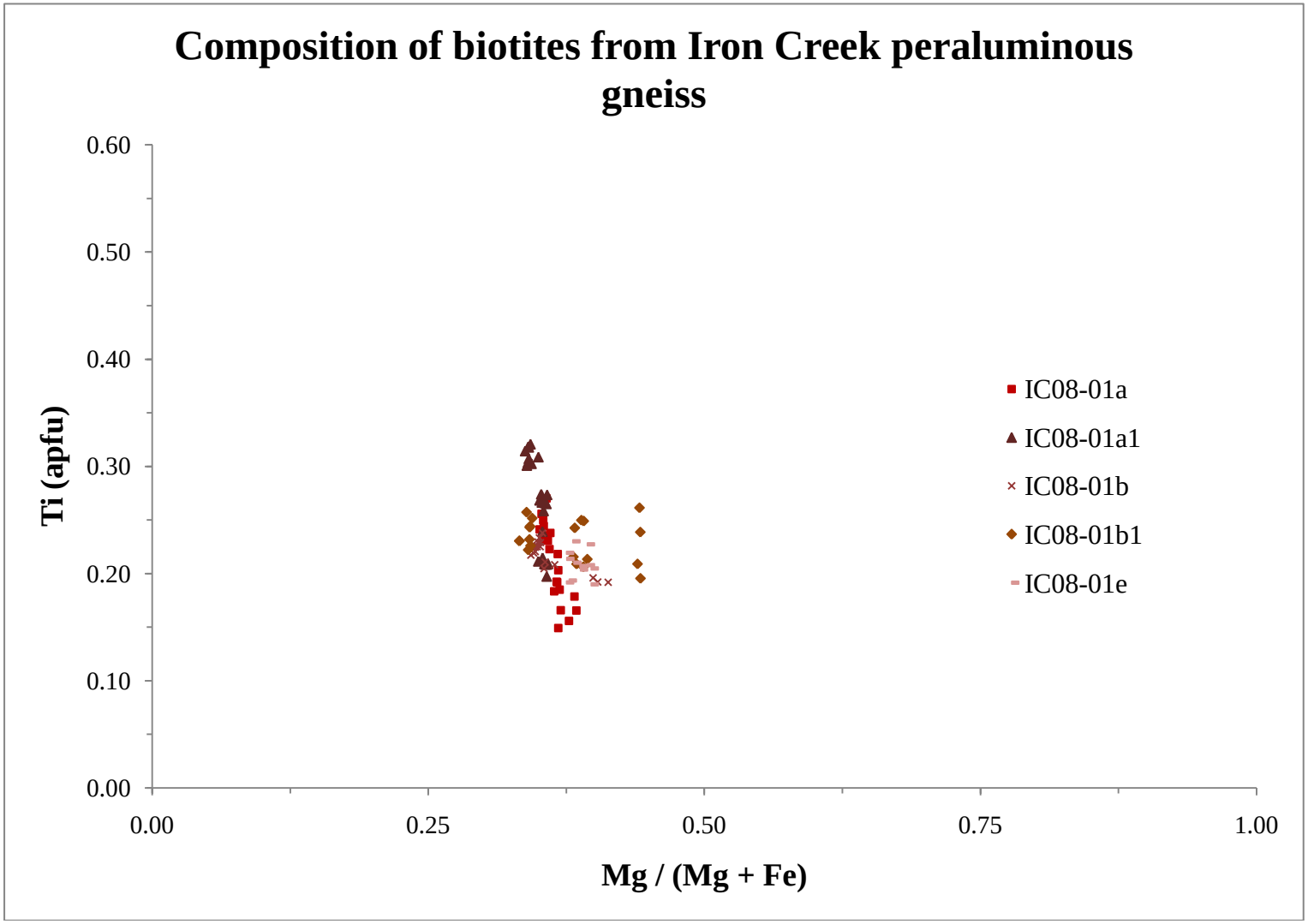

Figure 3.51: Compositions of biotite from the Iron Creek peraluminous gneiss displaying the limited range of composition. The matrix biotite of IC08-01b1 is slightly more Mg-rich.

Table 3.14: Compositional averages of muscovite in Iron Creek peraluminous gneiss.

	IC08-01a		IC08-01a1		IC08-01b		IC08-01b1		IC08-01e		
	Grain 1	Grain 2	Grain 1	Grain 2	Grain 1	Grain 2	Grain 1	Grain 2	Grain 1	Grain 2	Grain 3
wt %											
SiO_2	45.91	45.96	45.70	45.87	45.72	45.61	45.64	45.92	44.72	45.93	45.97
TiO_2	0.39	0.29	0.33	0.36	0.58	0.71	0.54	0.67	1.30	0.85	0.69
Al_2O_3	38.83	40.21	38.83	38.38	37.72	37.61	38.37	37.59	36.50	38.73	38.95
Cr_2O_3	0.06	0.06	0.06	0.07	0.05	0.06	0.02	0.03	0.06	0.04	0.04
FeO	1.29	1.21	1.06	1.08	1.11	1.29	0.94	1.11	1.24	1.01	1.06
MnO	0.02	0.01	0.01	0.01	0.00	0.01	0.01	0.02	0.01	0.01	0.01
MgO	0.77	0.53	0.54	0.64	0.62	0.71	0.49	0.63	0.64	0.58	0.57
CaO	0.00	0.01	0.00	0.00	0.00	0.01	0.01	0.00	0.00	0.00	0.00
BaO	0.20	0.42	0.23	0.20	0.46	0.45	0.45	0.47	0.48	0.38	0.30
Na_2O	0.76	0.89	0.69	0.66	1.23	1.26	1.35	1.23	0.85	0.68	0.77
K_2O	8.40	7.86	8.43	8.48	9.34	9.20	9.46	9.53	9.27	8.30	8.57
F	0.00	0.00	0.00	0.00	0.00	0.00	0.00	0.00	0.00	0.00	0.00
Total	96.61	97.44	95.88	95.76	96.82	96.92	97.28	97.20	95.05	96.49	96.92

Oxygens = 12

	Muscovite				muscovite						
	IC08-01a		IC08-01a1		IC08-01b		IC08-01b1		IC08-01e		
	Grain 1	Grain 2	Grain 1	Grain 2	Grain 1	Grain 2	Grain 1	Grain 2	Grain 1	Grain 2	Grain 3
apfu											
Si	3.05	3.07	3.01	3.02	3.07	3.07	3.08	3.10	2.96	3.04	3.06
Ti	0.02	0.01	0.02	0.02	0.03	0.04	0.03	0.03	0.06	0.04	0.03
Al	3.04	3.16	3.01	2.98	2.98	2.98	3.05	2.99	2.85	3.02	3.06
Cr	0.00	0.00	0.00	0.00	0.00	0.00	0.00	0.00	0.00	0.00	0.00
Fe^{2+}	0.07	0.07	0.06	0.06	0.06	0.07	0.05	0.06	0.07	0.06	0.06
Mn^{2+}	0.00	0.00	0.00	0.00	0.00	0.00	0.00	0.00	0.00	0.00	0.00
Mg	0.08	0.05	0.05	0.06	0.06	0.07	0.05	0.06	0.06	0.06	0.06
Ca	0.00	0.00	0.00	0.00	0.00	0.00	0.00	0.00	0.00	0.00	0.00
Ba	0.01	0.01	0.01	0.01	0.01	0.01	0.01	0.01	0.01	0.01	0.01
Na	0.10	0.12	0.09	0.08	0.16	0.16	0.18	0.16	0.11	0.09	0.10
K	0.71	0.67	0.71	0.71	0.80	0.79	0.81	0.82	0.78	0.70	0.73
F	0.00	0.00	0.00	0.00	0.00	0.00	0.00	0.00	0.00	0.00	0.00
OH	1.50	1.13	1.81	1.86	1.42	1.38	1.22	1.26	2.18	1.55	1.37

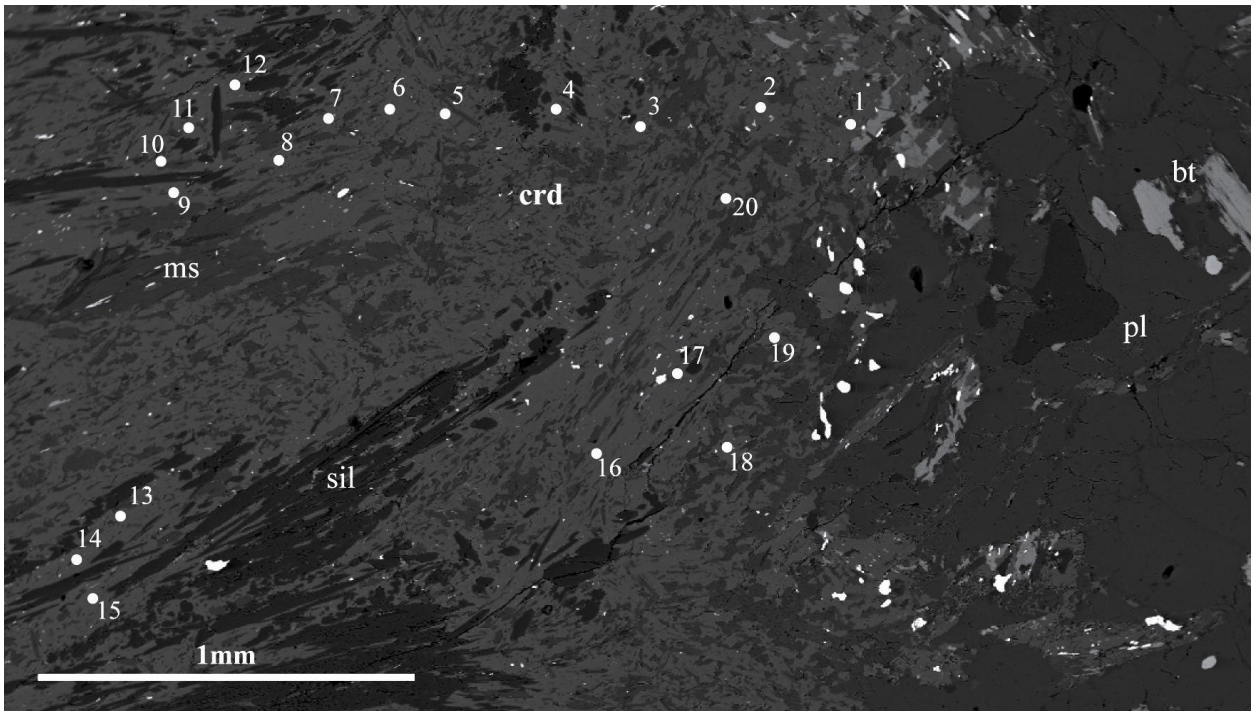

Figure 3.52: BSE image displaying analyses points on cordierite in IC08-01b.

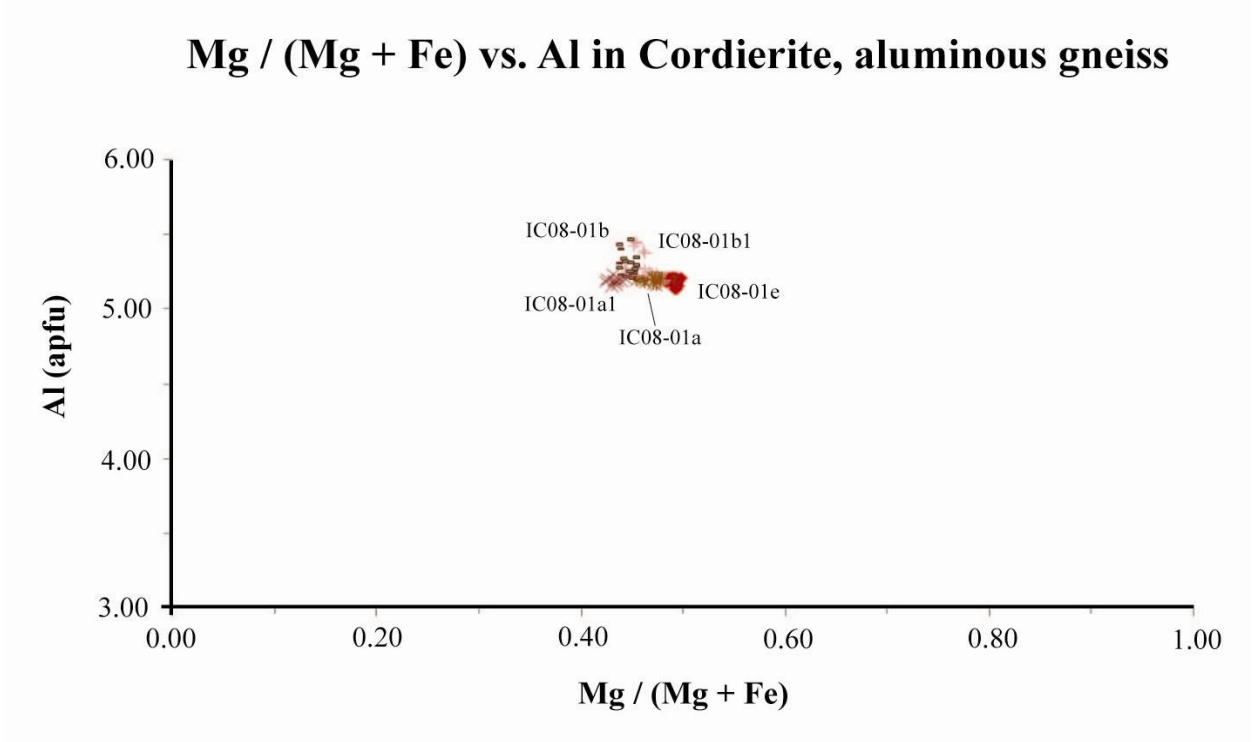

Figure 3.53: Composition of cordierite grains from Iron Creek peraluminous gneisses. Compositions are intermediate with respect to Fe-Mg.

Table 3.15: Compositional averages of cordierites in Iron Creek peraluminous gneisses.

	IC08-01a		IC08-01a1		IC08-01b		IC08-01b1		IC08-01e	
	low-X_{Mg}	high-X_{Mg}	Low-X_{Mg}	high-X_{Mg}	Low-X_{Mg}	high-X_{Mg}	Low-X_{Mg}	high-X_{Mg}	Low-X_{Mg}	high-X_{Mg}
wt %										
SiO_2	45.18	45.98	46.06	46.03	45.49	45.72	45.00	46.15	46.65	46.95
TiO_2	0.05	0.03	0.01	0.01	0.04	0.05	0.01	0.02	0.00	0.01
Al_2O_3	32.26	32.75	32.68	32.59	33.30	32.34	32.47	32.85	33.15	32.99
Cr_2O_3	0.00	0.00	0.00	0.08	0.03	0.00	0.04	0.03	0.02	0.02
FeO	12.30	11.43	12.99	12.47	10.91	11.96	12.24	11.88	12.07	11.66
MnO	0.44	0.52	0.57	0.58	0.17	0.21	0.18	0.23	0.33	0.36
MgO	5.75	6.21	5.38	5.50	4.71	5.72	5.50	6.21	6.35	6.42
CaO	0.03	0.01	0.05	0.04	0.10	0.06	0.12	0.07	0.06	0.01
BaO	0.00	0.00	0.00	0.02	0.10	0.00	0.04	0.00	0.01	0.00
Na_2O	0.27	0.27	0.29	0.36	0.54	0.52	0.47	0.35	0.24	0.26
K_2O	0.01	0.01	0.01	0.06	1.49	0.16	0.42	0.01	0.00	0.01
F	0.00	0.00	0.00	0.00	0.00	0.00	0.00	0.00	0.00	0.00
Total	96.29	97.21	98.04	97.74	96.88	96.74	96.49	97.80	98.88	98.69

Oxygens = 18

Cordierite

	IC08-01a		IC08-01a1		IC08-01b		IC08-01b1		IC08-01e	
	low-X_{Mg}	high-X_{Mg}	Low-X_{Mg}	high-X_{Mg}	Low-X_{Mg}	high-X_{Mg}	Low-X_{Mg}	high-X_{Mg}	Low-X_{Mg}	high-X_{Mg}
apfu										
Si	4.87	4.88	4.89	4.89	4.88	4.90	4.85	4.88	4.88	4.91
Ti	0.00	0.00	0.00	0.00	0.00	0.00	0.00	0.00	0.00	0.00
Al	4.10	4.10	4.09	4.08	4.21	4.08	4.13	4.09	4.09	4.07
Cr	0.00	0.00	0.00	0.01	0.00	0.00	0.00	0.00	0.00	0.00
Fe^{2+}	1.11	1.02	1.15	1.11	0.98	1.07	1.10	1.05	1.06	1.02
Mn^{2+}	0.04	0.05	0.05	0.05	0.02	0.02	0.02	0.02	0.03	0.03
Mg	0.92	0.98	0.85	0.87	0.75	0.91	0.88	0.98	0.99	1.00
Ca	0.00	0.00	0.01	0.00	0.01	0.01	0.01	0.01	0.01	0.00
Ba	0.00	0.00	0.00	0.00	0.00	0.00	0.00	0.00	0.00	0.00
Na	0.06	0.06	0.06	0.07	0.11	0.11	0.10	0.07	0.05	0.05
K	0.00	0.00	0.00	0.01	0.20	0.02	0.06	0.00	0.00	0.00
F	0.00	0.00	0.00	0.00	0.00	0.00	0.00	0.00	0.00	0.00
X_{Mg}	0.45	0.49	0.42	0.44	0.43	0.46	0.44	0.48	0.48	0.50

Table 3.16: Compositional averages of feldspars in Iron Creek peraluminous gneisses.

	IC08-01a				IC08-01a1		IC08-01b		IC08-01b1					IC08-01e	
	Grain 1	Grain 2	Grain 3	Grain 4	Grain 1	Grain 2	Grain 1	Grain 2	Grain 1	Grain 2	Grain 3	Grain 4	Grain 5	Grain 1	Grain 2
wt %															
SiO_2	59.15	62.27	58.90	58.43	58.24	58.38	58.50	59.04	59.60	59.18	59.34	60.04	59.70	57.22	57.51
Al_2O_3	25.66	23.69	26.10	26.28	26.34	25.99	25.79	25.71	25.65	25.89	25.85	25.29	25.56	27.00	27.20
CaO	7.03	4.78	7.43	7.51	7.52	7.39	7.26	7.03	6.88	7.01	6.88	6.57	6.55	8.61	8.64
BaO	0.01	0.01	0.02	0.02	0.02	0.00	0.03	0.01	0.00	0.02	0.03	0.01	0.05	0.02	0.01
Na_2O	6.87	8.20	6.67	6.67	6.65	6.73	7.15	7.24	7.18	7.08	7.12	7.13	7.33	6.02	6.03
K_2O	0.12	0.15	0.11	0.12	0.11	0.10	0.12	0.16	0.11	0.19	0.15	0.11	0.07	0.11	0.15
FeO	0.07	0.04	0.07	0.17	0.04	0.04	0.08	0.04	0.04	0.13	0.09	0.05	0.03	0.03	0.08
MgO	0.02	0.00	0.00	0.00	0.00	0.00	0.08	0.00	0.01	0.02	0.01	0.01	0.01	0.00	0.00
Total	98.94	99.15	99.29	99.20	98.92	98.63	99.01	99.23	99.48	99.53	99.45	99.21	99.30	99.01	99.61

Oxygens = 8

Feldspar

	IC08-01a				IC08-01a1		IC08-01b		IC08-01b1					IC08-01e	
	Grain 1	Grain 2	Grain 3	Grain 4	Grain 1	Grain 2	Grain 1	Grain 2	Grain 1	Grain 2	Grain 3	Grain 4	Grain 5	Grain 1	Grain 2
apfu															
Si	2.66	2.77	2.64	2.63	2.62	2.64	2.64	2.65	2.66	2.65	2.65	2.69	2.67	2.58	2.58
Al	1.36	1.24	1.38	1.39	1.40	1.38	1.37	1.36	1.35	1.37	1.36	1.33	1.35	1.44	1.44
Ca	0.34	0.23	0.36	0.36	0.36	0.36	0.35	0.34	0.33	0.34	0.33	0.31	0.31	0.42	0.42
Ba	0.00	0.00	0.00	0.00	0.00	0.00	0.00	0.00	0.00	0.00	0.00	0.00	0.00	0.00	0.00
Na	0.60	0.71	0.58	0.58	0.58	0.59	0.62	0.63	0.62	0.61	0.62	0.62	0.64	0.53	0.52
K	0.01	0.01	0.01	0.01	0.01	0.01	0.01	0.01	0.01	0.01	0.01	0.01	0.00	0.01	0.01
Fe^{2+}	0.00	0.00	0.00	0.01	0.00	0.00	0.00	0.00	0.00	0.00	0.00	0.00	0.00	0.00	0.00
Mg	0.00	0.00	0.00	0.00	0.00	0.00	0.01	0.00	0.00	0.00	0.00	0.00	0.00	0.00	0.00
X_{Ab}	0.63	0.75	0.61	0.61	0.61	0.62	0.64	0.64	0.65	0.64	0.65	0.66	0.67	0.55	0.55
X_{Or}	0.01	0.01	0.01	0.01	0.01	0.01	0.01	0.01	0.01	0.01	0.01	0.01	0.00	0.01	0.01
X_{An}	0.36	0.24	0.38	0.38	0.38	0.38	0.36	0.35	0.34	0.35	0.34	0.34	0.33	0.44	0.44

Figure 3.54: Outcrop of amphibole-pyroxene gneiss (Idaho M) displaying anastamosing, light-colored, felsic-dikes cross-cutting grey amphibole-pyroxene gneiss. Outcrops appear to be separated from surrounding gneiss by dikes such that it is a xenolith. Hammer at top for scale.

account for >5 modal percent. Amphiboles display diagnostic cleavage and exhibit brown-pleochroic cores with green rims. Small, < 0.2 mm, wedge shaped titanite grains account for < 5% modal amount.

The metamorphic texture suggests a metamorphic overprint. The gneissic foliation is poorly developed, defined by < 50 percent of tabular biotite grains with a preferred orientation (Fig. 3.55). Euhedral amphibole grains appear to overprint pyroxene and biotite. Amphibole rims partially replace clinopyroxene (Fig. 3.56).

Amphibole compositions were calculated for 38 analyses on three grains from one sample, Idaho M (Fig. 3.57, Appendix D). Due to the optical zoning of green rims and brown cores observed in thin section (Fig. 3.56), traverses across amphibole grains were conducted and analyses were grouped as green rims and brown cores (Table 3.17). A zoning pattern of Mg-rich

green rims and Mg-depleted brown cores was observed (Fig. 3.58). Green-rim compositions range from Mg/(Mg+Fe) = 0.69 – 0.75, Si = 7.32 – 7.63 apfu, Al = 0.46 – 0.97 apfu, and Ti = 0.01 – 0.03 apfu, and brown-core compositions range from Mg/(Mg+Fe) = 0.72 – 1.49, Si = 6.91 – 7.47 apfu, Al = 0.72 – 1.49 apfu, and Ti = 0.03 – 0.11 apfu. The structural formula for rims is: $Ca_{1.95}(Mg_{3.21}Fe^{2+}_{1.45})Al_{0.86}Ti_{0.03}Si_{7.37}O_{22}(OH)_2$ and core compositions of: $Ca_{1.95}(Mg_{2.87}Fe^{2+}_{1.64})(Al_{1.39}Fe^{3+}_{0.09})Ti_{0.09}Si_{6.96}O_{22}(OH)_2$. These range from magnesio-hornblende to actinolite.

Amphibole compositions represent three species. Green-rims contain higher Si-concentrations and plot as actinolite and actinolitic-hornblende. Brown-core compositions contain less Si compared to rims and plot as actinolitic-hornblende and magnesio-hornblende (Fig. 3.59, Leake et al., 1997).

Plagioclase compositions were calculated using 21 analyses on 2 grains in Idaho M (Fig. 3.60, Appendix C). No relationship between spatial distribution and composition was seen. Plagioclase compositions range from $Ab_{56-65}An_{37-43}Or_{1-2}$ and are classified as andesine (Fig. 3.20, Table 3.18).

Clinopyroxene compositions were calculated using 24 analyses on two grains in Idaho M (Fig. 3.61, Appendix F). Pyroxenes are dominantly calcic with $Wo_{49-51}En_{37-39}Fs_{13-15}$ (Table 3.19). The average pyroxene composition, $Ca_{1.0}(Mg_{0.74}Fe_{0.26})Si_2O_6$, plots as diopside (Fig. 3.28).

Biotite compositions were calculated with 21 analyses on two grains (Fig. 3.62, Appendix E). No chemical zoning of biotite was detected. Biotite analyses are Mg-rich and Al-poor containing X_{Mg} = 0.59 – 0.60, Al = 2.75 – 2.95 apfu and Ti = 0.20– 0.25 apfu. The chemical composition of biotite ranges from $K_{1.82}Na_{0.03}\square_{0.15}(Mg_{3.10}Fe^{2+}_{2.08}Mn_{0.02})(Al_{2.79}Ti_{0.20}Cr_{0.02}Si_{5.58})O_{20}(OH)_4$ to $K_{1.88}Na_{0.03}\square_{0.09}(Mg_{3.28}Fe^{2+}_{2.19}Mn_{0.03})(Al_{2.89}Ti_{0.25}Cr_{0.02}Si_{5.83})O_{20}(OH)_4$. All biotite grains from amphibole-pyroxene gneisses approach phlogopite composition (Fig. 3.23, Table 3.20).

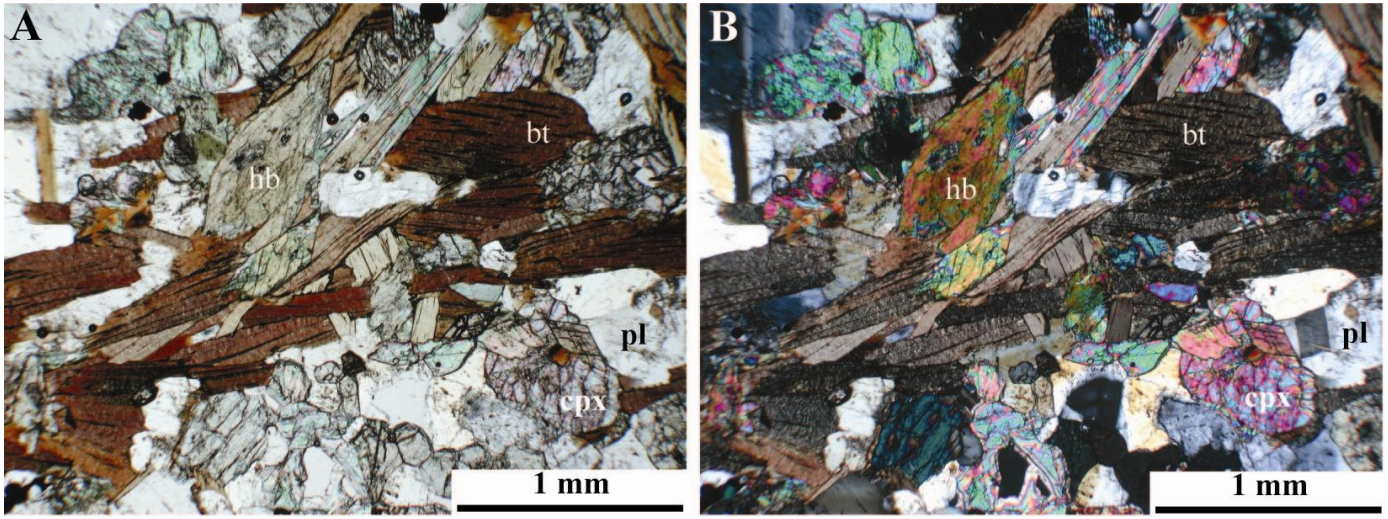

Figure 3.55: Photomicrographs of pyroxene-amphibole gneiss (Idaho M) in PPL (a) and XPL (b) displaying equant amphibole grains and weak-moderate gneissic texture identified by aligned biotite laths. Amphibole grains appear to cross-cut the foliation.

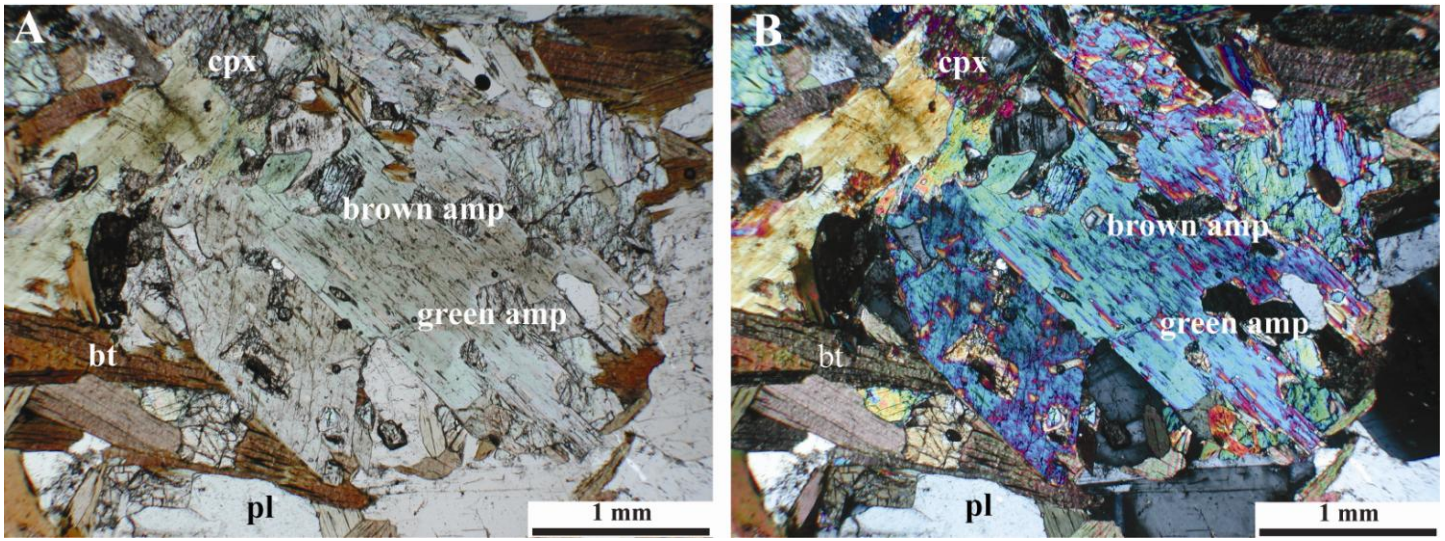

Figure 3.56: Photomicrographs of pyroxene-amphibole gneiss (Idaho M) in PPL (a) and XPL (b) displaying large equant amphibole with two stages of growth evidenced by brown cores and green rims including and partially replacing clinopyroxene.

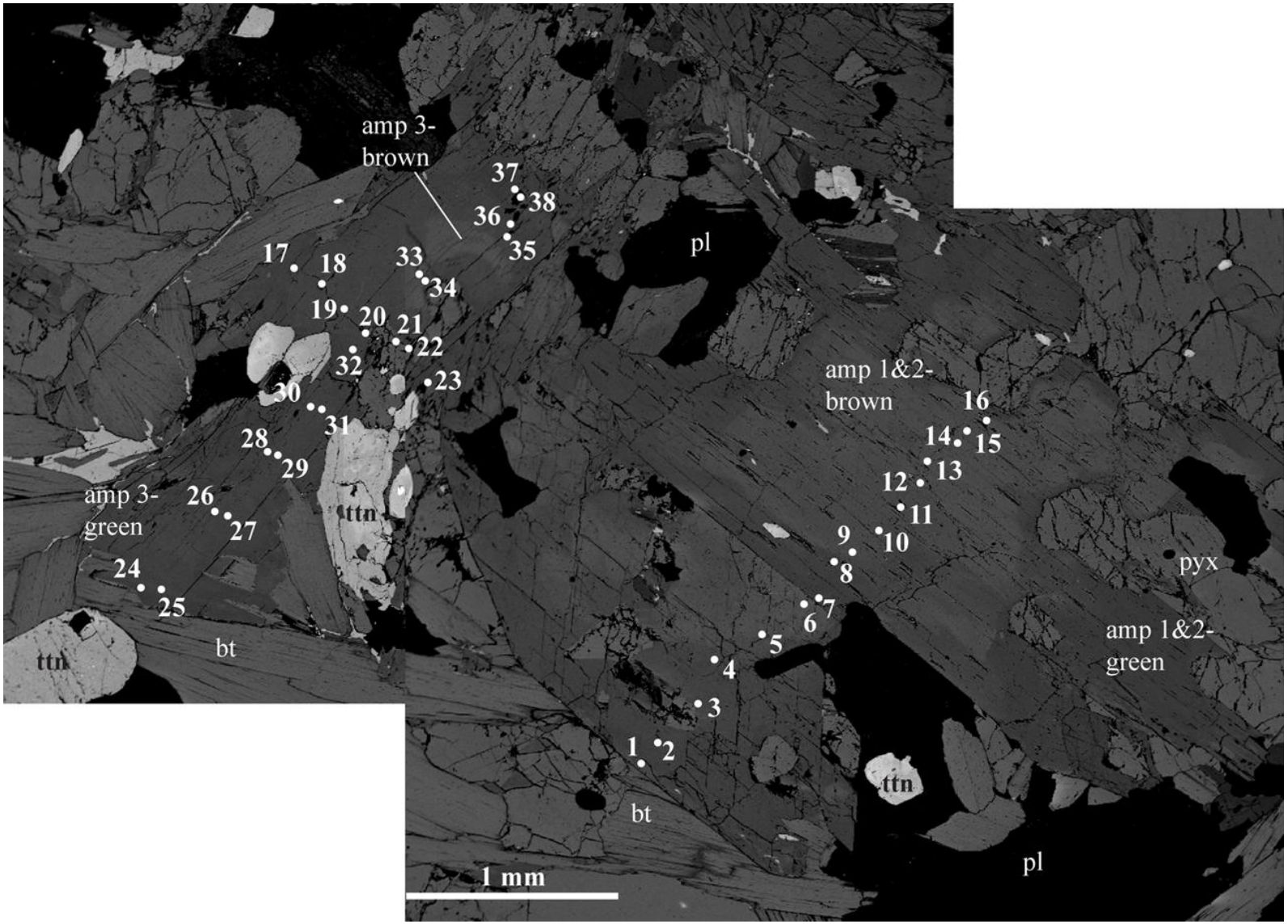

Figure 3.57: Composite BSE image of amphibole in Idaho M showing analysis point. Lighter-colored amphibole corresponds to brown-cores whereas the darker amphibole corresponds to green-rims. Rim and core compositions were separated by optical distinction in this BSE image (Table 3.17).

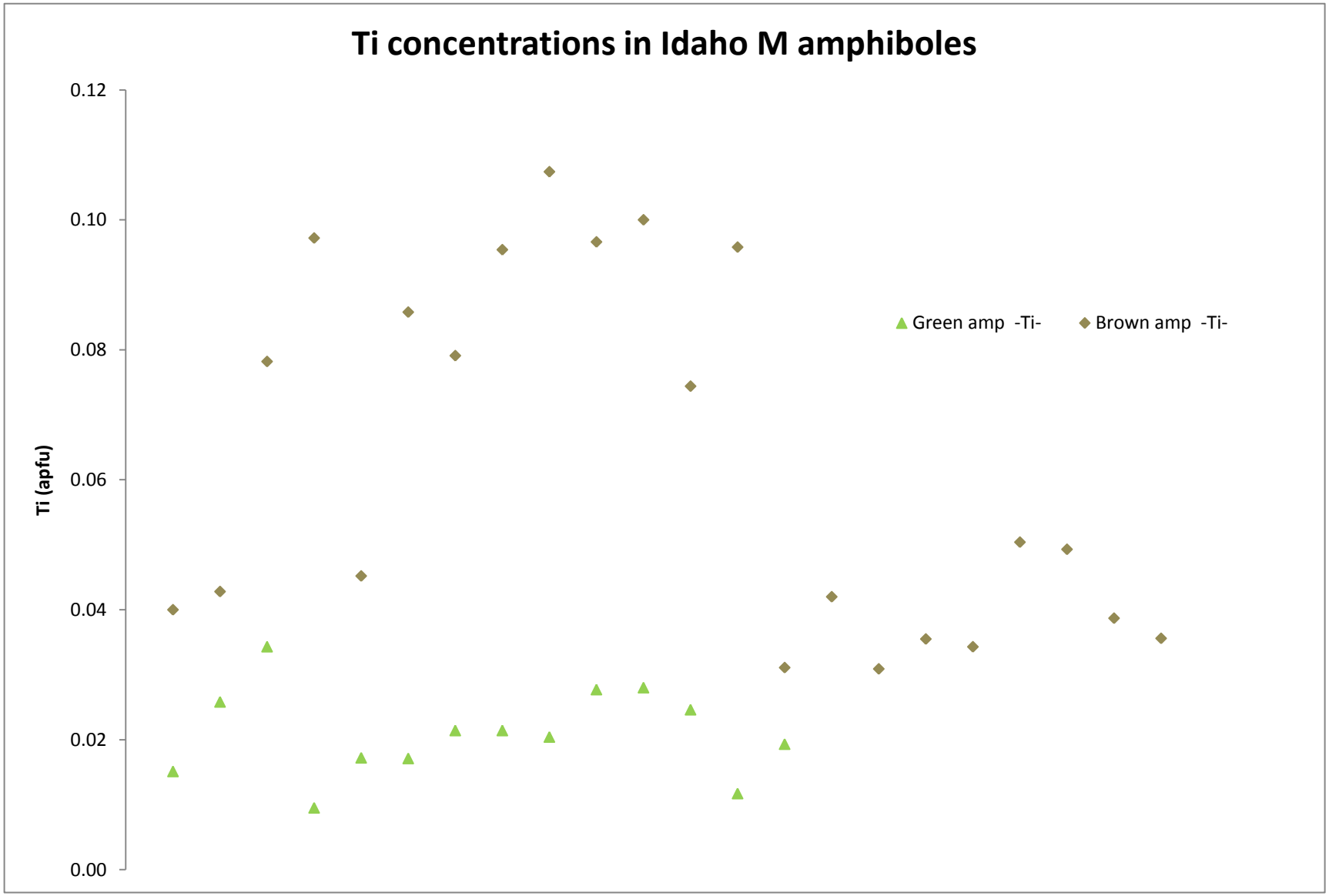

Figure 3.58: Plot of Ti concentration in amphibole (Idaho M) separated into brown-cores and green-rims. Brown amphibole cores contain higher Ti-concentrations with respect to green amphibole rims, suggesting that amphiboles were reset or two stages of amphibole growth have occurred.

Table 3.17: Core and rim compositions of amphibole grains in Idaho M.

	Idaho M Rim 1&2	Core 1&2	Idaho M Rim 3	Core 3
wt %				
SiO_2	51.60	47.98	53.00	51.41
TiO_2	0.23	0.85	0.19	0.39
Al_2O_3	5.11	8.16	3.80	5.36
Cr_2O_3	0.08	0.19	0.11	0.12
FeO	12.17	13.48	11.81	12.55
MnO	0.26	0.28	0.25	0.28
MgO	15.10	13.29	15.74	14.89
CaO	12.76	12.57	12.91	12.73
BaO	0.00	0.02	0.01	0.03
Na_2O	0.69	1.08	0.51	0.70
K_2O	0.38	0.81	0.29	0.45
Cl	0.02	0.04	0.01	0.02
Total	99.25	99.10	99.30	99.19

stoiched on 15 cations

	Idaho M Rim 1&2	Core 1&2	Idaho M Rim 3	Core 3
apfu				
Si	7.37	6.96	7.53	7.35
Ti	0.03	0.09	0.02	0.04
Al	0.86	1.39	0.64	0.90
Cr	0.01	0.02	0.01	0.01
Fe^{3+}	0.09	0.04	0.07	0.03
Fe^{2+}	1.45	1.64	1.40	1.50
Mn^{2+}	0.03	0.03	0.03	0.03
Mg	3.21	2.87	3.33	3.17
Ca	1.95	1.95	1.97	1.95
Ba	0.00	0.00	0.00	0.00
Na	0.19	0.30	0.14	0.19
K	0.07	0.15	0.05	0.08
Cl	0.00	0.01	0.00	0.01
X_{Mg}	0.69	0.64	0.70	0.68

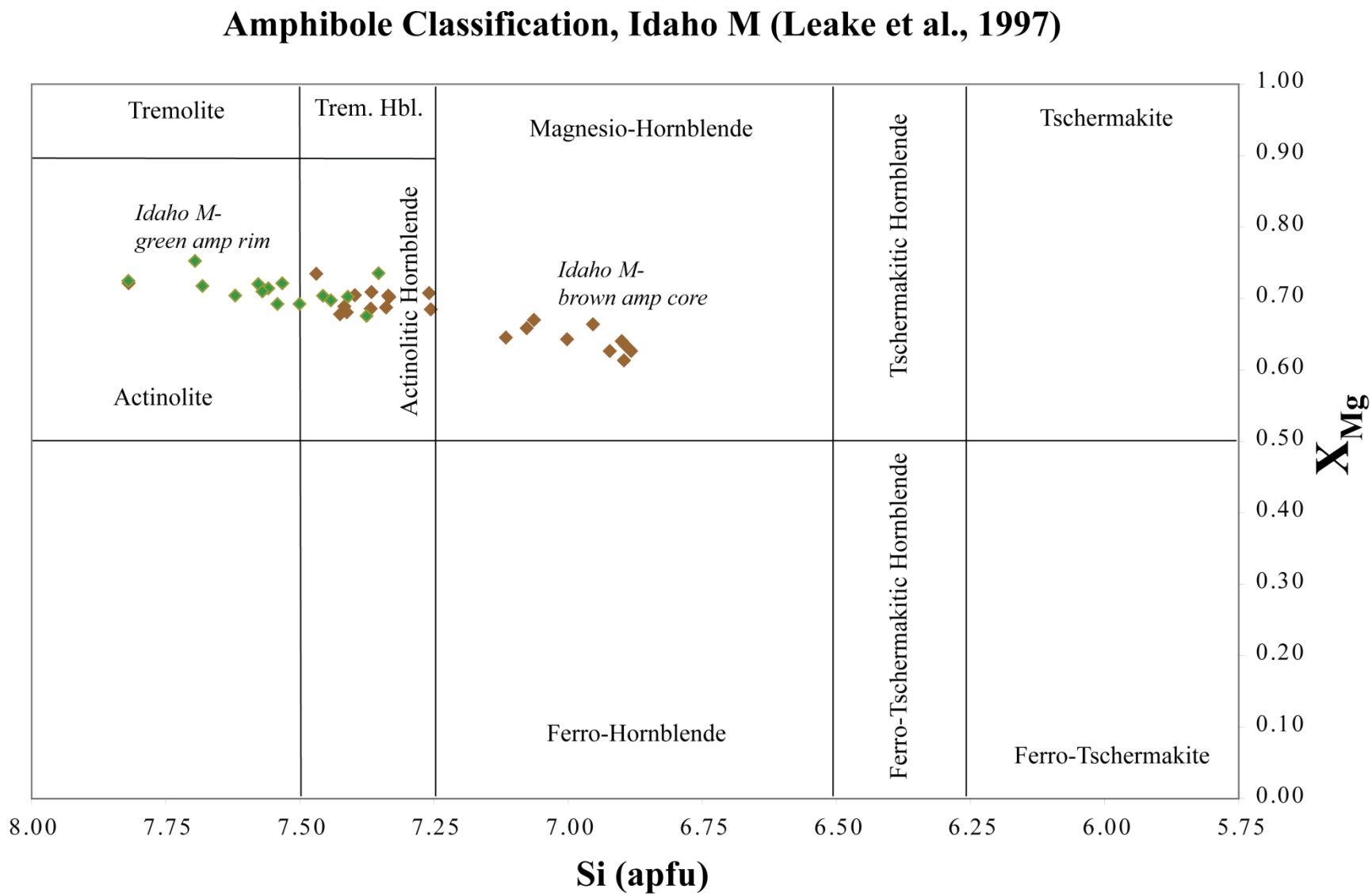

Figure 3.59: Classification of amphibole core and rim analyses in sample Idaho M. Amphiboles range from actinolitic to magnesio hornblende along a nearly continuous compositional series. Classification after Leake (1997).

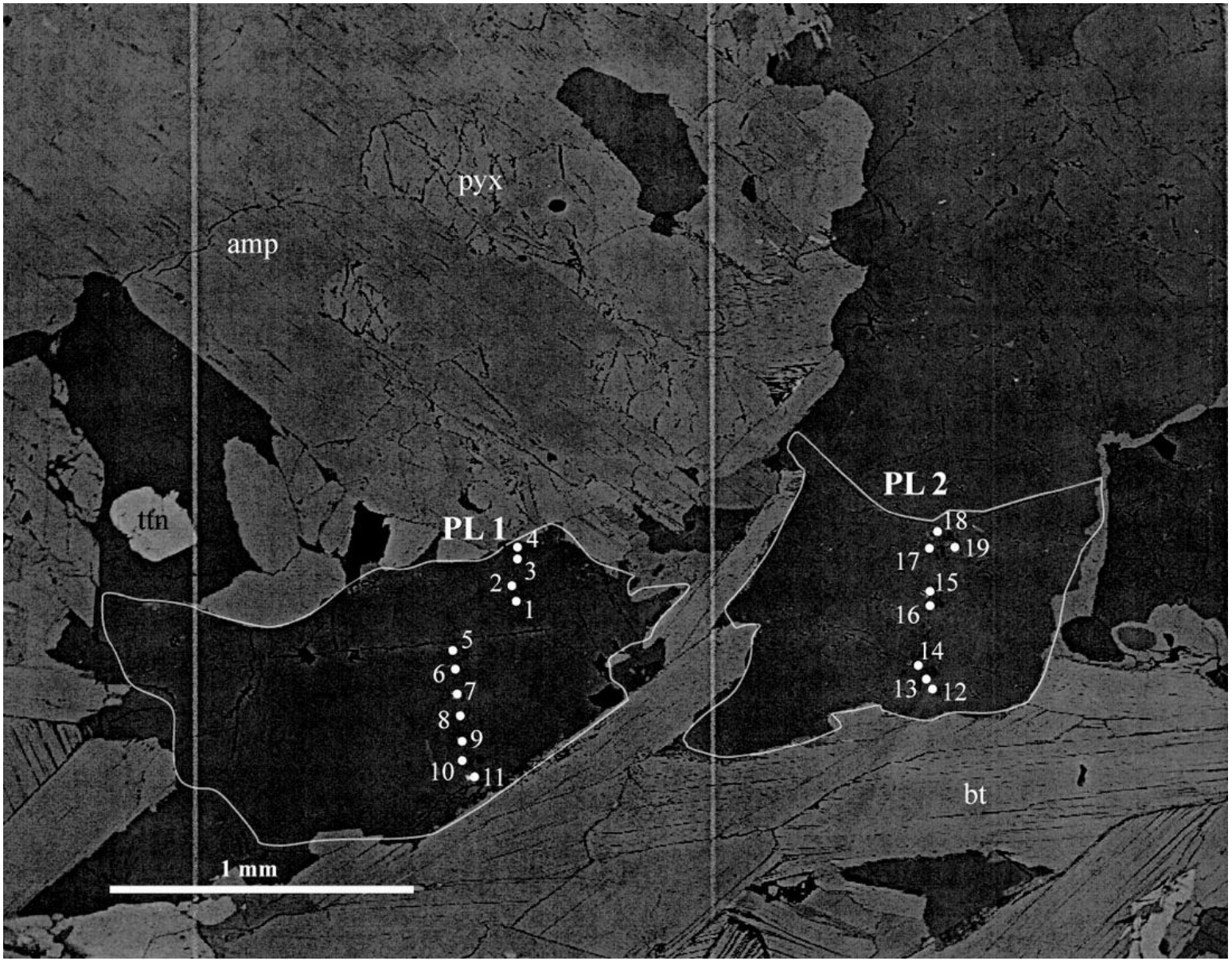

Figure 3.60: BSE image displaying analysis points on plagioclase in amphibole-pyroxene gneiss (Idaho M).

Table 3.18: Compositional averages of plagioclase grains analyzed in Idaho M.

	Idaho M	
	Grain 1	Grain 2
wt %		
SiO_2	58.17	58.84
Al_2O_3	26.53	26.18
CaO	7.95	7.4
BaO	0.02	0.01
Na_2O	6.19	6.69
K_2O	0.27	0.25
FeO	0.03	0.02
MgO	0.01	0
Total	99.17	99.39

Oxygens = 8

	Feldspar	
	Idaho M	
	Grain 1	Grain 2
apfu		
Si	2.61	2.64
Al	1.41	1.38
Ca	0.38	0.36
Ba	0.00	0.00
Na	0.54	0.58
K	0.02	0.01
Fe^{2+}	0.00	0.00
Mg	0.00	0.00
X_{Ab}	0.58	0.61
X_{Or}	0.02	0.02
X_{An}	0.41	0.37

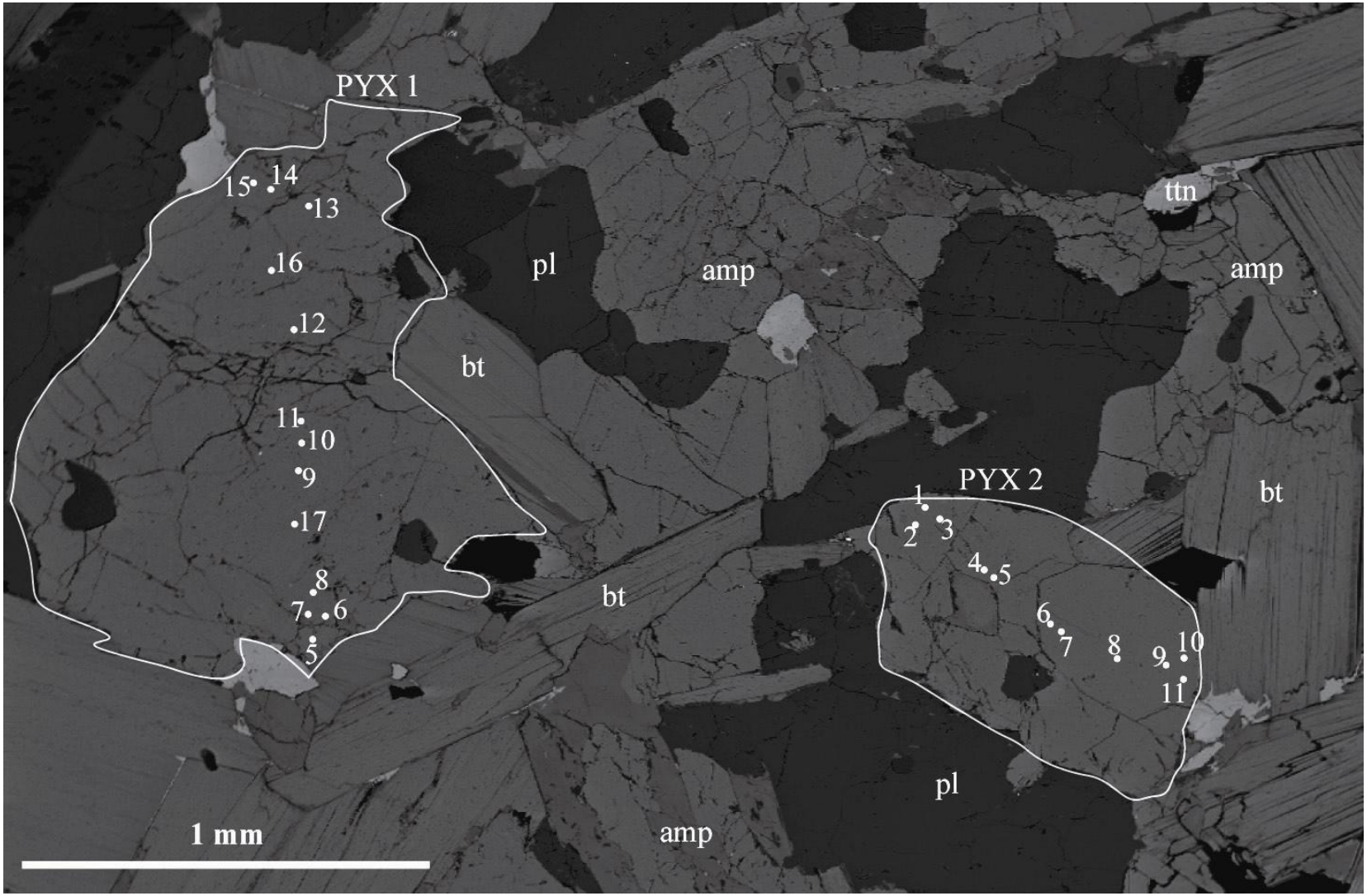

Figure 3.61: BSE image displaying analysis points on pyroxene (PYX) in amphibole-pyroxene gneiss (Idaho M, Table 3.19).

Table 3.19: Compositional averages of pyroxenes in Idaho M.

	Idaho M	
	Grain 1	Grain 2
wt %		
SiO_2	52.30	51.32
TiO_2	0.06	0.06
Al_2O_3	0.68	0.66
Cr_2O_3	0.04	0.03
FeO	8.58	8.88
MnO	0.35	0.35
MgO	13.37	13.32
CaO	24.93	24.69
Na_2O	0.26	0.26
K_2O	0.00	0.00
Total	100.58	99.57

Oxygens = 6

	Pyroxene	
	Idaho M	
	Grain 1	Grain 2
apfu		
Si	1.96	1.95
Ti	0.00	0.00
Al	0.03	0.03
Cr	0.00	0.00
Fe^{2+}	0.27	0.28
Mn^{2+}	0.01	0.01
Mg	0.75	0.75
Ca	1.00	1.00
Na	0.02	0.02
K	0.00	0.00
Fe^{3+}	0.00	0.00
X_{Mg}	0.74	0.73

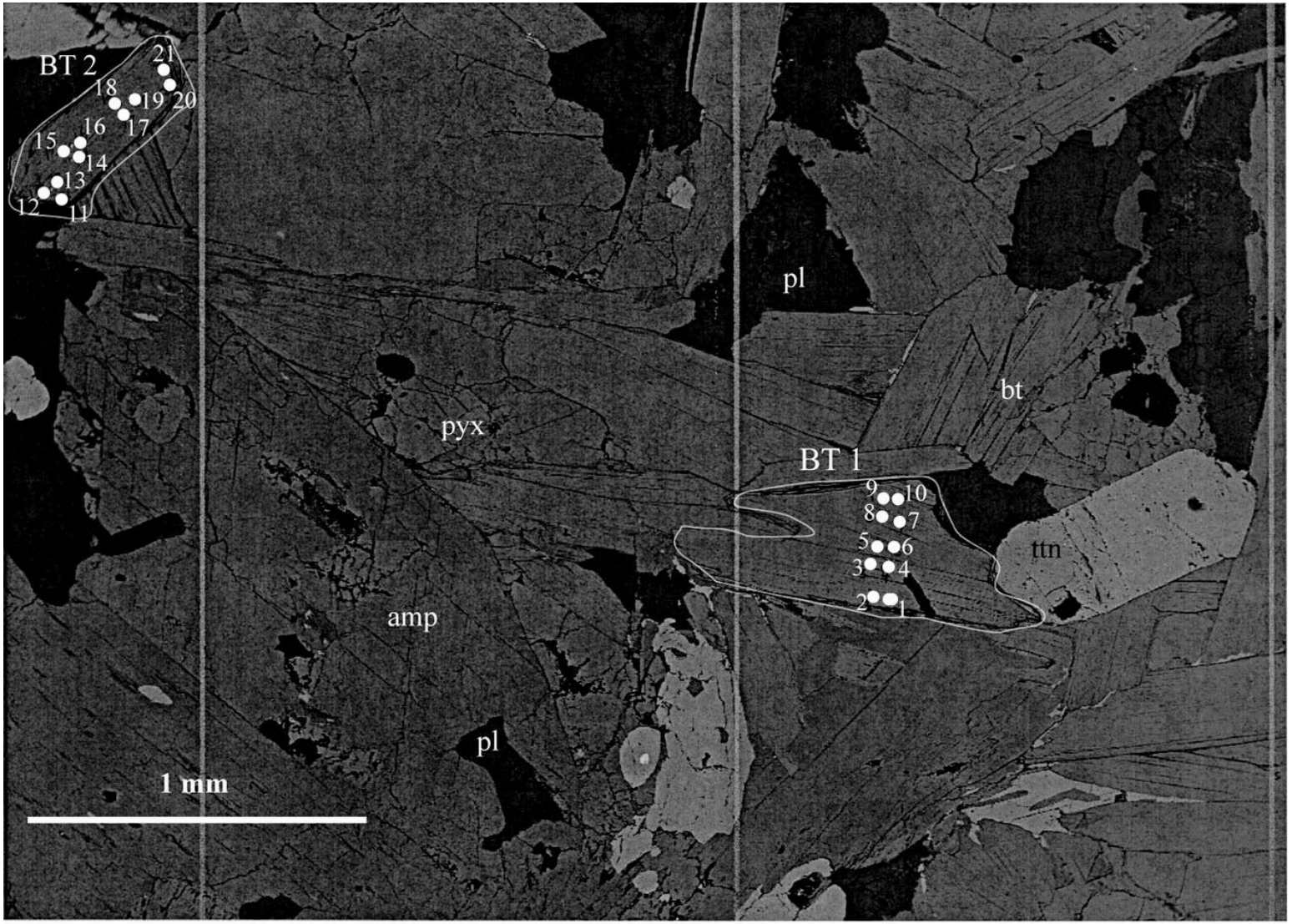

Figure 3.62: BSE image displaying analysis points on two biotite grains (BT) in amphibole-pyroxene gneiss (Idaho M, Table 3.20).

Table 3.20: Compositional range of biotites based on titanium in amphibole-pyroxene gneiss (Idaho M).

	Idaho M			
	Grain 1 - low-Ti	Grain 1 - High-Ti	Grain 2 - low-Ti	Grain 2 - High-Ti
wt %				
SiO_2	37.36	38.06	38.24	38.30
TiO_2	1.80	2.21	1.87	2.16
Al_2O_3	15.82	16.02	16.25	16.12
Cr_2O_3	0.21	0.13	0.10	0.11
FeO	16.66	17.07	17.06	16.96
MnO	0.19	0.21	0.22	0.18
MgO	13.93	14.36	14.09	14.02
CaO	0.00	0.01	0.08	0.00
BaO	0.24	0.24	0.16	0.25
Na_2O	0.09	0.10	0.07	0.09
K_2O	9.57	9.62	9.38	9.59
Total	95.87	98.03	97.52	97.78

Oxygens = 22

Biotite

	Idaho M			
	Grain 1 - low-Ti	Grain 1 - High-Ti	Grain 2 - low-Ti	Grain 2 - High-Ti
apfu				
Si	37.36	5.58	5.62	5.62
Ti	1.80	0.24	0.21	0.24
Al	15.82	2.77	2.81	2.79
Cr	0.21	0.02	0.01	0.01
Fe^{2+}	16.66	2.09	2.10	2.08
Mn^{2+}	0.19	0.03	0.03	0.02
Mg	13.93	3.14	3.08	3.07
Ca	0.00	0.00	0.01	0.00
Ba	0.24	0.01	0.01	0.01
Na	0.09	0.03	0.02	0.03
K	9.57	1.80	1.76	1.79
X_{Mg}	95.87	0.60	0.60	0.60

CHAPTER IV: DISCUSSION

The metamorphic history of the SMC can be interpreted through mineral assemblages, pressure-temperature calculations, and metamorphic textures. K_D plots provide a test of chemical equilibrium. Replacement textures provide a basis for interpreting changes in pressure and temperature through the metamorphic history. The comparison of the progression in mineral assemblages with a petrogenetic grid for the assemblages observed in the Iron Creek peraluminous gneiss and the Thompson Peak peraluminous gneiss provides equally important insights into the metamorphic evolution of the SMC. The following sections provide interpretations of the evolution of the SMC.

4.1 Chemical Equilibrium

Geothermobarometric calculations require minerals in chemical equilibrium. K_D plots compare Mg/Fe ratios to test for chemical equilibrium in garnet/biotite, cordierite/biotite, and garnet/cordierite in Iron Creek peraluminous gneisses. K_D were plotted for Mg/Fe ratios in amphibole/pyroxene in titanite-amphibole-biotite gneisses, biotite-amphibolites, amphibole-pyroxene gneiss, and metagabbros.

Plots of Mg/Fe^{2+} in peraluminous gneiss provide a K_D of approximately 0.31 for garnet/biotite (Fig. 4.1). Analyses of matrix biotite in IC08-01b and IC08-01b1 contain relatively high Mg/Fe^{2+} ratios (0.66 and 079 respectively) suggesting local reequilibration or sulfide-silicate interactions.

Mg/Fe^{2+} ratios in peraluminous gneiss provide a K_D of 0.21 for garnet/cordierite (Fig. 4.2). These data plot along a linear trend suggesting an approach to chemical equilibrium between garnet and cordierite in Iron Creek peraluminous gneiss.

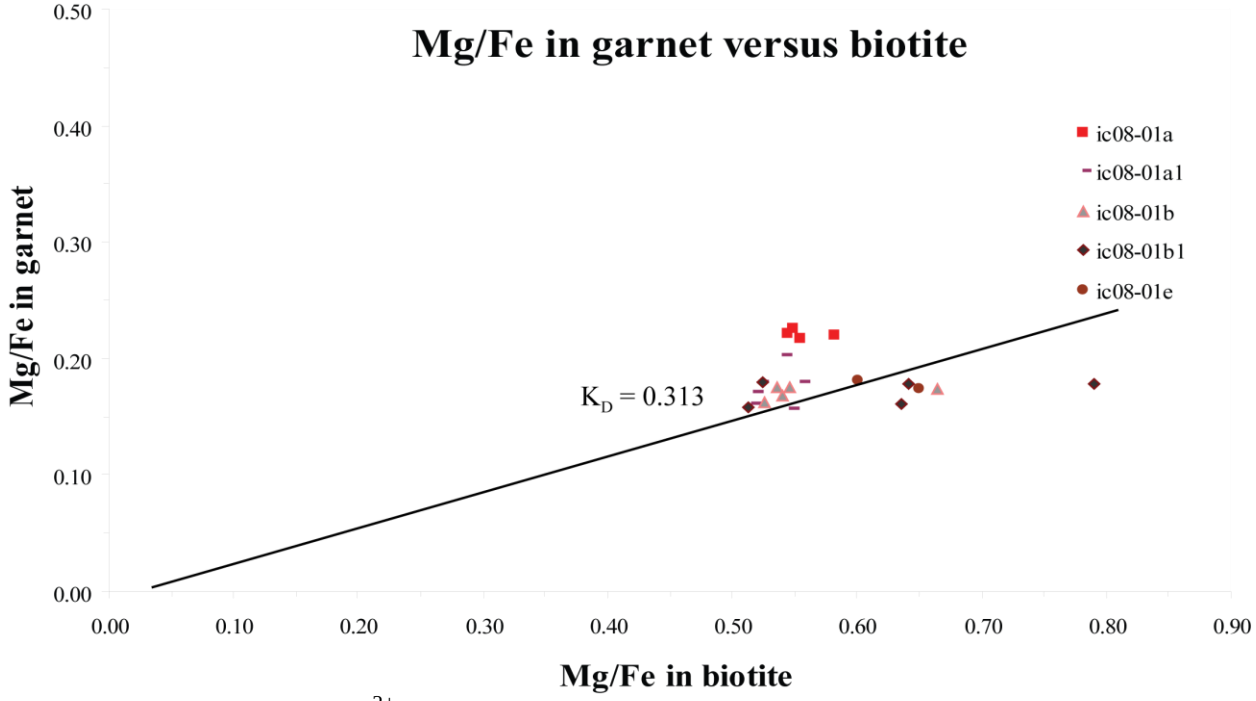

Figure 4.1: K_D plot of Mg/Fe^{2+} in garnet versus biotite in Iron Creek peraluminous gneiss. Analyses plot along a linear trend with a K_D between 0.5 and 0.25 suggesting an approach to chemical equilibrium. Matrix biotite in IC08-0b and IC08-01b1 contain high Mg/Fe^{2+} ratios that do not plot along the linear trend suggesting matrix biotite is not in chemical equilibrium with garnet.

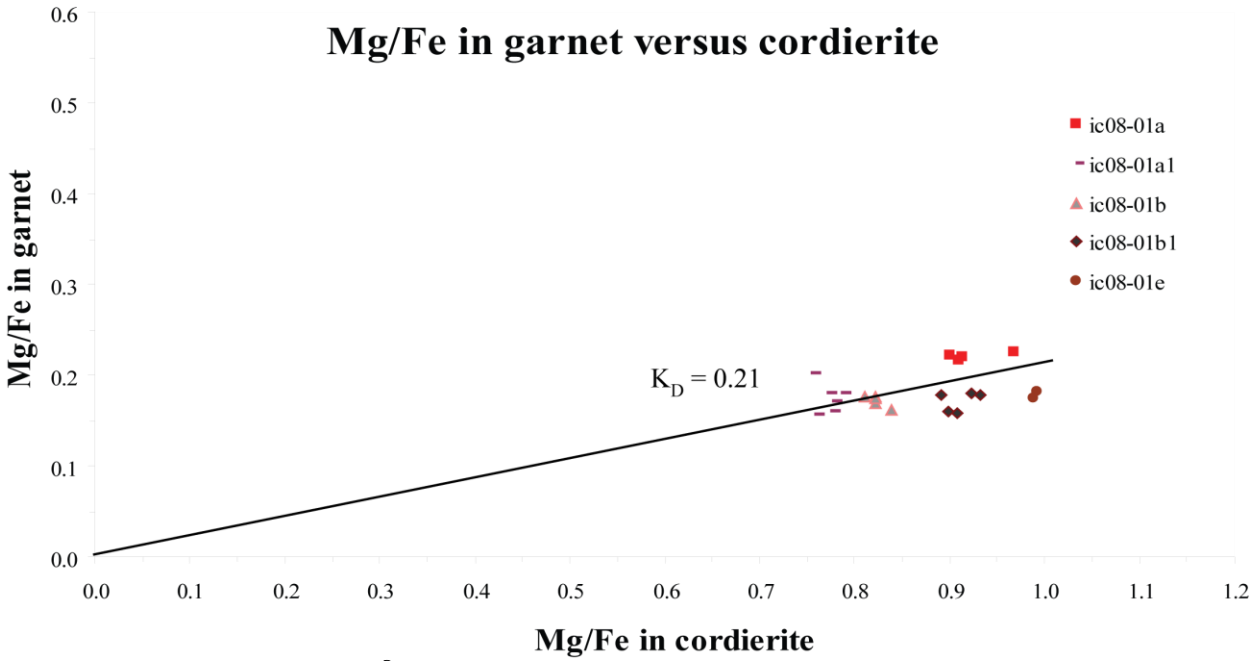

Figure 4.2: K_D plot of Mg/Fe^{2+} in garnet versus cordierite in Iron Creek peraluminous gneiss. Analyses plot along a linear trend with a K_D approximately 0.25 suggesting an approach to chemical equilibrium.

Plots of Mg/Fe^{2+} in peraluminous gneiss provide K_D of 1.49 for cordierite/biotite Fig. 4.3). Analyses of matrix biotite in IC08-01b and IC08-01b1 contain relatively high Mg/Fe^{2+} ratios (0.66 and 0.79 respectively) suggesting matrix biotite in these samples may reflect local equilibrium. Plagioclase and muscovite were assumed to be in chemical equilibrium (with garnet, biotite, cordierite, and sillimanite in all samples. No textural evidence for disequilibrium was present.

Mineral chemical analyses from phases in chemical equilibrium are used for geothermo-barometric calculations.

4.2 Geothermobarometry – Exchange Thermometers

4.2.1 Peraluminous Gneisses

Several geothermometers are available for calculating P-T conditions of peraluminous gneisses. The garnet-biotite (GB) thermometer calculates temperature conditions based on Mg – Fe exchange between garnet and biotite (Ferry and Spear, 1978). Three calibrations used in this study are: Bhattacharya et al. (1992), Dasgupta et al. (1991), and Holdaway & Lee (1977). These calibrations were applied to five samples of peraluminous gneiss from Iron Creek and yield temperatures from 635 – 769 ± 40 °C, 402 – 538 ± 40 °C, and 648 – 795 ± 40 °C respectively for calculations using inner rim garnet data, and 641 – 768 ± 40 °C, 400 – 549 ± 40 °C, and 643 – 798 ± 40 °C respectively for calculations using garnet core data with biotite near garnet (Table 4.1). The highest Ti-bearing biotite analyses were used in the calculations because these represent the highest temperature. Calculations using matrix biotite (1-3 cm away from garnet) resulted in lower temperatures (5 – 50 °C) relative to calculations utilizing biotite near garnet (1-2 mm) in the same sample. This suggests matrix biotite reflects local equilibrium or

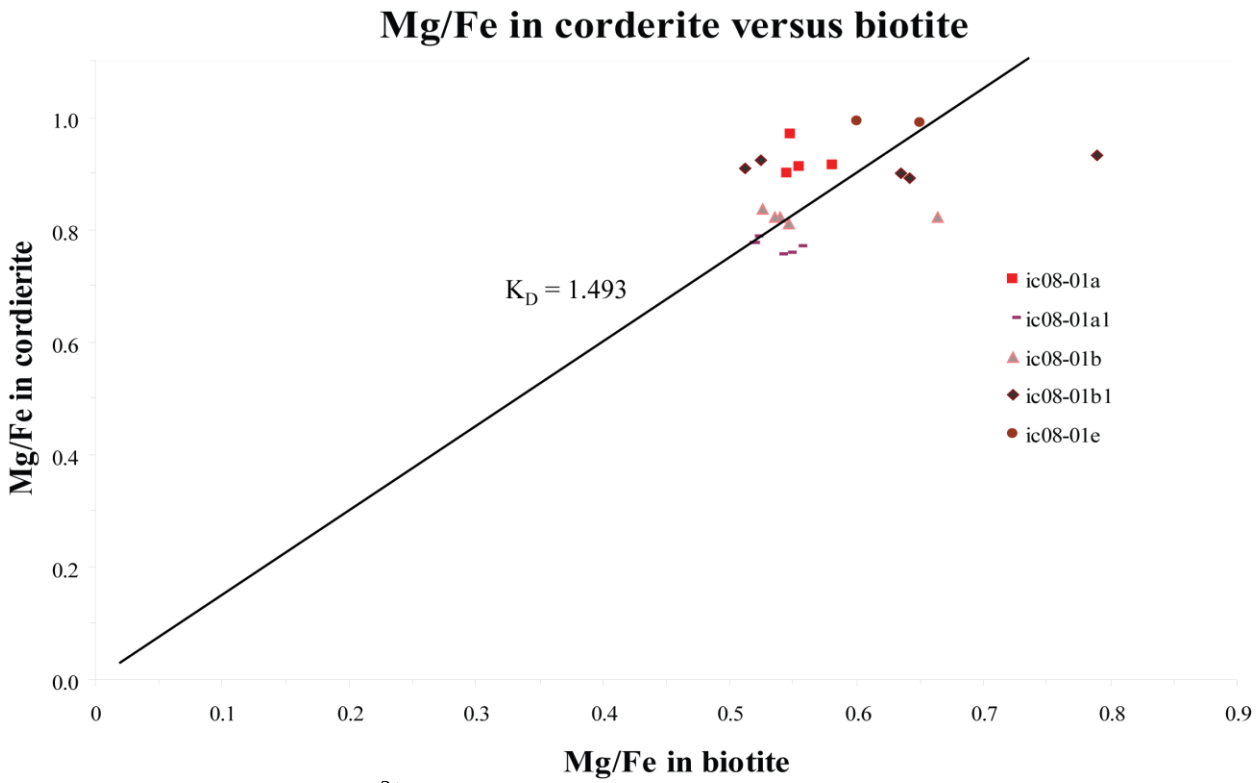

Figure 4.3: K_D plot of Mg/Fe^{2+} in cordierite versus biotite in Iron Creek peraluminous gneiss. Analyses plot along a linear trend with a K_D approximately 1.5 suggesting an approach to chemical equilibrium. Matrix biotite in IC08-0b and IC08-01b1 contain high Mg/Fe^{2+} ratios that do not plot along the linear trend suggesting matrix biotite is not in chemical equilibrium with cordierite.

Table 4.1: Temperature calculations from garnet-biotite calibrations for Iron Creek peraluminous gneiss (Fig. 3.3).

		GB thermometers (˚C)							
		B92-HW		B92-GS		Dasg91		HL77	
sample	grain	inner	rim	inner	rim	inner	rim	inner	rim
			core		core		core		core
ic08-01a	bt 1	717	765	714	768	495	549	743	798
	bt 2	705	751	702	753	484	536	728	782
ic08-01a1	bt 1	765	708	769	703	538	480	795	736
	bt 2	748	693	751	688	517	462	775	718
	matrix bt	745	691	748	686	519	464	772	716
ic08-01b	bt 1	683	712	680	712	444	473	701	732
	bt 2	681	710	678	710	440	469	699	729
	matrix bt	636	662	636	663	402	427	644	671
ic08-01b1	bt 1	703	723	700	723	451	470	727	747
	matrix bt	650	667	648	667	409	425	661	679
	grt 2	645	641	649	645	403	400	648	643
ic08-01e	bt 1	640	667	635	666	409	433	651	678

grt # = garnet grain #, bt # = biotite grain # with high-Ti value, m bt = matrix biotite
Reference P of 6.5 Kbar from intial work by Dutrow et al. (1995)
B92-HW & GS *= Bhattacharya et al. (1992) using models of Mg-Fe mixing*
in garnet from Hackler & Wood (1989) (HW) and Ganguley and Saxena (1984) (GS)
Dasg91 *= Dasgupta et al. (1991)*
HL77 *= Holdaway & Lee (1977)*

resetting. Differences in temperature between garnet in the same samples were less than 40˚C, the associated error. Results from the Dasgupta et al. (1991) calibration are approximately 200 °C lower than other calibrations suggesting it is not reflective of conditions for the Iron Creek peraluminous gneiss. Results from IC08-01a and IC08-01a1 are 50 – 100 °C higher than those from IC08-01b, IC08-01b1, and IC08-01e suggesting garnet and biotite compositions have not been reset in IC08-01a and IC08-01a1.

The garnet-muscovite (GM) thermometer calculates temperature based on the exchange between coexisting garnet and muscovite according to the reaction: pyrope + Fe-celadonite = almandine + Mg-celadonite using the empirical calibration of Wu & Zhao (2006). The same five

samples of peraluminous gneiss from Iron Creek result in temperatures lower than GB and range from 471 – 504 ± 70 °C using garnet core compositions and 550 – 590 ± 70 °C using garnet inner rim compositions (Table 4.2).

The TiB thermometer of Henry et al. (2005) calculates temperature based on Ti content in biotite. This thermometer is calibrated for graphitic, ilmenite-bearing peraluminous rocks that equilibrated between 4-6 kbar pressure and 480 - 800˚C. The Iron Creek peraluminous gneiss is not graphitic, but meets the other criteria suggesting this thermometer underestimates the temperature up to 50 ˚C (Henry et al., 2005). This thermometer yields temperatures from 568 – 624 ± 12 ˚C for IC08-01a, 600 – 651 ± 12 ˚C for IC08-01a1, 565 – 599 ± 12 ˚C for IC08-01b, 613 – 631 ± 12 ˚C for IC08-01b1, and 596 ± 12 ˚C for IC08-01e (Table 4.3). These lower temperature could be due to the lack of graphite in the rocks or resetting of biotite.

Pressures were calculated for five samples of peraluminous gneiss from Iron Creek using two net-transfer geobarometers. The GASP barometer is defined by the equilibrium: grossular + Al-silicate + quartz = 3anorthite (Ghent, 1976). This barometer yields pressures of 4.0 – 5.8 ± 1.5 kbar using inner rim garnet data and 4.3 – 5.8 ± 1.5 kbar using garnet core data (Table 4.4). An error of 1.5 kbar is assumed for all analyses. The reference temperature was taken from the GB calibration of Bhattacharya et al. (1992) for the respective sample. The variability between samples is interpreted as due to resetting of certain mineral phases. Garnet cores record pressure-temperature conditions approximately 20-50 °C and 0.1 – 0.5 kbar greater than inner rim analyses. Calculations using matrix biotite were 0.1 – 1.3 kbar lower than calculations using biotite in plagioclase halos. This could be due to differential resetting of biotite or growth at different pressure-temperature conditions.

The GMPQ barometer is defined by two equilibria: pyrope + grossular + muscovite + quartz = anorthite + Mg-celadonite, and almandine + grossular + muscovite + quartz = anorthite + Fe-celadonite (Wu and Zhao, 2006). The GMPQ barometer was applied to five samples of Iron Creek peraluminous gneiss using the calibration of Wu and Zhao (2006) with a reference temperature calculated with the GM thermometer of Wu and Zhao (2006). These pressure and temperatures were calculated synchronously through iteration pairs. The Mg- and Fe-models yield pressures from 1.2 – 2.5 ± 1.5 kbar for garnet core compositions and 2.7 – 3.8 ± 1.5 kbar for garnet inner-rim compositions (Table 4.2). The anomalously low pressures suggest this calibration is not valid for these rocks.

4.2.2 Amphibole-Bearing Assemblages

Two amphibole-plagioclase thermometers and barometers were used to calculate pressure – temperature conditions for titanite-amphibole-biotite gneisses, biotite-hornblende gneisses, amphibole-pyroxene gneisses, and metagabbros (Fig. 3.2).

The amphibole – plagioclase thermometer of Holland and Blundy (1994) uses the equilibria: edenite + albite = richterite + anorthite for non-quartz bearing assemblages and edenite + 4 quartz = tremolite + albite for quartz bearing assemblages. Temperatures were calculated using plagioclase grain averages with amphibole rim and core averages. These calibration yields temperatures from 658 – 739 °C for rim and 668 – 787 °C for core analyses of titanite- amphibole-biotite gneisses (n=5), 690 – 750 °C for rim and 726 – 754 °C for core analyses of biotite-amphibolites (n=6), and 628 – 631 °C for rim and 637 – 655 °C for core analyses of amphibole-pyroxene gneisses (n=2), with an error of ± 40 °C (Table 4.5).

The amphibole – plagioclase thermobarometer of Gerya et al. (1997) uses the equilibria: edenite + 4 quartz = tremolite + albite and pargasite + 4 quartz = hornblende + albite. This

Table 4.2: Temperature and pressure calculations for Iron Creek peraluminous gneiss using garnet-muscovite (GM) thermometer and garnet-muscovite-plagioclase-quartz (GMPQ) barometer calibrations from Wu and Zhao (2006). Results are subject to an error of ±70°C.

		GM thermometer and GMPQ barometer							
		with garnet core				with garnet inner rim			
		Model A- Mg-celadonite		Model B- Fe-celadonite		Model A- Mg-celadonite		Model B- Fe-celadonite	
Sample	Grain	T(ºC)	P(kbar)	T(ºC)	P(kbar)	T(ºC)	P(kbar)	T(ºC)	P(kbar)
IC08-01a	ms 1	478	1.9	499	2.2	580	3.5	574	3.4
	ms 2	481	2.1	483	2.1	590	3.8	561	3.3
IC08-01a1	ms 1	467	2.4	473	2.5	587	3.2	560	2.8
	ms 2	465	2.3	478	2.5	581	3.0	564	2.8
IC08-01b	ms 1	479	1.2	490	1.4	550	2.9	542	2.8
	ms 2	485	1.2	503	1.5	557	2.9	557	2.9
IC08-01b1	ms 1	471	1.6	472	1.6	552	3.1	531	2.7
	ms 2	474	1.5	487	1.7	554	2.9	546	2.8
IC08-01e	ms 1	511	2.0	520	2.2	562	3.1	557	3.1
	ms 2	500	2.0	501	2.0	549	3.1	536	2.9
	ms 3	504	2.1	503	2.1	554	3.2	539	3.0

Calibration of Wu and Zhao (2006)

Table 4.3: Temperature calculations for Iron Creek peraluminous gneiss using the titanium-in-biotite (TiB) thermometer of Henry et al. (2005). Results are subject to an error of ± 12°C.

TiB thermometer		
sample	grain	Temperature (˚C)
ic08-01a	near garnet	624
	Matrix	568
ic08-01a1	near garnet	600 - 651
	Matrix	620
ic08-01b	near garnet	580 - 600
	Matrix	565
ic08-01b1	near garnet	613
	Matrix	631
ic08-01e	near garnet	596

Ti-in-biotite thermometer from Henry et al. (2005)

Table 4.4: Pressure calculations for Iron Creek peraluminous gneiss using the GASP barometer (Ghent, 1976). Pressure calculations are subject to an assumed error of ±1.5 kbar.

		With Garnet Cores		**With Garnet Inner Rims**	
sample	grain	Reference T (°C) *Bhattacharya et al. 1992*	Pressure (kbar) GASP	Reference T (°C) *Bhattacharya et al. 1992*	Pressure (kbar) GASP
ic08-01a	near garnet	763	5.8	715	5.8
	Matrix bt	749	5.7	703	5.6
ic08-01a1	near garnet	690 - 710	4.4 - 4.6	745 - 760	5.2 - 5.5
	Matrix bt	689	4.4	743	5.2
ic08-01b	near garnet	705 - 710	5.7 - 5.8	680	5.2 - 5.3
	Matrix bt	660	5.0	635	4.6
ic08-01b1	near garnet	665 - 720	4.9 - 5.7	650 - 700	4.6 - 5.3
	Matrix bt	620	4.3	605	4.0
ic08-01e	near garnet	665	4.9	638	4.5

Calculated with Waters' program (http://www.earth.ox.ac.uk/~davewa/pt/pt04.html)

calibration requires plagioclase with greater than 10 percent albite component. Results were calculated using plagioclase grain averages with amphibole rim and core averages. This thermobarometer yields values from 566 – 644 °C and 4.2 – 5.2 kbar for rim and 559 – 654 °C and 4.2 – 5.3 kbar for core analyses from titanite-amphibole-biotite gneisses, 589 – 635 °C and 5.0 – 5.4 kbar for rim and 612 – 633 and 5.3 – 5.4 kbar for core analyses from biotite-amphibolites, 523 –547 °C and 3.5 – 3.9 kbar for rim and 552 – 560 °C and 3.9 – 4.0 kbar for core analyses from metagabbros, and 446 – 474 °C and 2.1 – 2.6 kbar for rim and 481 – 546 °C and 2.6 – 3.6 kbar for core analyses from amphibole-pyroxene gneiss (Table 4.6). All results are subject to an error of ± 40 °C and 1.2 kbar.

The amphibole – plagioclase barometer of Bhadra and Bhattacharya (2007) was used for all amphibole + plagioclase-bearing lithologies. This equilibria is based on the reaction: tremolite + tschermakite + 2 albite = 2 pargasite + 8 quartz. Results were calculated using plagioclase grain averages with amphibole (amp) rim and core averages. Pressures attained are higher and range from 7.2 – 12.2 kbar for amp rim and 6.4 – 10.8 kbar for amp core analyses in titanite-hornblende-biotite gneisses, 9.5 – 12.7 kbar for amp rim and 7.9 – 12.7 kbar for amp core analyses in biotite-amphibole gneisses, and 0.1 – 3.3 kbar for amp rim and 3.5 – 4.9 kbar for amp core analyses in amphibole-pyroxene gneiss (Table 4.7). All results are subject to an error of ± 2.0 kbar. The high-pressure conditions calculated suggest this calibration is not accurate for these rocks.

The low pressure-temperature conditions, 1-3 kbar 450 – 650 °C calculated for amphibole-pyroxene gneiss (Idaho M, Table 4.6, 4.7) are interpreted as reflecting the intrusion of the Sawtooth batholith at shallow levels in the crust. This sample was collected from a “mixed”

Table 4.5: Amphibole-plagioclase temperature calculations on four amphibole-bearing samples in the SMC. Temperatures were calculated for amphibole rim and core analyses.

Amphibole geothermometer from Holland and Blundy (1994)			
lithology	sample	texture/grain	T (°C)
bt-amp gneiss	**ST08-13a**	Rim	690-795
		Core	690-790
ttn-amp-bt gneiss*	**ST08-30a**	Rim	675 - 740
		Core	690 - 740
	ST08-45a	Rim	705-770
		Core	715 - 753
amp-pyx-gneiss*	**Idaho M**	Rim	670-730
		Core	690-735

*quartz-bearing assemblage

Table 4.6: Temperature and pressure calculations of amphibole-plagioclase bearing lithologies in the SMC using the amphibole-plagioclase geothermometer and geobarometer of Gerya et al. (1997).

Amphibole-plagioclase thermobarometry				
lithology	sample	texture	T [C]	P [kbar]
bt-amp gneiss	ST08-13a	Rim	590 - 635	5.0 - 5.4
		Core	610 - 635	5.3 - 5.4
metagabbro	*ST08-15d	Rim	520 - 550	3.5 - 3.9
		Core	550 - 560	4.0
ttn-amp-bt gneiss	ST08-30a	Rim	565 - 580	4.2 - 4.7
		Core	560 - 605	4.2 - 4.8
	ST08-45a	Rim	645	5.2
		Core	640 - 655	5.1 - 5.3
amp-pyx gneiss	Idaho M	Rim	445 - 475	2.1 - 2.6
		Core	480 - 550	2.6 - 3.6

*assumed plagioclase composition of $>Ab_{10}$ due to lack of plagioclase analysis

Table 4.7: Pressure calculations on amphibole and plagioclase bearing lithologies of the SMC using the geobarometer of Bhadra and Bhattacharya (2007).

Amphibole - plagioclase barometer of Bhadra and Bhattacharya (2007)				
lithology	sample	texture	P1 (kbar)	P2 (kbar)
bt-amp gneiss	ST08-13a	Rim	9.5 - 12.3	9.9 - 12.7
		Core	7.9 - 12.6	8.6 - 12.7
ttn-amp-bt gneiss	ST08-30a	Rim	7.2 - 8.4	7.7 - 8.6
		Core	6.4 - 8.8	6.9 - 9.1
	ST08-45a	Rim	10.5 - 11.8	11.1 - 12.2
		Core	9.5 - 10.3	10.2 - 10.8
amp-pyx gneiss	Idaho M	Rim	0.1 - 3	0.1 - 3.3
		Core	3.5 - 4.5	3.6 - 4.9

unit in the valley floor that was originally interpreted as near the contact between the SMC and the Sawtooth batholith. It appears this unit is composed of xenoliths of mafic calc- silicate gneiss of the SMC floating in more felsic material interpreted as the Sawtooth batholith (Fig. 3.54). Amphiboles in Idaho M contain brown magnesio-hornblende cores and green- actinolitic rims (Fig. 3.59). The actinolitic rims are attributed to resetting of the rock at lower pressure-temperature conditions during the intrusion of the Idaho and/or Sawtooth batholith(s).

4.3 Geothermobarometry – Multi-equilibria Approach (TWQ)

The multi-equilibria approach was used in addition to single equilibria geothermometers and geobarometers. Cordierite and plagioclase grain averages with garnet core compositions and high-Ti biotite analyses for each sample were calculated and used in Berman's TWQ program (Berman, 1991). These phases plus quartz and sillimanite represent the equilibrium assemblage of peraluminous gneisses. Zoning observed in garnet is interpreted as late-stage resorbtion of Mn into garnet rims (Henry, pers. comm.). Therefore, garnet core analyses were used in these calculations. The results were calculated for the KFMASH system. Minor components such as manganese were low and had minor affects on results.

Pressure-temperature conditions were developed for IC08-01a, IC08-01a1, IC08-01b, IC08-01b1, and IC08-01e using the intersection of phlogopite + almandine = annite + pyrope (GB) and the grossular + Al-silicate + quartz = 3 anorthite (GASP) equilibria. These intersections define a range of pressure-temperature conditions from 660 – 770 ˚C and 5.2 – 6.7 kbar with results from IC08-01a =724 ˚C and 6.7 kbar, IC08-01a1 = 770 ˚C and 6.0 kbar, IC08-01b = 690 ˚C and 5.6 kbar, IC08-01b1 = 704 ˚C and 5.7 kbar, and IC08-01e = 670 ˚C and 5.3 kbar (Fig. 4.4).

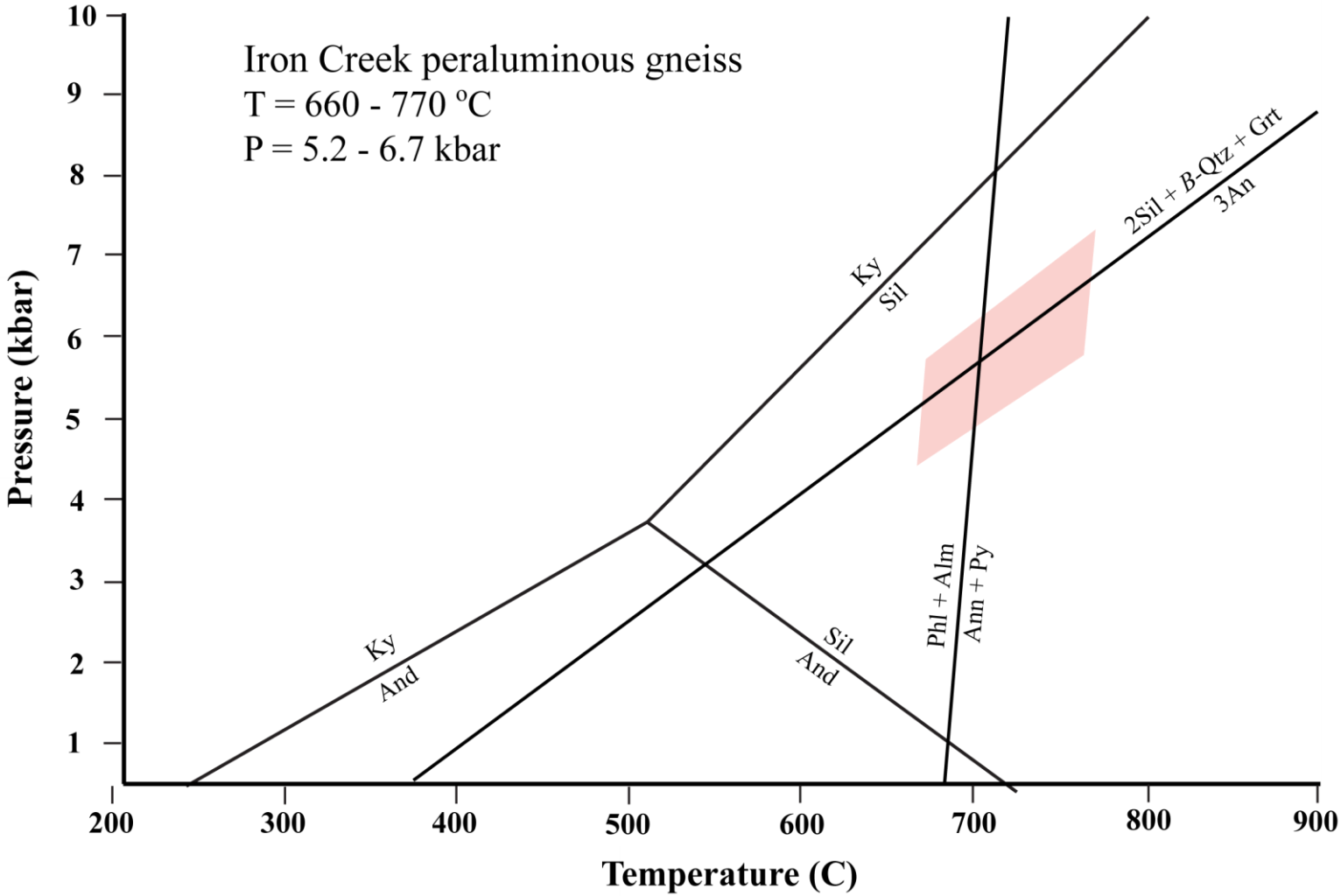

Figure 4.4: TWQ calculation displaying GB and GASP equilibria with Al_2SiO_5 phase boundaries. Intersections of these equilibria for five samples of Iron Creek peraluminous gneiss define a range from 660 – 770 °C and 5.2 – 6.7 kbar indicated by the red trapezoid.

Plots using the phases: garnet + biotite + plagioclase + cordierite + β-quartz + sillimanite for all peraluminous samples contain the following equilibria: (1) grs + β-qtz + 2 sil = 3 an, (2) 2 alm + 2 phl + 5 β-qtz + 4 sil = 3 crd + 2 ann, (3) 2 pyp + 5 β-qtz + 4 sil = 3 crd, (4) 2 ann + 3crd + 5 grs + 6 sil = 2 phl + 15 an + 2 alm, (5) 2 alm + 6 an + 2 phl + 3 β-qtz = 2 grs + 3 crd + 2 ann, (6) 3 crd + 5 grs + 6 sil = 2 pyp + 15 an, (7) 6 an + 2 pyp + 3 β-qtz = 2 grs + 3 crd, (8) alm+ phl = pyp + ann (Table 4.8). The intersection of these equilibria was analyzed by the winTERSX program of Berman (1993) for each sample. This program discards equilibria with slope differences less than 20˚ and intersections that occur ≥1.5 sigma outside the average. These analyses yield the following results: IC08-01a = 670 ± 40 ˚C and 5.8 ± 1.1 kbar (Fig. 4.5), IC08-01a1 = 825 ± 40 ˚C and 6.7 ± 0.5 kbar (Fig. 4.6), IC08-01b = 695 ± 5 ˚C and 5.7 ± 0.1 kbar (Fig. 4.7), IC08-01b1 = 695 ± 5 ˚C and 5.6 ± 0.2 kbar (Fig. 4.8), and IC08-01e = 670 ± 5 ˚C and 5.3 ± 0.2 kbar (Fig. 4.9). The intersections in IC08-01b are clustered most tightly and, therefore, provide the best estimate for pressure-temperature conditions for these samples. IC08-01a1 appears to be weathered, this may account for the high temperatures calculated.

The results from the multi-equilibria approach provide pressure-temperature conditions similar to the Bhattacharya et al. (1992) calibration of the garnet-biotite thermometer and the upper-end of the results from the titanium-in-biotite thermometer of Henry et al., (2005).

These data provide points in pressure – temperature space through which the SMC likely traveled (Fig. 4.10). Combining these data with metamorphic textural observations allow for a pressure – temperature evolutionary path to be interpreted.

Table 4.8: List of equilibria displayed in TWQ calculations of Iron Creek peraluminous gneiss using the minerals: garnet, biotite, plagioclase, cordierite, β-quartz, and sillimanite.

number	equilibria
1	grs + β-qtz + 2 sil = 3 an
2	2 alm + 2 phl + 5 β-qtz + 4 sil = 3 crd + 2 ann
3	2 pyp + 5 β-qtz + 4 sil = 3 crd
4	2 ann + 3 crd + 5 grs + 6 sil = 2 phl + 15 an + 2 alm
5	2 alm + 6 an + 2 phl + 3 β-qtz = 2 grs + 3 crd + 2 ann
6	3 crd + 5 grs + 6 sil = 2 pyp + 15 an
7	6 an + 2 pyp + 3 β-qtz = 2 grs + 3 crd
8	alm + phl = pyp + ann

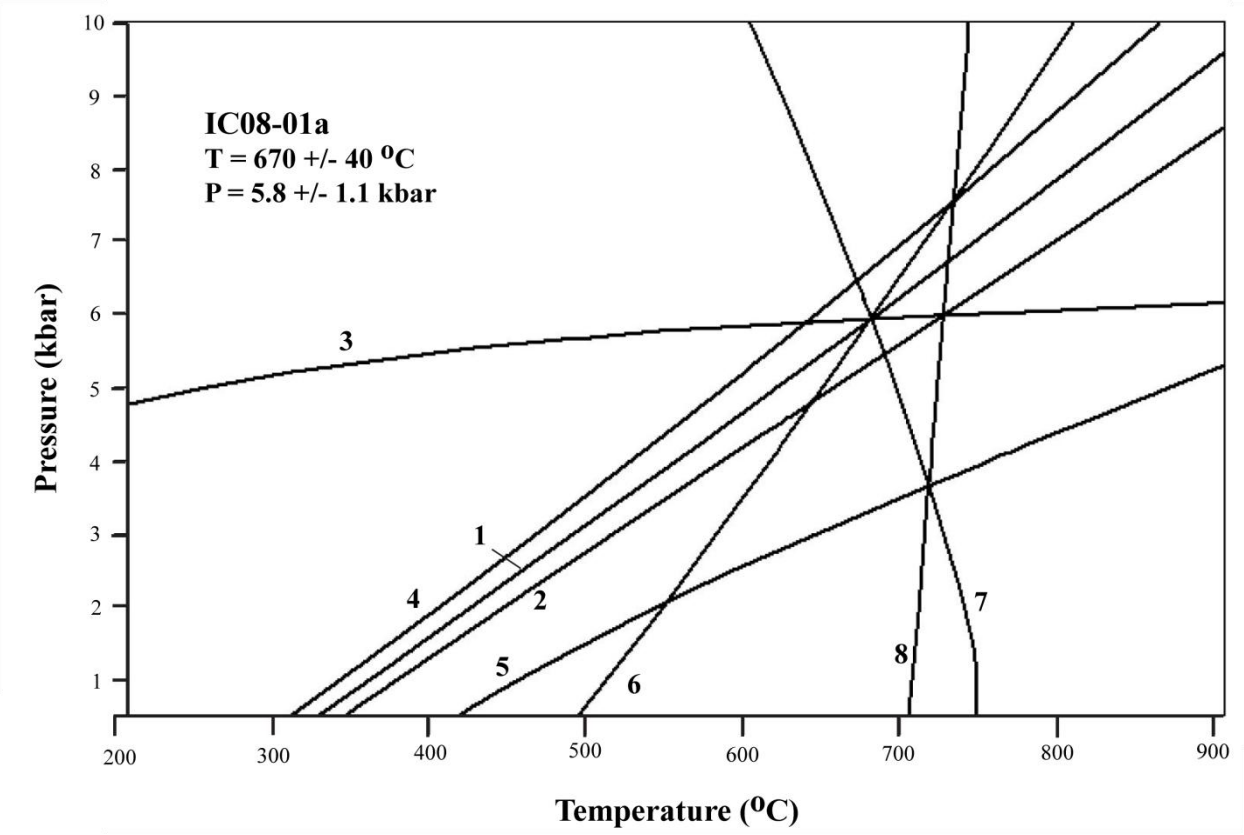

Figure 4.5: TWQ calculation displaying pressure-temperature (P-T) conditions using the phases: garnet, biotite, plagioclase, β-quartz, sillimanite, and cordierite. Multiple equilibria intersections provide a best-fit estimate of T = 670 +/- 40°C and P = 5.8 +/- 1.1 kbar for Iron Creek peraluminous gneiss (IC08-01a).

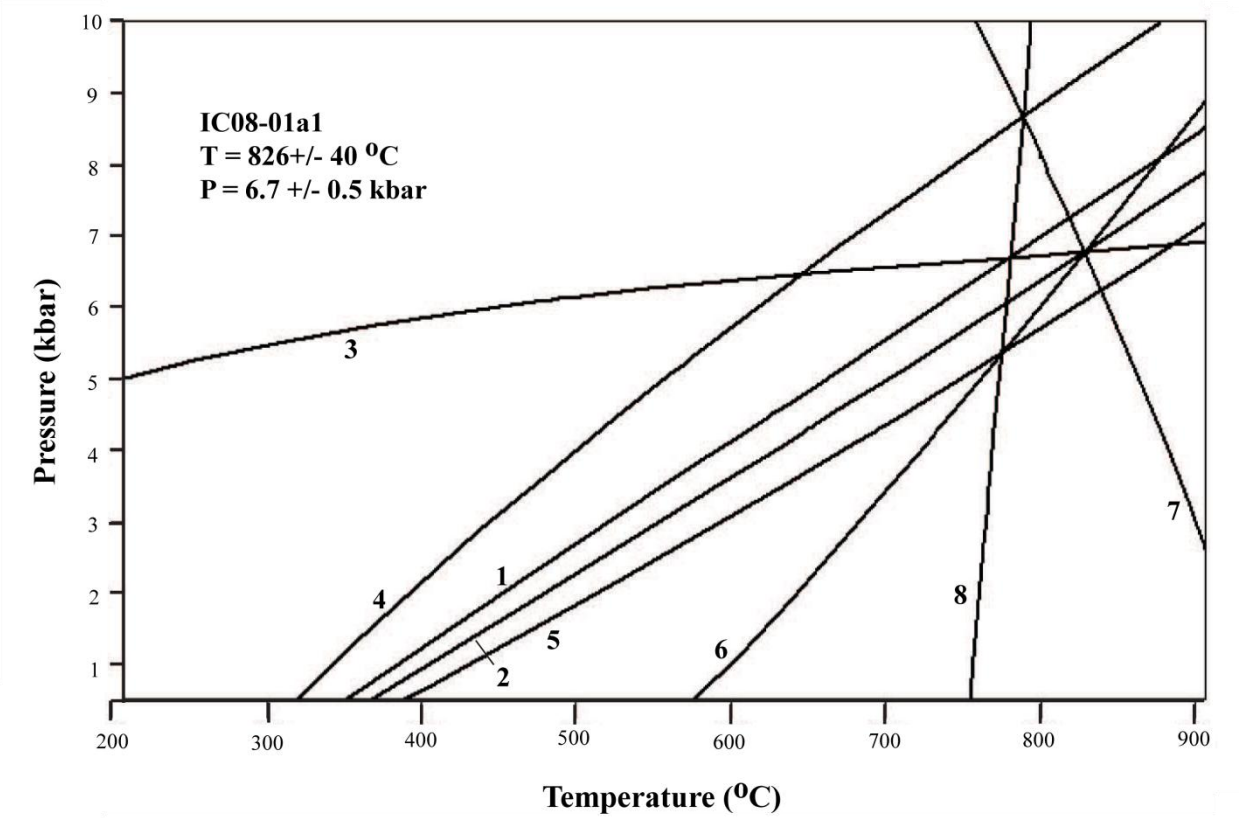

Figure 4.6: TWQ calculation displaying pressure-temperature (P-T) conditions using the phases: garnet, biotite, plagioclase, quartz, sillimanite, and cordierite. Multiple equilibria intersections provide a best-fit estimate of T = 826 +/- 40°C and P = 6.7 +/- 0.5 kbar for Iron Creek peraluminous gneiss (IC08-01a1).

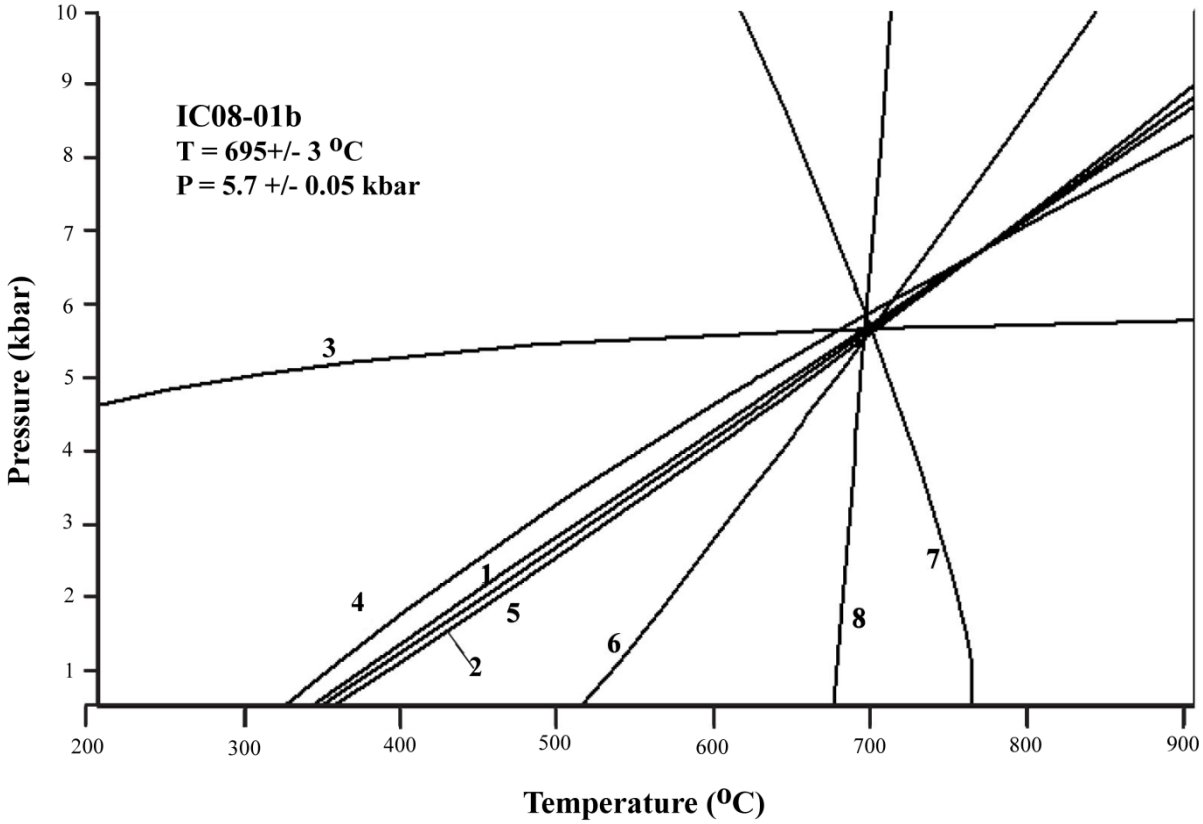

Figure 4.7: TWQ calculation displaying pressure-temperature (P-T) conditions using the phases: garnet, biotite, plagioclase, quartz, sillimanite, and cordierite. Multiple equilibria intersections provide a best-fit estimate of T = 695 +/- 3°C and P = 5.7 +/- 0.05 kbar for Iron Creek peraluminous gneiss (IC08-01b). The tight intersection of equilibria suggest this may be the best estimate of P-T conditions for Iron Creek peraluminous gneiss.

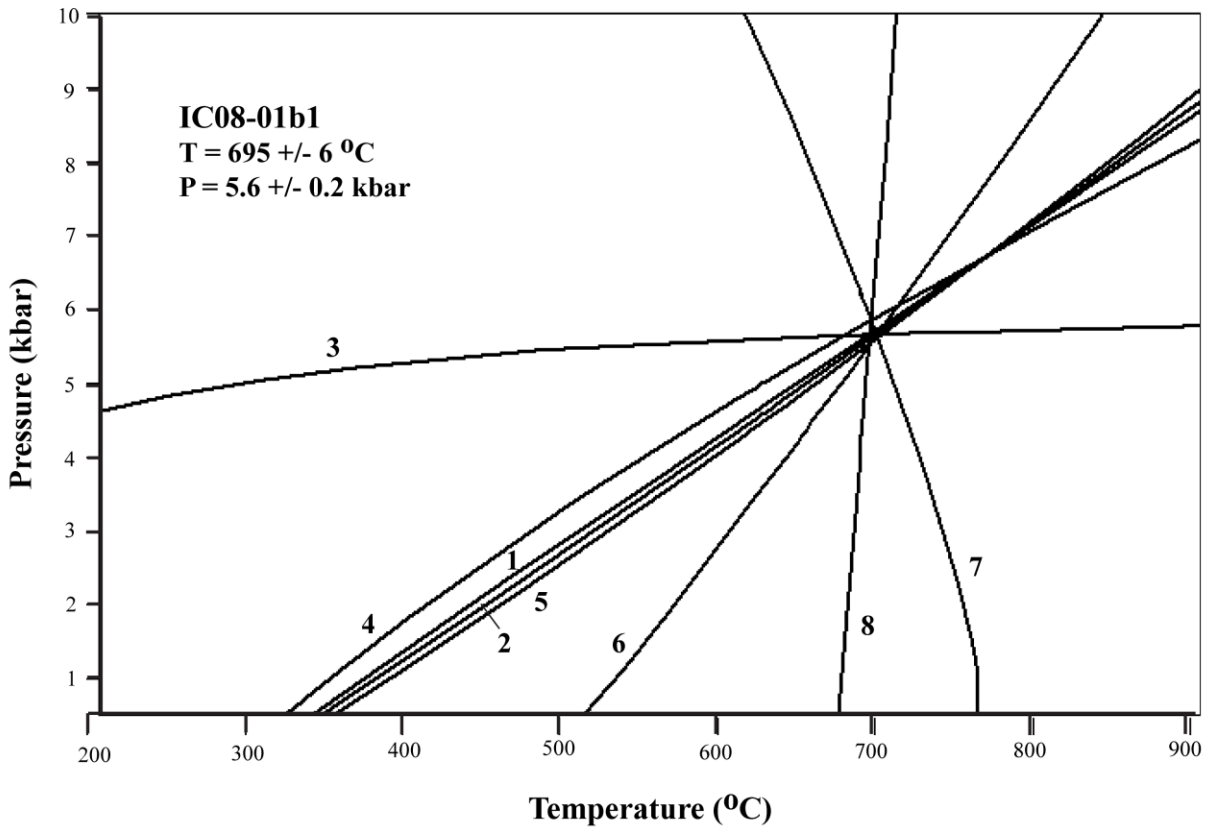

Figure 4.8: TWQ calculation displaying pressure-temperature (P-T) conditions using the phases: garnet, biotite, plagioclase, quartz, sillimanite, and cordierite. Multiple equilibria intersections provide a best-fit estimate of T = 695 +/- 6°C and P = 5.6 +/- 0.2 kbar for Iron Creek peraluminous gneiss (IC08-01b1).

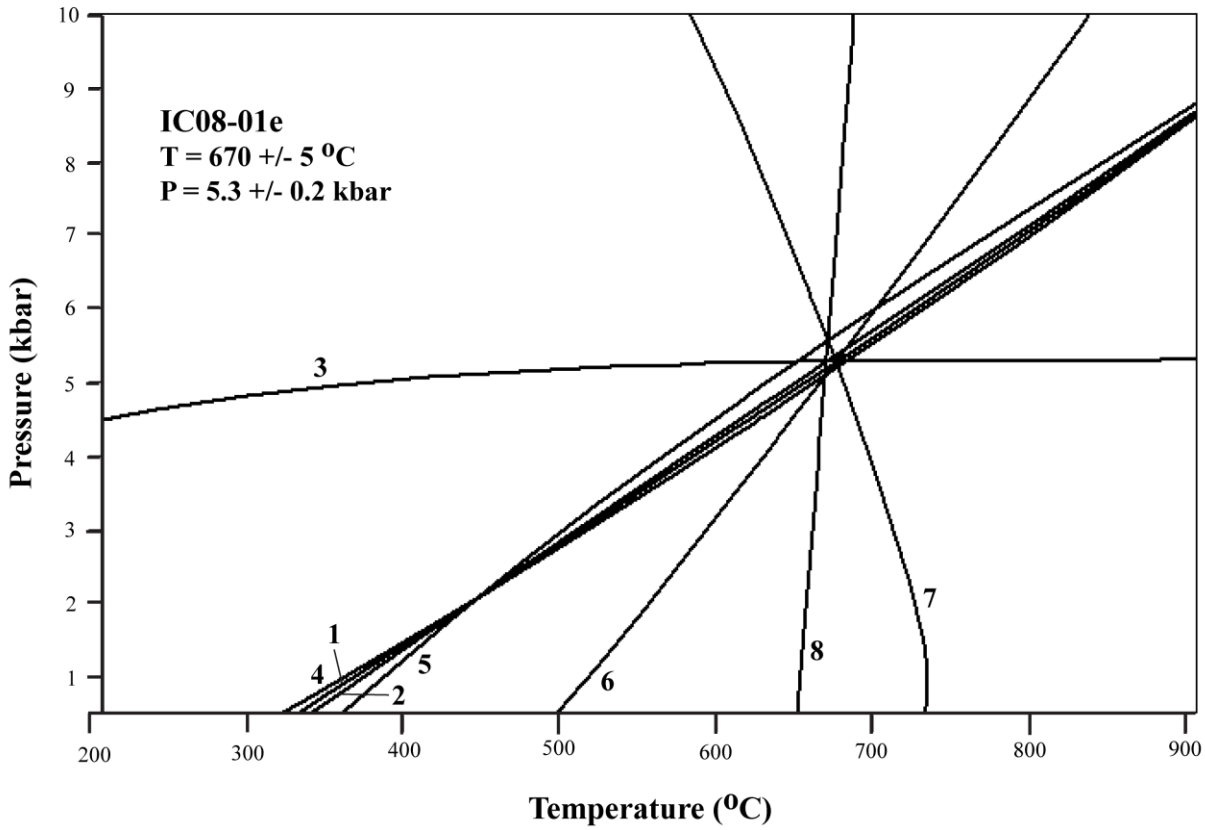

Figure 4.9: TWQ calculation displaying pressure-temperature (P-T) conditions using the phases: garnet, biotite, plagioclase, quartz, sillimanite, and cordierite. Multiple equilibria intersections provide a best-fit estimate of T = 670 +/- 5°C and P = 5.3 +/- 0.2 kbar for Iron Creek peraluminous gneiss (IC08-01e).

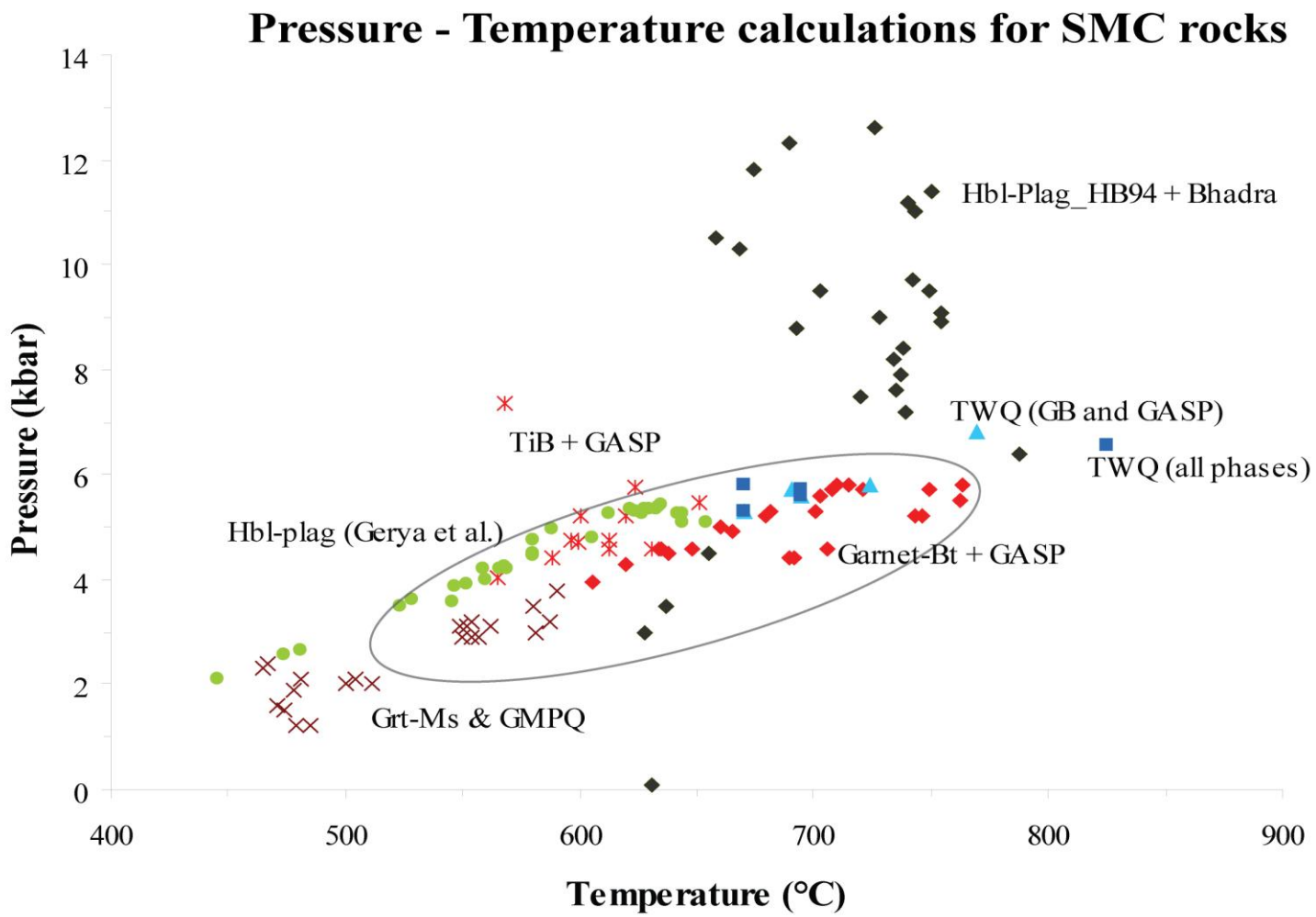

Figure 4.10: Plot of all pressure-temperature calculations for SMC rocks. Most analyses plot within the oval defining a range from ~500 – 800 °C and 3 – 6.5 kbar. Pressure calculations of Bhadra and Bhattacharya (Hbl-Plag_HB94 + Bhadra) are high and plot outside the oval. GM and GMPQ calculations plot at the low P-T side or outside the oval. The best fit conditions are described by GB – GASP thermobarometry and TWQ calculations at approximately 690 °C and 5.75 kbar.

4.4 Metamorphic Textures

Metamorphic textures in all samples of Iron Creek peraluminous gneiss provide insight into metamorphic history occurring through the pressure-temperature evolution of the SMC. Relative timing of these textures and associated reactions is interpreted through inclusion patterns, crosscutting relationships, and secondary mineral formation. In chronologic order, these textures are: (1) sillimanite in garnet, (2) embayed muscovite and K-feldspar with sillimanite, (3) disseminated sillimanite and biotite in cordierite, (4) deformation of cordierite + sillimanite + biotite + muscovite around garnet grains, (5) plagioclase halos around garnet, (6) sillimanite mats replacing cordierite, (8) tabular muscovite cross cutting deformational fabric, and (9) large euhedral andalusite crystal overprinting deformational fabric. These textures are described and interpreted below.

Aligned needles of sillimanite occur within garnet in Iron Creek peraluminous gneiss (Fig. 4.11). This suggests that sillimanite was present before and durring garnet growth, and that garnet grew within the sillimanite field.

The pelitic assemblage of Iron Creek peraluminous gneiss contains embayed muscovite parallel to the main foliation (Fig. 4.12) suggesting muscovite is breaking down and that temperature conditions are above muscovite stability. In addition, K-feldspar is present in the leucosome assemblage and occurs near sillimanite (Fig. 4.13) supporting the interpretation of muscovite decomposition through the dehydration reaction: muscovite + quartz → K-feldspar + sillimanite + H_2O. This reaction produces fluid that could promote partial melting and the beginning of migmatization.

Fine-grained sillimanite and biotite are disseminated throughout poikiloblastic cordierite suggesting cordierite growth at the expense of sillimanite and biotite (Fig. 4.14). This texture

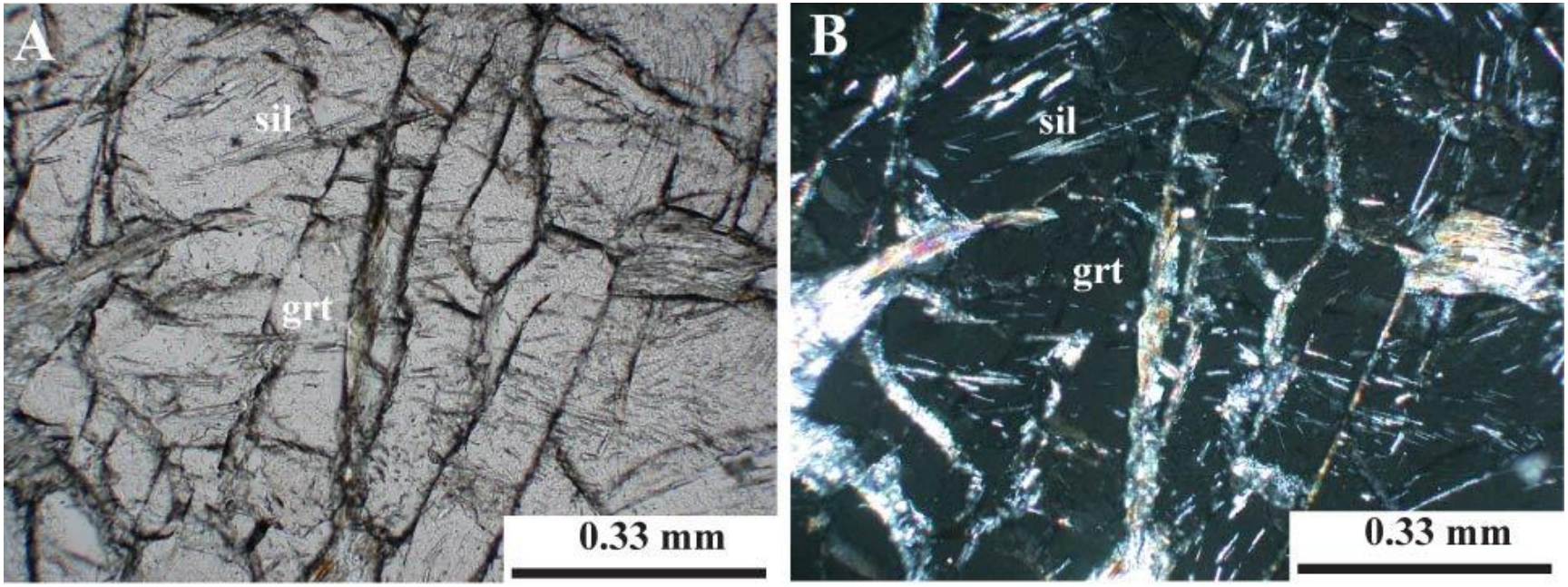

Figure 4.11: Photomicrographs in PPL (A) and XPL (B) of aligned sillimanite in garnet in Iron Creek peraluminous gneiss (IC08-01b1) indicating sillimanite was present before and during garnet growth.

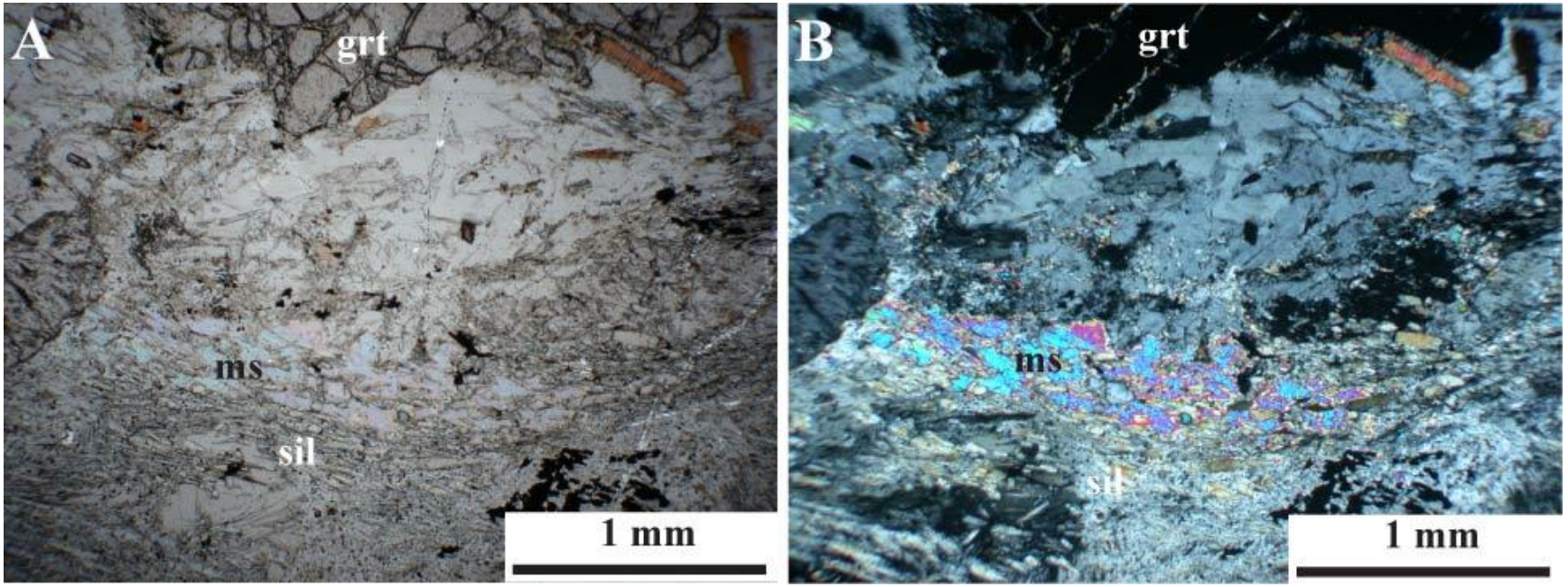

Figure 4.12: Photomicrographs in PPL (A) and XPL (B) of embayed muscovite in Iron Creek peraluminous gneiss (IC08-01b). Texture suggests the rocks attained temperatures above the muscovite stability field.

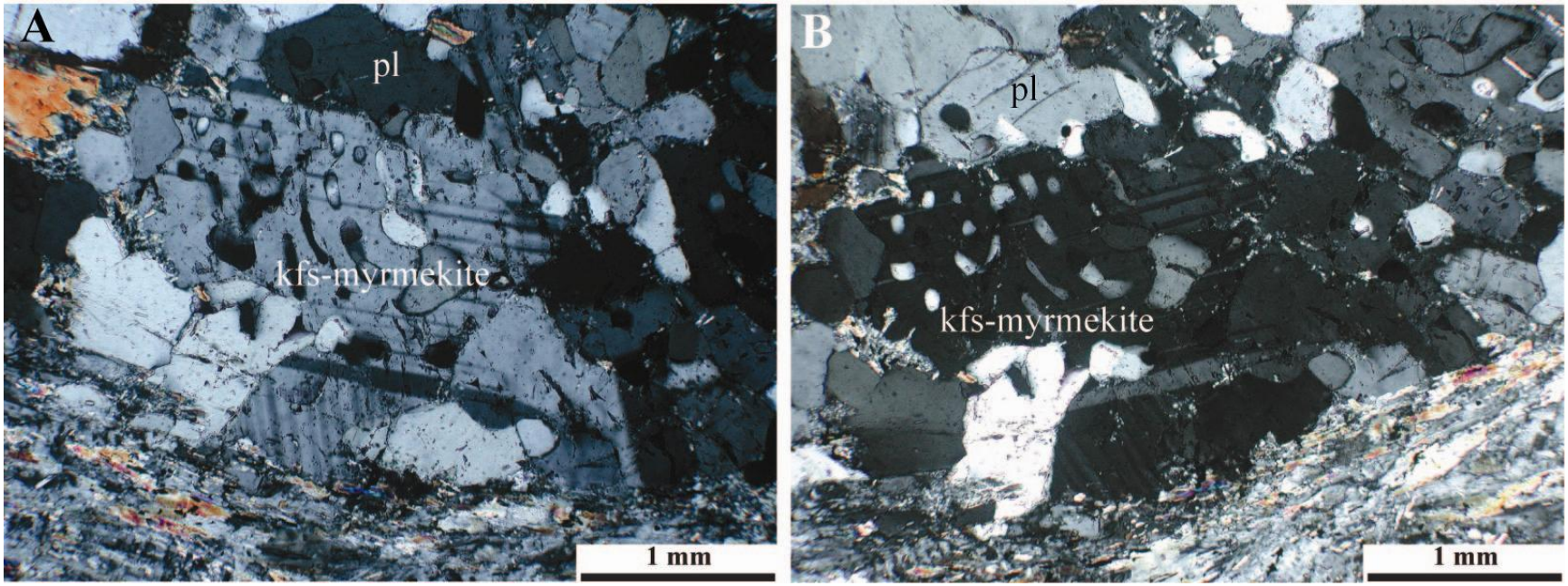

Figure 4.13: Photomicrographs in XPL of Iron Creek peraluminous gneiss (IC08-01b) displaying myrmekitic alkali-feldspar and sillimanite suggesting muscovite breakdown.

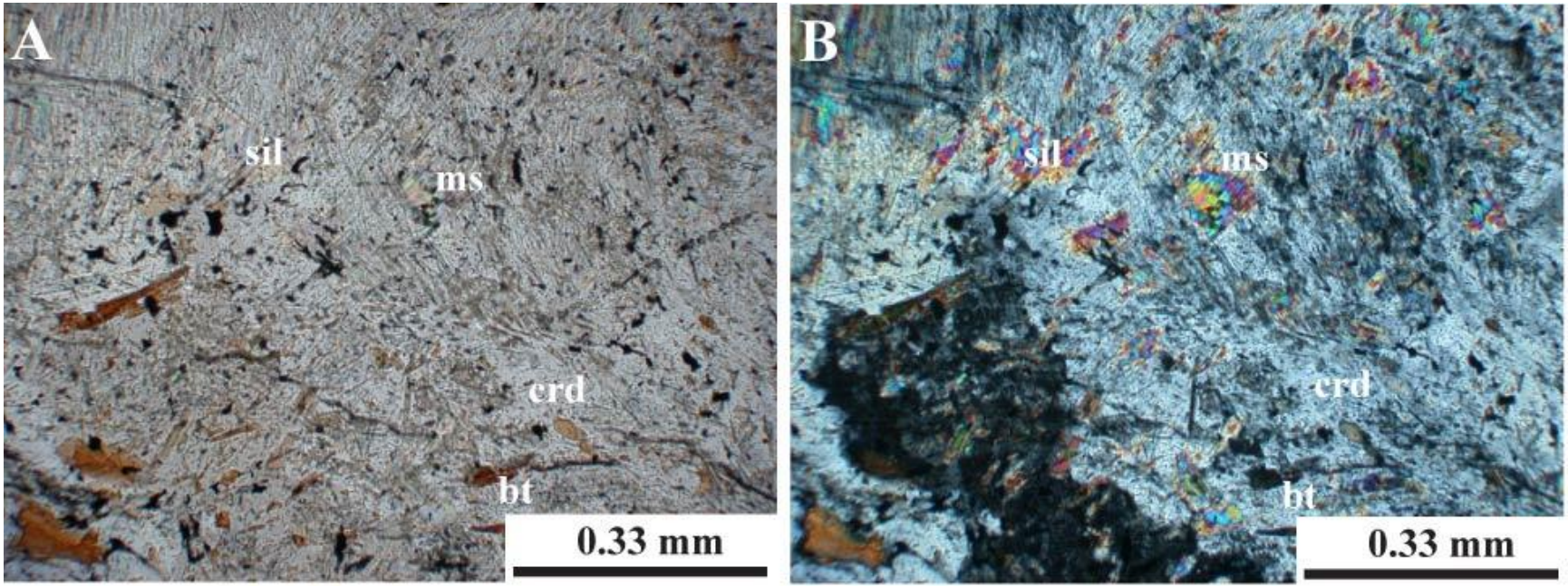

Figure 4.14: Photomicrographs in PPL (A) and XPL (B) of disseminated sillimanite and biotite in poikiloblastic colorless cordierite (IC08-01b). This texture suggests that cordierite growing at the expense of biotite and sillimanite through the reaction: biotite + sillimanite → garnet + cordierite + H_2O. This biotite dehydration reaction produces a large volume of H_2O that could be responsible for partial melting and migmitization and marks peak metamorphic conditions.

describes the dehydration reaction: biotite + sillimanite → garnet + cordierite + H_2O. This reaction produces large volumes of supercritical H_2O that allow for partial melting of felsic minerals and migmatization to occur. This is the highest pressure-temperature reaction recorded in the rocks, therefore, peak metamorphic conditions are marked by migmatization and partial melting interpreted at approximately T = 800 °C and P = 7 kbar.

After peak metamorphic conditions were reached, several metamorphic textures record retrograde metamorphic reactions. Fibrous mats of sillimanite occur in poikiloblastic cordierite (Fig. 4.15) suggesting a second phase of sillimanite growth through the reversal of the previously described reaction (i.e. garnet + cordierite + H_2O → biotite + sillimanite). This reaction requires the presence of H_2O to occur. Therefore, it is interpreted that this reaction did not reach completion because H_2O escaped the system and was not present in sufficient quantities, allowing the preservation of prograde textures.

The main deformation is marked by biotite, sillimanite, muscovite, and cordierite deforming around elongate garnet (Fig. 4.15). Because these phases are incorporated into the deformation, this indicates that deformation occurred after growth of the phases described previously. Plagioclase halos occur around garnet and appear to be replacing deformed garnet (Fig. 4.16) indicating a post-peak decompression texture (D. Henry, pers. comm..).

Tabular muscovite, perpendicular to the main foliation, cross-cuts the primary rock fabric (Fig. 4.17). This suggests the muscovite is secondary and that the rocks passed back into muscovite stability along the retrograde pressure-temperature path.

Large euhedral andalusite crystals (<1 – 6 mm in length) (Fig. 4.18) occur in all samples of peraluminous gneiss and indicate that the rocks passed through the andalusite field (less than 3.5 kbar) during their retrograde history.

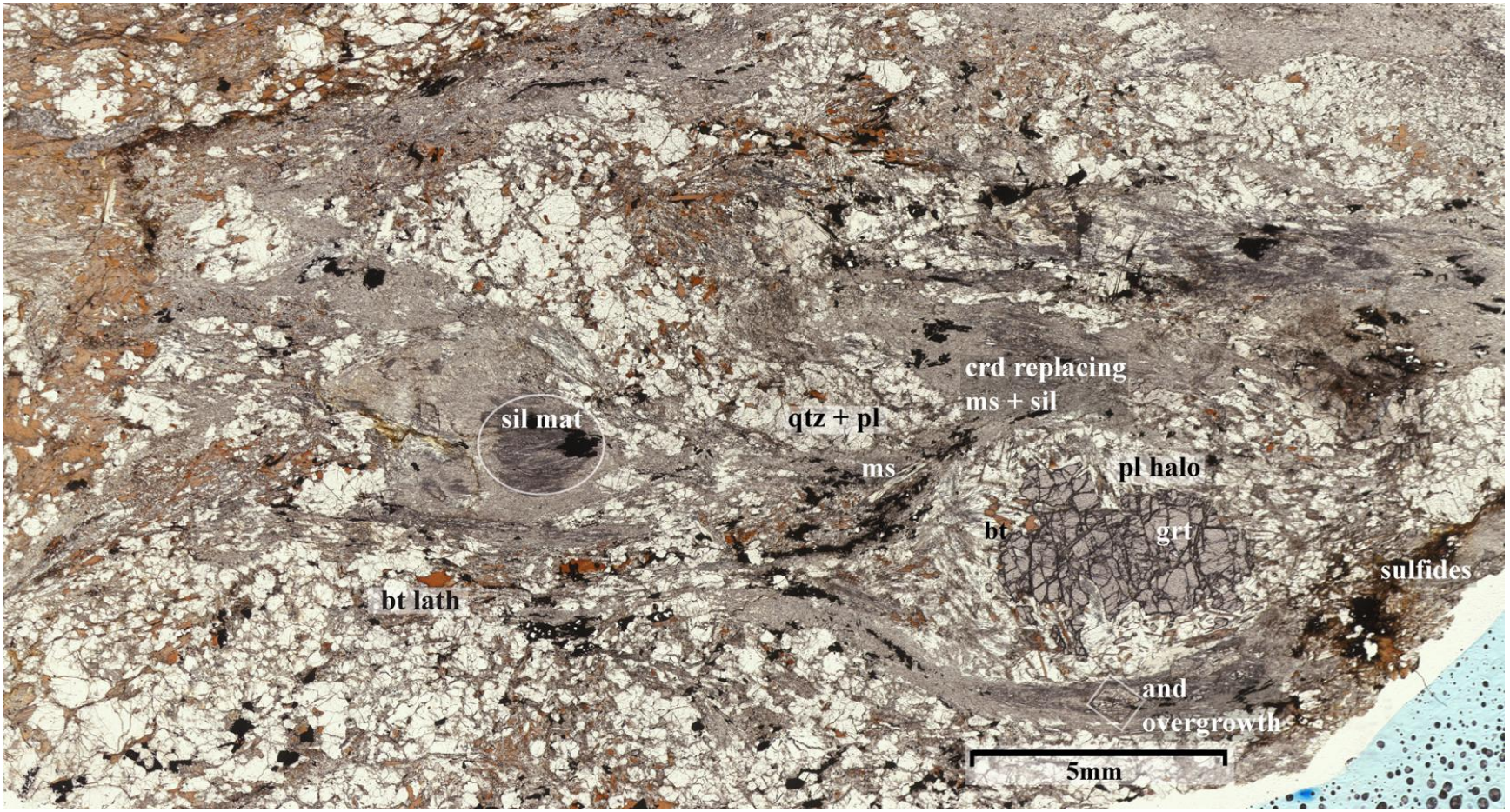

Figure 4.15: Thinsection scan of Iron Creek peraluminous gneiss (IC08-01b1) displaying main deformation/foliation, bimodal distribution of minerals, and sillimanite mat replacing cordierite. The main deformation is recorded by the pelitic assemblage deforming around garnet grains. Plagioclase halos surround and appear to be replacing deformed garnet.

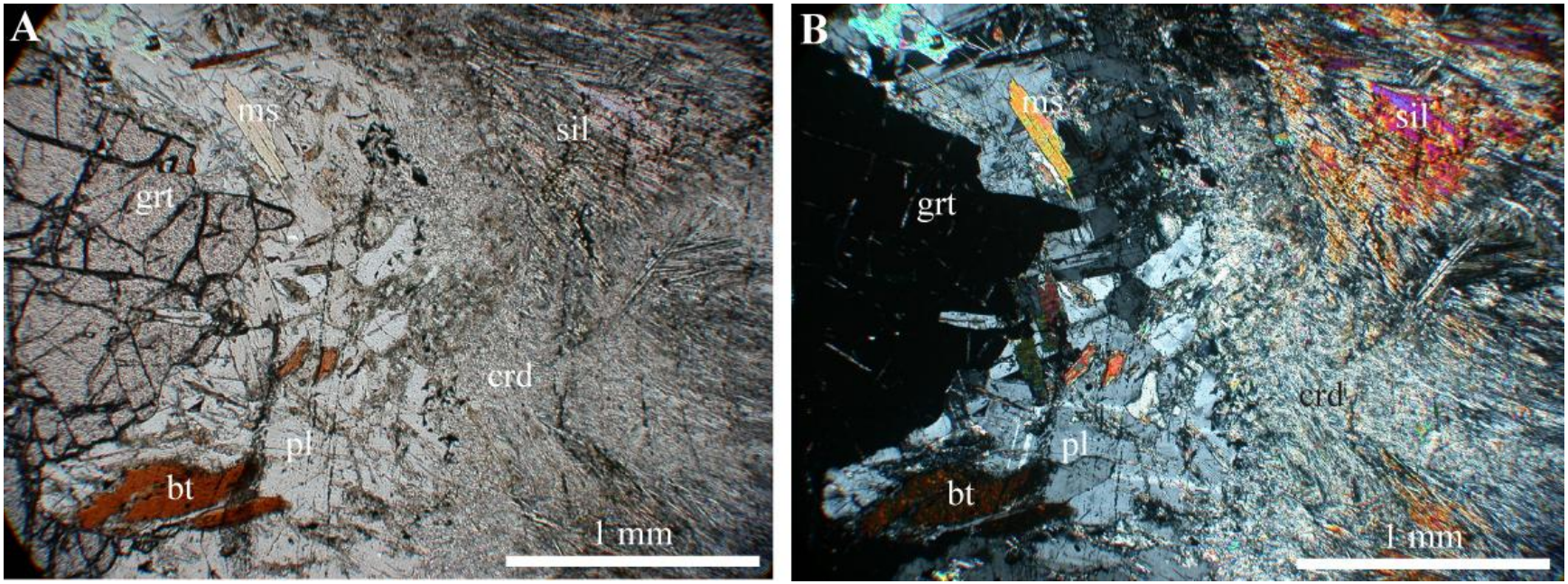

Figure 4.16: Photomicrographs in PPL (A) and XPL (B) of plagioclase halo surrounding garnet in Iron Creek peraluminous gneiss (IC08-01b). Plagioclase appears to be replacing deformed garnet. Tabular muscovite and biotite occur parallel with the main rock fabric within the halo. Cordierite and sillimanite fold around garnet/plagioclase defining the main foliation.

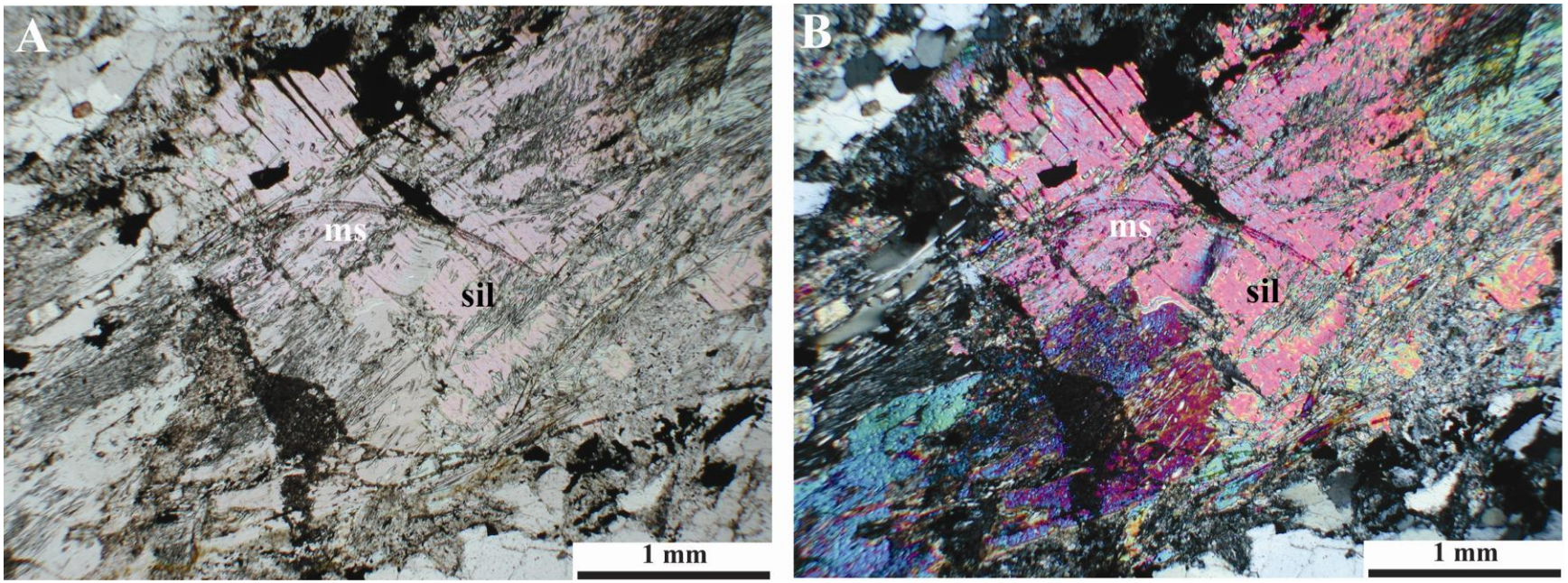

Figure 4.17: Photomicrographs in PPL (A) and XPL (B) displaying tabular muscovite cross-cutting the main foliation (IC08-01b1). This suggests muscovite grew after peak metamorphism.

Coupling metamorphic textures, interpreted reactions, and pressure-temperature (P-T) calculations define a clock-wise P-T path for the Iron Creek peraluminous gneisses (Fig. 4.19). A clock-wise P-T path suggests metamorphism through collisional processes. Little-to-no evidence of the prograde path is preserved in samples of the Iron Creek peraluminous gneiss, therefore, an interpreted prograde path of increasing pressure and temperature represents burial of the rocks. At some point along the prograde path, the rocks cross into the sillimanite field. In the sillimanite field, the rocks pass beyond muscovite stability such that dehydration melting occurs to produce isolated migmatites in the area. Approaching peak conditions, garnet + cordierite growth occurs through the dehydration of sillimanite and biotite generating fluid with partial melting and migmitization. Production of migmatites is interpreted as peak metamorphism along the partial melting curve at ~800 °C and 7 kbar. Subsequently, the rocks experience a decrease in pressure and temperature such that mats of sillimanite locally replace cordierite, plagioclase replaces garnet, and tabular muscovite replaces K-feldspar. A kink in the P-T path results from a pressure decrease. This is interpreted as tectonic de-roofing and is required for the rocks to drop into the andalusite field.

Comparing P-T paths across the SMC provides insight into the continuity of metamorphic history across the SMC. A composite P-T path generated by Dutrow et al. (1995) displays a clock-wise P-T metamorphic history for rocks from the Thompson-Peak area (Fig. 1.8). Overlaying the P-T path calculated from Iron Creek it is clear these parts of the SMC suggest similar peak and post-peak metamorphic conditions, but different retrograde paths (Fig. 4.20). The Thompson Peak rocks remained at high-pressure conditions (4 – 5 kbar), indicated by a kyanite pseudomorph after margarite, whereas, the Iron Creek rocks experienced lower pressure conditions (less than 3.5 kbar) in the andalusite field.

The garnet-sillimanite-biotite gneiss in the Thompson Peak area (mapped by Dutrow et al., 1995) is similar in bulk-rock composition to the Iron Creek peraluminous gneiss (Fig. 4.21). Plagioclase halos surround garnet (ibid.). However, the Thompson Peak samples contain greater modal amount of biotite (20 – 45 %) that define a moderate-strong foliation and include fine-grained sillimanite needles accounting for 5 – 20 modal amount. No cordierite is observed (ibid.). Lack of cordierite and abundance of tabular biotite suggests the Thompson Peak rocks did not record the reaction: biotite + sillimanite → garnet + cordierite + H_2O. This reaction produces H_2O and partial melting that allows the rocks to deform more readily. The foliation in the Thompson Peak rocks is weaker than in the Iron Creek rocks, suggesting Thompson Peak rocks did not experience the same deformational history. This could be attributed to the earlier uplift of the Iron Creek rocks, and/or lack of H_2O in Thompson Peak garnet-sillimanite-biotite gneiss.

Calculated pressure-temperature conditions are similar in Thompson Peak and Iron Creek. Thompson peak garnet-sillimanite-biotite gneisses TWQ calculations record conditions of 765 ± 10°C and 6.54 ± 0.11 kbar (Table 1.1, Dutrow et al., 1995), whereas Iron Creek peraluminous gneisses record conditions of 670 – 825 ± 40°C and 5.3 – 6.7 ± 0.5 kbar.

Similar bulk rock compositions, peak metamorphic conditions, post-peak metamorphic conditions, and interpreted prograde-peak P-T paths coupled with different textures and interpreted retrograde paths between Thompson Peak and Iron Creek suggest the SMC is composed of two or more tectonic slices of rock from the mid-lower crust that experienced similar peak metamorphic conditions, but different uplift / exhumation histories.

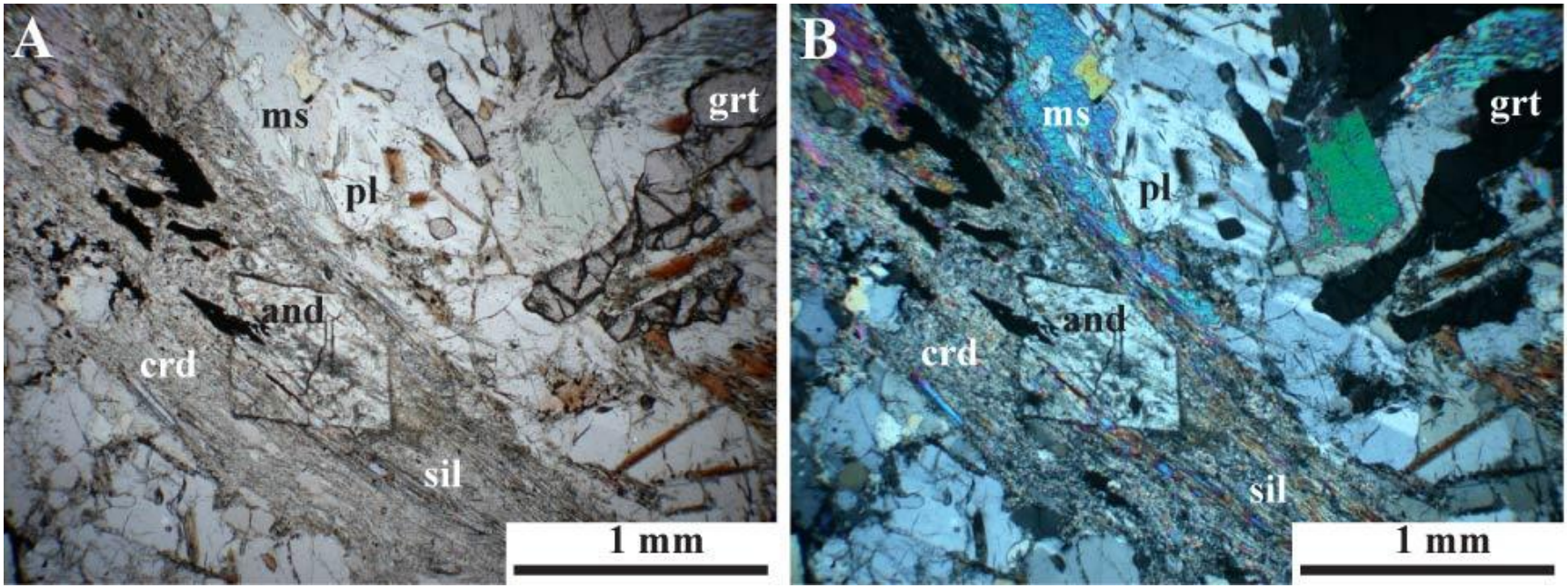

Figure 4.18: Photomicrographs in PPL (A) and XPL (B) of Iron Creek peraluminous gneiss (IC08-01b) displaying euhedral andalusite overprinting main foliation indicating post-peak and post-deformation overprinting.

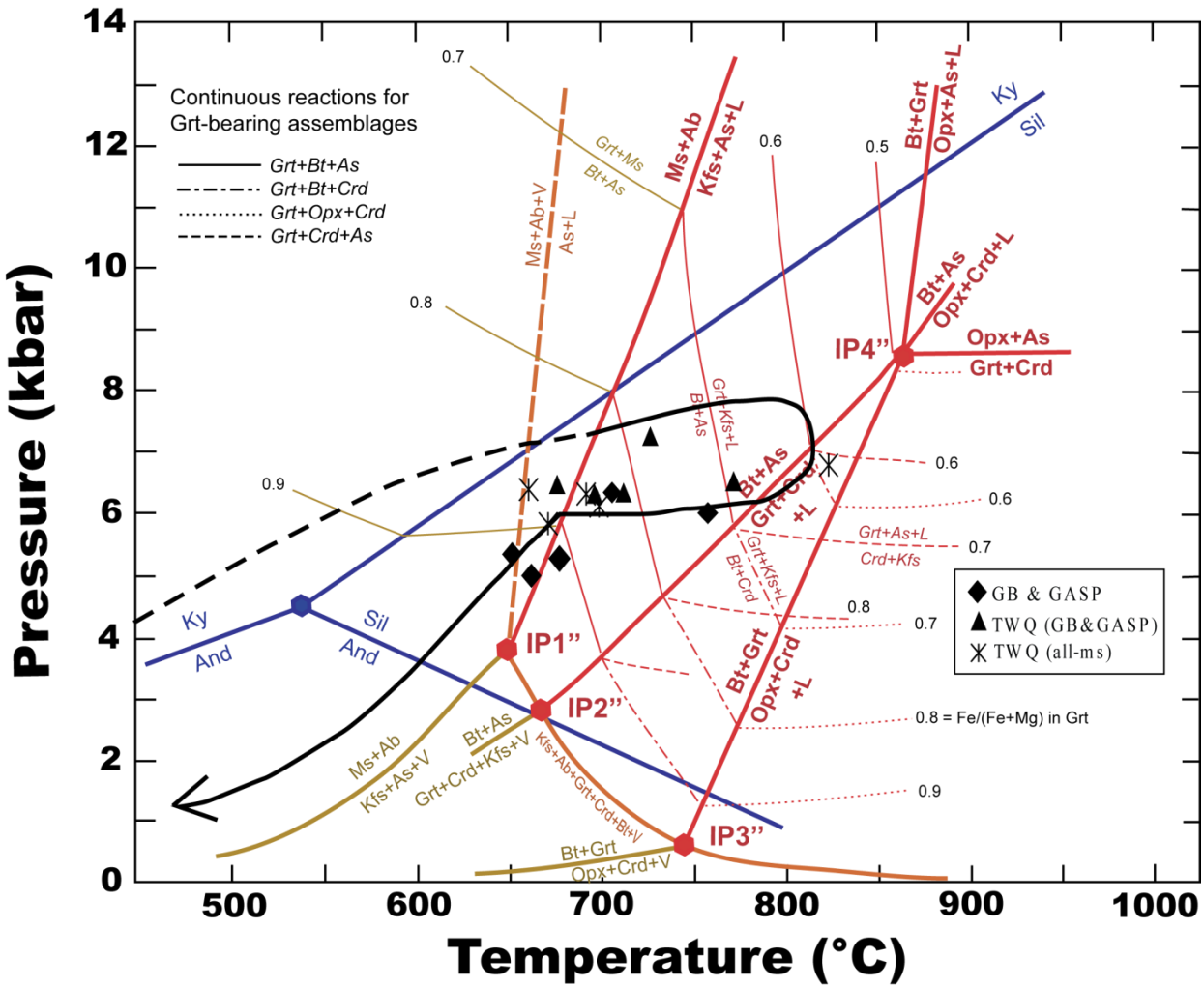

Figure 4.19: Petrogenetic grid displaying continuous reactions for garnet-bearing peraluminous gneiss (Spear et al., 1999), estimated pressure-temperature (P-T) path and calculated P-T conditions for five samples of Iron Creek peraluminous gneiss. The prograde path is represented by a dashed line due to a lack of evidence. The rocks cross into the sillimanite field followed by muscovite dehydration (first bold red-line). Here, partial melting occurs. Peak metamorphic conditions are estimated at ~800 °C and 7 kbar where garnet + cordierite occur (second bold line) And fluid isgenerated that contributes to partial melting and migmitization of the rocks. P-T conditions calculated from five samples of Iron Creek peraluminous gneiss record post-peak conditions from ~625-775 and 5-6.75 kbar. The rocks experienced a decrease in pressure and temperature to reside in the andalusite stability field A clockwise P-T path suggests metamorphism in a collisional environment followed by uplift and erosion during the Tertiary.

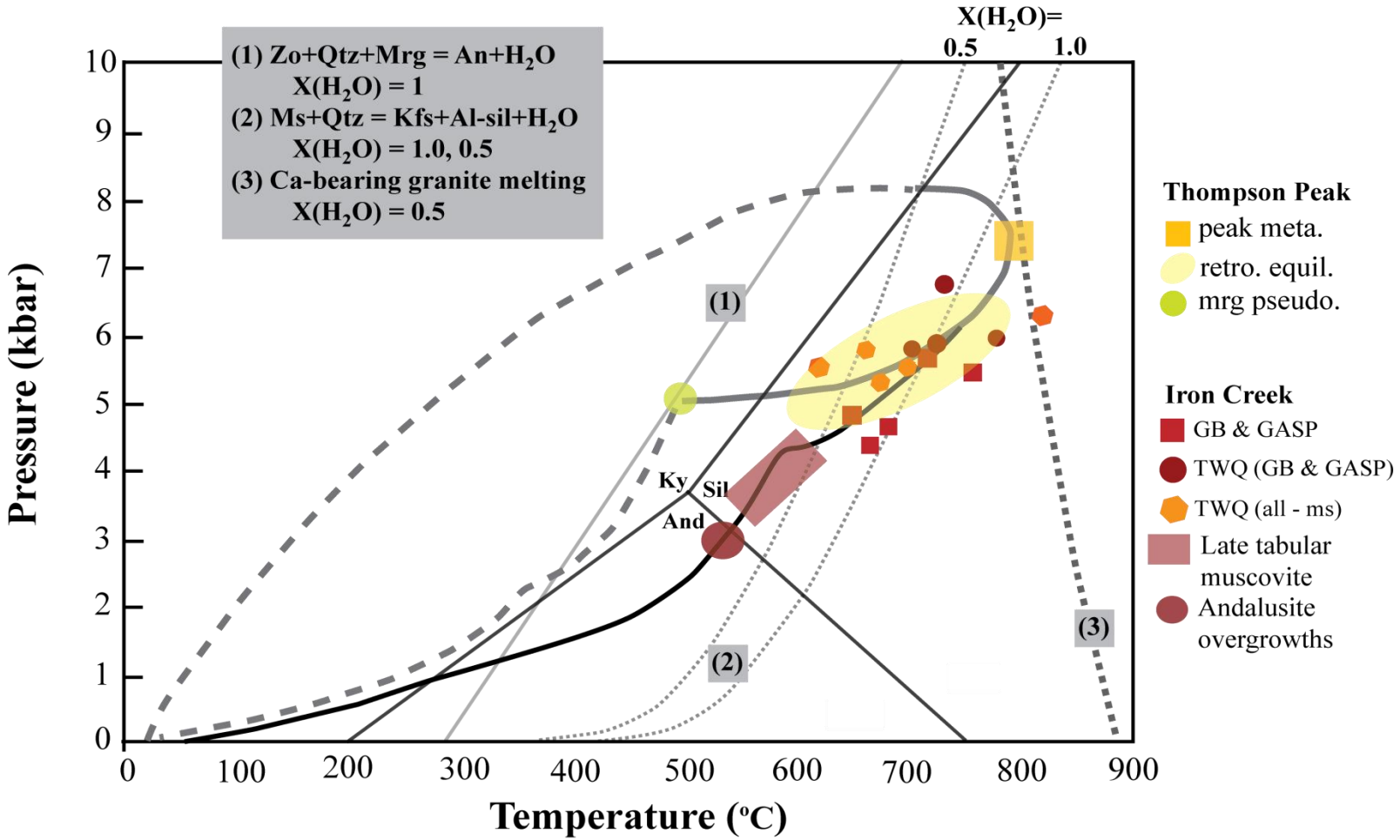

Figure 4.20: Comparison of P-T paths from Iron Creek (this study) with Thompson Peak (Dutrow et al., 1995). Similar peak conditions are observed at ~800 °C and 7 kbar, with post-peak conditions range from 625 – 825 °C and 4 – 6.75 kbar for Iron Creek rocks versus 625 – 775 ˚C and 5 – 7 kbar for Thompson Peak rocks. The Thompson Peak rocks remained at higher pressures as indicated by a margarite pseudomorph of kyanite (Dutrow et al., 1995), whereas the Iron Creek rocks passed through conditions of andalusite stability. The similarities suggest the two areas of the SMC experienced similar peak conditions, but the difference between the two retrograde paths suggests the SMC is composed of two or more tectonic slices of rock from the mid-lower crust.

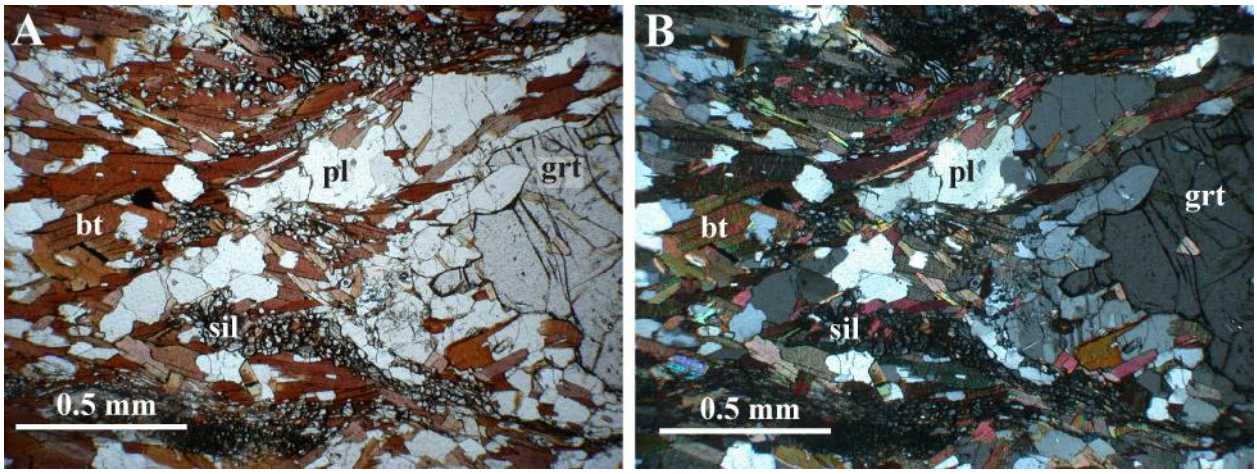

Figure 4.21: Photomicrographs in PPL (A) and XPL (B) of garnet-sillimanite-biotite gneiss (ST95-08) from the Thompson Peak area. Medium-grained tabular biotite is common throughout the sample and defines a moderate-strong foliation. Plagioclase halos surround deformed garnets. Coarse sillimanite crystals are present throughout the foliation.

4.5 Protolith Interpretations / Tectonic Setting

Bulk-rock compositions coupled with mineral textures are used as evidence for interpreting the protoliths within the SMC. Metamorphic textures used for interpreting the style of metamorphism (i.e. collisional) are coupled with lithologic associations and protolith interpretations to form a depositional setting and tectonic environment for the evolution of the SMC.

Bulk-rock compositions (i.e. quartzites, marbles, and peraluminous gneisses) suggest a sedimentary protolith for most SMC lithologies. Quartzites contain ≥ 90 percent quartz, suggestive of a pure quartz arenite protolith. Quartzites are often interlayered with quartzofeldspathic gneiss or grade into quartzofeldspathic gneiss along contacts with other units such as biotite-amphibole gneisses. Gradational contacts such as these suggest a sedimentary protolith. The abundance of quartz and feldspar components suggests an arkosic sandstone protolith. Peraluminous gneisses require an aluminous protolith, such as shale. Calc-silicate gneisses contain minor calcite and Ca-rich minerals, such as albite, Ca-amphibole, and

clinozoisite suggesting a protolith with carbonate and silicate minerals such as calcite-cemented arkosic sandstones. Marbles contain abundant fine-grained calcite and/or dolomite with accessory graphite suggestive of an organic-rich limestone protolith. Biotite-amphibolite and titanite-amphibole-biotite gneisses contain abundant amphibole and Ti-rich minerals such as titanite, ilmenite and rutile. These minerals suggest a volcano-clastic sandstone. Idaho M, the amphibole-pyroxene gneiss, contains abundant albite, diopside, calcic-amphibole, and quartz. These minerals are indicative of calc-silicate gneiss. However, abundant biotite suggests input from an aluminous source. Therefore, the protolith is interpreted as interbedded carbonate-cemented arkosic sandstone and shale. Actinolite present in this unit is interpreted as a later metamorphic event.

The depositional environment for SMC protoliths can be interpreted from unit characteristics and protolith types. Limestones suggest deposition in relatively shallow water with little-to-no clastic sediment input whereas shales suggest deposition in deep-water or a low-energy environment. Volcanic sandstones imply sediments were derived from a volcanic source. Gradational contacts preserve stratigraphic relationships, but more commonly, sharp contacts between units are intruded with Tertiary dikes from regional volcanic activity. Sharp contacts could represent tectonic mixing of original SMC rocks.

These rock types suggest deposition along the flanks of a magmatic arc. A volcanic source supplied pulses of sediment, that were controlled by tectonic processes (i.e. periods of accretion/uplift followed by tectonic quiescence).

This depositional setting coupled with the collisional (clock-wise) pressure-temperature path calculated for SMC metasedimentary rocks suggests that accretion of magmatic arc-like terranes buried the SMC protoliths to 21 – 28 km depth (~7 kbar) where they were subjected to

amphibolite to lower-granulite facies metamorphism. This tectonic model correlates with the model proposed for the Selway terrane by Foster et al. (2006). Therefore, the SMC in interpreted as a western extension of the Selway terrane.

CHAPTER V: CONCLUSIONS

The history of the SMC begins with the deposition of flysch-like sediments on a passive margin during the Proterozoic. These sedimentary rocks were intruded with mafic dikes now preserved as metagabbros. This package of rock was metamorphosed in a collisional tectonic setting, as recorded by a clockwise prograde P-T path (Fig. 4.19, 4.20). Peak metamorphic conditions are suggested by migmitization and estimated to be 800 °C and 7 kbar. Based on mineral assemblages and mineral chemistry, post-peak metamorphic conditions are calculated to be 650 – 700˚C and 5.5 – 7 kbar pressure. These conditions suggest the rocks were buried to depths over 20 km and subjected to amphibolite-granulite facies metamorphism. The main deformation occurred near peak conditions and is recorded by cordierite, biotite, and sillimanite deforming around garnet porphyroblasts. The retrograde path is marked by plagioclase halos replacing deformed garnet and sillimanite replacing cordierite. Further decrease in temperature brought the SMC back into the muscovite stability field, indicated by large tabular muscovite overprinting the main foliation. During retrograde metamorphism, the Iron Creek and Thompson Peak regions of the SMC experienced different histories. The Thompson Peak rocks remained at greater depths with higher-pressure kyanite aluminosilicate growths, whereas the Iron Creek rocks were brought to more shallow levels of the crust as indicated by the occurrence of lower-pressure andalusite overgrowths. These different retrograde paths suggest the SMC is composed of multiple tectonic slices of rock from the mid-lower crust. The presence of Cr-muscovite in quartzites is evidence for metamorphism in the Precambrian and is supported by Nd mantle-model ages (Dutrow et al., 1995). The SMC uplifted through Laramide and Sevier thrusting, intrusion of the Idaho and Sawtooth batholiths and basin and range faulting.

The clockwise P-T path is evidence for collisional metamorphism occurring along the southwestern margin of Laurentia. Protoliths of titanite-amphibole-biotite gneisses and biotite-amphibolites are volcanic sandstones suggesting sediments were sourced from a magmatic arc. Therefore, the SMC is interpreted to record accretion of magmatic arc like terranes in this region during the Precambrian. Furthermore, the area immediately surrounding the SMC had been very fertile for magma generation in the Tertiary (i.e. the Idaho and Sawtooth batholiths). Therefore, it is unlikely that thick Archean basement crust under-plates the region. These interpretations are consistent with characteristics of the Selway Terrane. Therefore, this study concludes that the Sawtooth Metamorphic Complex represents rock from the Selway Terrane.

REFERENCES

Alexander, J.T., Schmitz, M.D., and Northrup, C.J., 2006, Preliminary U/Pb zircon data from the House Mountain metamorphic complex in the Atlanta lobe of the Idaho batholith: Geological Society of America, Abstracts with Programs, v. 38, p. 483.

Anderson, S.D., 1995, Petrology of Precambrian roof pendants: Thompson Peak, Sawtooth Mountains, Idaho [Senior Thesis]: Baton Rouge, LA, Louisiana State University, p. 1-56.

Barnett, D., Bowman, J., and Smith, H., 1993, Petrologic and geochronologic studies in the Farmington Canyon complex, Wasatch Mountains, Utah: Utah Geological Survey Contract Report 93-5.

Berman, R.G., 1991, Thermobarometry using multi-equilibrium calculations - A new technique, with petrological applications: Canadian Mineralogist, v. 29, p. 833-855.

Bhadra, S., and Bhattacharya, A., 2007, The barometer tremolite plus tschermakite+2 albite=2 pargasite+8 quartz: Constraints from experimental data at unit silica activity, with application to garnet-free natural assemblages: American Mineralogist, v. 92, p. 491-502.

Bhattacharya, A., Mohanty, L., Maji, A., Sen, S.K., and Raith, M., 1992, Nonideal mixing in the phlogopite-annite binary - constraints from experimental-data on mg-fe partitioning and a reformulation of the biotite garnet geothermometer: Contributions to Mineralogy and Petrology, v. 111, p. 87-93.

Bleeker, W., 2003, The late Archean record: a puzzle in ca. 35 pieces: Lithos, v. 71, p. 99-134.

Bleeker, W., and Ernst, G.R., 2006, Short-lived mantle generated magmatic events and their dyke swarms: The key to unlocking Earth's paleogeographic record back to 2.6 Ga, *in* Hanski, E., ed., Dyke swarms- Time markers of crustal evolution: Rotterdamn, A.A. Balkema, p. 3-26.

Bryant, B., 1988, Geology of the Farmington Canyon complex, Wasatch Mountains, Utah, *in* Paper, U.G.S.P., ed., Volume 1476.

Carey, J.W., Rice, J.M., and Grover, T.W., 1992, Petrology of aluminous schist in the Boehls Butte region of northern Idaho: Geologic history and aluminum-silicate phase relations: American Journal of Science, v. 292, p. 455-473.

Chamberlain, K.R., Frost, C.D., and Frost, B.R., 2003, Early Archean to Mesoproterozoic evolution of the Wyoming Province: Archean origins to modern lithospheric architecture: Canadian Journal of Earth Sciences, v. 40, p. 1357-1374.

Cheney, J.T., Webb, A.A.G., Coath, C.D., and McKeegan, K.D., 2004, In situ ion microprobe 207Pb/206Pb dating of monazite from Precambrian metamorphic suits, Tobacco Root Mountains, Montana, *in* Brady, J., Burger, H., Cheney, J., and Harms, T., eds., Precambrian geology of the Tobacco Root Mountains, Montana, Volume 337, Geological Society of America, Special Paper, p. 151-179.

Corrigan, D., Hajnal, Z., Nemeth, B., and Lucas, S.B., 2005, Tectonic framework of a Paleoproterozoic arc-continent to continent-continent collisional zone, Trans-Hudson Orogen, from geological and seismic reflection studies: Canadian Journal of Earth Sciences, v. 42, p. 421-U57.

Dahl, P.S., Hamilton, M.A., Wooden, J.L., Foland, K.A., Frei, R., McCombs, J.A., and Holm, D.K., 2006, 2480 Ma mafic magmatism in the northern Black Hills, South Dakota: a new link connecting the Wyoming and Superior cratons: Canadian Journal of Earth Sciences, v. 43, p. 1579-1600.

Dasgupta, S., Sengupta, P., Guha, D., and Fukuoka, M., 1991, A refined garnet - biotite Fe-Mg exchange geothermometer and its application in amphibolites and granulites: Contributions to Mineralogy and Petrology, v. 109, p. 130-137.

Doughty, P.T., 1995, Tectonic evolution of the Priest River Complex and the age of basement gneisses: constraints from geochronology and metamorphic thermobarometry [Ph.D. thesis]: Kingston, Ont., Queen's University.

Doughty, P.T., Price, R.A., and Parrish, R.R., 1998, Geology and U-Pb geochronology of Archean basement and Proterozoic cover in the Priest River complex, northwestern United States, and their implications for Cordilleran structure and Precambrian continent reconstructions: Canadian Journal of Earth Sciences, v. 35, p. 39-54.

Durk, K.M., Link, P.K., and Fanning, C.M., 2007, Neoproterozoic 695 Ma felsic orthogneiss, Wildhorse Creek, Pioneer Mountains, south-central Idaho: new tie point in reconstruction of Rodinian rifting: Geological Society of America, Abstracts with Programs, v. 39, p. 613.

Dutrow, B., Anderson, S., Henry, D., Mueller, P., and Giaramita, M., 1995, A new Precambrian crustal province in south-central Idaho? EOS, Transactions, American Geophysical Union, 76:F678.

Egger, A.E., Dumitru, T.A., Miller, E.L., Savage, C.F.I., and Wooden, J.L., 2003, Timing and nature of Tertiary plutonism and extension in the Grouse Creek Mountains, Utah: International Geology Review, v. 45, p. 497-532.

Evans, K.V., Aleinikoff, J.N., Obradovich, J.D., and Fanning, C.M., 2000, SHRIMP U-Pb geochronology of volcanic rocks, Belt Supergroup, western Montana: evidence for rapid

deposition of sedimentary strata: Canadian Journal of Earth Sciences, v. 37, p. 1287-1300.

Evans, K.V., and Fischer, L.B., 1986, U-Pb geochronology of two augen gneiss terranes, Idaho - New data and tectonic implications: Canadian Journal of Earth Sciences, v. 23, p. 1919-1927.

Evans, K.V., and Green, G.N., 2003, Geologic Map of the Salmon National Forest, and vicinity, east-central Idaho, U.S. Geological Survey Geologic Investigations Series I-2765.

Fanning, C.M., Flint, R.B., Parker, A.J., Ludwig, K.R., and Blissett, A.H., 1988, Refined Proterozoic evolution of the Grawler Craton, south Australia, through U-Pb zircon geochronology: Precambrian Research, v. 40-1, p. 363-386.

Ferry, J.M., and Spear, F.S., 1978, Experimental calibration of partitioning of Fe and Mg between biotite and garnet: Contributions to Mineralogy and Petrology, v. 66, p. 113-117.

Fettes, D., and Desmons, J., 2007, Metamorphic Rocks: A Classification and Glossary of Terms, *in* Arkai, P., Brodie, I., Bryhni, I., Callegari, E., Coutinho, J., Davis, E., Desmons, J., Fettes, D., Grieve, R., Harte, B., Krautner, H., Pertsev, N., Rosen, O., Rusinov, V., Sassi, F., Schmid, R., Sen, S., Siivola, J., Smulikowski, W., Stoffler, D., Wimmenauer, W., and Zharikov, V., eds., Recommendations of the International Union of Geological Sciences Subcommission on the Systematics of Metamorphic Rocks: Cambridge, University Press, p. 1-244.

Foster, D.A., and Fanning, C.M., 1997, Geochronology of the northern Idaho batholith and the Bitterroot metamorphic core complex: Magmatism preceding and contemporaneous with extension: Geological Society of America Bulletin, v. 109, p. 379-394.

Foster, D.A., Mueller, P.A., Mogk, D.W., Wooden, J.L., and Vogl, J.J., 2006, Proterozoic evolution of the western margin of the Wyoming craton: implications for the tectonic and magmatic evolution of the northern Rocky Mountains: Canadian Journal of Earth Sciences, v. 43, p. 1601-1619.

Frost, B.R., Chamberlain, K.R., Swapp, S., Frost, C.D., and Hulsebosch, T.P., 2000, Late Archean structural and metamorphic history of the Wind River Range: Evidence for a long-lived active margin on the Archean Wyoming craton: Geological Society of America Bulletin, v. 112, p. 564-578.

Frost, C.D., 1993, Nd isotopic evidence for the antiquity of the Wyoming Province: Geology, v. 21, p. 351-354.

Frost, C.D., Frost, B.R., Chamberlain, K.R., and Hulsebosch, T.P., 1998, The Late Archean history of the Wyoming province as recorded by granitic magmatism in the Wind River Range, Wyoming: Precambrian Research, v. 89, p. 145-173.

Gaschnig, R., Vervoort, J., Lewis, R.S., and Dufrane, A., 2008, Utilizing U-Pb geochronology of inherited zircon in the Atlanta lobe of the Idaho batholith as a probe of the deep crust in southern Idaho: a progress report: Northwest Geology, v. 37, p. 101-110.

Gerya, T.V., Perchuk, L.L., Triboulet, C., Audren, C., and Sezko, A.I., 1997, Petrology of the Tumanshet zonal metamorphic complex, eastern Sayan: Petrology, v. 5, p. 503-533.

Ghent, E.D., 1976, Plagioclase-garnet-Al_2SiO_5-quartz: a potential geobarometer-geothermometer: American Mineralogist, v. 61, p. 710-714.

Giletti, B.J., 1966, Isotopic ages from southwestern Montana: Journal of Geophysical Research, v. 71, p. 4029.

Gonzalez-Alvarez, I., Kusiak, M.A., and Kerrich, R., 2006, A trace element and chemical Th-U total Pb dating study in the lower Belt-Purcell Supergroup, Western North America: Provenance and diagenetic implications: Chemical Geology, v. 230, p. 140-160.

Gorman, A.R., Clowes, R.M., Ellis, R.M., Henstock, T.J., Spence, G.D., Keller, G.R., Levander, A., Snelson, C.M., Burianyk, M.J.A., Kanasewich, E.R., Asudeh, I., Hajnal, Z., and Miller, K.C., 2002, Deep probe: imaging the roots of western North America: Canadian Journal of Earth Sciences, v. 39, p. 375-398.

Grover, T.W., Rice, J.M., and Carey, J.W., 1992, Petrology of aluminous schist in the Boehls Butte of Northern Idaho: Phase equilibria and P-T evolution: American Journal of Science, v. 292, p. 474-507.

Hackler, R.T., and Wood, B.J., 1989, Experimental-determination of Fe and Mg exchange between garnet and olivine and estimation of Fe-Mg mixing properties in garnet: American Mineralogist, v. 74, p. 994-999.

Harrison, J.E., 1972, Precambrian belt basin of northwestern United-States - its geometry, sedimentation, and copper occurrences: Geological Society of America Bulletin, v. 83, p. 1215.

Henry, D.J., Guidotti, C.V., and Thomson, J.A., 2005, The Ti-saturation surface for low-to-medium pressure metapelitic biotites: Implications for geothermometry and Ti-substitution mechanisms: American Mineralogist, v. 90, p. 316-328.

Henstock, T., Levander, A., Snelson, C., Keller, R., Miller, K., and al., S.He., 1998, Probing the Archean and Proterozoic Lithosphere of western North America: GSA Today, v. 8, p. 1-5.

Hietanen, A., 1956, Kyanite, andalusite, and sillimanite in the schist in Boehls Butte quadrangle, Idaho: American Mineralogist, v. 41, p. 1-27.

Hoffman, P.F., 1988, United Plates of America, the birth of a craton - Early Proterozoic assembly and growth of Laurentia: Annual Review of Earth and Planetary Sciences, v. 16, p. 543-603.

Hoffman, P.F., 1989, Speculations on Laurentia first gigayear (2.0 to 1.0 Ga): Geology, v. 17, p. 135-138.

Hoisch, T.D., 1990, Empirical calibration of 6 geobarometers for the mineral assemblage: quartz + muscovite + biotite + plagioclase + garnet: Contributions to Mineralogy and Petrology, v. 104, p. 225-234.

Holdaway, M.J., and Lee, S.M., 1977, Fe-Mg cordierite stability in high-grade pelitic rocks: Based on experimental, theoretical, and natural observation: Contributions to Mineralogy and Petrology, v. 63, p. 175-198.

Holland, T., and Blundy, J., 1994, Nonideal interactions in calcic amphiboles and their bearing on amphibole-plagioclase thermometry: Contributions to Mineralogy and Petrology, v. 116, p. 433-447.

Holland, T., and Powell, R., 1992, Plagioclase feldspars - activity-composition relations based upon Darken quadratic formalism and Landau theory: American Mineralogist, v. 77, p. 53-61.

King, E.M., and Valley, J.W., 2001, The source, magmatic contamination, and alteration of the Idaho Batholith: Contributions to Mineralogy and Petrology, v. 142, p. 77-88.

Kretz, R., 1983, Symbols for rock-forming minerals: American Mineralogist, v. 68, p. 277-279.

Leake, B.E., Woolley, A.R., Arps, C.E.S., Birch, W.D., Gilbert, M.C., Grice, J.D., Hawthorne, F.C., Kato, A., Kisch, H.J., Krivovichev, V.G., Linthout, K., Laird, J., Mandarino, J.A., Maresch, W.V., Nickel, E.H., Rock, N.M.S., Schumacher, J.C., Smith, D.C., Stephenson, N.C.N., Ungaretti, L., Whittaker, E.J.W., and Guo, Y.Z., 1997, Nomenclature of amphiboles: Report of the subcommittee on amphiboles of the International Mineralogical Association, Commission on New Minerals and Mineral Names: American Mineralogist, v. 82, p. 1019-1037.

Leeman, W.P., Menzies, M.A., Matty, D.J., and Embree, G.F., 1985, Strontium, neodymium and lead isotopic compositions of deep crustal xenoliths from the Snake River Plain - evidence for Archean basement: Earth and Planetary Science Letters, v. 75, p. 354-368.

Lemieux, S., Ross, G.M., and Cook, F.A., 2000, Crustal geometry and tectonic evolution of the Archean crystalline basement beneath the southern Alberta Plains, from new seismic reflection and potential-field studies: Canadian Journal of Earth Sciences, v. 37, p. 1473-1491.

Lewis, R.S., Kiilsgaard, T.H., Bennett, E.H., and Hall, W.E., 1987, Lithologic and chemical characteristics of the central and southeastern part of the southern lobe of the Idaho Batholith, *in* Vallier, T.L., and Brooks, H.C., eds., Geology of the Blue Mountains Region of Oregon, Idaho, and Washington: The Idaho Batholith and its border zone, U. S. Geological Survey Professional Paper, Volume 1436, p. 171-196.

Link, P.K., 2009, Age and Provenance of Precambrian Metamorphic Rocks in the Pioneer Metamorphic Core Complex, South-Central Idaho: the Southern Edge of the Lower Belt Supergroup, the Groups Creek Block, and Hints of a Proximal Grenville Source in the Northern Cordillera: Geological Society of America Abstracts with Programs, v. 41, p. 271.

Link, P. K., J. Welhan, et al. (2002). "http://imnh.isu.edu/digitalatlas/." accessed 03/2009.

Link, P.K., Durk, K.M., and Fanning, C.M., 2007, SHRIMP U-Pb ages for Archean orthogneiss, Mesoproterozoic paragneiss, and Eocene Boulder Creek pluton, Pioneer Mountains, south-central Idaho, part of the 2600 Grouse Creek block: Geological Society of America, Abstracts with Programs, v. 39, p. 613.

Luepke, J.J., and Lyons, T.W., 2001, Pre-Rodinian (Mesoproterozoic) supercontinental rifting along the western margin of Laurentia: Geochemical evidence from the Belt-Purcell Supergroup: Precambrian Research, v. 111, p. 79-90.

Lund, K., 1993, Metamorphic rocks of central Idaho: A progress report: Belt Symposium III: University of Idaho, Moscow, Department of Geology, and Idaho Bureau of Mines and Geology, v. 3, p. 116-132.

Mogk, D.W., 1990, A model for granulite-migmatite associations in the Archean basement of SW Montana: geochemical and tectonic implications., *in* Vielzeuf, D., and Vidal, P., eds., Granulites and Crustal Evolution. NATO ASI Series C, Volume 311: Dordrecht, Kluwer, p. 133-156.

Mogk, D.W., and Henry, D.J., 1988, Metamorphic petrology of the northern Archean Wyoming Province, southwestern Montana: evidence for Archean collisional tectonics, *in* Ernst, W.G., ed., Metamorphism and Crustal Evolution in the Western United States.: New York, Prentice-Hall, p. 363-382.

Mogk, D.W., Mueller, P.A., and Wooden, J.L., 1992, The nature of Archean terrane boundaries - An example from the northern Wyoming province: Precambrian Research, v. 55, p. 155-168.

Mueller, P.A., Burger, H.R., Wooden, J.L., Brady, J.B., Cheney, J.T., Harms, T.A., Heatherington, A.L., and Mogk, D.W., 2005, Paleoproterozoic metamorphism in the northern Wyoming province: Implications for the assembly of Laurentia: Journal of Geology, v. 113, p. 169-179.

Mueller, P.A., and Frost, C.D., 2006, The Wyoming Province: a distinctive Archean craton in Laurentian North America: Canadian Journal of Earth Sciences, v. 43, p. 1391-1397.

Mueller, P.A., Heatherington, A.L., Kelly, D.M., Wooden, J.L., and Mogk, D.W., 2002, Paleoproterozoic crust within the Great Falls tectonic zone: Implications for the assembly of southern Laurentia: Geology, v. 30, p. 127-130.

Mueller, P.A., Shuster, R.D., Wooden, J.L., Erslev, E.A., and Bowes, D.R., 1993, Age and composition of Archean crystalline rocks from the southern Madison range, Montana - Implications for crustal evolution in the Wyoming Craton: Geological Society of America Bulletin, v. 105, p. 437-446.

Mueller, P.A., and Wooden, J.L., 1988, Evidence for Archean subduction and crustal recycling, Wyoming Province: Geology, v. 16, p. 871-874.

Nelson, S.T., Harris, R.A., Dorais, M.J., Heizler, M., Constenius, K.N., and Barnett, D.E., 2002, Basement complexes in the Wasatch fault, Utah, provide new limits on crustal accretion: Geology, v. 30, p. 831-834.

O'Neill, J.M., Duncan, M.S., and Zartman, R.E., 1988, An Early Proterozoic gneiss dome in the Highland Mountains, southwestern Montana., *in* Lewis, S.E., and Berg, R.B., eds., Precambrian and Mesozoic plate margins, Volume 96, Montana Bureau of Mines and Geology, Special Publication, p. 81-88.

Percival, J.A., Bleeker, W., Cook, F.A., Rivers, T., Ross, G., and van Staal, C., 2004, PanLITHOPROBE Workshop IV: Intra-orogen correlations and comparative orogenic anatomy: Geoscience Canada, v. 31, p. 23-39.

Reid, R.R., 1963, Reconnaissance geology of the Sawtooth range, *in* Geology, Idaho.Bureau of Mines., ed., Volume 129.

Reid, R.R., Morrison, D.A., and Greenwood, W.R., 1973, The Clearwater Orogenic zone: a relict of Proterozoic orogeny in central and northern Idaho: Belt Symposium I: University of Idaho, Moscow, Department of Geology, and Idaho Bureau of Mines and Geology, v. 1, p. 10-56.

Roberts, H., Dahl, P., Kelley, S., and Frei, R., 2002, New Pb-207-Pb-206 and Ar-40-Ar-39 ages from SW Montana, USA: constraints on the Proterozoic and Archaean tectonic and depositional history of the Wyoming Province: Precambrian Research, v. 117, p. 119-143.

Ross, G.M., 2002, Evolution of Precambrian continental lithosphere in Western Canada: results from Lithoprobe studies in Alberta and beyond: Canadian Journal of Earth Sciences, v. 39, p. 413-437.

Ross, G.M., Parrish, R.R., Villeneuve, M.E., and Bowring, S.A., 1991, Geophysics and geochronology of the crystalline basement of the Alberta basin, western Canada: Canadian Journal of Earth Sciences, v. 28, p. 512-522.

Ross, G.M., Parrish, R.R., and Winston, D., 1992, Provenance and U-Pb geochronology of the Mesoproterozoic Belt Supergroup (northwestern United States): implications for age of deposition and pre-Panthalassa plate reconstructions: Earth and Planetary Science Letters, v. 113, p. 57-76.

Spear, F.S., 1993, Metamorphic phase equilibria and pressure-temperature-time paths: Washington, D.C., Mineralogical Society of America, p. xxii-799.

Spear, F.S., and Cheney, J.T., 1989, A petrogenetic grid for pelitic schists in the system SiO_2 - Al_2O_3 - FeO - MgO - K_2O - H_2O: Contributions to Mineralogy and Petrology, v. 101, p. 149-164.

Spear, F. S., M. J. Kohn, et al. (1999). P-T paths from anatectic pelites. Contributions to Mineralogy and Petrology 134: 17-32.

Stroud, M., Foster, David A., Mueller, Paul A., and Kamenov, George D., 2009, Isotopic analyses of the Grouse Creek Block: A Link to the Wyoming Craton: Geological Society of America *Abstracts with Programs*, v. 41, p. 1.

Thomas, M.D., Sharpton, V.L., and Grieve, R.A.F., 1987, Gravity patterns and Precambrian structure in the North-American Central Plains: Geology, v. 15, p. 489-492.

Trehu, A., Lillie, R., Goddard, C., Braunmiller, J., and LeBoeuf, C. (2009). " http://www.earthscope.org/", accessed 04/2010.

Vogl, J.J., 2004, Lithology and age of pre-belt Precambrian basement in the Little Belt Mountains, Montana; implications for the role of the Great Falls tectonic zone in the Paleoproterozoic assembly of North America, *in* Foster, D.A., Mueller, P.A., Wooden, J.L., and Mogk, D.W., eds., Northwest Geology, Volume 33: United States, University of Montana, Department of Geology : Missoula, MT, United States, p. 15.

Waters, D. J. (10/12/2004). "http://www.earth.ox.ac.uk/~davewa/pt/pt04.html." accessed 02/2010.

Whitmeyer, S.J., and Karlstrom, K.E., 2007, Tectonic model for the Proterozoic growth of North America: Geosphere, v. 3, p. 220-259.

Williams, T.J., Piccoli, P.M., Candela, P.A., and Simon, A., 2004, Minerals and reactions in miarolitic cavities in the Eocene Sawtooth batholith, south-central Idaho: Geological Society of America Abstracts with Programs, v. 36, p. 69.

Wolf, D.E., Leeman, W.P., and Vervoort, J.D., 2005, U-Pb zircon geochronology of crustal xenoliths confirms presence of Archean basement beneath the central and eastern Snake River plain, Geological Society of America *Abstracts with Programs*, Volume 37, p. 60.

Wooden, J.L., and Mueller, P.A., 1988, Pb, Sr, and Nd isotopic compositions of a suite of Late Archean, igneous rocks, eastern Bearthooth Moutnains - Implications for crust-mantle evolution: Earth and Planetary Science Letters, v. 87, p. 59-72.

Wright, J.E., and Snoke, A.W., 1993, Tertiary magmatism and mylonitization in the Ruby-East Humboldt metamorphic core complex, northeastern Nevada - U-Pb geochronology and Sr, Nd, and Pb isotope geochemistry: Geological Society of America Bulletin, v. 105, p. 935-952.

Wu, C.M., and Cheng, B.H., 2006, Valid garnet-biotite (GB) geothermometry and garnet-aluminum silicate-plagioclase-quartz (GASP) geobarometry in metapelitic rocks: Lithos, v. 89, p. 1-23.

Wu, C.M., Zhang, J., and Ren, L.D., 2004, Empirical garnet-muscovite-plagioclase-quartz geobarometry in medium- to high-grade metapelites: Lithos, v. 78, p. 319-332.

Wu, C.M., and Zhao, G.C., 2006, Recalibration of the garnet-muscovite (GM) geothermometer and the garnet-muscovite-plagioclase-quartz (GMPQ) geobarometer for metapelitic assemblages: Journal of Petrology, v. 47, p. 2357-2368.

APPENDIX A: SAMPLE, LOCATION, PREPARATION AND ANALYTICAL WORK

SAMPLE#	UTM		elevation (ft)	general location	USGS quadrangle	rock sample	rock cut	Thin Section	Thin Section Scan	Thin Section Polish	probed	outcrop picture	megascopic description
ST08-04a	661019	4890547	8281	Marshall Lake	Stanley	x	x	x				x	qfg
ST08-04b	661019	4890547	8281	Marshall Lake	Stanley	x	x	x				x	qfg
ST08-04c	661019	4890547	8281	Marshall Lake	Stanley	x	x	x				x	qfg
ST08-07b	661100	4890247	8450	Marshall Lake	Stanley	x	x	x					qfg
ST08-10a	661077	4890458	8331	Marshall Lake	Stanley	x	x	x					qfg
ST08-12a	660919	4890647	8548	Marshall Lake	Stanley	x	x	x					qfg
ST08-13a	660836	4890721	8589	Marshall Lake	Stanley	x	x	x	x	x	x	x	bt-gneiss
ST08-13b	660836	4890721	8589	Marshall Lake	Stanley	x	x	x		x			qfg
ST08-13c	660836	4890721	8589	Marshall Lake	Stanley	x	x	x		x			amphibolite
ST08-13d	660836	4890721	8589	Marshall Lake	Stanley	x	x	x		x			amphibolite
ST08-14a	660762	4890869	8473	Marshall Lake	Stanley	x	x	x					amphibolite
ST08-15a	660851	4890852	8377	Marshall Lake	Stanley	x	x	x				x	qfg
ST08-15b	660851	4890852	8377	Marshall Lake	Stanley	x	x	x				x	dark dike
ST08-15c	660851	4890852	8377	Marshall Lake	Stanley	x	x	x				x	bt-gneiss
ST08-15d	660851	4890852	8377	Marshall Lake	Stanley	x	x	x	x	x	x	x	meta-gabbro
ST08-18c	661054	4890213	8261	Marshall Lake	Stanley	x	x	x					qfg
ST08-24a	660715	4890542	9022	Marshall Lake	Stanley	x	x	x					calc-silicate
ST08-24b	660715	4890542	9022	Marshall Lake	Stanley	x	x	x					bt-gneiss
ST08-26a	660905	4890166	8231	Marshall Lake	Stanley	x	x	x					amphibolite
ST08-26b	660905	4890166	8231	Marshall Lake	Stanley	x	x	x					bt-gneiss
ST08-26c	660905	4890166	8231	Marshall Lake	Stanley	x	x	x		x			meta-gabbro
ST08-27	660871	4889994	8068	Marshall Lake	Stanley	x	x	x		x			amphibolite
ST08-28	660850	4889905	8067	Marshall Lake	Stanley	x	x	x					bt-gneiss
ST08-29a	660815	4889904	8074	Marshall Lake	Stanley	x	x	x				x	qfg
ST08-30a	660782	4889917	8160	Marshall Lake	Stanley	x	x	x	x	x	x	x	qfg
ST08-31a	660584	4890060	8381	Marshall Lake	Stanley	x	x	x					bt-gneiss
ST08-31c	660584	4890060	8381	Marshall Lake	Stanley	x	x	x					bt-gneiss
ST08-32b	660644	4890195	8446	Marshall Lake	Stanley	x	x	x				x	calc-silicate

Appendix A, cont'd

SAMPLE#	UTM		elevation (ft)	general location	USGS quadrangle	rock sample	rock cut	Thin Section	Thin Section Scan	Thin Section Polish	probed	outcrop picture	megascopic description
ST08-32c	660644	4890195	8446	Marshall Lake	Stanley	x	x	x				x	calc-silicate
ST08-32d	660644	4890195	8446	Marshall Lake	Stanley	x	x	x				x	calc-silicate
ST08-35a	660624	4890624	9170	Marshall Lake	Stanley	x	x	x				x	felsic vein
ST08-35b	660624	4890624	9170	Marshall Lake	Stanley	x	x	x				x	bt-gneiss
ST08-35c	660624	4890624	9170	Marshall Lake	Stanley	x	x	x				x	felsic dike
ST08-36a	660552	4890618	9259	Marshall Lake	Stanley	x	x	x					amphibolite
ST08-38	660458	4890587	9386	Marshall Lake	Stanley	x	x	x					bt-gneiss
ST08-40b	660364	4890544	9427	Marshall Lake	Stanley	x	x	x					bt-gneiss
ST08-40c	660364	4890544	9427	Marshall Lake	Stanley	x	x	x					bt-gneiss
ST08-42	660297	4890860	8756	Marshall Lake	Stanley	x	x	x					sawtooth dike
ST08-44b	660608	4891429	8310	Marshall Lake	Stanley	x	x	x					bt-schist
ST08-44c	660608	4891429	8310	Marshall Lake	Stanley	x	x	x					bt-schist
ST08-45a	660588	4891389	8339	Marshall Lake	Stanley	x	x	x	x	x	x	x	bt-gneiss
ST08-47b	660676	4891398	8151	Marshall Lake	Stanley	x	x	x					bt-schist
ST08-47c	660676	4891398	8151	Marshall Lake	Stanley	x	x	x					qfg
ST08-47d	660676	4891398	8151	Marshall Lake	Stanley	x	x	x					amphibolite
ST08-48a	660551	4890160	8552	Marshall Lake	Stanley	x	x	x				x	bt-schist
ST08-48b	660476	4890118	8648	Marshall Lake	Stanley	x	x	x				x	bt-schist
ST08-48c	660476	4890118	8648	Marshall Lake	Stanley	x	x	x				x	bt-schist
ST08-48d	660476	4890118	8648	Marshall Lake	Stanley	x	x	x				x	bt-schist
ST08-48e	660476	4890118	8648	Marshall Lake	Stanley	x	x	x				x	felsic dike
ST08-49	660384	489087	8699	Marshall Lake	Stanley	x	x	x					idaho batholith?
ST08-50	660262	4890037	8807	Marshall Lake	Stanley	x	x	x				x	dark dike
ST08-51	660121	4889910	8936	Thompson Peak	Stanley Lake	x	x	x					sawtooth dike
ST08-52b	660075	4889670	8991	Thompson Peak	Stanley Lake	x	x	x				x	calc-silicate
ST08-53a	660147	4889701	8908	Thompson Peak	Stanley Lake	x	x	x					marble mylonite
ST08-54	660176	4889786	8916	Thompson Peak	Stanley Lake	x	x	x				x	marble mylonite
ST08-55a	660177	4890154	8893	Thompson Peak	Stanley Lake	x	x	x					bt-schist
ST08-59c	660610	4891682	8497	Marshall Lake	Stanley	x	x	x					bt-gneiss
ST08-67b	659430	4901722	6372	Stanley Creek	Elk Meadow	x	x	x					calc-silicate

Appendix A, cont'd

SAMPLE#	UTM		elevation (ft)	general location	USGS quadrangle	rock sample	rock cut	Thin Section	Thin Section Scan	Thin Section Polish	probed	outcrop picture	megascopic description
STL08-04	654284	4893096	8991	Sawtooth Lake	Stanley Lake	x	x	x					qfg
STL08-07	654177	4892806	9059	Sawtooth Lake	Stanley Lake	x	x	x					idaho batholith?
STL08-08	656054	4890664	8298	Sawtooth Lake	Stanley Lake	x	x	x					bt-schist
Alpine Peak	n/a	n/a	--	Alpine Peak	Stanley Lake	x	x	x					Igneous
btw p&r	n/a	n/a	--	Marshall Lake	Stanley	x	x	x					xenolithic
idaho f	n/a	n/a	--	Sawtooth Lake	Stanley Lake	x	x	x					x-cutting felsic dikes
idaho m	n/a	n/a	--	Sawtooth Lake	Stanley Lake	x	x	x	x	x	x	x	mafix xenolith
TP08-08	659788	4890061	9374	Thompson Peak	Stanley Lake	x	x	x					calc-silicate
TP08-09	659689	489033	9442	Thompson Peak	Stanley Lake	x	x	x		x			calc-silicate
TP08-10	659663	4890024	9485	Thompson Peak	Stanley Lake	x	x	x					px-gneiss
TP08-11	659632	4890028	9541	Thompson Peak	Stanley Lake	x	x	x					quartzite
TP08-12	659613	4890033	9435	Thompson Peak	Stanley Lake	x	x	x					marble mylonite
TP08-13	n/a	n/a		Thompson Peak	Stanley Lake	x	x	x		x			amphibolite
IC08-01a	657447	4892450	8744	Iron Creek	Stanley Lake	x	x	x	x	x	x	x	pellitic gneiss
IC08-01a1	657447	4892450	8744	Iron Creek	Stanley Lake	x	x	x	x	x	x	x	pellitic gneiss
IC08-01b	657447	4892450	8744	Iron Creek	Stanley Lake	x	x	x	x	x	x	x	pellitic gneiss
IC08-01b1	657447	4892450	8744	Iron Creek	Stanley Lake	x	x	x	x	x	x	x	pellitic gneiss
IC08-01e	657447	4892450	8744	Iron Creek	Stanley Lake	x	x	x	x	x	x	x	pellitic gneiss
IC08-02a	657481	4892401	8828	Iron Creek	Stanley Lake	x	x	x					qfg with large ms books
IC08-02c	657481	4892401	8828	Iron Creek	Stanley Lake	x	x	x					qfg with large ms books

APPENDIX B: MINERAL ASSEMBLAGE OF SAMPLES FROM PETROGRAPHIC ANALYSIS

SAMPLE #		Minerals																				
	rock type	qtz	pl	kfs	bt	ms	chl	grt	amp	cpx	ep	sil	and	crd	cal	ilm	gr	rt	apt	aln	ttn	mnz	zrn
ST08-04a	qfg	x		x	x	x														x			x
ST08-04b	qfg	x		x	x	x	x																x
ST08-04c	quartzite	x		x	x	x																	
ST08-07b	quartzite	x		x	x	x																	x
ST08-10a	quartzite	x		x		x																	
ST08-12a	quartzite	x		x	x	x																	x
ST08-13a	bt-amp gneiss		x		x				x							x					x	x	x
ST08-14a	metagabbro		x						x														x
ST08-15a	quartzite	x		x	x	x																	
ST08-15c	bt-amp gneiss	x	x		x				x										x			x	x
ST08-15d	metagabbro			x	x				x	x													
ST08-18c	quartzite	x		x	x	x	x																
ST08-22b		x	x		x	x	x		x												x		x
ST08-23a	qfg	x	x		x		x												x			x	x
ST08-24a	quartzite	x		x		x																	
ST08-24b	qfg	x	x		x	x										x			x				x
ST08-26a	metagabbro		x		x	x	x		x		x											x	x
ST08-26b	ttn-amp-bt gneiss	x	x		x				x							x		x			x	x	x
ST08-26c	metagabbro				x		x		x	x	x								x		x		
ST08-27	metagabbro								x	x						x					x		
ST08-28	bt-amp gneiss		x		x				x							x					x	x	x
ST08-29a	quartzite	x		x	x	x	x															x	x

Appendix B, cont'd

SAMPLE #		Minerals																					
	rock type	qtz	pl	kfs	bt	ms	chl	grt	amp	cpx	ep	sil	and	crd	cal	ilm	gr	rt	apt	aln	ttn	mnz	zrn
ST08-29b	qfg	x	x		x															x			
ST08-30a	ttn-hb-bt gneiss		x		x				x	x								x	x		x		x
ST08-31a	calc-silicate	x	x		x					x	x						x		x		x		x
ST08-31c	qfg	x	x		x		x																x
ST08-32b	qfg	x	x		x	x	x		x												x	x	x
ST08-32c	calc-silicate	x	x				x			x	x	x							x		x		x
ST08-35a	qfg	x	x	x	x	x	x													x			x
ST08-35b	calc-silicate	x	x	x	x						x										x		
ST08-35c	quartzite	x		x																			
ST08-36a	metagabbro		x		x	x				x						x							
ST08-38a	qfg	x	x		x	x	x												x	x			x
ST08-40b	qfg	x	x		x														x	x	x		x
ST08-42a	calc-silicate		x	x						x	x					x			x		x		
ST08-44b	ttn-hb-bt gneiss	x	x		x				x							x		x			x		
ST08-44c	quartzite	x	x	x	x															x	x		x
ST08-45a	ttn-hb-bt gneiss	x	x						x									x	x		x		x
ST08-046a	qfg	x	x	x	x	x	x															x	x
ST08-47c	calc-silicate	x	x				x		x	x	x											x	x
ST08-47d	bt-amp gneiss		x		x		x		x														
ST08-48b	ttn-hb-bt gneiss	x	x		x	x												x					x
ST08-49	qfg	x	x	x	x																		x
ST08-50a	ttn-hb-bt gneiss	x	x		x																		
ST08-51a		x	x	x		x									x						x		

Appendix B, cont'd

SAMPLE #		Minerals																					
	rock type	qtz	pl	kfs	bt	ms	chl	grt	amp	cpx	ep	sil	and	crd	cal	ilm	gr	rt	apt	aln	ttn	mnz	zrn
ST08-29b	qfg	x	x		x															x			
ST08-30a	ttn-hb-bt gneiss		x		x				x	x								x	x		x		x
ST08-31a	calc-silicate	x	x		x					x	x						x		x		x		x
ST08-31c	qfg	x	x		x		x																x
ST08-32b	qfg	x	x		x	x	x		x												x	x	x
ST08-32c	calc-silicate	x	x				x			x	x	x							x		x		x
ST08-35a	qfg	x	x	x	x	x	x													x			x
ST08-35b	calc-silicate	x	x	x	x						x										x		
ST08-35c	quartzite	x		x																			
ST08-36a	metagabbro		x		x	x				x						x							
ST08-38a	qfg	x	x		x	x	x												x	x			x
ST08-40b	qfg	x	x		x														x	x	x		x
ST08-42a	calc-silicate		x	x						x	x					x			x		x		
ST08-44b	ttn-hb-bt gneiss	x	x		x				x							x		x			x		
ST08-44c	quartzite	x	x	x	x															x	x		x
ST08-45a	ttn-hb-bt gneiss	x	x						x									x	x		x		x
ST08-046a	qfg	x	x	x	x	x	x															x	x
ST08-47c	calc-silicate	x	x				x		x	x	x											x	x
ST08-47d	bt-amp gneiss		x		x		x		x														
ST08-48b	ttn-hb-bt gneiss	x	x		x	x												x					x
ST08-49	qfg	x	x	x	x																		x
ST08-50a	ttn-hb-bt gneiss	x	x		x																		
ST08-51a		x	x	x		x									x						x		

Appendix B, cont'd

SAMPLE #		Minerals																				
	rock type	**qtz**	**pl**	**kfs**	**bt**	**ms**	**chl**	**grt**	**amp**	**cpx**	**ep**	**sil**	**and**	**crd**	**cal**	**ilm**	**gr**	**rt**	**apt**	**aln**	**ttn**	**mnz**	**zrn**
ST08-52b	calc-silicate	x								x	x								x		x		x
ST08-53a	calc-silicate	x	x	x						x					x						x		x
ST08-54a	calc-silicate	x	x	x		x					x				x						x		x
ST08-55a	ttn-hb-bt gneiss	x	x		x		x		x									x	x		x		x
ST08-59c	qfg	x	x		x														x	x	x		x
ST08-67b	calc-silicate	x	x								x				x						x		x
STL08-04	qfg	x	x	x		x																	
STL08-07	qfg	x	x	x	x											x						x	
STL08-08	calc-silicate	x	x							x											x		x
Alpine Peak	qfg	x	x	x																			
btw p&r	qfg	x	x	x	x	x																	x
idaho f	qfg	x	x	x	x																		
idaho m	bt-amp-pyx gneiss	x	x		x				x	x	x					x		x			x	x	x

Appendix B, cont'd

SAMPLE #		Minerals																				
	rock type	**qtz**	**pl**	**kfs**	**bt**	**ms**	**chl**	**grt**	**amp**	**cpx**	**ep**	**sil**	**and**	**crd**	**cal**	**ilm**	**gr**	**rt**	**apt**	**aln**	**ttn**	**mnz**	**zrn**
TP08-08a	calc-silicate	x	x	x						x									x		x		
TP08-08b	calc-silicate	x								x		x			x						x		
TP08-09	calc-silicate	x		x	x				x	x											x		x
TP08-10	quartzite	x		x	x	x																	
TP08-11	quartzite	x		x	x	x																	x
TP08-12	calc-silicate	x		x		x				x	x	x			x								
TP08-13	bt-amp gneiss	x	x		x				x	x						?							
IC08-01a	peraluminous gneiss	x	x	x	x	x		x				x	x	x		x			x			x	x
IC08-01a1	peraluminous gneiss	x	x	x	x	x		x				x	x	x		x			x			x	x
IC08-01b	peraluminous gneiss	x	x	x	x	x		x				x	x	x		x			x			x	x
IC08-01b-1	peraluminous gneiss	x	x	x	x	x		x				x	x	x								x	x
IC08-01e	peraluminous gneiss	x	x	x	x	x		x				x	x	x									x
IC08-02a	qfg	x	x			x																	
IC08-02c	qfg	x	x			x																	

APPENDIX C: ELECTRON MICROPROBE ANALYSES – PLAGIOCLASE

	Plagioclase													
	ic08-01a													
	Wpl t1	Wpl t2	Wpl 1	Wpl 2	Wpl 3	Wpl 4	Wpl 5	Wpl 6	Wpl 7	Wpl 8	Wpl 9	Wpl 10	Wpl 11	Wpl 12
wt %														
SiO_2	58.86	62.67	58.56	59.01	58.62	58.90	58.63	58.82	58.28	62.54	62.10	62.56	62.09	62.35
Al_2O_3	25.88	23.57	25.96	25.86	26.03	25.84	25.71	25.94	26.16	23.44	23.59	23.65	23.42	23.63
CaO	7.30	4.56	7.23	7.28	7.23	7.58	7.20	7.37	7.53	4.74	4.59	4.79	4.60	4.61
BaO	0.00	0.03	0.00	0.02	0.02	0.00	0.04	0.02	0.00	0.04	0.04	0.01	0.00	0.01
Na_2O	6.53	8.17	6.90	6.98	6.60	6.74	6.65	6.57	6.65	8.19	8.34	8.11	8.24	8.26
K_2O	0.13	0.16	0.10	0.11	0.13	0.11	0.11	0.12	0.13	0.14	0.15	0.15	0.17	0.18
FeO	0.15	0.05	0.05	0.03	0.11	0.11	0.02	0.07	0.03	0.02	0.06	0.01	0.07	0.04
MgO	0.00	0.17	0.00	0.00	0.00	0.00	0.00	0.00	0.00	0.00	0.00	0.00	0.00	0.00
Total	98.85	99.38	98.80	99.29	98.74	99.28	98.36	98.91	98.78	99.11	98.87	99.28	98.59	99.08

Oxygens = 8

	Plagioclase													
	ic08-01a													
	Wpl t1	Wpl t2	Wpl 1	Wpl 2	Wpl 3	Wpl 4	Wpl 5	Wpl 6	Wpl 7	Wpl 8	Wpl 9	Wpl 10	Wpl 11	Wpl 12
apfu														
Si	2.65	2.78	2.64	2.65	2.64	2.64	2.65	2.65	2.63	2.78	2.77	2.78	2.78	2.78
Al	1.37	1.23	1.38	1.37	1.38	1.37	1.37	1.37	1.39	1.23	1.24	1.24	1.24	1.24
Ca	0.35	0.22	0.35	0.35	0.35	0.36	0.35	0.36	0.36	0.23	0.22	0.23	0.22	0.22
Ba	0.00	0.00	0.00	0.00	0.00	0.00	0.00	0.00	0.00	0.00	0.00	0.00	0.00	0.00
Na	0.57	0.70	0.60	0.61	0.58	0.59	0.58	0.57	0.58	0.71	0.72	0.70	0.72	0.71
K	0.01	0.01	0.01	0.01	0.01	0.01	0.01	0.01	0.01	0.01	0.01	0.01	0.01	0.01
Fe^{2+}	0.01	0.00	0.00	0.00	0.00	0.00	0.00	0.00	0.00	0.00	0.00	0.00	0.00	0.00
Mg	0.00	0.01	0.00	0.00	0.00	0.00	0.00	0.00	0.00	0.00	0.00	0.00	0.00	0.00
X_{Ab}	0.61	0.76	0.63	0.63	0.62	0.61	0.62	0.61	0.61	0.75	0.76	0.75	0.76	0.76
X_{Or}	0.01	0.01	0.01	0.01	0.01	0.01	0.01	0.01	0.01	0.01	0.01	0.01	0.01	0.01
X_{An}	0.38	0.23	0.36	0.36	0.37	0.38	0.37	0.38	0.38	0.24	0.23	0.24	0.23	0.23

Appendix C, cont'd

	Plagioclase								
	ic08-01a								
	Wpl 13	Wpl 14	Wpl 15	Wpl 16	Wpl 17	Wpl 18	Wpl 19	Wpl 20	Wpl 21
wt %									
SiO_2	62.20	62.02	62.34	62.03	62.27	58.91	59.16	58.85	58.70
Al_2O_3	23.99	23.88	23.91	23.99	23.84	26.14	25.93	26.08	26.25
CaO	4.95	5.14	4.85	5.25	4.62	7.61	7.24	7.47	7.41
BaO	0.02	0.00	0.00	0.02	0.03	0.02	0.00	0.01	0.03
Na_2O	8.28	8.10	8.09	8.12	8.39	6.65	6.62	6.67	6.71
K_2O	0.19	0.11	0.10	0.15	0.14	0.08	0.10	0.11	0.13
FeO	0.02	0.07	0.04	0.21	0.61	0.05	0.03	0.04	0.17
MgO	0.00	0.00	0.00	0.00	0.00	0.00	0.00	0.00	0.00
Total	99.65	99.32	99.33	99.77	99.90	99.46	99.08	99.23	99.40

Oxygens = 8

	Plagioclase								
	ic08-01a								
	Wpl 13	Wpl 14	Wpl 15	Wpl 16	Wpl 17	Wpl 18	Wpl 19	Wpl 20	Wpl 21
apfu									
Si	2.76	2.76	2.77	2.75	2.76	2.64	2.65	2.64	2.63
Al	1.25	1.25	1.25	1.25	1.25	1.38	1.37	1.38	1.39
Ca	0.24	0.25	0.23	0.25	0.22	0.36	0.35	0.36	0.36
Ba	0.00	0.00	0.00	0.00	0.00	0.00	0.00	0.00	0.00
Na	0.71	0.70	0.70	0.70	0.72	0.58	0.58	0.58	0.58
K	0.01	0.01	0.01	0.01	0.01	0.00	0.01	0.01	0.01
Fe^{2+}	0.00	0.00	0.00	0.01	0.02	0.00	0.00	0.00	0.01
Mg	0.00	0.00	0.00	0.00	0.00	0.00	0.00	0.00	0.00
X_{Ab}	0.74	0.74	0.75	0.73	0.76	0.61	0.62	0.61	0.62
X_{Or}	0.01	0.01	0.01	0.01	0.01	0.00	0.01	0.01	0.01
X_{An}	0.25	0.26	0.25	0.26	0.23	0.39	0.37	0.38	0.38

Appendix C, cont'd

	Plagioclase											
	ic08-01a											
	Mpl test	Mpl 1	Mpl 2	Mpl 3	Mpl 4	Mpl 5	Mpl 6	Mpl 7	Mpl 8	Mpl 9	Mpl 10	Mpl 11
wt %												
SiO_2	58.50	58.62	58.20	57.44	58.46	58.76	58.41	58.62	58.65	58.54	60.02	58.32
Al_2O_3	25.98	26.16	26.24	26.27	26.27	26.43	26.49	26.46	26.16	26.33	25.81	26.27
CaO	7.77	7.28	7.42	6.97	7.64	7.58	7.80	7.45	7.64	7.50	7.14	7.45
BaO	0.01	0.00	0.00	0.00	0.01	0.02	0.02	0.00	0.01	0.04	0.05	0.02
Na_2O	6.61	6.66	6.72	6.47	6.41	6.62	6.60	6.75	6.69	6.67	7.14	6.79
K_2O	0.14	0.12	0.13	0.10	0.13	0.14	0.14	0.15	0.11	0.11	0.10	0.11
FeO	0.01	0.04	0.04	1.73	0.01	0.02	0.04	0.02	0.01	0.12	0.13	0.04
MgO	0.00	0.00	0.00	0.03	0.00	0.00	0.00	0.00	0.00	0.01	0.00	0.00
Total	99.02	98.88	98.75	99.01	98.93	99.57	99.50	99.45	99.27	99.32	100.39	99.00

Oxygens = 8

	Plagioclase											
	ic08-01a											
	Mpl test	Mpl 1	Mpl 2	Mpl 3	Mpl 4	Mpl 5	Mpl 6	Mpl 7	Mpl 8	Mpl 9	Mpl 10	Mpl 11
apfu												
Si	2.63	2.64	2.63	2.60	2.63	2.63	2.62	2.62	2.63	2.63	2.66	2.62
Al	1.38	1.39	1.39	1.40	1.39	1.39	1.40	1.40	1.38	1.39	1.35	1.39
Ca	0.37	0.35	0.36	0.34	0.37	0.36	0.37	0.36	0.37	0.36	0.34	0.36
Ba	0.00	0.00	0.00	0.00	0.00	0.00	0.00	0.00	0.00	0.00	0.00	0.00
Na	0.58	0.58	0.59	0.57	0.56	0.57	0.57	0.59	0.58	0.58	0.61	0.59
K	0.01	0.01	0.01	0.01	0.01	0.01	0.01	0.01	0.01	0.01	0.01	0.01
Fe^{2+}	0.00	0.00	0.00	0.07	0.00	0.00	0.00	0.00	0.00	0.00	0.00	0.00
Mg	0.00	0.00	0.00	0.00	0.00	0.00	0.00	0.00	0.00	0.00	0.00	0.00
X_{Ab}	0.60	0.62	0.62	0.62	0.60	0.61	0.60	0.62	0.61	0.61	0.64	0.62
X_{Or}	0.01	0.01	0.01	0.01	0.01	0.01	0.01	0.01	0.01	0.01	0.01	0.01
X_{An}	0.39	0.37	0.38	0.37	0.39	0.38	0.39	0.38	0.38	0.38	0.35	0.37

Appendix C, cont'd

Plagioclase

	ic08-01a1		ic08-01a1												
	test 1	test -matri	Epl 1	Epl 2	Epl 3	Epl 4	Epl 5	Epl 6	E pl 7	Epl 8	Epl 9	Epl 10	Epl 11	Epl 12	Epl 13
wt %															
SiO_2	58.09	58.17	58.06	51.75	58.28	58.58	58.56	58.28	57.60	58.18	58.05	58.60	57.37	58.23	57.47
Al_2O_3	25.85	25.66	26.40	26.10	26.32	26.58	26.28	26.23	26.43	26.16	26.30	26.33	26.20	26.32	26.14
CaO	7.25	6.97	7.62	5.94	7.72	7.44	7.51	7.40	7.72	7.45	7.74	7.43	7.64	7.20	7.14
BaO	0.00	0.04	0.01	0.01	0.00	0.05	0.00	0.04	0.02	0.04	0.00	0.03	0.00	0.03	0.00
Na_2O	6.78	6.61	6.54	5.66	6.63	6.73	6.95	6.63	6.69	6.73	6.65	6.20	6.72	6.75	6.72
K_2O	0.05	0.12	0.08	0.09	0.14	0.12	0.11	0.09	0.10	0.10	0.12	0.10	0.08	0.11	0.13
FeO	0.36	0.47	0.02	7.44	0.05	0.04	0.02	0.02	0.04	0.06	0.03	0.05	0.05	0.11	1.18
MgO	0.00	0.00	0.00	1.98	0.00	0.00	0.00	0.00	0.00	0.00	0.00	0.00	0.00	0.00	0.48
Total	98.38	98.04	98.73	98.97	99.14	99.54	99.43	98.69	98.60	98.72	98.89	98.74	98.06	98.75	99.26

Oxygens = 8

Plagioclase

	ic08-01a1		ic08-01a1												
	test 1	test -matri	Epl 1	Epl 2	Epl 3	Epl 4	Epl 5	Epl 6	E pl 7	Epl 8	Epl 9	Epl 10	Epl 11	Epl 12	Epl 13
apfu															
Si	2.63	2.64	2.62	2.42	2.62	2.62	2.63	2.63	2.61	2.63	2.62	2.64	2.61	2.63	2.60
Al	1.38	1.37	1.40	1.44	1.39	1.40	1.39	1.39	1.41	1.39	1.40	1.40	1.40	1.40	1.39
Ca	0.35	0.34	0.37	0.30	0.37	0.36	0.36	0.36	0.37	0.36	0.37	0.36	0.37	0.35	0.35
Ba	0.00	0.00	0.00	0.00	0.00	0.00	0.00	0.00	0.00	0.00	0.00	0.00	0.00	0.00	0.00
Na	0.60	0.58	0.57	0.51	0.58	0.58	0.60	0.58	0.59	0.59	0.58	0.54	0.59	0.59	0.59
K	0.00	0.01	0.00	0.01	0.01	0.01	0.01	0.01	0.01	0.01	0.01	0.01	0.00	0.01	0.01
Fe^{2+}	0.01	0.02	0.00	0.29	0.00	0.00	0.00	0.00	0.00	0.00	0.00	0.00	0.00	0.00	0.04
Mg	0.00	0.00	0.00	0.14	0.00	0.00	0.00	0.00	0.00	0.00	0.00	0.00	0.00	0.00	0.03
X_{Ab}	0.63	0.63	0.61	0.63	0.60	0.62	0.62	0.62	0.61	0.62	0.60	0.60	0.61	0.62	0.63
X_{Or}	0.00	0.01	0.00	0.01	0.01	0.01	0.01	0.01	0.01	0.01	0.01	0.01	0.00	0.01	0.01
X_{An}	0.37	0.37	0.39	0.36	0.39	0.38	0.37	0.38	0.39	0.38	0.39	0.40	0.38	0.37	0.37

Appendix C, cont'd

	Plagioclase					
	ic08-01a1					
	Mpl 17	Mpl 18	Mpl 19	Mpl 20	Mpl 21	Mpl 22
wt %						
SiO_2	58.33	58.45	58.20	58.71	58.27	61.40
Al_2O_3	25.95	26.02	26.03	25.98	26.00	24.07
CaO	7.39	7.11	7.43	7.24	7.51	5.35
BaO	0.00	0.03	0.00	0.00	0.00	0.00
Na_2O	6.68	6.45	6.90	6.71	6.62	7.11
K_2O	0.13	0.11	0.10	0.08	0.11	0.15
FeO	0.05	0.02	0.02	0.06	0.03	0.06
MgO	0.00	0.00	0.00	0.00	0.00	0.00
Total	98.53	98.19	98.68	98.78	98.54	98.14

Oxygens = 8

	Plagioclase					
	ic08-01a1					
	Mpl 17	Mpl 18	Mpl 19	Mpl 20	Mpl 21	Mpl 22
apfu						
Si	2.64	2.64	2.63	2.64	2.63	2.76
Al	1.38	1.39	1.39	1.38	1.38	1.27
Ca	0.36	0.34	0.36	0.35	0.36	0.26
Ba	0.00	0.00	0.00	0.00	0.00	0.00
Na	0.59	0.57	0.60	0.59	0.58	0.62
K	0.01	0.01	0.01	0.00	0.01	0.01
Fe^{2+}	0.00	0.00	0.00	0.00	0.00	0.00
Mg	0.00	0.00	0.00	0.00	0.00	0.00
X_{Ab}	0.62	0.62	0.62	0.62	0.61	0.70
X_{Or}	0.01	0.01	0.01	0.00	0.01	0.01
X_{An}	0.38	0.38	0.37	0.37	0.38	0.29

Appendix C, cont'd

	Plagioclase													
	ic08-01b				ic08-01b									
	1-Npl-1	1-Npl-2	1-Npl-3	1-Npl-4	1-Npl-1	1-Npl-2	1-Npl-3	1-Npl-4	1-Npl-5	1-Npl-6	1-Npl-7	1-Npl-8	1-Npl-9	1-Npl-10
wt %				really pt 4										
SiO_2	58.29	58.89	59.10	58.94	58.16	58.62	58.89	58.49	58.11	57.15	58.20	58.08	58.05	58.25
Al_2O_3	25.27	25.46	25.15	25.44	25.24	25.16	25.55	25.50	25.53	25.14	25.67	25.66	25.74	25.49
CaO	6.29	6.81	6.45	6.87	6.43	6.81	6.58	6.92	6.60	6.97	6.64	7.03	6.92	7.01
BaO	0.00	0.00	0.00	0.01	0.04	0.00	0.09	0.00	0.01	0.00	0.07	0.00	0.07	0.01
Na_2O	7.27	7.16	7.10	7.10	6.99	6.90	7.02	7.06	7.04	6.83	6.82	6.98	6.87	7.05
K_2O	0.08	0.12	0.14	0.14	0.05	0.12	0.12	0.10	0.10	0.19	0.09	0.16	0.06	0.18
FeO	0.00	0.01	0.03	0.07	0.00	0.00	0.02	0.05	0.03	0.14	0.04	0.08	0.00	0.07
MgO	0.00	0.00	0.00	0.03	0.00	0.00	0.01	0.00	0.00	0.03	0.00	0.00	0.01	0.00
Total	97.20	98.45	97.97	98.60	96.91	97.61	98.28	98.12	97.42	96.45	97.53	97.99	97.72	98.06

Oxygens = 8

	Plagioclase													
	ic08-01b				ic08-01b									
	1-Npl-1	1-Npl-2	1-Npl-3	1-Npl-4	1-Npl-1	1-Npl-2	1-Npl-3	1-Npl-4	1-Npl-5	1-Npl-6	1-Npl-7	1-Npl-8	1-Npl-9	1-Npl-10
apfu				really pt 4										
Si	2.66	2.66	2.68	2.66	2.66	2.67	2.66	2.65	2.65	2.64	2.65	2.64	2.64	2.65
Al	1.36	1.36	1.34	1.35	1.36	1.35	1.36	1.36	1.37	1.37	1.38	1.37	1.38	1.36
Ca	0.31	0.33	0.31	0.33	0.32	0.33	0.32	0.34	0.32	0.35	0.32	0.34	0.34	0.34
Ba	0.00	0.00	0.00	0.00	0.00	0.00	0.00	0.00	0.00	0.00	0.00	0.00	0.00	0.00
Na	0.64	0.63	0.62	0.62	0.62	0.61	0.62	0.62	0.62	0.61	0.60	0.62	0.61	0.62
K	0.00	0.01	0.01	0.01	0.00	0.01	0.01	0.01	0.01	0.01	0.01	0.01	0.00	0.01
Fe^{2+}	0.00	0.00	0.00	0.00	0.00	0.00	0.00	0.00	0.00	0.01	0.00	0.00	0.00	0.00
Mg	0.00	0.00	0.00	0.00	0.00	0.00	0.00	0.00	0.00	0.00	0.00	0.00	0.00	0.00
X_{Ab}	0.67	0.65	0.66	0.65	0.66	0.64	0.65	0.64	0.65	0.63	0.65	0.64	0.64	0.64
X_{Or}	0.00	0.01	0.01	0.01	0.00	0.01	0.01	0.01	0.01	0.01	0.01	0.01	0.00	0.01
X_{An}	0.32	0.34	0.33	0.35	0.34	0.35	0.34	0.35	0.34	0.36	0.35	0.35	0.36	0.35

Appendix C, cont'd

Plagioclase

	ic08-01b								ic08-01b						
	1-Npl-11	1-Npl-12	1-Npl-13	1-Npl-14	1-Npl-15	1-Npl-16	1-Npl-17	1-Npl-17	1-Wpl-18	1-Wpl-19	1-Wpl-20	1-Wpl-21	1-Wpl-22	1-Wpl-23	1-Wpl-24
wt %															
SiO_2	58.91	58.18	58.70	58.22	58.52	57.40	10.56	57.94	58.53	58.34	58.45	58.01	58.34	58.05	58.44
Al_2O_3	25.59	25.53	25.47	25.26	25.98	25.47	6.59	25.80	25.64	25.74	25.85	25.73	26.14	25.68	25.92
CaO	6.62	6.81	6.49	6.98	6.63	6.71	1.20	6.91	7.14	7.02	7.39	6.98	7.41	6.81	7.17
BaO	0.04	0.00	0.09	0.00	0.05	0.10	0.00	0.03	0.02	0.03	0.04	0.05	0.04	0.00	0.00
Na_2O	7.11	7.05	7.10	7.07	7.18	7.03	1.38	6.80	6.78	6.59	6.80	6.67	6.63	6.83	6.55
K_2O	0.10	0.16	0.17	0.14	0.18	0.02	0.42	0.07	0.09	0.01	0.06	0.02	0.11	0.02	0.17
FeO	0.07	0.06	0.04	0.04	0.12	0.02	3.49	0.05	0.03	0.05	0.03	0.05	0.12	0.03	0.05
MgO	0.00	0.01	0.02	0.02	0.03	0.01	0.40	0.00	0.00	0.00	0.01	0.01	0.00	0.00	0.00
Total	98.44	97.80	98.08	97.73	98.69	96.76	24.04	97.60	98.23	97.78	98.63	97.52	98.79	97.42	98.30

Oxygens = 8

Plagioclase

	ic08-01b								ic08-01b						
	1-Npl-11	1-Npl-12	1-Npl-13	1-Npl-14	1-Npl-15	1-Npl-16	1-Npl-17	1-Npl-17	1-Wpl-18	1-Wpl-19	1-Wpl-20	1-Wpl-21	1-Wpl-22	1-Wpl-23	1-Wpl-24
apfu															
Si	2.66	2.65	2.66	2.65	2.64	2.64	2.16	2.64	2.65	2.65	2.64	2.64	2.63	2.65	2.64
Al	1.36	1.37	1.36	1.36	1.38	1.38	1.59	1.39	1.37	1.38	1.38	1.38	1.39	1.38	1.38
Ca	0.32	0.33	0.32	0.34	0.32	0.33	0.26	0.34	0.35	0.34	0.36	0.34	0.36	0.33	0.35
Ba	0.00	0.00	0.00	0.00	0.00	0.00	0.00	0.00	0.00	0.00	0.00	0.00	0.00	0.00	0.00
Na	0.62	0.62	0.62	0.62	0.63	0.63	0.55	0.60	0.60	0.58	0.60	0.59	0.58	0.60	0.57
K	0.01	0.01	0.01	0.01	0.01	0.00	0.11	0.00	0.01	0.00	0.00	0.00	0.01	0.00	0.01
Fe^{2+}	0.00	0.00	0.00	0.00	0.00	0.00	0.60	0.00	0.00	0.00	0.00	0.00	0.00	0.00	0.00
Mg	0.00	0.00	0.00	0.00	0.00	0.00	0.12	0.00	0.00	0.00	0.00	0.00	0.00	0.00	0.00
X_{Ab}	0.66	0.65	0.66	0.64	0.65	0.65	0.60	0.64	0.63	0.63	0.62	0.63	0.61	0.64	0.62
X_{Or}	0.01	0.01	0.01	0.01	0.01	0.00	0.12	0.00	0.01	0.00	0.00	0.00	0.01	0.00	0.01
X_{An}	0.34	0.34	0.33	0.35	0.33	0.34	0.29	0.36	0.37	0.37	0.37	0.37	0.38	0.35	0.37

Appendix C, cont'd

Plagioclase

	ic08-01b					ic08-01b			ic08-01b								
	1-Wpl-25	1-Wpl-26	1-Wpl-28	1-Wpl-29	1-Wpl-30	1-Epl-33	1-Epl-34	1-Epl-35	M-pl-1	M-pl-2	M-pl-3	M-pl-4	M-pl-5	M-pl-6	M-pl-7	M-pl-8	M-pl-9
wt %																	
SiO_2	57.69	58.70	58.73	58.59	58.49	58.53	58.72	58.06	58.88	59.09	59.43	59.25	58.97	58.79	58.91	59.02	58.93
Al_2O_3	25.73	25.84	25.92	25.82	26.12	25.65	25.83	25.68	25.28	25.49	25.31	25.24	25.33	25.54	25.37	25.66	25.10
CaO	7.03	7.30	7.23	7.04	7.28	6.73	7.16	6.88	6.59	6.85	6.49	6.82	6.40	6.99	6.61	6.98	6.69
BaO	0.05	0.00	0.01	0.00	0.06	0.00	0.00	0.00	0.03	0.01	0.02	0.03	0.06	0.01	0.00	0.04	0.00
Na_2O	6.61	6.66	6.78	6.79	6.53	6.68	6.83	6.81	6.66	6.89	6.93	7.12	6.86	6.61	6.75	6.90	6.90
K_2O	0.06	0.16	0.15	0.03	0.10	0.05	0.13	0.02	0.00	0.17	0.05	0.13	0.08	0.13	0.01	0.14	0.07
FeO	0.02	0.02	0.06	0.08	0.21	0.04	0.02	0.02	0.04	0.04	0.02	0.01	0.04	0.06	0.05	0.02	0.04
MgO	0.00	0.00	0.00	0.00	0.00	0.01	0.00	0.00	0.00	0.00	0.01	0.00	0.00	0.00	0.01	0.02	0.00
Total	97.19	98.68	98.88	98.35	98.79	97.69	98.69	97.47	97.48	98.54	98.26	98.60	97.74	98.13	97.71	98.78	97.73

Oxygens = 8

Plagioclase

	ic08-01b					ic08-01b			ic08-01b								
	1-Wpl-25	1-Wpl-26	1-Wpl-28	1-Wpl-29	1-Wpl-30	1-Epl-33	1-Epl-34	1-Epl-35	M-pl-1	M-pl-2	M-pl-3	M-pl-4	M-pl-5	M-pl-6	M-pl-7	M-pl-8	M-pl-9
apfu																	
Si	2.64	2.65	2.64	2.65	2.64	2.66	2.65	2.65	2.68	2.66	2.68	2.67	2.68	2.66	2.67	2.66	2.68
Al	1.39	1.37	1.37	1.38	1.39	1.37	1.37	1.38	1.35	1.35	1.35	1.34	1.35	1.36	1.36	1.36	1.34
Ca	0.34	0.35	0.35	0.34	0.35	0.33	0.35	0.34	0.32	0.33	0.31	0.33	0.31	0.34	0.32	0.34	0.33
Ba	0.00	0.00	0.00	0.00	0.00	0.00	0.00	0.00	0.00	0.00	0.00	0.00	0.00	0.00	0.00	0.00	0.00
Na	0.59	0.58	0.59	0.59	0.57	0.59	0.60	0.60	0.59	0.60	0.61	0.62	0.60	0.58	0.59	0.60	0.61
K	0.00	0.01	0.01	0.00	0.01	0.00	0.01	0.00	0.00	0.01	0.00	0.01	0.00	0.01	0.00	0.01	0.00
Fe^{2+}	0.00	0.00	0.00	0.00	0.01	0.00	0.00	0.00	0.00	0.00	0.00	0.00	0.00	0.00	0.00	0.00	0.00
Mg	0.00	0.00	0.00	0.00	0.00	0.00	0.00	0.00	0.00	0.00	0.00	0.00	0.00	0.00	0.00	0.00	0.00
X_{Ab}	0.63	0.62	0.62	0.63	0.62	0.64	0.63	0.64	0.65	0.64	0.66	0.65	0.66	0.63	0.65	0.64	0.65
X_{Or}	0.00	0.01	0.01	0.00	0.01	0.00	0.01	0.00	0.00	0.01	0.00	0.01	0.01	0.01	0.00	0.01	0.00
X_{An}	0.37	0.37	0.37	0.36	0.38	0.36	0.36	0.36	0.35	0.35	0.34	0.34	0.34	0.37	0.35	0.36	0.35

Appendix C, cont'd

Plagioclase

	ic08-01b1										ic08-01b1			
	1-Npl -1	1-Npl -2	1-Npl -3	1-Npl -4	1-Npl -5	1-Npl-6	1-Npl-7	1-Npl-8	1-Npl-9	1-Npl-10	1-Wpl-11	1-Wpl-12	1-Wpl-13	1-Wpl-14
wt %														
SiO_2	59.73	58.90	59.48	58.91	59.41	59.80	59.02	60.41	59.69	58.94	59.44	59.21	59.35	59.42
Al_2O_3	25.79	25.91	25.98	25.66	26.01	25.91	26.23	24.45	25.51	26.00	25.75	25.66	26.06	25.83
CaO	7.14	6.76	7.10	7.22	6.96	7.17	6.97	5.95	6.69	7.36	6.61	6.90	6.97	7.18
BaO	0.00	0.00	0.01	0.00	0.07	0.00	0.00	0.00	0.02	0.00	0.04	0.00	0.09	0.03
Na_2O	7.12	6.93	7.13	7.13	7.16	7.00	7.12	7.57	7.32	6.97	7.17	7.09	7.10	7.06
K_2O	0.12	0.36	0.22	0.10	0.10	0.06	0.13	0.09	0.16	0.10	0.14	0.17	0.10	0.17
FeO	0.07	0.41	0.08	0.02	0.03	0.01	0.01	0.11	0.02	0.04	0.20	0.08	0.07	0.03
MgO	0.00	0.06	0.01	0.00	0.00	0.01	0.00	0.02	0.01	0.00	0.00	0.01	0.01	0.00
Total	99.97	99.33	100.01	99.04	99.74	99.96	99.48	98.60	99.42	99.41	99.35	99.12	99.75	99.72

Oxygens = 8

Plagioclase

	ic08-01b1										ic08-01b1			
	1-Npl -1	1-Npl -2	1-Npl -3	1-Npl -4	1-Npl -5	1-Npl-6	1-Npl-7	1-Npl-8	1-Npl-9	1-Npl-10	1-Wpl-11	1-Wpl-12	1-Wpl-13	1-Wpl-14
apfu														
Si	2.66	2.64	2.65	2.65	2.65	2.66	2.64	2.72	2.67	2.64	2.66	2.66	2.65	2.65
Al	1.35	1.37	1.36	1.36	1.37	1.36	1.38	1.30	1.34	1.37	1.36	1.36	1.37	1.36
Ca	0.34	0.33	0.34	0.35	0.33	0.34	0.33	0.29	0.32	0.35	0.32	0.33	0.33	0.34
Ba	0.00	0.00	0.00	0.00	0.00	0.00	0.00	0.00	0.00	0.00	0.00	0.00	0.00	0.00
Na	0.61	0.60	0.62	0.62	0.62	0.60	0.62	0.66	0.63	0.61	0.62	0.62	0.61	0.61
K	0.01	0.02	0.01	0.01	0.01	0.00	0.01	0.01	0.01	0.01	0.01	0.01	0.01	0.01
Fe^{2+}	0.00	0.02	0.00	0.00	0.00	0.00	0.00	0.00	0.00	0.00	0.01	0.00	0.00	0.00
Mg	0.00	0.00	0.00	0.00	0.00	0.00	0.00	0.00	0.00	0.00	0.00	0.00	0.00	0.00
X_{Ab}	0.64	0.64	0.64	0.64	0.65	0.64	0.64	0.69	0.66	0.63	0.66	0.64	0.64	0.63
X_{Or}	0.01	0.02	0.01	0.01	0.01	0.00	0.01	0.01	0.01	0.01	0.01	0.01	0.01	0.01
X_{An}	35.41	34.26	35.04	35.67	34.74	36.01	34.84	30.11	33.24	36.63	33.46	34.62	34.96	35.62

Appendix C, cont'd

Plagioclase

	ic08-01b1						ic08-01b1						ic08-01b1		
	1-Wpl-15	1-Wpl-16	1-Wpl-17	1-Wpl-18	1-Wpl-19	1-Wpl-20	2-pl-21	2-pl-22	2-pl-23	2-pl-24	2-pl-25	2-pl-26	m-pl-27	m-pl-28	m-pl-28
wt %															
SiO_2	59.76	59.09	59.40	59.18	59.44	59.08	59.59	59.00	59.56	58.97	59.53	63.39	59.82	58.96	60.02
Al_2O_3	25.63	26.02	25.79	25.64	26.23	25.88	25.77	25.70	25.71	25.70	25.82	23.02	25.72	25.26	25.48
CaO	6.70	7.23	6.85	6.39	6.81	7.18	6.57	6.94	6.53	6.83	6.87	5.65	6.55	6.65	6.50
BaO	0.08	0.00	0.01	0.00	0.00	0.00	0.04	0.00	0.01	0.02	0.01	0.00	0.07	0.00	0.07
Na_2O	7.08	6.88	7.07	7.54	7.12	7.11	7.39	7.04	7.10	7.07	7.07	7.15	7.31	7.31	7.38
K_2O	0.10	0.16	0.16	0.25	0.10	0.13	0.13	0.13	0.10	0.14	0.10	0.05	0.06	0.12	0.07
FeO	0.18	0.11	0.08	0.06	0.03	0.04	0.06	0.07	0.04	0.00	0.07	0.08	0.06	0.02	0.02
MgO	0.00	0.00	0.00	0.01	0.03	0.03	0.02	0.02	0.01	0.00	0.00	0.00	0.00	0.00	0.02
Total	99.53	99.49	99.36	99.07	99.76	99.45	99.57	98.90	99.06	98.73	99.47	99.34	99.59	98.32	99.56

Oxygens = 8

Plagioclase

	ic08-01b1						ic08-01b1						ic08-01b1		
	1-Wpl-15	1-Wpl-16	1-Wpl-17	1-Wpl-18	1-Wpl-19	1-Wpl-20	2-pl-21	2-pl-22	2-pl-23	2-pl-24	2-pl-25	2-pl-26	m-pl-27	m-pl-28	m-pl-28
apfu															
Si	2.67	2.64	2.66	2.66	2.65	2.65	2.66	2.65	2.67	2.66	2.66	2.81	2.67	2.67	2.68
Al	1.35	1.37	1.36	1.36	1.38	1.37	1.36	1.36	1.36	1.36	1.36	1.20	1.35	1.35	1.34
Ca	0.32	0.35	0.33	0.31	0.33	0.34	0.31	0.33	0.31	0.33	0.33	0.27	0.31	0.32	0.31
Ba	0.00	0.00	0.00	0.00	0.00	0.00	0.00	0.00	0.00	0.00	0.00	0.00	0.00	0.00	0.00
Na	0.61	0.60	0.61	0.66	0.62	0.62	0.64	0.61	0.62	0.62	0.61	0.61	0.63	0.64	0.64
K	0.01	0.01	0.01	0.01	0.01	0.01	0.01	0.01	0.01	0.01	0.01	0.00	0.00	0.01	0.00
Fe^{2+}	0.01	0.00	0.00	0.00	0.00	0.00	0.00	0.00	0.00	0.00	0.00	0.00	0.00	0.00	0.00
Mg	0.00	0.00	0.00	0.00	0.00	0.00	0.00	0.00	0.00	0.00	0.00	0.00	0.00	0.00	0.00
X_{Ab}	0.65	0.63	0.65	0.67	0.65	0.64	0.67	0.64	0.66	0.65	0.65	0.69	0.67	0.66	0.67
X_{Or}	0.01	0.01	0.01	0.01	0.01	0.01	0.01	0.01	0.01	0.01	0.01	0.00	0.00	0.01	0.00
X_{An}	34.13	36.38	34.54	31.43	34.37	35.54	32.69	34.99	33.49	34.51	34.73	30.30	33.00	33.21	32.60

Appendix C, cont'd

	Plagioclase													
	ic08-01e													
	5-Wpl-1	5-Wpl-2	5-Wpl-3	5-Wpl-4	5-Wpl-5	5-Wpl-6	5-Wpl-7	5-Wpl-8	5-Wpl-9	5-Wpl-10	5-Wpl-11	5-Wpl-12	5-Wpl-13	5-Wpl-14
wt %														
SiO_2	57.70	57.49	57.38	57.80	56.94	57.31	57.20	57.12	56.92	57.43	56.55	57.41	57.08	57.11
Al_2O_3	26.50	26.82	26.59	26.69	26.76	26.83	26.99	26.97	26.94	27.09	27.27	27.06	27.18	27.15
CaO	8.14	8.40	8.30	8.42	8.39	8.77	8.62	8.71	8.50	8.70	8.68	8.70	8.35	8.88
BaO	0.00	0.00	0.04	0.01	0.00	0.00	0.04	0.03	0.00	0.02	0.09	0.00	0.04	0.00
Na_2O	6.10	6.13	6.12	6.12	6.08	5.98	5.84	5.93	6.21	5.95	5.93	6.24	6.01	5.88
K_2O	0.02	0.12	0.03	0.12	0.04	0.14	0.11	0.12	0.03	0.13	0.03	0.16	0.03	0.18
FeO	0.00	0.00	0.00	0.03	0.01	0.04	0.03	0.03	0.04	0.02	0.03	0.01	0.04	0.02
MgO	0.00	0.00	0.00	0.01	0.00	0.01	0.00	0.00	0.00	0.01	0.00	0.00	0.00	0.01
Total	98.46	98.96	98.46	99.20	98.22	99.08	98.83	98.91	98.64	99.35	98.58	99.58	98.73	99.23

Oxygens = 8

	Plagioclase													
	ic08-01e													
	5-Wpl-1	5-Wpl-2	5-Wpl-3	5-Wpl-4	5-Wpl-5	5-Wpl-6	5-Wpl-7	5-Wpl-8	5-Wpl-9	5-Wpl-10	5-Wpl-11	5-Wpl-12	5-Wpl-13	5-Wpl-14
apfu														
Si	2.61	2.59	2.60	2.60	2.59	2.58	2.58	2.58	2.58	2.58	2.56	2.58	2.58	2.57
Al	1.41	1.43	1.42	1.41	1.43	1.43	1.44	1.44	1.44	1.44	1.46	1.43	1.45	1.44
Ca	0.39	0.41	0.40	0.41	0.41	0.42	0.42	0.42	0.41	0.42	0.42	0.42	0.40	0.43
Ba	0.00	0.00	0.00	0.00	0.00	0.00	0.00	0.00	0.00	0.00	0.00	0.00	0.00	0.00
Na	0.53	0.54	0.54	0.53	0.54	0.52	0.51	0.52	0.55	0.52	0.52	0.54	0.53	0.51
K	0.00	0.01	0.00	0.01	0.00	0.01	0.01	0.01	0.00	0.01	0.00	0.01	0.00	0.01
Fe^{2+}	0.00	0.00	0.00	0.00	0.00	0.00	0.00	0.00	0.00	0.00	0.00	0.00	0.00	0.00
Mg	0.00	0.00	0.00	0.00	0.00	0.00	0.00	0.00	0.00	0.00	0.00	0.00	0.00	0.00
X_{Ab}	0.57	0.56	0.57	0.56	0.57	0.55	0.55	0.55	0.57	0.55	0.55	0.56	0.56	0.54
X_{Or}	0.00	0.01	0.00	0.01	0.00	0.01	0.01	0.01	0.00	0.01	0.00	0.01	0.00	0.01
X_{An}	0.42	0.43	0.43	0.43	0.43	0.44	0.45	0.44	0.43	0.44	0.45	0.43	0.43	0.45

Appendix C, cont'd

	Plagioclase						
	ic08-01e						
	1-Spl-1	1-Spl-2	1-Spl-3	1-Spl-4	1-Spl-5	1-Spl-6	1-Spl-7
wt %							
SiO_2	54.13	57.64	57.10	57.12	57.26	57.60	58.35
Al_2O_3	24.76	27.19	27.23	27.30	27.28	27.27	26.91
CaO	5.64	8.82	8.55	9.20	8.58	8.71	7.96
BaO	0.00	0.00	0.00	0.00	0.00	0.00	0.07
Na_2O	5.72	6.04	5.86	5.86	5.93	6.04	6.46
K_2O	1.47	0.27	0.14	0.11	0.12	0.15	0.09
FeO	5.76	0.11	0.06	0.06	0.06	0.12	0.08
MgO	1.27	0.00	0.00	0.00	0.00	0.00	0.00
Total	98.75	100.07	98.94	99.65	99.23	99.89	99.92

Oxygens = 8

	Plagioclase						
	ic08-01e						
	1-Spl-1	1-Spl-2	1-Spl-3	1-Spl-4	1-Spl-5	1-Spl-6	1-Spl-7
apfu							
Si	2.53	2.58	2.58	2.56	2.58	2.58	2.60
Al	1.36	1.43	1.45	1.44	1.45	1.44	1.42
Ca	0.28	0.42	0.41	0.44	0.41	0.42	0.38
Ba	0.00	0.00	0.00	0.00	0.00	0.00	0.00
Na	0.52	0.52	0.51	0.51	0.52	0.52	0.56
K	0.09	0.02	0.01	0.01	0.01	0.01	0.01
Fe^{2+}	0.23	0.00	0.00	0.00	0.00	0.00	0.00
Mg	0.09	0.00	0.00	0.00	0.00	0.00	0.00
X_{Ab}	0.58	0.54	0.55	0.53	0.55	0.55	0.59
X_{Or}	0.10	0.02	0.01	0.01	0.01	0.01	0.01
X_{An}	0.32	0.44	0.44	0.46	0.44	0.44	0.40

Appendix C, cont'd

	Plagioclase												
	st08-13a												
	1_1	1_2	1_3	1_4	1_5	1_6	1_7	1_8	1_9	1_10	1_11	1_12	1_13
wt %													
SiO_2	53.80	53.55	53.89	53.55	54.47	54.96	54.63	55.25	54.80	54.34	54.69	54.22	54.28
Al_2O_3	29.12	29.02	29.02	28.79	28.71	28.26	28.46	27.98	28.65	28.49	28.54	29.18	29.08
CaO	11.07	10.97	10.81	10.88	10.34	10.01	10.26	9.96	10.33	10.41	10.21	11.08	10.97
BaO	0.02	0.00	0.03	0.06	0.00	0.02	0.03	0.00	0.01	0.06	0.00	0.04	0.01
Na_2O	4.89	5.11	4.96	5.02	5.09	5.34	5.16	5.50	5.19	5.36	5.34	4.96	4.89
K_2O	0.12	0.07	0.10	0.08	0.08	0.12	0.07	0.11	0.06	0.12	0.12	0.07	0.10
FeO	0.10	0.06	0.05	0.06	0.08	0.03	0.02	0.02	0.00	0.03	0.05	0.04	0.13
MgO	0.00	0.02	0.01	0.00	0.00	0.00	0.00	0.03	0.00	0.00	0.02	0.00	0.01
Total	99.12	98.80	98.87	98.44	98.77	98.74	98.63	98.85	99.04	98.81	98.97	99.59	99.47

Oxygens = 8

	Plagioclase												
	st08-13a												
	1_1	1_2	1_3	1_4	1_5	1_6	1_7	1_8	1_9	1_10	1_11	1_12	1_13
apfu													
Si	2.45	2.44	2.46	2.45	2.48	2.50	2.49	2.51	2.49	2.48	2.48	2.45	2.46
Al	1.56	1.56	1.56	1.55	1.54	1.51	1.53	1.50	1.53	1.53	1.53	1.56	1.55
Ca	0.54	0.54	0.53	0.53	0.50	0.49	0.50	0.48	0.50	0.51	0.50	0.54	0.53
Ba	0.00	0.00	0.00	0.00	0.00	0.00	0.00	0.00	0.00	0.00	0.00	0.00	0.00
Na	0.43	0.45	0.44	0.45	0.45	0.47	0.46	0.48	0.46	0.47	0.47	0.44	0.43
K	0.01	0.00	0.01	0.00	0.00	0.01	0.00	0.01	0.00	0.01	0.01	0.00	0.01
Fe^{2+}	0.00	0.00	0.00	0.00	0.00	0.00	0.00	0.00	0.00	0.00	0.00	0.00	0.00
Mg	0.00	0.00	0.00	0.00	0.00	0.00	0.00	0.00	0.00	0.00	0.00	0.00	0.00
X_{Ab}	0.44	0.46	0.45	0.45	0.47	0.49	0.47	0.50	0.47	0.48	0.48	0.45	0.44
X_{Or}	0.01	0.00	0.01	0.00	0.00	0.01	0.00	0.01	0.00	0.01	0.01	0.00	0.01
X_{An}	0.55	0.54	0.54	0.54	0.53	0.51	0.52	0.50	0.52	0.51	0.51	0.55	0.55

Appendix C, cont'd

	Plagioclase						
	st08-13a						
	2_14	2_15	2_16	2_17	2_18	2_19	2_20
wt %							
SiO_2	54.58	54.72	54.92	56.10	54.65	54.93	55.05
Al_2O_3	28.95	28.67	28.53	27.85	28.93	28.46	28.79
CaO	10.65	10.51	10.30	9.69	10.64	10.09	10.47
BaO	0.00	0.02	0.02	0.00	0.01	0.05	0.03
Na_2O	5.05	5.14	4.91	5.47	5.26	5.29	5.17
K_2O	0.10	0.09	0.08	0.09	0.06	0.10	0.12
FeO	0.14	0.03	0.08	0.01	0.04	0.01	0.12
MgO	0.00	0.01	0.00	0.01	0.00	0.00	0.03
Total	99.47	99.19	98.84	99.22	99.59	98.93	99.78

Oxygens = 8

	Plagioclase						
	st08-13a						
	2_14	2_15	2_16	2_17	2_18	2_19	2_20
apfu							
Si	2.47	2.48	2.49	2.53	2.47	2.49	2.48
Al	1.54	1.53	1.53	1.48	1.54	1.52	1.53
Ca	0.52	0.51	0.50	0.47	0.52	0.49	0.51
Ba	0.00	0.00	0.00	0.00	0.00	0.00	0.00
Na	0.44	0.45	0.43	0.48	0.46	0.47	0.45
K	0.01	0.01	0.00	0.01	0.00	0.01	0.01
Fe^{2+}	0.01	0.00	0.00	0.00	0.00	0.00	0.00
Mg	0.00	0.00	0.00	0.00	0.00	0.00	0.00
X_{Ab}	0.46	0.47	0.46	0.50	0.47	0.48	0.47
X_{Or}	0.01	0.01	0.00	0.01	0.00	0.01	0.01
X_{An}	0.53	0.53	0.53	0.49	0.53	0.51	0.52

Appendix C, cont'd

	Plagioclase											
	st08-30a											
	1 _ 5	1 _6	1_7	1_8	1_9	1_10	1_11	1_12	1_13	1_14	1_15	1_16
wt %												
SiO_2	47.13	47.33	46.83	47.15	45.07	45.18	48.96	46.04	45.59	45.55	46.87	46.87
Al_2O_3	33.84	34.23	34.01	34.39	35.65	35.50	32.68	34.99	34.87	35.05	34.06	34.09
CaO	17.13	16.74	17.01	17.49	18.77	18.49	15.77	18.09	18.04	18.14	16.98	16.74
BaO	0.00	0.02	0.00	0.00	0.01	0.00	0.03	0.02	0.00	0.03	0.02	0.03
Na_2O	2.09	1.96	1.89	1.77	1.09	1.05	2.65	1.39	1.50	1.38	1.98	2.04
K_2O	0.04	0.05	0.03	0.02	0.01	0.05	0.05	0.05	0.03	0.04	0.04	0.06
FeO	0.00	0.06	0.03	0.04	0.07	0.10	0.05	0.06	0.03	0.04	0.08	0.04
MgO	0.01	0.00	0.02	0.00	0.01	0.02	0.00	0.00	0.00	0.00	0.00	0.00
Total	100.24	100.39	99.82	100.86	100.68	100.39	100.19	100.64	100.06	100.23	100.03	99.87

Oxygens = 8

	Plagioclase											
	st08-30a											
	1 _ 5	1 _6	1_7	1_8	1_9	1_10	1_11	1_12	1_13	1_14	1_15	1_16
apfu												
Si	2.16	2.16	2.15	2.15	2.07	2.08	2.24	2.11	2.10	2.10	2.15	2.15
Al	1.83	1.84	1.84	1.85	1.93	1.92	1.76	1.89	1.89	1.90	1.84	1.85
Ca	0.84	0.82	0.84	0.85	0.92	0.91	0.77	0.89	0.89	0.89	0.84	0.82
Ba	0.00	0.00	0.00	0.00	0.00	0.00	0.00	0.00	0.00	0.00	0.00	0.00
Na	0.19	0.17	0.17	0.16	0.10	0.09	0.23	0.12	0.13	0.12	0.18	0.18
K	0.00	0.00	0.00	0.00	0.00	0.00	0.00	0.00	0.00	0.00	0.00	0.00
Fe^{2+}	0.00	0.00	0.00	0.00	0.00	0.00	0.00	0.00	0.00	0.00	0.00	0.00
Mg	0.00	0.00	0.00	0.00	0.00	0.00	0.00	0.00	0.00	0.00	0.00	0.00
X_{Ab}	0.18	0.17	0.17	0.15	0.10	0.09	0.23	0.12	0.13	0.12	0.17	0.18
X_{Or}	0.00	0.00	0.00	0.00	0.00	0.00	0.00	0.00	0.00	0.00	0.00	0.00
X_{An}	0.82	0.82	0.83	0.84	0.90	0.90	0.76	0.88	0.87	0.88	0.82	0.82

Appendix C, cont'd

	Plagioclase																
	st08-30a							st08-30a									
	2_17	2_18	2_19	2_20	2_21	2_22	2_23	3_24	3_25	3_26	3_27	3_28	3_29	3_30	3_31	3_32	3_33
wt %																	
SiO_2	60.44	60.31	59.39	58.62	58.99	59.45	58.87	47.81	47.58	48.18	47.54	47.89	47.84	48.03	47.85	48.05	47.38
Al_2O_3	25.06	25.25	25.08	25.67	25.94	25.79	26.46	33.75	33.57	33.63	33.40	33.54	33.79	33.72	33.56	33.27	33.67
CaO	6.15	6.47	6.01	7.11	7.45	7.13	7.58	16.18	16.29	16.21	16.48	16.13	16.32	16.21	16.31	16.31	16.58
BaO	0.05	0.00	0.10	0.00	0.01	0.03	0.05	0.00	0.00	0.00	0.00	0.00	0.00	0.00	0.06	0.01	0.07
Na_2O	7.16	6.95	6.83	6.36	6.60	6.81	6.69	2.29	2.28	2.29	2.21	2.30	2.21	2.35	2.28	2.25	2.28
K_2O	0.24	0.21	0.77	0.22	0.19	0.17	0.12	0.04	0.03	0.06	0.09	0.07	0.06	0.04	0.04	0.05	0.01
FeO	0.01	0.05	0.04	0.45	0.02	0.03	0.03	0.04	0.09	0.09	0.06	0.12	0.07	0.01	0.03	0.03	0.04
MgO	0.00	0.02	0.01	0.01	0.01	0.00	0.01	0.00	0.03	0.01	0.00	0.00	0.00	0.00	0.00	0.00	0.02
Total	99.11	99.26	98.23	98.44	99.21	99.41	99.81	100.11	99.87	100.47	99.78	100.05	100.29	100.36	100.13	99.97	100.05

Oxygens = 8

	Plagioclase																
	st08-30a							st08-30a									
	2_17	2_18	2_19	2_20	2_21	2_22	2_23	3_24	3_25	3_26	3_27	3_28	3_29	3_30	3_31	3_32	3_33
apfu																	
Si	2.70	2.69	2.69	2.65	2.65	2.66	2.63	2.19	2.18	2.20	2.19	2.19	2.19	2.19	2.19	2.20	2.17
Al	1.32	1.33	1.34	1.37	1.37	1.36	1.39	1.82	1.82	1.81	1.81	1.81	1.82	1.81	1.81	1.80	1.82
Ca	0.29	0.31	0.29	0.34	0.36	0.34	0.36	0.79	0.80	0.79	0.81	0.79	0.80	0.79	0.80	0.80	0.82
Ba	0.00	0.00	0.00	0.00	0.00	0.00	0.00	0.00	0.00	0.00	0.00	0.00	0.00	0.00	0.00	0.00	0.00
Na	0.62	0.60	0.60	0.56	0.57	0.59	0.58	0.20	0.20	0.20	0.20	0.20	0.20	0.21	0.20	0.20	0.20
K	0.01	0.01	0.04	0.01	0.01	0.01	0.01	0.00	0.00	0.00	0.01	0.00	0.00	0.00	0.00	0.00	0.00
Fe^{2+}	0.00	0.00	0.00	0.02	0.00	0.00	0.00	0.00	0.00	0.00	0.00	0.00	0.00	0.00	0.00	0.00	0.00
Mg	0.00	0.00	0.00	0.00	0.00	0.00	0.00	0.00	0.00	0.00	0.00	0.00	0.00	0.00	0.00	0.00	0.00
X_{Ab}	0.67	0.65	0.64	0.61	0.61	0.63	0.61	0.20	0.20	0.20	0.19	0.20	0.20	0.21	0.20	0.20	0.20
X_{Or}	0.01	0.01	0.05	0.01	0.01	0.01	0.01	0.00	0.00	0.00	0.01	0.00	0.00	0.00	0.00	0.00	0.00
X_{An}	0.32	0.34	0.31	0.38	0.38	0.36	0.38	0.79	0.80	0.79	0.80	0.79	0.80	0.79	0.80	0.80	0.80

Appendix C, cont'd

	Plagioclase				
	st08-30a				
	3_34	3_35	3_36	3_37	3_38
wt %					
SiO_2	48.09	47.74	47.01	46.46	60.04
Al_2O_3	33.65	33.42	34.31	34.13	25.11
CaO	16.13	16.59	16.57	16.71	6.37
BaO	0.03	0.03	0.05	0.06	0.00
Na_2O	2.13	2.30	2.02	1.95	6.12
K_2O	0.06	0.00	0.03	0.14	0.16
FeO	0.00	0.03	0.10	0.06	0.05
MgO	0.00	0.01	0.00	0.01	0.00
Total	100.09	100.12	100.09	99.52	97.85

Oxygens = 8

	Plagioclase				
	st08-30a				
	3_34	3_35	3_36	3_37	3_38
apfu					
Si	2.20	2.19	2.16	2.15	2.71
Al	1.81	1.80	1.85	1.86	1.33
Ca	0.79	0.81	0.81	0.83	0.31
Ba	0.00	0.00	0.00	0.00	0.00
Na	0.19	0.20	0.18	0.17	0.54
K	0.00	0.00	0.00	0.01	0.01
Fe^{2+}	0.00	0.00	0.00	0.00	0.00
Mg	0.00	0.00	0.00	0.00	0.00
X_{Ab}	0.19	0.20	0.18	0.17	0.63
X_{Or}	0.00	0.00	0.00	0.01	0.01
X_{An}	0.80	0.80	0.82	0.82	0.36

Appendix C, cont'd

	Plagioclase											
	st08-45a											
	1_1	1_2	1_3	1_4	1_5	1_6	1_7	1_8	1_9	1_10	1_11	1_12
wt %												
SiO_2	60.07	60.18	60.21	59.50	60.82	60.59	59.50	59.25	60.23	59.49	59.89	59.82
Al_2O_3	25.88	25.59	25.60	25.33	25.61	25.32	25.26	25.36	25.46	25.45	25.57	25.56
CaO	6.98	6.64	6.84	6.41	6.28	6.32	6.29	6.58	6.61	6.46	6.53	6.62
BaO	0.01	0.00	0.06	0.03	0.07	0.00	0.02	0.00	0.03	0.00	0.00	0.00
Na_2O	6.90	7.09	7.06	7.08	7.13	7.17	7.05	6.99	6.95	7.11	7.04	7.03
K_2O	0.28	0.35	0.36	0.38	0.44	0.43	0.32	0.31	0.28	0.31	0.39	0.39
FeO	0.06	0.05	0.03	0.05	0.04	0.05	0.04	0.03	0.04	0.04	0.01	0.05
MgO	0.03	0.01	0.00	0.00	0.00	0.00	0.00	0.02	0.00	0.00	0.03	0.00
Total	100.21	99.91	100.16	98.78	100.39	99.88	98.48	98.54	99.60	98.86	99.46	99.47

Oxygens = 8

	Plagioclase											
	st08-45a											
	1_1	1_2	1_3	1_4	1_5	1_6	1_7	1_8	1_9	1_10	1_11	1_12
apfu												
Si	2.66	2.68	2.67	2.68	2.69	2.69	2.68	2.67	2.68	2.67	2.68	2.67
Al	1.35	1.34	1.34	1.34	1.33	1.33	1.34	1.35	1.34	1.35	1.35	1.35
Ca	0.33	0.32	0.33	0.31	0.30	0.30	0.30	0.32	0.32	0.31	0.31	0.32
Ba	0.00	0.00	0.00	0.00	0.00	0.00	0.00	0.00	0.00	0.00	0.00	0.00
Na	0.59	0.61	0.61	0.62	0.61	0.62	0.62	0.61	0.60	0.62	0.61	0.61
K	0.02	0.02	0.02	0.02	0.02	0.02	0.02	0.02	0.02	0.02	0.02	0.02
Fe^{2+}	0.00	0.00	0.00	0.00	0.00	0.00	0.00	0.00	0.00	0.00	0.00	0.00
Mg	0.00	0.00	0.00	0.00	0.00	0.00	0.00	0.00	0.00	0.00	0.00	0.00
X_{Ab}	0.63	0.65	0.64	0.65	0.65	0.66	0.66	0.65	0.64	0.65	0.65	0.64
X_{Or}	0.02	0.02	0.02	0.02	0.03	0.03	0.02	0.02	0.02	0.02	0.02	0.02
X_{An}	0.35	0.33	0.34	0.33	0.32	0.32	0.32	0.34	0.34	0.33	0.33	0.33

Appendix C, cont'd

	plagioclase								
	st08-45a								
	2_13	2_14	2_15	2_16	2_17	2_18	2_19	2_20	2_21
wt %									
SiO_2	59.86	59.26	60.22	60.01	59.77	58.87	59.47	59.21	60.21
Al_2O_3	25.64	25.57	25.67	25.50	25.66	25.51	26.05	26.02	25.98
CaO	6.82	6.79	6.73	6.56	6.63	6.76	7.03	7.02	6.98
BaO	0.00	0.04	0.05	0.03	0.07	0.00	0.00	0.00	0.00
Na_2O	6.91	7.04	6.88	7.12	6.98	7.02	6.74	6.86	6.63
K_2O	0.44	0.44	0.42	0.31	0.23	0.37	0.36	0.36	0.32
FeO	0.03	0.09	0.08	0.04	0.04	0.02	0.08	0.08	0.06
MgO	0.02	0.01	0.03	0.00	0.00	0.00	0.01	0.00	0.01
Total	99.72	99.24	100.08	99.57	99.38	98.55	99.74	99.55	100.19

Oxygens = 8

	plagioclase								
	st08-45a								
	2_13	2_14	2_15	2_16	2_17	2_18	2_19	2_20	2_21
apfu									
Si	2.67	2.66	2.68	2.68	2.67	2.66	2.65	2.65	2.67
Al	1.35	1.35	1.34	1.34	1.35	1.36	1.37	1.37	1.36
Ca	0.33	0.33	0.32	0.31	0.32	0.33	0.34	0.34	0.33
Ba	0.00	0.00	0.00	0.00	0.00	0.00	0.00	0.00	0.00
Na	0.60	0.61	0.59	0.62	0.60	0.61	0.58	0.59	0.57
K	0.03	0.03	0.02	0.02	0.01	0.02	0.02	0.02	0.02
Fe^{2+}	0.00	0.00	0.00	0.00	0.00	0.00	0.00	0.00	0.00
Mg	0.00	0.00	0.00	0.00	0.00	0.00	0.00	0.00	0.00
X_{Ab}	0.63	0.64	0.63	0.65	0.65	0.64	0.62	0.62	0.62
X_{Or}	0.03	0.03	0.03	0.02	0.01	0.02	0.02	0.02	0.02
X_{An}	0.34	0.34	0.34	0.33	0.34	0.34	0.36	0.35	0.36

Appendix C, cont'd

	Plagioclase										
	idaho m										
	1_1	1_2	1_3	1_4	1_5	1_6	1_7	1_8	1_9	1_10	1_11
wt %											
SiO_2	57.87	57.67	58.35	60.27	58.10	58.07	58.00	57.54	58.00	57.91	58.08
Al_2O_3	26.62	26.42	26.68	25.16	26.74	26.58	26.56	26.56	26.75	26.76	26.95
CaO	8.24	8.44	7.76	6.52	8.09	8.09	7.96	8.15	8.12	8.10	7.98
BaO	0.02	0.04	0.05	0.01	0.00	0.03	0.00	0.00	0.04	0.02	0.03
Na_2O	6.19	6.09	6.43	5.55	6.33	6.28	6.20	6.13	6.33	6.28	6.31
K_2O	0.28	0.22	0.24	0.14	0.33	0.33	0.35	0.32	0.30	0.26	0.24
FeO	0.03	0.01	0.01	0.07	0.02	0.04	0.01	0.00	0.05	0.05	0.08
MgO	0.00	0.00	0.00	0.00	0.00	0.00	0.00	0.00	0.03	0.02	0.03
Total	99.25	98.89	99.52	97.72	99.61	99.42	99.08	98.70	99.62	99.40	99.70

Oxygens = 8

	Plagioclase										
	idaho m										
	1_1	1_2	1_3	1_4	1_5	1_6	1_7	1_8	1_9	1_10	1_11
apfu											
Si	2.60	2.60	2.61	2.72	2.60	2.61	2.61	2.60	2.60	2.60	2.60
Al	1.41	1.41	1.41	1.34	1.41	1.41	1.41	1.42	1.41	1.42	1.42
Ca	0.40	0.41	0.37	0.31	0.39	0.39	0.38	0.39	0.39	0.39	0.38
Ba	0.00	0.00	0.00	0.00	0.00	0.00	0.00	0.00	0.00	0.00	0.00
Na	0.54	0.53	0.56	0.48	0.55	0.55	0.54	0.54	0.55	0.55	0.55
K	0.02	0.01	0.01	0.01	0.02	0.02	0.02	0.02	0.02	0.01	0.01
Fe^{2+}	0.00	0.00	0.00	0.00	0.00	0.00	0.00	0.00	0.00	0.00	0.00
Mg	0.00	0.00	0.00	0.00	0.00	0.00	0.00	0.00	0.00	0.00	0.00
X_{Ab}	0.57	0.56	0.59	0.60	0.57	0.57	0.57	0.57	0.57	0.57	0.58
X_{Or}	0.02	0.01	0.01	0.01	0.02	0.02	0.02	0.02	0.02	0.02	0.01
X_{An}	0.42	0.43	0.39	0.39	0.41	0.41	0.41	0.42	0.41	0.41	0.41

Appendix C, cont'd

	Plagioclase							
	idaho m							
	2_12	2_13	2_14	2_15	2_16	2_17	2_18	2_19
wt %								
SiO_2	58.72	58.41	58.61	59.74	59.88	58.39	58.68	58.26
Al_2O_3	26.28	26.47	26.52	25.40	25.56	26.38	26.23	26.57
CaO	7.60	7.65	7.60	6.73	6.62	7.75	7.56	7.70
BaO	0.05	0.01	0.01	0.01	0.00	0.01	0.00	0.00
Na_2O	6.71	6.74	6.50	7.00	7.04	6.51	6.46	6.53
K_2O	0.22	0.21	0.22	0.32	0.30	0.24	0.25	0.23
FeO	0.04	0.04	0.03	0.04	0.01	0.02	0.01	0.00
MgO	0.00	0.00	0.00	0.00	0.01	0.00	0.00	0.01
Total	99.62	99.53	99.49	99.24	99.42	99.30	99.19	99.30

Oxygens = 8

	Plagioclase							
	idaho m							
	2_12	2_13	2_14	2_15	2_16	2_17	2_18	2_19
apfu								
Si	2.63	2.62	2.62	2.68	2.68	2.62	2.63	2.62
Al	1.39	1.40	1.40	1.34	1.35	1.40	1.39	1.41
Ca	0.36	0.37	0.36	0.32	0.32	0.37	0.36	0.37
Ba	0.00	0.00	0.00	0.00	0.00	0.00	0.00	0.00
Na	0.58	0.59	0.56	0.61	0.61	0.57	0.56	0.57
K	0.01	0.01	0.01	0.02	0.02	0.01	0.01	0.01
Fe^{2+}	0.00	0.00	0.00	0.00	0.00	0.00	0.00	0.00
Mg	0.00	0.00	0.00	0.00	0.00	0.00	0.00	0.00
X_{Ab}	0.61	0.61	0.60	0.64	0.65	0.59	0.60	0.60
X_{Or}	0.01	0.01	0.01	0.02	0.02	0.01	0.02	0.01
X_{An}	0.38	0.38	0.39	0.34	0.34	0.39	0.39	0.39

APPENDIX D: ELECTRON MICROPROBE ANALYSES – AMPHIBOLE

	Amphibole																		
	st08-13a													st08-13a					
	1_1	1_2	1_3	1_4	1_5	1_7	1_8	1_9	1_10	1_11	1_12	1_13	1_14	2_15	2_16	2_17	2_18	2_19	2_20
wt %																			
SiO_2	42.50	42.88	42.68	42.65	42.69	42.34	42.15	42.57	42.66	42.44	42.85	41.94	42.62	42.99	42.88	42.32	43.08	43.28	43.20
TiO_2	1.38	1.37	1.64	1.64	1.51	1.80	1.87	1.74	1.74	1.73	1.72	1.67	1.64	1.64	1.16	1.88	1.77	1.72	1.71
Al_2O_3	13.21	13.50	13.41	13.43	13.41	13.25	13.29	13.53	13.36	13.03	13.38	13.33	13.24	13.75	11.46	13.57	13.64	13.61	13.38
Cr_2O_3	0.00	0.10	0.02	0.07	0.03	0.08	0.05	0.04	0.09	0.05	0.08	0.06	0.08	0.09	0.02	0.09	0.07	0.05	0.03
FeO	15.09	15.88	15.70	16.01	15.69	15.81	15.84	16.27	16.18	15.02	15.75	15.02	15.84	16.15	12.56	15.99	15.84	16.02	15.89
MnO	0.24	0.19	0.29	0.25	0.25	0.24	0.23	0.26	0.22	0.26	0.30	0.26	0.22	0.26	0.29	0.26	0.25	0.25	0.21
MgO	10.37	9.99	10.19	10.05	10.13	9.97	9.71	9.93	9.79	10.43	9.88	10.07	9.88	10.03	11.52	9.95	9.69	9.83	9.63
CaO	11.60	11.91	11.58	11.72	11.74	11.64	11.70	11.46	11.89	11.74	11.75	11.80	11.93	11.85	11.04	12.00	11.44	11.91	11.26
BaO	0.01	0.03	0.03	0.02	0.02	0.03	0.00	0.00	0.02	0.00	0.00	0.10	0.04	0.00	0.00	0.08	0.04	0.02	0.00
Na_2O	1.44	1.44	1.31	1.47	1.39	1.30	1.37	1.40	1.34	1.39	1.36	1.37	1.36	1.37	0.87	1.49	1.40	1.42	1.43
K_2O	0.85	0.87	0.97	0.89	0.95	0.96	0.96	1.02	0.94	0.94	0.85	0.93	0.88	1.02	0.80	1.05	0.96	1.01	0.93
F	0.00	0.00	0.00	0.00	0.00	0.00	0.00	0.00	0.00	0.00	0.00	0.00	0.00	0.00	0.00	0.00	0.00	0.00	0.00
Cl	0.18	0.18	0.21	0.19	0.23	0.18	0.17	0.20	0.20	0.17	0.19	0.18	0.18	0.19	0.12	0.22	0.22	0.16	0.15
Total	96.87	98.34	98.03	98.39	98.04	97.60	97.34	98.42	98.43	97.20	98.11	96.73	97.91	99.34	92.72	98.90	98.40	99.28	97.82

stoiched on 15 cations

	Amphibole																		
	st08-13a													st08-13a					
	1_1	1_2	1_3	1_4	1_5	1_7	1_8	1_9	1_10	1_11	1_12	1_13	1_14	2_15	2_16	2_17	2_18	2_19	2_20
apfu																			
Si	6.33	6.36	6.33	6.32	6.34	6.32	6.34	6.34	6.34	6.31	6.38	6.28	6.36	6.32	6.39	6.28	6.42	6.38	6.47
Ti	0.15	0.15	0.18	0.18	0.17	0.20	0.21	0.19	0.19	0.19	0.19	0.19	0.18	0.18	0.13	0.21	0.20	0.19	0.19
Al	2.32	2.36	2.34	2.35	2.35	2.33	2.36	2.37	2.34	2.28	2.35	2.35	2.33	2.38	2.01	2.37	2.39	2.37	2.36
Cr	0.00	0.01	0.00	0.01	0.00	0.01	0.01	0.00	0.01	0.01	0.01	0.01	0.01	0.01	0.00	0.01	0.01	0.01	0.00
Fe^{2+}	1.88	1.97	1.95	1.98	1.95	1.97	1.99	2.03	2.01	1.87	1.96	1.88	1.98	1.99	1.56	1.98	1.97	1.98	1.99
Mn^{2+}	0.03	0.02	0.04	0.03	0.03	0.03	0.03	0.03	0.03	0.03	0.04	0.03	0.03	0.03	0.04	0.03	0.03	0.03	0.03
Mg	2.30	2.21	2.25	2.22	2.24	2.22	2.18	2.20	2.17	2.31	2.19	2.25	2.20	2.20	2.56	2.20	2.15	2.16	2.15
Ca	1.85	1.89	1.84	1.86	1.87	1.86	1.89	1.83	1.89	1.87	1.87	1.89	1.91	1.87	1.76	1.91	1.83	1.88	1.81
Ba	0.00	0.00	0.00	0.00	0.00	0.00	0.00	0.00	0.00	0.00	0.00	0.01	0.00	0.00	0.00	0.00	0.00	0.00	0.00
Na	0.42	0.41	0.38	0.42	0.40	0.38	0.40	0.40	0.39	0.40	0.39	0.40	0.39	0.39	0.25	0.43	0.40	0.41	0.42
K	0.16	0.16	0.18	0.17	0.18	0.18	0.18	0.19	0.18	0.18	0.16	0.18	0.17	0.19	0.15	0.20	0.18	0.19	0.18
F	0.00	0.00	0.00	0.00	0.00	0.00	0.00	0.00	0.00	0.00	0.00	0.00	0.00	0.00	0.00	0.00	0.00	0.00	0.00
Cl	0.05	0.05	0.05	0.05	0.06	0.05	0.04	0.05	0.05	0.04	0.05	0.05	0.05	0.05	0.03	0.06	0.06	0.04	0.04
Fe^{3+}	0.13	0.02	0.07	0.05	0.06	0.05	0.00	0.00	0.01	0.13	0.00	0.13	0.00	0.03	0.54	0.00	0.00	0.00	0.00
X_{Mg}	0.55	0.53	0.54	0.53	0.54	0.53	0.52	0.52	0.52	0.55	0.53	0.54	0.53	0.53	0.62	0.53	0.52	0.52	0.52

Appendix D, cont'd

	Amphibole								
	st08-13a								
	3_21	3_22	3_23	3_24	3_25	3_26	3_28	3_29	3_30
wt %									
SiO_2	43.80	44.24	44.01	43.43	43.00	43.62	43.92	44.49	44.74
TiO_2	1.21	1.22	1.12	1.12	1.24	1.20	1.28	1.08	0.93
Al_2O_3	13.35	12.40	12.98	12.80	13.65	13.61	12.65	12.38	12.57
Cr_2O_3	0.08	0.07	0.00	0.09	0.00	0.05	0.06	0.02	0.04
FeO	16.04	16.02	15.42	15.15	15.58	16.09	15.22	15.22	14.73
MnO	0.28	0.24	0.26	0.28	0.28	0.31	0.25	0.26	0.31
MgO	9.97	10.24	10.02	9.91	9.82	9.90	9.96	10.30	10.04
CaO	11.90	11.70	11.76	11.57	11.68	11.52	11.50	12.08	11.53
BaO	0.00	0.03	0.02	0.00	0.00	0.00	0.00	0.02	0.04
Na_2O	1.40	1.25	1.36	1.40	1.41	1.52	1.25	1.16	1.04
K_2O	0.82	0.70	0.79	0.72	0.80	0.79	0.74	0.73	0.62
F	0.00	0.00	0.00	0.00	0.00	0.00	0.00	0.00	0.00
Cl	0.18	0.20	0.17	0.15	0.21	0.19	0.15	0.19	0.12
Total	99.03	98.31	97.91	96.62	97.67	98.80	96.98	97.93	96.71

stoiched on 15 cations

	Amphibole								
	st08-13a								
	3_21	3_22	3_23	3_24	3_25	3_26	3_28	3_29	3_30
apfu									
Si	6.46	6.56	6.55	6.55	6.42	6.45	6.59	6.60	6.70
Ti	0.13	0.14	0.13	0.13	0.14	0.13	0.14	0.12	0.10
Al	2.32	2.17	2.28	2.27	2.40	2.37	2.24	2.16	2.22
Cr	0.01	0.01	0.00	0.01	0.00	0.01	0.01	0.00	0.00
Fe^{2+}	1.98	1.99	1.92	1.91	1.95	1.99	1.91	1.89	1.84
Mn^{2+}	0.04	0.03	0.03	0.04	0.04	0.04	0.03	0.03	0.04
Mg	2.19	2.26	2.22	2.23	2.19	2.18	2.23	2.28	2.24
Ca	1.88	1.86	1.87	1.87	1.87	1.83	1.85	1.92	1.85
Ba	0.00	0.00	0.00	0.00	0.00	0.00	0.00	0.00	0.00
Na	0.40	0.36	0.39	0.41	0.41	0.44	0.36	0.33	0.30
K	0.15	0.13	0.15	0.14	0.15	0.15	0.14	0.14	0.12
F	0.00	0.00	0.00	0.00	0.00	0.00	0.00	0.00	0.00
Cl	0.05	0.05	0.04	0.04	0.05	0.05	0.04	0.05	0.03
Fe^{3+}	0.00	0.00	0.00	0.00	0.00	0.00	0.00	0.00	0.00
X_{Mg}	0.53	0.53	0.54	0.54	0.53	0.52	0.54	0.55	0.55

Appendix D, cont'd

	Amphibole												
	st08-13a					st08-13a							
	4_31	4_32	4_33	4_34	4_37	5_38	5_39	5_40	5_41	5_42	5_43	5_44	5_45
wt %													
SiO_2	43.11	43.68	43.72	43.62	43.51	43.75	43.79	43.12	51.28	43.88	43.34	42.98	43.60
TiO_2	1.30	1.58	1.55	1.41	1.53	1.40	1.19	1.60	0.15	1.51	1.67	1.58	1.42
Al_2O_3	13.34	13.51	13.55	13.81	13.83	13.49	13.38	13.68	4.68	12.97	13.58	13.16	13.34
Cr_2O_3	0.02	0.03	0.02	0.01	0.00	0.00	0.00	0.05	0.01	0.04	0.05	0.05	0.02
FeO	15.87	15.79	15.74	16.09	16.07	16.21	15.70	15.90	14.85	16.10	15.88	16.00	16.11
MnO	0.26	0.25	0.21	0.27	0.29	0.25	0.24	0.29	0.27	0.25	0.30	0.26	0.22
MgO	10.20	10.02	10.22	10.24	10.01	9.96	10.30	9.89	12.46	10.06	10.26	10.10	10.38
CaO	11.65	11.69	11.70	11.84	11.33	11.62	12.10	11.99	13.03	12.20	11.89	11.83	11.79
BaO	0.06	0.00	0.00	0.02	0.00	0.08	0.01	0.02	0.00	0.00	0.04	0.02	0.04
Na_2O	1.56	1.45	1.41	1.54	1.43	1.54	1.39	1.37	0.25	1.29	1.48	1.41	1.47
K_2O	0.88	0.81	0.93	0.85	1.08	0.84	0.84	0.95	0.18	0.82	1.07	0.91	0.95
F	0.00	0.00	0.00	0.00	0.00	0.00	0.00	0.00	0.00	0.00	0.00	0.00	0.00
Cl	0.19	0.16	0.18	0.20	0.21	0.18	0.18	0.21	0.00	0.15	0.20	0.16	0.17
Total	98.44	98.97	99.23	99.90	99.29	99.32	99.12	99.07	97.16	99.27	99.76	98.46	99.51

stoiched on 15 cations

	Amphibole												
	st08-13a					st08-13a							
	4_31	4_32	4_33	4_34	4_37	5_38	5_39	5_40	5_41	5_42	5_43	5_44	5_45
apfu													
Si	6.40	6.44	6.43	6.38	6.42	6.45	6.43	6.37	7.41	6.43	6.36	6.37	6.40
Ti	0.15	0.18	0.17	0.16	0.17	0.16	0.13	0.18	0.02	0.17	0.18	0.18	0.16
Al	2.33	2.35	2.35	2.38	2.40	2.34	2.32	2.38	0.80	2.24	2.35	2.30	2.31
Cr	0.00	0.00	0.00	0.00	0.00	0.00	0.00	0.01	0.00	0.00	0.01	0.01	0.00
Fe^{2+}	1.97	1.95	1.94	1.97	1.98	2.00	1.93	1.96	1.79	1.97	1.95	1.98	1.98
Mn^{2+}	0.03	0.03	0.03	0.03	0.04	0.03	0.03	0.04	0.03	0.03	0.04	0.03	0.03
Mg	2.26	2.20	2.24	2.23	2.20	2.19	2.26	2.18	2.68	2.20	2.24	2.23	2.27
Ca	1.85	1.85	1.84	1.85	1.79	1.84	1.90	1.90	2.02	1.92	1.87	1.88	1.85
Ba	0.00	0.00	0.00	0.00	0.00	0.00	0.00	0.00	0.00	0.00	0.00	0.00	0.00
Na	0.45	0.41	0.40	0.44	0.41	0.44	0.40	0.39	0.07	0.37	0.42	0.41	0.42
K	0.17	0.15	0.17	0.16	0.20	0.16	0.16	0.18	0.03	0.15	0.20	0.17	0.18
F	0.00	0.00	0.00	0.00	0.00	0.00	0.00	0.00	0.00	0.00	0.00	0.00	0.00
Cl	0.05	0.04	0.04	0.05	0.05	0.05	0.04	0.05	0.00	0.04	0.05	0.04	0.04
Fe^{3+}	0.00	0.00	0.00	0.00	0.00	0.00	0.00	0.00	0.25	0.04	0.00	0.02	0.00
X_{Mg}	0.53	0.53	0.54	0.53	0.53	0.52	0.54	0.53	0.60	0.53	0.54	0.53	0.53

Appendix D, cont'd

	Amphibole																	
	st08-15d																	
	test	1_1	1_2	1_3	1_4	1_5	1_6	1_7	1_8	1_9	1_10	1_11	1_12	1_13	1_14	1_15	1_16	1_17
wt %																		
SiO_2	48.39	48.23	48.02	48.43	48.69	47.86	49.29	47.85	46.11	48.20	48.88	51.80	47.88	48.72	48.59	47.76	48.24	48.16
TiO_2	1.06	1.03	1.18	1.08	1.15	1.05	0.90	1.05	0.74	1.00	1.00	0.36	1.14	0.93	1.08	1.03	1.05	0.69
Al_2O_3	8.73	8.86	9.21	8.76	9.72	9.87	8.68	9.10	9.73	9.09	8.93	5.50	9.41	8.99	8.96	9.53	8.97	9.27
Cr_2O_3	0.14	0.06	0.15	0.13	0.10	0.16	0.08	0.14	0.11	0.14	0.16	0.04	0.15	0.08	0.12	0.06	0.14	0.09
FeO	11.14	11.18	11.08	10.97	11.28	11.33	11.05	11.64	9.60	10.98	10.75	9.40	11.53	11.12	11.30	11.09	11.10	10.69
MnO	0.24	0.21	0.24	0.23	0.22	0.24	0.18	0.18	0.20	0.21	0.20	0.22	0.25	0.28	0.23	0.20	0.20	0.22
MgO	14.80	15.04	14.72	15.08	15.06	14.49	15.29	14.62	14.13	14.66	15.39	16.52	14.64	15.24	14.72	14.50	14.74	15.09
CaO	12.15	11.89	12.19	11.98	12.12	12.02	12.35	11.81	12.27	11.79	12.27	12.75	12.10	11.82	12.44	11.78	12.26	11.97
BaO	0.00	0.00	0.05	0.05	0.00	0.00	0.09	0.00	0.00	0.00	0.00	0.04	0.07	0.02	0.00	0.05	0.00	0.02
Na_2O	1.09	1.00	1.08	1.01	1.18	1.16	0.95	1.01	1.03	1.03	1.03	0.51	1.17	1.03	1.01	1.12	1.04	1.07
K_2O	0.60	0.56	0.64	0.53	0.66	0.71	0.46	0.52	0.42	0.50	0.53	0.25	0.53	0.39	0.51	0.54	0.63	0.49
F	0.00	0.00	0.00	0.00	0.00	0.00	0.00	0.00	0.00	0.00	0.00	0.00	0.00	0.00	0.00	0.00	0.00	0.00
Cl	0.08	0.10	0.08	0.05	0.03	0.04	0.06	0.04	0.02	0.07	0.04	0.03	0.07	0.03	0.04	0.05	0.05	0.07
Total	98.42	98.16	98.64	98.30	100.21	98.93	99.38	97.96	94.36	97.67	99.18	97.42	98.94	98.65	99.00	97.71	98.42	97.83

stoiched on 15 cations

	Amphibole																	
	st08-15d																	
	test	1_1	1_2	1_3	1_4	1_5	1_6	1_7	1_8	1_9	1_10	1_11	1_12	1_13	1_14	1_15	1_16	1_17
apfu																		
Si	6.97	6.94	6.90	6.96	6.88	6.87	6.99	6.91	6.79	6.98	6.93	7.32	6.87	6.95	6.94	6.92	6.94	6.93
Ti	0.11	0.11	0.13	0.12	0.12	0.11	0.10	0.11	0.08	0.11	0.11	0.04	0.12	0.10	0.12	0.11	0.11	0.07
Al	1.48	1.50	1.56	1.48	1.62	1.67	1.45	1.55	1.69	1.55	1.49	0.92	1.59	1.51	1.51	1.63	1.52	1.57
Cr	0.02	0.01	0.02	0.01	0.01	0.02	0.01	0.02	0.01	0.02	0.02	0.00	0.02	0.01	0.01	0.01	0.02	0.01
Fe^{2+}	1.34	1.35	1.33	1.32	1.33	1.36	1.31	1.40	1.18	1.33	1.27	1.11	1.38	1.33	1.35	1.34	1.34	1.29
Mn^{2+}	0.03	0.03	0.03	0.03	0.03	0.03	0.02	0.02	0.02	0.03	0.02	0.03	0.03	0.03	0.03	0.02	0.02	0.03
Mg	3.18	3.23	3.15	3.23	3.17	3.10	3.23	3.15	3.10	3.16	3.25	3.48	3.13	3.24	3.14	3.13	3.16	3.24
Ca	1.87	1.83	1.88	1.85	1.84	1.85	1.88	1.83	1.93	1.83	1.86	1.93	1.86	1.81	1.90	1.83	1.89	1.85
Ba	0.00	0.00	0.00	0.00	0.00	0.00	0.01	0.00	0.00	0.00	0.00	0.00	0.00	0.00	0.00	0.00	0.00	0.00
Na	0.30	0.28	0.30	0.28	0.32	0.32	0.26	0.28	0.29	0.29	0.28	0.14	0.33	0.28	0.28	0.31	0.29	0.30
K	0.11	0.10	0.12	0.10	0.12	0.13	0.08	0.10	0.08	0.09	0.10	0.05	0.10	0.07	0.09	0.10	0.12	0.09
F	0.00	0.00	0.00	0.00	0.00	0.00	0.00	0.00	0.00	0.00	0.00	0.00	0.00	0.00	0.00	0.00	0.00	0.00
Cl	0.02	0.02	0.02	0.01	0.01	0.01	0.01	0.01	0.01	0.02	0.01	0.01	0.02	0.01	0.01	0.01	0.01	0.02
Fe^{3+}	0.00	0.00	0.00	0.00	0.00	0.00	0.00	0.02	0.19	0.00	0.04	0.17	0.00	0.02	0.00	0.00	0.00	0.02
X_{Mg}	0.70	0.71	0.70	0.71	0.70	0.70	0.71	0.69	0.72	0.70	0.72	0.76	0.69	0.71	0.70	0.70	0.70	0.72

Appendix D, cont'd

	Amphibole															
	st08-15d								st08-15d							
	2_18	2_19	2_20	2_21	2_22	2_23	2_24	2_25	3_26	3_27	2_28	3_29	3_30	2_31	3_32	3_33
wt %																
SiO_2	49.55	47.73	47.94	45.97	47.82	48.58	48.35	49.35	51.52	47.78	47.79	47.42	47.29	48.80	49.43	48.46
TiO_2	0.67	1.02	1.02	0.92	1.06	0.87	1.06	0.87	0.39	1.22	1.14	1.32	1.36	0.76	0.66	1.00
Al_2O_3	8.21	9.28	9.16	8.82	9.21	8.69	9.48	8.27	6.45	9.36	9.61	9.42	9.67	8.63	8.57	8.02
Cr_2O_3	0.13	0.17	0.11	0.15	0.20	0.15	0.15	0.08	0.28	0.15	0.13	0.06	0.14	0.09	0.07	0.13
FeO	10.87	11.48	11.42	10.90	11.17	10.84	11.49	10.80	12.07	11.33	11.09	11.22	10.86	10.79	10.56	11.08
MnO	0.19	0.28	0.20	0.21	0.20	0.23	0.23	0.24	0.21	0.20	0.22	0.23	0.18	0.19	0.21	0.23
MgO	15.49	14.50	14.72	13.35	14.76	14.45	14.84	15.33	15.22	14.60	14.65	14.55	14.29	15.04	15.37	15.11
CaO	12.07	11.87	12.13	11.55	12.35	11.80	12.26	12.09	12.45	11.82	12.10	11.67	12.43	11.88	12.50	11.60
BaO	0.07	0.00	0.05	0.01	0.00	0.02	0.00	0.00	0.01	0.00	0.00	0.03	0.05	0.01	0.00	0.00
Na_2O	0.98	1.19	1.10	0.99	1.16	0.96	1.09	1.03	0.92	1.11	1.17	1.19	1.30	1.05	0.99	1.11
K_2O	0.45	0.64	0.61	0.54	0.66	0.60	0.68	0.49	0.29	0.66	0.63	0.56	0.68	0.47	0.40	0.54
F	0.00	0.00	0.00	0.00	0.00	0.00	0.00	0.00	0.00	0.00	0.00	0.00	0.00	0.00	0.00	0.00
Cl	0.04	0.10	0.07	0.08	0.09	0.04	0.07	0.05	0.11	0.08	0.08	0.07	0.05	0.08	0.05	0.06
Total	98.72	98.26	98.53	93.49	98.68	97.23	99.70	98.60	99.92	98.31	98.61	97.74	98.30	97.79	98.81	97.34

stoiched on 15 cations

	Amphibole															
	st08-15d								st08-15d							
	2_18	2_19	2_20	2_21	2_22	2_23	2_24	2_25	3_26	3_27	2_28	3_29	3_30	2_31	3_32	3_33
apfu																
Si	7.07	6.90	6.90	6.98	6.86	7.07	6.87	7.06	7.29	6.90	6.87	6.88	6.84	7.04	7.02	7.04
Ti	0.07	0.11	0.11	0.11	0.11	0.10	0.11	0.09	0.04	0.13	0.12	0.14	0.15	0.08	0.07	0.11
Al	1.38	1.58	1.55	1.58	1.56	1.49	1.59	1.39	1.08	1.59	1.63	1.61	1.65	1.47	1.43	1.37
Cr	0.01	0.02	0.01	0.02	0.02	0.02	0.02	0.01	0.03	0.02	0.01	0.01	0.02	0.01	0.01	0.01
Fe^{2+}	1.30	1.39	1.37	1.38	1.34	1.32	1.37	1.29	1.43	1.37	1.33	1.36	1.31	1.30	1.25	1.35
Mn^{2+}	0.02	0.03	0.02	0.03	0.02	0.03	0.03	0.03	0.03	0.02	0.03	0.03	0.02	0.02	0.03	0.03
Mg	3.30	3.13	3.16	3.02	3.16	3.14	3.15	3.27	3.21	3.14	3.14	3.15	3.08	3.24	3.25	3.27
Ca	1.85	1.84	1.87	1.88	1.90	1.84	1.87	1.85	1.89	1.83	1.86	1.82	1.93	1.84	1.90	1.81
Ba	0.00	0.00	0.00	0.00	0.00	0.00	0.00	0.00	0.00	0.00	0.00	0.00	0.00	0.00	0.00	0.00
Na	0.27	0.33	0.31	0.29	0.32	0.27	0.30	0.29	0.25	0.31	0.33	0.33	0.36	0.29	0.27	0.31
K	0.08	0.12	0.11	0.10	0.12	0.11	0.12	0.09	0.05	0.12	0.12	0.10	0.13	0.09	0.07	0.10
F	0.00	0.00	0.00	0.00	0.00	0.00	0.00	0.00	0.00	0.00	0.00	0.00	0.00	0.00	0.00	0.00
Cl	0.01	0.02	0.02	0.02	0.02	0.01	0.02	0.01	0.03	0.02	0.02	0.02	0.01	0.02	0.01	0.01
Fe^{3+}	0.00	0.00	0.00	0.00	0.02	0.00	0.00	0.00	0.00	0.00	0.00	0.00	0.00	0.00	0.03	0.00
X_{Mg}	0.72	0.69	0.70	0.69	0.70	0.70	0.70	0.72	0.69	0.70	0.70	0.70	0.70	0.71	0.72	0.71

Appendix D, cont'd

	Amphibole												
	st08-30a												
	1_1	1_2	1_3	1_5	1_6	1_7	1_9	1_10	1_11	1_12	1_13	1_14	1_15
wt %													
SiO_2	45.81	46.16	44.26	44.32	45.48	44.97	45.13	43.98	43.92	44.86	45.02	44.88	45.57
TiO_2	0.94	1.02	1.76	1.69	1.36	1.60	0.82	1.76	1.73	1.63	1.59	1.33	1.08
Al_2O_3	10.93	10.34	11.87	11.72	11.81	11.66	13.30	12.02	11.88	11.39	11.01	10.97	11.09
Cr_2O_3	0.03	0.00	0.02	0.00	0.06	0.05	0.00	0.00	0.02	0.00	0.01	0.03	0.00
FeO	15.82	16.10	16.59	16.74	16.70	16.53	16.06	16.45	17.02	16.94	16.65	15.84	15.81
MnO	0.28	0.24	0.28	0.30	0.27	0.30	0.28	0.24	0.28	0.29	0.26	0.28	0.29
MgO	10.65	11.03	10.03	10.10	10.98	10.36	9.77	10.25	10.05	9.98	10.49	10.75	10.68
CaO	12.15	11.58	11.86	11.73	9.55	11.76	11.62	11.96	11.80	11.70	11.66	12.04	12.30
BaO	0.07	0.03	0.04	0.00	0.05	0.09	0.01	0.07	0.02	0.00	0.00	0.05	0.03
Na_2O	0.83	0.75	1.14	1.13	0.80	1.09	0.77	0.96	1.13	1.06	1.12	1.00	0.99
K_2O	0.77	0.75	1.12	1.10	2.33	1.03	0.82	1.28	1.12	1.09	1.02	1.06	0.85
F	0.00	0.00	0.00	0.00	0.00	0.00	0.00	0.00	0.00	0.00	0.00	0.00	0.00
Cl	0.14	0.11	0.13	0.13	0.12	0.15	0.11	0.13	0.13	0.16	0.11	0.12	0.13
Total	98.42	98.11	99.10	98.96	99.51	99.59	98.69	99.10	99.10	99.10	98.94	98.35	98.82

stoiched on 15 cations

	Amphibole												
	st08-30a												
	1_1	1_2	1_3	1_5	1_6	1_7	1_9	1_10	1_11	1_12	1_13	1_14	1_15
apfu													
Si	6.74	6.75	6.55	6.56	6.74	6.61	6.63	6.47	6.50	6.64	6.65	6.60	6.66
Ti	0.10	0.11	0.20	0.19	0.15	0.18	0.09	0.19	0.19	0.18	0.18	0.15	0.12
Al	1.89	1.78	2.07	2.05	2.06	2.02	2.30	2.08	2.07	1.99	1.92	1.90	1.91
Cr	0.00	0.00	0.00	0.00	0.01	0.01	0.00	0.00	0.00	0.00	0.00	0.00	0.00
Fe^{2+}	1.95	1.97	2.05	2.07	2.07	2.03	1.97	2.02	2.11	2.10	2.06	1.95	1.93
Mn^{2+}	0.03	0.03	0.04	0.04	0.03	0.04	0.03	0.03	0.04	0.04	0.03	0.03	0.04
Mg	2.33	2.40	2.21	2.23	2.42	2.27	2.14	2.25	2.22	2.20	2.31	2.36	2.33
Ca	1.91	1.81	1.88	1.86	1.52	1.85	1.83	1.88	1.87	1.86	1.85	1.90	1.92
Ba	0.00	0.00	0.00	0.00	0.00	0.01	0.00	0.00	0.00	0.00	0.00	0.00	0.00
Na	0.24	0.21	0.33	0.32	0.23	0.31	0.22	0.27	0.32	0.30	0.32	0.29	0.28
K	0.14	0.14	0.21	0.21	0.44	0.19	0.15	0.24	0.21	0.21	0.19	0.20	0.16
F	0.00	0.00	0.00	0.00	0.00	0.00	0.00	0.00	0.00	0.00	0.00	0.00	0.00
Cl	0.03	0.03	0.03	0.03	0.03	0.04	0.03	0.03	0.03	0.04	0.03	0.03	0.03
Fe^{3+}	0.04	0.14	0.00	0.00	0.00	0.00	0.00	0.07	0.00	0.00	0.00	0.11	0.10
X_{Mg}	0.55	0.55	0.52	0.52	0.54	0.53	0.52	0.53	0.51	0.51	0.53	0.55	0.55

Appendix D, cont'd

	Amphibole								
	st08-30a								
	2_16	2_17	2_18	2_19	2_21	2_22	2_23	2_24	2_25
wt %									
SiO_2	40.19	44.53	45.51	43.62	45.02	46.83	46.87	45.97	46.39
TiO_2	3.16	1.21	0.99	1.05	1.20	1.03	1.00	0.88	1.01
Al_2O_3	17.47	12.09	10.53	11.18	11.34	9.82	10.07	10.50	10.65
Cr_2O_3	0.02	0.13	0.10	0.02	0.05	0.05	0.02	0.10	0.03
FeO	10.42	15.90	15.30	16.45	15.98	15.41	16.24	14.57	16.09
MnO	0.16	0.26	0.23	0.26	0.27	0.28	0.23	0.27	0.26
MgO	6.16	10.20	10.55	9.57	10.55	11.32	11.15	11.08	10.90
CaO	18.16	12.18	12.54	11.71	12.12	12.53	12.17	12.58	12.35
BaO	0.00	0.00	0.00	0.09	0.02	0.02	0.00	0.03	0.00
Na_2O	0.50	0.98	0.87	0.93	1.00	0.87	0.93	0.81	0.95
K_2O	0.55	0.96	0.80	0.88	0.97	0.78	0.74	0.81	0.81
F	0.00	0.00	0.00	0.00	0.00	0.00	0.00	0.00	0.00
Cl	0.09	0.17	0.14	0.13	0.15	0.13	0.11	0.14	0.11
Total	96.88	98.61	97.56	95.89	98.67	99.07	99.53	97.74	99.55

stoiched on 15 cations

	Amphibole								
	st08-30a								
	2_16	2_17	2_18	2_19	2_21	2_22	2_23	2_24	2_25
apfu									
Si	5.95	6.55	6.69	6.59	6.61	6.80	6.83	6.71	6.75
Ti	0.35	0.13	0.11	0.12	0.13	0.11	0.11	0.10	0.11
Al	3.05	2.10	1.82	1.99	1.96	1.68	1.73	1.81	1.83
Cr	0.00	0.02	0.01	0.00	0.01	0.01	0.00	0.01	0.00
Fe^{2+}	1.29	1.96	1.88	2.08	1.96	1.87	1.98	1.78	1.96
Mn^{2+}	0.02	0.03	0.03	0.03	0.03	0.03	0.03	0.03	0.03
Mg	1.36	2.24	2.31	2.16	2.31	2.45	2.42	2.41	2.36
Ca	2.88	1.92	1.97	1.90	1.91	1.95	1.90	1.97	1.93
Ba	0.00	0.00	0.00	0.01	0.00	0.00	0.00	0.00	0.00
Na	0.14	0.28	0.25	0.27	0.28	0.25	0.26	0.23	0.27
K	0.10	0.18	0.15	0.17	0.18	0.14	0.14	0.15	0.15
F	0.00	0.00	0.00	0.00	0.00	0.00	0.00	0.00	0.00
Cl	0.02	0.04	0.03	0.03	0.04	0.03	0.03	0.03	0.03
Fe^{3+}	0.09	0.05	0.18	0.13	0.08	0.09	0.00	0.18	0.03
X_{Mg}	0.51	0.53	0.55	0.51	0.54	0.57	0.55	0.58	0.55

Appendix D, cont'd

	Amphibole															
	st08-30a							st08-30a								
	3_26	3_27	3_28	3_29	3_30	3_31	3_32	4_33	4_34	4_35	4_36	4_37	4_38	4_39	4_40	
wt %																
SiO_2	46.44	46.84	45.75	46.71	45.48	45.85	46.01	46.31	45.89	46.01	46.53	46.61	46.67	46.75	45.62	
TiO_2	1.02	0.98	1.00	1.01	1.00	0.99	0.99	0.97	1.02	1.01	0.47	0.62	0.61	0.56	0.56	
Al_2O_3	9.94	9.65	10.05	10.08	10.07	10.33	10.45	9.86	10.18	9.85	9.47	10.06	10.43	10.37	9.98	
Cr_2O_3	0.08	0.05	0.03	0.05	0.05	0.05	0.06	0.06	0.07	0.06	0.01	0.00	0.07	0.02	0.03	
FeO	15.57	15.69	15.29	16.37	14.95	15.65	15.46	15.63	16.45	15.09	13.44	14.61	14.85	15.04	14.17	
MnO	0.26	0.29	0.31	0.30	0.26	0.28	0.24	0.27	0.31	0.30	0.23	0.24	0.27	0.25	0.27	
MgO	11.43	11.29	11.00	11.23	10.99	10.77	11.05	11.29	10.99	11.44	11.79	11.34	11.37	11.57	11.10	
CaO	12.21	12.16	12.25	12.00	12.42	12.23	12.08	12.14	11.65	11.99	12.28	12.61	12.40	11.73	12.56	
BaO	0.02	0.03	0.00	0.07	0.03	0.05	0.02	0.05	0.02	0.00	0.00	0.01	0.00	0.07	0.00	
Na_2O	1.01	0.85	0.94	0.99	0.97	0.84	0.78	0.99	0.92	0.99	0.66	0.94	0.89	0.78	0.99	
K_2O	0.83	0.66	0.82	0.76	0.84	0.82	0.86	0.77	0.96	0.74	0.66	0.64	0.74	0.59	0.70	
F	0.00	0.00	0.00	0.00	0.00	0.00	0.00	0.00	0.00	0.00	0.00	0.00	0.00	0.00	0.00	
Cl	0.11	0.12	0.17	0.14	0.15	0.17	0.19	0.11	0.14	0.13	0.08	0.06	0.08	0.11	0.13	
Total	98.92	98.61	97.61	99.71	97.21	98.03	98.19	98.45	98.60	97.61	95.62	97.74	98.38	97.84	96.11	

stoiched on 15 cations

	Amphibole															
	st08-30a							st08-30a								
	3_26	3_27	3_28	3_29	3_30	3_31	3_32	4_33	4_34	4_35	4_36	4_37	4_38	4_39	4_40	
apfu																
Si	6.75	6.83	6.73	6.80	6.70	6.72	6.74	6.77	6.75	6.71	6.80	6.77	6.75	6.79	6.74	
Ti	0.11	0.11	0.11	0.11	0.11	0.11	0.11	0.11	0.11	0.11	0.05	0.07	0.07	0.06	0.06	
Al	1.70	1.66	1.74	1.73	1.75	1.78	1.80	1.70	1.77	1.69	1.63	1.72	1.78	1.77	1.74	
Cr	0.01	0.01	0.00	0.01	0.01	0.01	0.01	0.01	0.01	0.01	0.00	0.00	0.01	0.00	0.00	
Fe^{2+}	1.89	1.91	1.88	1.99	1.84	1.92	1.89	1.91	2.03	1.84	1.64	1.77	1.80	1.83	1.75	
Mn^{2+}	0.03	0.04	0.04	0.04	0.03	0.03	0.03	0.03	0.04	0.04	0.03	0.03	0.03	0.03	0.03	
Mg	2.48	2.45	2.41	2.44	2.41	2.35	2.41	2.46	2.41	2.49	2.57	2.45	2.45	2.50	2.44	
Ca	1.90	1.90	1.93	1.87	1.96	1.92	1.89	1.90	1.84	1.87	1.92	1.96	1.92	1.82	1.99	
Ba	0.00	0.00	0.00	0.00	0.00	0.00	0.00	0.00	0.00	0.00	0.00	0.00	0.00	0.00	0.00	
Na	0.28	0.24	0.27	0.28	0.28	0.24	0.22	0.28	0.26	0.28	0.19	0.26	0.25	0.22	0.28	
K	0.15	0.12	0.15	0.14	0.16	0.15	0.16	0.14	0.18	0.14	0.12	0.12	0.14	0.11	0.13	
F	0.00	0.00	0.00	0.00	0.00	0.00	0.00	0.00	0.00	0.00	0.00	0.00	0.00	0.00	0.00	
Cl	0.03	0.03	0.04	0.03	0.04	0.04	0.05	0.03	0.03	0.03	0.02	0.01	0.02	0.03	0.03	
Fe^{3+}	0.12	0.10	0.14	0.01	0.20	0.16	0.12	0.12	0.05	0.24	0.35	0.23	0.19	0.19	0.25	
X_{Mg}	0.57	0.56	0.56	0.55	0.57	0.55	0.56	0.56	0.54	0.57	0.61	0.58	0.58	0.58	0.58	

Appendix D, cont'd

	Amphibole											
	st08-45a											
	1_5	1_6	1_7	1_8	1_9	1_10	1_11	1_12	1_13	1_14	1_15	1_16
wt %												
SiO_2	40.69	39.48	40.75	39.52	40.63	39.94	40.15	39.99	40.18	39.43	38.43	39.77
TiO_2	1.59	1.62	1.64	1.26	1.00	1.39	1.29	1.23	1.46	1.21	1.17	1.26
Al_2O_3	11.92	12.35	11.81	12.32	12.19	12.42	12.48	12.37	12.23	12.07	12.41	12.34
Cr_2O_3	0.07	0.03	0.05	0.14	0.03	0.05	0.06	0.02	0.05	0.05	0.09	0.02
FeO	21.93	21.61	22.50	21.32	20.15	21.65	20.57	21.00	21.15	22.78	20.48	21.69
MnO	0.30	0.26	0.29	0.36	0.32	0.31	0.42	0.35	0.35	0.35	0.30	0.38
MgO	5.74	5.58	5.75	5.57	6.11	5.72	5.89	5.75	5.73	5.49	5.45	5.58
CaO	12.08	11.69	11.92	11.45	12.06	11.44	12.14	11.60	12.18	10.24	11.06	11.41
BaO	0.00	0.03	0.00	0.04	0.00	0.02	0.03	0.04	0.04	0.00	0.00	0.00
Na_2O	1.23	1.31	1.31	1.24	1.12	1.25	1.24	1.18	1.24	1.17	1.07	1.24
K_2O	1.85	1.79	1.87	1.75	1.68	1.69	1.81	1.62	1.86	1.76	1.81	1.79
F	0.00	0.00	0.00	0.00	0.00	0.00	0.00	0.00	0.00	0.00	0.00	0.00
Cl	0.32	0.38	0.37	0.28	0.28	0.33	0.21	0.26	0.33	0.34	0.28	0.34
Total	97.72	96.13	98.26	95.25	95.57	96.21	96.29	95.41	96.80	94.89	92.55	95.82

stoiched on 15 cations

	Amphibole											
	st08-45a											
	1_5	1_6	1_7	1_8	1_9	1_10	1_11	1_12	1_13	1_14	1_15	1_16
apfu												
Si	6.22	6.16	6.26	6.15	6.21	6.22	6.16	6.21	6.17	6.21	6.06	6.21
Ti	0.18	0.19	0.19	0.15	0.11	0.16	0.15	0.14	0.17	0.14	0.14	0.15
Al	2.15	2.27	2.14	2.26	2.20	2.28	2.26	2.26	2.21	2.24	2.31	2.27
Cr	0.01	0.00	0.01	0.02	0.00	0.01	0.01	0.00	0.01	0.01	0.01	0.00
Fe^{2+}	2.81	2.82	2.89	2.77	2.57	2.82	2.64	2.73	2.72	3.00	2.70	2.83
Mn^{2+}	0.04	0.03	0.04	0.05	0.04	0.04	0.05	0.05	0.05	0.05	0.04	0.05
Mg	1.31	1.30	1.32	1.29	1.39	1.33	1.35	1.33	1.31	1.29	1.28	1.30
Ca	1.98	1.95	1.96	1.91	1.97	1.91	2.00	1.93	2.00	1.73	1.87	1.91
Ba	0.00	0.00	0.00	0.00	0.00	0.00	0.00	0.00	0.00	0.00	0.00	0.00
Na	0.36	0.40	0.39	0.37	0.33	0.38	0.37	0.36	0.37	0.36	0.33	0.38
K	0.36	0.36	0.37	0.35	0.33	0.34	0.35	0.32	0.36	0.35	0.36	0.36
F	0.00	0.00	0.00	0.00	0.00	0.00	0.00	0.00	0.00	0.00	0.00	0.00
Cl	0.08	0.10	0.10	0.07	0.07	0.09	0.05	0.07	0.09	0.09	0.07	0.09
Fe^{3+}	0.30	0.26	0.19	0.41	0.50	0.24	0.39	0.35	0.36	0.35	0.59	0.27
X_{Mg}	0.32	0.32	0.31	0.32	0.35	0.32	0.34	0.33	0.33	0.30	0.32	0.31

Appendix D, cont'd

	Amphibole								
	st08-45a								
	2_17	2_18	2_19	2_20	2_21	2_22	2_23	2_24	2_25
wt %									
SiO_2	39.49	40.27	39.87	39.45	40.11	39.38	40.27	38.85	39.19
TiO_2	1.27	1.42	1.37	2.04	2.06	2.00	1.93	1.98	2.00
Al_2O_3	12.18	12.17	12.41	12.21	11.98	12.14	11.76	12.24	12.06
Cr_2O_3	0.01	0.07	0.08	0.12	0.10	0.12	0.07	0.14	0.11
FeO	20.91	22.35	21.19	22.85	22.78	22.32	22.33	21.77	21.76
MnO	0.30	0.30	0.39	0.34	0.33	0.35	0.32	0.35	0.29
MgO	5.59	5.59	5.52	5.37	5.53	5.43	5.50	5.30	5.37
CaO	11.86	11.48	12.19	11.43	11.88	11.50	12.16	11.59	12.09
BaO	0.02	0.01	0.01	0.04	0.00	0.04	0.00	0.02	0.06
Na_2O	1.23	1.24	1.31	1.39	1.37	1.31	1.22	1.31	1.30
K_2O	1.82	1.77	1.88	1.83	1.93	1.81	1.99	1.79	1.99
F	0.00	0.00	0.00	0.00	0.00	0.00	0.00	0.00	0.00
Cl	0.40	0.37	0.37	0.44	0.38	0.45	0.47	0.40	0.41
Total	95.08	97.04	96.59	97.51	98.45	96.85	98.02	95.74	96.63

stoiched on 15 cations

	Amphibole								
	st08-45a								
	2_17	2_18	2_19	2_20	2_21	2_22	2_23	2_24	2_25
apfu									
Si	6.18	6.26	6.13	6.17	6.19	6.17	6.24	6.11	6.12
Ti	0.15	0.17	0.16	0.24	0.24	0.24	0.22	0.23	0.24
Al	2.25	2.23	2.25	2.25	2.18	2.24	2.15	2.27	2.22
Cr	0.00	0.01	0.01	0.01	0.01	0.01	0.01	0.02	0.01
Fe^{2+}	2.74	2.91	2.72	2.99	2.94	2.92	2.89	2.86	2.84
Mn^{2+}	0.04	0.04	0.05	0.05	0.04	0.05	0.04	0.05	0.04
Mg	1.30	1.30	1.27	1.25	1.27	1.27	1.27	1.24	1.25
Ca	1.99	1.91	2.01	1.91	1.96	1.93	2.02	1.95	2.02
Ba	0.00	0.00	0.00	0.00	0.00	0.00	0.00	0.00	0.00
Na	0.37	0.37	0.39	0.42	0.41	0.40	0.37	0.40	0.39
K	0.36	0.35	0.37	0.36	0.38	0.36	0.39	0.36	0.40
F	0.00	0.00	0.00	0.00	0.00	0.00	0.00	0.00	0.00
Cl	0.11	0.10	0.10	0.12	0.10	0.12	0.12	0.11	0.11
Fe^{3+}	0.35	0.17	0.41	0.13	0.16	0.18	0.16	0.26	0.25
X_{Mg}	0.32	0.31	0.32	0.30	0.30	0.30	0.31	0.30	0.31

Appendix D, cont'd

	Amphibole															
	idaho m						idaho m									
	1_1	1_2	1_3	1_4	1_5	1_6	2_7	2_8	2_9	2_10	2_11	2_12	2_13	2_14	2_15	2_16
wt %																
SiO_2	51.17	51.70	50.64	51.75	48.39	47.04	51.93	50.94	48.16	48.95	48.55	47.43	47.47	47.83	48.89	47.32
TiO_2	0.14	0.24	0.37	0.40	0.72	0.88	0.32	0.42	0.79	0.73	0.88	0.98	0.88	0.92	0.68	0.88
Al_2O_3	5.73	4.59	5.30	5.66	7.36	8.60	5.01	5.37	8.08	7.43	7.84	8.67	8.59	8.67	6.81	8.91
Cr_2O_3	0.06	0.13	0.12	0.13	0.27	0.18	0.05	0.10	0.21	0.13	0.16	0.17	0.15	0.21	0.15	0.18
FeO	12.42	11.55	11.75	12.47	12.54	14.26	12.55	11.77	13.30	13.09	13.50	13.76	13.56	13.84	14.01	13.62
MnO	0.26	0.26	0.26	0.29	0.31	0.27	0.26	0.23	0.28	0.26	0.26	0.29	0.28	0.26	0.35	0.32
MgO	14.46	15.40	15.12	14.93	13.76	12.52	15.44	15.19	13.67	13.85	13.52	12.94	12.94	13.12	13.32	12.89
CaO	12.88	12.92	12.66	12.74	12.61	12.44	12.47	12.73	12.48	12.55	12.74	12.51	12.66	12.56	12.41	12.67
BaO	0.00	0.00	0.00	0.00	0.06	0.01	0.00	0.01	0.02	0.01	0.00	0.00	0.00	0.03	0.00	0.04
Na_2O	0.65	0.69	0.82	0.80	0.89	1.21	0.72	0.76	1.13	0.96	1.06	1.13	1.11	1.11	0.88	1.14
K_2O	0.33	0.37	0.47	0.48	0.78	0.86	0.43	0.45	0.84	0.65	0.77	0.86	0.93	0.81	0.73	0.89
F	0.00	0.00	0.00	0.00	0.00	0.00	0.00	0.00	0.00	0.00	0.00	0.00	0.00	0.00	0.00	0.00
Cl	0.03	0.02	0.05	0.02	0.03	0.05	0.00	0.01	0.04	0.03	0.02	0.05	0.06	0.06	0.10	0.04
Total	98.13	97.87	97.56	99.67	97.72	98.32	99.18	97.98	99.00	98.64	99.30	98.79	98.63	99.42	98.33	98.90

stoiched on 15 cations

	Amphibole															
	idaho m						idaho m									
	1_1	1_2	1_3	1_4	1_5	1_6	2_7	2_8	2_9	2_10	2_11	2_12	2_13	2_14	2_15	2_16
apfu																
Si	7.32	7.38	7.28	7.36	6.99	6.91	7.40	7.29	6.96	7.05	7.00	6.91	6.93	6.91	7.11	6.85
Ti	0.02	0.03	0.04	0.04	0.08	0.10	0.03	0.05	0.09	0.08	0.10	0.11	0.10	0.10	0.07	0.10
Al	0.97	0.77	0.90	0.95	1.25	1.49	0.84	0.91	1.38	1.26	1.33	1.49	1.48	1.48	1.17	1.52
Cr	0.01	0.01	0.01	0.01	0.03	0.02	0.01	0.01	0.02	0.01	0.02	0.02	0.02	0.02	0.02	0.02
Fe^{2+}	1.48	1.38	1.41	1.48	1.51	1.75	1.50	1.41	1.61	1.58	1.63	1.68	1.65	1.67	1.70	1.65
Mn^{2+}	0.03	0.03	0.03	0.04	0.04	0.03	0.03	0.03	0.03	0.03	0.03	0.04	0.03	0.03	0.04	0.04
Mg	3.08	3.28	3.24	3.17	2.96	2.74	3.28	3.24	2.94	2.98	2.91	2.81	2.81	2.83	2.89	2.78
Ca	1.97	1.98	1.95	1.94	1.95	1.96	1.90	1.95	1.93	1.94	1.97	1.95	1.98	1.94	1.93	1.96
Ba	0.00	0.00	0.00	0.00	0.00	0.00	0.00	0.00	0.00	0.00	0.00	0.00	0.00	0.00	0.00	0.00
Na	0.18	0.19	0.23	0.22	0.25	0.34	0.20	0.21	0.32	0.27	0.30	0.32	0.31	0.31	0.25	0.32
K	0.06	0.07	0.09	0.09	0.14	0.16	0.08	0.08	0.15	0.12	0.14	0.16	0.17	0.15	0.14	0.16
F	0.00	0.00	0.00	0.00	0.00	0.00	0.00	0.00	0.00	0.00	0.00	0.00	0.00	0.00	0.00	0.00
Cl	0.01	0.00	0.01	0.00	0.01	0.01	0.00	0.00	0.01	0.01	0.00	0.01	0.01	0.01	0.02	0.01
Fe^{3+}	0.13	0.15	0.13	0.00	0.19	0.00	0.00	0.13	0.04	0.07	0.02	0.00	0.00	0.01	0.06	0.08
X_{Mg}	0.67	0.70	0.70	0.68	0.66	0.61	0.69	0.70	0.65	0.65	0.64	0.63	0.63	0.63	0.63	0.63

Appendix D, cont'd

	Amphibole																			
	idaho m																			
	3_17	3_19	3_20	3_21	3_22	3_24	3_25	3_26	3_27	3_28	3_29	3_30	3_31	3_32	3_33	3_34	3_35	3_36	3_37	3_38
wt %																				
SiO_2	53.85	52.02	51.45	52.74	51.86	53.48	53.24	52.57	52.90	52.94	52.06	52.06	52.77	52.24	50.53	51.02	51.79	51.82	53.98	53.14
TiO_2	0.09	0.29	0.39	0.29	0.33	0.16	0.16	0.20	0.20	0.19	0.26	0.26	0.23	0.32	0.47	0.46	0.36	0.33	0.11	0.18
Al_2O_3	3.17	4.91	5.04	4.31	4.91	3.39	3.46	3.83	3.81	4.03	4.82	4.70	4.22	4.95	5.91	5.98	5.12	5.19	2.79	3.57
Cr_2O_3	0.13	0.11	0.15	0.08	0.13	0.12	0.14	0.15	0.14	0.09	0.18	0.11	0.11	0.14	0.13	0.11	0.08	0.09	0.03	0.06
FeO	9.80	12.34	12.50	11.72	12.53	11.82	11.51	11.27	11.85	12.47	12.20	12.38	12.44	12.53	11.95	12.94	12.87	12.52	11.81	12.39
MnO	0.21	0.26	0.28	0.30	0.29	0.27	0.24	0.24	0.25	0.25	0.26	0.26	0.27	0.29	0.25	0.25	0.26	0.33	0.29	0.26
MgO	16.73	15.32	15.02	15.89	14.97	15.78	16.15	15.80	15.85	15.28	15.41	15.14	15.37	15.10	15.04	14.72	14.96	14.61	16.02	15.56
CaO	13.30	12.77	12.82	12.69	12.89	12.93	12.92	13.00	12.77	12.93	12.83	12.72	12.93	12.71	12.61	12.79	12.52	12.75	12.93	12.79
BaO	0.04	0.01	0.03	0.00	0.07	0.00	0.01	0.00	0.04	0.00	0.02	0.02	0.00	0.00	0.01	0.07	0.00	0.00	0.00	0.01
Na_2O	0.31	0.67	0.76	0.50	0.67	0.51	0.56	0.53	0.50	0.44	0.74	0.69	0.60	0.77	0.83	0.84	0.56	0.51	0.31	0.44
K_2O	0.12	0.42	0.44	0.37	0.39	0.23	0.27	0.31	0.33	0.31	0.38	0.34	0.39	0.42	0.51	0.51	0.45	0.40	0.21	0.28
F	0.00	0.00	0.00	0.00	0.00	0.00	0.00	0.00	0.00	0.00	0.00	0.00	0.00	0.00	0.00	0.00	0.00	0.00	0.00	0.00
Cl	0.01	0.03	0.03	0.00	0.00	0.00	0.00	0.01	0.03	0.01	0.00	0.00	0.01	0.01	0.02	0.05	0.00	0.03	0.00	0.02
Total	97.76	99.15	98.91	98.89	99.04	98.69	98.66	97.91	98.67	98.94	99.16	98.68	99.34	99.48	98.26	99.74	98.97	98.58	98.48	98.70

stoiched on 15 cations

	Amphibole																			
	idaho m																			
	3_17	3_19	3_20	3_21	3_22	3_24	3_25	3_26	3_27	3_28	3_29	3_30	3_31	3_32	3_33	3_34	3_35	3_36	3_37	3_38
apfu																				
Si	7.54	7.42	7.38	7.47	7.42	7.63	7.55	7.47	7.52	7.55	7.38	7.46	7.51	7.44	7.20	7.27	7.41	7.44	7.63	7.57
Ti	0.01	0.03	0.04	0.03	0.04	0.02	0.02	0.02	0.02	0.02	0.03	0.03	0.02	0.03	0.05	0.05	0.04	0.04	0.01	0.02
Al	0.52	0.83	0.85	0.72	0.83	0.57	0.58	0.64	0.64	0.68	0.81	0.79	0.71	0.83	0.99	1.00	0.86	0.88	0.46	0.60
Cr	0.01	0.01	0.02	0.01	0.01	0.01	0.02	0.02	0.02	0.01	0.02	0.01	0.01	0.02	0.01	0.01	0.01	0.01	0.00	0.01
Fe^{2+}	1.15	1.47	1.50	1.39	1.50	1.41	1.36	1.34	1.41	1.49	1.45	1.48	1.48	1.49	1.42	1.54	1.54	1.50	1.40	1.48
Mn^{2+}	0.02	0.03	0.03	0.04	0.04	0.03	0.03	0.03	0.03	0.03	0.03	0.03	0.03	0.04	0.03	0.03	0.03	0.04	0.03	0.03
Mg	3.49	3.26	3.21	3.36	3.19	3.35	3.41	3.35	3.36	3.25	3.26	3.24	3.26	3.21	3.20	3.13	3.19	3.13	3.37	3.31
Ca	2.00	1.95	1.97	1.93	1.98	1.98	1.96	1.98	1.94	1.98	1.95	1.95	1.97	1.94	1.93	1.95	1.92	1.96	1.96	1.95
Ba	0.00	0.00	0.00	0.00	0.00	0.00	0.00	0.00	0.00	0.00	0.00	0.00	0.00	0.00	0.00	0.00	0.00	0.00	0.00	0.00
Na	0.08	0.19	0.21	0.14	0.19	0.14	0.15	0.15	0.14	0.12	0.20	0.19	0.17	0.21	0.23	0.23	0.16	0.14	0.08	0.12
K	0.02	0.08	0.08	0.07	0.07	0.04	0.05	0.06	0.06	0.06	0.07	0.06	0.07	0.08	0.09	0.09	0.08	0.07	0.04	0.05
F	0.00	0.00	0.00	0.00	0.00	0.00	0.00	0.00	0.00	0.00	0.00	0.00	0.00	0.00	0.00	0.00	0.00	0.00	0.00	0.00
Cl	0.00	0.01	0.01	0.00	0.00	0.00	0.00	0.00	0.01	0.00	0.00	0.00	0.00	0.00	0.00	0.01	0.00	0.01	0.00	0.00
Fe^{3+}	0.24	0.00	0.00	0.07	0.00	0.00	0.07	0.15	0.06	0.00	0.08	0.00	0.00	0.00	0.16	0.02	0.00	0.00	0.13	0.03
X_{Mg}	0.75	0.69	0.68	0.71	0.68	0.70	0.71	0.71	0.70	0.69	0.69	0.69	0.69	0.68	0.69	0.67	0.67	0.68	0.71	0.69

APPENDIX E: ELECTRON MICROPROBE ANALYSES – BIOTITE

	Biotite																					
	ic08-01a																ic08-01a					
	Wbt 1	Wbt 2	Wbt 3	Wbt 4	Wbt 5	Wbt 6	Wbt 7	Wbt 8	Wbt 9	Wbt 10	Wbt 11	Wbt 12	Wbt 13	Wbt 14	Wbt 15	Wbt 16	Mbt 1	Mbt 2	Mbt 3	Mbt 4	Mbt 5	Mbt 6
wt %																						
SiO_2	34.33	34.41	34.32	34.60	34.71	34.97	34.79	34.99	34.67	34.81	34.33	34.48	33.95	35.26	35.43	34.59	34.64	34.92	34.37	34.77	34.88	34.75
TiO_2	1.94	2.08	2.04	1.91	2.12	2.15	2.25	2.08	2.37	2.20	2.02	1.60	1.66	1.57	1.46	2.02	1.78	1.70	1.61	1.46	1.32	1.37
Al_2O_3	20.25	20.49	20.29	20.33	20.10	20.15	20.07	20.46	20.00	20.41	20.32	20.30	20.24	20.16	20.34	20.07	20.32	20.49	20.34	20.56	20.83	20.75
Cr_2O_3	0.09	0.11	0.06	0.05	0.08	0.06	0.07	0.08	0.12	0.09	0.04	0.15	0.17	0.09	0.06	0.07	0.06	0.07	0.06	0.05	0.07	0.09
FeO	23.52	23.27	23.68	23.13	24.12	23.73	23.86	23.54	23.64	23.47	23.92	23.56	23.04	22.89	22.93	23.83	23.35	24.02	23.14	23.90	23.95	23.17
MnO	0.14	0.19	0.16	0.20	0.13	0.13	0.14	0.11	0.15	0.15	0.13	0.12	0.08	0.14	0.12	0.12	0.12	0.13	0.09	0.10	0.11	0.12
MgO	7.41	7.36	7.27	7.53	7.31	7.31	7.29	7.30	7.36	7.22	7.33	7.56	7.47	7.95	8.02	7.46	7.62	7.80	7.59	7.87	7.81	7.88
CaO	0.01	0.01	0.00	0.00	0.02	0.01	0.00	0.00	0.03	0.00	0.02	0.00	0.01	0.02	0.02	0.00	0.00	0.02	0.00	0.00	0.01	0.00
BaO	0.24	0.20	0.17	0.20	0.18	0.19	0.19	0.20	0.19	0.25	0.19	0.18	0.20	0.09	0.14	0.26	0.20	0.22	0.15	0.14	0.16	0.19
Na_2O	0.24	0.19	0.22	0.24	0.20	0.25	0.22	0.24	0.23	0.20	0.25	0.20	0.19	0.23	0.20	0.20	0.16	0.21	0.25	0.14	0.15	0.20
K_2O	8.60	8.62	8.66	8.89	8.82	8.81	8.96	8.89	8.75	8.83	8.48	8.63	8.66	8.39	8.42	8.70	9.01	8.82	8.88	8.90	8.86	8.86
F	0.00	0.00	0.00	0.00	0.00	0.00	0.00	0.00	0.00	0.00	0.00	0.00	0.00	0.00	0.00	0.00	0.00	0.00	0.00	0.00	0.00	0.00
Total	96.77	96.93	96.87	97.08	97.79	97.76	97.84	97.89	97.51	97.63	97.03	96.78	95.67	96.79	97.14	97.32	97.26	98.40	96.48	97.89	98.15	97.38

Oxygens = 22

	Biotite																					
	ic08-01a																ic08-01a					
	Wbt 1	Wbt 2	Wbt 3	Wbt 4	Wbt 5	Wbt 6	Wbt 7	Wbt 8	Wbt 9	Wbt 10	Wbt 11	Wbt 12	Wbt 13	Wbt 14	Wbt 15	Wbt 16	Mbt 1	Mbt 2	Mbt 3	Mbt 4	Mbt 5	Mbt 6
apfu																						
Si	5.24	5.23	5.24	5.26	5.25	5.28	5.26	5.27	5.25	5.26	5.23	5.26	5.24	5.34	5.34	5.26	5.26	5.25	5.25	5.25	5.25	5.25
Ti	0.22	0.24	0.23	0.22	0.24	0.24	0.26	0.24	0.27	0.25	0.23	0.18	0.19	0.18	0.17	0.23	0.20	0.19	0.19	0.17	0.15	0.16
Al	3.64	3.67	3.65	3.64	3.59	3.59	3.58	3.63	3.57	3.64	3.65	3.65	3.68	3.60	3.61	3.59	3.64	3.63	3.67	3.66	3.69	3.70
Cr	0.01	0.01	0.01	0.01	0.01	0.01	0.01	0.01	0.01	0.01	0.00	0.02	0.02	0.01	0.01	0.01	0.01	0.01	0.01	0.01	0.01	0.01
Fe^{2+}	3.00	2.96	3.02	2.94	3.05	3.00	3.02	2.97	3.00	2.97	3.05	3.00	2.97	2.90	2.89	3.03	2.96	3.02	2.96	3.02	3.01	2.93
Mn^{2+}	0.02	0.02	0.02	0.03	0.02	0.02	0.02	0.01	0.02	0.02	0.02	0.02	0.01	0.02	0.02	0.02	0.02	0.02	0.01	0.01	0.01	0.02
Mg	1.69	1.67	1.65	1.71	1.65	1.65	1.64	1.64	1.66	1.63	1.66	1.72	1.72	1.79	1.80	1.69	1.72	1.75	1.73	1.77	1.75	1.78
Ca	0.00	0.00	0.00	0.00	0.00	0.00	0.00	0.00	0.00	0.00	0.00	0.00	0.00	0.00	0.00	0.00	0.00	0.00	0.00	0.00	0.00	0.00
Ba	0.01	0.01	0.01	0.01	0.01	0.01	0.01	0.01	0.01	0.01	0.01	0.01	0.01	0.01	0.01	0.02	0.01	0.01	0.01	0.01	0.01	0.01
Na	0.07	0.06	0.07	0.07	0.06	0.07	0.06	0.07	0.07	0.06	0.07	0.06	0.06	0.07	0.06	0.06	0.05	0.06	0.07	0.04	0.04	0.06
K	1.67	1.67	1.69	1.72	1.70	1.70	1.73	1.71	1.69	1.70	1.65	1.68	1.70	1.62	1.62	1.69	1.74	1.69	1.73	1.71	1.70	1.71
F	0.00	0.00	0.00	0.00	0.00	0.00	0.00	0.00	0.00	0.00	0.00	0.00	0.00	0.00	0.00	0.00	0.00	0.00	0.00	0.00	0.00	0.00
X_{Mg}	0.36	0.36	0.35	0.37	0.35	0.35	0.35	0.36	0.36	0.35	0.35	0.36	0.37	0.38	0.38	0.36	0.37	0.37	0.37	0.37	0.37	0.38

Appendix E, cont'd

	Biotite																
	ic08-01a1									ic08-01a1							
	Wbt 5	Wbt 6	Wbt 7	Wbt 8	Wbt 9	Wbt 10	Wbt 11	Wbt 12	Wbt 13	Sbt 14	Sbt 15	Sbt 16	Sbt 17	Sbt 18	Sbt 19	Sbt 20	Sbt 21
wt %																	
SiO_2	34.50	34.46	34.55	34.44	34.47	34.81	34.65	34.44	34.24	34.26	33.83	34.04	34.04	33.92	33.88	34.24	33.76
TiO_2	2.62	2.68	2.77	2.76	2.64	2.65	2.69	2.73	2.79	1.81	1.79	1.70	2.06	1.79	1.79	1.83	1.83
Al_2O_3	19.45	19.49	19.36	19.46	19.45	19.61	19.47	19.29	19.46	20.37	19.94	20.21	20.02	20.33	20.02	20.26	19.77
Cr_2O_3	0.09	0.06	0.02	0.08	0.09	0.02	0.04	0.07	0.07	0.06	0.07	0.08	0.10	0.07	0.06	0.10	0.08
FeO	24.13	24.15	23.75	23.84	23.79	23.92	23.60	24.09	24.02	23.30	23.05	23.09	23.10	22.36	23.12	23.28	22.95
MnO	0.21	0.23	0.22	0.20	0.25	0.17	0.20	0.22	0.20	0.13	0.13	0.18	0.17	0.13	0.14	0.14	0.14
MgO	6.95	7.01	6.88	6.92	6.88	7.02	7.12	6.89	7.02	7.22	7.12	7.20	7.08	7.01	7.21	7.02	7.04
CaO	0.02	0.00	0.02	0.00	0.01	0.00	0.00	0.00	0.01	0.01	0.02	0.00	0.00	0.02	0.02	0.00	0.00
BaO	0.19	0.22	0.19	0.18	0.25	0.25	0.18	0.20	0.26	0.20	0.20	0.19	0.18	0.24	0.20	0.22	0.20
Na_2O	0.23	0.23	0.28	0.10	0.22	0.20	0.23	0.21	0.26	0.19	0.22	0.24	0.27	0.20	0.22	0.26	0.21
K_2O	8.80	9.01	8.95	8.75	9.03	8.95	8.69	8.86	8.88	8.69	8.69	8.65	8.55	8.54	8.71	8.76	8.72
F	0.00	0.00	0.00	0.00	0.00	0.00	0.00	0.00	0.00	0.00	0.00	0.00	0.00	0.00	0.00	0.00	0.00
Total	97.19	97.54	96.99	96.73	97.08	97.60	96.87	97.00	97.21	96.24	95.06	95.58	95.57	94.61	95.37	96.11	94.70

Oxygens = 22

	Biotite																
	ic08-01a1									ic08-01a1							
	Wbt 5	Wbt 6	Wbt 7	Wbt 8	Wbt 9	Wbt 10	Wbt 11	Wbt 12	Wbt 13	Sbt 14	Sbt 15	Sbt 16	Sbt 17	Sbt 18	Sbt 19	Sbt 20	Sbt 21
apfu																	
Si	5.27	5.25	5.28	5.27	5.27	5.28	5.29	5.27	5.23	5.25	5.26	5.26	5.26	5.27	5.25	5.26	5.27
Ti	0.30	0.31	0.32	0.32	0.30	0.30	0.31	0.31	0.32	0.21	0.21	0.20	0.24	0.21	0.21	0.21	0.21
Al	3.50	3.50	3.49	3.51	3.51	3.51	3.50	3.48	3.51	3.68	3.65	3.68	3.64	3.72	3.66	3.67	3.64
Cr	0.01	0.01	0.00	0.01	0.01	0.00	0.00	0.01	0.01	0.01	0.01	0.01	0.01	0.01	0.01	0.01	0.01
Fe^{2+}	3.08	3.08	3.04	3.05	3.04	3.04	3.01	3.08	3.07	2.99	3.00	2.98	2.98	2.91	3.00	2.99	3.00
Mn^{2+}	0.03	0.03	0.03	0.03	0.03	0.02	0.03	0.03	0.03	0.02	0.02	0.02	0.02	0.02	0.02	0.02	0.02
Mg	1.58	1.59	1.57	1.58	1.57	1.59	1.62	1.57	1.60	1.65	1.65	1.66	1.63	1.62	1.67	1.61	1.64
Ca	0.00	0.00	0.00	0.00	0.00	0.00	0.00	0.00	0.00	0.00	0.00	0.00	0.00	0.00	0.00	0.00	0.00
Ba	0.01	0.01	0.01	0.01	0.02	0.01	0.01	0.01	0.02	0.01	0.01	0.01	0.01	0.01	0.01	0.01	0.01
Na	0.07	0.07	0.08	0.03	0.07	0.06	0.07	0.06	0.08	0.06	0.07	0.07	0.08	0.06	0.07	0.08	0.06
K	1.71	1.75	1.75	1.71	1.76	1.73	1.69	1.73	1.73	1.70	1.72	1.70	1.68	1.69	1.72	1.72	1.74
F	0.00	0.00	0.00	0.00	0.00	0.00	0.00	0.00	0.00	0.00	0.00	0.00	0.00	0.00	0.00	0.00	0.00
X_{Mg}	0.34	0.34	0.34	0.34	0.34	0.34	0.35	0.34	0.34	0.36	0.36	0.36	0.35	0.36	0.36	0.35	0.35

Appendix E, cont'd

	Biotite						
	ic08-01a1						
	Mbt 22	Mbt 23	Mbt 24	Mbt 25	Mbt 26	Mbt 27	Mbt 28
wt %							
SiO_2	34.37	34.12	33.94	33.92	33.92	34.17	34.17
TiO_2	2.30	2.32	2.36	2.22	2.29	2.37	2.31
Al_2O_3	19.80	19.69	19.59	19.46	19.54	19.75	19.71
Cr_2O_3	0.02	0.08	0.08	0.04	0.03	0.08	0.04
FeO	23.22	23.59	23.37	23.28	23.28	22.99	23.41
MnO	0.12	0.15	0.16	0.11	0.07	0.13	0.12
MgO	7.23	7.15	7.13	7.17	7.20	7.18	7.16
CaO	0.01	0.00	0.01	0.03	0.02	0.04	0.02
BaO	0.23	0.20	0.27	0.18	0.25	0.23	0.24
Na_2O	0.34	0.27	0.35	0.61	0.61	0.72	0.67
K_2O	8.74	8.69	8.66	8.67	8.73	8.74	8.81
F	0.00	0.00	0.00	0.00	0.00	0.00	0.00
Total	96.38	96.26	95.92	95.69	95.94	96.40	96.66

Oxygens = 22

	Biotite						
	ic08-01a1						
	Mbt 22	Mbt 23	Mbt 24	Mbt 25	Mbt 26	Mbt 27	Mbt 28
apfu							
Si	5.27	5.25	5.24	5.25	5.24	5.24	5.24
Ti	0.27	0.27	0.27	0.26	0.27	0.27	0.27
Al	3.58	3.57	3.57	3.55	3.56	3.57	3.56
Cr	0.00	0.01	0.01	0.00	0.00	0.01	0.00
Fe^{2+}	2.98	3.03	3.02	3.01	3.01	2.95	3.00
Mn^{2+}	0.02	0.02	0.02	0.01	0.01	0.02	0.02
Mg	1.65	1.64	1.64	1.65	1.66	1.64	1.64
Ca	0.00	0.00	0.00	0.01	0.00	0.01	0.00
Ba	0.01	0.01	0.02	0.01	0.02	0.01	0.01
Na	0.10	0.08	0.10	0.18	0.18	0.21	0.20
K	1.71	1.71	1.71	1.71	1.72	1.71	1.72
F	0.00	0.00	0.00	0.00	0.00	0.00	0.00
X_{Mg}	0.36	0.35	0.35	0.35	0.36	0.36	0.35

Appendix E, cont'd

Biotite

	ic08-01b							ic08-01b								ic08-01b		
	N-bt 1	N-bt 2	N-bt 3	N-bt 4	N-bt 5	N-bt 6	N-bt 7	E-bt 1	E-bt 2	E-bt 3	E-bt 4	E-bt 5	E-bt 6	E-bt 7	E-bt 8	M-bt 1	M-bt 2	M-bt 3
wt %																		
SiO_2	33.70	34.99	34.51	34.40	33.96	34.81	33.82	35.32	34.74	35.04	34.40	34.88	34.21	34.50	34.28	35.59	34.81	34.53
TiO_2	2.01	1.98	1.96	1.92	1.95	1.79	1.92	2.02	1.96	1.84	1.88	1.92	1.99	1.84	2.06	1.71	1.68	1.71
Al_2O_3	20.49	20.55	20.43	20.43	19.85	20.64	19.95	20.43	20.28	20.43	19.84	20.27	20.27	20.48	20.36	20.87	20.37	20.33
Cr_2O_3	0.09	0.03	0.07	0.07	0.05	0.04	0.07	0.10	0.07	0.05	0.11	0.09	0.05	0.10	0.07	0.11	0.07	0.07
FeO	23.45	23.47	23.70	23.77	23.82	23.33	23.51	23.57	23.31	23.94	24.11	23.86	23.62	23.52	23.11	21.59	21.77	22.19
MnO	0.08	0.07	0.07	0.04	0.06	0.09	0.08	0.08	0.08	0.07	0.04	0.09	0.06	0.05	0.04	0.07	0.06	0.06
MgO	7.10	7.13	7.06	7.08	7.02	7.20	6.95	7.17	7.00	7.70	7.06	7.06	7.11	7.29	7.08	8.52	8.26	8.27
CaO	0.01	0.01	0.03	0.02	0.03	0.09	0.04	0.00	0.00	0.01	0.00	0.01	0.03	0.01	0.03	0.01	0.01	0.00
BaO	0.20	0.29	0.21	0.23	0.19	0.18	0.21	0.19	0.22	0.17	0.21	0.31	0.26	0.20	0.16	0.28	0.26	0.21
Na_2O	0.28	0.28	0.27	0.27	0.30	0.29	0.22	0.25	0.24	0.28	0.31	0.25	0.31	0.28	0.27	0.25	0.31	0.25
K_2O	8.22	8.46	8.49	8.27	8.25	8.02	8.46	8.30	8.38	8.33	8.36	8.46	8.34	8.46	8.30	8.44	8.43	8.34
F	0.00	0.00	0.00	0.00	0.00	0.00	0.00	0.00	0.00	0.00	0.00	0.00	0.00	0.00	0.00	0.00	0.00	0.00
Total	95.63	97.26	96.80	96.50	95.48	96.48	95.23	97.43	96.28	97.86	96.32	97.20	96.25	96.73	95.76	97.44	96.03	95.96

Oxygens = 22

Biotite

	ic08-01b							ic08-01b								ic08-01b		
	N-bt 1	N-bt 2	N-bt 3	N-bt 4	N-bt 5	N-bt 6	N-bt 7	E-bt 1	E-bt 2	E-bt 3	E-bt 4	E-bt 5	E-bt 6	E-bt 7	E-bt 8	M-bt 1	M-bt 2	M-bt 3
apfu																		
Si	5.20	5.29	5.26	5.26	5.26	5.29	5.25	5.32	5.31	5.27	5.28	5.30	5.25	5.26	5.26	5.31	5.30	5.27
Ti	0.23	0.23	0.22	0.22	0.23	0.20	0.22	0.23	0.23	0.21	0.22	0.22	0.23	0.21	0.24	0.19	0.19	0.20
Al	3.73	3.66	3.67	3.68	3.62	3.70	3.65	3.63	3.65	3.62	3.59	3.63	3.66	3.68	3.68	3.67	3.65	3.65
Cr	0.01	0.00	0.01	0.01	0.01	0.00	0.01	0.01	0.01	0.01	0.01	0.01	0.01	0.01	0.01	0.01	0.01	0.01
Fe^{2+}	3.03	2.97	3.02	3.04	3.08	2.97	3.05	2.97	2.98	3.01	3.10	3.03	3.03	3.00	2.97	2.70	2.77	2.83
Mn^{2+}	0.01	0.01	0.01	0.01	0.01	0.01	0.01	0.01	0.01	0.01	0.01	0.01	0.01	0.01	0.01	0.01	0.01	0.01
Mg	1.63	1.61	1.60	1.61	1.62	1.63	1.61	1.61	1.59	1.73	1.62	1.60	1.63	1.66	1.62	1.90	1.87	1.88
Ca	0.00	0.00	0.00	0.00	0.01	0.01	0.01	0.00	0.00	0.00	0.00	0.00	0.00	0.00	0.00	0.00	0.00	0.00
Ba	0.01	0.02	0.01	0.01	0.01	0.01	0.01	0.01	0.01	0.01	0.01	0.02	0.02	0.01	0.01	0.02	0.02	0.01
Na	0.08	0.08	0.08	0.08	0.09	0.09	0.07	0.07	0.07	0.08	0.09	0.07	0.09	0.08	0.08	0.07	0.09	0.07
K	1.62	1.63	1.65	1.61	1.63	1.56	1.68	1.60	1.63	1.60	1.64	1.64	1.63	1.64	1.63	1.61	1.64	1.62
F	0.00	0.00	0.00	0.00	0.00	0.00	0.00	0.00	0.00	0.00	0.00	0.00	0.00	0.00	0.00	0.00	0.00	0.00
X_{Mg}	0.35	0.35	0.35	0.35	0.34	0.35	0.35	0.35	0.35	0.36	0.34	0.35	0.35	0.36	0.35	0.41	0.40	0.40

Appendix E, cont'd

Biotite

	ic08-01b1									ic08-01b1							ic08-01b1			
	1-bt 1	1-bt 2	1-bt 3	1-bt 4	1-bt 5	1- bt 6	1-bt 7	1-bt 8	1-bt 8	2- bt 1	2- bt 2	2- bt 3	2- bt 4	2- bt 5	2- bt 6	2- bt 7	m- b1 1	m- bt 2	m- bt 3	m- bt 4
wt %																				
SiO_2	36.12	34.42	34.74	34.58	34.24	34.69	34.70	34.43	34.43	34.51	34.82	35.06	35.11	34.43	34.95	34.80	34.96	34.60	35.05	34.36
TiO_2	2.29	2.20	2.14	2.14	2.02	1.98	1.95	2.01	2.01	2.17	2.18	2.13	1.88	1.89	1.84	1.81	2.31	1.83	1.73	2.06
Al_2O_3	20.73	20.49	20.67	20.41	20.54	20.42	20.57	20.33	20.33	20.01	20.24	19.95	20.47	20.50	20.48	20.61	20.51	20.18	20.40	19.35
Cr_2O_3	0.10	0.07	0.06	0.08	0.10	0.12	0.08	0.09	0.09	0.08	0.04	0.05	0.07	0.05	0.08	0.06	0.08	0.07	0.03	0.07
FeO	22.50	23.69	23.90	24.17	23.85	24.09	24.18	24.31	24.31	22.10	21.93	22.61	22.10	22.93	22.68	22.21	20.42	21.00	21.09	20.54
MnO	0.07	0.07	0.08	0.05	0.09	0.09	0.07	0.10	0.10	0.06	0.08	0.07	0.05	0.08	0.05	0.06	0.04	0.03	0.08	0.05
MgO	6.47	6.97	6.96	7.05	6.94	7.04	7.00	6.79	6.79	7.88	7.89	7.86	8.06	7.93	7.94	7.98	9.05	9.24	9.38	9.13
CaO	0.21	0.00	0.03	0.02	0.02	0.00	0.00	0.02	0.02	0.00	0.01	0.02	0.00	0.01	0.00	0.02	0.00	0.00	0.00	0.00
BaO	0.20	0.25	0.28	0.26	0.21	0.16	0.23	0.22	0.22	0.18	0.21	0.18	0.21	0.18	0.26	0.25	0.19	0.26	0.19	0.15
Na_2O	0.73	0.31	0.31	0.31	0.33	0.25	0.29	0.23	0.23	0.32	0.29	0.34	0.32	0.39	0.30	0.35	0.24	0.24	0.31	0.22
K_2O	8.16	8.48	8.36	8.25	8.29	8.26	8.31	8.47	8.47	8.23	8.59	8.57	8.54	8.51	8.50	8.32	8.58	8.41	8.53	8.61
F	0.00	0.00	0.00	0.00	0.00	0.00	0.00	0.00	0.00	0.00	0.00	0.00	0.00	0.00	0.00	0.00	0.00	0.00	0.00	0.00
Total	97.58	96.95	97.53	97.32	96.63	97.10	97.38	97.00	97.00	95.54	96.28	96.84	96.81	96.90	97.08	96.47	96.38	95.86	96.79	94.54

Oxygens = 22

Biotite

	ic08-01b1									ic08-01b1							ic08-01b1			
	1-bt 1	1-bt 2	1-bt 3	1-bt 4	1-bt 5	1- bt 6	1-bt 7	1-bt 8	1-bt 8	2- bt 1	2- bt 2	2- bt 3	2- bt 4	2- bt 5	2- bt 6	2- bt 7	m- b1 1	m- bt 2	m- bt 3	m- bt 4
apfu																				
Si	5.40	5.24	5.25	5.25	5.23	5.27	5.26	5.25	5.25	5.28	5.29	5.31	5.30	5.23	5.28	5.28	5.26	5.26	5.27	5.30
Ti	0.26	0.25	0.24	0.24	0.23	0.23	0.22	0.23	0.23	0.25	0.25	0.24	0.21	0.22	0.21	0.21	0.26	0.21	0.20	0.24
Al	3.65	3.68	3.68	3.65	3.70	3.65	3.67	3.66	3.66	3.61	3.63	3.56	3.64	3.67	3.65	3.68	3.64	3.61	3.62	3.52
Cr	0.01	0.01	0.01	0.01	0.01	0.01	0.01	0.01	0.01	0.01	0.00	0.01	0.01	0.01	0.01	0.01	0.01	0.01	0.00	0.01
Fe^{2+}	2.81	3.02	3.02	3.07	3.05	3.06	3.06	3.10	3.10	2.83	2.79	2.86	2.79	2.91	2.87	2.82	2.57	2.67	2.65	2.65
Mn^{2+}	0.01	0.01	0.01	0.01	0.01	0.01	0.01	0.01	0.01	0.01	0.01	0.01	0.01	0.01	0.01	0.01	0.01	0.00	0.01	0.01
Mg	1.44	1.58	1.57	1.59	1.58	1.59	1.58	1.54	1.54	1.80	1.79	1.78	1.81	1.79	1.79	1.80	2.03	2.09	2.10	2.10
Ca	0.03	0.00	0.00	0.00	0.00	0.00	0.00	0.00	0.00	0.00	0.00	0.00	0.00	0.00	0.00	0.00	0.00	0.00	0.00	0.00
Ba	0.01	0.01	0.02	0.02	0.01	0.01	0.01	0.01	0.01	0.01	0.01	0.01	0.01	0.01	0.02	0.01	0.01	0.02	0.01	0.01
Na	0.21	0.09	0.09	0.09	0.10	0.07	0.09	0.07	0.07	0.10	0.09	0.10	0.09	0.11	0.09	0.10	0.07	0.07	0.09	0.07
K	1.56	1.65	1.61	1.60	1.62	1.60	1.61	1.65	1.65	1.61	1.67	1.66	1.65	1.65	1.64	1.61	1.65	1.63	1.64	1.69
F	0.00	0.00	0.00	0.00	0.00	0.00	0.00	0.00	0.00	0.00	0.00	0.00	0.00	0.00	0.00	0.00	0.00	0.00	0.00	0.00
X_{Mg}	0.34	0.34	0.34	0.34	0.34	0.34	0.34	0.33	0.33	0.39	0.39	0.38	0.39	0.38	0.38	0.39	0.44	0.44	0.44	0.44

Appendix E, cont'd

	Biotite											
	ic08-01e											
	1	2	4	5	6	7	8	9	11	12	13	14
wt %												
SiO_2	34.31	34.82	34.25	34.80	34.77	34.96	35.44	34.22	34.01	34.43	34.51	34.87
TiO_2	1.69	1.93	1.67	1.81	1.79	1.83	1.68	1.77	1.95	2.01	1.84	1.88
Al_2O_3	20.38	20.39	20.74	20.46	20.53	20.63	20.71	20.47	20.02	20.27	20.76	20.71
Cr_2O_3	0.05	0.08	0.07	0.02	0.02	0.02	0.01	0.03	0.08	0.06	0.05	0.04
FeO	23.07	22.92	22.59	22.06	22.53	21.97	21.77	21.42	21.32	22.62	22.41	22.53
MnO	0.13	0.13	0.12	0.11	0.10	0.11	0.07	0.09	0.09	0.11	0.12	0.16
MgO	7.86	7.72	7.61	7.83	8.01	8.02	8.06	7.93	7.78	7.81	7.77	7.60
CaO	0.02	0.00	0.03	0.01	0.02	0.00	0.00	0.00	0.00	0.00	0.00	0.01
BaO	0.21	0.17	0.14	0.17	0.10	0.20	0.09	0.20	0.22	0.21	0.14	0.19
Na_2O	0.25	0.31	0.31	0.33	0.23	0.32	0.28	0.31	0.31	0.22	0.25	0.30
K_2O	8.90	8.89	8.86	8.51	8.84	8.87	8.84	8.64	8.81	9.00	8.79	8.83
F	0.00	0.00	0.00	0.00	0.00	0.00	0.00	0.00	0.00	0.00	0.00	0.00
Total	96.87	97.36	96.39	96.11	96.94	96.93	96.95	95.08	94.59	96.74	96.64	97.12

Oxygens = 22

	Biotite											
	ic08-01e											
	1	2	4	5	6	7	8	9	11	12	13	14
apfu												
Si	5.23	5.26	5.23	5.30	5.26	5.28	5.33	5.26	5.27	5.24	5.24	5.27
Ti	0.19	0.22	0.19	0.21	0.20	0.21	0.19	0.20	0.23	0.23	0.21	0.21
Al	3.66	3.63	3.73	3.67	3.66	3.67	3.67	3.71	3.66	3.64	3.72	3.69
Cr	0.01	0.01	0.01	0.00	0.00	0.00	0.00	0.00	0.01	0.01	0.01	0.00
Fe^{2+}	2.94	2.90	2.88	2.81	2.85	2.78	2.74	2.76	2.76	2.88	2.85	2.85
Mn^{2+}	0.02	0.02	0.02	0.01	0.01	0.01	0.01	0.01	0.01	0.01	0.02	0.02
Mg	1.79	1.74	1.73	1.78	1.81	1.81	1.81	1.82	1.80	1.77	1.76	1.71
Ca	0.00	0.00	0.00	0.00	0.00	0.00	0.00	0.00	0.00	0.00	0.00	0.00
Ba	0.01	0.01	0.01	0.01	0.01	0.01	0.01	0.01	0.01	0.01	0.01	0.01
Na	0.07	0.09	0.09	0.10	0.07	0.09	0.08	0.09	0.09	0.07	0.07	0.09
K	1.73	1.71	1.73	1.65	1.71	1.71	1.70	1.70	1.74	1.75	1.70	1.70
F	0.00	0.00	0.00	0.00	0.00	0.00	0.00	0.00	0.00	0.00	0.00	0.00
X_{Mg}	0.38	0.38	0.38	0.39	0.39	0.39	0.40	0.40	0.39	0.38	0.38	0.38

Appendix E, cont'd

	Biotite								
	st08-13a								
	1_3	1_4	1_5	1_6	1_7	1_8	1_9	1_10	1_11
wt %									
SiO_2	36.32	36.36	35.88	34.21	36.45	35.11	36.45	36.33	36.62
TiO_2	1.73	1.76	2.05	1.81	2.02	1.95	2.28	2.09	2.16
Al_2O_3	17.45	17.19	16.79	17.49	17.02	17.90	17.03	17.27	17.09
Cr_2O_3	0.04	0.10	0.04	0.07	0.08	0.05	0.01	0.02	0.03
FeO	19.39	19.59	20.30	21.11	19.24	20.18	20.40	19.47	19.69
MnO	0.17	0.17	0.17	0.13	0.18	0.20	0.14	0.14	0.20
MgO	12.26	12.33	12.23	13.03	12.21	12.62	11.74	11.80	11.86
CaO	0.25	0.29	0.07	0.07	0.14	0.16	0.03	0.16	0.11
BaO	0.26	0.17	0.27	0.18	0.20	0.16	0.33	0.19	0.22
Na_2O	0.26	0.24	0.10	0.11	0.16	0.15	0.15	0.24	0.18
K_2O	6.64	6.52	7.92	6.03	7.64	6.04	8.72	7.84	8.34
F	0.00	0.00	0.00	0.00	0.00	0.00	0.00	0.00	0.00
Total	94.77	94.72	95.82	94.24	95.34	94.52	97.28	95.55	96.50

Oxygens = 22

	Biotite								
	st08-13a								
	1_3	1_4	1_5	1_6	1_7	1_8	1_9	1_10	1_11
apfu									
Si	5.49	5.50	5.43	5.25	5.50	5.33	5.46	5.48	5.49
Ti	0.20	0.20	0.23	0.21	0.23	0.22	0.26	0.24	0.24
Al	3.11	3.06	3.00	3.16	3.03	3.20	3.00	3.07	3.02
Cr	0.00	0.01	0.00	0.01	0.01	0.01	0.00	0.00	0.00
Fe^{2+}	2.45	2.48	2.57	2.71	2.43	2.56	2.55	2.46	2.47
Mn^{2+}	0.02	0.02	0.02	0.02	0.02	0.03	0.02	0.02	0.03
Mg	2.76	2.78	2.76	2.98	2.75	2.86	2.62	2.65	2.65
Ca	0.04	0.05	0.01	0.01	0.02	0.03	0.00	0.03	0.02
Ba	0.02	0.01	0.02	0.01	0.01	0.01	0.02	0.01	0.01
Na	0.08	0.07	0.03	0.03	0.05	0.04	0.04	0.07	0.05
K	1.28	1.26	1.53	1.18	1.47	1.17	1.66	1.51	1.60
F	0.00	0.00	0.00	0.00	0.00	0.00	0.00	0.00	0.00
X_{Mg}	0.53	0.53	0.52	0.52	0.53	0.53	0.51	0.52	0.52

Appendix E, cont'd

	Biotite														
	st08-13a										st08-13a				
	2_12	2_13	2_14	2_15	2_16	2_17	2_18	2_19	2_20	2_21	3_24	3_25	3_26	3_27	3_28
wt %															
SiO_2	34.77	34.14	35.95	35.80	36.25	36.28	36.54	36.66	36.46	36.89	35.95	35.56	35.86	35.49	34.51
TiO_2	1.91	1.77	1.99	2.08	2.04	2.19	2.22	2.21	2.07	2.13	1.86	1.99	1.87	1.70	1.59
Al_2O_3	17.50	17.31	17.64	17.20	17.28	16.95	17.03	17.24	17.44	16.99	17.17	17.07	17.34	17.34	17.29
Cr_2O_3	0.04	0.06	0.07	0.03	0.01	0.01	0.00	0.00	0.04	0.02	0.06	0.00	0.01	0.01	0.01
FeO	21.86	22.02	19.97	20.52	20.08	20.62	20.60	19.67	19.86	19.86	21.09	20.87	21.01	21.18	21.65
MnO	0.15	0.14	0.18	0.17	0.19	0.15	0.11	0.18	0.12	0.19	0.14	0.14	0.17	0.14	0.10
MgO	12.91	12.59	12.44	12.47	11.75	11.74	11.80	11.77	11.75	11.67	11.72	11.66	12.07	12.06	12.43
CaO	0.10	0.08	0.29	0.14	0.09	0.06	0.03	0.33	0.17	0.15	0.16	0.14	0.21	0.15	0.16
BaO	0.25	0.24	0.21	0.17	0.21	0.30	0.32	0.23	0.29	0.14	0.27	0.24	0.25	0.22	0.29
Na_2O	0.07	0.17	0.15	0.13	0.23	0.14	0.15	0.19	0.22	0.21	0.21	0.20	0.23	0.23	0.19
K_2O	5.88	5.81	6.66	6.89	7.83	8.58	8.48	7.35	7.71	8.10	7.51	7.45	7.30	6.95	6.52
F	0.00	0.00	0.00	0.00	0.00	0.00	0.00	0.00	0.00	0.00	0.00	0.00	0.00	0.00	0.00
Total	95.44	94.33	95.55	95.60	95.96	97.02	97.28	95.83	96.13	96.35	96.14	95.32	96.32	95.47	94.74

Oxygens = 22

	Biotite														
	st08-13a										st08-13a				
	2_12	2_13	2_14	2_15	2_16	2_17	2_18	2_19	2_20	2_21	3_24	3_25	3_26	3_27	3_28
apfu															
Si	5.27	5.25	5.40	5.40	5.46	5.45	5.46	5.50	5.47	5.53	5.43	5.42	5.40	5.39	5.30
Ti	0.22	0.20	0.23	0.24	0.23	0.25	0.25	0.25	0.23	0.24	0.21	0.23	0.21	0.19	0.18
Al	3.13	3.14	3.13	3.06	3.07	3.00	3.00	3.05	3.09	3.00	3.06	3.06	3.08	3.10	3.13
Cr	0.00	0.01	0.01	0.00	0.00	0.00	0.00	0.00	0.00	0.00	0.01	0.00	0.00	0.00	0.00
Fe^{2+}	2.77	2.83	2.51	2.59	2.53	2.59	2.58	2.47	2.49	2.49	2.66	2.66	2.65	2.69	2.78
Mn^{2+}	0.02	0.02	0.02	0.02	0.02	0.02	0.01	0.02	0.02	0.02	0.02	0.02	0.02	0.02	0.01
Mg	2.92	2.89	2.79	2.81	2.64	2.63	2.63	2.63	2.63	2.61	2.64	2.65	2.71	2.73	2.84
Ca	0.02	0.01	0.05	0.02	0.01	0.01	0.00	0.05	0.03	0.02	0.03	0.02	0.03	0.02	0.03
Ba	0.01	0.01	0.01	0.01	0.01	0.02	0.02	0.01	0.02	0.01	0.02	0.01	0.01	0.01	0.02
Na	0.02	0.05	0.04	0.04	0.07	0.04	0.04	0.06	0.06	0.06	0.06	0.06	0.07	0.07	0.06
K	1.14	1.14	1.28	1.33	1.51	1.64	1.62	1.41	1.48	1.55	1.45	1.45	1.40	1.35	1.28
F	0.00	0.00	0.00	0.00	0.00	0.00	0.00	0.00	0.00	0.00	0.00	0.00	0.00	0.00	0.00
X_{Mg}	0.51	0.50	0.53	0.52	0.51	0.50	0.51	0.52	0.51	0.51	0.50	0.50	0.51	0.50	0.51

Appendix E, cont'd

	Biotite									
	st08-30a									
	1_1	1_2	1_10	1_11	1_12	1_13	1_14	1_15	1_16	1_17
wt %										
SiO_2	36.24	36.43	36.26	35.98	36.88	36.36	36.80	36.35	36.21	36.19
TiO_2	2.46	1.77	2.09	2.28	1.73	1.74	1.53	1.46	1.69	1.61
Al_2O_3	17.18	17.45	17.23	17.31	17.92	17.35	17.93	17.73	17.48	17.93
Cr_2O_3	0.03	0.02	0.00	0.02	0.01	0.00	0.01	0.07	0.03	0.02
FeO	20.41	20.68	20.46	20.69	20.73	20.48	20.31	20.34	20.28	19.96
MnO	0.20	0.20	0.14	0.18	0.18	0.23	0.18	0.24	0.21	0.23
MgO	10.94	11.20	11.37	10.92	11.63	11.52	11.85	11.49	11.24	11.31
CaO	0.09	0.07	0.06	0.07	0.05	0.09	0.06	0.07	0.03	0.02
BaO	0.81	0.84	0.90	0.83	0.88	0.59	0.54	0.49	0.78	0.82
Na_2O	0.06	0.11	0.13	0.11	0.15	0.13	0.12	0.14	0.09	0.12
K_2O	9.15	8.79	9.02	9.08	8.82	8.52	8.72	8.83	9.00	9.03
F	0.00	0.00	0.00	0.00	0.00	0.00	0.00	0.00	0.00	0.00
Total	97.57	97.56	97.66	97.47	98.98	97.01	98.05	97.21	97.04	97.24

Oxygens = 22

	Biotite									
	st08-30a									
	1_1	1_2	1_10	1_11	1_12	1_13	1_14	1_15	1_16	1_17
apfu										
Si	5.44	5.46	5.44	5.42	5.44	5.46	5.46	5.45	5.46	5.44
Ti	0.28	0.20	0.24	0.26	0.19	0.20	0.17	0.16	0.19	0.18
Al	3.04	3.08	3.05	3.07	3.12	3.07	3.13	3.13	3.11	3.17
Cr	0.00	0.00	0.00	0.00	0.00	0.00	0.00	0.01	0.00	0.00
Fe^{2+}	2.56	2.59	2.57	2.61	2.56	2.57	2.52	2.55	2.56	2.51
Mn^{2+}	0.03	0.03	0.02	0.02	0.02	0.03	0.02	0.03	0.03	0.03
Mg	2.45	2.50	2.54	2.45	2.56	2.58	2.62	2.57	2.53	2.53
Ca	0.01	0.01	0.01	0.01	0.01	0.01	0.01	0.01	0.00	0.00
Ba	0.05	0.05	0.05	0.05	0.05	0.03	0.03	0.03	0.05	0.05
Na	0.02	0.03	0.04	0.03	0.04	0.04	0.03	0.04	0.03	0.03
K	1.75	1.68	1.73	1.74	1.66	1.63	1.65	1.69	1.73	1.73
F	0.00	0.00	0.00	0.00	0.00	0.00	0.00	0.00	0.00	0.00
X_{Mg}	0.49	0.49	0.50	0.48	0.50	0.50	0.51	0.50	0.50	0.50

Appendix E, cont'd

	Biotite																	
	st08-30a										st08-30a							
	2_1	2_1	2_2	2_3	2_4	2_5	2_6	2_7	2_8	2_9	3_18	3_19	3_20	3_21	3_22	3_23	3_24	3_25
wt %																		
SiO_2	36.68	35.65	35.96	36.59	36.48	34.96	35.95	36.15	36.46	36.08	36.38	36.46	36.79	36.99	36.82	36.24	36.00	35.81
TiO_2	1.45	0.99	1.09	1.05	1.46	1.07	1.02	1.47	1.44	1.56	1.45	1.72	1.65	1.93	2.22	1.61	2.20	1.38
Al_2O_3	17.73	18.51	18.31	18.24	17.83	18.82	18.45	17.73	17.22	17.42	17.15	17.44	16.89	17.72	17.45	17.41	17.39	18.14
Cr_2O_3	0.03	0.02	0.02	0.03	0.08	0.04	0.00	0.01	0.06	0.03	0.00	0.00	0.03	0.05	0.00	0.03	0.02	0.03
FeO	19.92	20.55	19.93	20.25	19.96	20.44	20.64	19.86	20.51	20.75	20.86	20.47	20.56	20.67	20.39	20.76	20.68	20.54
MnO	0.20	0.23	0.15	0.20	0.24	0.15	0.24	0.21	0.23	0.23	0.20	0.23	0.21	0.16	0.22	0.21	0.18	0.25
MgO	11.92	11.48	11.81	12.12	11.78	11.80	11.73	11.64	11.58	11.78	11.36	11.29	11.66	11.33	11.17	11.39	11.23	11.87
CaO	0.02	0.19	0.12	0.10	0.05	0.09	0.15	0.06	0.06	0.07	0.06	0.03	0.04	0.05	0.02	0.06	0.04	0.05
BaO	0.79	0.10	0.17	0.25	0.67	0.25	0.25	0.81	0.50	0.95	0.58	0.68	0.50	0.72	0.74	0.56	0.89	0.54
Na_2O	0.07	0.11	0.18	0.12	0.09	0.11	0.15	0.09	0.11	0.12	0.03	0.11	0.16	0.18	0.10	0.14	0.11	0.15
K_2O	8.81	7.53	8.30	8.65	8.89	8.10	8.26	9.15	9.03	8.79	9.29	9.11	9.34	9.14	9.25	9.08	9.08	8.93
F	0.00	0.00	0.00	0.00	0.00	0.00	0.00	0.00	0.00	0.00	0.00	0.00	0.00	0.00	0.00	0.00	0.00	0.00
Total	97.62	95.36	96.04	97.60	97.53	95.83	96.84	97.18	97.20	97.78	97.36	97.54	97.83	98.94	98.38	97.49	97.82	97.69

Oxygens = 22

	Biotite																	
	st08-30a										st08-30a							
	2_1	2_1	2_2	2_3	2_4	2_5	2_6	2_7	2_8	2_9	3_18	3_19	3_20	3_21	3_22	3_23	3_24	3_25
apfu																		
Si	5.47	5.40	5.42	5.44	5.45	5.30	5.39	5.44	5.48	5.41	5.48	5.47	5.50	5.46	5.47	5.44	5.40	5.36
Ti	0.16	0.11	0.12	0.12	0.16	0.12	0.12	0.17	0.16	0.18	0.16	0.19	0.19	0.21	0.25	0.18	0.25	0.16
Al	3.12	3.31	3.25	3.19	3.14	3.36	3.26	3.14	3.05	3.08	3.04	3.08	2.98	3.09	3.06	3.08	3.08	3.20
Cr	0.00	0.00	0.00	0.00	0.01	0.00	0.00	0.00	0.01	0.00	0.00	0.00	0.00	0.01	0.00	0.00	0.00	0.00
Fe^{2+}	2.48	2.60	2.51	2.52	2.49	2.59	2.59	2.50	2.58	2.60	2.63	2.57	2.57	2.55	2.53	2.61	2.60	2.57
Mn^{2+}	0.03	0.03	0.02	0.03	0.03	0.02	0.03	0.03	0.03	0.03	0.03	0.03	0.03	0.02	0.03	0.03	0.02	0.03
Mg	2.65	2.59	2.65	2.68	2.62	2.67	2.62	2.61	2.60	2.64	2.55	2.52	2.60	2.50	2.47	2.55	2.51	2.65
Ca	0.00	0.03	0.02	0.02	0.01	0.01	0.02	0.01	0.01	0.01	0.01	0.00	0.01	0.01	0.00	0.01	0.01	0.01
Ba	0.05	0.01	0.01	0.01	0.04	0.01	0.01	0.05	0.03	0.06	0.03	0.04	0.03	0.04	0.04	0.03	0.05	0.03
Na	0.02	0.03	0.05	0.03	0.03	0.03	0.04	0.03	0.03	0.03	0.01	0.03	0.05	0.05	0.03	0.04	0.03	0.04
K	1.68	1.46	1.60	1.64	1.69	1.57	1.58	1.76	1.73	1.68	1.79	1.74	1.78	1.72	1.75	1.74	1.74	1.71
F	0.00	0.00	0.00	0.00	0.00	0.00	0.00	0.00	0.00	0.00	0.00	0.00	0.00	0.00	0.00	0.00	0.00	0.00
X_{Mg}	0.52	0.50	0.51	0.52	0.51	0.51	0.50	0.51	0.50	0.50	0.49	0.50	0.50	0.49	0.49	0.49	0.49	0.51

Appendix E, cont'd

	Biotite									
	idaho m									
	1_1	1_2	1_3	1_4	1_5	1_6	1_7	1_8	1_9	1_10
wt %										
SiO_2	37.74	37.29	38.06	37.75	36.78	37.71	38.01	37.96	37.36	38.06
TiO_2	2.15	2.16	2.21	2.08	1.94	1.98	1.96	1.92	1.80	1.99
Al_2O_3	15.60	16.27	16.02	16.22	15.74	16.12	15.81	15.63	15.82	15.52
Cr_2O_3	0.16	0.13	0.13	0.17	0.12	0.15	0.17	0.14	0.21	0.17
FeO	16.96	16.56	17.07	16.74	16.65	16.91	16.87	16.63	16.66	17.30
MnO	0.20	0.16	0.21	0.24	0.19	0.20	0.22	0.20	0.19	0.18
MgO	13.75	13.95	14.36	13.98	14.03	14.22	14.03	13.98	13.93	13.91
CaO	0.01	0.01	0.01	0.03	0.00	0.00	0.00	0.02	0.00	0.01
BaO	0.26	0.22	0.24	0.30	0.22	0.22	0.21	0.23	0.24	0.24
Na_2O	0.14	0.08	0.10	0.10	0.10	0.05	0.10	0.06	0.09	0.05
K_2O	9.52	9.36	9.62	9.47	9.36	9.60	9.83	9.60	9.57	9.79
F	0.00	0.00	0.00	0.00	0.00	0.00	0.00	0.00	0.00	0.00
Total	96.49	96.19	98.03	97.08	95.13	97.16	97.21	96.37	95.87	97.22

Oxygens = 22

	Biotite									
	idaho m									
	1_1	1_2	1_3	1_4	1_5	1_6	1_7	1_8	1_9	1_10
apfu										
Si	5.62	5.56	5.58	5.58	5.56	5.57	5.62	5.65	5.60	5.64
Ti	0.24	0.24	0.24	0.23	0.22	0.22	0.22	0.21	0.20	0.22
Al	2.74	2.86	2.77	2.83	2.80	2.81	2.76	2.74	2.79	2.71
Cr	0.02	0.02	0.02	0.02	0.01	0.02	0.02	0.02	0.02	0.02
Fe^{2+}	2.11	2.06	2.09	2.07	2.10	2.09	2.09	2.07	2.09	2.14
Mn^{2+}	0.03	0.02	0.03	0.03	0.02	0.03	0.03	0.03	0.02	0.02
Mg	3.05	3.10	3.14	3.08	3.16	3.13	3.09	3.10	3.11	3.07
Ca	0.00	0.00	0.00	0.00	0.00	0.00	0.00	0.00	0.00	0.00
Ba	0.02	0.01	0.01	0.02	0.01	0.01	0.01	0.01	0.01	0.01
Na	0.04	0.02	0.03	0.03	0.03	0.01	0.03	0.02	0.03	0.01
K	1.81	1.78	1.80	1.79	1.80	1.81	1.85	1.82	1.83	1.85
F	0.00	0.00	0.00	0.00	0.00	0.00	0.00	0.00	0.00	0.00
X_{Mg}	0.59	0.60	0.60	0.60	0.60	0.60	0.60	0.60	0.60	0.59

Appendix E, cont'd

	Biotite										
	idaho m										
	2_11	2_12	2_13	2_14	2_15	2_16	2_17	2_18	2_19	2_20	2_21
wt %											
SiO_2	38.08	37.70	38.23	37.94	38.08	38.26	38.27	37.78	38.30	38.24	38.46
TiO_2	1.87	1.97	1.91	2.09	2.07	2.14	2.16	2.03	2.16	1.87	1.99
Al_2O_3	16.20	15.84	16.00	16.38	15.89	15.92	16.06	16.13	16.12	16.25	16.14
Cr_2O_3	0.27	0.18	0.22	0.24	0.18	0.22	0.20	0.20	0.11	0.10	0.20
FeO	16.71	16.97	17.49	16.89	17.19	17.52	17.22	16.85	16.96	17.06	17.11
MnO	0.19	0.21	0.17	0.19	0.17	0.21	0.19	0.21	0.18	0.22	0.17
MgO	13.90	13.74	14.08	14.07	13.90	14.02	13.91	13.94	14.02	14.09	13.99
CaO	0.02	0.03	0.01	0.01	0.00	0.00	0.00	0.00	0.00	0.08	0.00
BaO	0.29	0.24	0.30	0.31	0.20	0.24	0.24	0.28	0.25	0.16	0.25
Na_2O	0.06	0.12	0.13	0.07	0.11	0.12	0.10	0.07	0.09	0.07	0.05
K_2O	9.68	9.47	9.61	9.60	9.81	9.70	9.46	9.62	9.59	9.38	9.75
F	0.00	0.00	0.00	0.00	0.00	0.00	0.00	0.00	0.00	0.00	0.00
Total	97.27	96.47	98.15	97.79	97.60	98.35	97.81	97.11	97.78	97.52	98.11

Oxygens = 22

	Biotite										
	idaho m										
	2_11	2_12	2_13	2_14	2_15	2_16	2_17	2_18	2_19	2_20	2_21
apfu											
Si	5.62	5.61	5.61	5.57	5.61	5.60	5.62	5.59	5.62	5.62	5.63
Ti	0.21	0.22	0.21	0.23	0.23	0.24	0.24	0.23	0.24	0.21	0.22
Al	2.82	2.78	2.77	2.83	2.76	2.75	2.78	2.81	2.79	2.81	2.78
Cr	0.03	0.02	0.03	0.03	0.02	0.03	0.02	0.02	0.01	0.01	0.02
Fe^{2+}	2.06	2.11	2.14	2.07	2.12	2.15	2.11	2.08	2.08	2.10	2.09
Mn^{2+}	0.02	0.03	0.02	0.02	0.02	0.03	0.02	0.03	0.02	0.03	0.02
Mg	3.06	3.05	3.08	3.08	3.05	3.06	3.04	3.07	3.07	3.08	3.05
Ca	0.00	0.00	0.00	0.00	0.00	0.00	0.00	0.00	0.00	0.01	0.00
Ba	0.02	0.01	0.02	0.02	0.01	0.01	0.01	0.02	0.01	0.01	0.01
Na	0.02	0.03	0.04	0.02	0.03	0.03	0.03	0.02	0.03	0.02	0.01
K	1.82	1.80	1.80	1.80	1.84	1.81	1.77	1.82	1.79	1.76	1.82
F	0.00	0.00	0.00	0.00	0.00	0.00	0.00	0.00	0.00	0.00	0.00
X_{Mg}	0.60	0.59	0.59	0.60	0.59	0.59	0.59	0.60	0.60	0.60	0.59

APPENDIX F: ELECTRON MICROPROBE ANALYSES – CPX

	Pyroxene										
	st08-045a				st08-045a						
	1_1	1_2	1_3	1_4	1_1	1_2	1_3	1_4	1_5	1_6	1_7
wt %											
SiO_2	51.28	51.47	51.48	50.75	50.61	50.83	51.28	51.31	51.10	50.69	51.22
TiO_2	0.05	0.04	0.06	0.05	0.06	0.06	0.05	0.03	0.04	0.05	0.05
Al_2O_3	0.64	0.63	0.65	0.66	0.64	0.63	0.66	0.63	0.61	0.49	0.47
Cr_2O_3	0.04	0.00	0.04	0.03	0.05	0.01	0.00	0.00	0.06	0.05	0.04
FeO	16.11	16.72	17.10	16.70	16.31	16.35	16.22	16.17	16.01	16.33	16.13
MnO	0.42	0.47	0.47	0.40	0.42	0.44	0.41	0.42	0.41	0.45	0.43
MgO	8.56	8.47	8.68	8.60	8.64	8.41	8.36	8.62	8.55	8.47	8.37
CaO	23.39	23.87	23.48	23.13	23.45	23.55	23.34	23.49	23.71	23.72	23.84
Na_2O	0.34	0.25	0.31	0.21	0.26	0.19	0.26	0.21	0.25	0.11	0.24
K_2O	0.00	0.01	0.01	0.01	0.00	0.01	0.01	0.01	0.00	0.00	0.00
Total	100.83	101.93	102.28	100.54	100.44	100.48	100.59	100.89	100.74	100.36	100.79

Oxygens = 6

	Pyroxene										
	st08-045a				st08-045a						
	1_1	1_2	1_3	1_4	1_1	1_2	1_3	1_4	1_5	1_6	1_7
apfu											
Si	1.97	1.97	1.96	1.97	1.96	1.97	1.98	1.97	1.97	1.97	1.98
Ti	0.00	0.00	0.00	0.00	0.00	0.00	0.00	0.00	0.00	0.00	0.00
Al	0.03	0.03	0.03	0.03	0.03	0.03	0.03	0.03	0.03	0.02	0.02
Cr	0.00	0.00	0.00	0.00	0.00	0.00	0.00	0.00	0.00	0.00	0.00
Fe^{2+}	0.52	0.53	0.55	0.54	0.53	0.53	0.52	0.52	0.52	0.53	0.52
Mn^{2+}	0.01	0.02	0.02	0.01	0.01	0.01	0.01	0.01	0.01	0.01	0.01
Mg	0.49	0.48	0.49	0.50	0.50	0.49	0.48	0.49	0.49	0.49	0.48
Ca	0.97	0.98	0.96	0.96	0.97	0.98	0.97	0.97	0.98	0.99	0.99
Na	0.03	0.02	0.02	0.02	0.02	0.01	0.02	0.02	0.02	0.01	0.02
K	0.00	0.00	0.00	0.00	0.00	0.00	0.00	0.00	0.00	0.00	0.00
Fe^{3+}	0.00	0.00	0.00	0.00	0.00	0.00	0.00	0.00	0.00	0.00	0.00
X_{Mg}	0.25	0.24	0.25	0.25	0.25	0.24	0.24	0.25	0.25	0.24	0.24
X_{Ca}	0.49	0.49	0.48	0.48	0.49	0.49	0.49	0.49	0.49	0.49	0.50
X_{Fe}	0.26	0.27	0.27	0.27	0.26	0.27	0.27	0.26	0.26	0.26	0.26

Appendix F, cont'd

	Pyroxene																	
	st08-45a									st08-45a								
	2_8	2_9	2_10	2_11	2_12	2_13	2_14	2_15	2_16	4_9	4_10	4_11	4_12	4_13	4_14	4_15	4_16	4_17
wt %																		
SiO_2	51.09	50.80	51.02	51.28	51.19	51.06	50.76	50.81	48.62	50.62	51.09	50.72	50.30	50.79	45.38	50.93	51.41	50.97
TiO_2	0.11	0.08	0.05	0.04	0.06	0.03	0.05	0.07	0.01	0.14	0.00	0.15	0.12	0.10	0.22	0.08	0.01	0.08
Al_2O_3	0.90	0.83	0.40	0.34	0.61	0.54	0.62	0.58	2.27	1.06	0.22	0.99	0.87	0.94	7.18	0.80	0.31	0.79
Cr_2O_3	0.03	0.03	0.05	0.09	0.00	0.07	0.04	0.05	0.05	0.00	0.05	0.00	0.03	0.00	0.02	0.00	0.02	0.13
FeO	16.76	16.33	16.47	16.27	16.20	16.41	16.57	16.45	14.94	17.80	16.86	17.53	17.23	17.46	23.17	16.35	16.40	16.57
MnO	0.47	0.47	0.46	0.42	0.42	0.47	0.46	0.49	0.45	0.42	0.47	0.46	0.44	0.45	0.31	0.40	0.48	0.50
MgO	8.31	8.34	8.50	8.55	8.71	8.47	8.30	8.30	8.27	7.77	8.15	7.75	7.83	7.55	6.68	8.18	8.35	7.97
CaO	23.64	23.17	24.04	23.77	23.74	23.93	23.76	23.42	23.06	22.89	24.11	23.38	23.62	23.42	14.32	23.77	24.29	23.67
Na_2O	0.30	0.35	0.24	0.19	0.25	0.21	0.27	0.23	0.13	0.29	0.12	0.32	0.23	0.31	0.97	0.29	0.16	0.29
K_2O	0.00	0.01	0.01	0.01	0.00	0.00	0.00	0.00	0.02	0.00	0.00	0.01	0.01	0.01	0.41	0.00	0.01	0.01
Total	101.61	100.41	101.24	100.96	101.18	101.19	100.83	100.40	97.82	100.99	101.07	101.31	100.68	101.03	98.66	100.80	101.44	100.98

Oxygens = 6

	Pyroxene																	
	st08-45a									st08-45a								
	2_8	2_9	2_10	2_11	2_12	2_13	2_14	2_15	2_16	4_9	4_10	4_11	4_12	4_13	4_14	4_15	4_16	4_17
apfu																		
Si	1.96	1.97	1.97	1.98	1.97	1.97	1.96	1.97	1.93	1.96	1.97	1.96	1.96	1.97	1.82	1.97	1.98	1.97
Ti	0.00	0.00	0.00	0.00	0.00	0.00	0.00	0.00	0.00	0.00	0.00	0.00	0.00	0.00	0.01	0.00	0.00	0.00
Al	0.04	0.04	0.02	0.02	0.03	0.02	0.03	0.03	0.11	0.05	0.01	0.05	0.04	0.04	0.34	0.04	0.01	0.04
Cr	0.00	0.00	0.00	0.00	0.00	0.00	0.00	0.00	0.00	0.00	0.00	0.00	0.00	0.00	0.00	0.00	0.00	0.00
Fe^{2+}	0.54	0.53	0.53	0.52	0.52	0.53	0.54	0.53	0.50	0.58	0.55	0.57	0.56	0.57	0.78	0.53	0.53	0.54
Mn^{2+}	0.02	0.02	0.02	0.01	0.01	0.02	0.02	0.02	0.02	0.01	0.02	0.02	0.01	0.01	0.01	0.01	0.02	0.02
Mg	0.48	0.48	0.49	0.49	0.50	0.49	0.48	0.48	0.49	0.45	0.47	0.45	0.45	0.44	0.40	0.47	0.48	0.46
Ca	0.97	0.96	0.99	0.98	0.98	0.99	0.98	0.97	0.98	0.95	1.00	0.97	0.98	0.97	0.61	0.98	1.00	0.98
Na	0.02	0.03	0.02	0.01	0.02	0.02	0.02	0.02	0.01	0.02	0.01	0.02	0.02	0.02	0.08	0.02	0.01	0.02
K	0.00	0.00	0.00	0.00	0.00	0.00	0.00	0.00	0.00	0.00	0.00	0.00	0.00	0.00	0.02	0.00	0.00	0.00
Fe^{3+}	0.00	0.00	0.00	0.00	0.00	0.00	0.00	0.00	0.00	0.00	0.00	0.00	0.00	0.00	0.00	0.00	0.00	0.00
X_{Mg}	0.24	0.24	0.24	0.25	0.25	0.24	0.24	0.24	0.25	0.23	0.23	0.23	0.23	0.22	0.22	0.24	0.24	0.23
X_{Ca}	0.49	0.49	0.49	0.49	0.49	0.49	0.49	0.49	0.50	0.48	0.50	0.49	0.49	0.49	0.34	0.50	0.50	0.50
X_{Fe}	0.27	0.27	0.26	0.26	0.26	0.26	0.27	0.27	0.25	0.29	0.27	0.29	0.28	0.29	0.43	0.27	0.26	0.27

Appendix F, cont'd

	Pyroxene												
	Idaho M												
	1_5	1_6	1_7	1_8	1_9	1_10	1_11	1_12	1_13	1_14	1_15	1_16	1_17
wt %													
SiO_2	52.72	52.65	52.52	52.81	52.26	52.11	52.41	51.91	52.43	52.58	52.27	51.29	51.96
TiO_2	0.01	0.03	0.03	0.02	0.12	0.11	0.07	0.04	0.09	0.10	0.04	0.12	0.06
Al_2O_3	0.37	0.51	0.33	0.42	0.85	0.86	0.83	0.79	0.81	0.79	0.75	0.77	0.73
Cr_2O_3	0.02	0.05	0.00	0.04	0.08	0.03	0.00	0.08	0.04	0.05	0.06	0.04	0.02
FeO	9.09	8.59	8.28	8.17	8.44	8.50	8.72	8.88	8.55	8.79	8.90	8.42	8.16
MnO	0.35	0.31	0.36	0.31	0.40	0.39	0.35	0.38	0.32	0.34	0.38	0.32	0.36
MgO	13.09	13.54	13.47	13.65	13.31	13.21	13.38	13.35	13.35	13.43	13.24	13.46	13.37
CaO	25.50	25.35	25.32	25.49	24.88	24.95	24.54	24.80	24.43	24.63	24.70	24.54	24.91
Na_2O	0.20	0.26	0.20	0.18	0.32	0.27	0.26	0.36	0.31	0.27	0.19	0.37	0.24
K_2O	0.00	0.00	0.00	0.01	0.00	0.01	0.00	0.00	0.00	0.01	0.00	0.00	0.00
Total	101.35	101.29	100.51	101.10	100.66	100.44	100.56	100.59	100.33	100.99	100.53	99.33	99.81

Oxygens = 6

	Pyroxene												
	Idaho M												
	1_5	1_6	1_7	1_8	1_9	1_10	1_11	1_12	1_13	1_14	1_15	1_16	1_17
apfu													
Si	1.96	1.96	1.97	1.96	1.95	1.95	1.96	1.95	1.96	1.96	1.96	1.95	1.96
Ti	0.00	0.00	0.00	0.00	0.00	0.00	0.00	0.00	0.00	0.00	0.00	0.00	0.00
Al	0.02	0.02	0.01	0.02	0.04	0.04	0.04	0.03	0.04	0.03	0.03	0.03	0.03
Cr	0.00	0.00	0.00	0.00	0.00	0.00	0.00	0.00	0.00	0.00	0.00	0.00	0.00
Fe^{2+}	0.28	0.27	0.26	0.25	0.26	0.27	0.27	0.28	0.27	0.27	0.28	0.27	0.26
Mn^{2+}	0.01	0.01	0.01	0.01	0.01	0.01	0.01	0.01	0.01	0.01	0.01	0.01	0.01
Mg	0.73	0.75	0.75	0.76	0.74	0.74	0.75	0.75	0.75	0.75	0.74	0.76	0.75
Ca	1.02	1.01	1.02	1.02	1.00	1.00	0.98	1.00	0.98	0.98	0.99	1.00	1.01
Na	0.01	0.02	0.01	0.01	0.02	0.02	0.02	0.03	0.02	0.02	0.01	0.03	0.02
K	0.00	0.00	0.00	0.00	0.00	0.00	0.00	0.00	0.00	0.00	0.00	0.00	0.00
Fe^{3+}	0.00	0.00	0.00	0.00	0.00	0.00	0.00	0.00	0.00	0.00	0.00	0.00	0.00
X_{Mg}	0.36	0.37	0.37	0.37	0.37	0.37	0.37	0.37	0.37	0.37	0.37	0.38	0.37
X_{Ca}	0.50	0.50	0.50	0.50	0.50	0.50	0.49	0.49	0.49	0.49	0.49	0.49	0.50
X_{Fe}	0.14	0.13	0.13	0.13	0.13	0.13	0.14	0.14	0.13	0.14	0.14	0.13	0.13

Appendix F, cont'd

	Pyroxene										
	Idaho m										
	2_1	2_2	2_3	2_4	2_5	2_6	2_7	2_8	2_9	2_10	2_11
wt %											
SiO_2	51.26	51.90	50.60	51.76	51.19	51.09	51.86	52.21	50.95	51.38	50.27
TiO_2	0.08	0.08	0.07	0.10	0.08	0.06	0.04	0.05	0.04	0.05	0.03
Al_2O_3	0.82	0.86	0.83	0.83	0.78	0.63	0.60	0.45	0.48	0.49	0.49
Cr_2O_3	0.03	0.05	0.01	0.05	0.06	0.01	0.05	0.00	0.02	0.03	0.00
FeO	8.75	8.53	8.91	8.55	8.60	8.73	8.75	9.32	9.09	9.18	9.29
MnO	0.34	0.37	0.31	0.33	0.37	0.37	0.30	0.36	0.36	0.36	0.36
MgO	13.33	13.42	13.31	13.49	13.58	13.42	13.50	13.18	12.99	13.12	13.14
CaO	24.59	24.62	24.45	24.34	24.85	24.61	24.64	24.71	25.04	24.64	25.07
Na_2O	0.26	0.30	0.26	0.28	0.35	0.27	0.21	0.24	0.20	0.27	0.26
K_2O	0.00	0.00	0.00	0.00	0.00	0.00	0.01	0.00	0.00	0.01	0.01
Total	99.46	100.13	98.75	99.73	99.86	99.19	99.96	100.52	99.17	99.53	98.92

Oxygens = 6

	Pyroxene										
	Idaho m										
	2_1	2_2	2_3	2_4	2_5	2_6	2_7	2_8	2_9	2_10	2_11
apfu											
Si	1.94	1.95	1.94	1.95	1.94	1.94	1.95	1.96	1.95	1.95	1.93
Ti	0.00	0.00	0.00	0.00	0.00	0.00	0.00	0.00	0.00	0.00	0.00
Al	0.04	0.04	0.04	0.04	0.03	0.03	0.03	0.02	0.02	0.02	0.02
Cr	0.00	0.00	0.00	0.00	0.00	0.00	0.00	0.00	0.00	0.00	0.00
Fe^{2+}	0.28	0.27	0.29	0.27	0.27	0.28	0.28	0.29	0.29	0.29	0.30
Mn^{2+}	0.01	0.01	0.01	0.01	0.01	0.01	0.01	0.01	0.01	0.01	0.01
Mg	0.75	0.75	0.76	0.76	0.77	0.76	0.76	0.74	0.74	0.74	0.75
Ca	1.00	0.99	1.00	0.98	1.01	1.00	0.99	0.99	1.02	1.00	1.03
Na	0.02	0.02	0.02	0.02	0.03	0.02	0.02	0.02	0.01	0.02	0.02
K	0.00	0.00	0.00	0.00	0.00	0.00	0.00	0.00	0.00	0.00	0.00
Fe^{3+}	0.00	0.00	0.00	0.00	0.00	0.00	0.00	0.00	0.00	0.00	0.00
X_{Mg}	0.37	0.37	0.37	0.38	0.37	0.37	0.37	0.36	0.36	0.36	0.36
X_{Ca}	0.49	0.49	0.49	0.49	0.49	0.49	0.49	0.49	0.50	0.49	0.50
X_{Fe}	0.14	0.13	0.14	0.13	0.13	0.14	0.14	0.14	0.14	0.14	0.14

APPENDIX G: ELECTRON MICROPROBE ANALYSES – GARNET

	Garnet																	
	ic08-01a																	
	1	2	3	4	5	6	7	8	9	10	11	12	13	14	15	16	17	18
wt %																		
SiO_2	36.65	37.30	37.09	37.13	37.00	37.26	36.84	36.97	36.90	37.20	36.49	37.10	36.88	37.27	37.07	37.34	36.74	37.33
TiO_2	0.00	0.01	0.01	0.01	0.00	0.01	0.00	0.01	0.01	0.03	0.00	0.02	0.00	0.00	0.00	0.03	0.00	0.00
Al_2O_3	20.54	20.85	20.71	20.47	20.49	20.83	20.70	20.76	20.86	20.82	20.03	21.02	20.57	21.02	20.53	21.12	20.41	21.12
Cr_2O_3	0.01	0.04	0.04	0.02	0.04	0.04	0.06	0.02	0.02	0.01	0.00	0.05	0.02	0.01	0.00	0.01	0.00	0.01
FeO	33.79	33.13	33.67	33.60	33.93	33.97	34.03	33.84	33.44	33.89	33.66	33.82	32.75	33.78	33.08	34.51	34.05	34.17
MnO	4.11	3.05	2.53	3.41	1.52	1.54	1.86	2.74	1.62	1.74	1.67	1.58	1.73	1.86	1.24	1.01	1.02	1.02
MgO	1.95	3.03	3.20	2.82	3.87	3.83	3.44	2.87	3.91	4.21	4.10	4.28	4.05	4.01	4.08	4.04	4.07	3.90
CaO	1.79	1.67	1.61	1.61	1.55	1.55	1.59	1.57	1.42	1.41	1.41	1.40	1.53	1.55	1.84	1.76	1.80	1.76
Total	98.84	99.08	98.86	99.07	98.40	99.03	98.52	98.78	98.18	99.31	97.36	99.27	97.53	99.50	97.84	99.82	98.09	99.31

Oxygens = 12

	Garnet																	
	ic08-01a																	
	1	2	3	4	5	6	7	8	9	10	11	12	13	14	15	16	17	18
apfu																		
Si	3.01	3.02	3.01	3.02	3.01	3.01	3.00	3.01	3.00	3.00	3.01	2.99	3.02	3.00	3.02	2.99	3.00	3.00
Ti	0.00	0.00	0.00	0.00	0.00	0.00	0.00	0.00	0.00	0.00	0.00	0.00	0.00	0.00	0.00	0.00	0.00	0.00
Al	1.99	1.99	1.98	1.96	1.97	1.98	1.99	1.99	2.00	1.98	1.95	2.00	1.98	1.99	1.97	2.00	1.97	2.00
Cr	0.00	0.00	0.00	0.00	0.00	0.00	0.00	0.00	0.00	0.00	0.00	0.00	0.00	0.00	0.00	0.00	0.00	0.00
Fe^{2+}	2.32	2.24	2.29	2.29	2.31	2.30	2.32	2.31	2.28	2.28	2.32	2.28	2.24	2.27	2.26	2.31	2.33	2.30
Mn^{2+}	0.29	0.21	0.17	0.24	0.10	0.11	0.13	0.19	0.11	0.12	0.12	0.11	0.12	0.13	0.09	0.07	0.07	0.07
Mg	0.24	0.37	0.39	0.34	0.47	0.46	0.42	0.35	0.47	0.51	0.50	0.51	0.49	0.48	0.50	0.48	0.50	0.47
Ca	0.16	0.15	0.14	0.14	0.14	0.13	0.14	0.14	0.12	0.12	0.12	0.12	0.13	0.13	0.16	0.15	0.16	0.15
Fe^{3+}	0.00	0.00	0.00	0.00	0.00	0.00	0.00	0.00	0.00	0.00	0.00	0.00	0.00	0.00	0.00	0.00	0.00	0.00
X_{Mg}	0.09	0.14	0.14	0.13	0.17	0.17	0.15	0.13	0.17	0.18	0.18	0.18	0.18	0.17	0.18	0.17	0.18	0.17

Appendix G, cont'd

	Garnet									
	ic08-01a									
	19	20	21	22	23	24	25	26	27	28
wt %										
SiO_2	36.89	36.58	36.95	37.21	36.32	37.12	36.61	34.38	37.03	37.23
TiO_2	0.03	0.00	0.01	0.01	0.00	0.02	0.00	0.00	0.02	0.01
Al_2O_3	20.60	20.56	20.99	21.27	20.42	20.98	20.83	19.30	21.09	20.67
Cr_2O_3	0.00	0.02	0.04	0.04	0.00	0.01	0.00	0.05	0.00	0.03
FeO	34.10	33.42	33.60	34.10	34.29	33.71	33.03	34.40	33.13	32.99
MnO	2.99	4.48	1.87	1.61	3.22	1.59	3.33	4.82	2.58	2.39
MgO	2.91	2.10	3.63	3.78	2.28	4.23	3.07	1.33	3.43	3.30
CaO	1.74	1.74	1.58	1.60	1.61	1.39	1.77	1.39	1.84	1.84
Total	99.26	98.90	98.67	99.62	98.14	99.05	98.64	95.67	99.12	98.46

Oxygens = 12

	Garnet									
	ic08-01a									
	19	20	21	22	23	24	25	26	27	28
apfu										
Si	3.00	3.00	3.00	2.99	3.00	3.00	2.99	2.96	3.00	3.03
Ti	0.00	0.00	0.00	0.00	0.00	0.00	0.00	0.00	0.00	0.00
Al	1.98	1.99	2.01	2.01	1.99	2.00	2.00	1.96	2.01	1.98
Cr	0.00	0.00	0.00	0.00	0.00	0.00	0.00	0.00	0.00	0.00
Fe^{2+}	2.32	2.29	2.28	2.29	2.37	2.27	2.26	2.48	2.24	2.24
Mn^{2+}	0.21	0.31	0.13	0.11	0.23	0.11	0.23	0.35	0.18	0.16
Mg	0.35	0.26	0.44	0.45	0.28	0.51	0.37	0.17	0.41	0.40
Ca	0.15	0.15	0.14	0.14	0.14	0.12	0.15	0.13	0.16	0.16
Fe^{3+}	0.00	0.00	0.00	0.00	0.00	0.00	0.00	0.00	0.00	0.00
X_{Mg}	0.13	0.10	0.16	0.17	0.11	0.18	0.14	0.06	0.16	0.15

Appendix G, cont'd

	Garnet																	
	ic08-01a1																	
	1	2	3	4	5	6	7	8	9	10	11	12	13	14	15	16	17	18
wt %																		
SiO_2	37.22	36.86	37.32	37.36	37.22	37.28	37.36	37.15	36.93	36.17	37.24	36.91	37.43	37.19	37.29	37.30	36.68	36.56
TiO_2	0.03	0.02	0.00	0.01	0.00	0.01	0.00	0.00	0.01	0.00	0.01	0.04	0.00	0.01	0.01	0.02	0.03	0.03
Al_2O_3	20.92	20.47	20.54	20.89	20.71	20.74	20.96	20.61	20.64	20.64	20.75	20.32	21.07	20.78	21.01	20.57	20.77	20.23
Cr_2O_3	0.03	0.03	0.00	0.00	0.02	0.02	0.05	0.00	0.03	0.02	0.04	0.00	0.02	0.00	0.05	0.03	0.00	0.00
FeO	33.44	33.55	34.32	34.14	34.43	34.33	33.87	34.34	33.75	33.91	33.04	34.00	33.50	33.65	33.68	34.02	33.26	33.47
MnO	3.59	3.63	1.74	1.75	1.78	1.72	2.60	2.58	2.21	2.09	3.19	2.21	1.80	1.64	1.72	1.51	2.35	3.59
MgO	2.83	2.84	3.70	3.59	3.58	3.57	3.08	3.09	3.24	3.42	2.90	3.42	3.80	4.01	3.61	3.69	3.26	2.58
CaO	1.70	1.71	1.40	1.56	1.53	1.44	1.48	1.49	1.47	1.55	1.55	1.51	1.57	1.53	1.58	1.54	1.46	1.65
Total	99.76	99.11	99.02	99.30	99.27	99.11	99.40	99.26	98.28	97.80	98.72	98.41	99.19	98.81	98.95	98.68	97.81	98.11

Oxygens = 12

	Garnet																	
	ic08-01a1																	
	1	2	3	4	5	6	7	8	9	10	11	12	13	14	15	16	17	18
apfu																		
Si	3.01	3.01	3.02	3.01	3.01	3.02	3.02	3.02	3.02	2.98	3.03	3.02	3.01	3.01	3.01	3.03	3.01	3.01
Ti	0.00	0.00	0.00	0.00	0.00	0.00	0.00	0.00	0.00	0.00	0.00	0.00	0.00	0.00	0.00	0.00	0.00	0.00
Al	1.99	1.97	1.96	1.99	1.97	1.98	2.00	1.97	1.99	2.00	1.99	1.96	2.00	1.98	2.00	1.97	2.01	1.97
Cr	0.00	0.00	0.00	0.00	0.00	0.00	0.00	0.00	0.00	0.00	0.00	0.00	0.00	0.00	0.00	0.00	0.00	0.00
Fe^{2+}	2.26	2.29	2.32	2.30	2.33	2.32	2.29	2.33	2.31	2.34	2.25	2.32	2.26	2.28	2.28	2.31	2.28	2.31
Mn^{2+}	0.25	0.25	0.12	0.12	0.12	0.12	0.18	0.18	0.15	0.15	0.22	0.15	0.12	0.11	0.12	0.10	0.16	0.25
Mg	0.34	0.35	0.45	0.43	0.43	0.43	0.37	0.37	0.39	0.42	0.35	0.42	0.46	0.48	0.43	0.45	0.40	0.32
Ca	0.15	0.15	0.12	0.13	0.13	0.12	0.13	0.13	0.13	0.14	0.14	0.13	0.14	0.13	0.14	0.13	0.13	0.15
Fe^{3+}	0.00	0.00	0.00	0.00	0.00	0.00	0.00	0.00	0.00	0.00	0.00	0.00	0.00	0.00	0.00	0.00	0.00	0.00
X_{Mg}	0.13	0.13	0.16	0.16	0.16	0.16	0.14	0.14	0.15	0.15	0.14	0.15	0.17	0.18	0.16	0.16	0.15	0.12

Appendix G, cont'd

	Garnet																	
	ic08-01b																	
	1	2	3	4	5	6	7	8	9	10	11	12	13	14	15	16	17	18
wt %																		
SiO_2	36.76	36.74	36.84	36.86	37.10	36.94	36.58	36.87	37.21	36.65	37.18	36.96	36.95	36.97	37.04	37.01	37.07	37.04
TiO_2	0.00	0.01	0.00	0.01	0.01	0.03	0.01	0.03	0.00	0.01	0.01	0.00	0.00	0.04	0.01	0.03	0.03	0.01
Al_2O_3	21.00	20.96	21.06	20.64	21.14	20.76	20.81	21.08	21.31	20.69	21.42	20.98	20.64	20.74	21.03	20.29	20.88	20.66
Cr_2O_3	0.04	0.03	0.00	0.00	0.03	0.00	0.00	0.03	0.00	0.00	0.00	0.02	0.02	0.00	0.06	0.00	0.02	0.05
FeO	34.48	34.27	35.06	34.33	34.72	34.49	34.30	34.54	34.33	34.75	34.61	34.44	34.97	34.26	34.42	35.52	34.55	34.84
MnO	3.27	3.06	2.77	2.38	2.37	2.41	1.90	1.83	1.66	1.61	1.53	1.58	1.60	1.41	1.28	1.31	1.53	1.60
MgO	2.24	2.53	1.92	2.78	2.79	2.81	3.04	3.08	3.09	3.21	3.20	3.25	3.18	3.38	3.39	3.46	3.27	3.34
CaO	1.61	1.66	1.64	1.66	1.60	1.74	1.65	1.68	1.72	1.66	1.71	1.71	1.69	1.67	1.62	1.73	1.66	1.66
Total	99.40	99.26	99.29	98.66	99.76	99.18	98.29	99.14	99.32	98.58	99.66	98.94	99.05	98.47	98.85	99.35	99.01	99.20

Oxygens = 12

	Garnet																	
	ic08-01b																	
	1	2	3	4	5	6	7	8	9	10	11	12	13	14	15	16	17	18
apfu																		
Si	2.99	2.99	3.00	3.01	3.00	3.00	3.00	2.99	3.00	2.99	2.99	3.00	3.00	3.01	3.00	3.01	3.01	3.00
Ti	0.00	0.00	0.00	0.00	0.00	0.00	0.00	0.00	0.00	0.00	0.00	0.00	0.00	0.00	0.00	0.00	0.00	0.00
Al	2.02	2.01	2.02	1.99	2.01	1.99	2.01	2.02	2.03	1.99	2.03	2.01	1.98	1.99	2.01	1.94	2.00	1.98
Cr	0.00	0.00	0.00	0.00	0.00	0.00	0.00	0.00	0.00	0.00	0.00	0.00	0.00	0.00	0.00	0.00	0.00	0.00
Fe^{2+}	2.35	2.33	2.39	2.35	2.35	2.35	2.35	2.34	2.32	2.37	2.33	2.34	2.38	2.33	2.33	2.41	2.34	2.36
Mn^{2+}	0.23	0.21	0.19	0.16	0.16	0.17	0.13	0.13	0.11	0.11	0.10	0.11	0.11	0.10	0.09	0.09	0.11	0.11
Mg	0.27	0.31	0.23	0.34	0.34	0.34	0.37	0.37	0.37	0.39	0.38	0.39	0.39	0.41	0.41	0.42	0.40	0.40
Ca	0.14	0.14	0.14	0.15	0.14	0.15	0.14	0.15	0.15	0.15	0.15	0.15	0.15	0.15	0.14	0.15	0.14	0.14
Fe^{3+}	0.00	0.00	0.00	0.00	0.00	0.00	0.00	0.00	0.00	0.00	0.00	0.00	0.00	0.00	0.00	0.00	0.00	0.00
X_{Mg}	0.10	0.12	0.09	0.13	0.13	0.13	0.14	0.14	0.14	0.14	0.14	0.14	0.14	0.15	0.15	0.15	0.14	0.15

Appendix G, cont'd

	Garnet														
	ic08-01b														
	19	20	21	22	27	28	29	30	31	32	33	34	35	36	37
wt %															
SiO_2	37.24	36.83	37.02	36.78	36.63	36.70	36.99	36.91	37.53	37.05	36.76	36.78	37.05	36.53	36.83
TiO_2	0.01	0.00	0.01	0.02	0.00	0.03	0.00	0.03	0.03	0.02	0.00	0.00	0.00	0.01	0.00
Al_2O_3	20.78	20.85	20.43	20.30	20.37	20.50	20.78	20.82	21.66	21.14	21.18	21.21	21.51	21.04	21.24
Cr_2O_3	0.02	0.00	0.03	0.03	0.02	0.01	0.01	0.00	0.04	0.01	0.01	0.02	0.03	0.03	0.02
FeO	34.51	34.87	34.66	34.48	34.26	34.59	35.10	34.78	35.17	35.45	34.42	34.59	34.34	34.27	34.71
MnO	1.79	2.17	2.65	3.11	3.26	2.30	1.19	0.74	0.93	0.94	2.18	2.80	2.38	3.14	3.15
MgO	3.16	2.91	2.72	2.34	2.36	2.74	3.33	3.74	3.60	3.60	2.99	2.76	2.83	2.47	2.18
CaO	1.63	1.72	1.67	1.65	1.56	1.59	1.67	1.79	1.67	1.67	1.76	1.65	1.67	1.66	1.70
Total	99.14	99.35	99.19	98.71	98.46	98.46	99.07	98.81	100.63	99.88	99.30	99.81	99.81	99.15	99.83

Oxygens = 12

	Garnet														
	ic08-01b														
	19	20	21	22	27	28	29	30	31	32	33	34	35	36	37
apfu															
Si	3.02	2.99	3.02	3.02	3.01	3.01	3.00	3.00	2.99	2.98	2.98	2.98	2.99	2.98	2.99
Ti	0.00	0.00	0.00	0.00	0.00	0.00	0.00	0.00	0.00	0.00	0.00	0.00	0.00	0.00	0.00
Al	1.98	2.00	1.96	1.96	1.97	1.98	1.99	1.99	2.03	2.01	2.02	2.02	2.04	2.02	2.03
Cr	0.00	0.00	0.00	0.00	0.00	0.00	0.00	0.00	0.00	0.00	0.00	0.00	0.00	0.00	0.00
Fe^{2+}	2.34	2.37	2.36	2.37	2.36	2.37	2.38	2.36	2.34	2.39	2.33	2.34	2.31	2.34	2.35
Mn^{2+}	0.12	0.15	0.18	0.22	0.23	0.16	0.08	0.05	0.06	0.06	0.15	0.19	0.16	0.22	0.22
Mg	0.38	0.35	0.33	0.29	0.29	0.33	0.40	0.45	0.43	0.43	0.36	0.33	0.34	0.30	0.26
Ca	0.14	0.15	0.15	0.15	0.14	0.14	0.15	0.16	0.14	0.14	0.15	0.14	0.14	0.15	0.15
Fe^{3+}	0.00	0.00	0.00	0.00	0.00	0.00	0.00	0.00	0.00	0.00	0.00	0.00	0.00	0.00	0.00
X_{Mg}	0.14	0.13	0.12	0.11	0.11	0.12	0.14	0.16	0.15	0.15	0.13	0.12	0.13	0.11	0.10

Appendix G, cont'd

	Garnet																			
	ic08-01b1																			
	1	2	3	4	5	6	7	8	9	10	11	12	13	14	15	16	17	18	19	20
wt %																				
SiO_2	36.81	36.38	37.02	36.78	36.74	36.55	37.17	36.65	36.88	36.44	36.69	36.38	36.90	36.90	37.24	36.60	36.82	36.90	37.36	36.38
TiO_2	0.02	0.00	0.00	0.00	0.02	0.01	0.00	0.00	0.02	0.00	0.00	0.01	0.00	0.02	0.01	0.00	0.02	0.01	0.00	0.00
Al_2O_3	21.30	21.24	21.34	21.31	21.25	21.24	21.54	21.29	21.50	20.88	20.93	20.84	21.14	20.80	21.33	20.85	20.99	21.28	21.44	20.27
Cr_2O_3	0.00	0.04	0.00	0.05	0.06	0.00	0.03	0.04	0.01	0.09	0.06	0.01	0.04	0.02	0.01	0.02	0.04	0.02	0.03	0.00
FeO	34.59	34.45	34.55	34.27	34.21	34.47	34.43	34.48	34.66	34.51	34.50	34.13	34.81	34.52	34.70	34.64	34.61	34.44	35.73	36.00
MnO	2.45	2.37	2.44	2.28	2.17	2.04	2.17	3.71	2.83	1.98	2.44	3.57	3.00	2.05	2.14	2.50	2.13	2.66	3.10	3.15
MgO	3.08	3.20	3.06	3.24	3.26	3.31	3.42	2.55	3.06	3.49	3.11	2.53	2.91	3.29	3.40	3.06	3.41	3.06	2.03	2.00
CaO	1.57	1.64	1.57	1.63	1.67	1.59	1.51	1.59	1.53	1.58	1.53	1.57	1.57	1.61	1.56	1.60	1.67	1.63	1.62	1.57
Total	99.82	99.32	99.98	99.56	99.38	99.21	100.27	100.31	100.49	98.97	99.26	99.04	100.37	99.21	100.39	99.27	99.69	100.00	101.31	99.37

Oxygens = 12

	Garnet																			
	ic08-01b1																			
	1	2	3	4	5	6	7	8	9	10	11	12	13	14	15	16	17	18	19	20
apfu																				
Si	2.97	2.96	2.98	2.97	2.97	2.97	2.98	2.96	2.96	2.97	2.98	2.98	2.97	2.99	2.98	2.98	2.98	2.98	2.99	2.99
Ti	0.00	0.00	0.00	0.00	0.00	0.00	0.00	0.00	0.00	0.00	0.00	0.00	0.00	0.00	0.00	0.00	0.00	0.00	0.00	0.00
Al	2.03	2.03	2.03	2.03	2.03	2.03	2.03	2.03	2.04	2.00	2.00	2.01	2.01	1.99	2.01	2.00	2.00	2.02	2.02	1.96
Cr	0.00	0.00	0.00	0.00	0.00	0.00	0.00	0.00	0.00	0.01	0.00	0.00	0.00	0.00	0.00	0.00	0.00	0.00	0.00	0.00
Fe^{2+}	2.34	2.34	2.33	2.32	2.32	2.34	2.31	2.33	2.33	2.35	2.34	2.34	2.35	2.34	2.32	2.36	2.34	2.32	2.39	2.47
Mn^{2+}	0.17	0.16	0.17	0.16	0.15	0.14	0.15	0.25	0.19	0.14	0.17	0.25	0.20	0.14	0.15	0.17	0.15	0.18	0.21	0.22
Mg	0.37	0.39	0.37	0.39	0.39	0.40	0.41	0.31	0.37	0.42	0.38	0.31	0.35	0.40	0.41	0.37	0.41	0.37	0.24	0.25
Ca	0.14	0.14	0.14	0.14	0.14	0.14	0.13	0.14	0.13	0.14	0.13	0.14	0.14	0.14	0.13	0.14	0.14	0.14	0.14	0.14
Fe^{3+}	0.00	0.00	0.00	0.00	0.00	0.00	0.00	0.00	0.00	0.00	0.00	0.00	0.00	0.00	0.00	0.00	0.00	0.00	0.00	0.00
X_{Mg}	0.14	0.14	0.14	0.14	0.15	0.15	0.15	0.12	0.14	0.15	0.14	0.12	0.13	0.15	0.15	0.14	0.15	0.14	0.09	0.09

Appendix G, cont'd

	Garnet														
	ic08-01e						ic08-01e					ic08-01e			
	5.1	5.2	5.3	5.4	5.5	5.6	3.1	3.2	3.3	3.4	3.5	4.1	4.2	4.3	4.4
wt %															
SiO_2	37.34	37.07	37.34	37.20	37.24	36.95	36.75	37.24	37.15	37.24	36.99	37.14	37.24	37.16	36.99
TiO_2	0.00	0.02	0.01	0.00	0.02	0.02	0.02	0.01	0.02	0.00	0.00	0.03	0.03	0.01	0.02
Al_2O_3	21.04	21.06	21.16	20.84	20.79	20.56	20.65	20.68	20.66	20.65	20.70	20.77	21.03	20.88	21.14
Cr_2O_3	0.01	0.00	0.00	0.01	0.00	0.03	0.02	0.00	0.00	0.00	0.06	0.03	0.03	0.04	0.03
FeO	34.06	34.07	34.28	34.14	34.39	33.99	34.49	33.63	34.09	34.16	34.24	33.94	34.03	34	33.94
MnO	3.53	2.96	2.25	2.09	1.90	3.43	3.02	1.94	1.40	1.43	2.48	1.77	1.57	2.25	2.12
MgO	2.31	2.81	3.00	3.24	3.19	2.39	2.09	3.11	3.46	3.59	3.14	3.26	3.33	3.07	3.11
CaO	1.93	2.04	2.08	2.06	1.99	1.91	2.13	2.44	2.29	2.18	2.06	2.16	2.22	2.01	2.01
Total	100.22	100.03	100.12	99.58	99.52	99.28	99.17	99.05	99.07	99.25	99.67	99.10	99.48	99.42	99.36

Oxygens = 12

	Garnet														
	ic08-01e						ic08-01e					ic08-01e			
	5.1	5.2	5.3	5.4	5.5	5.6	3.1	3.2	3.3	3.4	3.5	4.1	4.2	4.3	4.4
apfu															
Si	3.01	2.99	3.00	3.00	3.01	3.01	3.00	3.02	3.01	3.01	2.99	3.01	3.00	3.01	2.99
Ti	0.00	0.00	0.00	0.00	0.00	0.00	0.00	0.00	0.00	0.00	0.00	0.00	0.00	0.00	0.00
Al	2.00	2.00	2.00	1.98	1.98	1.97	1.99	1.98	1.97	1.97	1.97	1.98	2.00	1.99	2.01
Cr	0.00	0.00	0.00	0.00	0.00	0.00	0.00	0.00	0.00	0.00	0.00	0.00	0.00	0.00	0.00
Fe^{2+}	2.30	2.30	2.30	2.31	2.32	2.32	2.36	2.28	2.31	2.31	2.32	2.30	2.29	2.30	2.30
Mn^{2+}	0.24	0.20	0.15	0.14	0.13	0.24	0.21	0.13	0.10	0.10	0.17	0.12	0.11	0.15	0.15
Mg	0.28	0.34	0.36	0.39	0.38	0.29	0.25	0.38	0.42	0.43	0.38	0.39	0.40	0.37	0.37
Ca	0.17	0.18	0.18	0.18	0.17	0.17	0.19	0.21	0.20	0.19	0.18	0.19	0.19	0.17	0.17
Fe^{3+}	0.00	0.00	0.00	0.00	0.00	0.00	0.00	0.00	0.00	0.00	0.00	0.00	0.00	0.00	0.00
X_{Mg}	0.11	0.13	0.13	0.14	0.14	0.11	0.10	0.14	0.15	0.16	0.14	0.15	0.15	0.14	0.14

APPENDIX H: ELECTRON MICROPROBE ANALYSES – MUSCOVITE

	Muscovite											
	ic08-01a											
	1_1	1_2	1_3	1_4	1_5	1_6	1_7	1_8	1_9	1_10	1_11	1_12
wt %												
SiO_2	46.78	46.02	46.41	45.95	45.71	45.81	46.43	45.70	45.38	45.57	45.65	45.47
TiO_2	0.44	0.28	1.04	0.46	0.48	0.21	0.23	0.28	0.18	0.33	0.33	0.40
Al_2O_3	36.86	37.73	36.00	37.40	39.66	40.54	38.14	39.65	39.40	40.31	40.05	40.18
Cr_2O_3	0.06	0.10	0.05	0.11	0.07	0.02	0.07	0.00	0.07	0.04	0.04	0.05
FeO	1.71	1.61	1.89	1.97	1.05	0.88	1.53	1.02	1.19	0.91	0.83	0.93
MnO	0.00	0.02	0.01	0.00	0.00	0.03	0.04	0.03	0.01	0.02	0.03	0.00
MgO	1.34	1.06	1.22	1.08	0.56	0.41	0.99	0.50	0.65	0.42	0.46	0.51
CaO	0.01	0.00	0.00	0.00	0.00	0.00	0.00	0.00	0.00	0.00	0.00	0.00
BaO	0.25	0.17	0.19	0.22	0.18	0.12	0.16	0.17	0.28	0.17	0.18	0.25
Na_2O	0.53	0.24	0.50	0.40	0.96	0.82	0.65	0.79	0.78	1.11	1.25	1.10
K_2O	8.60	9.03	8.23	8.76	8.27	8.44	8.30	8.57	8.52	7.91	8.28	7.85
F	0.00	0.00	0.00	0.00	0.00	0.00	0.00	0.00	0.00	0.00	0.00	0.00
Total	96.58	96.26	95.54	96.35	96.94	97.28	96.54	96.71	96.46	96.79	97.10	96.74

Oxygens = 22

	Muscovite											
	ic08-01a											
	1_1	1_2	1_3	1_4	1_5	1_6	1_7	1_8	1_9	1_10	1_11	1_12
apfu												
Si	6.09	6.02	6.10	6.01	5.90	5.89	6.03	5.92	5.91	5.88	5.89	5.87
Ti	0.04	0.03	0.10	0.05	0.05	0.02	0.02	0.03	0.02	0.03	0.03	0.04
Al	5.66	5.81	5.58	5.77	6.04	6.14	5.83	6.05	6.04	6.13	6.09	6.12
Cr	0.01	0.01	0.01	0.01	0.01	0.00	0.01	0.00	0.01	0.00	0.00	0.01
Fe^{2+}	0.19	0.18	0.21	0.22	0.11	0.09	0.17	0.11	0.13	0.10	0.09	0.10
Mn^{2+}	0.00	0.00	0.00	0.00	0.00	0.00	0.00	0.00	0.00	0.00	0.00	0.00
Mg	0.26	0.21	0.24	0.21	0.11	0.08	0.19	0.10	0.13	0.08	0.09	0.10
Ca	0.00	0.00	0.00	0.00	0.00	0.00	0.00	0.00	0.00	0.00	0.00	0.00
Ba	0.01	0.01	0.01	0.01	0.01	0.01	0.01	0.01	0.01	0.01	0.01	0.01
Na	0.13	0.06	0.13	0.10	0.24	0.20	0.16	0.20	0.20	0.28	0.31	0.28
K	1.43	1.51	1.38	1.46	1.36	1.38	1.37	1.42	1.41	1.30	1.36	1.29
F	0.00	0.00	0.00	0.00	0.00	0.00	0.00	0.00	0.00	0.00	0.00	0.00
X_{Mg}	0.58	0.54	0.54	0.49	0.49	0.45	0.54	0.47	0.49	0.45	0.50	0.49

Appendix H, cont'd

	Muscovite								
	ic08-01a								
	2_1	2_2	2_3	2_4	2_5	2_6	2_7	2_8	2_9
wt %									
SiO_2	45.67	46.04	46.37	46.67	46.54	45.33	45.50	45.56	45.93
TiO_2	0.38	0.30	0.05	0.08	0.26	0.26	0.50	0.39	0.37
Al_2O_3	40.50	40.96	39.21	40.46	40.09	40.03	39.56	40.73	40.37
Cr_2O_3	0.13	0.00	0.02	0.02	0.07	0.02	0.06	0.12	0.06
FeO	1.08	0.93	1.64	1.17	2.37	0.91	1.04	0.89	0.88
MnO	0.01	0.00	0.00	0.00	0.01	0.01	0.02	0.00	0.02
MgO	0.46	0.37	0.68	0.56	0.88	0.45	0.52	0.39	0.43
CaO	0.01	0.01	0.04	0.00	0.03	0.01	0.00	0.01	0.02
BaO	0.41	0.45	0.33	0.49	0.45	0.38	0.46	0.42	0.37
Na_2O	1.00	1.01	0.48	0.58	0.71	1.35	0.96	0.96	0.97
K_2O	7.57	7.91	7.08	8.53	8.06	7.60	7.68	8.29	7.98
F	0.00	0.00	0.00	0.00	0.00	0.00	0.00	0.00	0.00
Total	97.22	97.98	95.90	98.56	99.47	96.35	96.30	97.76	97.40

Oxygens = 22

	Muscovite								
	ic08-01a								
	2_1	2_2	2_3	2_4	2_5	2_6	2_7	2_8	2_9
apfu									
Si	5.87	5.87	6.01	5.93	5.89	5.88	5.91	5.84	5.89
Ti	0.04	0.03	0.00	0.01	0.02	0.03	0.05	0.04	0.04
Al	6.13	6.16	5.99	6.06	5.98	6.12	6.05	6.16	6.11
Cr	0.01	0.00	0.00	0.00	0.01	0.00	0.01	0.01	0.01
Fe^{2+}	0.12	0.10	0.18	0.12	0.25	0.10	0.11	0.10	0.09
Mn^{2+}	0.00	0.00	0.00	0.00	0.00	0.00	0.00	0.00	0.00
Mg	0.09	0.07	0.13	0.11	0.17	0.09	0.10	0.07	0.08
Ca	0.00	0.00	0.01	0.00	0.00	0.00	0.00	0.00	0.00
Ba	0.02	0.02	0.02	0.02	0.02	0.02	0.02	0.02	0.02
Na	0.25	0.25	0.12	0.14	0.17	0.34	0.24	0.24	0.24
K	1.24	1.29	1.17	1.38	1.30	1.26	1.27	1.36	1.31
F	0.00	0.00	0.00	0.00	0.00	0.00	0.00	0.00	0.00
X_{Mg}	0.43	0.42	0.42	0.46	0.40	0.47	0.47	0.44	0.47

Appendix H, cont'd

	Muscovite										
	ic08-01a1										
	1_25	1_26	1_27	1_28	1_29	1_30	1_31	1_32	1_33	1_34	1_35
wt %											
SiO_2	92.10	45.38	44.84	45.22	45.48	45.48	46.00	45.91	45.53	46.46	46.40
TiO_2	0.17	0.24	0.24	0.59	0.38	0.59	0.24	0.27	0.29	0.28	0.31
Al_2O_3	39.27	39.50	39.65	38.09	39.01	37.92	39.26	38.06	40.39	37.30	38.68
Cr_2O_3	0.09	0.05	0.07	0.10	0.05	0.08	0.08	0.05	0.06	0.00	0.02
FeO	1.20	0.90	0.90	0.96	0.97	1.03	1.16	1.00	0.89	1.54	1.06
MnO	0.01	0.00	0.00	0.01	0.01	0.00	0.01	0.02	0.01	0.03	0.03
MgO	0.62	0.42	0.43	0.47	0.41	0.53	0.60	0.59	0.41	0.82	0.63
CaO	0.00	0.00	0.01	0.00	0.01	0.00	0.00	0.00	0.00	0.00	0.00
BaO	0.25	0.21	0.22	0.22	0.24	0.30	0.19	0.24	0.22	0.26	0.18
Na_2O	0.62	0.81	0.91	0.67	0.76	0.72	0.58	0.72	0.73	0.58	0.45
K_2O	8.50	8.55	8.25	8.35	8.47	8.53	8.35	8.62	8.48	8.37	8.31
F	0.00	0.00	0.00	0.00	0.02	0.00	0.00	0.00	0.00	0.00	0.00
Total	96.78	96.06	95.52	94.68	95.81	95.18	96.47	95.48	97.01	95.64	96.07

Oxygens = 22

	Muscovite										
	ic08-01a1										
	1_25	1_26	1_27	1_28	1_29	1_30	1_31	1_32	1_33	1_34	1_35
apfu											
Si	5.96	5.92	5.88	5.98	5.95	6.00	5.96	6.03	5.87	6.09	6.03
Ti	0.02	0.02	0.02	0.06	0.04	0.06	0.02	0.03	0.03	0.03	0.03
Al	5.99	6.07	6.12	5.94	6.01	5.89	6.00	5.89	6.14	5.76	5.92
Cr	0.01	0.01	0.01	0.01	0.01	0.01	0.01	0.01	0.01	0.00	0.00
Fe^{2+}	0.13	0.10	0.10	0.11	0.11	0.11	0.13	0.11	0.10	0.17	0.12
Mn^{2+}	0.00	0.00	0.00	0.00	0.00	0.00	0.00	0.00	0.00	0.00	0.00
Mg	0.12	0.08	0.08	0.09	0.08	0.10	0.12	0.12	0.08	0.16	0.12
Ca	0.00	0.00	0.00	0.00	0.00	0.00	0.00	0.00	0.00	0.00	0.00
Ba	0.01	0.01	0.01	0.01	0.01	0.02	0.01	0.01	0.01	0.01	0.01
Na	0.16	0.20	0.23	0.17	0.19	0.18	0.15	0.18	0.18	0.15	0.11
K	1.40	1.42	1.38	1.41	1.41	1.43	1.38	1.44	1.40	1.40	1.38
F	0.00	0.00	0.00	0.00	0.01	0.00	0.00	0.00	0.00	0.00	0.00
X_{Mg}	0.48	0.45	0.46	0.47	0.43	0.48	0.48	0.51	0.45	0.49	0.51

Appendix H, cont'd

	Muscovite									
	ic08-01a1									
	2_1	2_2	2_3	2_4	2_5	2_6	2_7	2_8	2_9	2_10
wt %										
SiO_2	45.96	45.41	45.81	45.98	45.70	46.04	45.83	45.80	45.70	46.49
TiO_2	0.50	0.51	0.50	0.47	0.50	0.16	0.21	0.33	0.28	0.12
Al_2O_3	38.15	39.22	37.69	38.19	38.23	39.24	37.97	38.96	37.39	38.79
Cr_2O_3	0.08	0.02	0.05	0.03	0.13	0.07	0.13	0.09	0.05	0.09
FeO	1.03	0.97	1.03	1.08	1.18	0.85	1.16	1.22	1.17	1.13
MnO	0.03	0.00	0.01	0.00	0.00	0.00	0.00	0.03	0.02	0.01
MgO	0.66	0.56	0.62	0.66	0.67	0.50	0.60	0.71	0.73	0.64
CaO	0.00	0.00	0.00	0.00	0.00	0.00	0.00	0.00	0.00	0.00
BaO	0.20	0.19	0.29	0.31	0.27	0.16	0.17	0.15	0.18	0.08
Na_2O	0.67	0.74	0.76	0.61	0.66	0.69	0.68	0.53	0.60	0.67
K_2O	8.13	8.32	8.76	8.48	8.45	8.33	8.65	8.59	8.63	8.48
F	0.00	0.00	0.00	0.00	0.00	0.00	0.00	0.00	0.00	0.00
Total	95.41	95.94	95.52	95.81	95.79	96.04	95.40	96.41	94.75	96.50

Oxygens = 22

	Muscovite									
	ic08-01a1									
	2_1	2_2	2_3	2_4	2_5	2_6	2_7	2_8	2_9	2_10
apfu										
Si	6.02	5.92	6.02	6.01	5.98	5.98	6.02	5.95	6.05	6.02
Ti	0.05	0.05	0.05	0.05	0.05	0.02	0.02	0.03	0.03	0.01
Al	5.89	6.03	5.84	5.89	5.90	6.01	5.88	5.97	5.83	5.92
Cr	0.01	0.00	0.01	0.00	0.01	0.01	0.01	0.01	0.01	0.01
Fe^{2+}	0.11	0.11	0.11	0.12	0.13	0.09	0.13	0.13	0.13	0.12
Mn^{2+}	0.00	0.00	0.00	0.00	0.00	0.00	0.00	0.00	0.00	0.00
Mg	0.13	0.11	0.12	0.13	0.13	0.10	0.12	0.14	0.14	0.12
Ca	0.00	0.00	0.00	0.00	0.00	0.00	0.00	0.00	0.00	0.00
Ba	0.01	0.01	0.02	0.02	0.01	0.01	0.01	0.01	0.01	0.00
Na	0.17	0.19	0.19	0.15	0.17	0.17	0.17	0.13	0.15	0.17
K	1.36	1.38	1.47	1.41	1.41	1.38	1.45	1.42	1.46	1.40
F	0.00	0.00	0.00	0.00	0.00	0.00	0.00	0.00	0.00	0.00
X_{Mg}	0.53	0.51	0.52	0.52	0.50	0.51	0.48	0.51	0.53	0.50

Appendix H, cont'd

	Muscovite													
	ic08-01b													
	W-Ms 1	W-Ms 2	W-Ms 3	W-Ms 4	W-Ms 5	W-Ms 6	W-Ms 7	W-Ms 8	W-Ms 9	W-Ms 10	W-Ms 11	W-Ms 12	W-Ms 13	W-Ms 14
wt %														
SiO_2	45.85	45.80	45.70	45.43	45.53	45.62	45.85	45.93	45.44	45.82	46.11	45.71	45.85	45.51
TiO_2	0.66	0.73	0.56	0.56	0.51	0.36	0.56	0.49	0.79	0.59	0.60	0.61	0.48	0.56
Al_2O_3	37.48	37.10	37.25	37.75	37.62	37.87	37.89	37.83	37.61	37.69	37.50	38.40	38.51	37.54
Cr_2O_3	0.04	0.06	0.07	0.07	0.07	0.03	0.03	0.02	0.08	0.04	0.05	0.04	0.00	0.03
FeO	1.19	1.21	1.15	1.03	1.03	1.21	1.03	1.08	1.08	1.24	1.21	0.95	0.83	1.27
MnO	0.00	0.03	0.00	0.00	0.00	0.00	0.00	0.01	0.00	0.00	0.02	0.00	0.00	0.00
MgO	0.64	0.74	0.68	0.56	0.67	0.69	0.56	0.67	0.61	0.61	0.61	0.50	0.42	0.70
CaO	0.00	0.00	0.00	0.00	0.00	0.00	0.00	0.00	0.00	0.00	0.00	0.00	0.00	0.00
BaO	0.46	0.43	0.47	0.49	0.49	0.45	0.48	0.48	0.44	0.46	0.49	0.43	0.41	0.48
Na_2O	1.09	1.18	1.22	1.18	1.19	1.18	1.14	1.28	1.15	1.08	1.23	1.31	1.56	1.34
K_2O	9.38	9.25	9.26	9.46	9.43	9.38	9.65	9.34	9.45	9.46	9.32	9.32	9.02	8.96
F	0.00	0.00	0.00	0.00	0.00	0.00	0.00	0.00	0.00	0.00	0.00	0.00	0.00	0.00
Total	96.79	96.53	96.36	96.53	96.54	96.79	97.19	97.13	96.65	96.99	97.14	97.27	97.08	96.39

Oxygens = 22

	Muscovite													
	ic08-01b													
	W-Ms 1	W-Ms 2	W-Ms 3	W-Ms 4	W-Ms 5	W-Ms 6	W-Ms 7	W-Ms 8	W-Ms 9	W-Ms 10	W-Ms 11	W-Ms 12	W-Ms 13	W-Ms 14
apfu														
Si	6.00	6.01	6.01	5.96	5.98	5.97	5.98	5.99	5.96	5.99	6.01	5.94	5.96	5.97
Ti	0.07	0.07	0.06	0.06	0.05	0.04	0.06	0.05	0.08	0.06	0.06	0.06	0.05	0.06
Al	5.78	5.74	5.77	5.84	5.82	5.84	5.82	5.81	5.81	5.80	5.76	5.88	5.90	5.81
Cr	0.00	0.01	0.01	0.01	0.01	0.00	0.00	0.00	0.01	0.00	0.01	0.00	0.00	0.00
Fe^{2+}	0.13	0.13	0.13	0.11	0.11	0.13	0.11	0.12	0.12	0.14	0.13	0.10	0.09	0.14
Mn^{2+}	0.00	0.00	0.00	0.00	0.00	0.00	0.00	0.00	0.00	0.00	0.00	0.00	0.00	0.00
Mg	0.12	0.14	0.13	0.11	0.13	0.13	0.11	0.13	0.12	0.12	0.12	0.10	0.08	0.14
Ca	0.00	0.00	0.00	0.00	0.00	0.00	0.00	0.00	0.00	0.00	0.00	0.00	0.00	0.00
Ba	0.02	0.02	0.02	0.03	0.03	0.02	0.02	0.02	0.02	0.02	0.03	0.02	0.02	0.02
Na	0.28	0.30	0.31	0.30	0.30	0.30	0.29	0.32	0.29	0.27	0.31	0.33	0.39	0.34
K	1.57	1.55	1.55	1.58	1.58	1.57	1.61	1.55	1.58	1.58	1.55	1.55	1.50	1.50
F	0.00	0.00	0.00	0.00	0.00	0.00	0.00	0.00	0.00	0.00	0.00	0.00	0.00	0.00
X_{Mg}	0.49	0.52	0.51	0.49	0.54	0.50	0.49	0.53	0.50	0.47	0.47	0.48	0.47	0.50

Appendix H, cont'd

	Muscovite									
	ic08-01b									
	N-Ms 1	N-Ms 2	N-Ms 3	N-Ms 4	N-Ms 5	N-Ms 6	N-Ms 7	N-Ms 8	N-Ms 9	N-Ms 10
wt %										
SiO_2	45.73	45.31	45.66	45.64	46.01	45.13	45.81	45.88	45.42	45.52
TiO_2	0.50	0.54	0.73	0.78	0.86	0.78	0.66	0.80	0.70	0.80
Al_2O_3	37.58	38.26	37.56	37.56	37.05	36.95	37.98	37.76	37.65	37.75
Cr_2O_3	0.05	0.03	0.04	0.04	0.10	0.08	0.07	0.03	0.06	0.05
FeO	2.10	1.31	1.05	1.10	1.35	1.59	1.12	1.12	1.13	1.04
MnO	0.00	0.02	0.00	0.01	0.00	0.00	0.00	0.03	0.00	0.01
MgO	0.95	0.69	0.59	0.62	0.83	0.89	0.62	0.67	0.67	0.60
CaO	0.05	0.02	0.02	0.01	0.00	0.04	0.00	0.00	0.00	0.00
BaO	0.34	0.38	0.45	0.52	0.41	0.50	0.48	0.49	0.49	0.49
Na_2O	1.26	1.39	1.31	1.31	1.29	1.19	1.21	1.17	1.22	1.27
K_2O	8.54	8.78	9.35	9.22	9.16	9.37	9.44	9.38	9.45	9.30
F	0.00	0.00	0.00	0.00	0.00	0.00	0.00	0.00	0.00	0.00
Total	97.10	96.73	96.76	96.81	97.06	96.52	97.39	97.33	96.79	96.83

Oxygens = 22

	Muscovite									
	ic08-01b									
	N-Ms 1	N-Ms 2	N-Ms 3	N-Ms 4	N-Ms 5	N-Ms 6	N-Ms 7	N-Ms 8	N-Ms 9	N-Ms 10
apfu										
Si	5.96	5.92	5.98	5.97	6.01	5.95	5.96	5.97	5.95	5.96
Ti	0.05	0.05	0.07	0.08	0.08	0.08	0.06	0.08	0.07	0.08
Al	5.77	5.89	5.80	5.79	5.70	5.74	5.82	5.79	5.82	5.82
Cr	0.01	0.00	0.00	0.00	0.01	0.01	0.01	0.00	0.01	0.01
Fe^{2+}	0.23	0.14	0.12	0.12	0.15	0.18	0.12	0.12	0.12	0.11
Mn^{2+}	0.00	0.00	0.00	0.00	0.00	0.00	0.00	0.00	0.00	0.00
Mg	0.18	0.13	0.12	0.12	0.16	0.18	0.12	0.13	0.13	0.12
Ca	0.01	0.00	0.00	0.00	0.00	0.01	0.00	0.00	0.00	0.00
Ba	0.02	0.02	0.02	0.03	0.02	0.03	0.02	0.03	0.03	0.03
Na	0.32	0.35	0.33	0.33	0.33	0.30	0.31	0.30	0.31	0.32
K	1.42	1.46	1.56	1.54	1.53	1.58	1.57	1.56	1.58	1.55
F	0.00	0.00	0.00	0.00	0.00	0.00	0.00	0.00	0.00	0.00
X_{Mg}	0.45	0.48	0.50	0.50	0.52	0.50	0.50	0.52	0.51	0.51

Appendix H, cont'd

	Muscovite									
	ic08-01b1									
	1-N-Ms 1	1-N-Ms 2	1-N-Ms 3	1-N-Ms 4	1-N-Ms 5	1-N-Ms 6	1-N-Ms 7	1-N-Ms 8	1-N-Ms 9	1-N-Ms 10
wt %										
SiO_2	45.56	45.28	45.39	45.41	45.88	45.71	45.65	45.58	45.87	46.10
TiO_2	0.55	0.43	0.47	0.54	0.69	0.57	0.60	0.57	0.45	0.48
Al_2O_3	38.86	38.50	38.76	38.16	37.88	38.34	38.38	38.40	38.48	37.95
Cr_2O_3	0.03	0.01	0.00	0.03	0.04	0.00	0.04	0.05	0.02	0.00
FeO	0.80	0.86	0.96	0.95	1.01	1.13	1.06	0.96	0.86	0.80
MnO	0.00	0.02	0.02	0.02	0.00	0.00	0.01	0.00	0.00	0.01
MgO	0.40	0.41	0.47	0.50	0.61	0.52	0.52	0.48	0.45	0.50
CaO	0.00	0.01	0.00	0.00	0.00	0.01	0.00	0.01	0.00	0.05
BaO	0.44	0.39	0.44	0.48	0.53	0.43	0.48	0.47	0.45	0.41
Na_2O	1.53	1.48	1.38	1.18	1.29	1.45	1.26	1.30	1.37	1.25
K_2O	9.07	9.27	9.47	9.61	9.54	9.56	9.57	9.49	9.54	9.54
F	0.00	0.00	0.00	0.00	0.00	0.00	0.00	0.00	0.00	0.00
Total	97.24	96.66	97.36	96.88	97.47	97.72	97.57	97.31	97.49	97.09

Oxygens = 22

	Muscovite									
	ic08-01b1									
	1-N-Ms 1	1-N-Ms 2	1-N-Ms 3	1-N-Ms 4	1-N-Ms 5	1-N-Ms 6	1-N-Ms 7	1-N-Ms 8	1-N-Ms 9	1-N-Ms 10
apfu										
Si	5.92	5.92	5.91	5.94	5.97	5.93	5.93	5.93	5.96	6.00
Ti	0.05	0.04	0.05	0.05	0.07	0.06	0.06	0.06	0.04	0.05
Al	5.95	5.94	5.94	5.88	5.81	5.87	5.88	5.89	5.89	5.82
Cr	0.00	0.00	0.00	0.00	0.00	0.00	0.00	0.01	0.00	0.00
Fe^{2+}	0.09	0.09	0.10	0.10	0.11	0.12	0.12	0.10	0.09	0.09
Mn^{2+}	0.00	0.00	0.00	0.00	0.00	0.00	0.00	0.00	0.00	0.00
Mg	0.08	0.08	0.09	0.10	0.12	0.10	0.10	0.09	0.09	0.10
Ca	0.00	0.00	0.00	0.00	0.00	0.00	0.00	0.00	0.00	0.01
Ba	0.02	0.02	0.02	0.02	0.03	0.02	0.02	0.02	0.02	0.02
Na	0.39	0.38	0.35	0.30	0.33	0.37	0.32	0.33	0.34	0.32
K	1.50	1.55	1.57	1.60	1.58	1.58	1.59	1.58	1.58	1.58
F	0.00	0.00	0.00	0.00	0.00	0.00	0.00	0.00	0.00	0.00
X_{Mg}	0.47	0.46	0.47	0.48	0.52	0.45	0.47	0.47	0.48	0.53

Appendix H, cont'd

	Muscovite				
	ic08-01b1				
	W-Ms 1	W-Ms 2	W- Ms 3	W - Ms 4	W-Ms 5
wt %					
SiO_2	45.96	46.05	45.86	45.86	45.87
TiO_2	0.76	0.58	0.58	0.68	0.77
Al_2O_3	37.70	37.34	37.65	37.61	37.66
Cr_2O_3	0.04	0.04	0.02	0.07	0.00
FeO	1.06	1.08	1.14	1.10	1.15
MnO	0.03	0.00	0.00	0.07	0.01
MgO	0.60	0.66	0.67	0.62	0.59
CaO	0.00	0.00	0.00	0.00	0.00
BaO	0.53	0.50	0.41	0.48	0.45
Na_2O	1.28	1.29	1.20	1.25	1.15
K_2O	9.31	9.47	9.64	9.60	9.62
F	0.00	0.00	0.00	0.00	0.00
Total	97.27	97.01	97.17	97.34	97.27

Oxygens = 22

	Muscovite				
	ic08-01b1				
	W-Ms 1	W-Ms 2	W- Ms 3	W - Ms 4	W-Ms 5
apfu					
Si	5.98	6.02	5.98	5.98	5.98
Ti	0.07	0.06	0.06	0.07	0.08
Al	5.79	5.75	5.79	5.78	5.79
Cr	0.00	0.00	0.00	0.01	0.00
Fe^{2+}	0.12	0.12	0.12	0.12	0.13
Mn^{2+}	0.00	0.00	0.00	0.01	0.00
Mg	0.12	0.13	0.13	0.12	0.11
Ca	0.00	0.00	0.00	0.00	0.00
Ba	0.03	0.03	0.02	0.02	0.02
Na	0.32	0.33	0.30	0.32	0.29
K	1.55	1.58	1.60	1.60	1.60
F	0.00	0.00	0.00	0.00	0.00
X_{Mg}	0.50	0.52	0.51	0.50	0.48

Appendix H, cont'd

	Muscovite												
	ic08-01e										ic08-01e		
	1_4	1_5	1_6	1_7	1_8	1_9	1_10	1_11	1_12	1_13	2_6	2_7	2_8
wt %													
SiO_2	46.02	44.87	45.10	44.60	44.61	44.87	44.85	44.10	45.22	42.91	45.86	46.35	45.64
TiO_2	1.13	1.17	1.11	1.36	1.41	1.42	1.32	1.24	1.33	1.48	1.11	0.74	0.43
Al_2O_3	36.43	36.06	36.52	36.01	36.20	35.89	36.48	36.36	36.66	38.37	38.06	39.21	39.17
Cr_2O_3	0.08	0.02	0.00	0.02	0.08	0.07	0.08	0.04	0.09	0.07	0.09	0.00	0.01
FeO	1.19	1.28	1.34	1.17	1.25	1.32	1.23	1.13	1.18	1.30	0.93	1.06	0.94
MnO	0.00	0.00	0.00	0.00	0.02	0.01	0.01	0.01	0.03	0.00	0.00	0.01	0.00
MgO	0.59	0.61	0.73	0.60	0.63	0.69	0.64	0.58	0.63	0.69	0.59	0.62	0.53
CaO	0.00	0.00	0.00	0.01	0.00	0.00	0.00	0.00	0.00	0.00	0.01	0.00	0.00
BaO	0.35	0.39	0.39	0.50	0.47	0.49	0.55	0.48	0.51	0.62	0.48	0.38	0.33
Na_2O	0.95	0.80	0.92	0.79	1.05	0.64	0.97	0.71	0.89	0.81	0.59	0.73	0.66
K_2O	8.65	9.85	9.02	9.59	9.02	9.72	8.93	9.92	8.24	9.77	8.27	8.28	8.10
F	0.00	0.00	0.00	0.00	0.00	0.00	0.00	0.00	0.00	0.00	0.00	0.00	0.00
Total	95.39	95.05	95.13	94.65	94.74	95.12	95.06	94.57	94.78	96.02	95.99	97.38	95.81

Oxygens = 22

	Muscovite												
	ic08-01e										ic08-01e		
	1_4	1_5	1_6	1_7	1_8	1_9	1_10	1_11	1_12	1_13	2_6	2_7	2_8
apfu													
Si	6.07	6.00	6.00	5.99	5.97	6.00	5.98	5.94	6.01	5.71	5.99	5.96	5.95
Ti	0.11	0.12	0.11	0.14	0.14	0.14	0.13	0.13	0.13	0.15	0.11	0.07	0.04
Al	5.67	5.69	5.72	5.70	5.71	5.66	5.73	5.77	5.74	6.02	5.86	5.94	6.02
Cr	0.01	0.00	0.00	0.00	0.01	0.01	0.01	0.00	0.01	0.01	0.01	0.00	0.00
Fe^{2+}	0.13	0.14	0.15	0.13	0.14	0.15	0.14	0.13	0.13	0.14	0.10	0.11	0.10
Mn^{2+}	0.00	0.00	0.00	0.00	0.00	0.00	0.00	0.00	0.00	0.00	0.00	0.00	0.00
Mg	0.12	0.12	0.14	0.12	0.13	0.14	0.13	0.12	0.12	0.14	0.11	0.12	0.10
Ca	0.00	0.00	0.00	0.00	0.00	0.00	0.00	0.00	0.00	0.00	0.00	0.00	0.00
Ba	0.02	0.02	0.02	0.03	0.02	0.03	0.03	0.03	0.03	0.03	0.02	0.02	0.02
Na	0.24	0.21	0.24	0.21	0.27	0.17	0.25	0.19	0.23	0.21	0.15	0.18	0.17
K	1.46	1.68	1.53	1.64	1.54	1.66	1.52	1.70	1.40	1.66	1.38	1.36	1.35
F	0.00	0.00	0.00	0.00	0.00	0.00	0.00	0.00	0.00	0.00	0.00	0.00	0.00
X_{Mg}	0.47	0.46	0.49	0.48	0.47	0.48	0.48	0.48	0.49	0.49	0.53	0.51	0.50

Appendix H, cont'd

	Muscovite									
	ic08-01e									
	3_9	3_10	3_11	3_12	3_13	3_14	3_15	3_16	3_17	3_18
wt %										
SiO_2	45.85	46.12	46.13	45.69	45.85	46.09	46.35	45.82	46.07	45.59
TiO_2	1.10	0.45	1.04	1.07	0.33	0.35	1.12	0.40	0.41	1.02
Al_2O_3	38.48	39.39	38.58	37.97	39.78	38.98	38.58	38.92	39.84	38.47
Cr_2O_3	0.04	0.02	0.04	0.02	0.04	0.02	0.00	0.08	0.03	0.07
FeO	1.12	1.16	1.14	1.21	0.97	0.90	1.17	0.95	0.96	1.12
MnO	0.01	0.01	0.01	0.00	0.00	0.00	0.00	0.02	0.02	0.00
MgO	0.59	0.58	0.60	0.62	0.54	0.50	0.60	0.55	0.49	0.61
CaO	0.00	0.00	0.00	0.00	0.00	0.00	0.00	0.00	0.00	0.00
BaO	0.33	0.32	0.25	0.35	0.30	0.26	0.33	0.30	0.31	0.32
Na_2O	0.74	0.89	0.74	0.87	0.94	0.69	0.71	0.79	0.65	0.64
K_2O	8.53	8.55	8.41	8.78	8.37	8.51	8.42	8.84	8.45	8.82
F	0.00	0.00	0.00	0.00	0.00	0.00	0.00	0.00	0.00	0.00
Total	96.79	97.49	96.94	96.58	97.12	96.30	97.28	96.67	97.23	96.66

Oxygens = 22

	Muscovite									
	ic08-01e									
	3_9	3_10	3_11	3_12	3_13	3_14	3_15	3_16	3_17	3_18
apfu										
Si	5.95	5.94	5.97	5.96	5.91	5.99	5.98	5.95	5.93	5.93
Ti	0.11	0.04	0.10	0.11	0.03	0.03	0.11	0.04	0.04	0.10
Al	5.88	5.98	5.88	5.84	6.05	5.97	5.86	5.96	6.04	5.90
Cr	0.00	0.00	0.00	0.00	0.00	0.00	0.00	0.01	0.00	0.01
Fe^{2+}	0.12	0.13	0.12	0.13	0.10	0.10	0.13	0.10	0.10	0.12
Mn^{2+}	0.00	0.00	0.00	0.00	0.00	0.00	0.00	0.00	0.00	0.00
Mg	0.11	0.11	0.12	0.12	0.10	0.10	0.12	0.11	0.09	0.12
Ca	0.00	0.00	0.00	0.00	0.00	0.00	0.00	0.00	0.00	0.00
Ba	0.02	0.02	0.01	0.02	0.02	0.01	0.02	0.02	0.02	0.02
Na	0.19	0.22	0.19	0.22	0.24	0.17	0.18	0.20	0.16	0.16
K	1.41	1.40	1.39	1.46	1.38	1.41	1.38	1.47	1.39	1.46
F	0.00	0.00	0.00	0.00	0.00	0.00	0.00	0.00	0.00	0.00
X_{Mg}	0.48	0.47	0.48	0.48	0.50	0.50	0.48	0.51	0.48	0.49

APPENDIX I: ELECTRON MICROPROBE ANALYSES – CORDIERITE

	Cordierite													
	ic08-01a													
	4	5	6	7	8	9	10	11	12	13	14	15	16	17
wt %														
SiO_2	45.71	45.72	45.15	45.98	45.91	46.23	45.67	45.87	45.43	45.60	44.92	45.90	45.18	45.73
TiO_2	0.00	0.04	0.02	0.03	0.00	0.01	0.04	0.01	0.03	0.02	0.15	0.03	0.05	0.14
Al_2O_3	32.34	32.21	32.30	32.75	32.67	33.08	32.37	32.64	32.06	32.52	31.91	32.56	32.26	32.85
Cr_2O_3	0.00	0.00	0.03	0.00	0.00	0.02	0.03	0.00	0.00	0.00	0.01	0.04	0.00	0.00
FeO	12.09	11.86	11.63	11.43	11.92	11.77	12.00	11.92	11.72	11.75	11.73	12.18	12.30	11.99
MnO	0.52	0.47	0.45	0.52	0.50	0.50	0.45	0.47	0.58	0.54	0.56	0.54	0.44	0.57
MgO	5.85	5.99	5.94	6.21	6.11	6.08	5.76	5.98	5.86	5.91	5.64	5.88	5.75	5.96
CaO	0.06	0.02	0.06	0.01	0.05	0.04	0.02	0.03	0.02	0.03	0.05	0.03	0.03	0.02
BaO	0.00	0.00	0.00	0.00	0.00	0.05	0.04	0.00	0.04	0.05	0.00	0.00	0.00	0.01
Na_2O	0.35	0.26	0.37	0.27	0.31	0.24	0.38	0.27	0.31	0.29	0.29	0.21	0.27	0.28
K_2O	0.00	0.02	0.01	0.01	0.01	0.01	0.00	0.00	0.01	0.00	0.02	0.01	0.01	0.03
F	0.00	0.00	0.00	0.00	0.00	0.00	0.00	0.00	0.00	0.00	0.00	0.00	0.00	0.00
Total	96.92	96.59	95.96	97.21	97.48	98.03	96.76	97.19	96.06	96.71	95.28	97.38	96.29	97.58

Oxygens = 18

	Cordierite													
	ic08-01a													
	4	5	6	7	8	9	10	11	12	13	14	15	16	17
apfu														
Si	4.89	4.90	4.87	4.88	4.88	4.88	4.89	4.88	4.90	4.88	4.88	4.89	4.87	4.86
Ti	0.00	0.00	0.00	0.00	0.00	0.00	0.00	0.00	0.00	0.00	0.01	0.00	0.00	0.01
Al	4.08	4.07	4.11	4.10	4.09	4.11	4.09	4.10	4.07	4.10	4.09	4.08	4.10	4.11
Cr	0.00	0.00	0.00	0.00	0.00	0.00	0.00	0.00	0.00	0.00	0.00	0.00	0.00	0.00
Fe^{2+}	1.08	1.06	1.05	1.02	1.06	1.04	1.07	1.06	1.06	1.05	1.07	1.08	1.11	1.07
Mn^{2+}	0.05	0.04	0.04	0.05	0.05	0.04	0.04	0.04	0.05	0.05	0.05	0.05	0.04	0.05
Mg	0.93	0.96	0.96	0.98	0.97	0.96	0.92	0.95	0.94	0.94	0.91	0.93	0.92	0.94
Ca	0.01	0.00	0.01	0.00	0.01	0.00	0.00	0.00	0.00	0.00	0.01	0.00	0.00	0.00
Ba	0.00	0.00	0.00	0.00	0.00	0.00	0.00	0.00	0.00	0.00	0.00	0.00	0.00	0.00
Na	0.07	0.05	0.08	0.06	0.06	0.05	0.08	0.06	0.06	0.06	0.06	0.04	0.06	0.06
K	0.00	0.00	0.00	0.00	0.00	0.00	0.00	0.00	0.00	0.00	0.00	0.00	0.00	0.00
F	0.00	0.00	0.00	0.00	0.00	0.00	0.00	0.00	0.00	0.00	0.00	0.00	0.00	0.00
X_{Mg}	0.46	0.47	0.48	0.49	0.48	0.48	0.46	0.47	0.47	0.47	0.46	0.46	0.45	0.47

Appendix I, cont'd

	Cordierite										
	ic08-01a1										
	4	5	6	7	8	9	10	11	12	13	14
wt %											
SiO_2	46.30	45.95	46.07	46.16	46.03	45.84	45.91	46.40	46.06	46.05	46.19
TiO_2	0.03	0.00	0.03	0.00	0.01	0.02	0.02	0.01	0.01	0.00	0.00
Al_2O_3	32.63	32.59	32.67	32.52	32.59	32.79	32.92	32.67	32.68	32.39	32.93
Cr_2O_3	0.00	0.02	0.00	0.02	0.08	0.06	0.00	0.00	0.00	0.00	0.03
FeO	12.55	12.76	12.73	12.25	12.47	12.47	13.19	12.90	12.99	12.96	12.57
MnO	0.46	0.59	0.55	0.53	0.58	0.55	0.58	0.52	0.57	0.49	0.56
MgO	5.46	5.47	5.43	5.34	5.50	5.31	5.50	5.58	5.38	5.49	5.63
CaO	0.04	0.01	0.02	0.01	0.04	0.10	0.07	0.02	0.05	0.02	0.02
BaO	0.00	0.00	0.00	0.02	0.02	0.01	0.02	0.00	0.00	0.00	0.00
Na_2O	0.25	0.39	0.34	0.46	0.36	0.44	0.27	0.42	0.29	0.33	0.25
K_2O	0.41	0.01	0.00	0.02	0.06	0.20	0.01	0.02	0.01	0.03	0.01
F	0.00	0.00	0.00	0.00	0.00	0.00	0.00	0.00	0.00	0.00	0.00
Total	98.13	97.79	97.84	97.33	97.74	97.79	98.49	98.54	98.04	97.76	98.19

Oxygens = 18

	Cordierite										
	ic08-01a1										
	4	5	6	7	8	9	10	11	12	13	14
apfu											
Si	4.91	4.89	4.89	4.92	4.89	4.88	4.86	4.90	4.89	4.90	4.88
Ti	0.00	0.00	0.00	0.00	0.00	0.00	0.00	0.00	0.00	0.00	0.00
Al	4.07	4.08	4.09	4.08	4.08	4.11	4.11	4.06	4.09	4.06	4.10
Cr	0.00	0.00	0.00	0.00	0.01	0.01	0.00	0.00	0.00	0.00	0.00
Fe^{2+}	1.11	1.13	1.13	1.09	1.11	1.11	1.17	1.14	1.15	1.15	1.11
Mn^{2+}	0.04	0.05	0.05	0.05	0.05	0.05	0.05	0.05	0.05	0.04	0.05
Mg	0.86	0.87	0.86	0.85	0.87	0.84	0.87	0.88	0.85	0.87	0.89
Ca	0.00	0.00	0.00	0.00	0.00	0.01	0.01	0.00	0.01	0.00	0.00
Ba	0.00	0.00	0.00	0.00	0.00	0.00	0.00	0.00	0.00	0.00	0.00
Na	0.05	0.08	0.07	0.10	0.07	0.09	0.06	0.09	0.06	0.07	0.05
K	0.06	0.00	0.00	0.00	0.01	0.03	0.00	0.00	0.00	0.00	0.00
F	0.00	0.00	0.00	0.00	0.00	0.00	0.00	0.00	0.00	0.00	0.00
X_{Mg}	0.44	0.43	0.43	0.44	0.44	0.43	0.43	0.44	0.42	0.43	0.44

Appendix I, cont'd

	Cordierite																			
	ic08-01b																			
	1	2	3	4	5	6	7	8	9	10	11	12	13	14	15	16	17	18	19	20
wt %																				
SiO_2	45.72	45.19	45.68	46.09	45.49	45.63	45.93	45.99	45.74	45.18	45.55	45.44	45.34	45.36	45.89	45.45	45.60	45.90	45.77	45.58
TiO_2	0.05	0.00	0.06	0.01	0.04	0.02	0.03	0.03	0.03	0.06	0.02	0.06	0.00	0.06	0.00	0.03	0.05	0.01	0.01	0.02
Al_2O_3	32.34	32.29	32.73	32.50	33.30	32.40	33.20	32.68	32.81	32.75	33.11	33.95	33.16	32.59	32.80	33.05	33.60	32.98	33.07	33.05
Cr_2O_3	0.00	0.00	0.00	0.00	0.03	0.02	0.02	0.00	0.01	0.02	0.00	0.02	0.02	0.01	0.01	0.03	0.00	0.03	0.00	0.01
FeO	11.96	12.39	12.21	12.18	10.91	12.32	11.88	12.39	12.26	11.15	11.95	12.13	12.45	12.04	12.59	11.70	10.62	12.32	12.26	11.84
MnO	0.21	0.26	0.19	0.23	0.17	0.20	0.20	0.23	0.21	0.20	0.20	0.17	0.22	0.20	0.20	0.22	0.18	0.23	0.21	0.22
MgO	5.72	5.50	5.56	5.62	4.71	5.79	5.48	5.63	5.55	5.14	5.27	5.26	5.38	5.21	5.47	5.15	4.79	5.55	5.62	5.34
CaO	0.06	0.07	0.08	0.07	0.10	0.05	0.07	0.06	0.07	0.07	0.07	0.07	0.08	0.04	0.05	0.07	0.06	0.06	0.07	0.09
BaO	0.00	0.00	0.02	0.00	0.10	0.01	0.00	0.00	0.01	0.00	0.03	0.00	0.01	0.03	0.00	0.00	0.06	0.00	0.00	0.00
Na_2O	0.52	0.47	0.44	0.39	0.54	0.31	0.38	0.35	0.38	0.42	0.43	0.35	0.42	0.43	0.38	0.47	0.51	0.33	0.34	0.44
K_2O	0.16	0.06	0.26	0.02	1.49	0.02	0.34	0.01	0.16	0.92	0.62	0.22	0.06	0.56	0.17	0.64	1.51	0.03	0.02	0.38
F	0.00	0.00	0.00	0.00	0.00	0.00	0.00	0.00	0.00	0.00	0.00	0.00	0.00	0.00	0.00	0.00	0.00	0.00	0.00	0.00
Total	96.74	96.23	97.23	97.11	96.88	96.77	97.53	97.37	97.23	95.91	97.25	97.67	97.14	96.53	97.56	96.81	96.98	97.44	97.37	96.97

Oxygens = 18

	Cordierite																			
	ic08-01b																			
	1	2	3	4	5	6	7	8	9	10	11	12	13	14	15	16	17	18	19	20
apfu																				
Si	4.90	4.88	4.88	4.91	4.88	4.89	4.88	4.89	4.88	4.88	4.86	4.82	4.84	4.88	4.88	4.87	4.87	4.88	4.87	4.87
Ti	0.00	0.00	0.00	0.00	0.00	0.00	0.00	0.00	0.00	0.00	0.00	0.00	0.00	0.00	0.00	0.00	0.00	0.00	0.00	0.00
Al	4.08	4.11	4.12	4.08	4.21	4.09	4.15	4.10	4.12	4.17	4.17	4.24	4.18	4.13	4.11	4.17	4.23	4.13	4.15	4.16
Cr	0.00	0.00	0.00	0.00	0.00	0.00	0.00	0.00	0.00	0.00	0.00	0.00	0.00	0.00	0.00	0.00	0.00	0.00	0.00	0.00
Fe^{2+}	1.07	1.12	1.09	1.09	0.98	1.10	1.05	1.10	1.09	1.01	1.07	1.08	1.11	1.08	1.12	1.05	0.95	1.10	1.09	1.06
Mn^{2+}	0.02	0.02	0.02	0.02	0.02	0.02	0.02	0.02	0.02	0.02	0.02	0.02	0.02	0.02	0.02	0.02	0.02	0.02	0.02	0.02
Mg	0.91	0.88	0.88	0.89	0.75	0.92	0.87	0.89	0.88	0.83	0.84	0.83	0.86	0.84	0.87	0.82	0.76	0.88	0.89	0.85
Ca	0.01	0.01	0.01	0.01	0.01	0.01	0.01	0.01	0.01	0.01	0.01	0.01	0.01	0.00	0.01	0.01	0.01	0.01	0.01	0.01
Ba	0.00	0.00	0.00	0.00	0.00	0.00	0.00	0.00	0.00	0.00	0.00	0.00	0.00	0.00	0.00	0.00	0.00	0.00	0.00	0.00
Na	0.11	0.10	0.09	0.08	0.11	0.06	0.08	0.07	0.08	0.09	0.09	0.07	0.09	0.09	0.08	0.10	0.11	0.07	0.07	0.09
K	0.02	0.01	0.04	0.00	0.20	0.00	0.05	0.00	0.02	0.13	0.08	0.03	0.01	0.08	0.02	0.09	0.21	0.00	0.00	0.05
F	0.00	0.00	0.00	0.00	0.00	0.00	0.00	0.00	0.00	0.00	0.00	0.00	0.00	0.00	0.00	0.00	0.00	0.00	0.00	0.00
X_{Mg}	0.46	0.44	0.45	0.45	0.43	0.46	0.45	0.45	0.45	0.45	0.44	0.44	0.44	0.44	0.44	0.44	0.45	0.45	0.45	0.45

Appendix I, cont'd

	Cordierite																				
	ic08-01b1																				
	1	2	3	4	5	6	7	8	9	10	11	12	13	14	15	16	17	18	19	20	21	22
wt %																						
SiO_2	45.78	46.29	45.54	45.71	46.27	46.07	45.90	46.15	45.26	45.73	45.43	45.98	45.80	45.61	46.37	46.12	45.87	46.10	45.00	45.87	45.17	45.57
TiO_2	0.01	0.04	0.01	0.03	0.06	0.00	0.06	0.02	0.08	0.02	0.03	0.00	0.00	0.03	0.00	0.02	0.00	0.02	0.01	0.05	0.00	0.02
Al_2O_3	32.96	32.92	34.00	32.70	32.81	33.02	32.74	32.85	32.33	32.76	32.57	32.95	34.20	33.82	33.19	32.71	33.14	32.95	32.47	33.38	34.02	33.42
Cr_2O_3	0.01	0.01	0.00	0.02	0.07	0.02	0.05	0.03	0.01	0.00	0.02	0.00	0.00	0.04	0.02	0.00	0.01	0.00	0.04	0.02	0.00	0.03
FeO	11.77	12.04	11.71	11.85	12.02	11.78	12.05	11.88	11.98	11.66	12.10	12.41	11.30	11.63	11.94	11.99	12.01	12.34	12.24	12.72	11.41	10.77
MnO	0.22	0.22	0.21	0.24	0.25	0.24	0.20	0.23	0.21	0.21	0.19	0.23	0.25	0.19	0.21	0.22	0.21	0.24	0.18	0.20	0.19	0.18
MgO	5.69	6.05	5.62	6.04	6.22	5.94	6.03	6.21	5.78	5.73	5.77	5.83	5.28	5.63	5.93	6.13	5.61	5.77	5.50	5.68	5.34	4.99
CaO	0.07	0.07	0.07	0.09	0.07	0.09	0.05	0.07	0.12	0.07	0.10	0.12	0.09	0.06	0.09	0.08	0.11	0.07	0.12	0.10	0.12	0.09
BaO	0.04	0.00	0.03	0.04	0.00	0.01	0.06	0.00	0.00	0.02	0.02	0.02	0.04	0.03	0.00	0.05	0.03	0.04	0.04	0.01	0.04	0.05
Na_2O	0.50	0.27	0.39	0.39	0.41	0.38	0.43	0.35	0.53	0.38	0.48	0.45	0.45	0.38	0.39	0.32	0.51	0.37	0.47	0.35	0.50	0.48
K_2O	0.22	0.03	0.24	0.02	0.12	0.15	0.08	0.01	0.95	0.36	0.07	0.15	0.34	0.16	0.19	0.14	0.29	0.02	0.42	0.08	0.72	1.16
F	0.00	0.00	0.00	0.00	0.00	0.00	0.00	0.00	0.00	0.00	0.00	0.00	0.00	0.00	0.00	0.00	0.00	0.00	0.00	0.00	0.00	0.00
Total	97.27	97.94	97.82	97.13	98.30	97.70	97.65	97.80	97.25	96.94	96.78	98.14	97.75	97.58	98.33	97.78	97.79	97.92	96.49	98.46	97.51	96.76

Oxygens = 18

	Cordierite																				
	ic08-01b1																				
	1	2	3	4	5	6	7	8	9	10	11	12	13	14	15	16	17	18	19	20	21	22
apfu																						
Si	4.87	4.89	4.82	4.87	4.88	4.88	4.87	4.88	4.85	4.88	4.87	4.86	4.84	4.83	4.88	4.88	4.86	4.88	4.85	4.84	4.80	4.88
Ti	0.00	0.00	0.00	0.00	0.00	0.00	0.00	0.00	0.01	0.00	0.00	0.00	0.00	0.00	0.00	0.00	0.00	0.00	0.00	0.00	0.00	0.00
Al	4.14	4.10	4.24	4.11	4.08	4.12	4.10	4.09	4.09	4.12	4.11	4.11	4.26	4.22	4.12	4.08	4.14	4.11	4.13	4.15	4.26	4.21
Cr	0.00	0.00	0.00	0.00	0.01	0.00	0.00	0.00	0.00	0.00	0.00	0.00	0.00	0.00	0.00	0.00	0.00	0.00	0.00	0.00	0.00	0.00
Fe^{2+}	1.05	1.06	1.04	1.06	1.06	1.04	1.07	1.05	1.07	1.04	1.08	1.10	1.00	1.03	1.05	1.06	1.07	1.09	1.10	1.12	1.01	0.96
Mn^{2+}	0.02	0.02	0.02	0.02	0.02	0.02	0.02	0.02	0.02	0.02	0.02	0.02	0.02	0.02	0.02	0.02	0.02	0.02	0.02	0.02	0.02	0.02
Mg	0.90	0.95	0.89	0.96	0.98	0.94	0.95	0.98	0.92	0.91	0.92	0.92	0.83	0.89	0.93	0.97	0.89	0.91	0.88	0.89	0.85	0.80
Ca	0.01	0.01	0.01	0.01	0.01	0.01	0.01	0.01	0.01	0.01	0.01	0.01	0.01	0.01	0.01	0.01	0.01	0.01	0.01	0.01	0.01	0.01
Ba	0.00	0.00	0.00	0.00	0.00	0.00	0.00	0.00	0.00	0.00	0.00	0.00	0.00	0.00	0.00	0.00	0.00	0.00	0.00	0.00	0.00	0.00
Na	0.10	0.06	0.08	0.08	0.08	0.08	0.09	0.07	0.11	0.08	0.10	0.09	0.09	0.08	0.08	0.07	0.10	0.08	0.10	0.07	0.10	0.10
K	0.03	0.00	0.03	0.00	0.02	0.02	0.01	0.00	0.13	0.05	0.01	0.02	0.05	0.02	0.03	0.02	0.04	0.00	0.06	0.01	0.10	0.16
F	0.00	0.00	0.00	0.00	0.00	0.00	0.00	0.00	0.00	0.00	0.00	0.00	0.00	0.00	0.00	0.00	0.00	0.00	0.00	0.00	0.00	0.00
X_{Mg}	0.46	0.47	0.46	0.48	0.48	0.47	0.47	0.48	0.46	0.47	0.46	0.46	0.45	0.46	0.47	0.48	0.45	0.45	0.44	0.44	0.45	0.45

Appendix I, cont'd

	Cordierite														
	ic08-01e														
	4	5	6	7	8	9	10	11	12	13	14	15	16	17	18
wt %															
SiO_2	45.91	46.51	46.36	46.41	46.02	46.17	45.80	46.95	46.99	46.24	46.97	46.50	46.74	46.65	46.93
TiO_2	0.03	0.03	0.02	0.02	0.03	0.02	0.02	0.01	0.03	0.01	0.00	0.01	0.02	0.00	0.01
Al_2O_3	32.96	33.25	32.74	33.34	33.04	33.22	32.84	32.99	32.77	33.05	32.75	32.98	33.04	33.15	33.29
Cr_2O_3	0.00	0.14	0.00	0.02	0.03	0.04	0.00	0.02	0.00	0.01	0.01	0.01	0.01	0.02	0.03
FeO	11.57	11.85	11.64	11.75	11.69	11.75	11.70	11.66	11.71	11.75	11.69	11.79	11.74	12.07	11.65
MnO	0.32	0.33	0.31	0.38	0.33	0.35	0.33	0.36	0.38	0.32	0.33	0.34	0.35	0.33	0.37
MgO	6.44	6.52	6.30	6.52	6.30	6.41	6.23	6.42	6.36	6.34	6.39	6.28	6.29	6.35	6.38
CaO	0.08	0.09	0.03	0.10	0.07	0.09	0.06	0.01	0.02	0.05	0.05	0.05	0.02	0.06	0.04
BaO	0.03	0.03	0.00	0.04	0.05	0.00	0.02	0.00	0.00	0.00	0.01	0.04	0.05	0.01	0.00
Na_2O	0.40	0.26	0.40	0.35	0.35	0.27	0.37	0.26	0.30	0.22	0.28	0.35	0.35	0.24	0.29
K_2O	0.02	0.00	0.01	0.02	0.10	0.03	0.00	0.01	0.02	0.02	0.01	0.02	0.00	0.00	0.02
F	0.00	0.00	0.00	0.00	0.00	0.00	0.00	0.00	0.00	0.00	0.00	0.00	0.00	0.00	0.00
Total	97.76	99.01	97.81	98.95	98.01	98.35	97.37	98.69	98.58	98.01	98.49	98.37	98.61	98.88	99.01

Oxygens = 18

	Cordierite														
	ic08-01e														
	4	5	6	7	8	9	10	11	12	13	14	15	16	17	18
apfu															
Si	4.86	4.86	4.90	4.85	4.86	4.85	4.86	4.91	4.92	4.87	4.92	4.89	4.90	4.88	4.89
Ti	0.00	0.00	0.00	0.00	0.00	0.00	0.00	0.00	0.00	0.00	0.00	0.00	0.00	0.00	0.00
Al	4.11	4.09	4.08	4.11	4.11	4.12	4.11	4.07	4.04	4.11	4.04	4.09	4.08	4.09	4.09
Cr	0.00	0.01	0.00	0.00	0.00	0.00	0.00	0.00	0.00	0.00	0.00	0.00	0.00	0.00	0.00
Fe^{2+}	1.02	1.04	1.03	1.03	1.03	1.03	1.04	1.02	1.03	1.04	1.02	1.04	1.03	1.06	1.02
Mn^{2+}	0.03	0.03	0.03	0.03	0.03	0.03	0.03	0.03	0.03	0.03	0.03	0.03	0.03	0.03	0.03
Mg	1.02	1.02	0.99	1.02	0.99	1.00	0.99	1.00	0.99	1.00	1.00	0.98	0.98	0.99	0.99
Ca	0.01	0.01	0.00	0.01	0.01	0.01	0.01	0.00	0.00	0.01	0.01	0.01	0.00	0.01	0.00
Ba	0.00	0.00	0.00	0.00	0.00	0.00	0.00	0.00	0.00	0.00	0.00	0.00	0.00	0.00	0.00
Na	0.08	0.05	0.08	0.07	0.07	0.06	0.08	0.05	0.06	0.05	0.06	0.07	0.07	0.05	0.06
K	0.00	0.00	0.00	0.00	0.01	0.00	0.00	0.00	0.00	0.00	0.00	0.00	0.00	0.00	0.00
F	0.00	0.00	0.00	0.00	0.00	0.00	0.00	0.00	0.00	0.00	0.00	0.00	0.00	0.00	0.00
X_{Mg}	0.50	0.50	0.49	0.50	0.49	0.49	0.49	0.50	0.49	0.49	0.49	0.49	0.49	0.48	0.49

APPENDIX J: TRANSMITTED LIGHT AND BACKSCATTER ELECTRON IMAGES DISPLAYING ELECTRON MICROPROBE ANALYSES – IRON CREEK PERALUMINOUS GNIESS

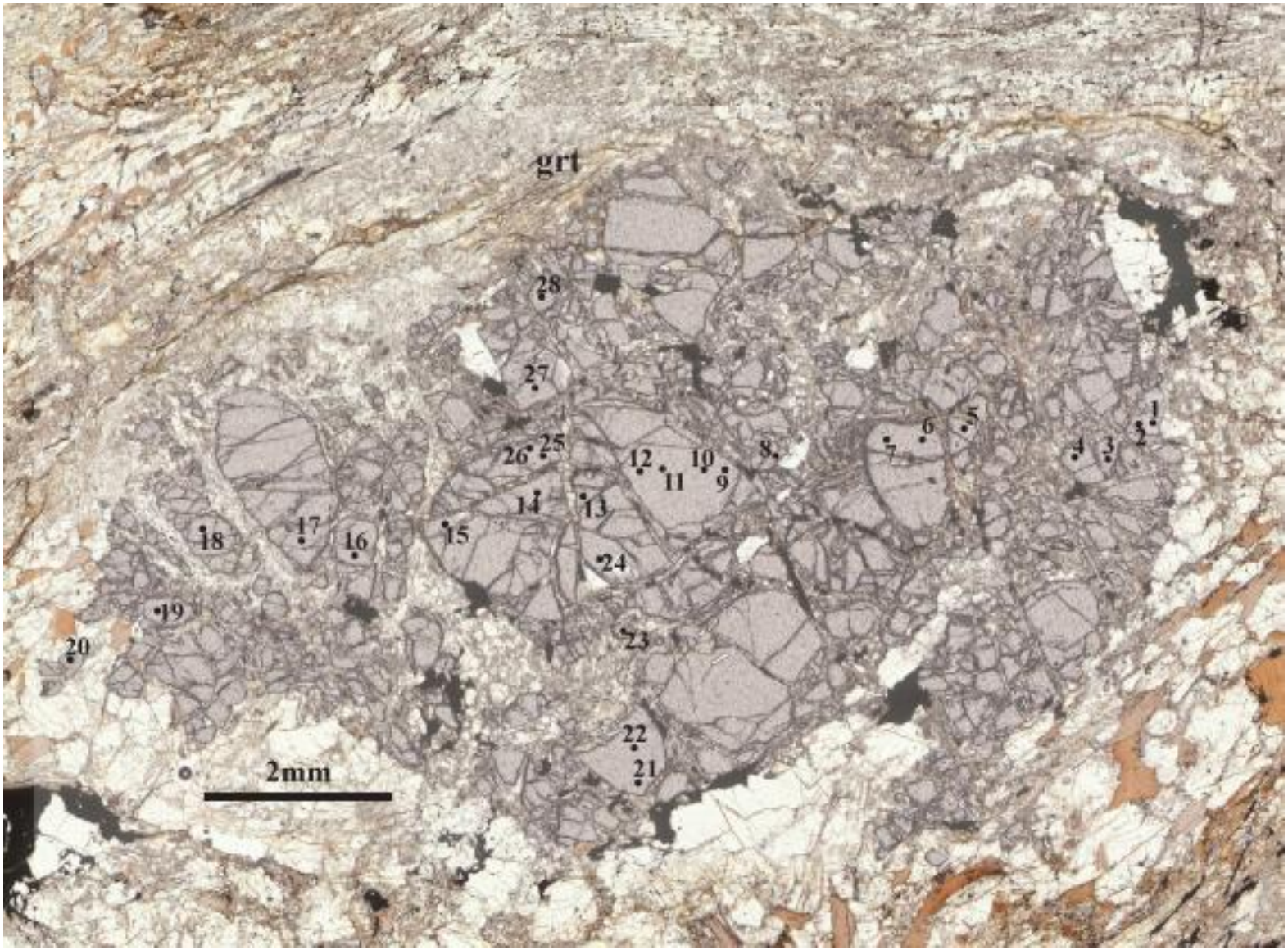

Appendix J, cont'd

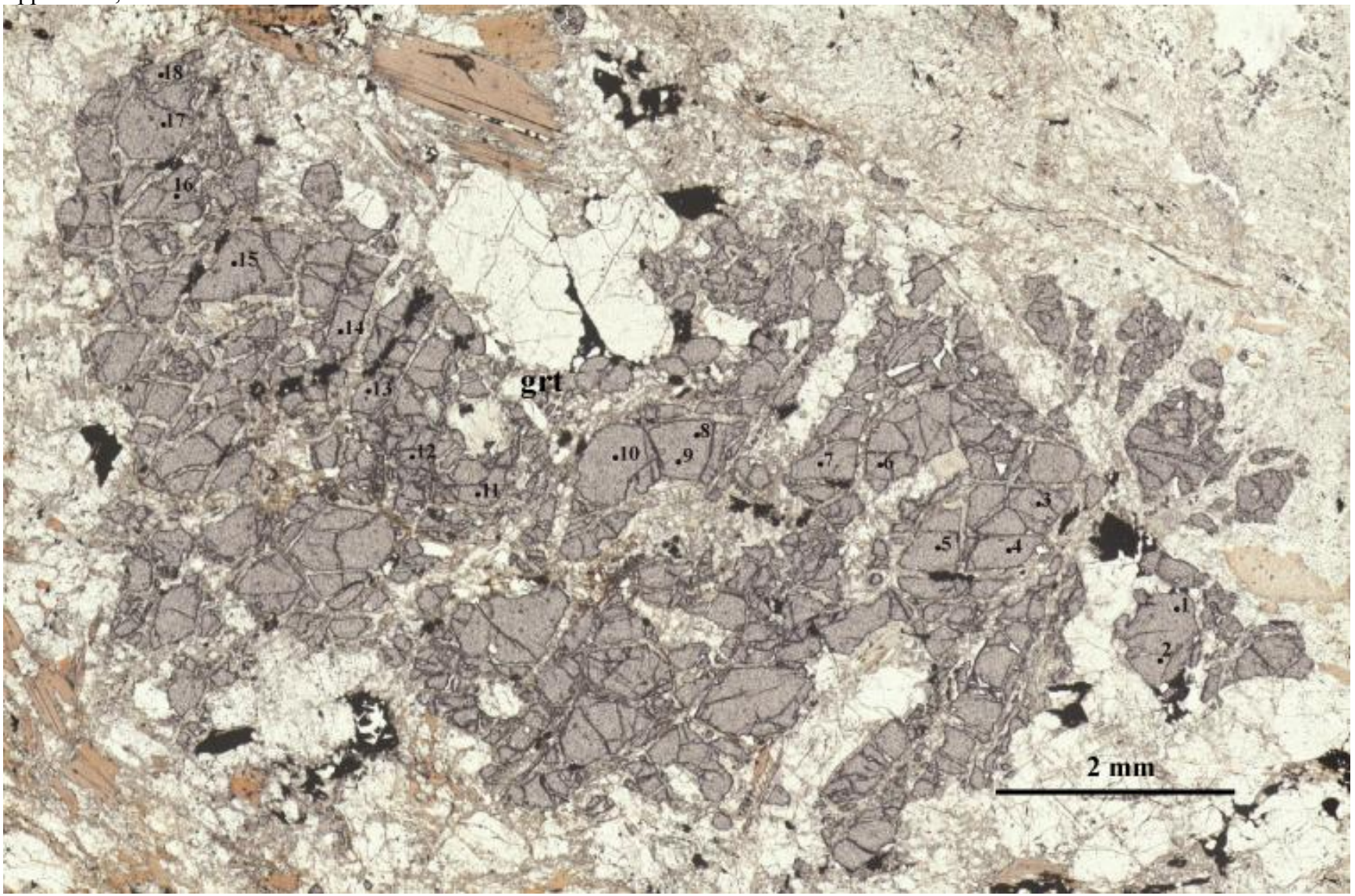

Appendix J, cont'd

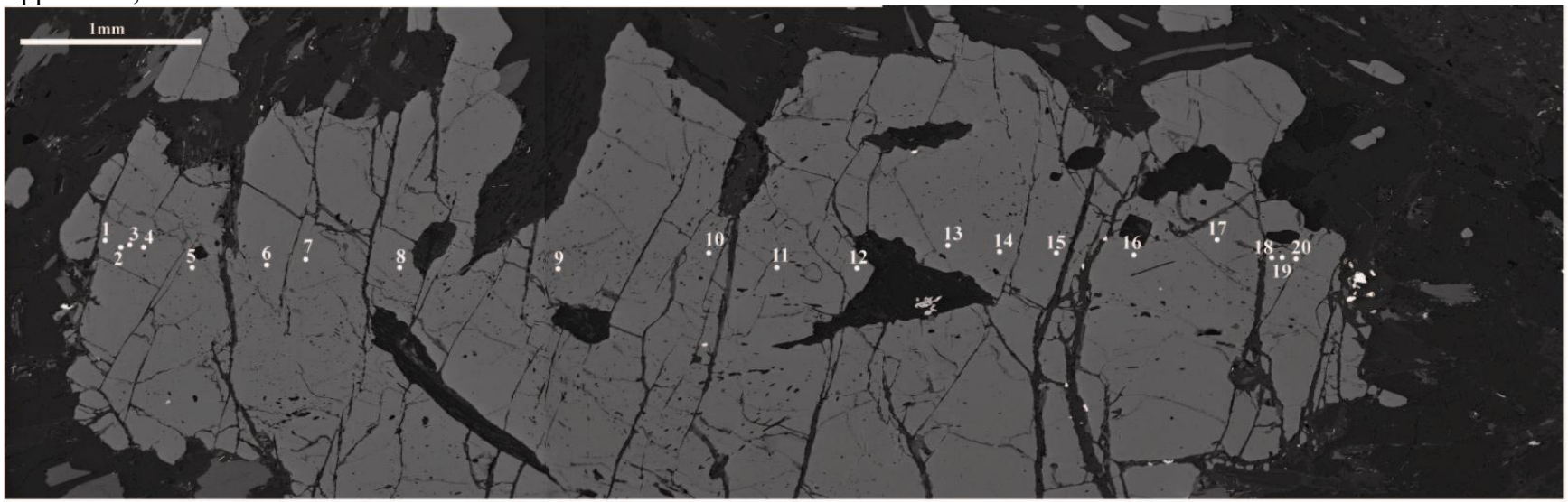

Appendix J, cont'd

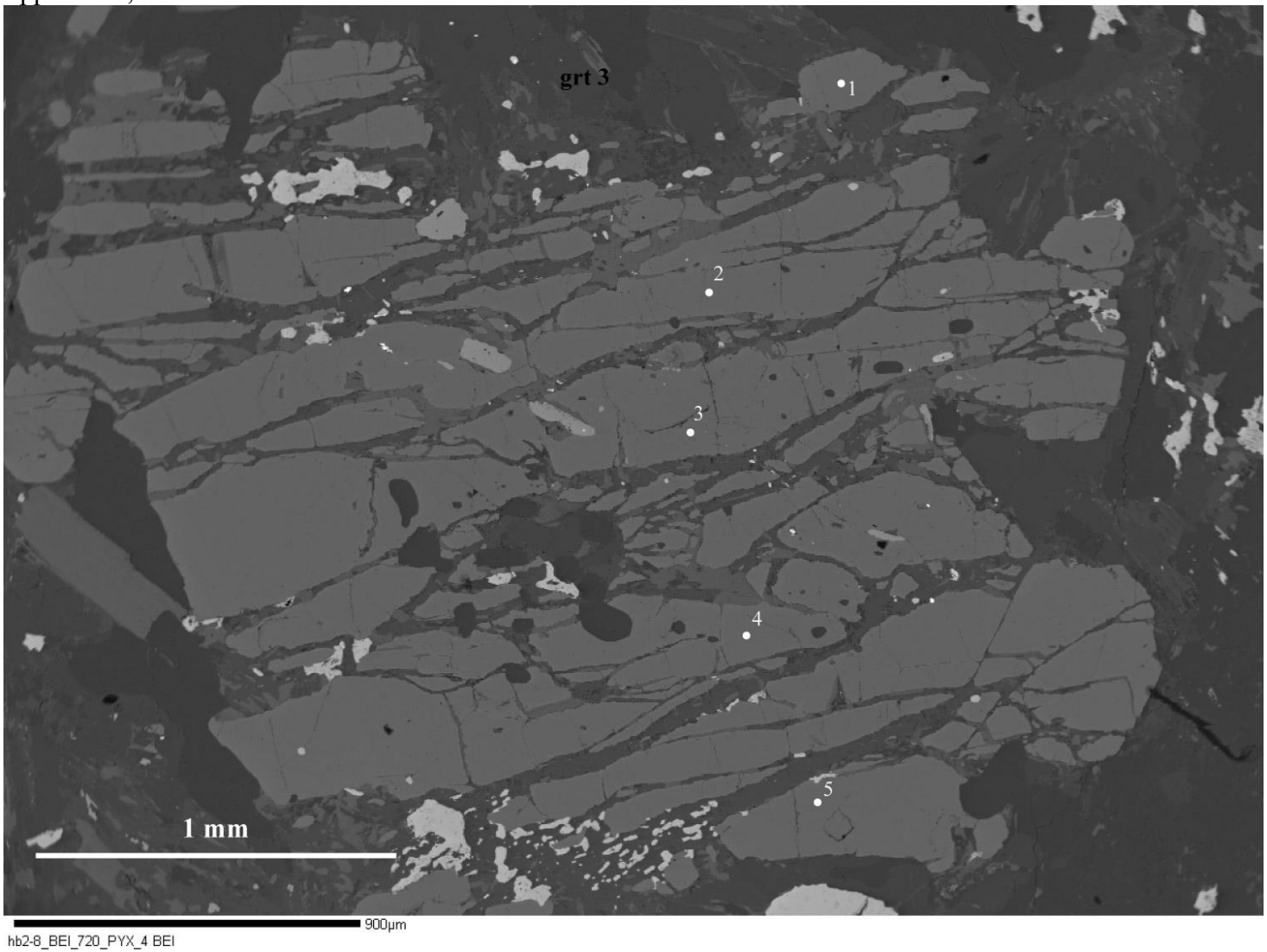

Appendix J, cont'd

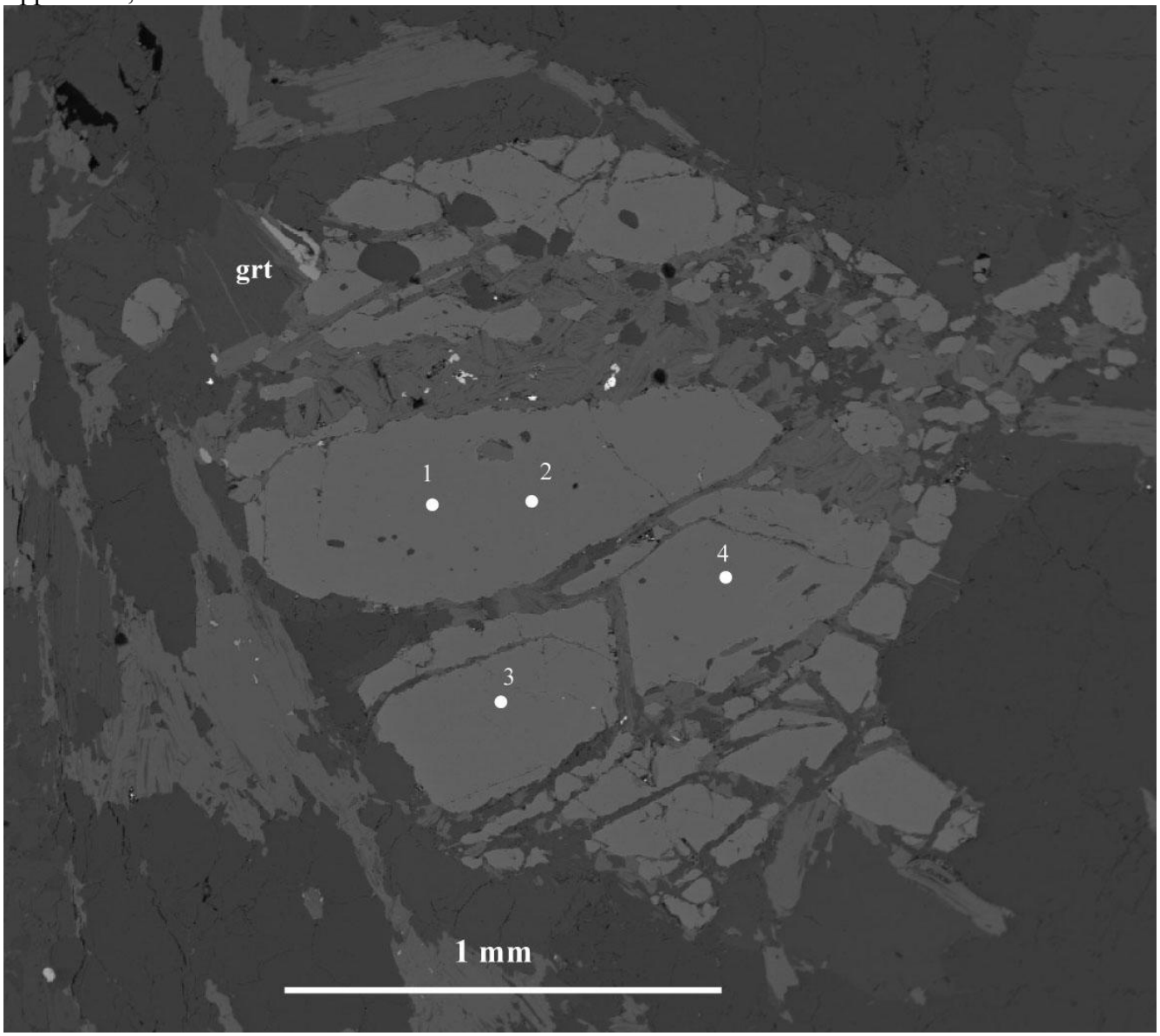

Appendix J, cont'd

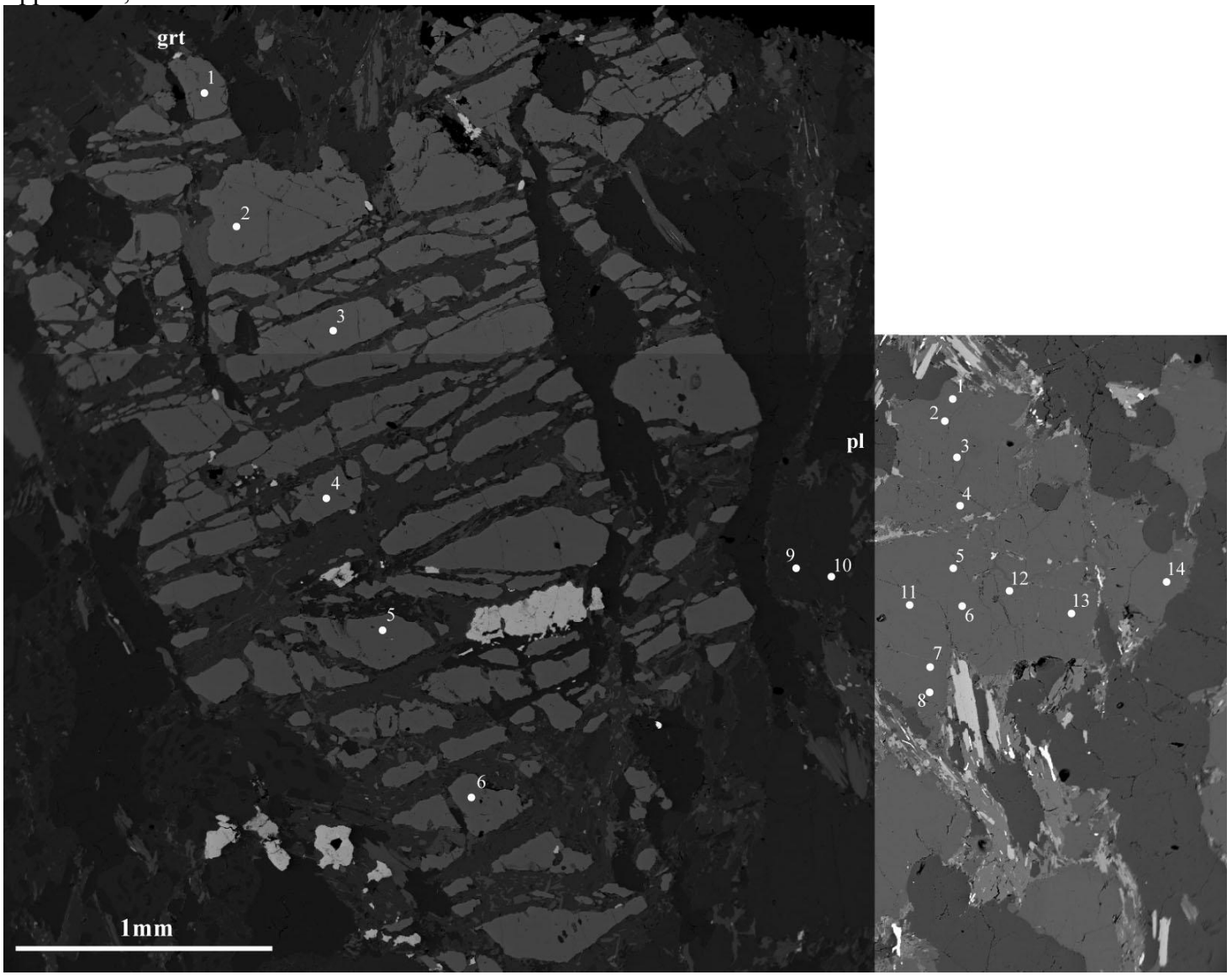

Appendix J, cont'd

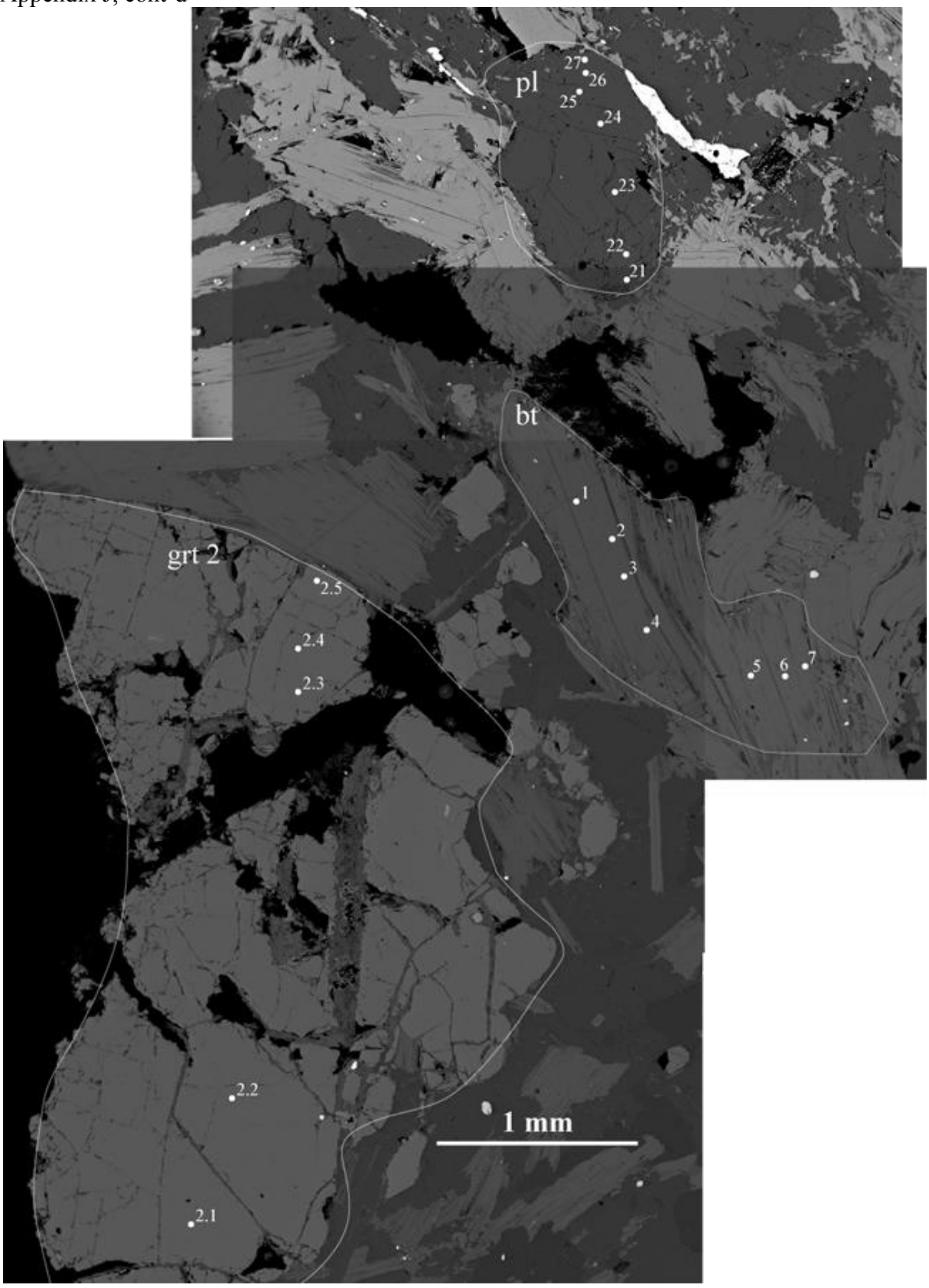

Appendix J, cont'd

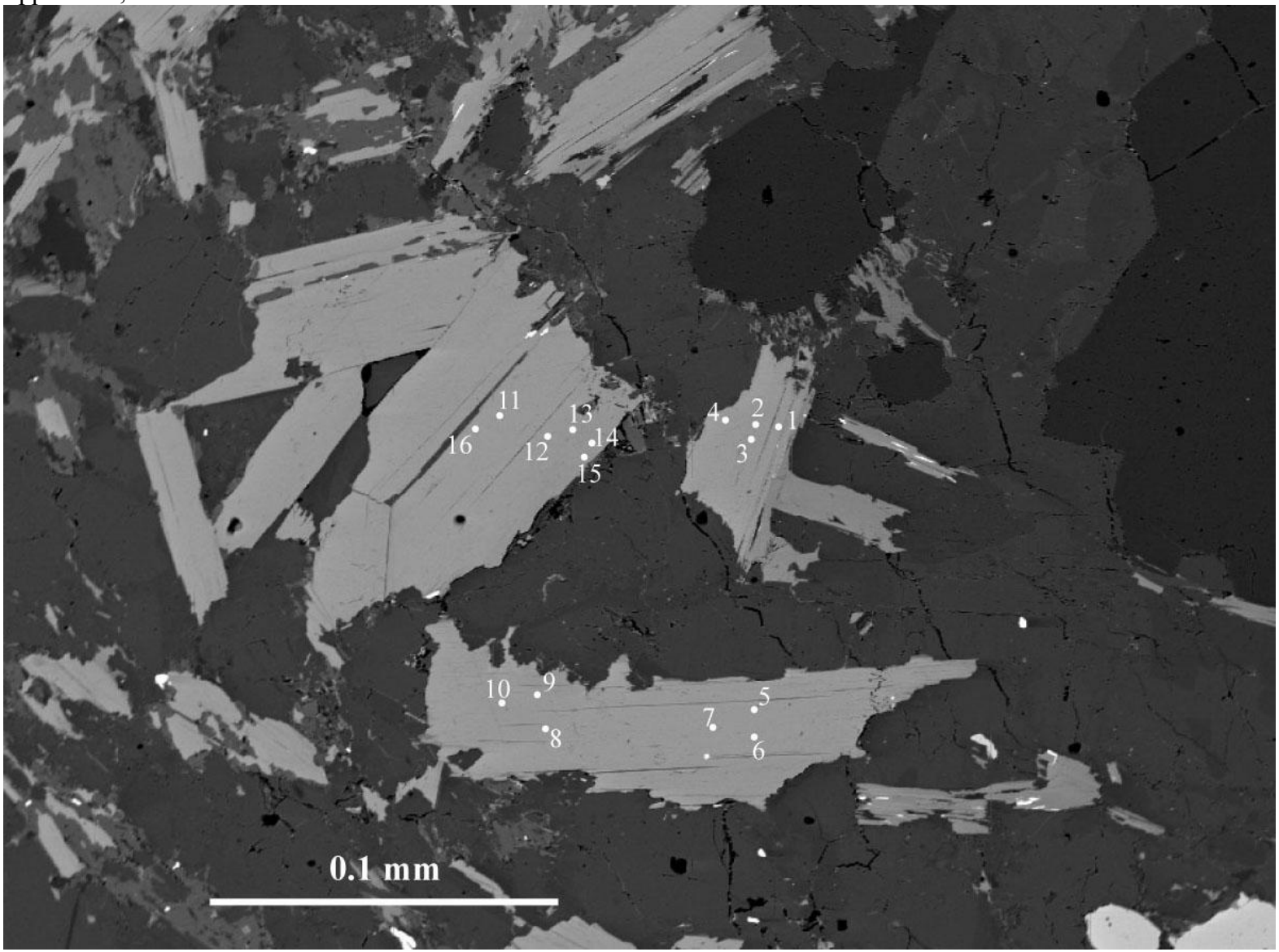

Appendix J, cont'd

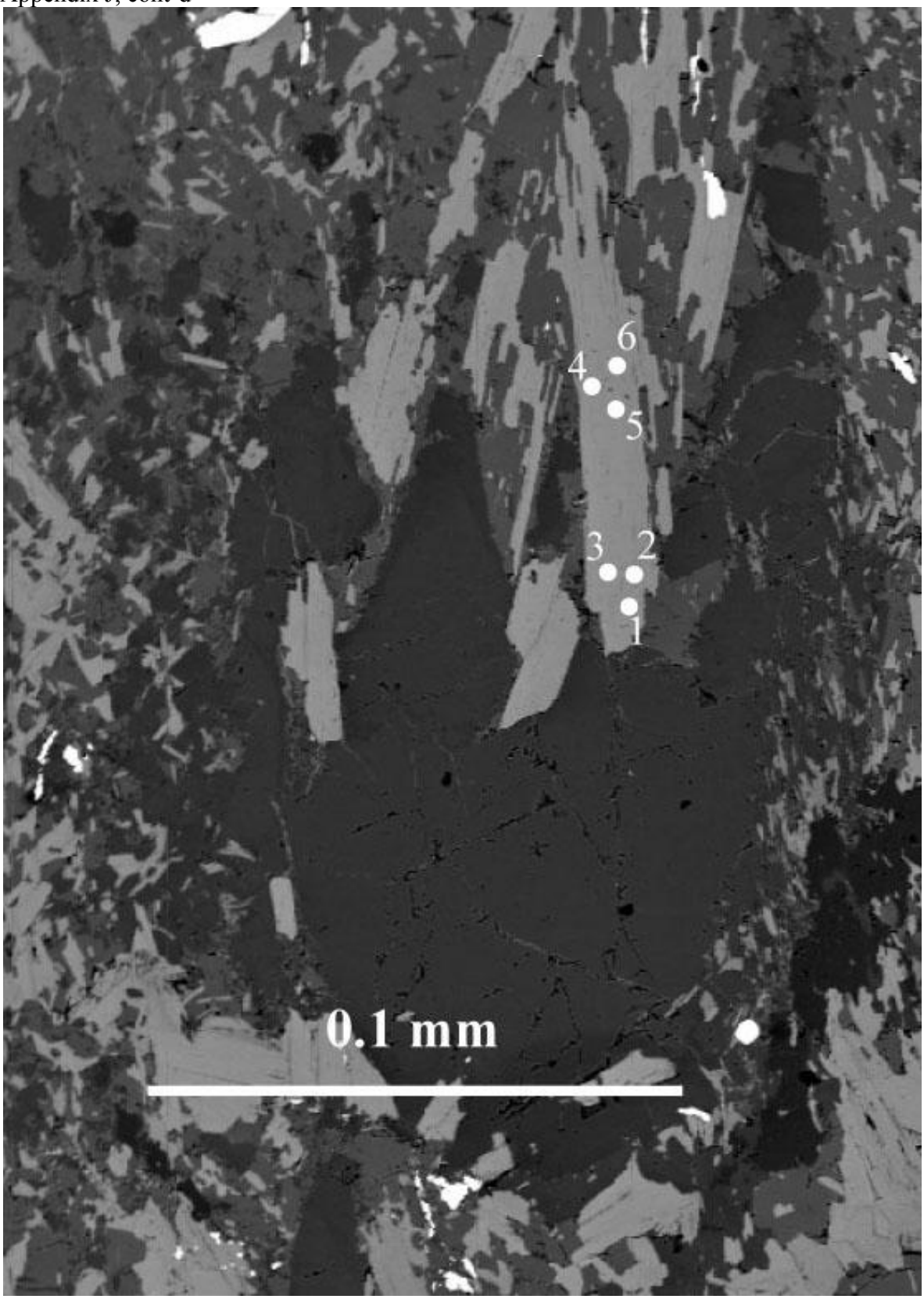

Appendix J, cont'd

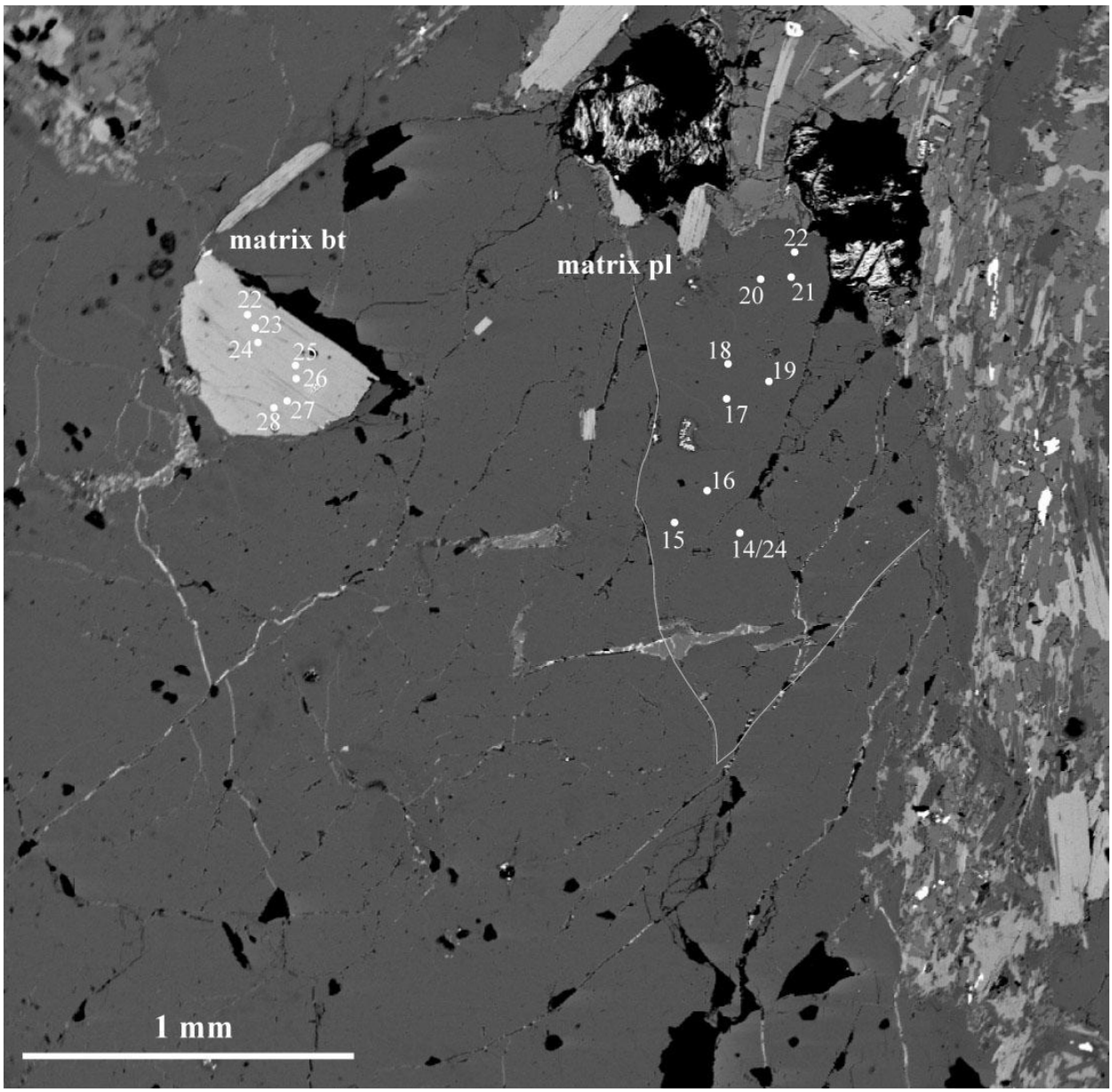

Appendix J, cont'd

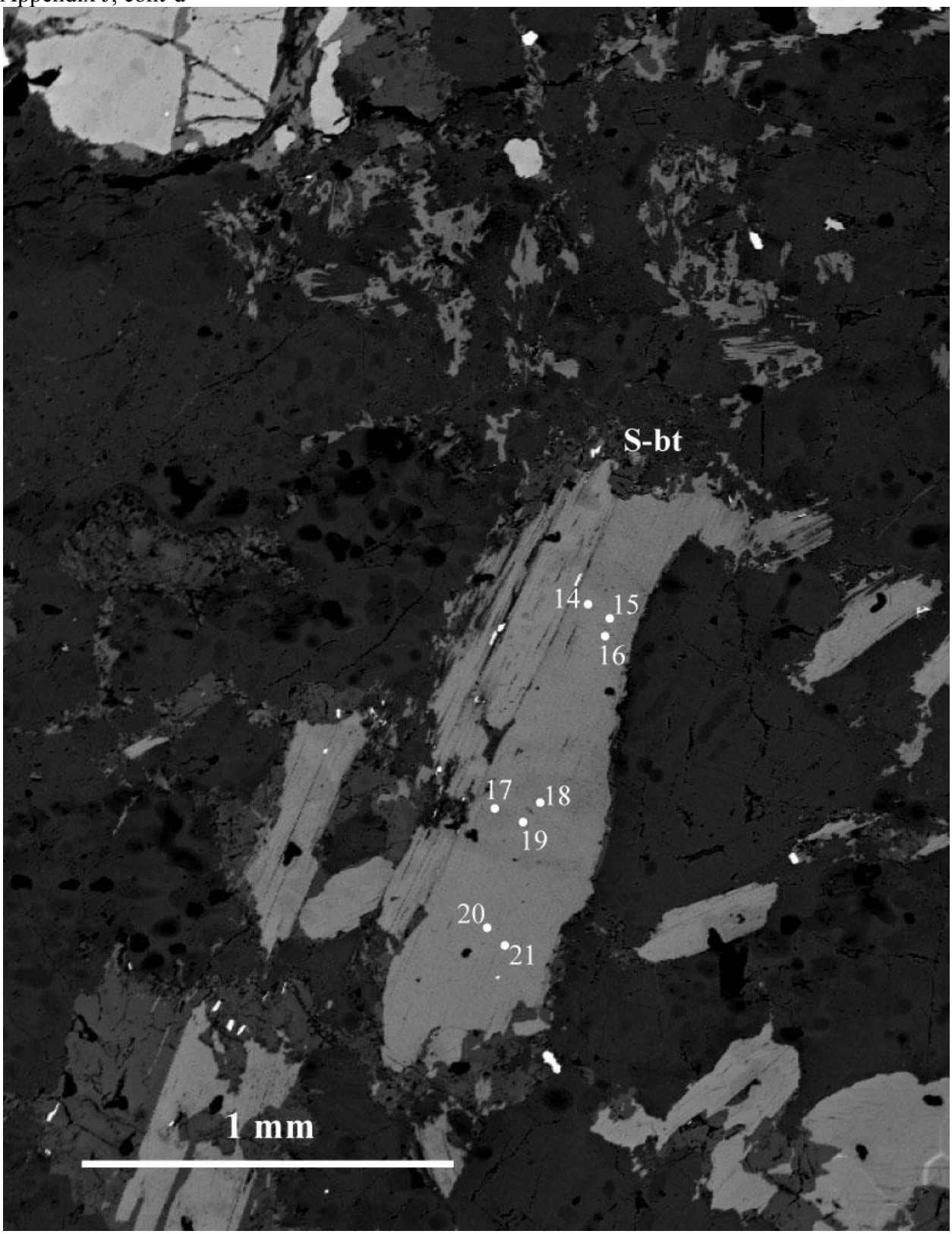

Appendix J, cont'd

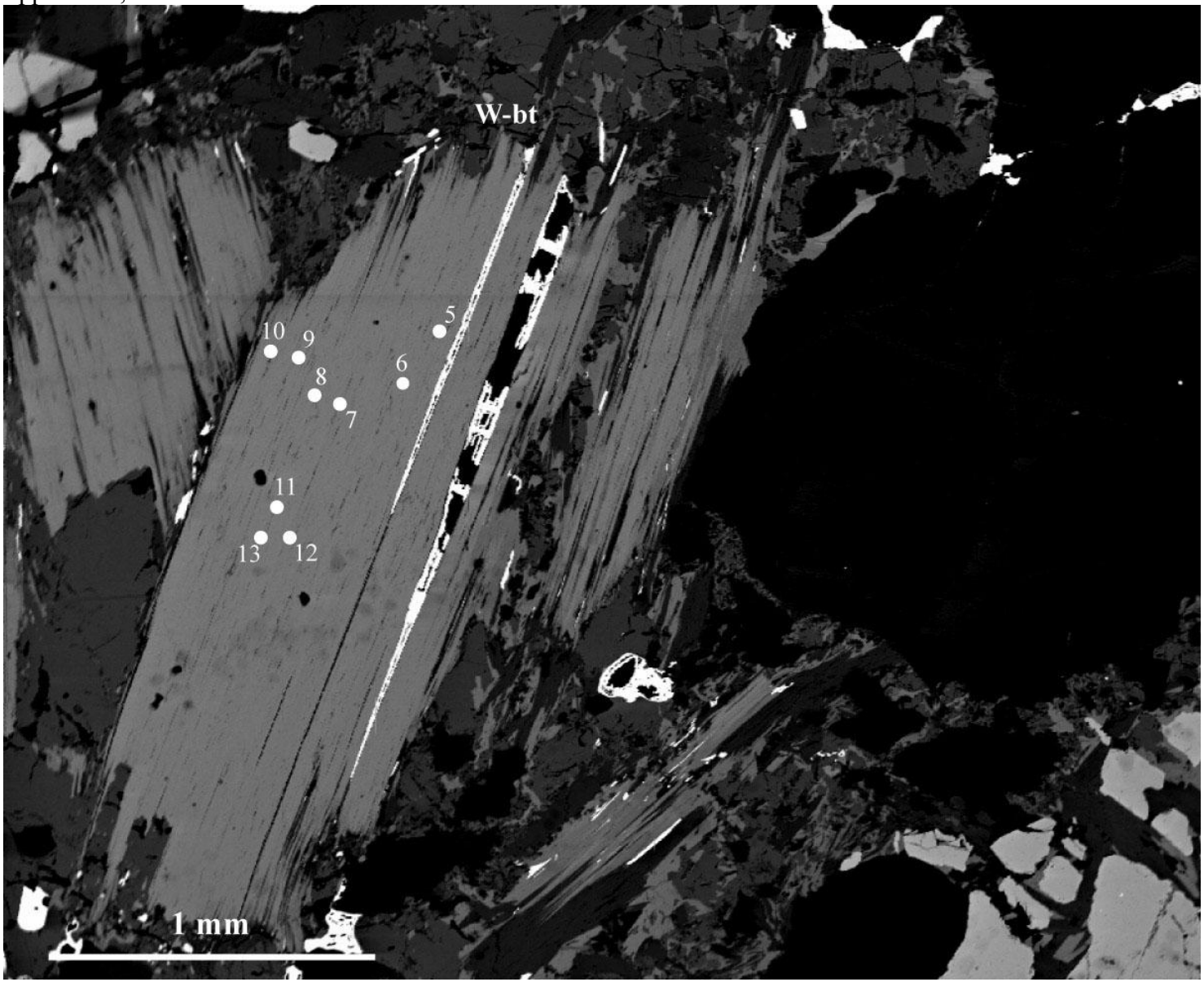

Appendix J, cont'd

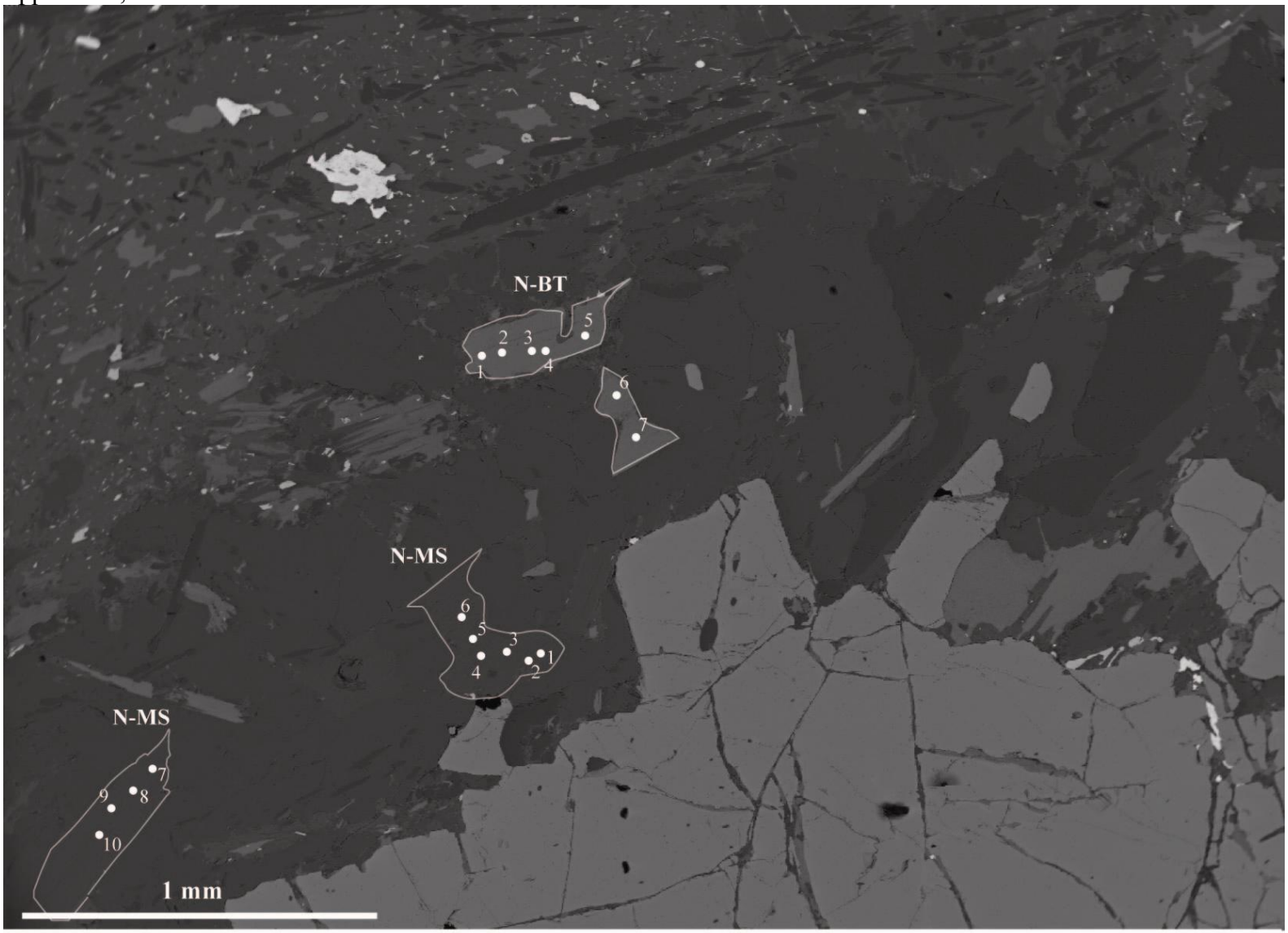

Appendix J, cont'd

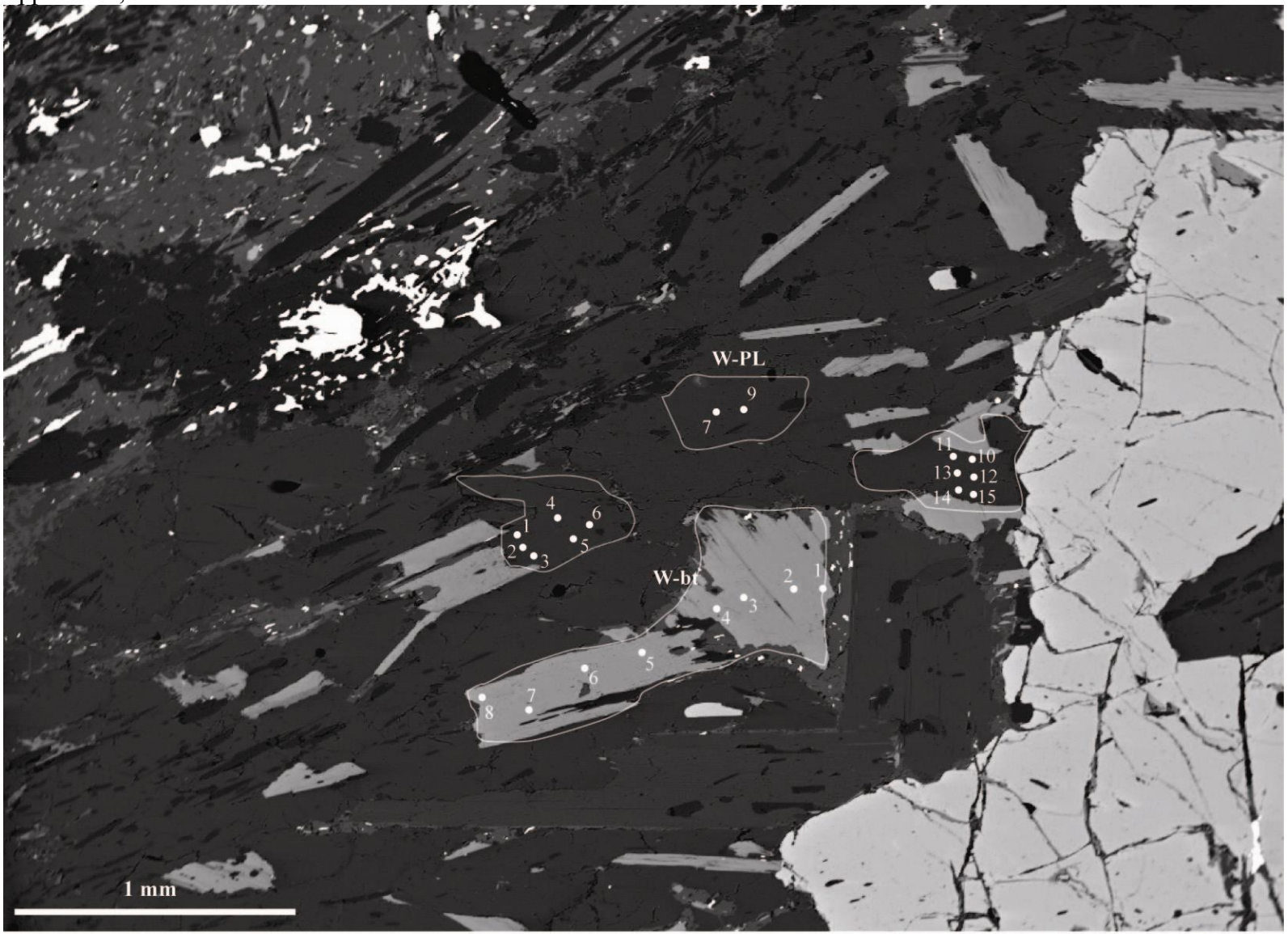

Appendix J, cont'd

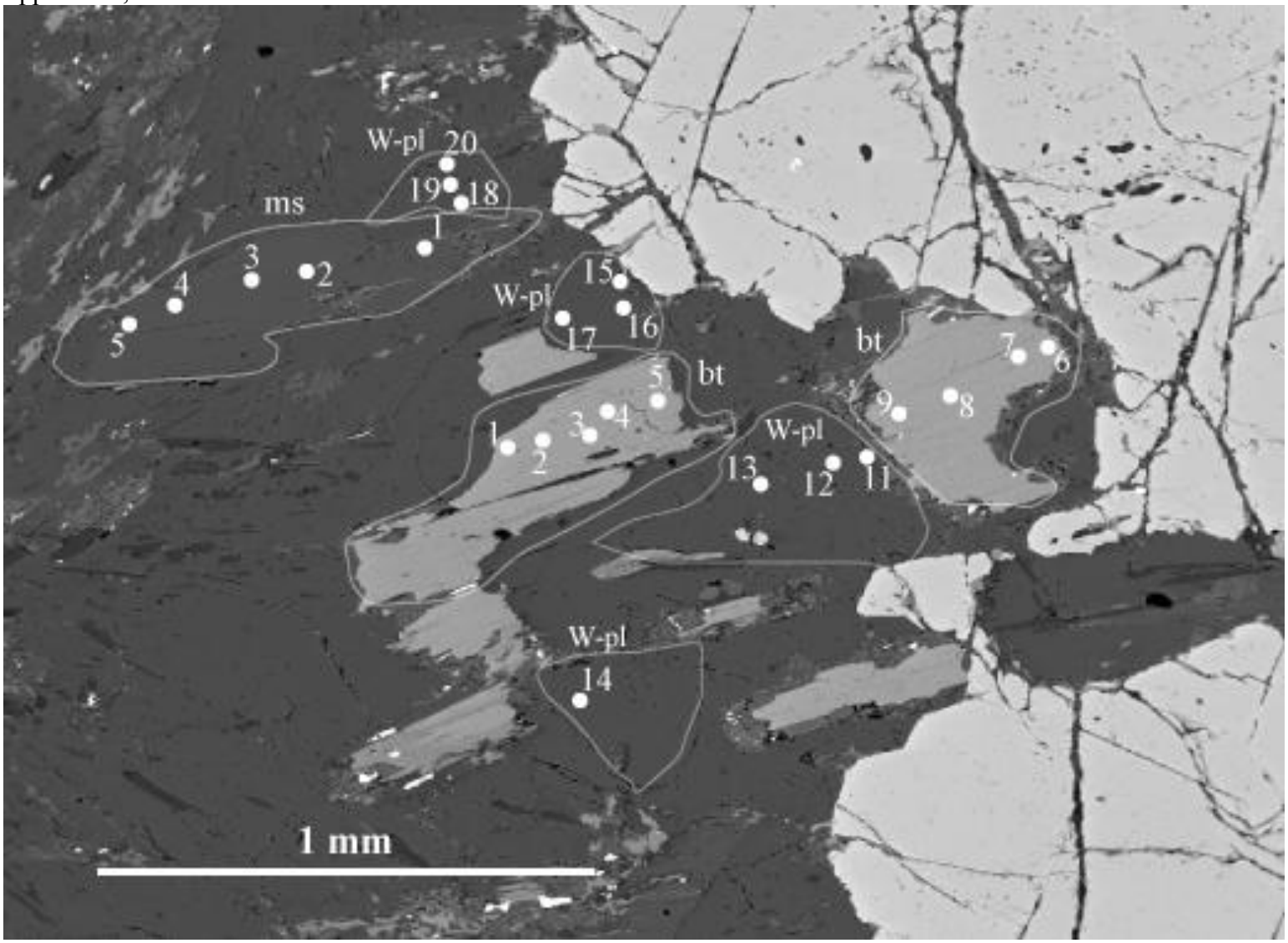

Appendix J, cont'd

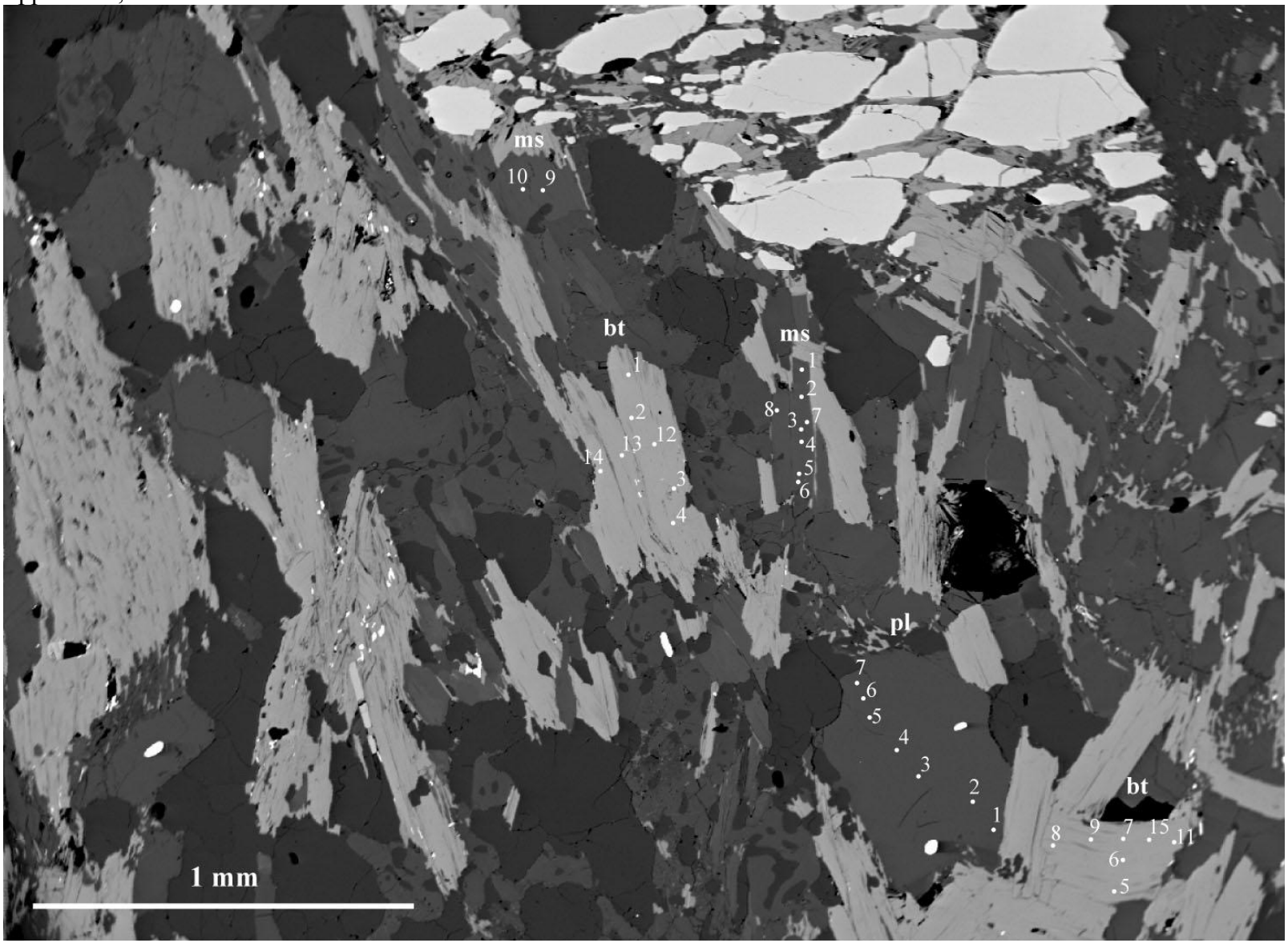

Appendix J, cont'd

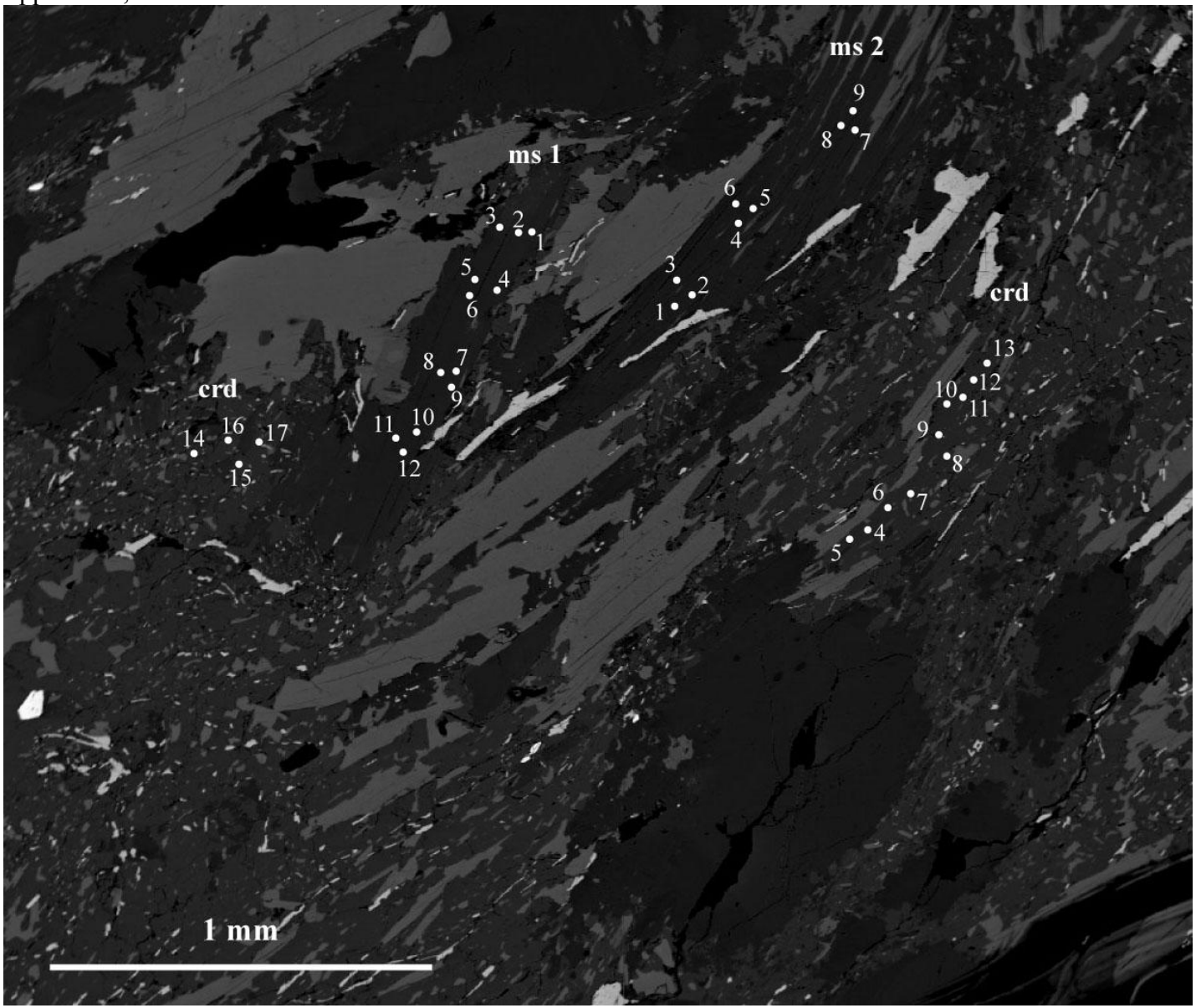

Appendix J, cont'd

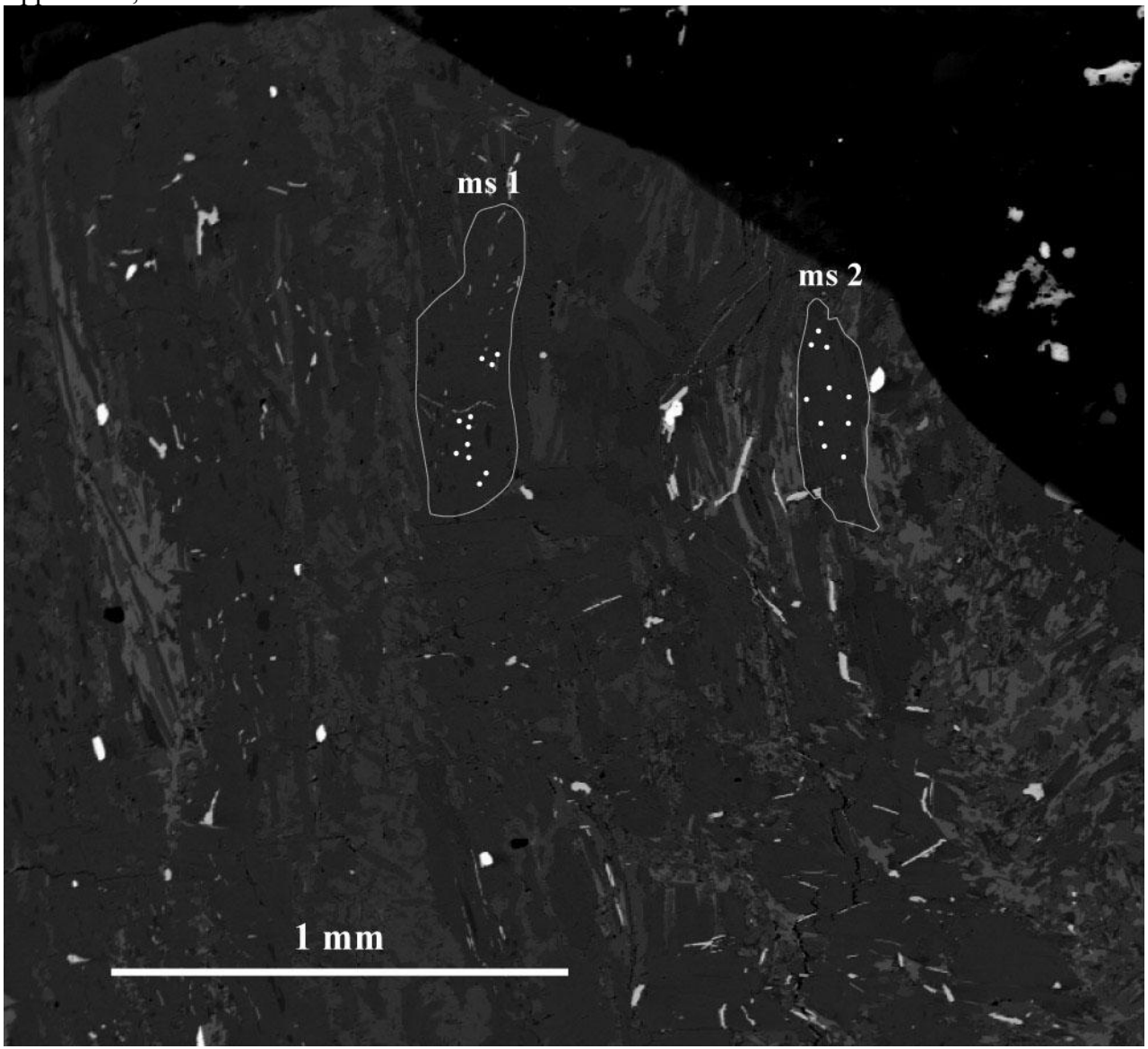

Appendix J, cont'd

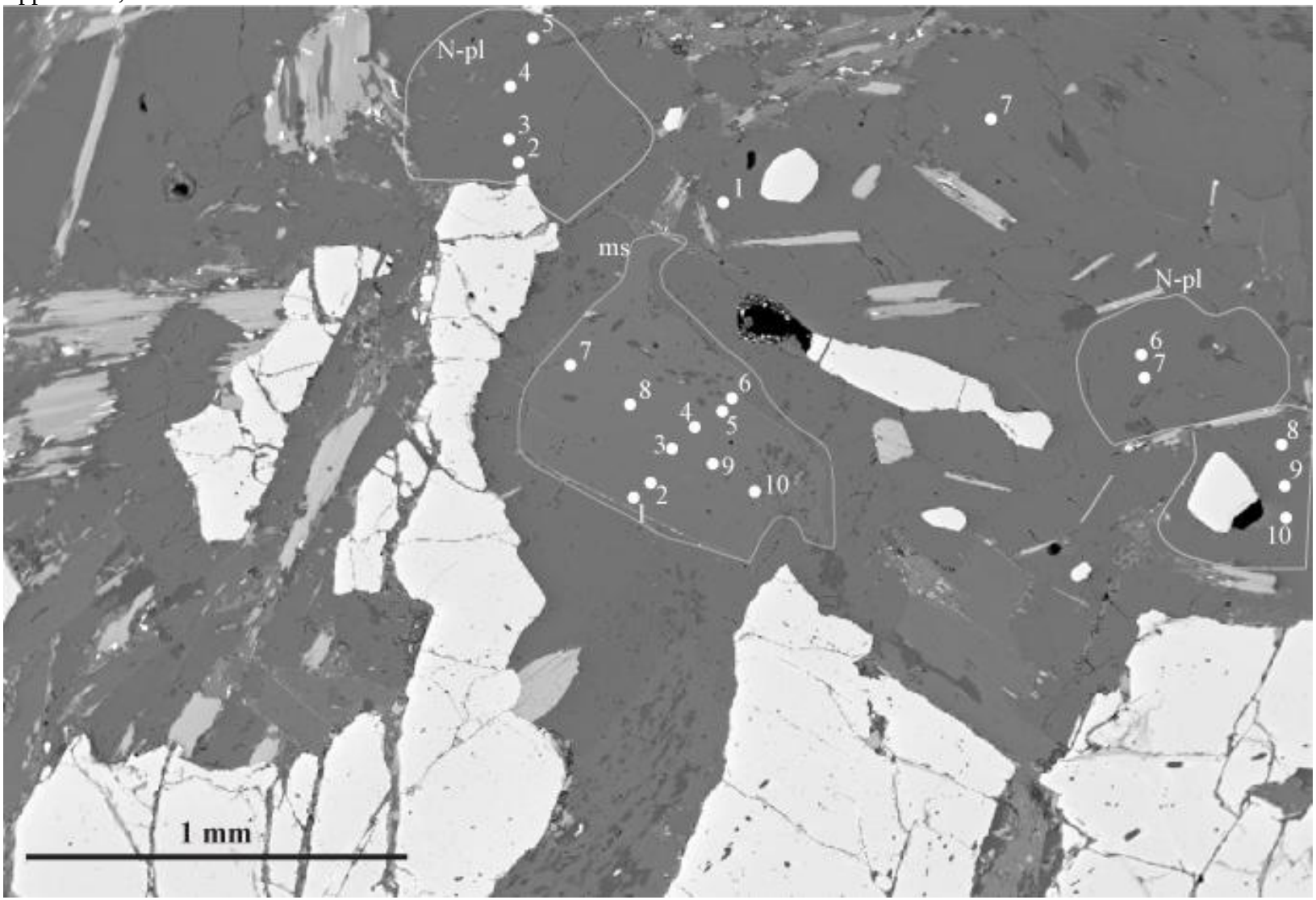

Appendix J, cont'd

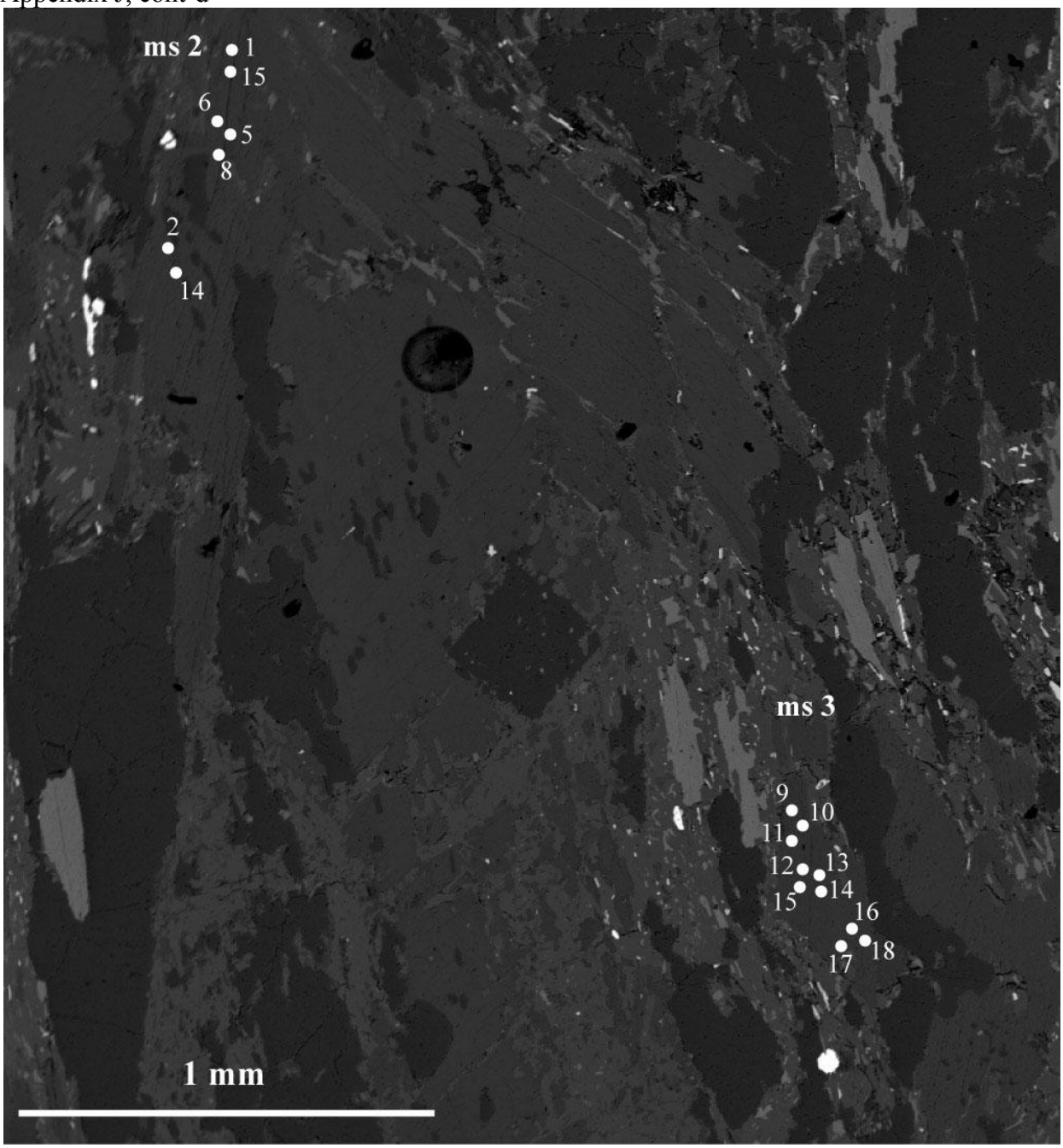

Appendix J, cont'd

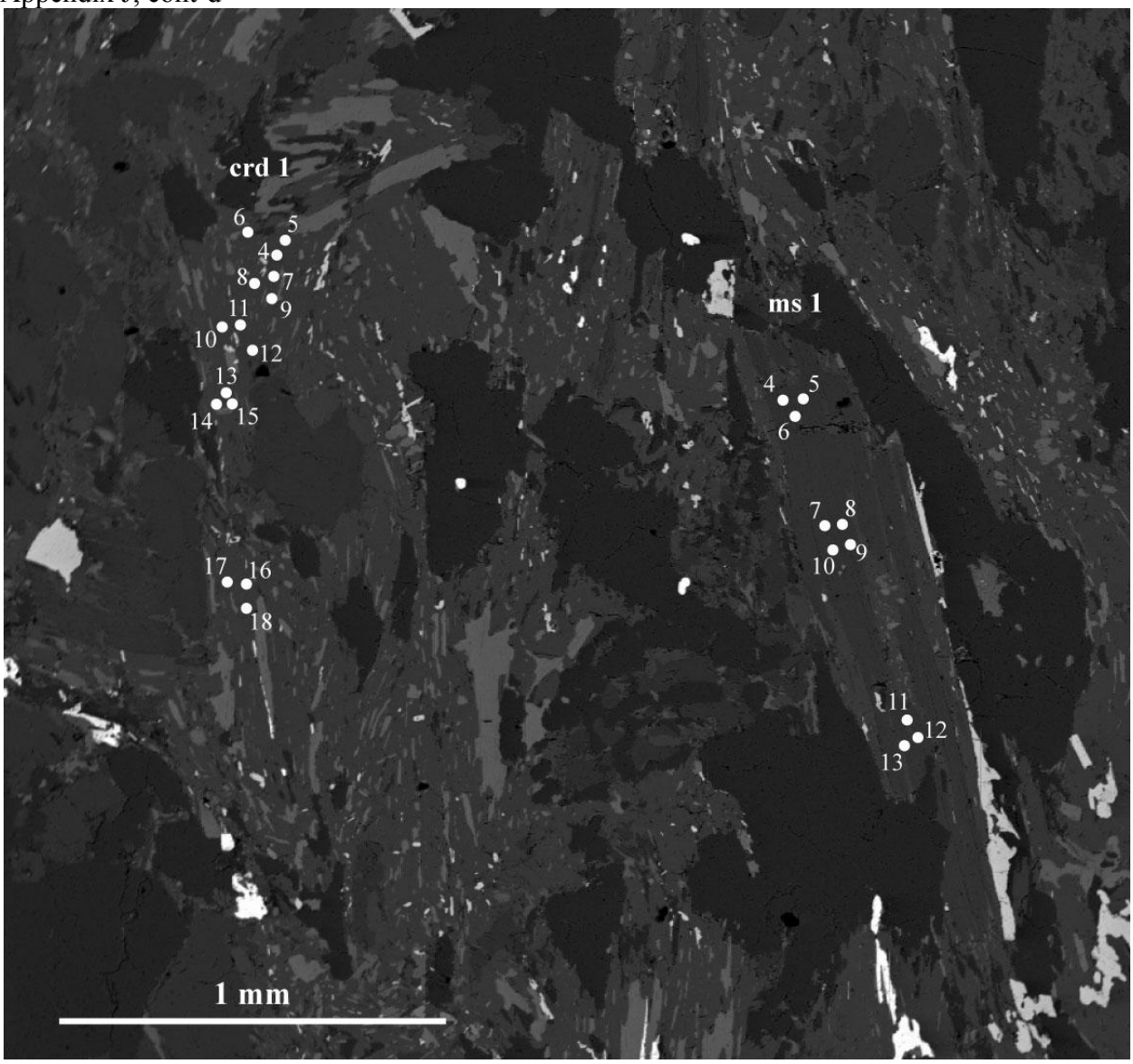

Appendix J, cont'd

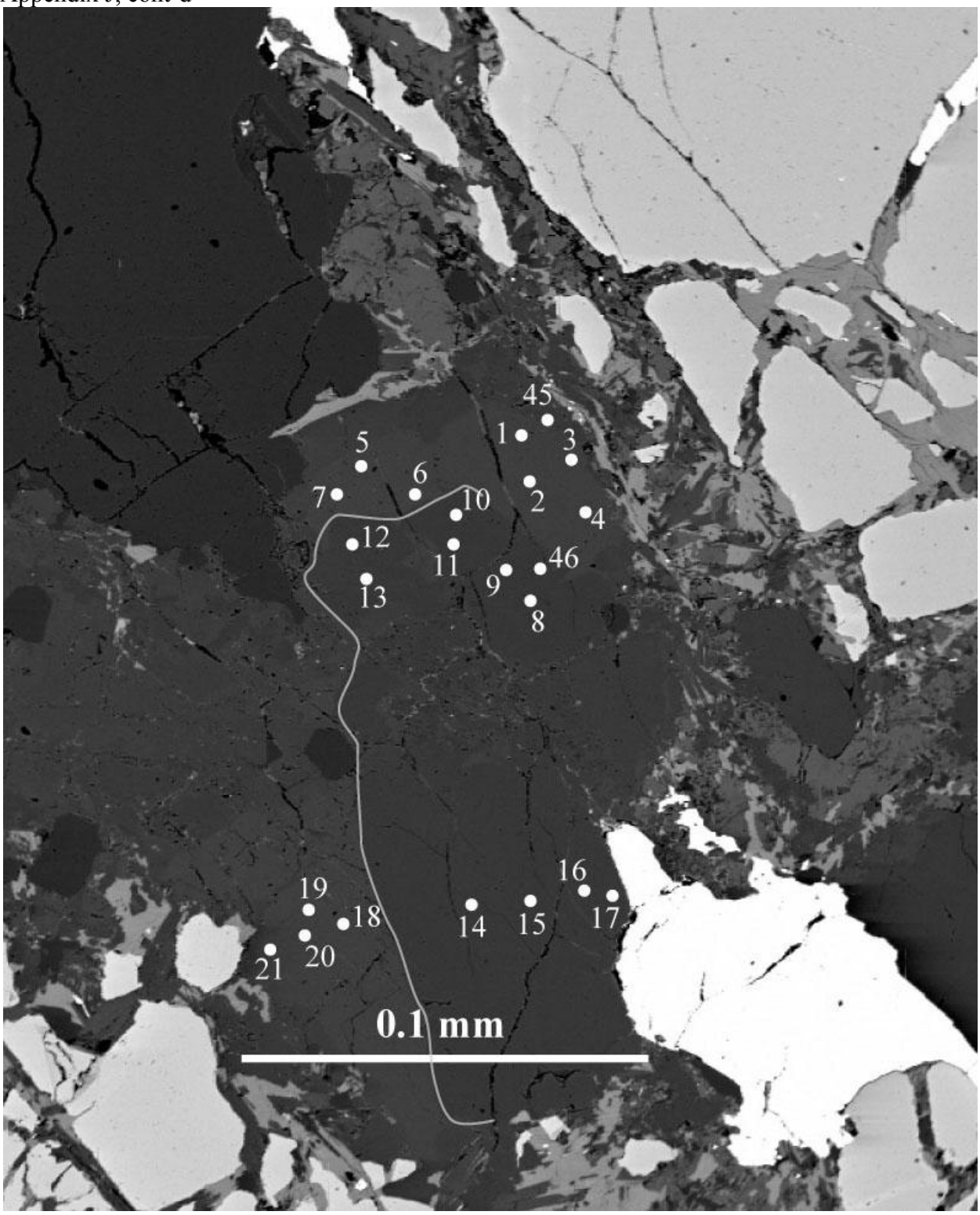

Appendix J, cont'd

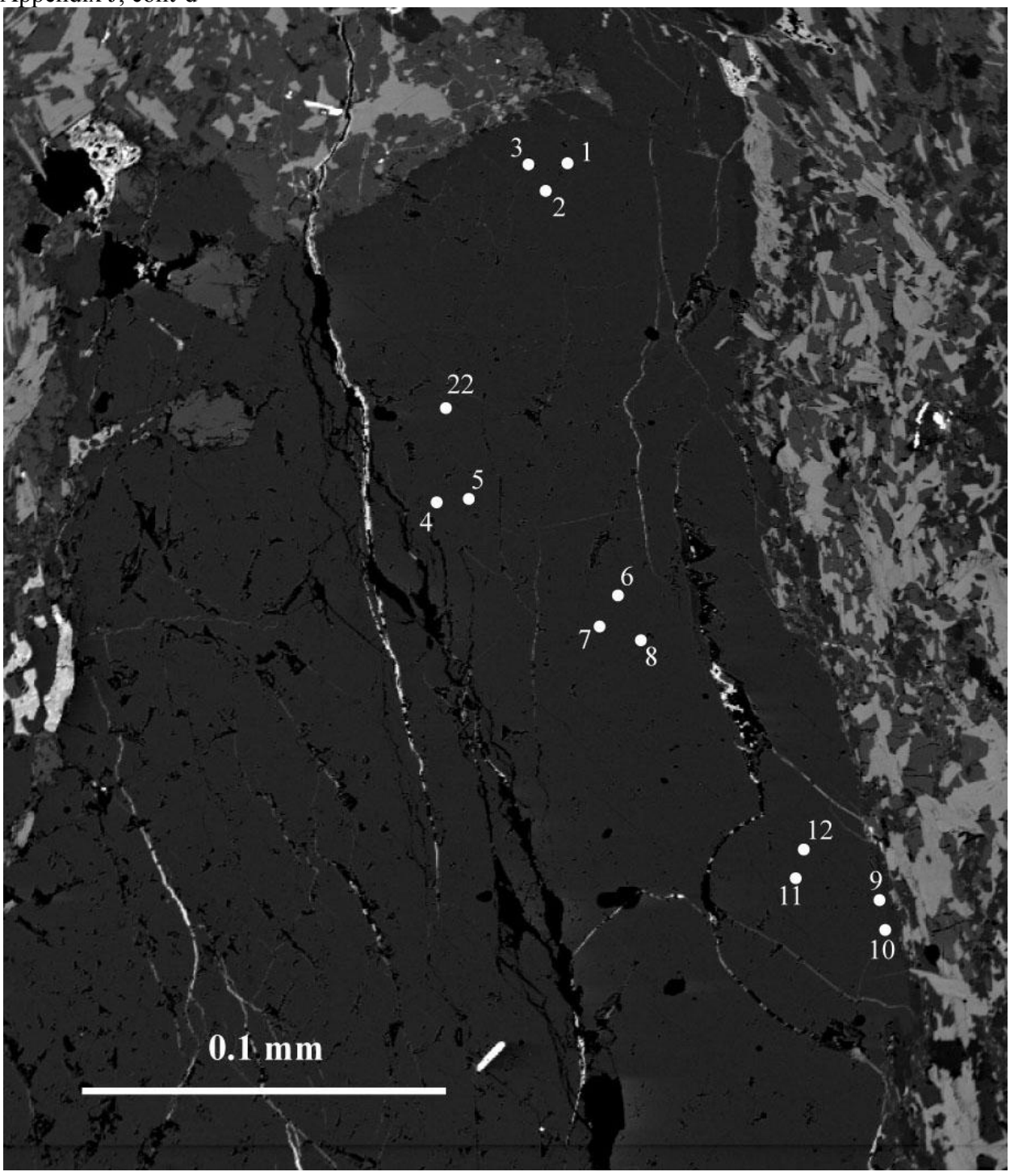

Appendix J, cont'd

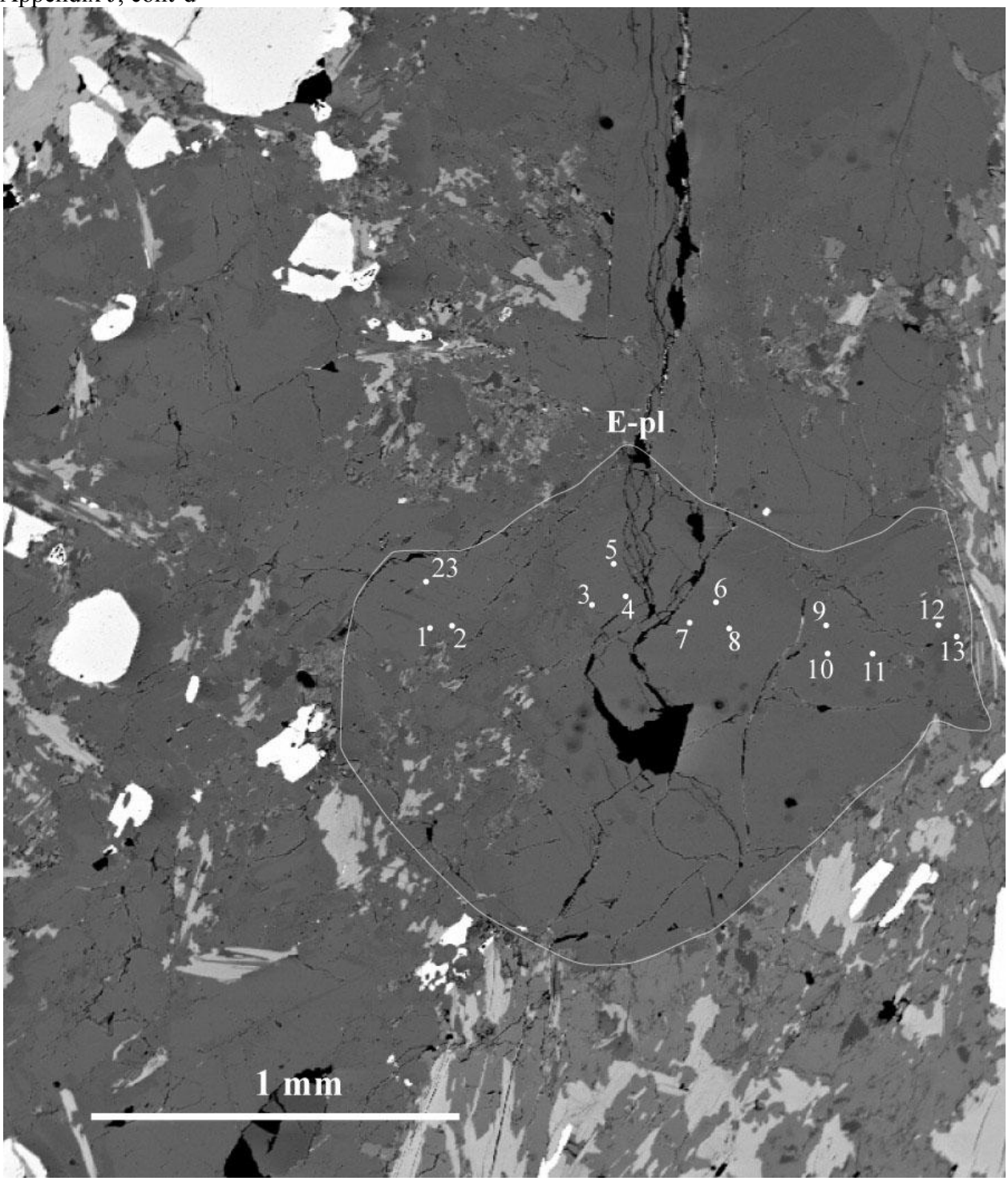

Appendix J, cont'd

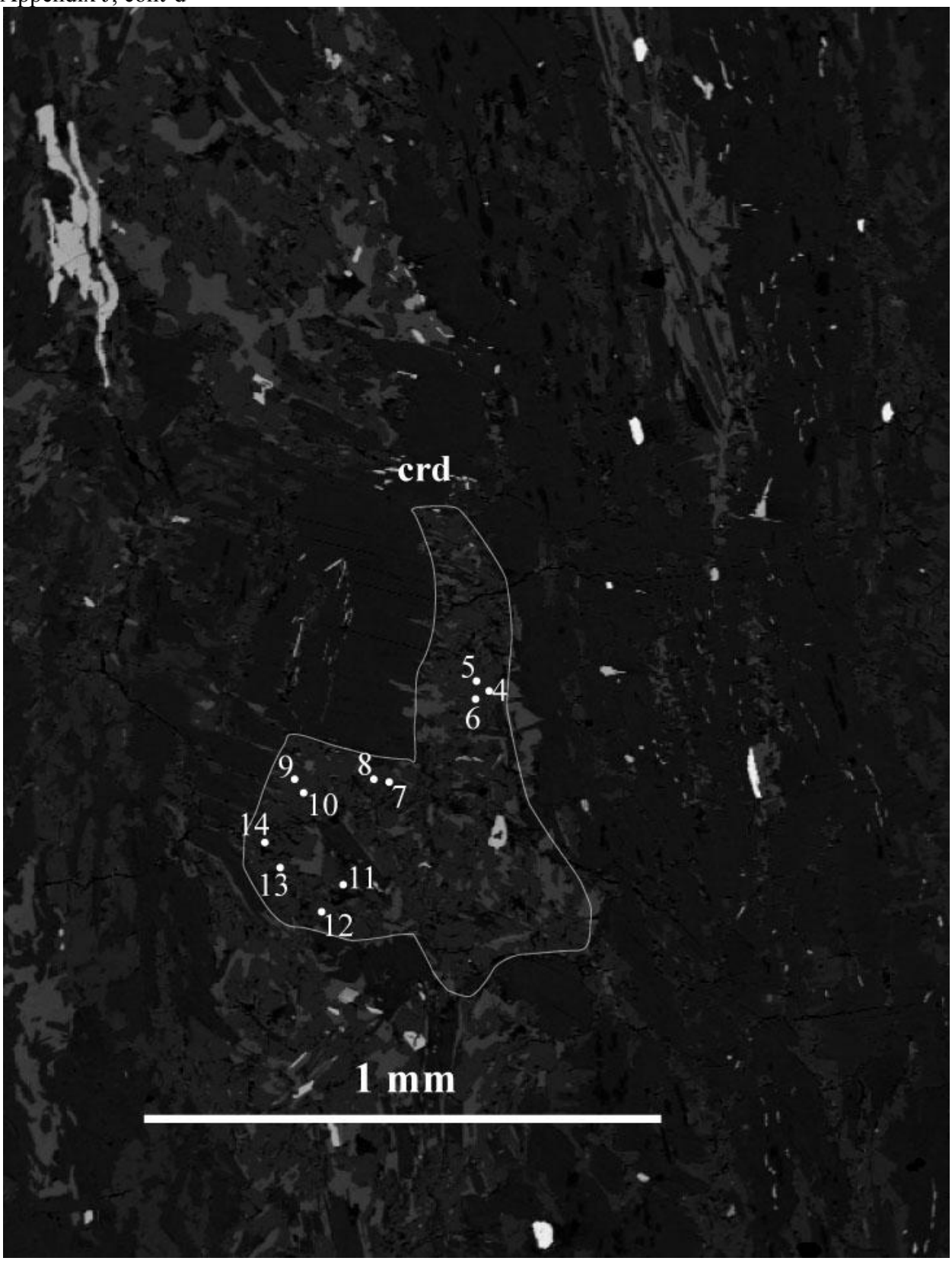

Appendix J, cont'd

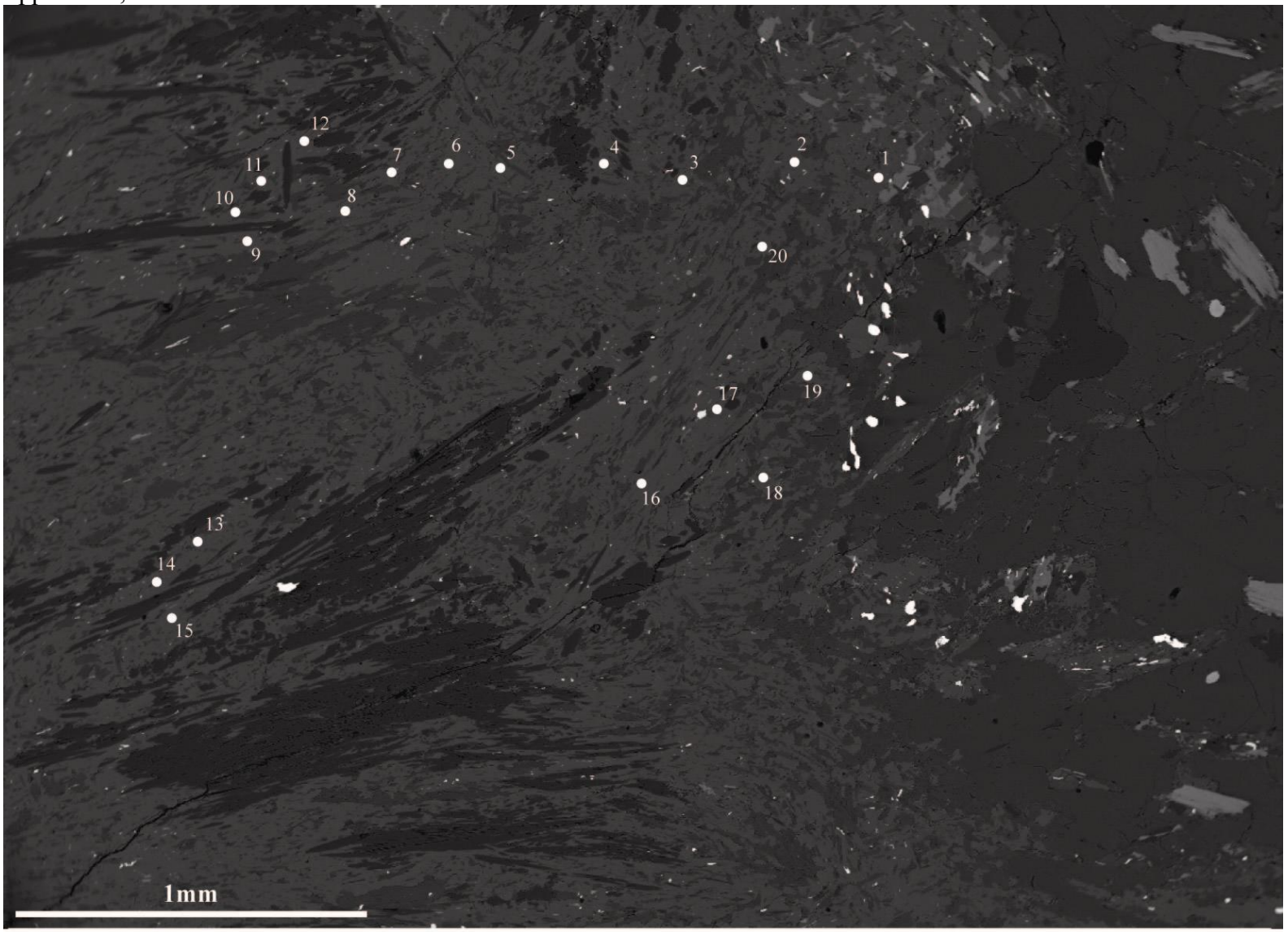

Appendix J, cont'd

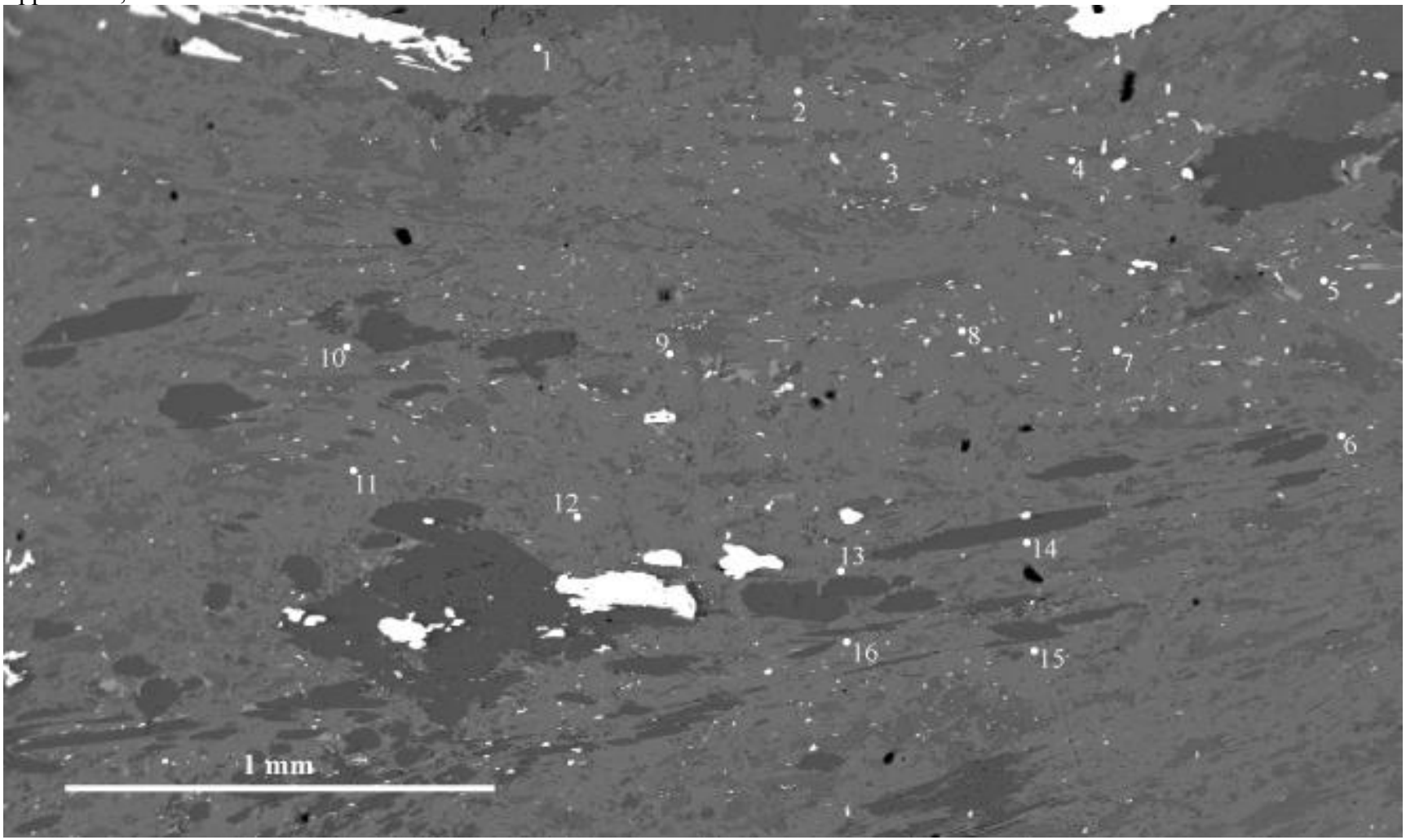

Appendix J, cont'd

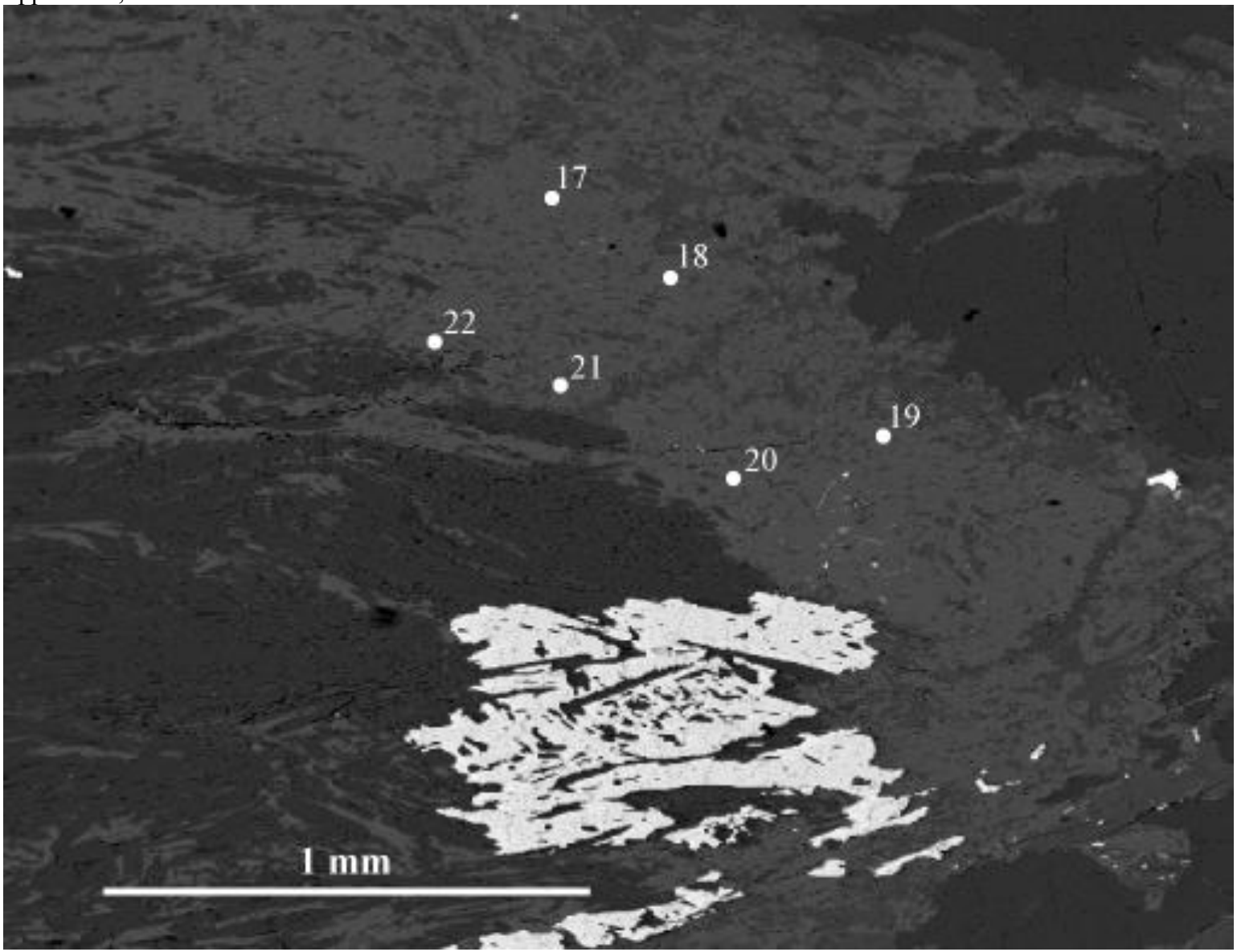

VITA

Kyle Michael Metz was born in February 1985, in Round Rock, Texas. He graduated from Round Rock High School in May, 2003, and was accepted to Texas Tech University as an engineering student. Following his first geology class, instructed by Aaron Yoshinobu, he changed his major to geology. Kyle was involved with Geoscience Society and served as president from August 2006 to May 2007. His senior thesis focused on studying the structural evolution of Precambrian metamorphic rocks with respect to the Priest Pluton in the Manzano Mountains, New Mexico. He graduated with honors from Texas Tech University in May, 2007 with a Bachelor of Science in geology.

In August 2007 Kyle entered the master's program at Louisiana State University. He was recruited by Dr. William Blanford to assist with a hydrogeology project outside Irbid, Jordan, in the summer of 2007. Once at Louisiana State University he was active in the Department of Geology and Geophysics. Kyle was accepted to the program as an ADG fellow from August 2007 – May 2009 and was a teaching assistant for structural geology in the spring of 2008 and mineralogy in the fall of 2008. He was able to participate in a research cruise in the Ross Sea, Antarctica, with Dr. Phil Bart in February, 2008. Kyle worked as an intern with Hess Oil Corporation in the summer of 2009.

Upon completion of his master's degree Kyle will enter the workforce with Marathon Oil Corporation in Oklahoma City, Oklahoma.